FERMILAB-DESIGN-1984-01

DESIGN REPORT TEVATRON 1 PROJECT

SEPTEMBER 1984

FERMI NATIONAL ACCELERATOR LABORATORY
BATAVIA, ILLINOIS

Operated by Universities Research Association Inc.,
under contract with the U.S. Department of Energy

TABLE OF CONTENTS

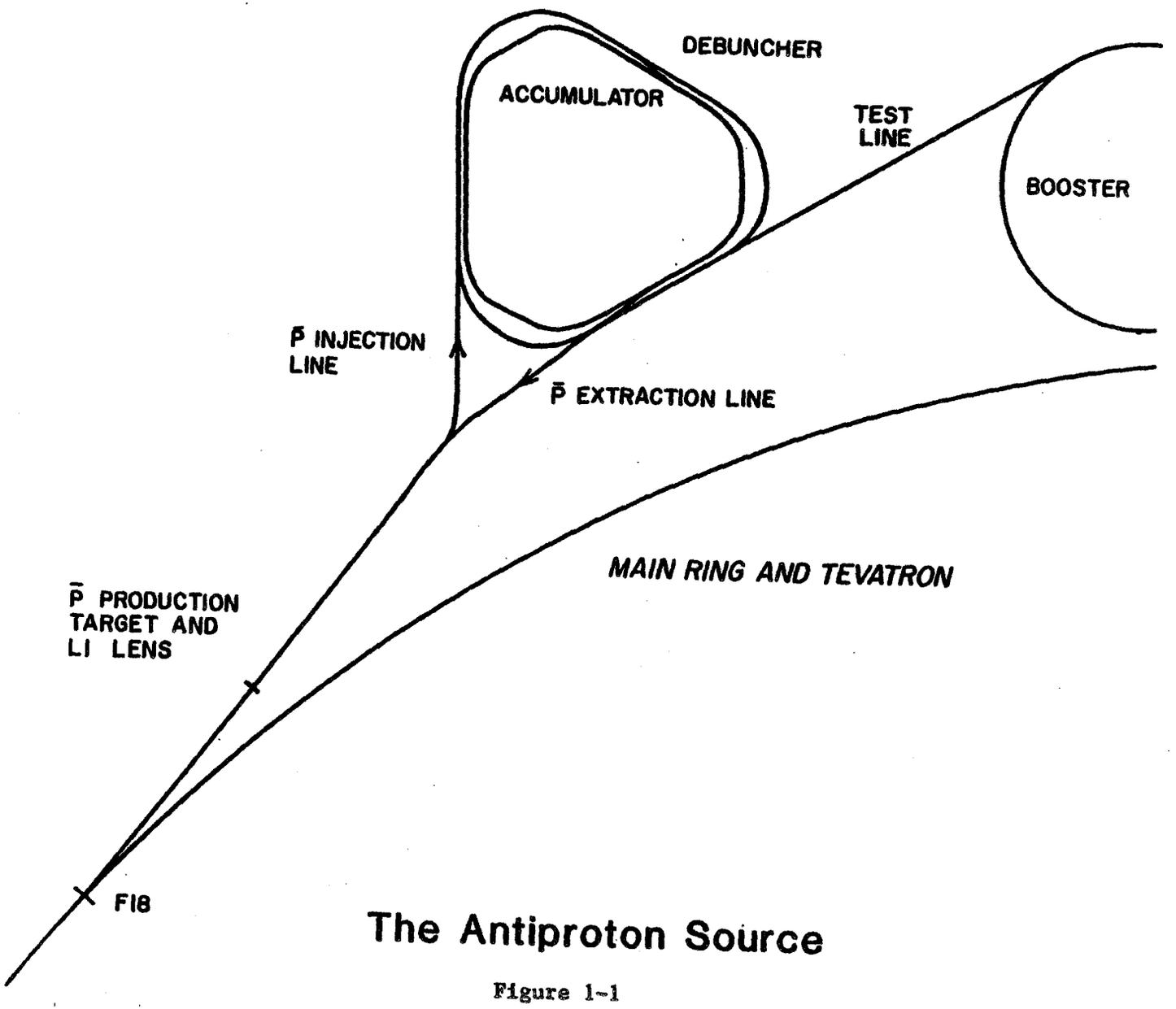

The Antiproton Source

Figure 1-1

CHAPTER 1

INTRODUCTION AND OVERVIEW

This report describes the design of the Tevatron I Project, which will enable Fermilab to produce proton-antiproton collisions in the Tevatron accelerator. Center-of-mass energies near 2 TeV, by far the highest available anywhere in the world for high-energy physics research until at least the decade of the 1990's, will provide enormous opportunities for exciting new physics.

After the energy, the most important parameter determining the utility of a colliding-beam facility is the luminosity, or interaction rate per unit cross section. The first goal of the Tevatron I project is to achieve a peak luminosity of $10^{30}cm^{-2}sec^{-1}$ for proton-antiproton collisions at the maximum energy in the Tevatron.

The luminosity depends on the intensity and phase space density of the interacting beams. The design luminosity of $10^{30}cm^{-2}sec^{-1}$ can be achieved with as few as 1.8×10^{11} protons and 1.8×10^{11} antiprotons of appropriate phase space density. The number and phase-space density of antiprotons produced by bombarding a dense target with one pulse of protons from the Main Ring are too small by orders of magnitude to achieve the design luminosity. Thus it is necessary to collect many pulses of antiprotons in an accumulator ring and to increase their phase-space density, i. e. to cool them, by roughly six orders of magnitude. To minimize user frustration and maximize the average luminosity, the accumulation time should be as short as possible, at least short compared to the luminosity lifetime, which is expected to be larger than twenty hours. The second goal of the project is to accumulate and cool the required number of antiprotons in five hours or less, starting with no antiprotons in the Accumulator.

The design presented here to meet these goals is based on the method of stochastic cooling developed by van der Meer, Thorndahl, and coworkers.[1] This method generates a non-uniform phase-space density distribution of the accumulated antiprotons, with only the high-density core useful for colliding beams. Thus the source has been designed to accumulate a total of 4.3×10^{11} antiprotons in 4 hours, of which typically 1.8×10^{11} antiprotons from the high-density core will be injected into the Tevatron. Subsequent accumulation cycles starting with the antiprotons left from the previous cycle will require considerably shorter times to achieve the necessary core density.

The amount of cooling to be done depends on the phase-space density at production. The higher the initial density, the easier it is to achieve the final density. The yield of antiprotons per incident proton is proportional to the product of the spatial solid angle and the momentum spread accepted by the beam-transport system, and the initial phase-space density can therefore be increased only by decreasing the spot size and

time spread of the antiprotons. The initial protons that produce the antiprotons determine these parameters and it is therefore useful to reduce the proton spot size and time spread.

The proton rms spot size will be reduced to 0.38 mm by the use of standard quadrupole lenses. Further reduction would provide little gain because the apparent spot size is ultimately dominated by the large antiproton beam divergence and the finite length of the target.[2] The first collection lens must match the large angular divergence of the antiproton beam at the target into the small angular admittance that is characteristic of a beam-transport system or a storage ring. This is achieved by using a lithium lens of the type developed by the Institute of Nuclear Physics at Novosibirsk.[3]

The time spread can be minimized by rf manipulation of the proton beam in the Main Ring just prior to extraction. The narrow time spread and large energy spread of the resulting antiproton bunches can be transformed into bunches with a much lower energy spread by rf phase rotation in a separate ring called the Debuncher. The rf phase-rotation system[4] makes it possible to start with a large momentum spread from the target, thereby increasing the antiproton flux. The reduced energy spread also greatly simplifies the design of the magnets and cooling systems of the Accumulator ring.

The design thus uses two fixed energy rings, the Debuncher and the Accumulator, located south of the Booster as shown in Fig. 1-1. The Accumulator has the same circumference as the Booster; the Debuncher is slightly larger. Both rings operate at a kinetic energy of 8 GeV, the Booster energy. The sequence of operations leading to colliding beams involves seven steps:

1. Proton Acceleration for Antiproton Production. Every two seconds, one Booster batch containing 2×10^{12} protons in 82 rf bunches is accelerated in the Main Ring to 120 GeV and held at that energy while the rf manipulation described in the next step is carried out.

2. Preparation of Protons for Targeting. The proton bunches at the beginning of the 120-GeV Main Ring flattop are matched to buckets produced by 1 MV per turn. When the rf is turned off for about 160 turns, the bunches shear so that the particles of extreme momentum spread reach a point that lies on a phase-space contour of $\Delta E = \pm 185$ MeV for 4 MV per turn of rf.[5] At this time the rf is turned back on at the 4 MV per turn level so that the sheared distribution is rotated slightly more than one quarter of a synchrotron oscillation to become a narrow distribution with energy spread $\Delta E = \pm 185$ MeV and a width of approximately 0.7 nsec. This train of short bunches is extracted from the Main Ring at F17 as soon as the rotation has produced the minimum bunch width.

3. Antiproton Production and Transport. The short proton bunches strike a tungsten target, producing a train of 82 equally short antiproton bunches. The peak energy deposition in the target is the same as that used successfully at CERN. 7×10^7 8.9-GeV/c antiprotons are collected by the lithium lens and transported to the Debuncher. The momentum spread of the beam is 3% and the transverse beam emittances are 20π mm-mrad in each plane.

4. Bunch Rotation in the Debuncher. The antiprotons are injected into 53-MHz rf buckets in the Debuncher. The rf voltage is large enough that the antiproton bunches rotate just as the proton bunches rotated in the previous step. After a quarter of a synchrotron oscillation, the narrow time structure and large momentum spread have been transformed into a small momentum spread and a broad time structure. The rf voltage is then rapidly lowered to match the bucket to the rotated bunch, and finally adiabatically lowered to reduce the momentum spread to 0.2%.

5. Transverse Cooling in the Debuncher. After the rf manipulations, the horizontal and vertical transverse emittances are stochastically cooled in the Debuncher from 20π mm-mrad to 7π mm-mrad during the almost two seconds before the next antiprotons are to be injected.

6. Antiproton Accumulation and Cooling. The antiprotons are extracted from the Debuncher and injected into the Accumulator. Successive batches are accumulated by rf stacking each batch at the edge of the stack. Between injection cycles, the stack is stochastically cooled using a combination of longitudinal and transverse cooling systems similar to the types developed by CERN for the AA ring.[6] A new batch of antiprotons with a density of about 7 antiprotons per eV is deposited at the stack tail every 2 sec. The fresh batch is moved by the coherent force of the stochastic-cooling system away from the injection channel and toward the center of the stack. The strength of the coherent force diminishes exponentially as the particles move away from the edge of the tail, causing the particle density to increase. Diffusion forces resulting from the Schottky noise of the antiproton stack and the thermal noise of the amplifiers cause the antiprotons to migrate from the high-density region toward the low-density region. As long as the coherent force is greater than the diffusion forces, the stack builds up in intensity until it reaches the core region where the coherent force is zero. Some antiprotons are lost during transfer and rf stacking and some diffuse away from the stack into the chamber walls. Allowing for losses, 6×10^7 antiprotons are stacked in each pulse. In 4 hours, the core will grow to a density of 1.0×10^5 antiprotons per eV. The total number of antiprotons in the core will be 4.3×10^{11}. During this time the transverse cooling systems will have reduced the horizontal and vertical emittances to 2π mm-mrad.

7. Filling the Tevatron. After accumulation is complete, antiproton bunches of the desired intensity are individually extracted from the core, transferred to the Main Ring, accelerated to 150 GeV and injected into the Tevatron. The same number of proton bunches of similar intensity are prepared in the Main Ring and injected into the Tevatron. Whether it is better to inject the protons or antiprotons first will be determined empirically. Both beams are then simultaneously accelerated to the desired energy.

Sufficient antiprotons for a luminosity of $10^{30}cm^{-2}sec^{-1}$ can be produced in 4 hours by this sequence, even with reasonable losses in production, cooling, and beam transfer. The project includes Main Ring beam overpasses at B0 and D0 to allow antiproton accumulation to proceed in parallel with colliding beams in the Tevatron. The design luminosity can be achieved without exceeding a beam-beam tune shift of 0.0018 per crossing. As the Tevatron and the Antiproton Source become more reliable, longer collection times will become practical, resulting in higher luminosity.

Beam-accumulation techniques are developing rapidly and it seems highly advisable to design an antiproton source that can accommodate future improvements. Accordingly, the third goal of this design is to incorporate flexibility for future improvements so that the Antiproton Source may ultimately achieve a luminosity of $10^{31}cm^{-2}sec^{-1}$. The potential for luminosity of the proposed source is exhibited in Table 1-I, which shows the relationship between the number of accumulated antiprotons and the luminosity.

The peak luminosity and accumulation rate are limited not by the antiproton production rate but by the cooling systems of the Accumulator Ring. Higher luminosities may be achieved through improvements in these cooling systems. The present design uses less than a half of the total number of particles collected in each accumulation cycle to reach its design luminosity of $10^{30}cm^{-2}sec^{-1}$. If future improvements can increase the final density by a factor of three, it will be possible to approach a luminosity of $10^{31}cm^{-2}sec^{-1}$. The design of the rings therefore includes provisions (aperture and straight-section space) for:

(i) Momentum precooling in the Debuncher.

(ii) Improved stochastic cooling in the Accumulator.

(iii) Improved Main Ring extraction for antiproton production.

(iv) Intermediate energy electron cooling in the Accumulator.

These features are not part of the initial design because it is difficult to foresee which improvements will be most feasible and cost-effective. The most beneficial choices will be clear only after some experience in operating the collider.

The design of each system are described in greater detail in the following sections.

TABLE 1-I LUMINOSITY PROGRESSION

$N_{\bar{p}}$ (10^{11})	N_p (10^{11})	N_B	N_T (10^{11})	L ($10^{30}cm^{-2}sec^{-1}$)
0.8	0.8	1	0.8	0.65
0.6	0.6	3	1.8	1.0 (design goal)
0.8	0.8	3	2.4	2.0
1.0	1.0	3	3.0	3.0
1.0	1.0	6	6.0	6.0

$N_{\bar{p}}$ and N_p are the numbers of antiprotons and protons per bunch, N_B is the number of bunches, N_T is the total number of antiprotons, $\beta^* = 1$ m is the value of β at the center of the interaction region, and L is the luminosity.

References

1. S. van der Meer, Stochastic Damping of Betatron Oscillations in the ISR CERN/ISR-PO/72-31 (1972) (unpublished).

   D. Mohl, G. Petrucci, L. Thorndahl, and S. van der Meer, Physics Reports 58, p. 73 (1980).

2. C. Hojvat and A. Van Ginneken, Fermilab $\bar{p}$ Note 139, July 16, 1981 (unpublished).

3. B. F. Bayanov et al., Nucl. Inst. Methods 190, 9 (1981).

4. A. G. Ruggiero, Fermilab $\bar{p}$ Note 102, January, 1981 (unpublished).

5. J. Griffin and J. MacLachlan, Fermilab TM-1258, May, 1984 (unpublished).

6. S. van der Meer, Stochastic Stacking in the Antiproton Accumulator CERN/PS/AA/78-22 (1978) (unpublished).

CHAPTER 2

PROTON ACCELERATION AND EXTRACTION FOR ANTIPROTON PRODUCTION

The production of antiprotons is done by bombarding a target with protons that have been accelerated to 120 GeV in the Main Ring. This chapter describes the acceleration of protons in the Main Ring and their subsequent extraction at F17.

2.1 Proton Acceleration

The accumulation cycle begins by accelerating a single Booster batch of protons in the Main Ring to 120 GeV with the existing rf system. This Booster batch consists of a string of 82 bunches spaced 5.6 m apart; its total length is 457 m. A single batch fills less than one-thirteenth of the Main Ring circumference. The Booster intensity record for a single batch is 3.4×10^{12}. For the purpose of this report, it is assumed that an intensity 2.0×10^{12} protons per Booster batch will be standard operating intensity for $\bar{p}$ production. The minimum time needed to accelerate a single batch to 120 GeV in the Main Ring can be reduced to 1.87 seconds. A flat-top of 0.13 sec is added to provide time for the rf beam manipulation before extraction. The cycle time is 2 seconds. The major beam properties are given in Table 2-I.

TABLE 2-I MAIN RING BEAM PARAMETERS

Proton Beam Kinetic Energy @ Extraction	120 GeV
Relativistic Factors: β	0.99997
γ	128.9318
$B\rho$, magnetic rigidity	4035.506 kG-m
Momentum, p	120.9347 GeV/c
Number of Booster batches accelerated	1
Number of Proton Bunches	82
Total number of protons per Batch	2.0×10^{12}
Main Ring Cycle Time	2.0 sec
Betatron Emittance, 95% of beam, (H and V)	0.2π mm-mrad
Longitudinal Emittance, 95% of beam at 120 GeV	0.3 eV-sec
RF harmonic number (h)	1113
RF Frequency @ 120 GeV	53.1035 Mhz
Revolution Period @ 120 GeV	20.96 μsec
Booster Batch Time Length	1.56 μsec
Transition Energy (γ_t)	18.75
Betatron tune number (H and V)	19.4
$\eta = \gamma^{-2} - \gamma_t^{-2}$	-0.0028
Maximum RF voltage	4.0 MV
Average Radius	1000 m

A reasonable estimate for the normalized betatron emittance, based on measurements,[1] is 24π mm-mrad. This value includes 95% of the beam. If $\sigma_{H,V}$ denotes the rms beam size and $\beta_{H,V}$ the lattice amplitude function, the emittance can be expressed in terms of these quantities as

$$\varepsilon_{H,V} = 6\pi \frac{\sigma^2_{H,V}}{\beta_{H,V}} .$$

The longitudinal phase-space area S of individual bunches in a Booster batch has been measured to be 0.3 eV-sec or less.[2] If the particle distribution is biGaussian in these variables, this value includes 95% of the beam. There is reason to believe this number can be reduced to <0.2 eV-sec in the future when improvements are made to the Main Ring and the Booster rf systems.

For energies well above the transition energy, a bunch area S half as large as the bucket area, and a bunch shape matched to the rf bucket, the rms bunch length σ_e and rms momentum spread σ_p/p are

$$\sigma_e = (142\text{cm})\sqrt{\frac{S}{\sqrt{VE}}} \qquad \sigma_p/p = (0.0112)\sqrt{\frac{S}{\sqrt{E^3/V}}} .$$

The bunch area can be expressed in terms of these quantities as

$$S = 6\pi\beta E \frac{\sigma_e}{c}\frac{\sigma_p}{p} .$$

The bucket area of a stationary bucket B and the phase-oscillation period T_s are respectively

$$B = (0.34\ \text{eV-sec})\ \sqrt{VE} \qquad T_s = (1\text{msec})\ \sqrt{E/V} .$$

In all these equations E is in GeV, V in MV and S in eV-sec.

For a fixed antiproton momentum spread, the bunch area of the antiprotons is minimized by making the time spread of the extracted proton bunches as narrow as possible. At the end of acceleration when the rf voltage is 4 MV the relevant beam parameters are $T_s = 5.6$ msec, $\sigma_e = 16$ cm, $\sigma_p/p = 2.4 \times 10^{-4}$ for a longitudinal emittance of 0.3 eV-sec.

The rf voltage is quickly turned off from its normal flattop value of 1 MV per turn for 2.9 msec (ε_ℓ = 0.3 eV-sec value) so that the bunch shears to the extent required for a subsequent rotation. The rf voltage is then turned on quickly to rotate the sheared distribution. Both the turning off and the turning on are accomplished in about 40 μsec. After 1.6 msec, the distribution has rotated to its narrowest projection. At that moment the phase-oscillation period T_s = 5.6 msec, σ_e = 6.8 cm, and $\sigma_p/p = 6.8 \times 10^{-4}$. After these operations have been completed, a momentum spread of 0.3% contains 95% of the beam. The bunch-narrowing process is illustrated in Figure 2-1.

The results of recent bunch-narrowing experiments in the Main Ring at 120 GeV, March 1982,[2] are shown in Fig. 2-2. In these experiments the maximum rf voltage was limited to 3.6 MV. Shorter bunches can be obtained by using the full available 4 MV.

Measurements made in the Main Ring[3] have shown that the available momentum aperture is ±0.27% for 90% beam transmission at 120 GeV with extraction equipment for the Tevatron in place. The loss of beam due to the 0.4% momentum spread is expected to be small, since very little of the beam will extend into the bad-field region of the aperture. As soon as the bunch rotation is complete, all 82 bunches are ejected at F17 into the 120-GeV transport line.

2.2 Extraction at F17

The dynamics of the process of proton extraction for $\bar{p}$ production is relatively straightforward. The proton energy at extraction will be in the range of 120 to 150 GeV (although for all the calculations discussed below, 149 GeV has been assumed.) A new kicker at E17 is energized to produce coherent betatron oscillations, which result in a beam displacement of roughly -42 mm at F17.

The kicker magnet will be a copy of the present 75-in. Main Ring abort kicker, which is a lumped inductance system with a tape-wound core. The necessary kick angle of approximately 450 μrad is expected to require approximately 5 kA. The half-sine-wave current pulse will have a risetime of approximately 15 μsec and a flat-top uniformity of ±.2% during the beam pulse. The kicker action is sufficient to cross the magnetic septum of a Lambertson placed at F17. Prior to extraction, the closed orbit between D38 and F14 is modified by energizing small dipoles at these locations (an existing magnet at D38 and a new one at F14.) The resulting orbit bumps are roughly out of phase with the kicker coherent oscillation, and serve to minimize excursions from the nominal Main Ring center until F17. Additional steering of the circulating beam horizontal position (of up to 13 mm) at F17 is provided by the F14 dipole and another new one at F19. The F14-F19 bump could be used to keep the accelerated beam away from the septum during acceleration, if necessary, and turned off as the D38-F14 pair is energized to prepare for extraction.

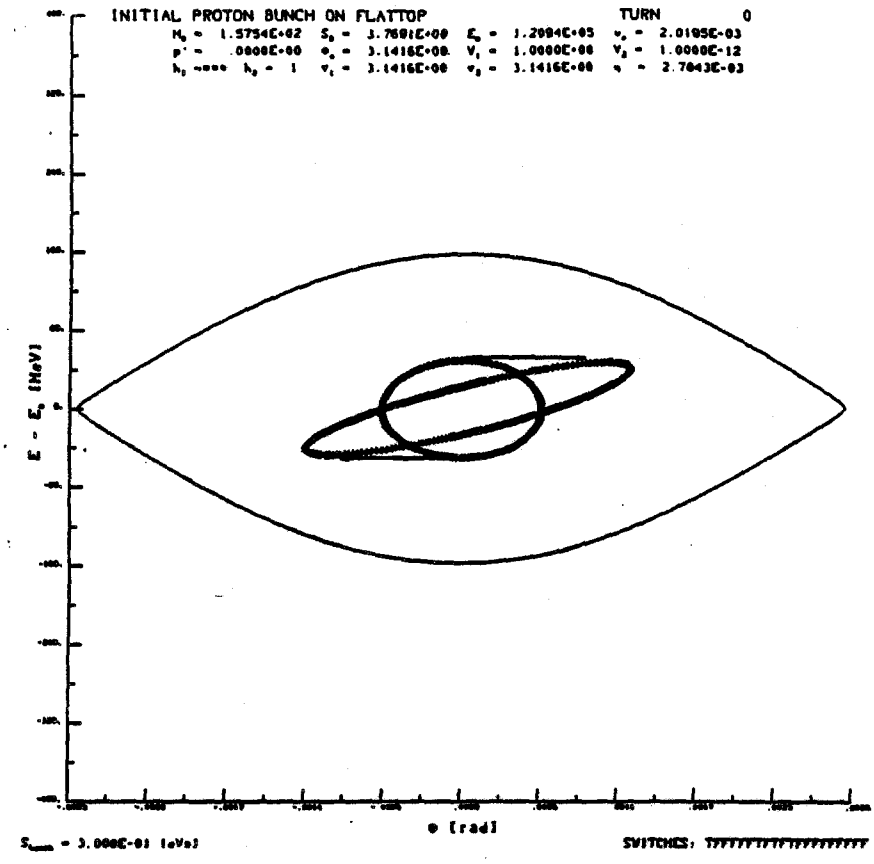

a) Outline of a Main Ring bunch of 0.3 eV-sec phase-space area matched to a bucket produced by 1 mV of rf at 120 GeV and the outline of the same bunch after 2.9 ms (140 turns) of drift with the rf off.

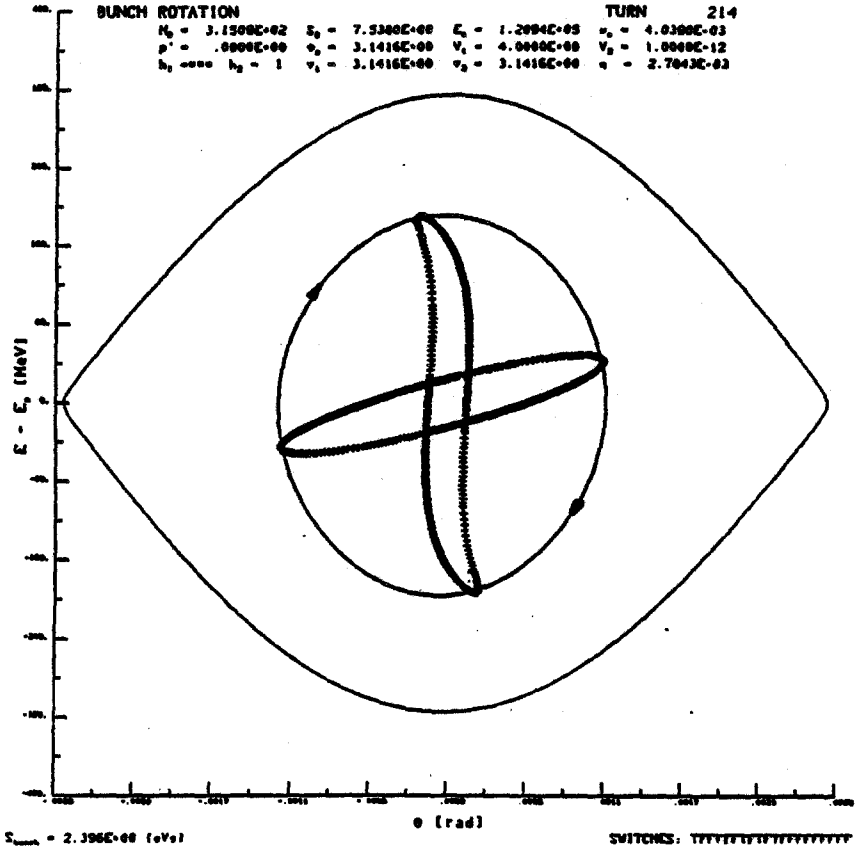

b) Rotation of the drifted bunch (a) in a bucket produced by 4 mV over a 1.6 msec interval.

Figure 2-1 Bunch narrowing for $\bar{p}$ production.

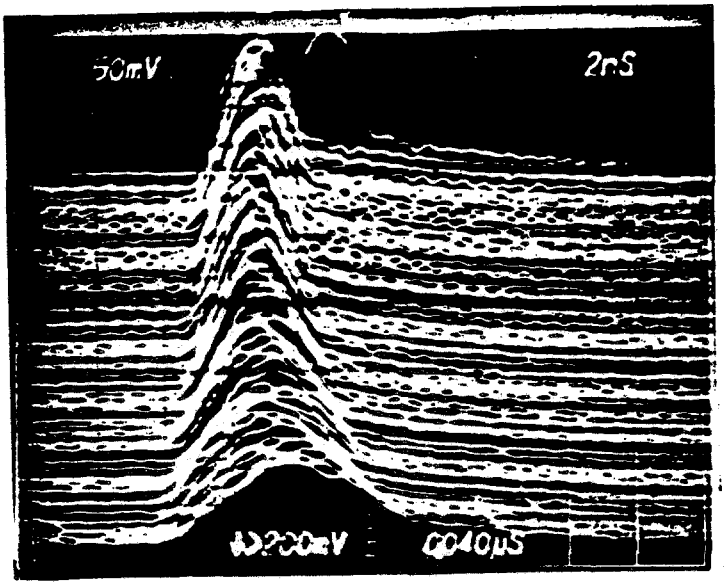

a) Bunch broadening. Time progresses downward, and total debunching time is 100 ms. The final bunch length is about 9 ns.

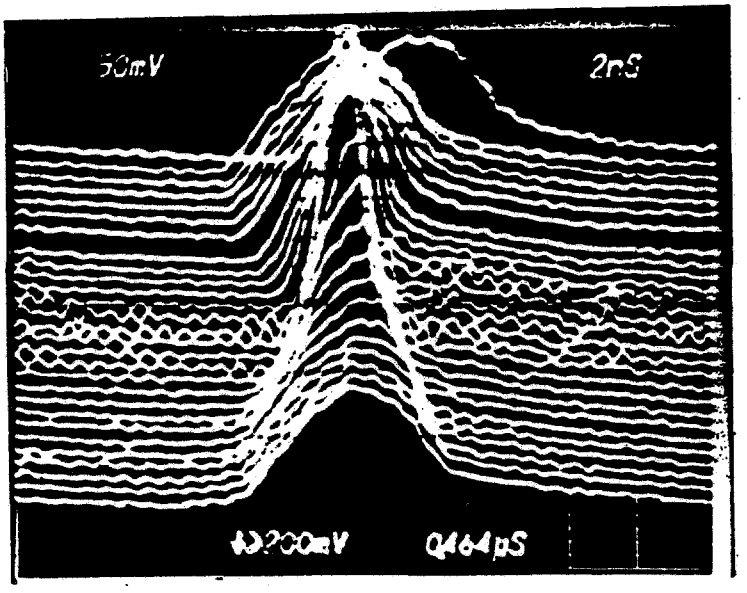

b) Rotation of mismatched bunch following sudden increase of the RF voltage to 1 MV. Time progresses downward, and traces are separated by about 100 ms. The topmost trace results from a mistrigger.

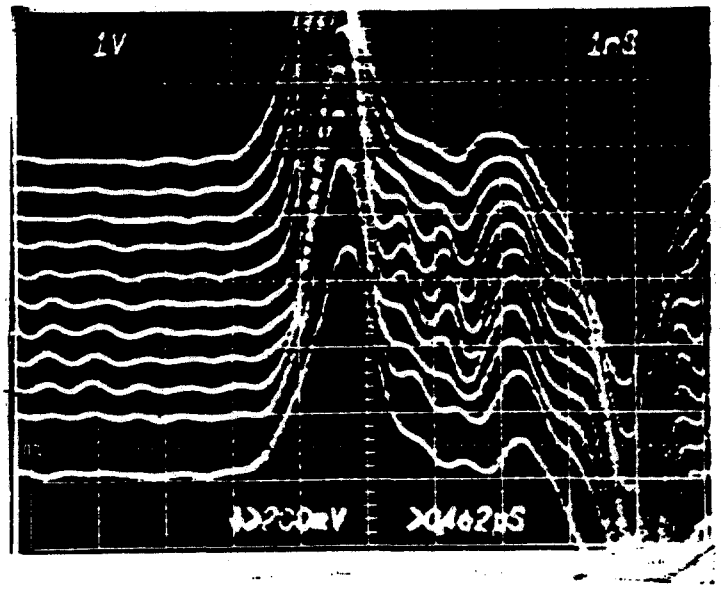

c) Bunch lengths near the time of narrowest bunches. Traces are taken at the beam rotation frequency, every 20.9 μs. The bunch pickup is a broadband transmission line, so inverted reflections from the downstream end of the pickup also appear. In this experiment the maximum RF voltage was 3.6 MV. Narrower bunches would be obtained with nominal 4 MV. A bunch with a 95% full time width of 1 ns has a length of 7.5 cm rms.

Figure 2-2 Debunching and Bunch Rotation.
Time base is 20 ms per major division.

The extraction channel is formed by two 162-in. Lambertsons, followed by two 118.4-in. C-magnets. The extraction magnets kick the beam vertically up by 32.6 mrad, which is sufficient to allow the extracted beam to pass above the next Main Ring dipole. The total vertical distance above Main Ring center at the end of the extraction channel is 9.7 in. The Lambertsons operate at approximately 10.6 kG and the C-magnets at 12.7 kG. The extraction magnets will be excited in series by a resonant LC pulser resulting in one cycle of a sine-wave of period 70 msec and peak amplitude 3000 A.

To make room for the system, the Main Ring B2's at slots F17-4 and F17-5 are replaced with a modified B2, which has twice the number of turns, and which is run in series with the rest of the Main Ring. Additional components of the system are a horizontal trim magnet located 140 in. downstream from the second C-magnet and a trim magnet located after the new B2. The first trim is intended to compensate for the difference in angle at F17 between the extracted and injected beams. The second trim compensates for small field differences between the modified B2 and the original standard B2's. The layout of the system is shown in Fig. 2-3.

The following calculations have been done for a momentum of 150 GeV/c, using a normalized emittance of 25 π mm-mrad, and a momentum spread of $\pm 0.2\%$.

Figure 2-4 shows the closed orbit with the D38, F14 pair; Figure 2-5 shows the D38, F14 bumps plus the extraction orbit produced by adding the E17 kicker.

Figure 2-6 shows the region near F17 in detail, indicating both the circulating and kicked beam envelopes. Note that the extracted beam explores nearly the full inner limit of the physical aperture of the dipoles and quad upstream of F17. The residual angle of 0.8 mrad of the extracted beam at the entrance to the first Lambertson is taken out by rolling the magnet by 5.2 deg (see dotted line.)

Figures 2-7, 2-8 and 2-9 show the beam spot(s) at the F17-1 quad, the Lambertsons and the C-magnets; both the circulating and the extracted beams are shown. In the figures, the dotted line indicates the beam spot when the F14-F19 pair is energized to its nominal value (13 mm offset.) In Fig. 2-8 the beam in the extraction channel is shown at the entrance of the first and exit of the second Lambertson. Fig. 2-9, shows the beam envelopes at the entrance and exit to the C-magnets, as well as the circulating beam. The C-magnets are pitched at roughly 1.2 deg vertically, so that the beam exits near the middle of the downstream aperture.

The residual field in the field-free region of the Lambertson is estimated to be 30 G at 150 GeV. The fields below the C-magnet, in the region of the circulating beam, are roughly a few tenths of a Gauss at 8 GeV, rising to less than 80 G at 150 GeV. It is planned to further suppress these by using a magnetically shielded beam pipe in this area.

F17 SCHEMATIC
ELEVATION

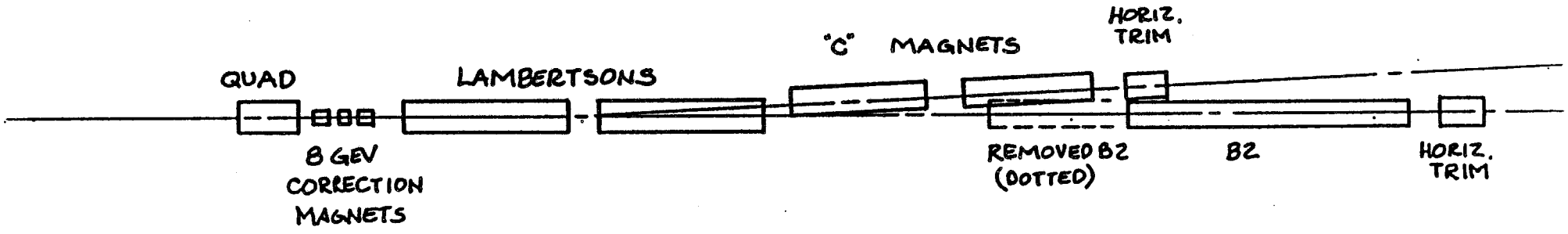

Figure 2-3

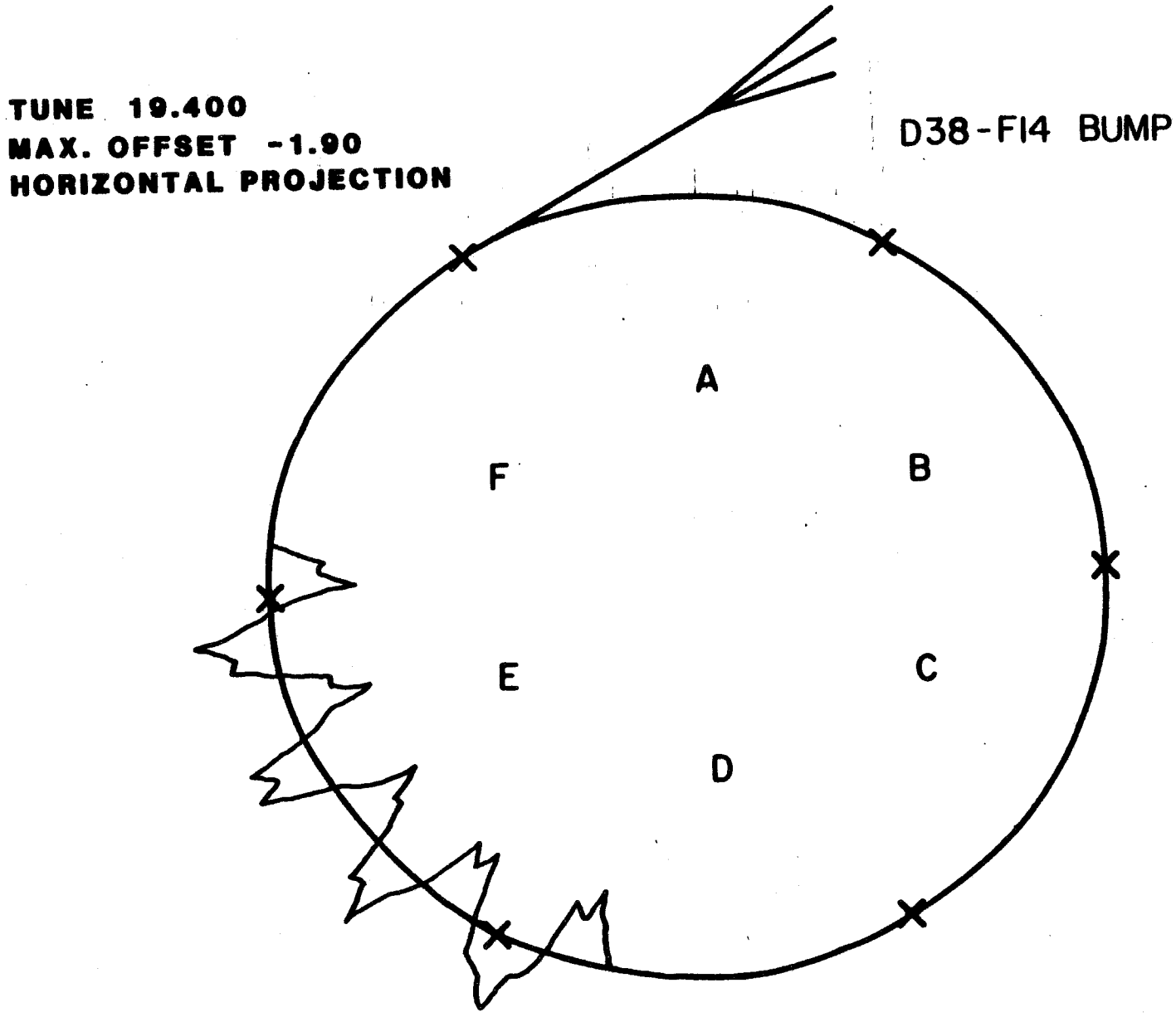
TUNE 19.400
MAX. OFFSET -1.90
HORIZONTAL PROJECTION
D38-F14 BUMP
A
B
C
D
E
F

Figure 2-4

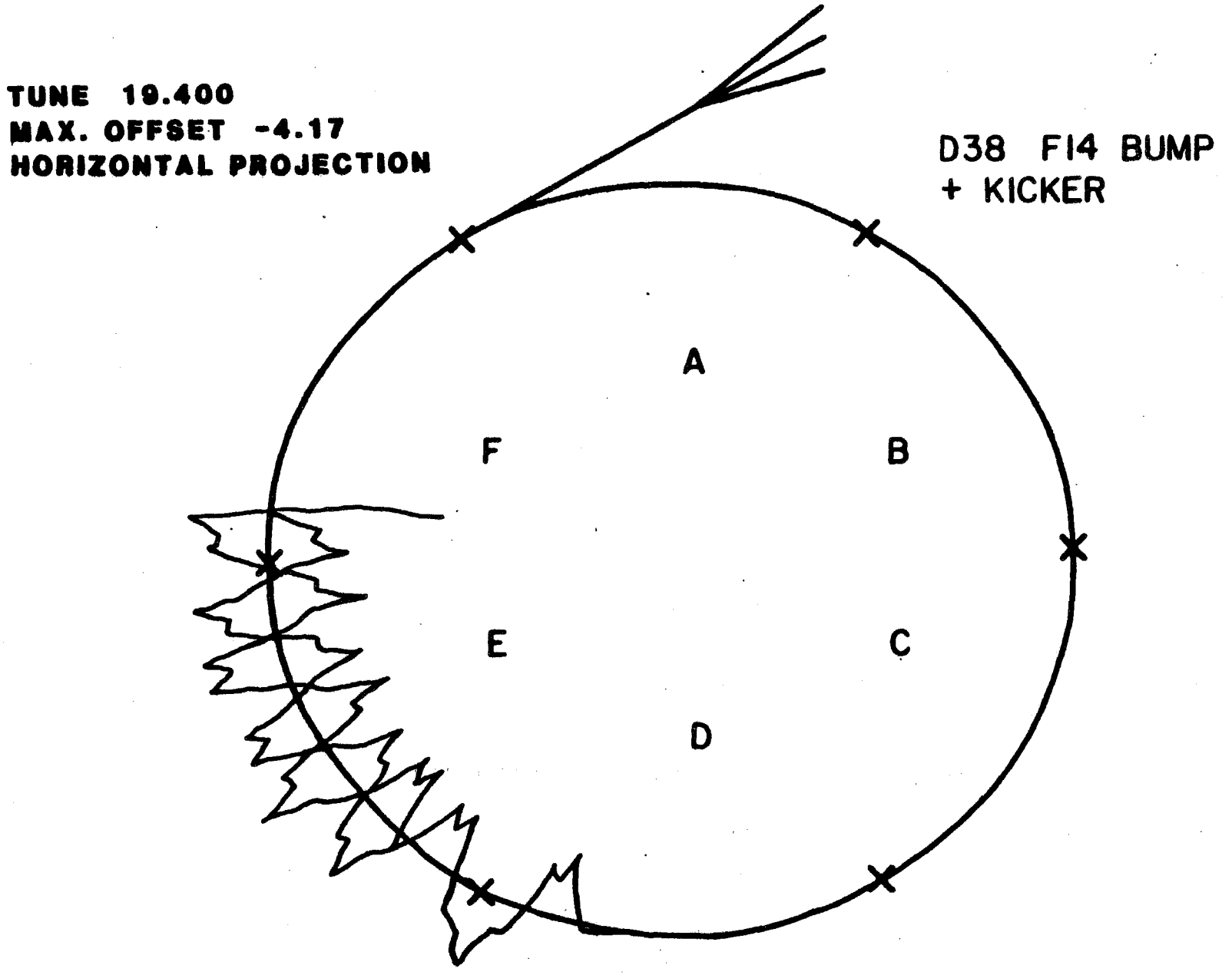
TUNE 19.400
MAX. OFFSET -4.17
HORIZONTAL PROJECTION
D38 F14 BUMP
+ KICKER
A
B
C
D
E
F

Figure 2-5

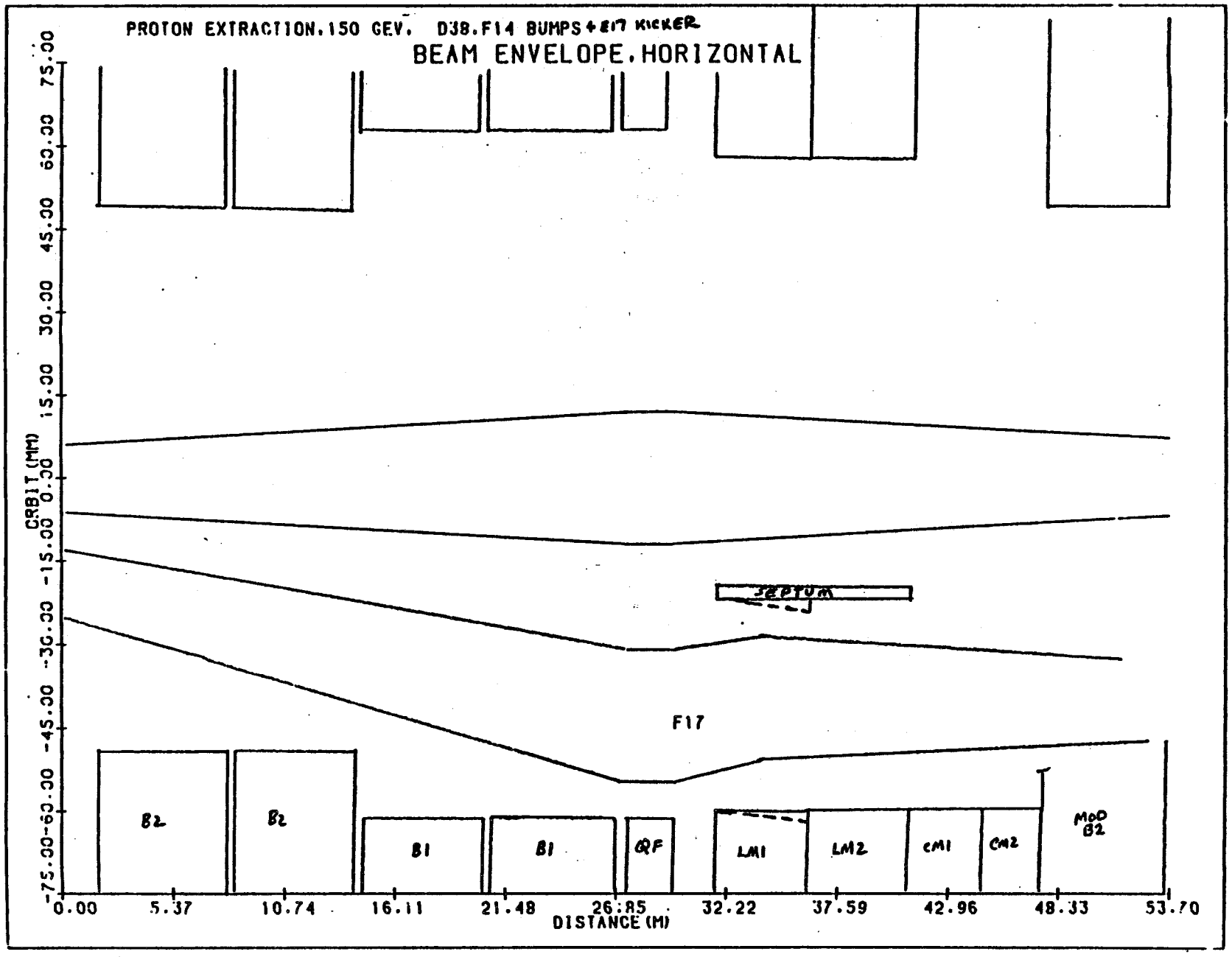
PROTON EXTRACTION, 150 GEV. D38, F14 BUMPS & E17 KICKER
BEAM ENVELOPE, HORIZONTAL
ORBIT (MM)
75.00
60.00
45.00
30.00
15.00
0.00
-15.00
-30.00
-45.00
-60.00
-75.00
SEPTUM
F17
B2
B2
B1
B1
QF
LM1
LM2
CM1
CM2
MOD B2
0.00
5.37
10.74
16.11
21.48
26.85
32.22
37.59
42.96
48.33
53.70
DISTANCE (M)

Figure 2-6

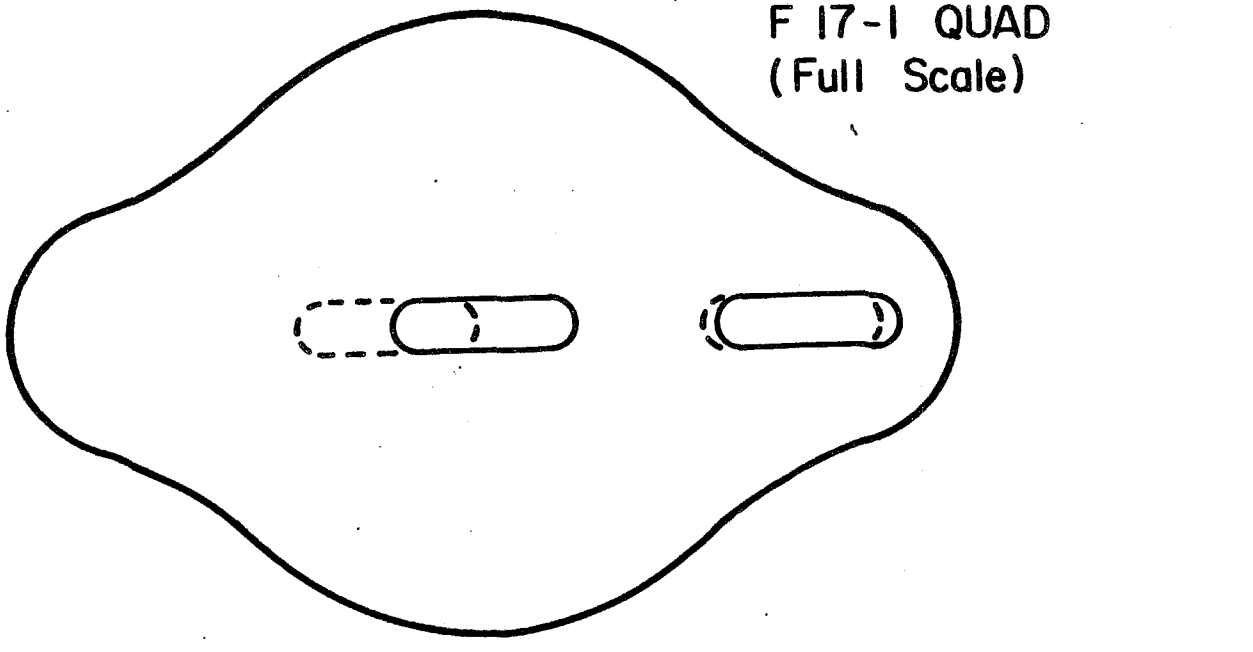

Figure 2-7

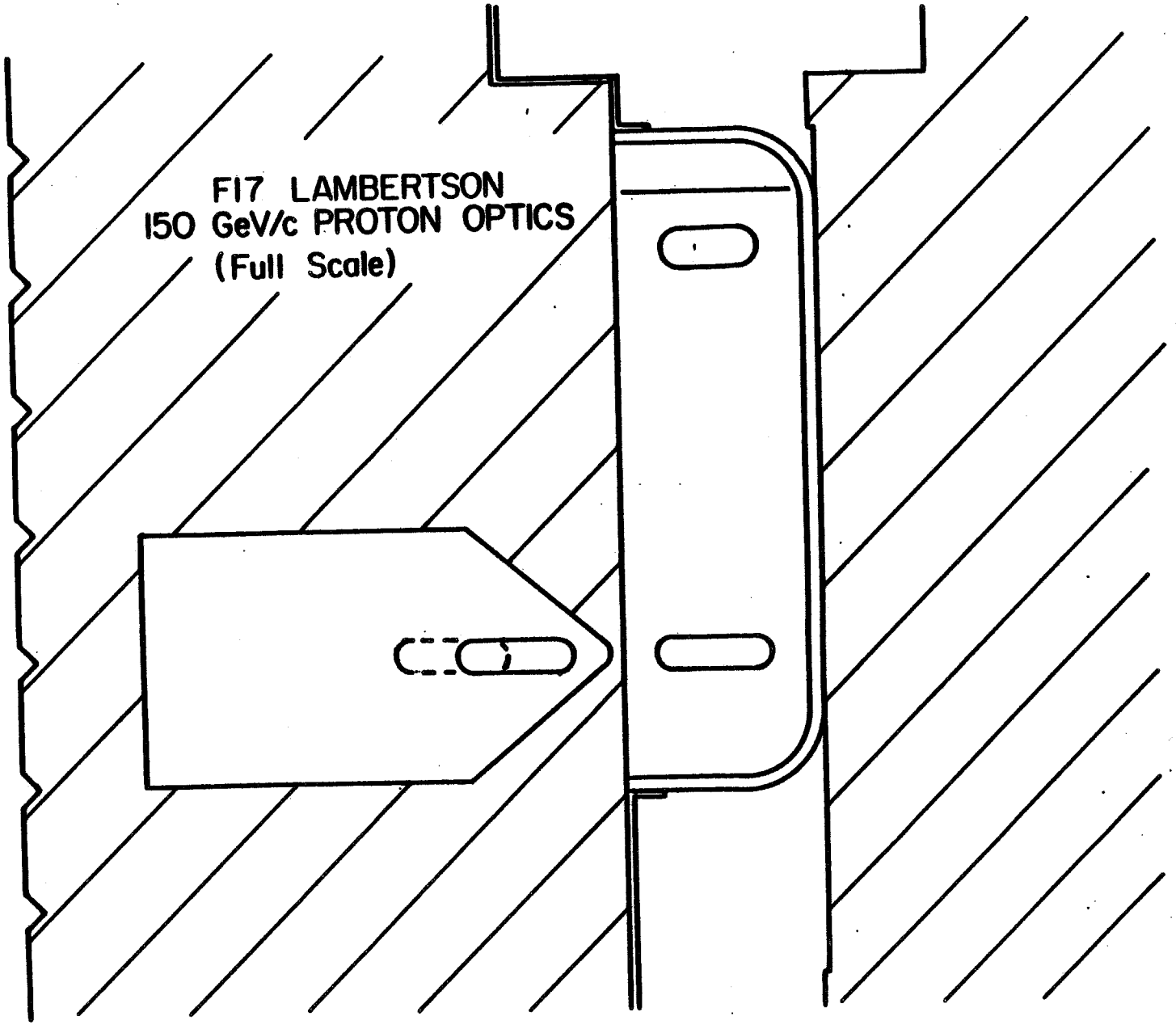

Figure 2-8

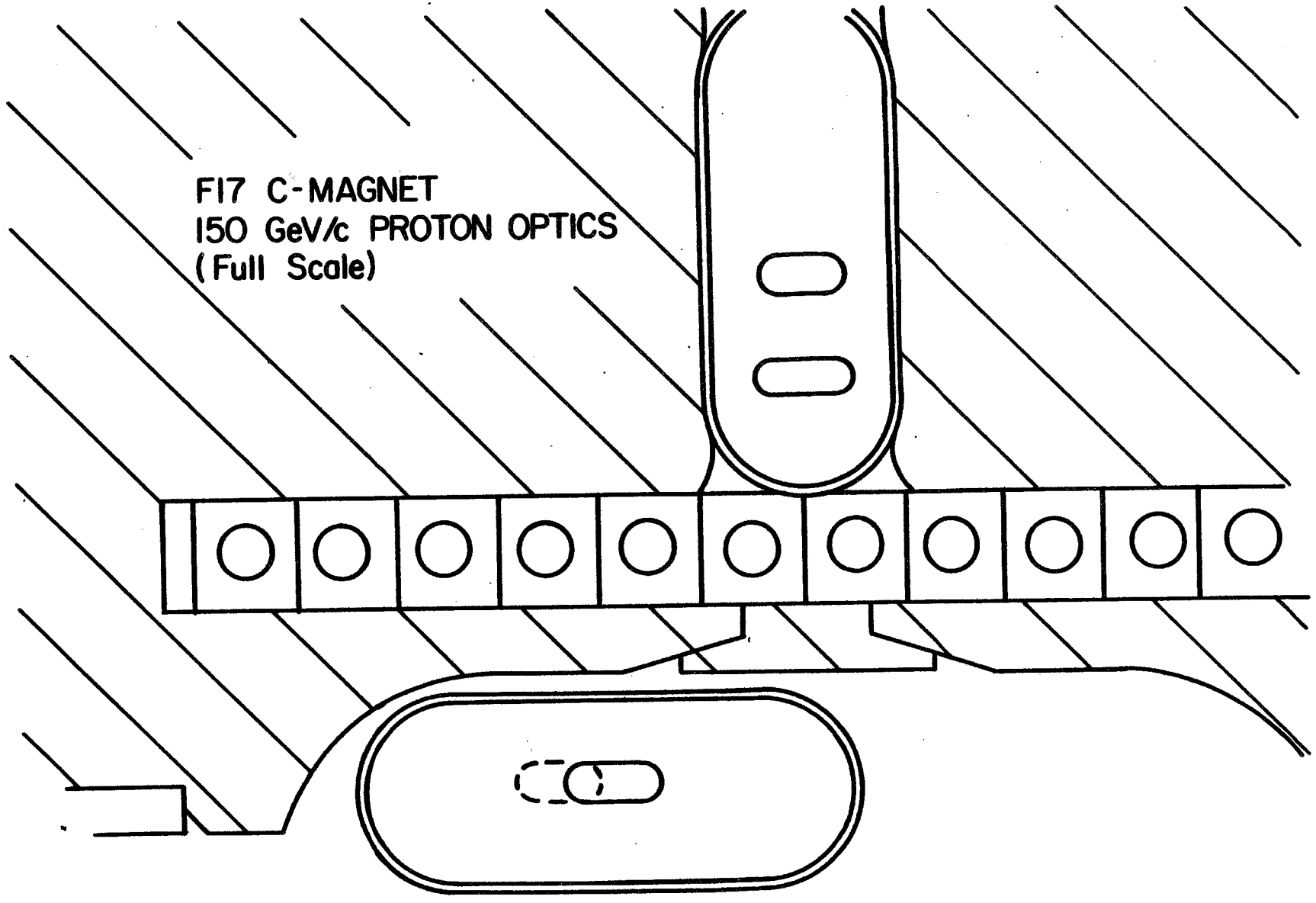

Figure 2-9

Transport of the 120-GeV protons to the target is discussed in Sec. 11.1.

References

1. C. Moore et al., Fermilab EXP Note 101, February 1980 (unpublished).

2. J. Griffin (unpublished).

3. J. Griffin, Fermilab Report, 7, July 1982.

CHAPTER 3

ANTIPROTON PRODUCTION

3.1 Antiproton Yields and Targeting

The choice of the antiproton energy and that of the protons for their production depend on the production cross sections and practical considerations relative to the existing facilities at the Laboratory. This section describes the present targeting scenario for the production of antiprotons, based on the discussion of the three following topics:

1. details of the production cross sections obtained from existing experimental data;
2. the choice of primary proton energy, antiproton momentum, antiproton longitudinal acceptance and antiproton transverse acceptance; and
3. limitations introduced by targeting and the antiproton collection system.

3.1.1 Antiproton Production Cross Sections. The available experimental data on the cross sections for the production of antiprotons have been described by a phenomenological formula that includes the dependence on the incident proton energy, the antiproton momentum and the target nucleus.[1] For example, the yields of antiprotons from a tungsten target collected within a laboratory angle of 60 mrad for various proton energies are shown in Fig. 3-1. It can be seen that there is a plateau at 120 GeV for the production of antiprotons between 8 and 13 GeV/c.

3.1.2 Proton Energy. The yield of antiprotons per unit volume of phase space per unit time changes very slowly with proton energy above 150 GeV, when the Main Ring cycle time is taken into consideration. Although some gain in yield could be obtained by going to a higher energy, a proton energy of 120 GeV was chosen because it is the maximum energy that can be extracted from a medium straight section such as F17. F17 provides a convenient location for the Antiproton Source. The choice was also influenced by the rapid increase in operating cost as the energy of the Main Ring is increased. The energy of 120 GeV is also compatible with the Colliding Beams Detector overpass. The B0 overpass is described in Chapter 7.

3.1.3 Antiproton Momentum. The optimum antiproton momentum is 10.0 GeV/c for an incident proton energy of 120 GeV. The yield is more than 90% of the optimum yield throughout the range from 7.5 GeV/c to 13.0 GeV/c. Since the normal injection momentum of the Main Ring, 8.89 GeV/c, is within this range of momenta, it is a reasonable choice. It has the advantage of

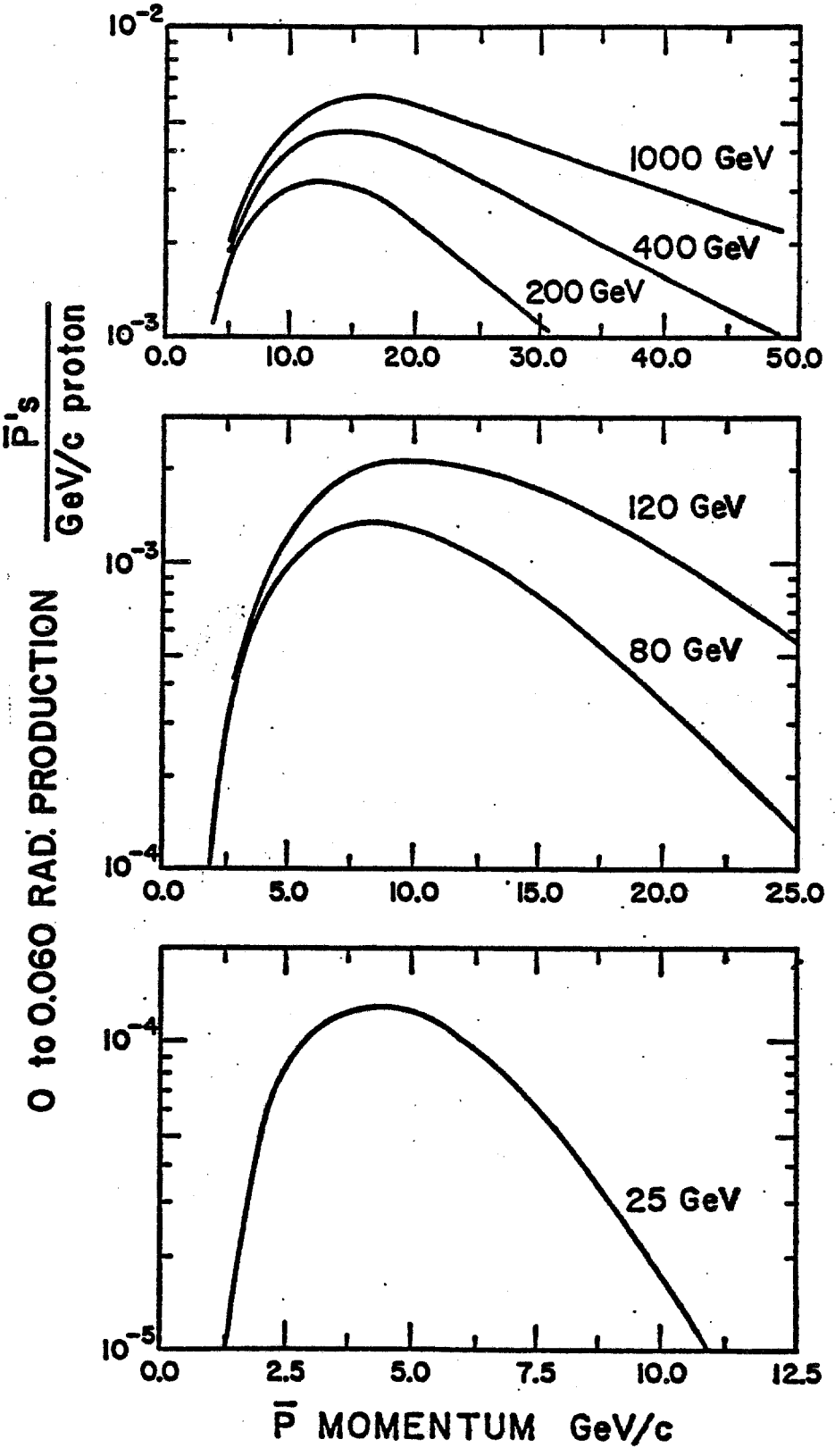
10^{-2}
10^{-3}
1000 GeV
400 GeV
200 GeV
0.0
10.0
20.0
30.0
40.0
50.0
10^{-3}
10^{-4}
120 GeV
80 GeV
0.0
5.0
10.0
15.0
20.0
25.0
10^{-4}
10^{-5}
25 GeV
0.0
2.5
5.0
7.5
10.0
12.5
$\frac{\bar{P}'s}{GeV/c\ proton}$
0 to 0.060 RAD. PRODUCTION
$\bar{P}$ MOMENTUM GeV/c

Figure 3-1

permitting the transfer of antiprotons directly from the Accumulator to the Main Ring. In addition, it opens the possibility of utilizing protons directly from the Booster as an alternative source of particles during commissioning of the source.

3.1.4 Antiproton Longitudinal Acceptance. Stochastic- cooling performance depends critically on the flux of p's injected into the Accumulator and on the particle density per unit of energy spread. This density, which is inversely proportional to the longitudinal emittance of the antiprotons, is determined in part by the time spread of the $\bar{p}$'s at production, as discussed in Chapter 2.

In the Debuncher, a total momentum spread of approximately 3% can be reduced to a momentum spread that can be accommodated by the Accumulator. Although a larger momentum spread will result in a larger flux the Accumulator is not able to cool the larger flux. The $\bar{p}$ collection and transport system is designed to accept 4% total momentum spread. The momentum spread of the $\bar{p}$'s transported to the Debuncher will be adjusted by collimation in the beam transport.

3.1.5 Antiproton Transverse Acceptance. The calculation of expected antiproton yields depends crucially on the collection system downstream of the target. A comparison of different collection systems has been performed[2], taking into account the large momentum spread of the antiproton beam. The advantages of a device such as the lithium lens that was developed at the INP in Novosibirsk[3] are clear. It has a very short focal length and it focuses in both transverse planes. Based on the INP experience, the parameters of the lithium lens collector were chosen to be: Radius = 1 cm, Gradient = 1000 T/m, Length = 15 cm. Within the present technology developed at Novosibirsk, a repetition rate of 1 Hz is feasible. The lens has a focal distance of 14.5 cm. The short focal distance requires the use of a dense target.

Antiprotons yields have been calculated with a Monte Carlo program[1] that includes the phenomenological description of the production cross section, the development of hadronic showers in the target and $\bar{p}$ production by secondaries, multiple scattering and absorption. The result of these calculations is shown in Fig. 3-2 for two different rms proton beam spot sizes, $\sigma_x = \sigma_y = 0.038$ cm and $\sigma_x = \sigma_y = 0.22$ cm. The number of antiprotons increases approximately linearly with the transverse acceptance above 20π mm-mrad for σ=0.038 cm. For the smaller beam size, the departure from linearity above 20π mm-mrad is caused by the finite lithium lens radius and the variation of field gradient. The optimum target length is approximately 5 cm.

3.1.6 Targeting Limitations. Decreasing the proton beam size at the target increases the transverse phase-space density of the produced

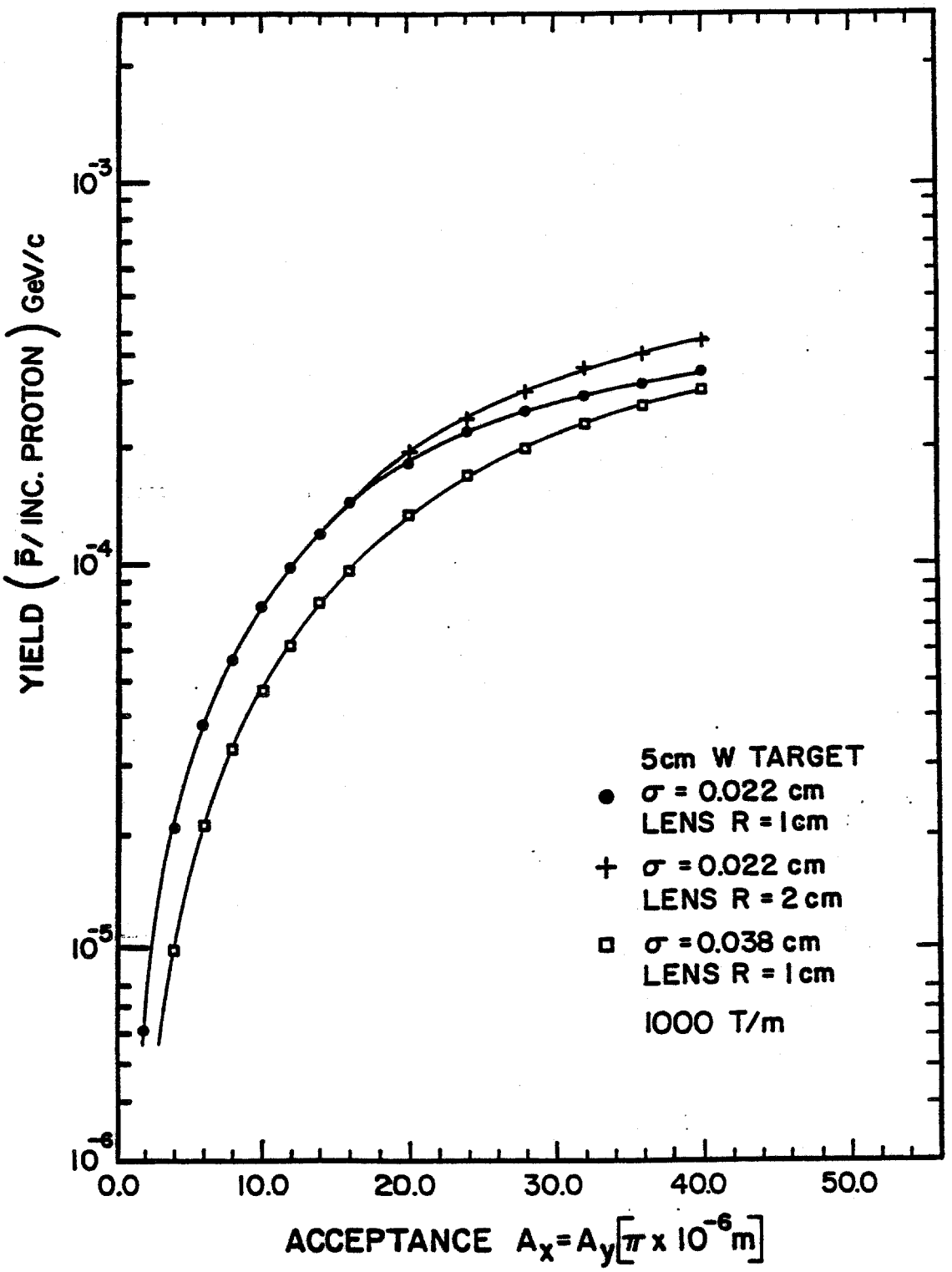
YIELD ($\bar{P}$/ INC. PROTON) GeV/c
10^{-3}
10^{-4}
10^{-5}
10^{-6}
0.0
10.0
20.0
30.0
40.0
50.0
ACCEPTANCE $A_x = A_y [\pi \times 10^{-6} m]$
5cm W TARGET
● σ = 0.022 cm
LENS R = 1cm
+ σ = 0.022 cm
LENS R = 2 cm
□ σ = 0.038 cm
LENS R = 1 cm
1000 T/m

Figure 3-2

antiprotons, resulting in a larger yield within a given acceptance. The diameter of the proton beam cannot be reduced arbitrarily because the energy deposited by the beam per unit volume increases as the beam area decreases, causing the target to overheat.

The subject of high energy density deposition in targets was the subject of a Fermilab Workshop[5]. It was generally agreed that metal targets can sustain energy density deposition up to 200 Joules gm^{-1} before the apparent onset of shock waves that could result in the destruction of the target. Calculations indicate that the CERN Antiproton Accumulator target sustains a maximum energy deposition of approximately 185 Joules/gm for tungsten. Both copper and rhenium (instead of tungsten) have been used at CERN for some time with no failures. The energy density deposited by a 120-GeV proton beam in tungsten has been calculated using the program MAXIM[4]. The maximum energy density deposited within a 5-cm long target is shown in Fig. 3-3 versus the rms size of the proton beam, σ. Within the errors of the calculation, it varies as σ^{-2}. Also shown is the maximum number of protons per pulse vs rms beam size, under the condition that the maximum allowable energy density is 200 Joules/gm.

Table 3-I shows the expected number of antiprotons per pulse as a function of beam size and maximum permissible proton intensity.

A feasibility study was carried out[6] on sweeping the proton beam across the target to decrease the energy density deposited in the material. The antiproton acceptance must be simultaneously swept to track the proton beam spot. If the sweeping covers several proton-beam diameters, it is possible to target 3×10^{12} protons on beam spots corresponding to $\beta < 3$ m, which will give an increased number of antiprotons accepted per proton. The design of the target area makes it possible to incorporate a beam-sweeping system in the future.

TABLE 3-I NUMBER OF ANTIPROTONS PER PULSE

β^*(m)$^+$	$\sigma_x = \sigma_y$ (cm)	Np(Max)	$\bar{p}/p^{++}$	$\bar{p}$/pulse
1.55	0.023	6.0×10^{11}	5.1×10^{-5}	3.1×10^{7}
3.07	0.032	1.2×10^{12}	4.3×10^{-5}	5.2×10^{7}
4.62	0.039	1.8×10^{12}	3.7×10^{-5}	6.7×10^{7}
8.00	0.052	3.0×10^{12}	2.5×10^{-5}	7.5×10^{7}

Notes: + β^* is for the proton beam at the center of the target ($\beta = \beta_y = \beta^*$)

++ The yield in $\bar{p}$/proton is for 3% $\Delta p/p$ and 20π mm-mrad.

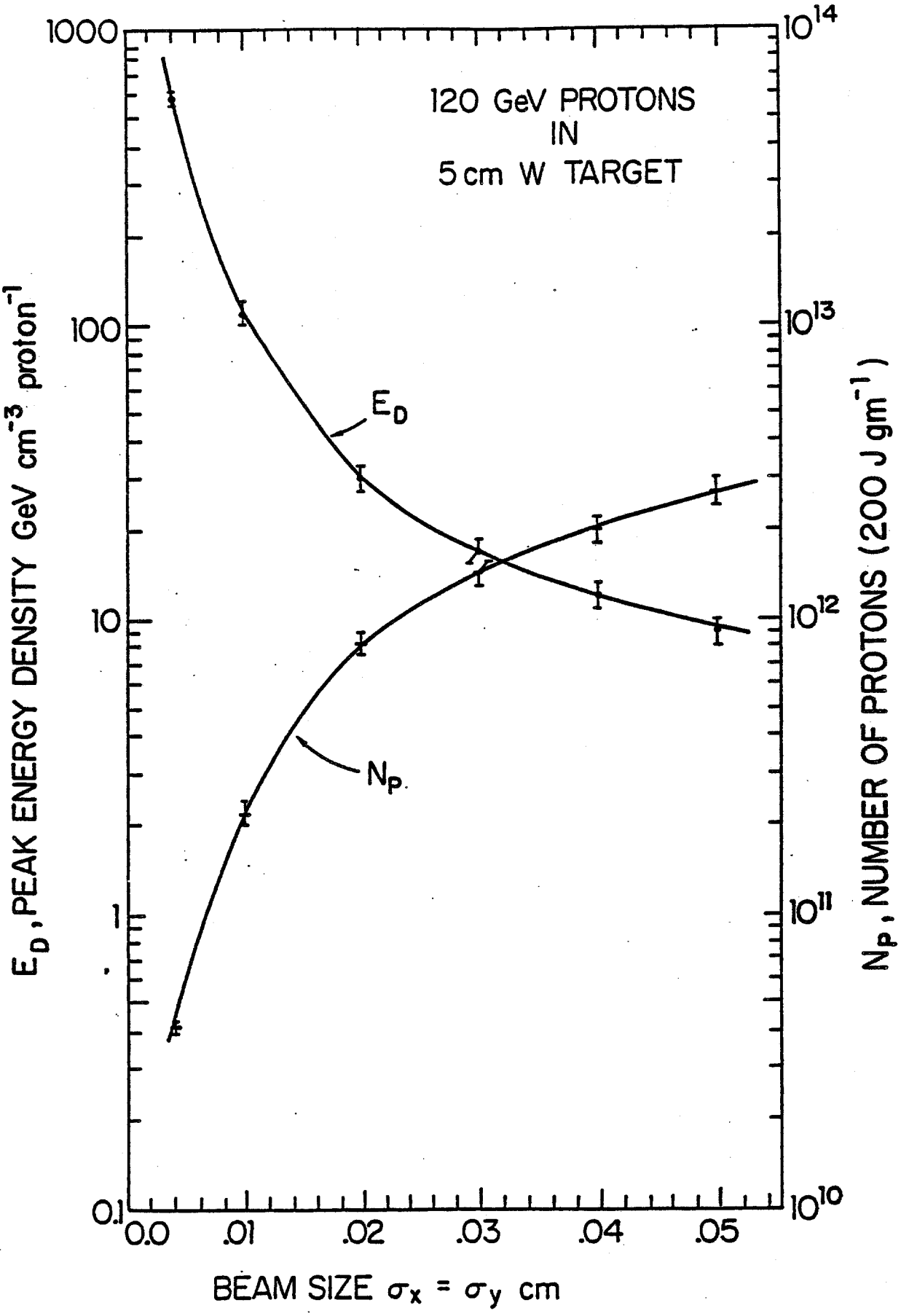
120 GeV PROTONS
IN
5 cm W TARGET
E_D
N_P
E_D, PEAK ENERGY DENSITY GeV cm^{-3} proton^{-1}
N_p, NUMBER OF PROTONS (200 J gm^{-1})
BEAM SIZE $\sigma_x = \sigma_y$ cm
1000
100
10
1
0.1
10^{14}
10^{13}
10^{12}
10^{11}
10^{10}
0.0
.01
.02
.03
.04
.05

Figure 3-3

3.2 Antiproton Target System Components

The principal components of the target system are the target itself and the antiproton collection device. This section discusses the design and limitations of these two components.

3.2.1 Antiproton Production Target The computer code MAXIM[4] has been used to calculate radial and longitudinal energy density distributions in a stationary tungsten target for an rms beam size of 0.038 cm. The results are plotted in Fig. 3-4. The temperature rise of tungsten corresponding to an energy deposition in Joules/gm may be estimated from the enthalpy reserve curve given in Fig. 3-5. As is shown in Fig. 3-4, it is expected that local peak energy densities will be approximately 200 Joules/gm for the present design parameters σ=.038 cm and 2×10^{12} protons per pulse. To decrease the number of thermal and stress cycles in the volume of material struck by the beam, the target will be rotated continuously, exposing a new volume of material to each beam pulse. Two possible configurations are shown in Figs. 3-6 and 3-7. During the target development stage the wedges shown in Fig. 3-6 will contain different materials to allow for comparative testing. Provision is also being made to test stationary targets of the CERN design.

The target must have a high density and high melting point. A compilation of mechanical properties for different materials was performed. A figure of merit to compare the mechanical properties is given by the yield stress divided by the coefficient of thermal expansion and the modulus of elasticity. On this basis rhenium, tungsten and tungsten-rhenium alloys are in increasing order for this figure of merit. The coefficient of heat conductivity could also be included in the figure of merit without significantly altering the choice of material.

The high-temperature behavior of tungsten-rhenium alloys shows considerable increase of yield stresses with respect to tungsten, but little change in the coefficient of thermal expansion or the modulus of elasticity. Tungsten-rhenium alloys are utilized in industry for high-temperature applications such as incandescent-lamp wire and targets for high-power x-ray tubes. A significant amount of experience with the technology for their fabrication exists. Tungsten has been used for all $\bar{p}$ yield calculations, although a number of target configurations will be tested during the R & D phase of the target-station development. A summary of the target parameters is given in Table 3-II.

TABLE 3-II TARGET PARAMETERS

Target Material	Tungsten/Tungsten Alloys
Length	5 cm
120 GeV protons/pulse	2.0×10^{12}
Total Beam Energy	3.46×10^{4} Joules
Repetition Rate	0.5 Hz

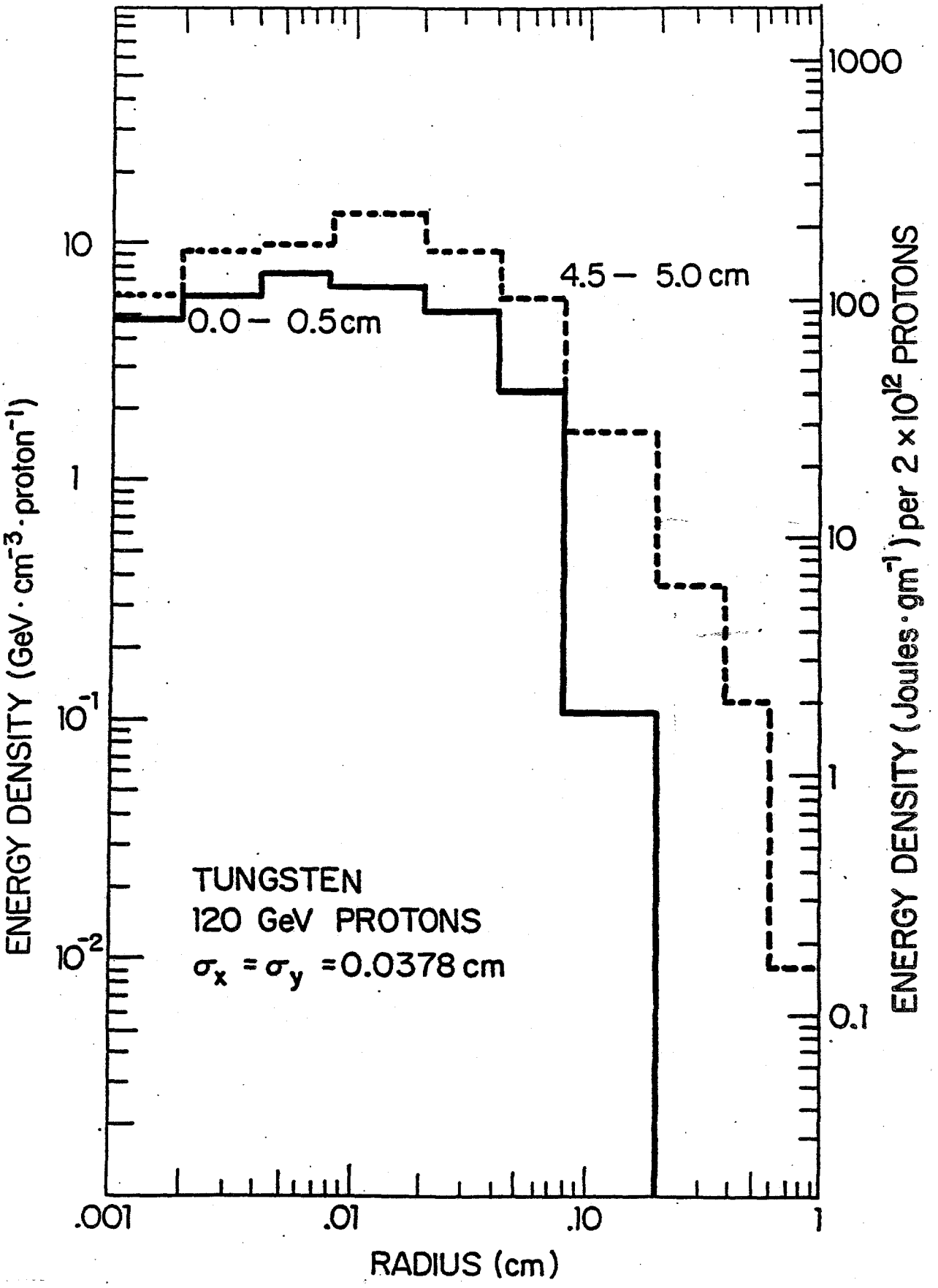
4.5 – 5.0 cm
0.0 – 0.5 cm
TUNGSTEN
120 GeV PROTONS
$\sigma_x = \sigma_y = 0.0378$ cm
ENERGY DENSITY (GeV · cm^{-3} · proton^{-1})
ENERGY DENSITY (Joules · gm^{-1}) per 2×10^{12} PROTONS
RADIUS (cm)
10
1
10^{-1}
10^{-2}
1000
100
10
1
0.1
.001
.01
.10
1

Figure 3-4

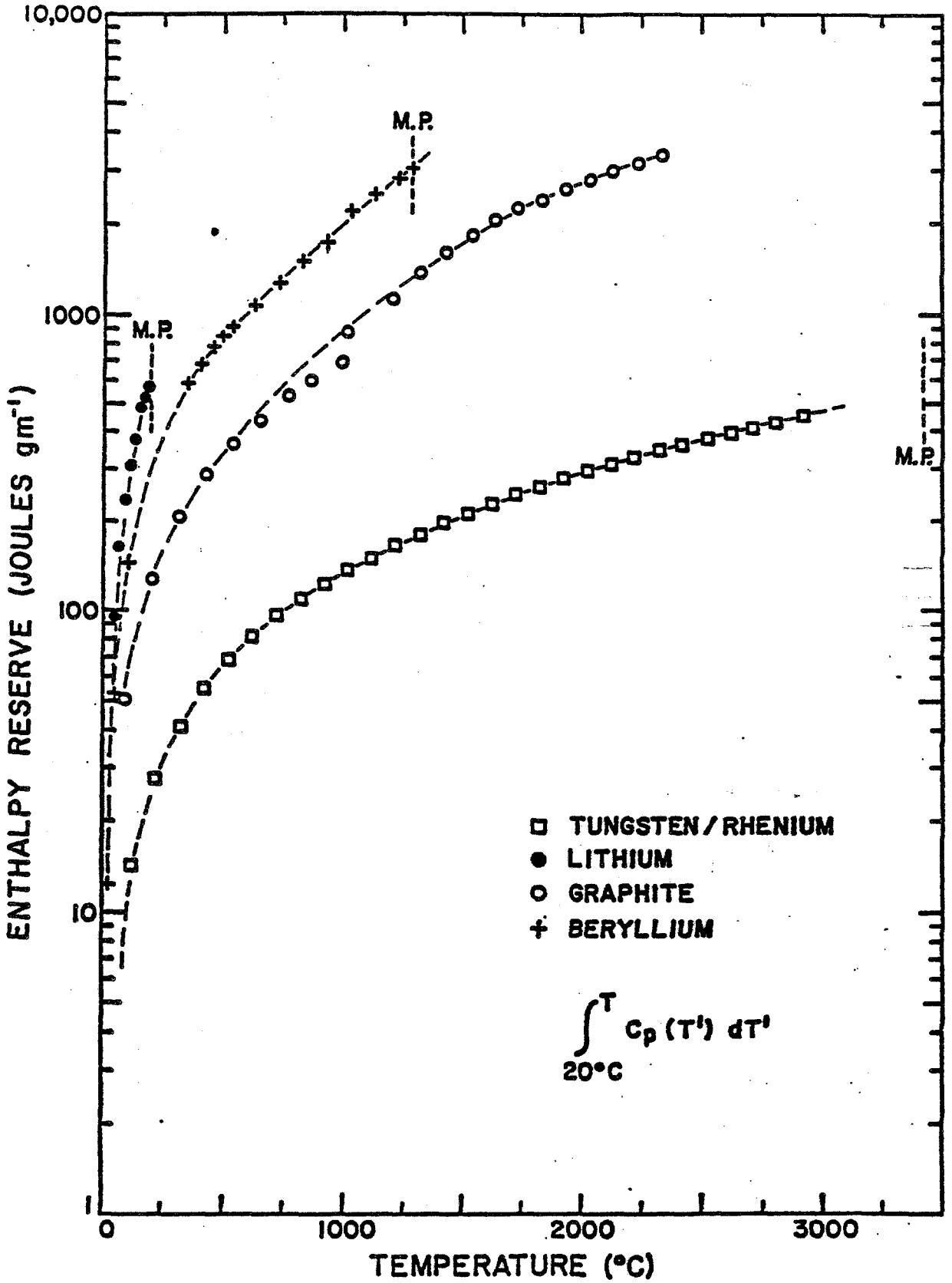
10,000
1000
100
10
1
ENTHALPY RESERVE (JOULES gm⁻¹)
M.P.
M.P.
M.P.
0
1000
2000
3000
TEMPERATURE (°C)
TUNGSTEN / RHENIUM
LITHIUM
GRAPHITE
BERYLLIUM
$\int_{20°C}^{T} C_p(T')\,dT'$

Figure 3-5

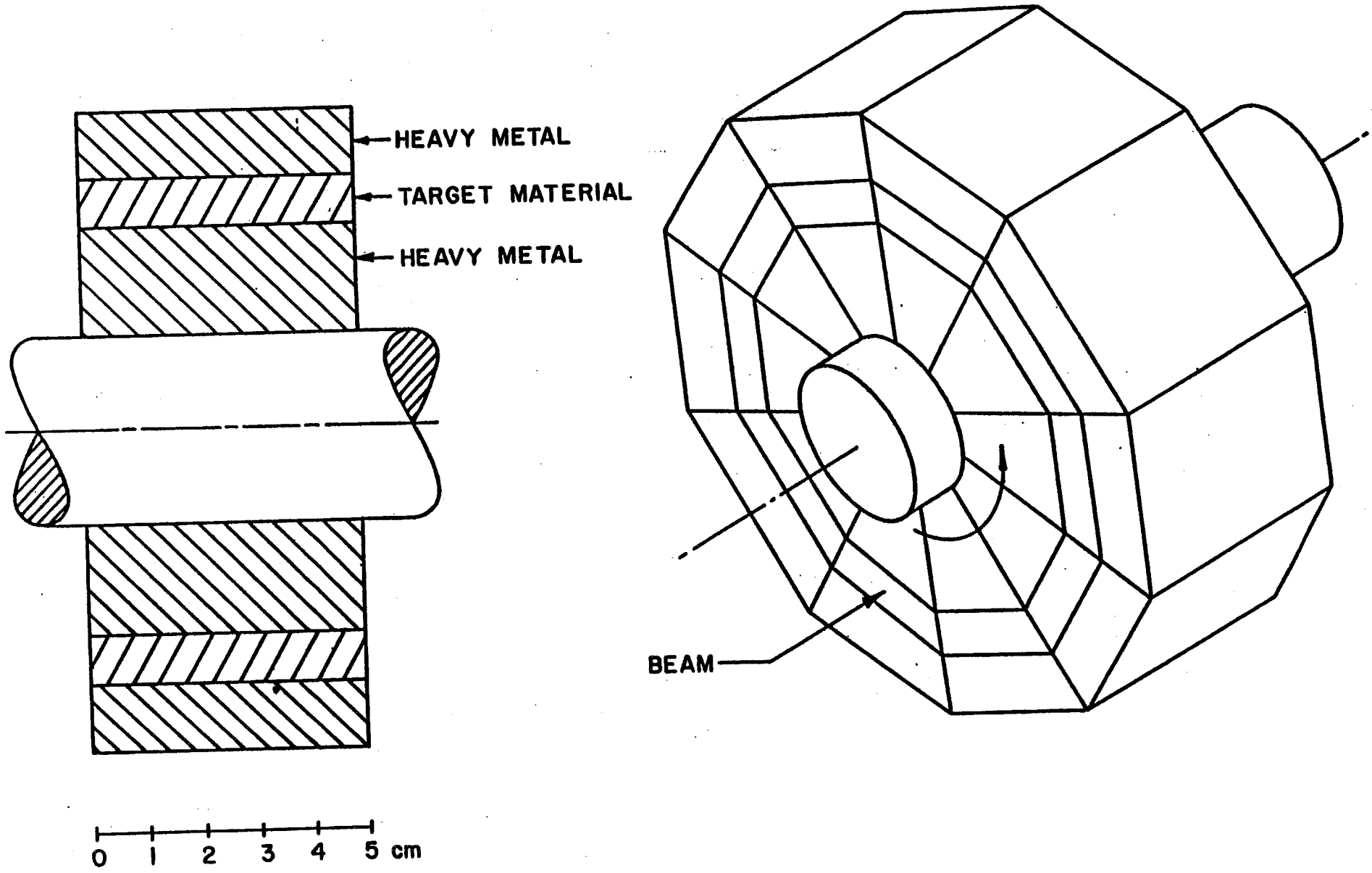

Figure 3-6

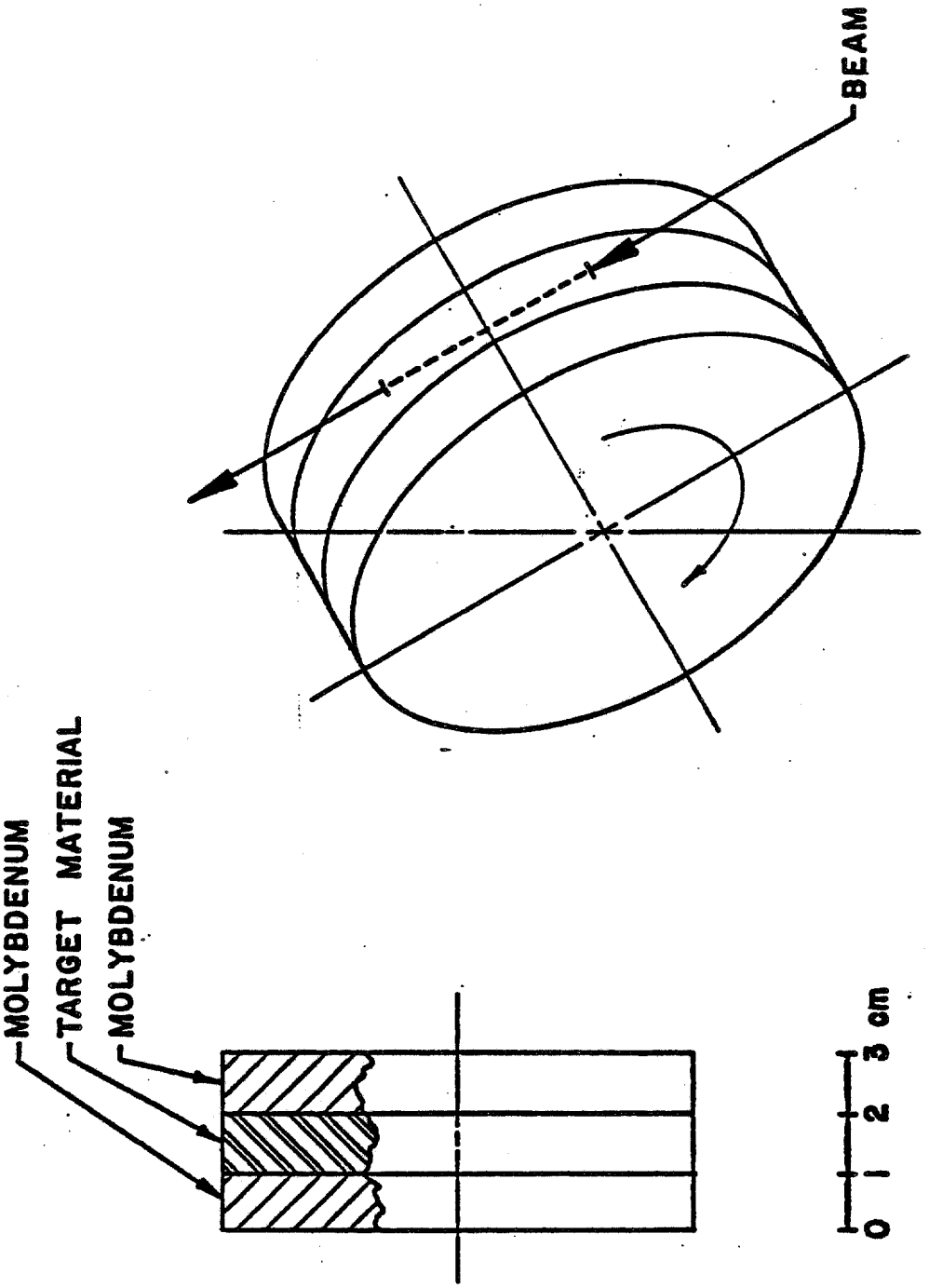

Figure 3-7

Beam Pulse Duration	1.6×10^{-6} sec
Energy Deposited/proton	1.26 GeV (1.81×10^{-10} Joules)
Energy Deposited/pulse	346 Joules
Power Deposited	173 Watts
Average Temperature	100°C
Beam Size($\sigma_x=\sigma_y$)	0.038 cm
Peak Energy Density/proton	13.4 GeV/cm^3
Peak Energy Density/pulse	200.0 Joules/gm
Peak Temperature Rise	<1500.0°C

CERN

Peak Energy Density[+]	>185 Joules/gm
Peak Temperature Rise	1500°C
Average Temperature	800°C

[+]This rhenium target has been used for some time with no failures.

3.2.2 Antiproton Collection; the Lithium Lens. A study has been made of the relative merits of $\bar{p}$ collection schemes that utilize a lithium lens, a pulsed quadrupole multiplet, or a conventional quadrupole triplet.[2] Since it was found that the lithium lens is far more efficient for the collection of $\bar{p}$'s, this section concentrates on the lens. The other options that are discussed will be pursued if the lens development lags.

The basic physical principle of the lithium lens is that a uniformly distributed electric current in a cylindrical conductor produces an azimuthal magnetic field with a constant radial gradient. Charged beam particles traversing the length of such a conductor experience a force that focuses them toward the axis. Lithium is an appropriate material for such a focusing device because it is the least-dense solid conductor, thereby minimizing $\bar{p}$ absorption and multiple scattering.[3] The lens under development uses a 15-cm long lithium cylinder of radius 1 cm and requires a current of 0.5 MA to produce the desired gradient of 1000 T/m. Joule heating caused by direct current in the lithium is prohibitively large, so a 0.6 msec full-width unipolar sine-like pulse of amplitude 0.5 MA will be applied every 2 sec. Each pulse will generate about 6000 Joules of heat and the problem of removing this heat dominates the mechanical design of the lens. It is desirable to keep the average temperature well below the 180°C melting point of lithium because the 1.5% volume expansion that occurs upon melting could shorten the lifetime of the lens. The magnetic induction H created by the pulsed current does not have a constant radial gradient, due to the skin effect. Fig. 3-8 shows the variation of H/H_{max} during one pulse.[7]

Energy deposition in a lithium lens located 14.5 cm (one focal length) downstream of a 5-cm tungsten target was calculated using the program MAXIM. Contributions from secondaries emerging from the target as well as from non-interacting 120 GeV protons were included. The heating due to the beam was found to be small compared to Joule heating.[8]

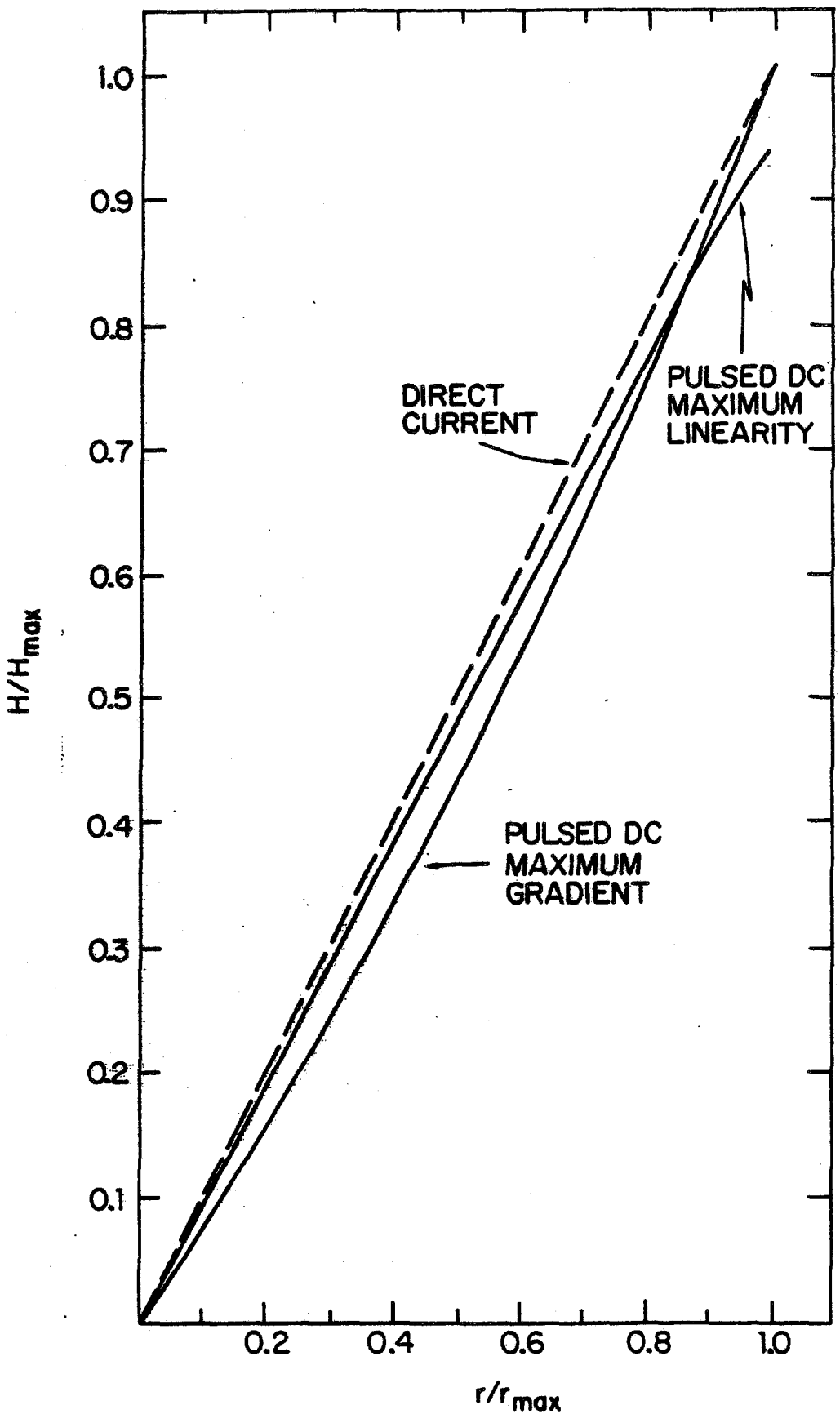
1.0
0.9
0.8
0.7
0.6
0.5
0.4
0.3
0.2
0.1
H/H_max
0.2
0.4
0.6
0.8
1.0
r/r_max
DIRECT CURRENT
PULSED DC MAXIMUM LINEARITY
PULSED DC MAXIMUM GRADIENT

In case the lithium-lens development lags, linear and non-linear horns of the types developed for the CERN AA ring could be utilized. To optimize the $\bar{p}$ rate, they require significantly longer targets. Preliminary results indicate that horns would not provide as good a collection efficiency as the proposed lithium lens at our $\bar{p}$ energy. The larger currents required for the 8.89 GeV/c $\bar{p}$'s, as compared with 3.5 GeV/c at CERN, may make the horn construction very difficult. Another option would be to install a 5Q36 triplet.[2] This would limit the $\bar{p}$ production system to small momentum spreads and emittances, but could be useful in the early stages of running.

3.2.3 Antiproton Selection. Downstream of the lithium lens, a pulsed dipole magnet will be used to select negative particles of energies near 8 GeV. Particles not selected, the remnants of the 120 GeV proton beam and other interaction products, continue towards the beam dump. The 8 GeV antiprotons pass through a channel in the beam dump and then into the transport line to the debuncher ring.

The pulsed magnet will be a dipole powered by a capacitive discharge supply similiar to that of the lithium lens. The current pulse will be a half sine wave with ω = 1200 hz. The magnet aperture will be 3 x 3 cm, and the field integral will be 1.55 Tesla-meter. This will provide a 3° bend in the antiproton beam.

3.3 Target Hall

The antiproton production target, proton beam dump and the lithium lens for antiproton collection will be located in a vault downstream of the final quadrupole focusing system in the 120-GeV proton line. The dimensions of this vault are planned to be 7 ft by 33 ft with the floor located at 17 ft below grade, as shown in Fig. 3-9a, and 3-9b.

The upstream end of the hall is separated from the proton-beam transport tunnel by 3 ft of steel shielding. Further shielding is placed around the external walls of the vault in the earth. Below the vault two separate impermeable membranes are used to collect irradiated ground water. Shielding configurations that limit the irradiations of the soil and the above-ground fluxes to permissible values have been designed to allow operation at an intensity of 10^{13} protons per second.

Downstream of the upstream end of the shield, within the target vault, a 3 ft high by 8 ft long and 2 ft wide volume of space is available for components. The space between this volume and the concrete walls and floors of the vault is filled with steel shielding. Access to the target station components is accomplished by raising one of a set of solid steel elevators into the Target Service Building. Each elevator segment extends 10 in. along the beam direction and 24 in. transverse to the beam. Each is 7 ft long in the vertical direction. The components are suspended from the bottom of the elevator. The 7 ft length makes it possible to place electronics and control systems immediately above each elevator segment without danger of radiation damage. An additional 3 ft of concrete is

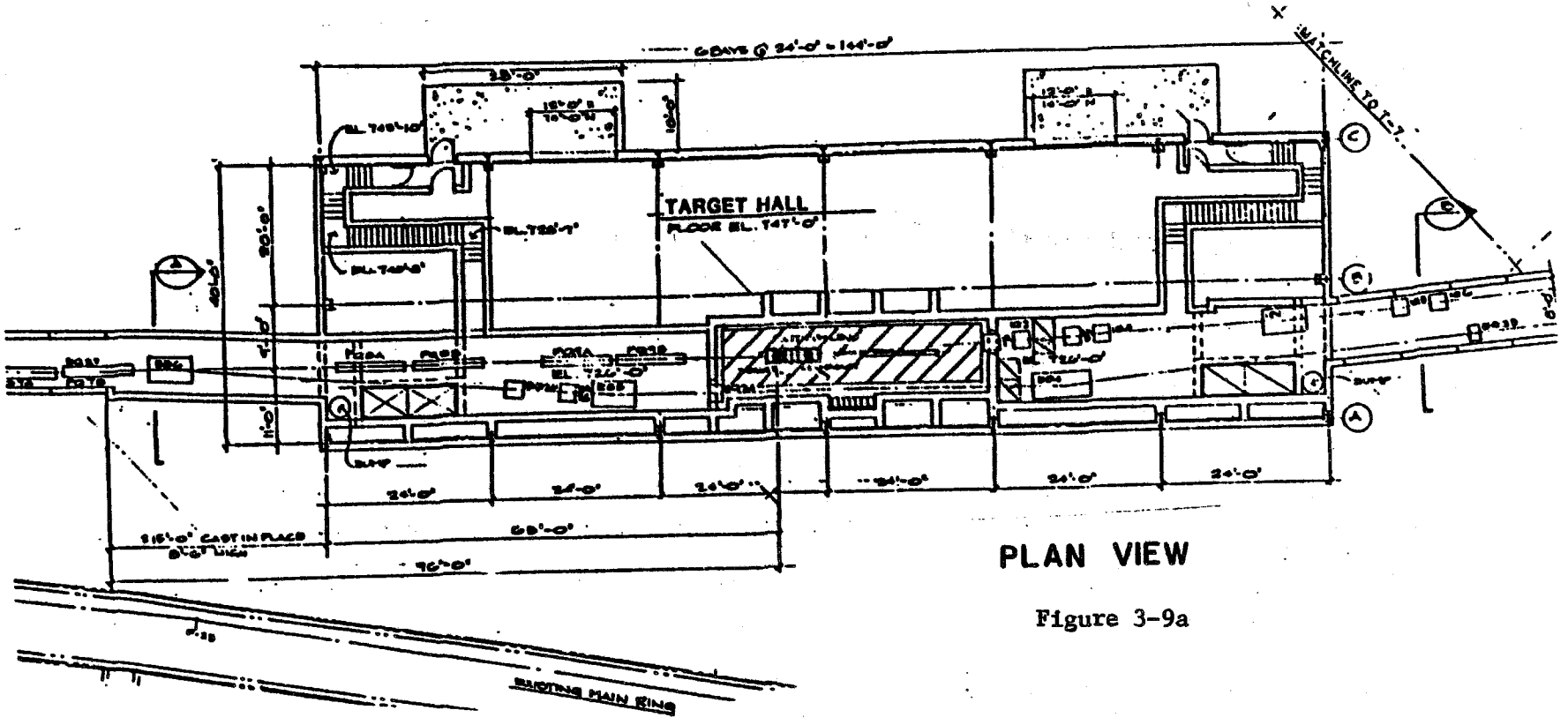

Figure 3-9a

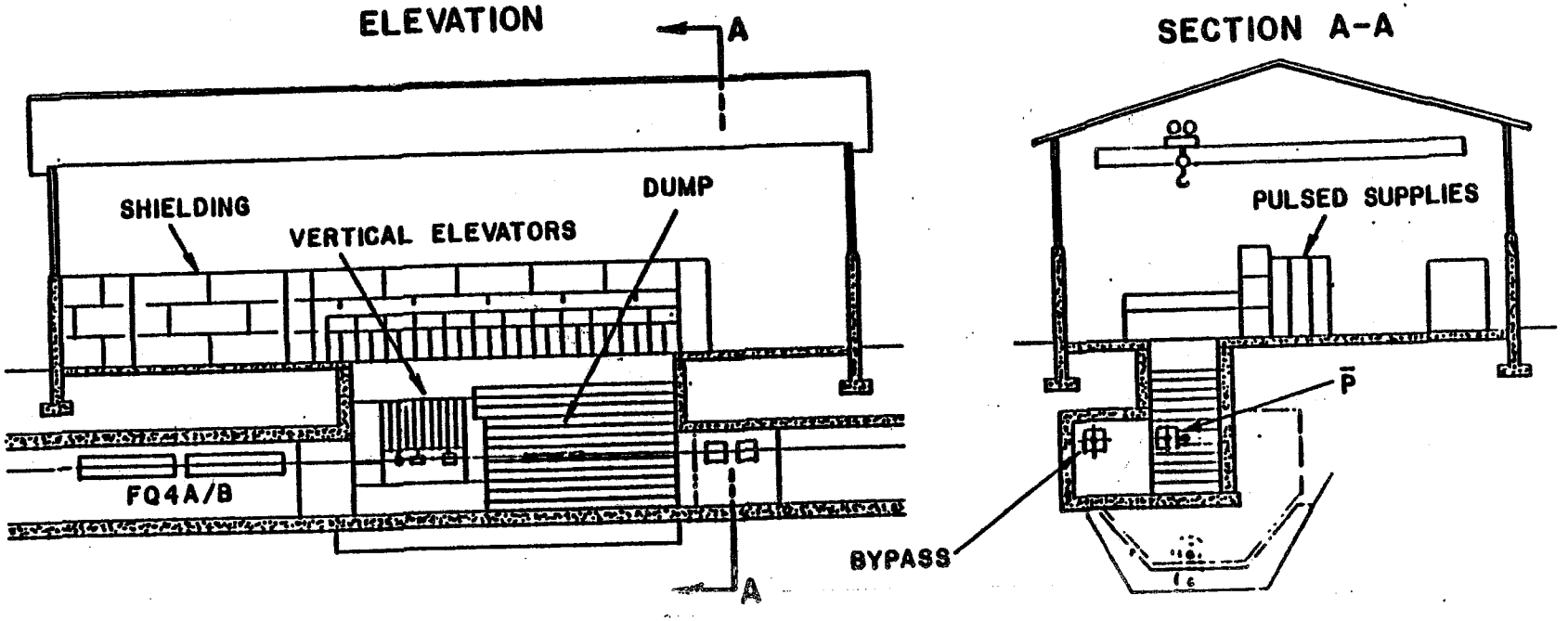

Figure 3-9b

required to keep the above-ground radiation levels within the Target Service Building below the maximum permissible level. Within the Target Service Building and surrounding the vault, a shielded area incorporating thick windows will be used to exchange elevator segments remotely. Work will be performed on components with remote manipulators. The manipulators will be used to exchange targets routinely. Access to the electronics at the top of the elevator segments will be possible when beam is not being delivered to the target station.

The last component in the beam before the dump is a pulsed magnet to bend the $\bar{p}$'s to the right by 3°, in order to separate them from the protons. The dump is a water-cooled graphite core 6 ft long surrounded by a steel jacket which fills the inside of the vault. The steel extends for 22 ft along the proton beam. The construction is similar to the dump developed for the Tevatron abort system.

Transport of the 8-GeV antiprotons to the Debuncher is discussed in Sec. 11.2.

References

1. "Calculation of Yields for the Fermilab Antiproton Source" Carlos Hojvat and A. Van Ginneken, Fermilab-Pub-82/43, 1982 (submitted to Nucl. Inst. Meth.)

2. E. Colton, "More on Antiproton Collectors," $\bar{p}$ note #120, Fermilab (unpublished).

3. B. F. Bayanov et al., "A Lithium Lens for Axially Symmetric Focusing of High Energy Particle Beams," Nuc. Inst. Meth., 1909(1981).

4. "MAXIM - Program to Simulate Cascades in Bulk Matter." A. Van Ginneken, Fermilab FN-272 (January 1975).

5. "High Intensity Targeting Workshop," Fermilab April 28-30, 1980.

6. F. Krienen and F. Mills, Spreading the Hot Spot on the Target, $\bar{p}$ Note 70. E. Colton, $\bar{p}$ Note 107.

7. "Skin Effect in Electrically Pulsed Cylindrical Conductors used as Focusing Devices," A.J. Lennox, Fermilab Report FN-379, January, 1983. "Optical Properties of Cylindrical Lenses," T.A. Vsevolozhskaya et al, Sov. Phys. Tech. Phys., Volume 20, No 12, 1556 (1976).

8. "Energy Deposition in the Lithium Lenses," A.J. Lennox, $\bar{p}$ Note 204, Fermilab 1982 (unpublished).

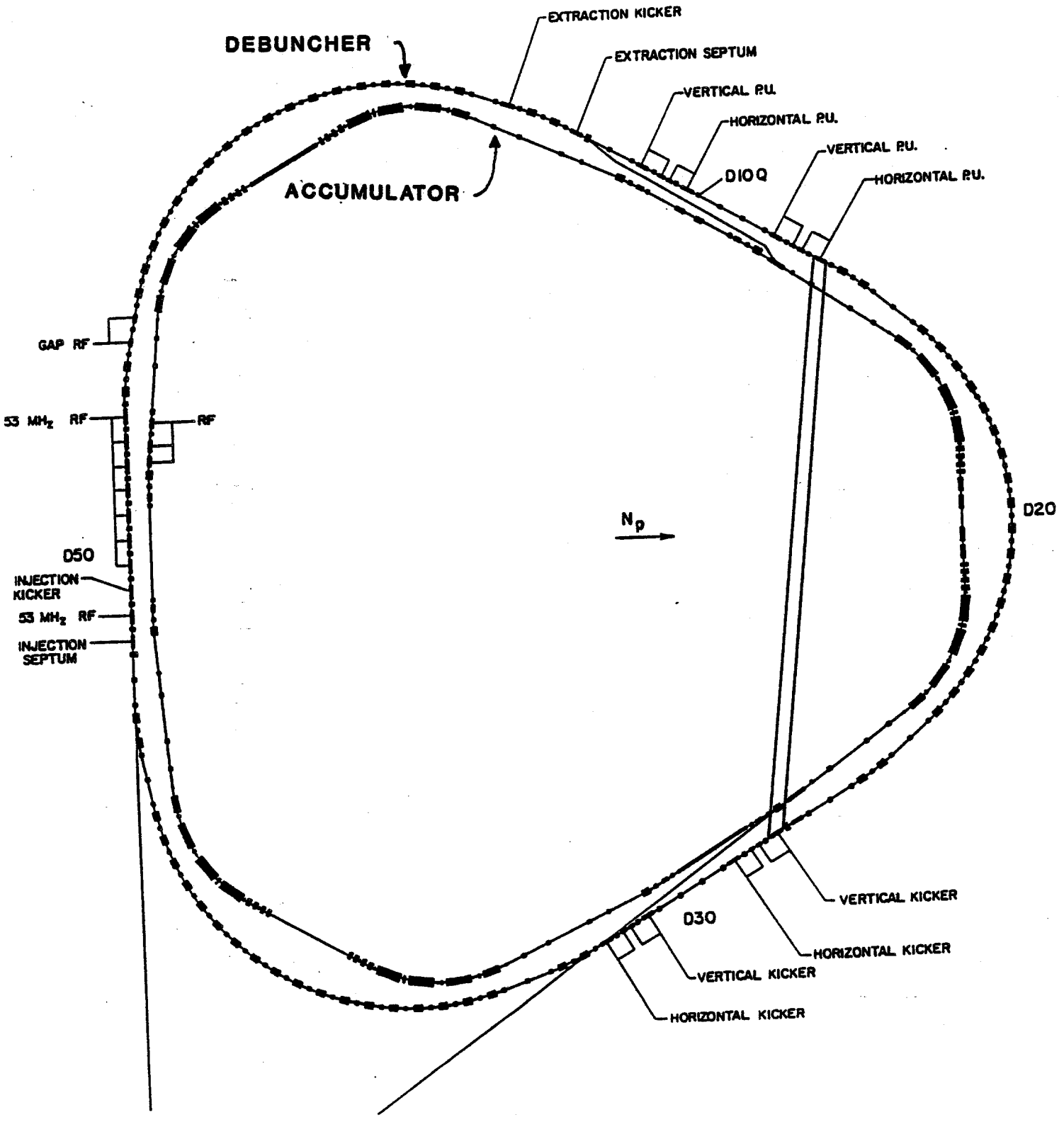

DEBUNCHER LAYOUT

CHAPTER 4

DEBUNCHER RING

4.1 Purpose of the Debuncher

The primary purpose of the Debuncher is to reduce the large momentum spread of the 8-GeV $\bar{p}$ beam at production to 0.2% or less prior to injection into the Accumulator. This reduction is done by rf bunch rotation and adiabatic debunching after the $\bar{p}$ beam is injected into stationary 53-MHz buckets in the Debuncher. The debunching time is only slightly longer than 10 msec, and there are therefore nearly two seconds available for cooling before the beam is transferred to the Accumulator. Stochastic cooling of betatron amplitudes has been shown to be feasible, and a betatron cooling system to reduce the emittance by a factor of 3 in both planes in 2 sec is included in the design.

A possible addition that is still being examined is a fast momentum stochastic precooling step to reduce even further the momentum spread by a factor of 2 or possibly 3, in 2 sec.

Table 4-I gives parameters of the Debuncher.

TABLE 4-I THE DEBUNCHER RING

Kinetic Energy	8.0 GeV
γ_t, transition energy	7.6482
$\eta = 1/\gamma_t^2 - 1/\gamma^2$	0.00608
Average Radius	80.42 m
RF Frequency	53.103 MHz
Maximum rf voltage	5 MV
Number of $\bar{p}$ bunches injected	80
Harmonic number	90
Beam Gap for Injection Kicker	200 nsec
Momentum Aperture, $\Delta p/p$	4%
Betatron Acceptance, h and v	20π mm-mrad
Betatron Tunes, h and v	9.75
Natural Chromaticity, h and v	-10
Periodicity	3, each with mirror symmetry
Max amplitude function β	20 m
Max dispersion value	2.1 m
Phase Advance per Cell, h and v	60°

4.2 Requirements of the Design

As shown in Fig. 4-1, the Debuncher ring surrounds the Accumulator. Because of the triangular shape of the latter, a periodicity of three was chosen for the Debuncher, each period with mirror symmetry.

The Debuncher operates at a kinetic energy of 8 GeV. Its circumference must be at least as long as each antiproton pulse, made of 80 narrow bunches with a separation frequency of 53.1 MHz. The circumference was chosen to be 505 m, which corresponds to an rf harmonic number of 90. This arrangement allows a separation of 12 ft between the Debuncher and the Accumulator in the long straight sections so that these portions of the two rings can be accommodated in the same wide tunnel.

Each superperiod includes a long straight section. These accommodate: (i) injection, (ii) extraction, (iii) rf cavities for the bunch rotation, (iv) pickups and kickers for stochastic cooling. The phase advance between pickups and kickers should be an integer number of betatron waves $\pm 90°$. This gives only a few possible choices for betatron tunes, which we take to be approximately the same in the two planes. The value 9.75 was finally chosen.

Another requirement is that the three long straight sections must have zero dispersion, an important requirement for the performance of stochastic cooling and for avoiding betatron-synchrotron coupling.

Finally the Debuncher is capable of accepting a momentum spread of $\pm 2\%$ and has a betatron acceptance of at least 20π mm-mrad in both planes.

4.3 Choice of Transition Energy

The most important parameter in the design of the Debuncher is the dispersion

$$\eta = 1/\gamma_t^2 - 1/\gamma^2$$

where γ is the relativistic energy factor and γ_t corresponds to the transition energy. The rf voltage needed for bunch rotation is proportional to $|\eta|$. If $|\eta|$ is less than 0.002, the variation of η with momentum will degrade the final momentum spread. On the other hand, a larger value of $|\eta|$ helps betatron cooling and is needed if momentum precooling is to be done in the future. We have reached a compromise by setting $\eta = 0.006$, which corresponds to $\gamma_t = 7.65$, a solution which gives ν_H, ν_V approximately 9.75. This choice corresponds to operating the Debuncher Ring above the transition energy.

We could also have chosen to operate below the transition energy (larger value of γ_t) because only the absolute value of η enters. We considered this possibility at the beginning of the design, but rejected it for the following reasons. A larger value of γ_t, and therefore of the strength of the lattice focusing, is desirable because it makes the dispersion and betatron amplitude functions small, which would also make the physical aperture of the magnets smaller. But larger values of γ_t would also lead to an unfortunately large natural chromaticity. To correct this, too much sextupole correction was required considering the smaller

dispersion around the ring. To eliminate problems intrinsic to sextupoles and chromaticity, we had to decrease the focusing of the ring to the present value of γ_t=7.65. When this was done, the dispersion of the ring doubled, but we could still manage to achieve the required momentum and betatron acceptance with reasonably small-aperture magnets.

With this choice of η, one still requires 5 MV peak rf voltage at 53 MHz for bunch rotation.

4.4 Lattice

We have opted for a smooth lattice to help stability of the ring against sextupoles and chromatic effects. The ring is divided into 57 FODO cells, each with a phase advance of 60° in each plane. One half a superperiod is shown in Fig. 4-2 with beta- and dispersion-function plots. In the curved sections of the ring, the cells are regular; bending magnets are placed exactly halfway between quads. The long straight sections are made of 6 cells, each without bending magnets. A "dispersion-killer" cell is located at each end of the long straight section. Zero dispersion is achieved by eliminating the two bending magnets just before the last regular cell. A regular cell is shown in Fig. 4-3.

Two fortunate features are obtained with this lattice: (i) the beta functions never exceed 20 m in either plane. This makes the beam size in the long straight sections small enough to fit in the aperture of stochastic-cooling pickups and kickers, which have a gap between plates of 30 mm (suitable for 2-4 GHz bandwidth). (ii) The chromaticity of the ring is reduced to a minimum of -10. In an earlier design, each long straight section was made of three consecutive low-beta insertions. To do this, four quadrupole triplets were required to provide room for stochastic-cooling devices, rf cavities and injection and extraction equipment. It has been found that these triplets added substantially to the natural chromaticity and it was therefore decided to bridge the long straight sections with regular FODO cells.

The beam envelope is shown in Fig. 4-4 for half of a superperiod. It corresponds to a momentum spread of 3% and an emittance of 20π mm-mrad in both planes.

4.5 Magnets

There is only one kind of dipole in the design. The dipoles are 1.66 m long (effective length), have a full gap of 6 cm and have a strength of 17 kG. There are three kinds of quadrupoles. The dipole and quadrupoles are described in Table 4-II. There is one kind of sextupole. The sextupoles are discussed in Sec. 4.7.

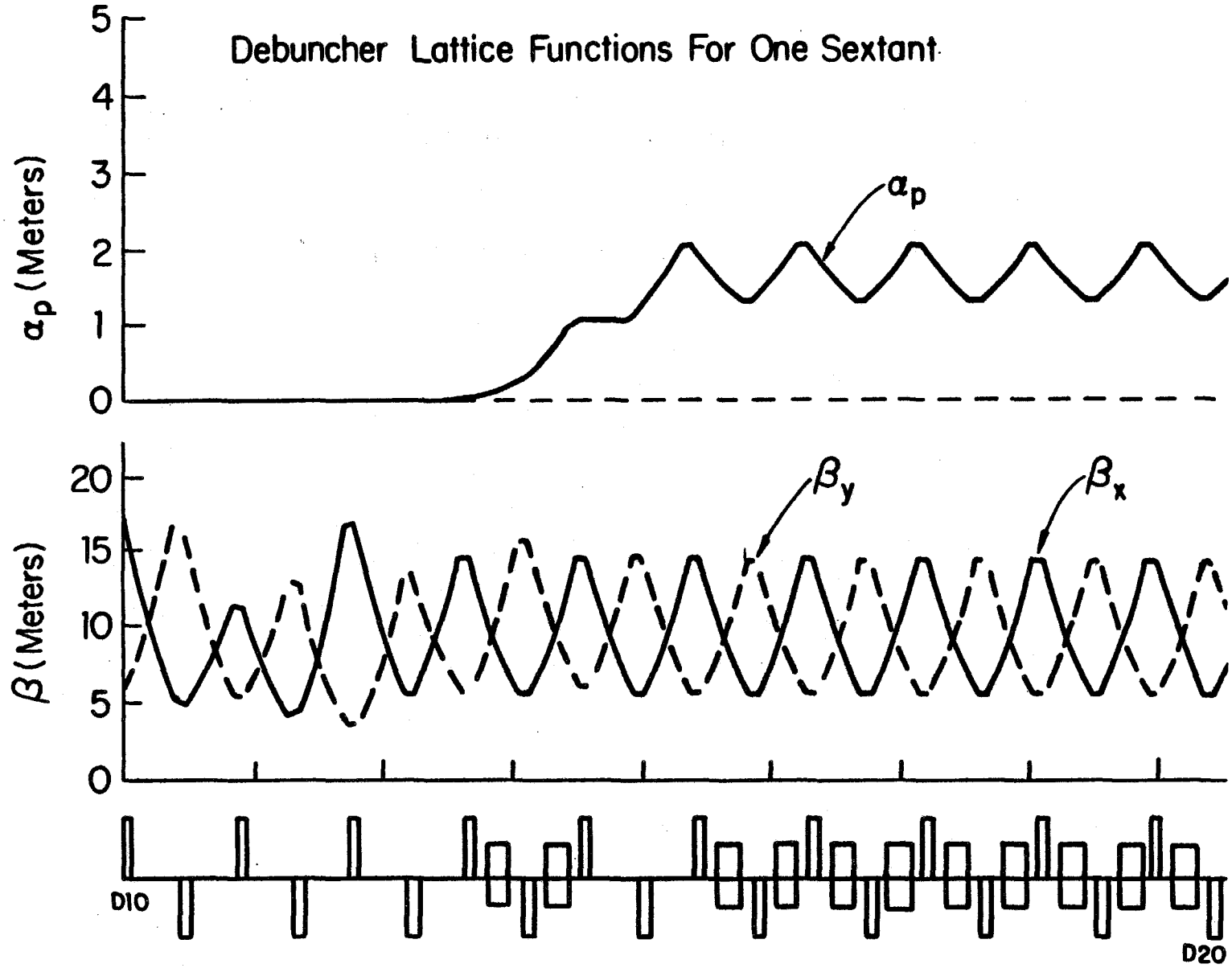
Debuncher Lattice Functions For One Sextant
α_p (Meters)
5
4
3
2
1
0
α_p
β (Meters)
20
15
10
5
0
β_y
β_x
D10
D20

Figure 4-2

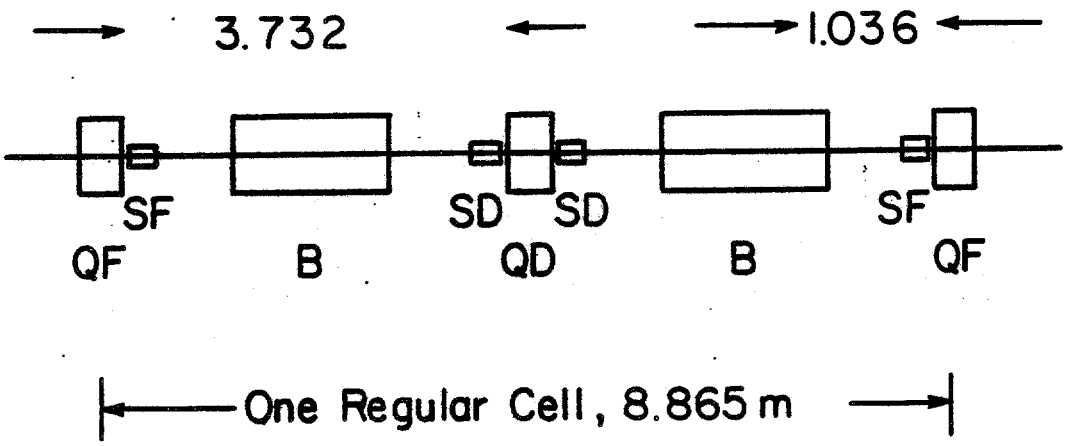

Figure 4-3

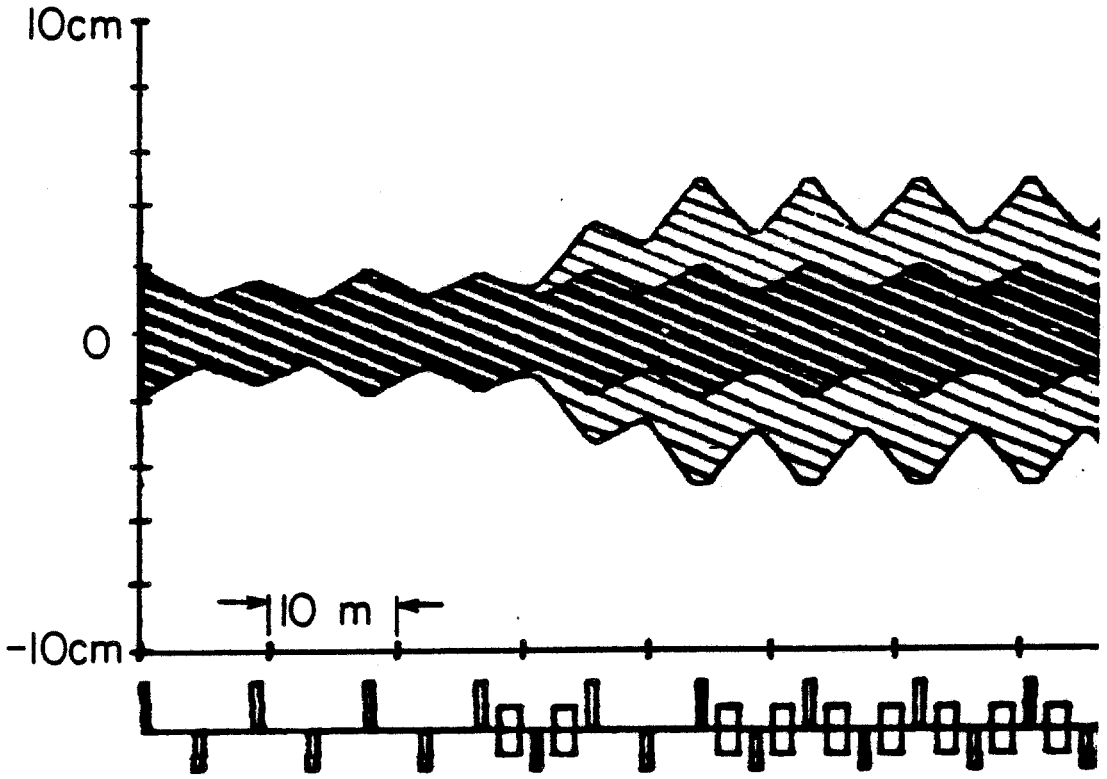

Horizontal Beam Envelopes for $\Delta P/P = 3\%$ and $E = 20\pi$ mm-mrad Before and After Debunching

Figure 4-4

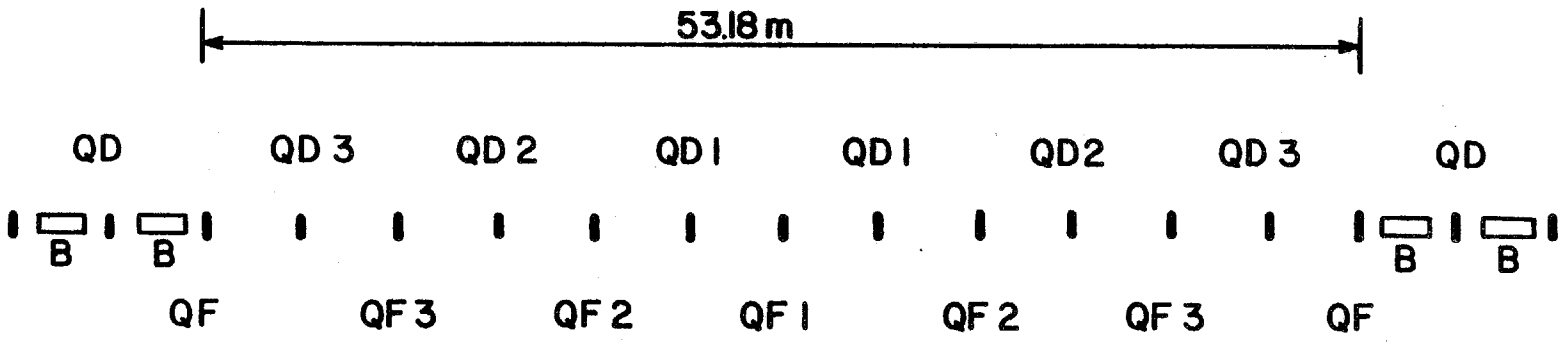

QUADRUPOLE LENGTHS: QF1, QF2, QD1, QD2 = 27.6 in

QF3, QD3 = 32.6 in

DISTANCE BETWEEN QUADRUPOLE CENTERS = 4.43 m

DEBUNCHER LONG STRAIGHT SECTION

Figure 4-5

TABLE 4-II DEBUNCHER MAGNETS

	Number	Effective Length	Strength	Gap or Poletip Radius
Dipoles:				
B	66	1.6604 m	1.7 T	.66 mm
Quadrupoles:				
I. QF, QD QF1, QD1 QF2, QD2	102	27.6 in.	12 T/m	44.5 mm
II. QF3, QD3 small aperture	9	32.6 in.	10.5 T/m	44.5 mm
III. QF3,QD3 large aperture	3	32.6 in.	10.5 T/m	84.1 mm

There are two effective quadrupole lengths: 27.6 in. and 32.6 in. The longer quadrupoles are located in pairs at both ends of each long straight section as shown in Fig. 4-5 which shows a long straight section with the neighboring regular cells. All the other quadrupoles are shorter. All quadrupoles have the same aperture, with a poletip radius of 44.5 mm, except for three special ones that have a poletip radius of 84.1 mm. These quadrupoles are marked with an L -in Fig. 4-1 and are also used in conjunction with beam transfer from and to several directions. The maximum gradient required is 12 T/m and somewhat less for the large aperture quadrupoles. The total magnet power to operate the ring at 8 GeV is 1.1 MW.

A detailed set of specifications for the magnets is given in Chapter 12.

4.6 Tuning

A nominal tuning mode has been worked out with betatron numbers ν_H=9.73 and ν_V=9.77. To obtain this, the regular cells have exactly 60° phase advance in both planes to give zero dispersion in the long straight sections. The quadrupoles in the long straight sections have been adjusted to get the required tune values with proper matching at the transition between the curved and straight sections. A waist is introduced in the middle of each long straight section and curved sector. The settings for all the magnets are given in Table 4-III for the nominal tune.

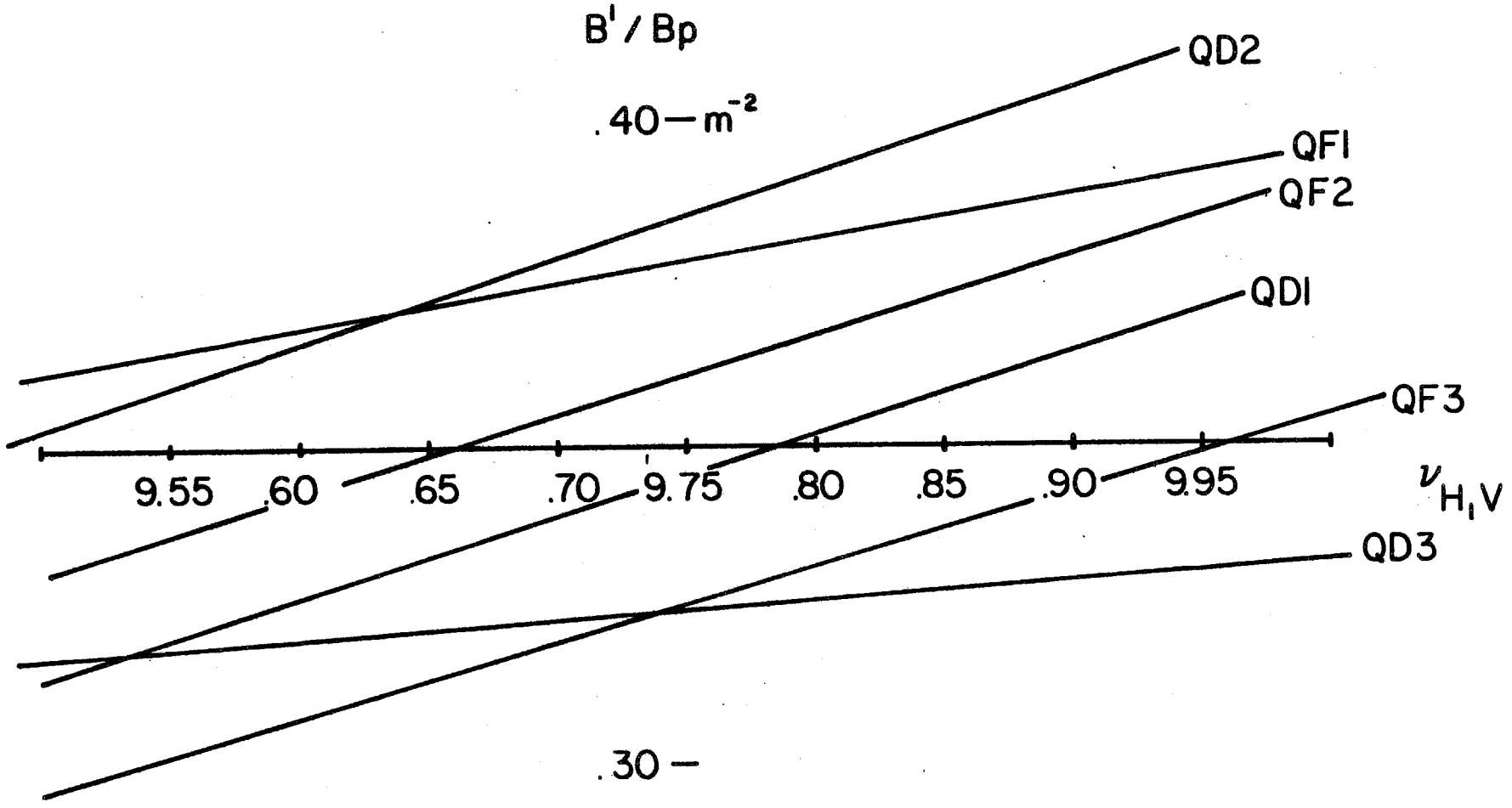

Variation Of B' /B For Each Type Of Quadrupole

Figure 4-6

TABLE 4-III MAGNET SETTING FOR THE TUNING MODE: ν_H=9.73, $\nu_.$=9.77

B = 1.7 T
Bρ = 29.6501 T-m

Quadrupoles		$B_0/B\rho$	Current	Voltage
QF		0.33652 m^{-2}	240 A	9.7 V
QD		0.32928	235	9.5
QF1		0.37747	270	10.9
QD1		0.34714	248	10.0
QF2		0.35881	256	10.3
QD2		0.38679	276	11.1
QF3	large	0.32494	1313	10.5
QD3	aperture	0.32459	1311	10.5
QF3	small	0.32494	232	10.4
QD3	aperture	0.32459	232	10.4

To achieve other betatron tune values, the strength of the regular quadrupoles QF and QD in the bending section is left unchanged, so that the phase advance/cell will remain 60°. With this mode of operation, the "dispersion killer" is always effective and the dispersion in the long straight section is always cancelled. To change the betatron tune, only the strengths of the six quadrupoles QF1, QD1, QF2, QD2, QF3 and QD3 in the long straight sections are varied. The search for the quadrupole setting is done by imposing the condition of matching between the long straight sections and the curved sections and of waists in the middle of both of them. It is possible to vary both tunes over the range from 9.5 to 10.0 by keeping them equal. The variation of $B_0/B\rho$ for each quad is shown in Fig. 4-6. The transition energy remains unchanged in this range. The variation of β_H and β_V, the maximum values of the horizontal and vertical beta functions in the space occupied by the pickups and kickers for the stochastic cooling, is given in Fig. 4-7. In the same figure, we give the variations of the natural horizontal and vertical chromaticities.

4.7 Sextupoles

Sextupoles are located next to each quadrupole, usually on both sides, as shown in Fig. 4-2. They are divided in two groups: those next to the horizontally focusing quads (SF) and those next to the vertically focusing quads (SD). The main purpose of these sextupoles is to correct and adjust the natural chromaticity of the ring. They are therefore elements of primary importance and are on an equal footing with the dipoles and quadrupoles. They are not intended to correct magnet errors and imperfections.

Their strength has been calculated with PATRIS, a particle tracking code that is a heavily modified version of PATRICIA suitable for protons.

Variation Of Lattice Functions Across A Cooling Straight Section

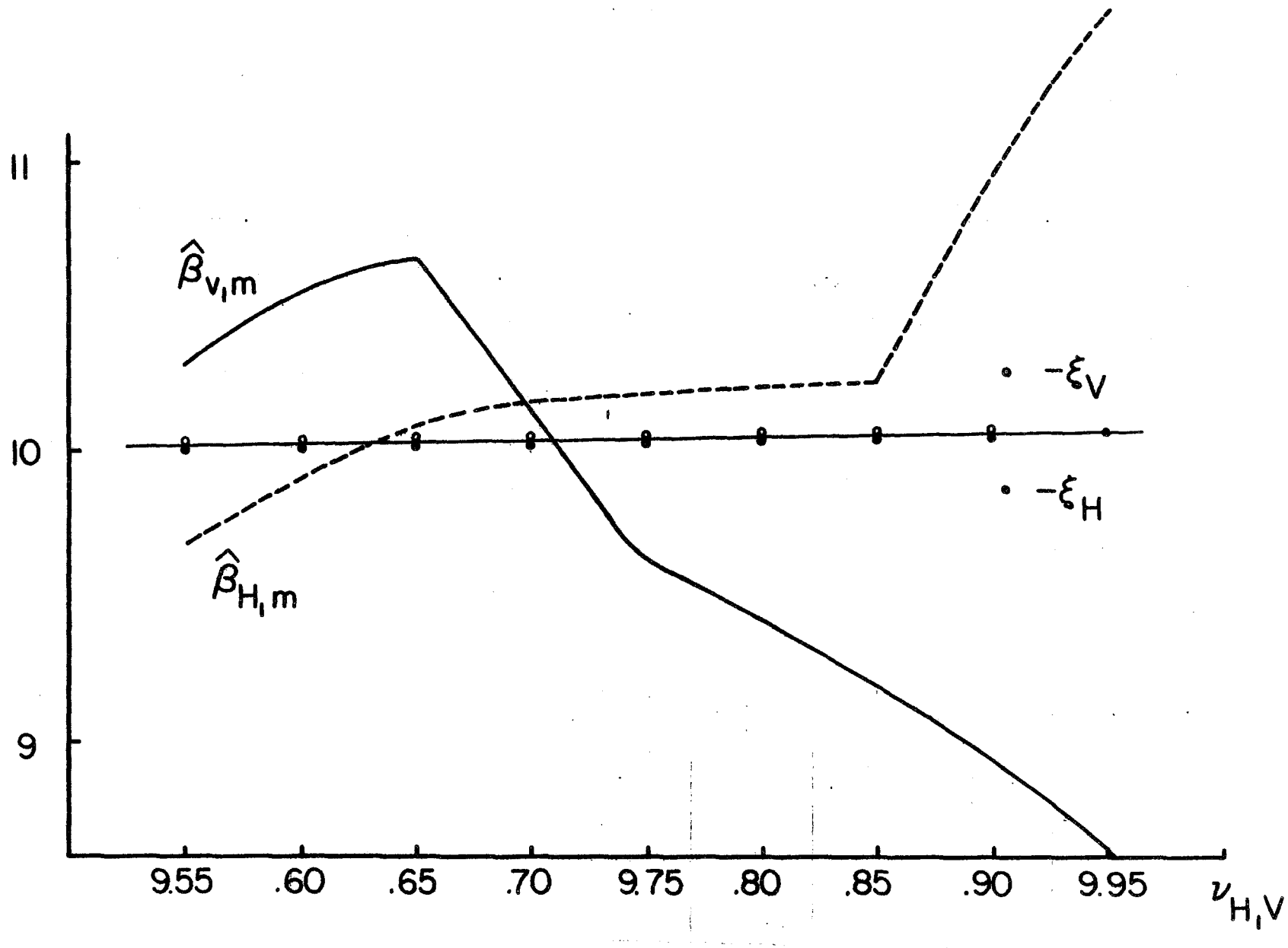

Figure 4-7

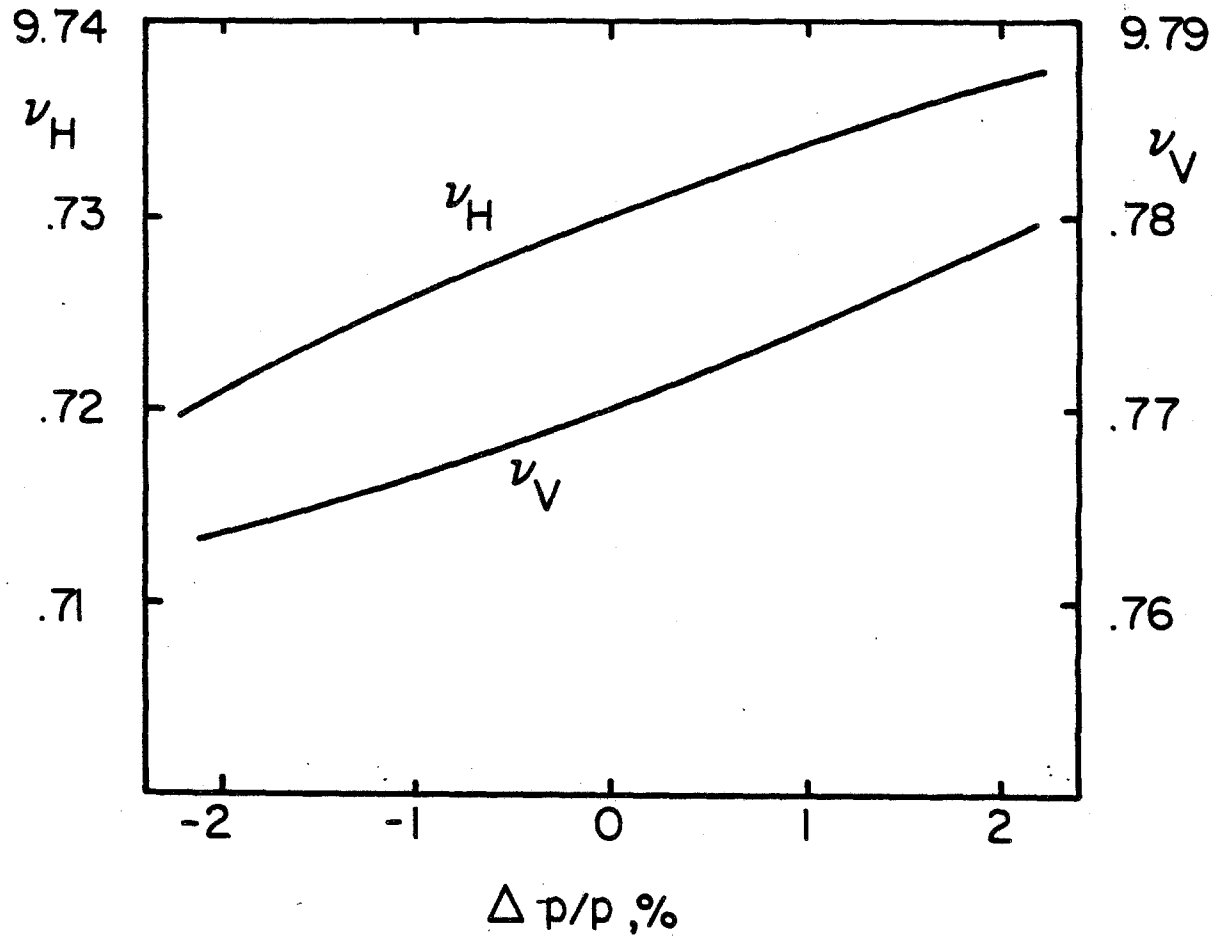

Variation Of Tunes With Momentum

Figure 4-8

The thin-lens approximation has been used. The sextupole strength given in Table 4-IV corresponds to zero chromaticity. The lattice variations with momentum have then been calculated with SYNCH. The results are shown in Fig. 4-8, which gives the variation of the betatron tunes with momentum, Fig. 4-9, which gives the change of $\alpha=1/\gamma_t^2$, the momentum compaction factor, and Fig. 4-10 which gives β_H, β_V and α_p versus $\Delta p/p$ at the downstream end of the injection kicker. Figure 4-11 gives the tune diagram with the working point for the reference tuning mode and the tune spread for ±2% beam momentum spread. Finally, Fig. 4-12 gives the variation of β with momentum along the ring circumference for half of a superperiod. As one can see, the variations are very modest, less than 10%.

TABLE 4-IV DEBUNCHER SEXTUPOLE DISTRIBUTION

Type	SF	SD
Number	72	66
$B''\ell/B\rho$	0.141 m^{-2}	-0.213 m^{-2}

The design specifications for the sextupoles are given in Table 4-V. The power per magnet is so small that no water cooling is needed.

TABLE 4-V DEBUNCHER SEXTUPOLE MAGNETS

Maximum strength, $B''\ell/B\rho$		0.22 m^{-2}
Bore radius		70 mm
Effective length		0.2 m
Maximum field, B''		33 T/m^2
Ampere-turns		1555 AT/pole
Current		256 A
Turns		6 turns/pole
Conductor size	0.3294" square, 0.18" hole dia., area	0.07723 $in.^2$
Current density		3.35 $kA/in.^2$
Resistance		5 mΩ/magnet
Voltage Drop		1.45 V/magnet
Thermal loss		375 W/magnet

4.8 Magnet Power Supplies

The layouts of the magnet power supplies and their circuits are dictated by the operating mode of the Debuncher Ring. The situation can be summarized as follows

i) There will be one individually controlled power supply bus for each family of sextupoles, SF and SD. The current is 80 A and 120 A respectively with a regulation of 0.1%. A tunability range of ±10% is desirable for chromaticity control over a wider range.

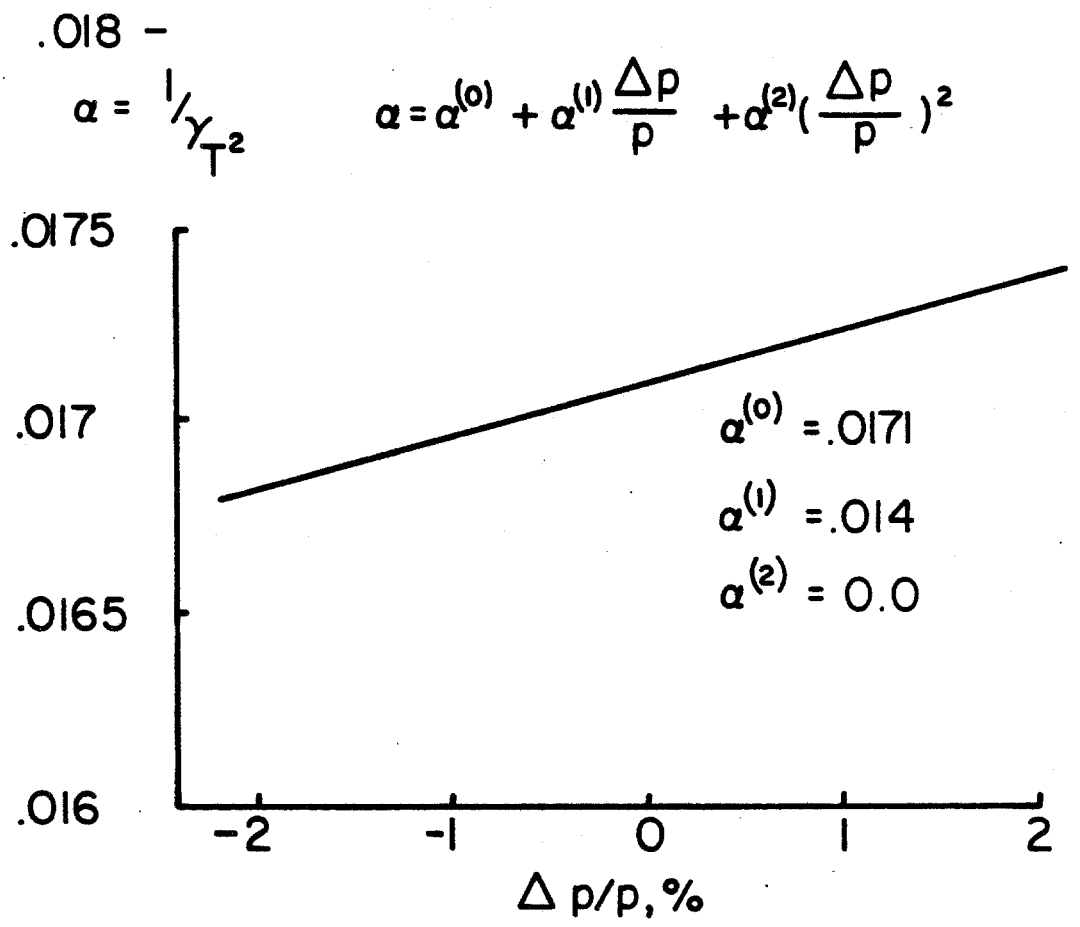

Variation Of Momentum-Compaction Factor With Momentum

Figure 4-9

Variation Of Lattice Functions With Momentum At The Injection Kicker

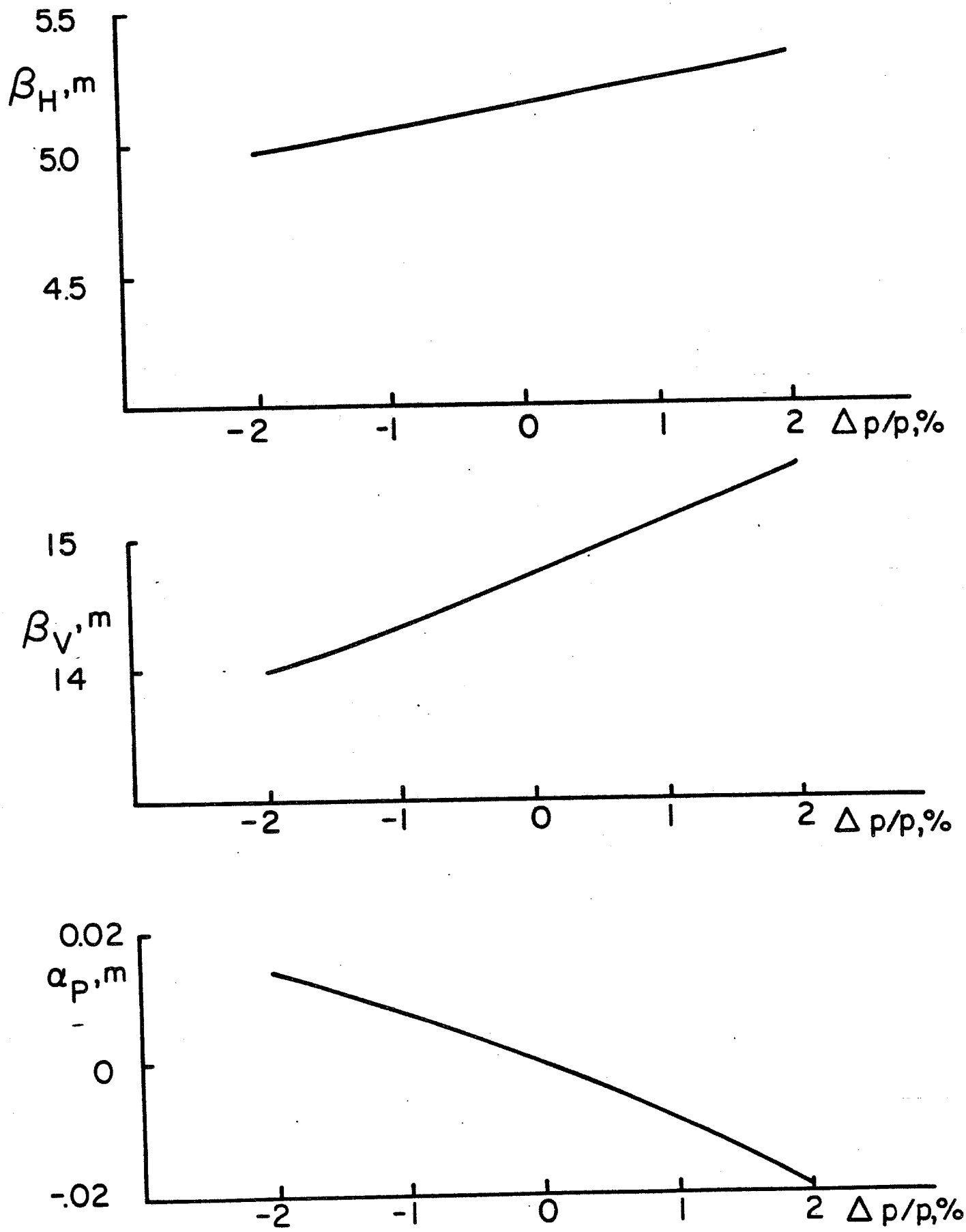

Figure 4-10

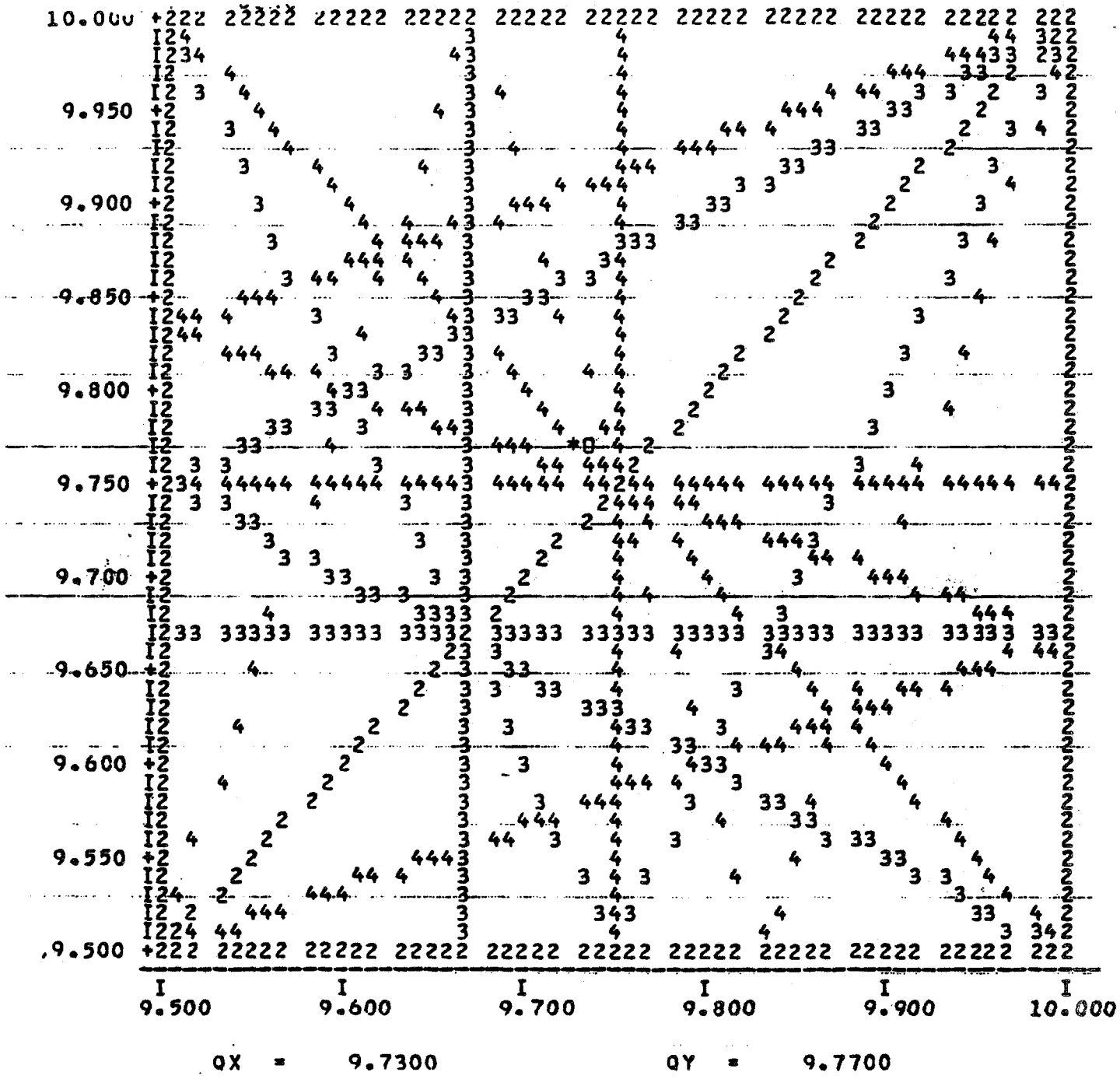

Tune Diagram

Figure 4-11

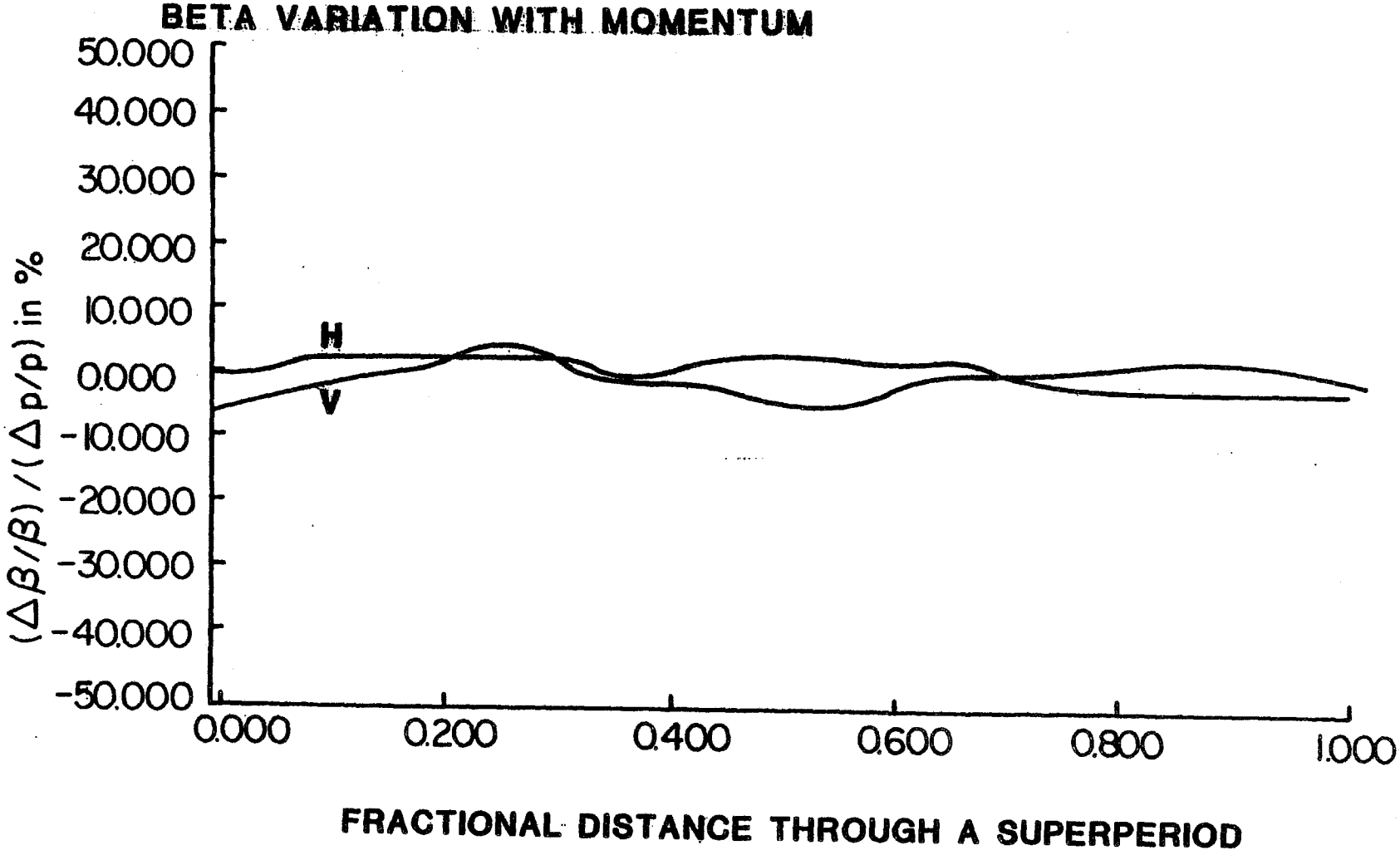
BETA VARIATION WITH MOMENTUM
50.000
40.000
30.000
20.000
10.000
0.000
-10.000
-20.000
-30.000
-40.000
-50.000
(Δβ/β) / (Δp/p) in %
H
V
0.000
0.200
0.400
0.600
0.800
1.000
FRACTIONAL DISTANCE THROUGH A SUPERPERIOD

Figure 4-12

ii) Only one current bus is required for all the dipoles. The current is 1175.6 A and a regulation of 0.01%. No shunts are needed, even for closed-orbit correction.

iii) There is one bus for the regular horizontally focusing quads (QF) and one for the vertically focusing quads (QD). The two buses are individually controlled. The current is 240 for QF and 235 for QD Power supply regulation is 0.01%. No shunts are required. Once the 60° phase advance/cell has been empirically obtained during the early days of operation, these quadrupole settings should remain unchanged.

iv) The special quadrupoles QF1, QF2, QD1 and QD2 in the long straight sections are connected together to a common power supply bus with a maximum current of 290 A; each of them has a shunt to drive the current down 55 A. The regulation is, as usual, 0.01% in current.

v) The special large-aperture quadrupoles QF3 and QD3 are connected to the dipole bus, which provides 1175.6 A, but on top of this individual power supplies for the range -50 to 100 A are added. The regulation requirement for this addition is 0.05%.

vi) The small aperture quads QF3 and QD3 in the long straight sections are connected respectively to the QF and the QD buses, but each of them carries an individual shunt with a current range of -40 A and a regulation of 0.05%.

4.9 Bunch Rotation and Other RF Manipulation

In order to evaluate the effectiveness of the debunching process and thus to determine the momentum spread of $\bar{p}$'s that can be accepted at production, extensive computer simulations of the rotation and debunching sequences have been carried out. The following features have been included:

(i) The antiproton bunches, at the moment they have been generated at the target, have the same longitudinal distribution as the proton bunches, that is, an rms bunch length of 5 cm.

(ii) The $\bar{p}$'s traverse a dispersionless drift of nearly 300 m between the target and the first rf cavity. The rf voltage is to be generated by eight cavities located immediately following the injection septum.

(iii) Three values of η were used to test the dependence of the rotation effectiveness versus the magnitude of η. A value of -0.002 was used with an rf voltage of 2 MV and a value of -0.004 was used with an rf voltage of 4 MV. For these two

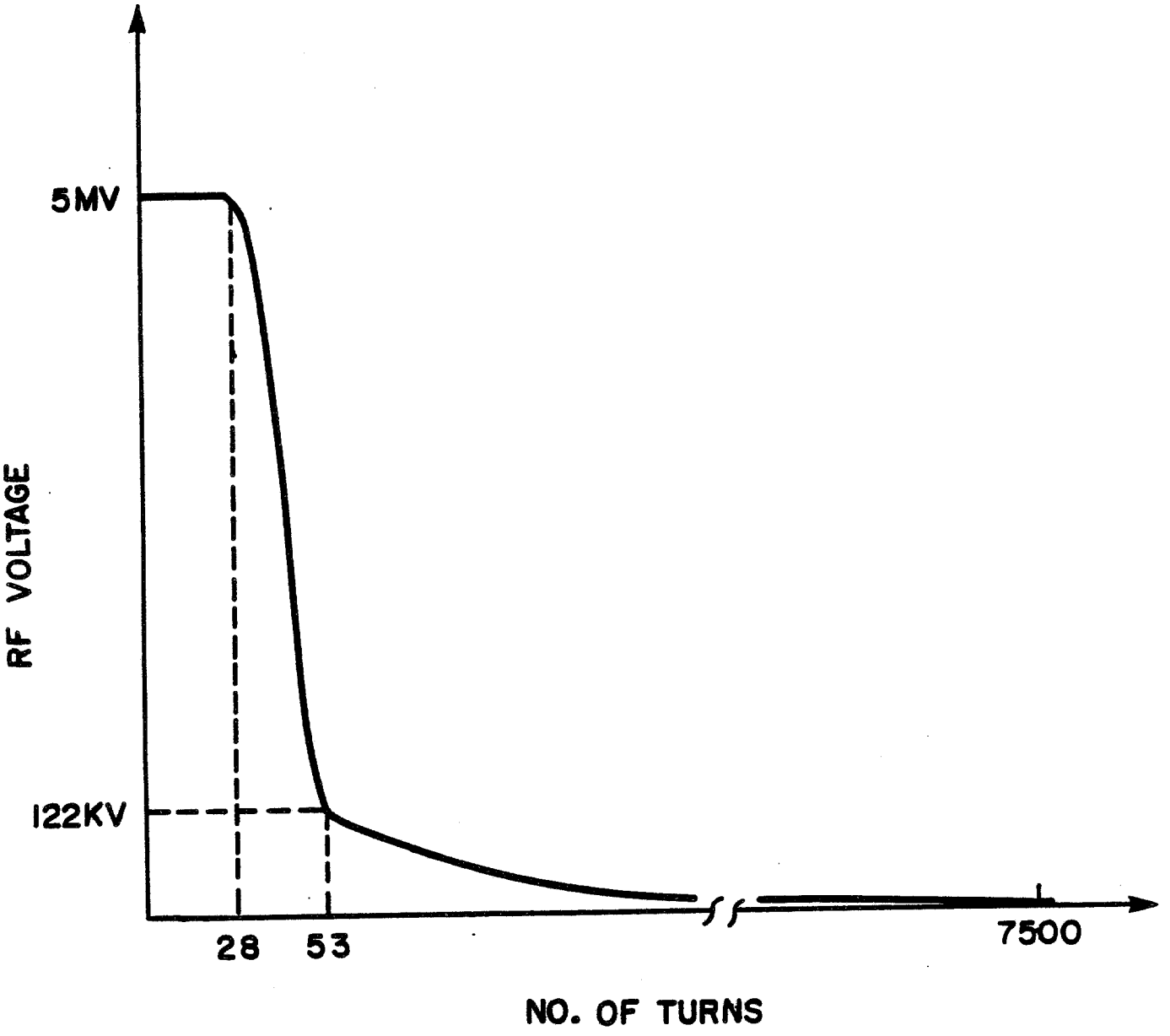

Figure 4-13 RF voltage program for the high gradient system in the Debuncher.

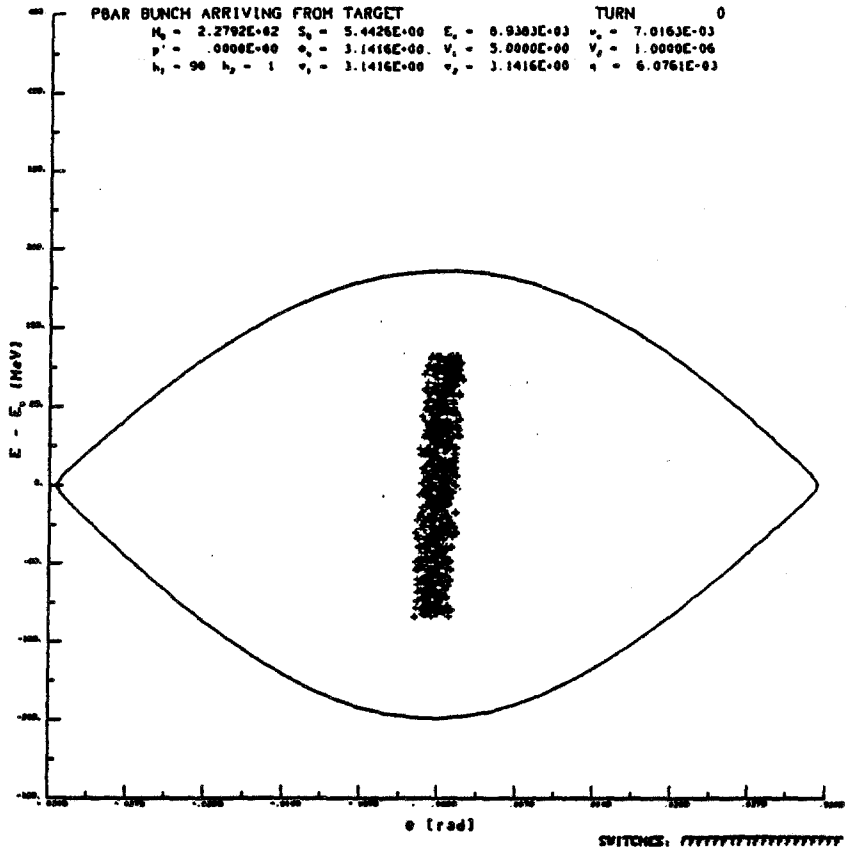

a) Antiproton bunch at injection into a Debuncher bucket produced by 5 mV

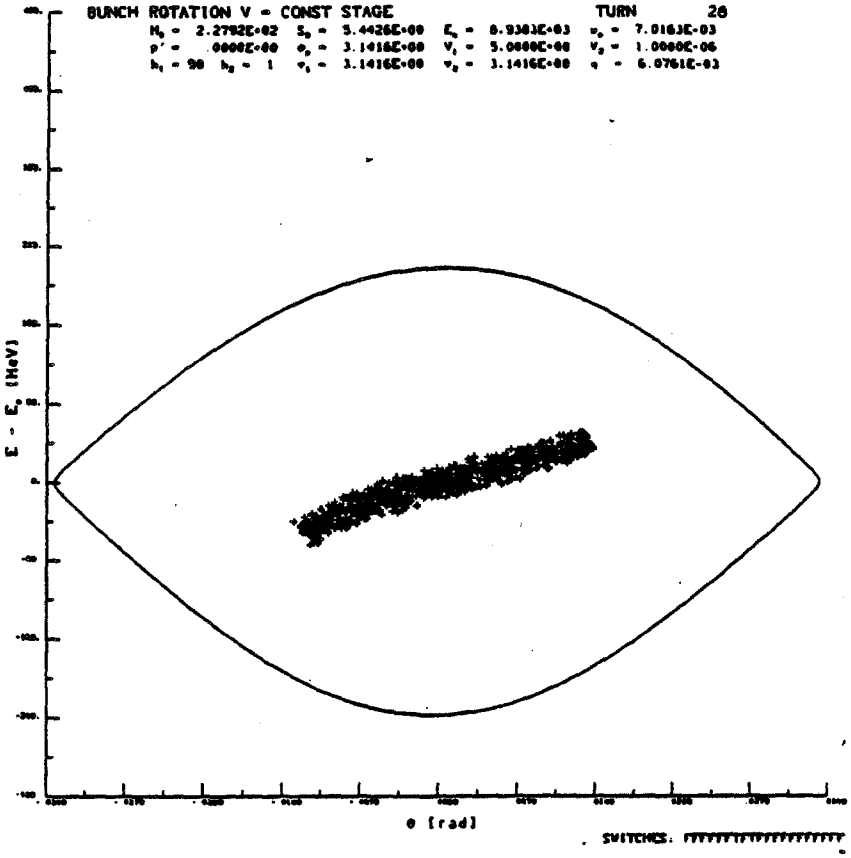

b) Bunch after 47.5 μsec, at end of 5 mV portion of rf voltage program.

Figure 4-14 Phase-space during debunching.

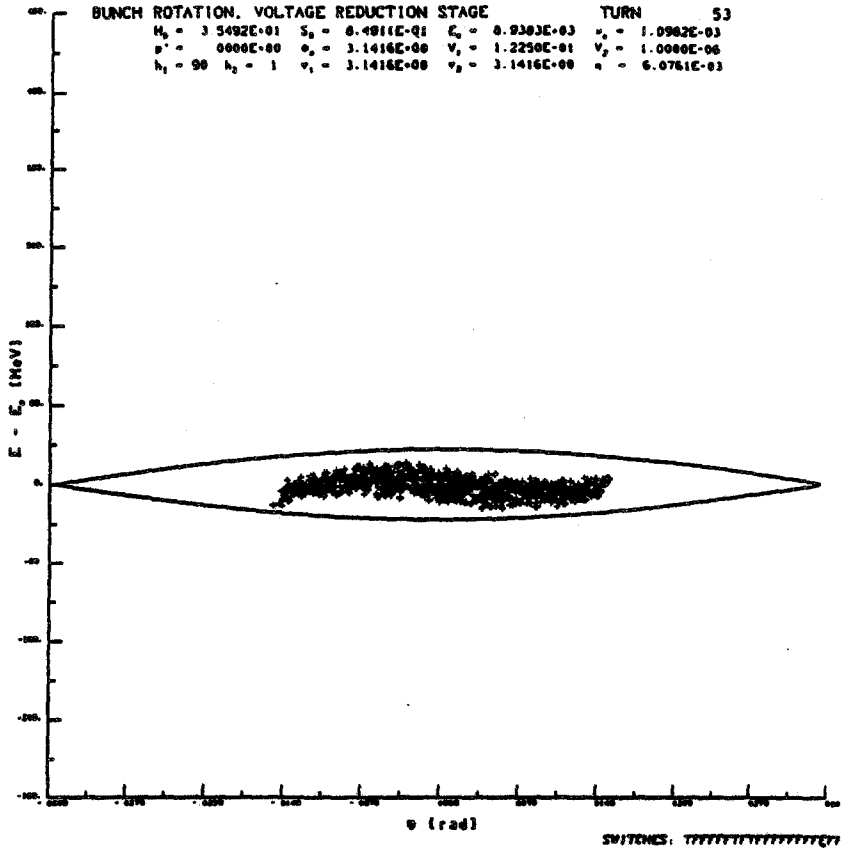

c) Bunch after 90 μsec, at beginning of the adiabatic debunching portion of the rf voltage program.

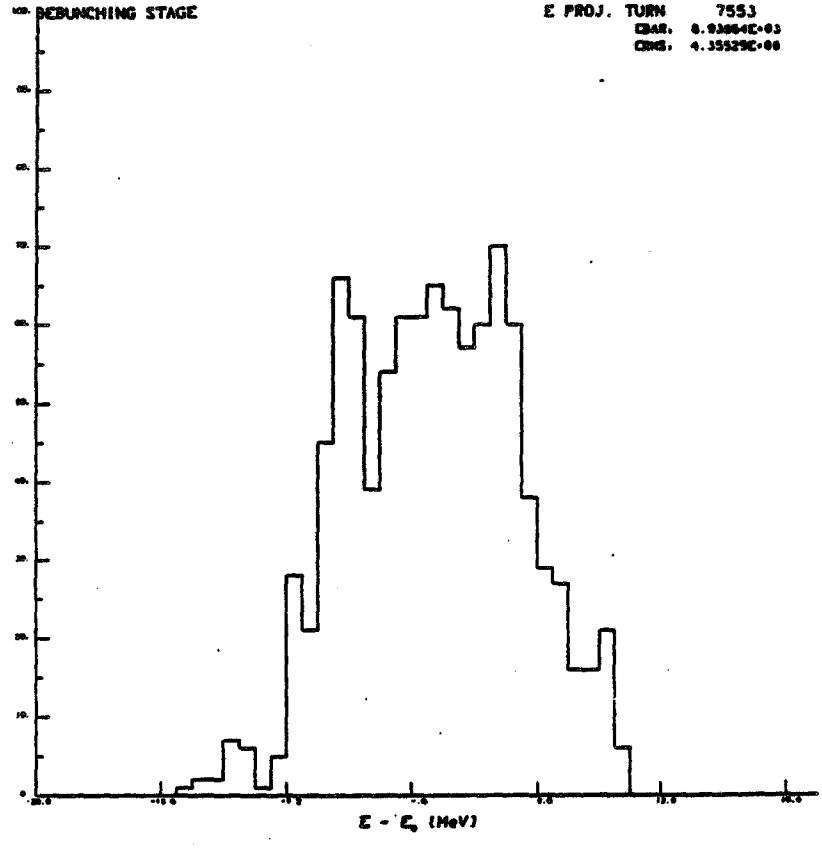

d) Energy distribution of the bunch after 128 msec, the end of the debunching.

Figure 4-14 c&d

cases an initial $\Delta p/p=4\%$ was assumed. The simulation for the actual design case has $\eta=0.006$ and an initial momentum spread of 3%; the maximum rf voltage was taken to be 5 MV. The results do not depend very much on the value of η although the case of $\eta=-0.002$ is somewhat worse.

(iv) The bunches are allowed to rotate for 20-35 turns while the voltage is kept constant. The rotation was about 45-60°.

(v) The voltage is then dropped to approximately 100-120 kV in 30-35 turns (1 turn = 1.6 μsec) to form a bucket matched in shape to the beam bunch, which has evolved into a distorted S-shape that extends over ±90° in synchrotron phase.

(vi) The voltage is slowly reduced to 5 kV and then abruptly turned off.

A debunching time of 12 msec was chosen, since longer times did not significantly reduce the momentum spread, while shorter times did increase the momentum spread. The final momentum spread is not sensitive to the other details of the time dependence of the rf voltage except during the early stage of rotation. The rf voltage program for the rotation and debunching operations is shown in Fig. 4-13 for the actual design case of $\eta=-0.006$ and $\Delta p/p=3\%$. Figures 4-14 shows the beam shape at the end of some of the steps for $\Delta p/p=3\%$. If the debunching could be done without dilution, 95% of the beam would be contained within a momentum spread of 0.17%. Computer simulations show that the debunched momentum spread is 0.23%. The 30% factor of dilution has several causes. It is caused in part by nonlinearities of phase oscillations of particles captured within an rf bucket and in part by the variations of γ^{-2} of the particles and the momentum compaction factor γ_t^{-2} with energy. These variations and the presence of sextupole corrections in the ring lattice were taken into account in the simulations (see Fig. 4-9).

Calculations were done with other initial momentum spreads for the design case. The initial rf voltage of 5 MV and the final rf voltage of 5 kV were kept fixed for these calculations. These results are shown in Fig. 4-15. The numbers in brackets are a measure of the dilution. The choice of 5 MV seems to be optimal for $\Delta p/p=3\%$. The momentum spread of the $\bar{p}$ beam will be limited to 3% by collimation prior to injection into the Debuncher. The Debuncher itself has a momentum aperture of over 4%. It may be possible to reduce the debunched beam momentum spread further if the rf voltage can be reduced adiabatically to a value much less than 5 kV.

Harmonics of twice and three times the fundamental frequency were added in the simulations. Significant improvement was found only for larger initial momentum spread.

A summary of the rf parameters is given in Table 4-VI.

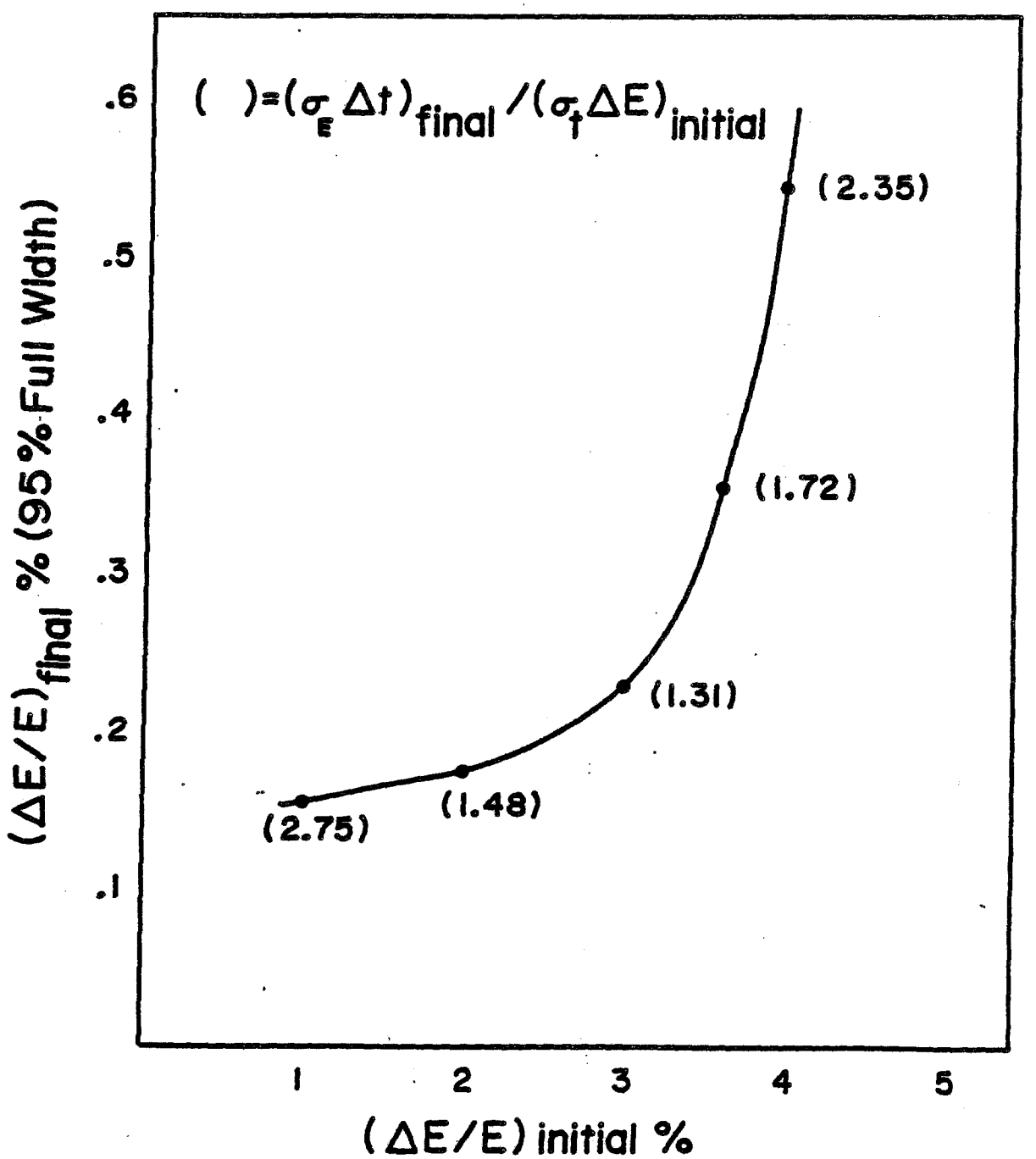
( )=(σ_E Δt)_final /(σ_t ΔE)_initial
(2.35)
(1.72)
(1.31)
(1.48)
(2.75)
.6
.5
.4
.3
.2
.1
1
2
3
4
5
(ΔE/E)_final % (95% Full Width)
(ΔE/E) initial %

Figure 4-15

TABLE 4-VI DEBUNCHER RF PARAMETERS

Kinetic Energy	8.0 GeV
Number of antiproton bunches	80
Total number of antiprotons ($\Delta p/p$=3%)	7×10^7
Momentum aperture, $\Delta p/p$ (full width)	4%
Bunch width (full)	<1 nsec
Transition γ (γ_t)	7.65
Mixing factor, $\eta = \gamma_t^{-2} - \gamma^{-2}$	.006
RF frequency	53.1035 MHz
RF harmonic number (h)	90
Revolution period	1.695 μsec
Maximum voltage	5.0 MV
RF voltage, end of rotation	122.5 kV
RF voltage, end of debunching	5.0 kV
Time required for rotation	.103 msec
Time required for debunching	12.712 msec

A broad-band, low-frequency rf system is operated to preserve a gap in the otherwise debunched beam. A 200 nsec gap is needed if the beam is to be transferred to the smaller Accumulator without loss. The rf system to make such a gap is described in Section 4.11.

4.10 RF Systems for Bunch Rotation and Debunching

The design criteria for the antiproton Debuncher rf are:

(i) Voltage gain per turn approximately 5 MV.

(ii) Maximum pulse length 100 μsec (duty factor 5×10^{-5}).

(iii) RF voltage pulse fall time from 5.0 MV to 120 kV, 50 μsec.

(iv) Pulse repetition rate 0.5 Hz.

(v) Minimum voltage gain per turn ≤5 kV.

(vi) Adiabatic reduction of voltage from 120 kV to ≤5 kV in a time of 5 to 20 msec under program control.

A representative rf voltage waveform was shown in Fig. 4-13. The design is simplified by the fact that the beam intensity will not exceed 10^{10} particles when the rf voltage is on. Of the particles that emerge from the production target when it is struck by 2×10^{12} 120-GeV protons, approximately 2×10^{10} are within the acceptance of the beam transport and the Debuncher. Some 90% of these particles are mesons, of which 50% decay before reaching the injection straight section. After each successive turn, 63% of the remaining mesons decay. The remainder of the particles that reach the center of the injection straight section consist of muons,

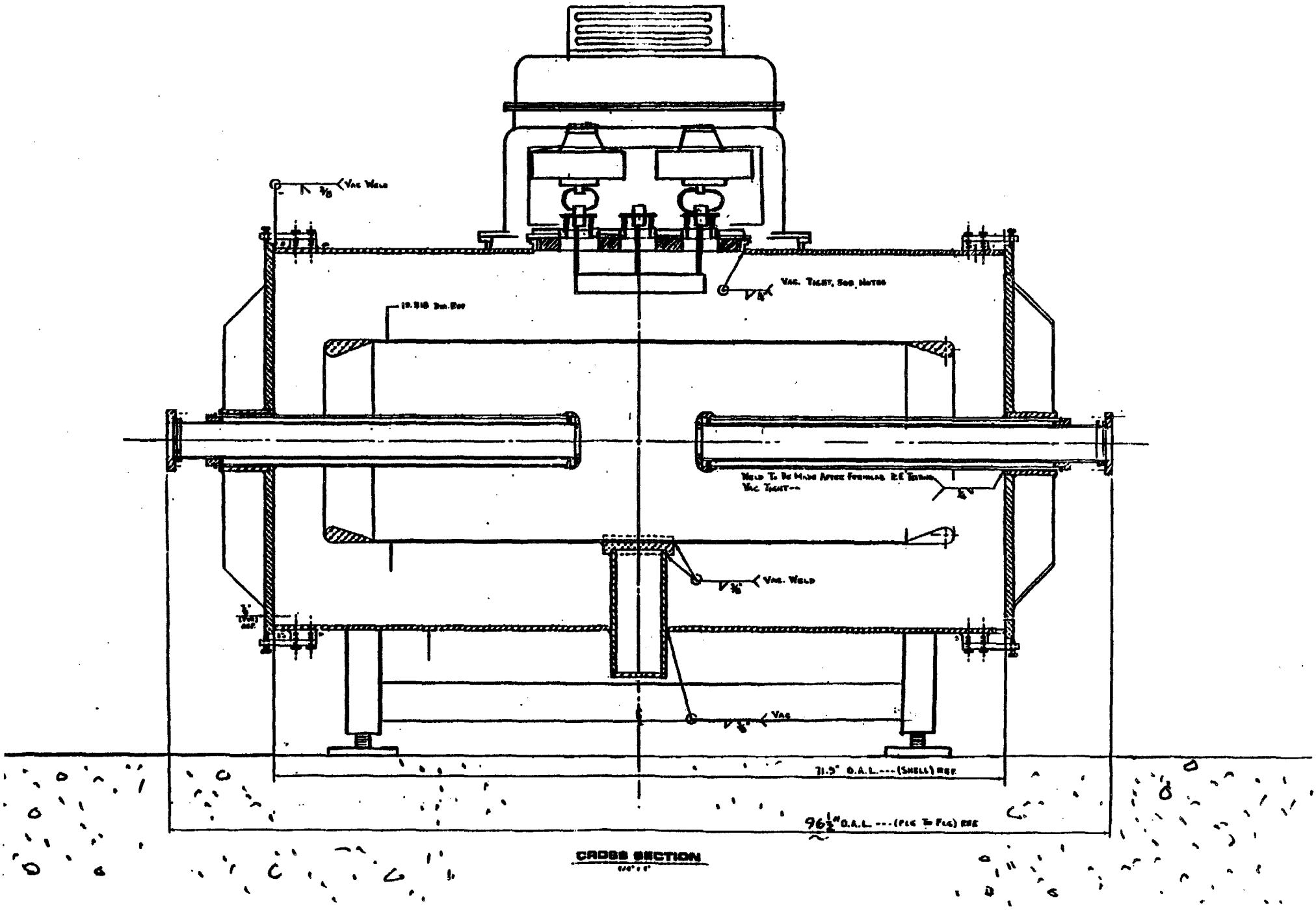
VAC. WELD
VAC. TIGHT, SEE NOTES
VAC. WELD
VAC
71.5" O.A.L. --- (SHELL) REF
CROSS SECTION

Figure 4-16a

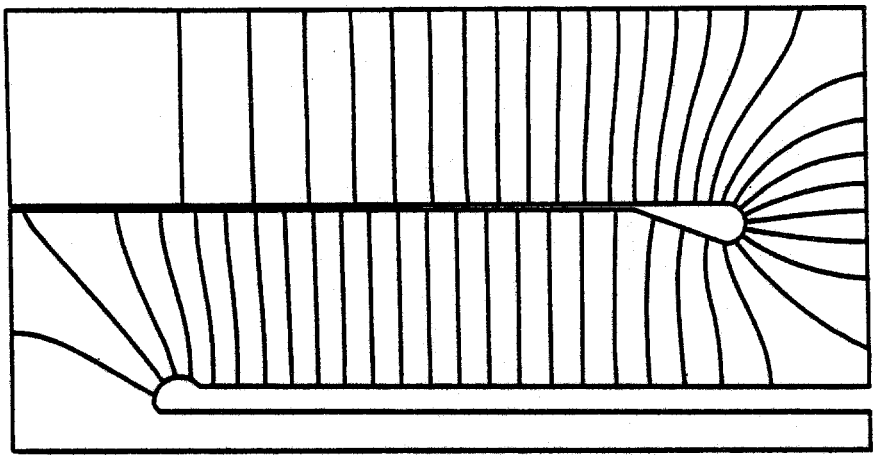

Figure 4-16b Electric field multiplied by radius as calculated by the program SUPERFISH

principally from pion decay, and electrons produced in showers in the target. The electrons lose 30 MeV per turn through synchrotron radiation and spiral out of the vacuum chamber within 20 turns.

The large rf voltage, low beam loading and small duty factor favor an accelerating cavity with a very high Q, hence a high shunt impedance, which requires very little rf drive power. But the short fall time of the rf voltage pulse is not obtained easily with a high-Q structure. Moreover, the physical size of high Q structures operating in the 53-MHz region would require much larger enclosures than are under consideration.

A compromise structure, which contains an intermediate cylinder that reduces both the Q and the physical size, is shown in Fig. 4-16a. Fig. 4-16b shows a SUPERFISH plot of the electric fields within one-quarter of the structure. The entire volume of each cavity will be evacuated, with rf power coupled through two small ceramic windows at the top. The plate through which rf power is introduced serves as a bedplate for the high-power driver amplifiers, which are mounted directly on top of the cavity and are completely enclosed. Thus high-power rf transmission lines are not needed and rf leakage is less likely. This may be important because rf noise could adversely affect stochastic cooling. Each cavity is driven by two relatively small 10-kW triodes operating in a cathode-driven grounded-grid configuration. In this configuration, the tubes are capable of delivering very large peak rf currents during the short pulse. Because the pulse is short and the duty factor is low, the average anode dissipation is only a few hundred watts.

The rf voltage is reduced quickly by reversing the phase of the power-amplifier excitation and raising the excitation amplitude to a very high level. The high peak-power capability of the tubes is used to "drive" the cavities off, even though the cavity time-constant is longer than the required turn-off time of 50 μsec.

The peak rf voltage that each cavity can develop has been calculated to be larger than 650 kV. Eight of these 1.8 m long cavities provide the required 5 MV. They are located in the long straight section immediately following injection from the target. The location of these cavities is shown in Fig. 4-17.

In order to reduce the rf voltage down to 5 kV or less during the adiabatic-debunching part of the rf program, six of the cavities are turned off and two of the cavities are held at 100 kV and their relative phases each changed by 90° in opposite directions. The resultant rf voltage gradually reaches a small value. This is done to avoid instabilities at low rf voltage that might arise from multipactoring.

In order to provide the structural rigidity necessary for complete evacuation and to reduce material costs, the cavities will be constructed from aluminum.

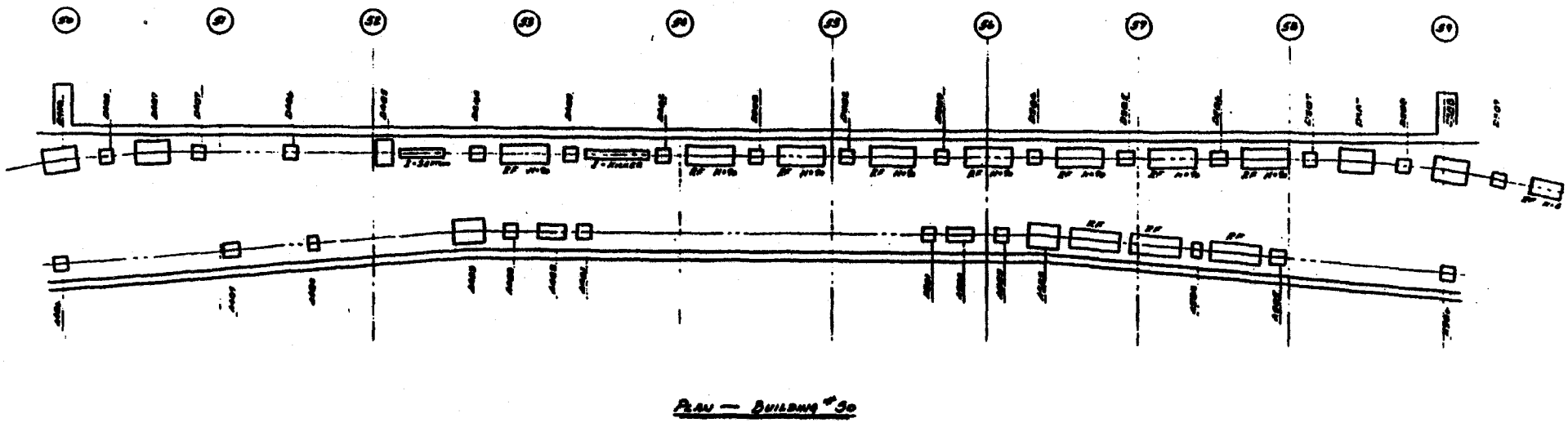

PLAN — BUILDING 30

Injection Straight Section Of The Debuncher

Figure 4-17

4.11 Gap-Preserving RF

Because the Debuncher circumference is larger than that of the Accumulator, antiprotons will be lost in the transfer to the Accumulator unless there is a gap in the Debuncher beam. Given the difference in circumference between the two rings and the need to allow for the fall time of the injection kicker, a gap greater than 200 nsec is needed.

An adequate gap can be created in the beam by a "barrier bucket" that excludes particles from its interior. It is created by a voltage that traces out a single complete sinusoidal oscillation for one-quarter of the rotation period and then becomes zero for the remaining three-quarters of the period. A sketch of this waveform is shown in Fig. 4-18. The voltage waveform repeats itself every turn. The phase of the voltage is chosen so that it establishes an unstable fixed point between two back-to-back half-bucket separatrices. If the bucket height exceeds the beam energy spread, the beam will be forced away from the unstable fixed point by a distance determined by the ratio of the bucket height to the energy spread. The rf voltage is chosen so that the beam is excluded from a region between $\pm\pi/2$ radians in the "barrier bucket". This will create a gap of 221 nsec, as shown in Fig. 4-18. The peak amplitude required is 890 V. The Fourier series expansion of such a voltage waveform is given by

$$V(t) = 890\,\frac{2h}{\pi}\sum_{n=1}^{\infty}\frac{\sin\pi\, n/h}{h^2 - n^2}\,\sin\,(n\omega_o t),$$

where $\omega_o = 2\pi f = 3.59\times10^6$ rad/sec and h=4. At frequencies above the 31st harmonic (17.7 MHz) the required amplitudes are reduced by more than three orders of magnitude. Amplifiers with a bandwidth between 0.1 and 30 MHz which are capable of delivering 300 W in a 50-ohm load are readily available. The required rf system can be broken into 450-V units, each consisting of a ceramic gap loaded with a 50-ohm resistor and surrounded by a shielding enclosure containing about ten large MnZn ferrite rings. The average power delivered to this system is very small. Since the physical size of each unit is dictated by the volume of ferrite required, each unit is 0.5 m in length. Their location is shown in Fig. 4-17.

An additional bonus associated with installation of the "barrier bucket" rf system is that it can be used in the "normal" h=4 mode to accelerate or decelerate 8-GeV protons across the ring aperture in tune-up testing of closed orbits and stochastic-cooling systems.

4.12 Beam Injection and Extraction

4.12.1 Injection from the Target Station. The beam enters the Debuncher in the vertical plane at an angle of 50 mrad to the closed orbit. The injection path is exactly aligned with the central closed orbit of the

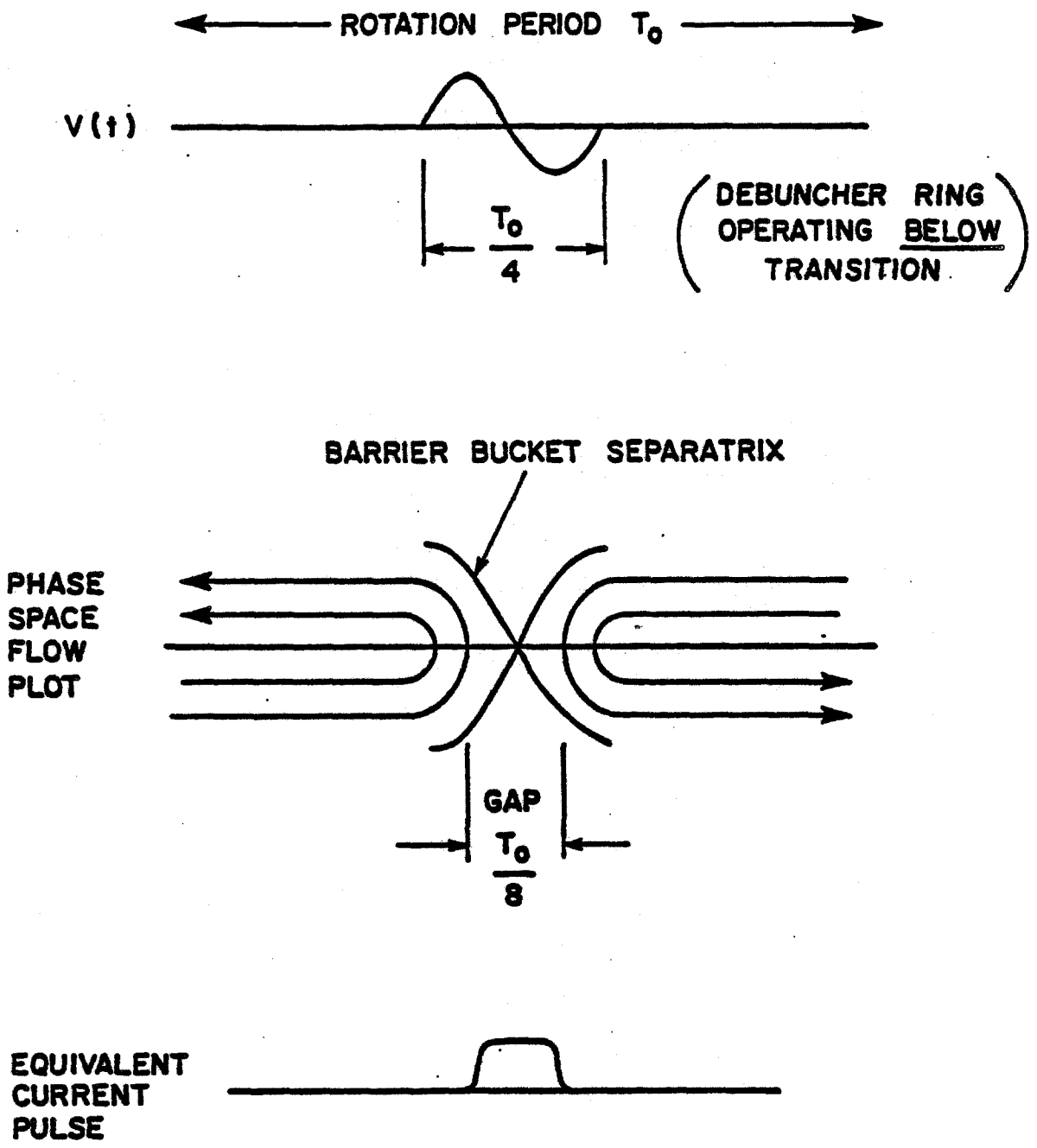

Gap Preserving RF

Figure 4-18

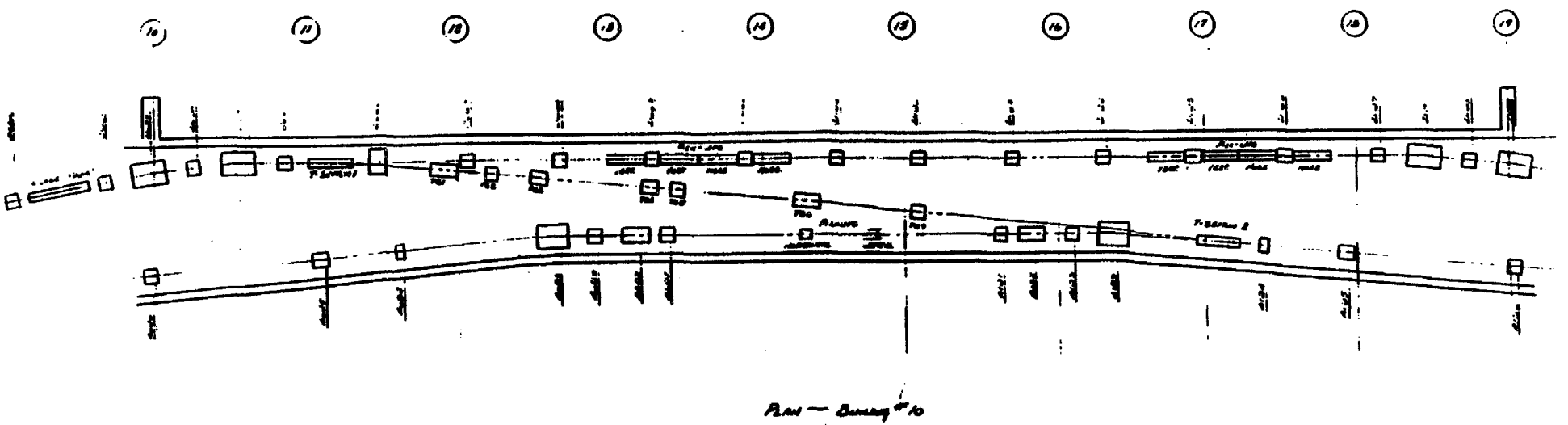

Beam Transfer From Debuncher To Accumulator

Figure 4-19

Debuncher. The beam first enters QF3, which has a large aperture to accommodate both the injected and the circulating beam. The circulating beam goes through the center of the quad, but the injected beam enters the quad with a vertical displacement of 5 in. at the upstream end and an angle of 50 mrad. A septum magnet located after QF3 brings the beam down to a vertical separation of 2 in. and parallel to the ring orbit. A kicker magnet between QF2 and QD1 brings finally the beam onto the reference orbit. The kicker and septum magnets parameters are given in Table 4-VII and are shown in Fig. 4-17. The injection channel has been designed to accommodate a beam with momentum spread of 4% and transverse emittances of 20π mm-mrad.

4.12.2 Debuncher to Accumulator Transfer. The beam transfer between the Debuncher and the Accumulator is a horizontal transfer taking place in the 10 straight section. Extraction from the Debuncher is accomplished with a kicker and a septum magnet, as shown in Fig. 4-19. The quadrupole after the septum magnet, QD3, has a large aperture to accommodate both the circulating and the extracted beam. This quad kicks the beam further to the inside of the ring toward the Accumulator. The horizontal displacement of the extracted beam from the magnet axis is 5 in. After extraction, the beam is transported to the Accumulator with no further bending through a string of 6 quadrupoles. At the Accumulator, the beam is injected onto a path displaced from the central momentum by $\Delta p=+0.93\%$ with an 12-kG 7-ft long pulsed septum placed between A1B3 and A1S3. Finally the beam is kicked onto the proper orbit in the Accumulator with a 500-G, 7-ft long shutter kicker placed in the A20 straight section. The elements are discussed in more detail in Sec. 11.3. A plot of the lattice functions of the transfer line is shown in Fig. 11-5 and the list of elements is given in Table 11-IV.

4.12.3 Injection from the Booster. Injection into the Debuncher from the Booster is exactly the same as injection from the Target Hall. The beam is transported to the upstream end of the 30 straight section and injected downward into the Debuncher at an angle of 50 mrad, again passing through a large-aperture quadrupole D2Q5 and then into a septum magnet. Finally a kicker located between D2Q3 and D2Q2 puts the beam onto the reference orbit.

4.13 Betatron Cooling

4.13.1 Design Goal. The goal of the stochastic cooling in the Debuncher is to cool the beam emittance from 20π mm-mrad to 7π mm-mrad in both the horizontal and vertical planes. An emittance of 7π mm-mrad is the assumed beam size that can be reliably transferred into the 10π mm-mrad acceptance Accumulator ring with negligible beam loss. In addition to cooling the beam to fit into the Accumulator, it is desirable to make the beam injected into the Accumulator as small as possible. In the Accumulator the momentum stacking is done in part by a pickup that senses a particle's momentum by observing its position in a region of high dispersion. Betatron oscillations add undesired noise to this process.

4.13.2 Design Considerations. The betatron-cooling system is conceptually simple. It consists of a pickup that senses the positions in a zero-dispersion region and therefore measures only the betatron amplitudes of the particles. The signal is amplified and applied to a kicker an odd multiple of 90° away in betatron phase. At the kicker, the position displacement that was sensed has been converted into an angular displacement. This angular displacement is decreased by a correcting kick, which thus decreases the betatron amplitude. As is well known, the cooling of a single particle is hampered by the presence of the other particles, that create a noise signal (Schottky noise) that heats the particle. For a properly designed system, the net effect over many turns is that cooling is achieved.

The process of betatron cooling is conventionally described by the equation

$$\frac{d\varepsilon}{dt} = -\frac{W}{N}(2g-g^2(M+U))\varepsilon, \qquad (4.1)$$

where ε is the betatron amplitude, W the amplifier bandwidth, N the number of particles, g the system gain, M the mixing factor and U the ratio of noise to signal power. The mixing factor M is given by

$$M = \frac{f^2\psi(f)\Lambda}{2WN}, \qquad (4.2)$$

where $\psi(f)$ is the density of particles (number per Hz), f is the revolution frequency, and Λ is a constant of order unity ($\Lambda=\ln 2$ if the gain is independent of frequency).

Stochastic cooling during the 2-sec Debuncher cycle is difficult because the mixing factor M is large compared to 1. M is inversely proportional to the dispersion $\eta\alpha$, where

$$\frac{\Delta f}{f} = \eta\frac{\Delta p}{p}, \qquad (4.3)$$

The choice of the value of η was a compromise between the rf requirement for the bunch rotation (which favors a small η) and stochastic cooling (which favors a large η). The choice of $\eta = +0.006$ leads to a mixing factor M of about 10 for the particles near the central momentum of the Debuncher, assuming a parabolic momentum distribution with a full width of $\Delta p/p=0.3\%$.

Another problem is that the noise-to-signal ratio U tends to be large. The techniques to make U small are: 1) increase the beam signal as much as possible by using a large number of high-impedance pickups and 2) decrease the noise temperature by cooling the pickup terminating resistors and the preamplifiers.

The criterion for the thermal noise to be negligible is U<<M. With the parameters of Table 4-VII below,

$$U = \frac{2K\,(\theta_R+\theta_A)h^2}{d^2 Z_o e^2 f_o n_p N \beta_p \bar{\varepsilon}} \qquad (4.4)$$

$$= 1.8 \text{ (initially)} \ ,$$

where $K=1.38\times10^{-23}$ Joules/°K, $f_o=1/T$=revolution frequency, $\bar{\varepsilon}$=average beam size=8π mm-mrad initially. But, as the beam is cooled to $\bar{\varepsilon}=0.8\pi$ mm-mrad, U will grow to 18, twice the value of M, the mixing factor. Thus cooling will initially proceed not limited by thermal noise, but as the beam cools, the effect of the Schottky and thermal noise become comparable (note that the cooling equation (4.1) is written in a deceptive form because it does not explicitly show the dependence of U on $\bar{\varepsilon}$).

A practical problem that occurs in fast stochastic cooling is that the power requirements are often very high. In the Debuncher, the best cooling rate is obtained for a power level of 1800W. But, as can be seen from Eq. (4.1), the gain can be decreased by a factor of 2 and the cooling rate will be only $2g-g^2=3/4$ of the optimum rate. In the absence of suppression, the power will decrease by a factor of 4. In the case that signal suppression is important, the decrease in power can be even greater, because the system gain g increases more slowly than linearly with the amplifier gain. In a system with bad mixing like the Debuncher, most of the thermal power is between Schottky bands and is largely unaffected by signal suppression. In this case, the thermal power is therefore more nearly proportional to amplifier gain squared than to system gain squared (g^2).

4.13.3 Hardware. For each of the two betatron-cooling systems, 4 sets of 32 pickup pairs are installed in straight section D10, and a similar set of kickers are installed in straight section D30. Both straight sections have zero dispersion. The pickup arrays are spaced out between the quadrupoles in a manner such that 2 sets are roughtly 180° out of phase with the other two. These signals are therefore combined with inverted phase. The signal is then amplified and sent to the kicker region which is 3 1/4 betatron oscillations away. The pickup termination resistors are cooled to 77°K, as are the preamplifiers. A block diagram of the betatron cooling system is shown in Fig. 4-20. In brief, the pickup signal from 32 upper plate pickups is combined with 32 lower plate signals to provide a difference

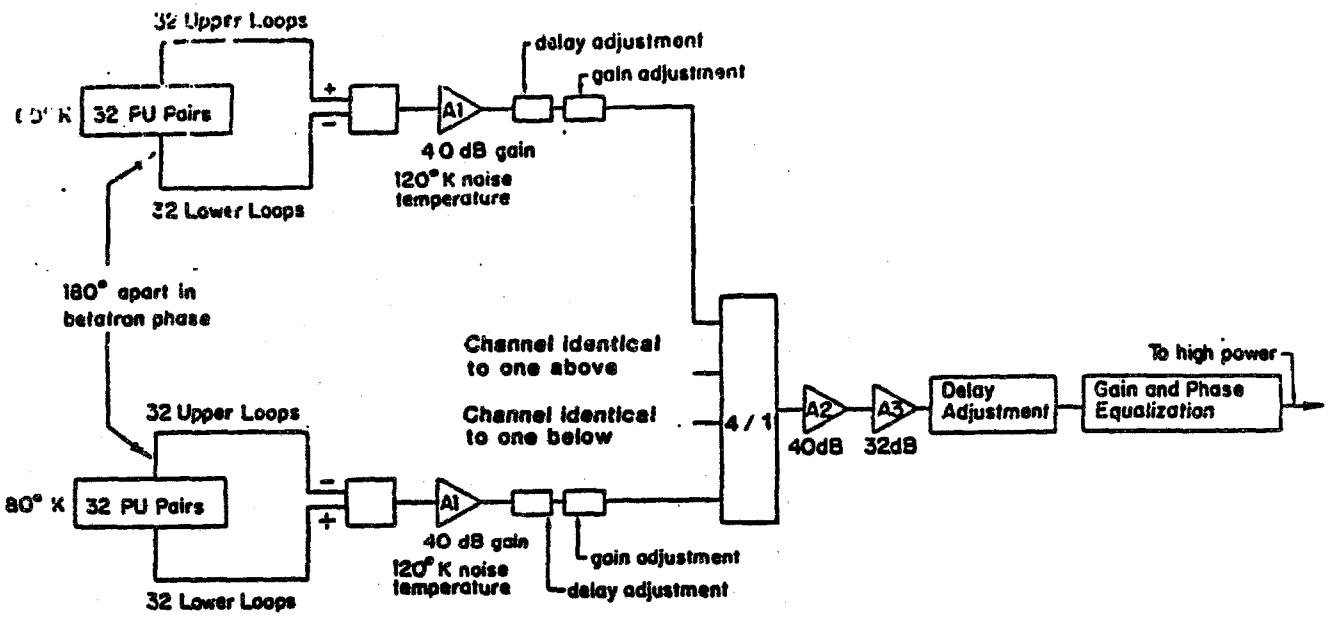

Debuncher Betatron Cooling Systems

2-4 GHz Horizontal and Vertical Systems are identical.

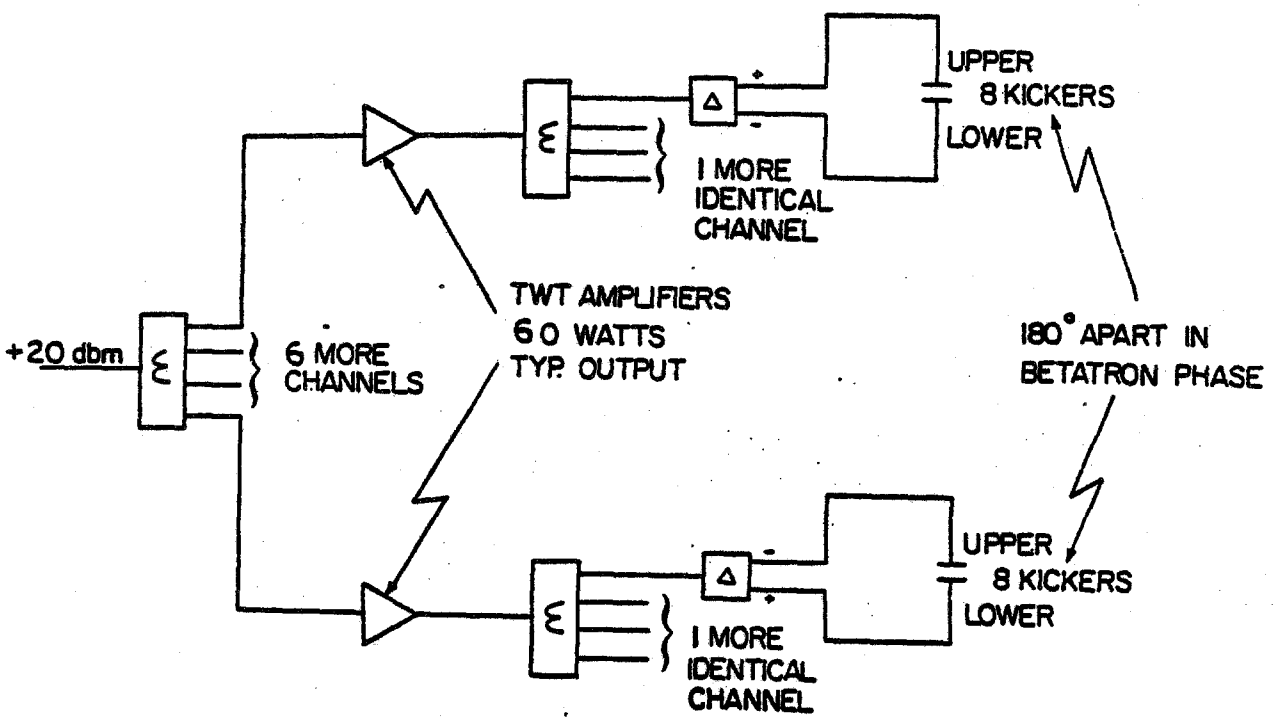

Figure 4-20

signal proportional to the position displacement of the beam. The signals from each set of 32 pickups amplified 40 dB are combined in an 4-fold combiner. Each combiner input has an adjustment for amplitude and delay. After combination the signal is further amplified by 72 dB to a level of about 25 dBm. An overall delay adjustment is followed by a gain and phase compensating circuit, to partially cancel the variations in the TWT (traveling wave tube) gain characteristics. The power is then split to drive two sets of TWT's, each of which drives an array of 16 kickers.

Table 4-VII lists some of the parameters of the betatron cooling systems. The characteristics of the hardware components are similar to those in the Accumulator, these characteristics are discussed in more detail in Section 5.4. The overall layout of the stochastic cooling system in one straight section was shown in Fig. 4-7.

4.13.4 Computer Simulation[5]. A simulation of the betatron cooling in the Debuncher was made to calculate the expected system performance. Included in the simulation were the pickup and kicker response functions, transit-time differences of the electrical signal and particles between pickup and kicker, and signal suppression. The amplifier was modeled as a physically unrealizable ideal amplifier having a gain g_A from 2 to 4 GHz and zero elsewhere. It was assumed that g_A was purely real. While the amplifier model was not realistic, measurements of the TWT tube amplifiers in the 1-2 GHz range show that, when externally phase compensated, these tubes can provide gain and phase characteristics that lead to cooling rates equal to or better than the 1-2 GHz "ideal" amplifier model used above. The initial $\bar{p}$ distribution was taken from Fig. 3-4. It was assumed that the Debuncher had an acceptance of 25π mm-mrad but that the transport line had already limited the beam size to 20π mm-mrad. The total output power was limited to 500W. The gain was continually adjusted to provide the best cooling within the 500W limit.

Figure 4-21 shows the initial and final beam distributions for particles at the central momentum. Ninety-nine per cent of the particles fall within an emittance of 7π -mm-mrad. Also shown is the final curve for particles with a momentum offset of 0.075%, or halfway to the edge of the distribution. The cooling of these particles is somewhat better since they have a somewhat lower density, i.e., less Schottky noise. Since the noise figure assumed is somewhat speculative, Fig. 4-22 compares the final spectrum for design case $\theta_A+\theta_R=200°K$. If the noise figures were worse because of the pickup sensitivity being less than supposed, the kickers would presumably be less sensitive in the same ratio. In this case, the total dissipated power would be larger than the design case of 500W. Figure 4-23 is a comparison of the final distribution for different power levels assuming the design case noise figure ($\theta_A+\theta_R=200°K$). As Rreviously stated, there is little advantage in running at power levels corresponding to the optimum gain.

As designed, the stochastic cooling system for the Debuncher will cool the beam emittance by about an order of magnitude. If the system fails to

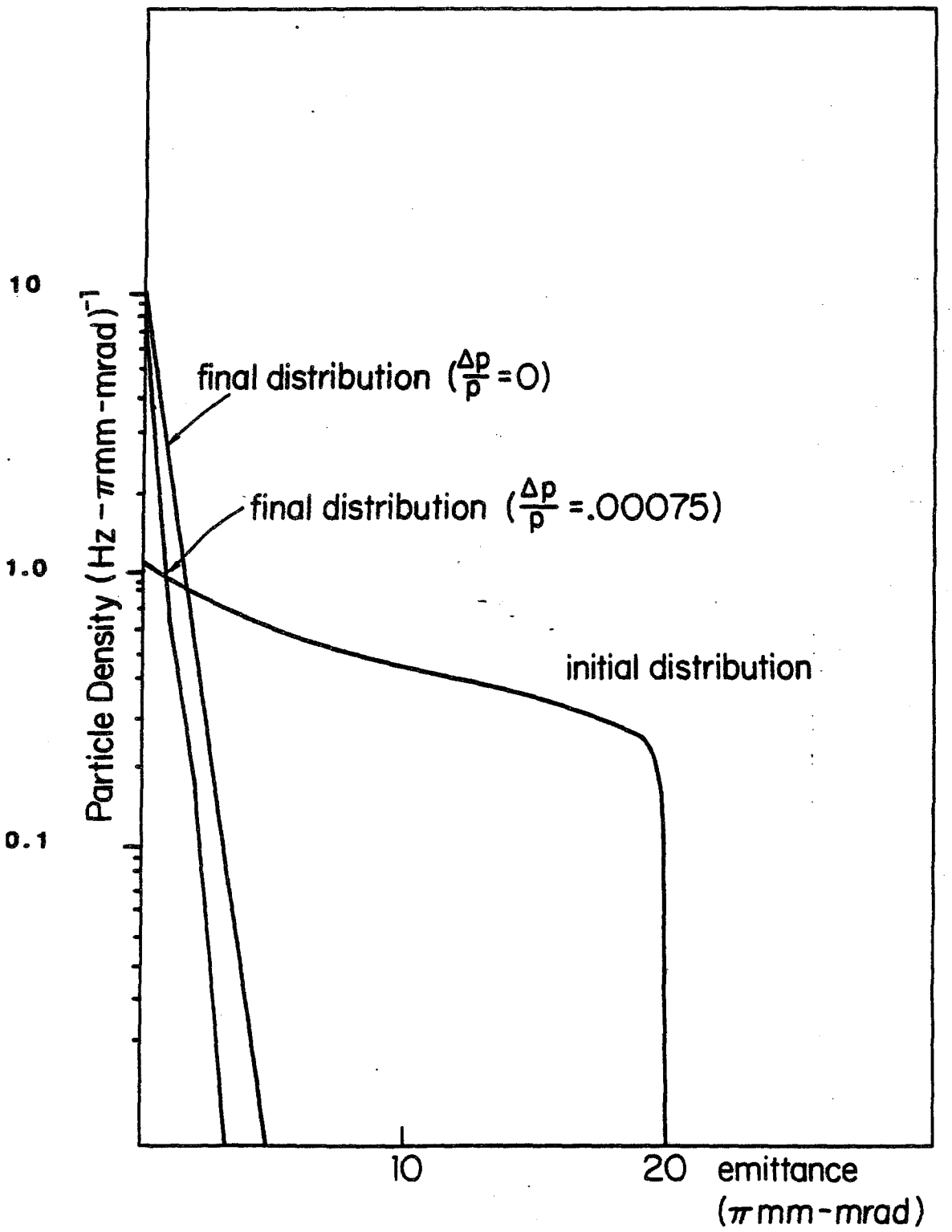
10
1.0
0.1
Particle Density (Hz - πmm-mrad)⁻¹
final distribution (Δp/p = 0)
final distribution (Δp/p = .00075)
initial distribution
10
20
emittance
(π mm-mrad)

Figure 4-21

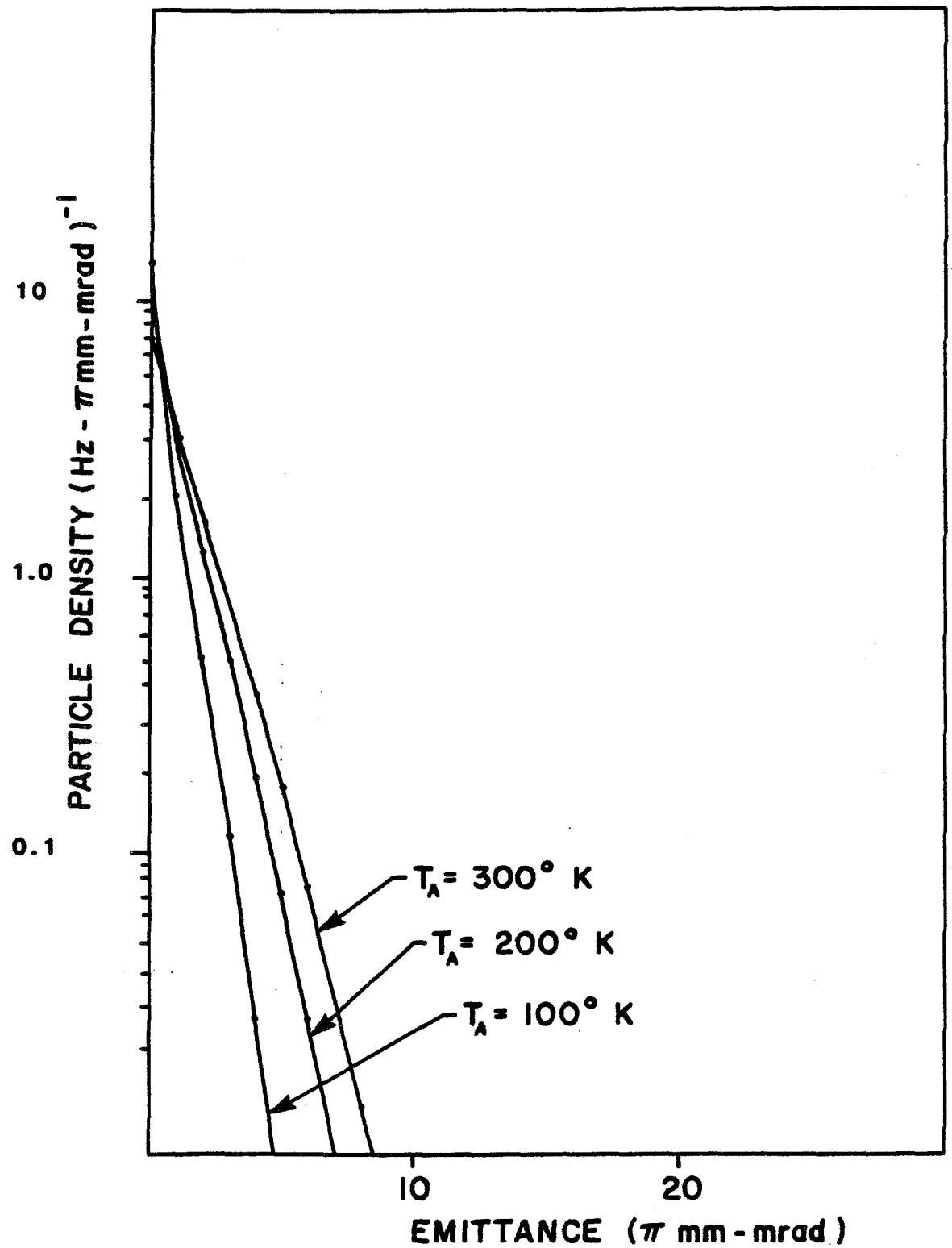
PARTICLE DENSITY (Hz - π mm - mrad)⁻¹
10
1.0
0.1
T_A = 300° K
T_A = 200° K
T_A = 100° K
10
20
EMITTANCE (π mm - mrad)

Figure 4-22

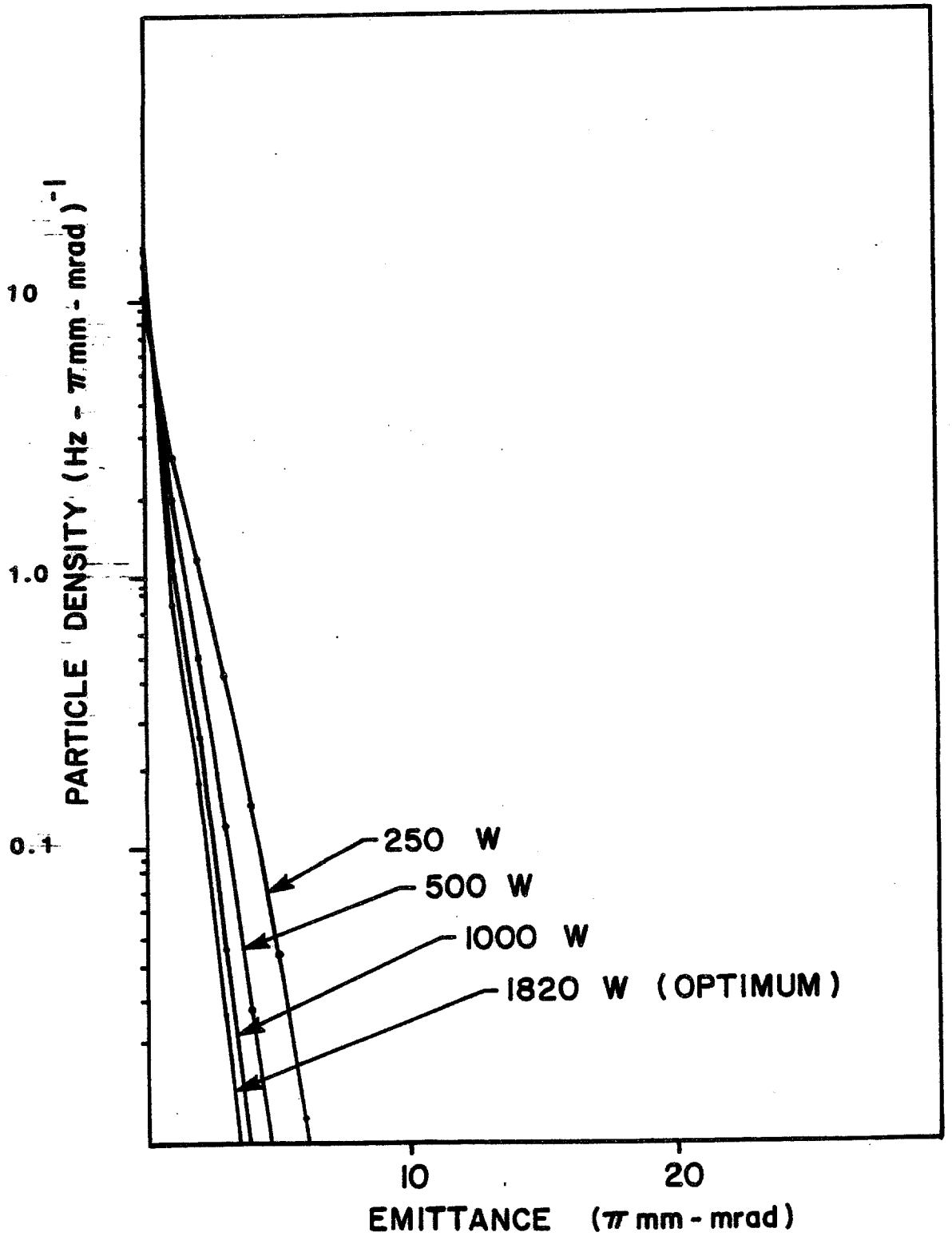
PARTICLE DENSITY (Hz - π mm - mrad)⁻¹
10
1.0
0.1
250 W
500 W
1000 W
1820 W (OPTIMUM)
10
20
EMITTANCE (π mm - mrad)

Figure 4-23

perform as designed, there is a substantial margin of safety in getting the beam to 7π mm-mrad for transfer into the accumulator.

TABLE 4-VII BETATRON-COOLING SYSTEM PARAMETERS (EACH SYSTEM)

Frequency band	2-4 GHz
Number of pickup pairs (loops)	128
Pickup Characteristic Impedance (odd mode)	83Ω
Pickup Sensitivity d(0,0)	1.59
Pickup resistor noise temperature (θ_R)	80K
Amplifier equivalent noise temperature (θ_A)	40K
Amplifier gain (net) (variable)	138 dB (variable)
Output Power	
-Schottky	100 W (typical)
-Thermal	400 W (typical)
-Total	500 W
Number of TWT's	8
Number of kicker pairs (loops)	128
Kicker characteristic impedance	83Ω
Kicker sensitivity d(0,0)	1.59
Spare time delay with foam heliax (β=0.89)	45 ns

CHAPTER 5

ACCUMULATOR RING

5.1 Accumulator - Functional Summary

The first function of the Accumulator is to accept a pulse of $\bar{p}$'s every 2 seconds. In order to make room for this pulse, the $\bar{p}$'s must be compressed (cooled) into a smaller area of phase space. A technique to accomplish the continuous $\bar{p}$ accumulation and compression has been developed at CERN and is the basis of this design. The technique consists of establishing a stack of $\bar{p}$'s with an energy density that rises approximately exponentially from the injection density (the low-density end is referred to as the "stack tail") and then culminates in a roughly Gaussian high-density region (the "core"). Betatron amplitudes are also cooled during the stacking process. The design criteria for the accumulation process are given in Table 5-1, and the parameters of the Accumulator are given in Table 5-II.

TABLE 5-I ANTIPROTON STACK PARAMETERS

Injected Pulse	
Number of $\bar{p}$'s	8×10^7
$\Delta p/p$	0.2%
Horizontal and vertical emittance	$<10\pi$ mm-mrad
Time between injections	2 sec
Fraction of beam accepted	>85% of injected pulse
Flux	4×10^7 $\bar{p}$/sec
Final Stack	
Number of $\bar{p}$'s	5×10^{11}
$\Delta p/p$	0.05%
Horizontal and vertical emittance	2π mm-mrad
Peak density	1×10^5 eV^{-1}
Core width (Gaussian part)	1.7 MeV (rms)
Total stacking time	5 hours

TABLE 5-II ACCUMULATOR RING PARAMETERS

Kinetic energy	7.9 GeV
γ_t, transition energy	5.43
$\eta = 1/\gamma_t^2 - 1/\gamma^2$	0.023
Average radius	75.45 m
RF frequency	52.812 MHz

Maximum rf voltage	120 kV
Harmonic number	84
Beam gap for injection kicker	115 nsec
Momentum aperture, $\Delta p/p$	2.5%
Betatron acceptance, h and v	10π mm-mrad
Betatron tunes, ν_H	6.611
ν_V	8.611
Natural chromaticities ζ_H	-8.48
ζ_V	-12.88
Periodicity	3, each with mirror symmetry
Maximum amplitude function, β	33 m
Maximum dispersion value, α_p	8.9 m

5.2 Design Requirements

The lattice of the Accumulator has been designed to accept the injection of antiprotons every few seconds at an energy of 8 GeV, momentum stack and stochastically cool the antiprotons, accumulate over a period of several hours a very dense core of antiprotons, and, finally extract a high-intensity beam to re-inject into the Main Ring and Tevatron. The requirements on the lattice are twofold. The Accumulator must be a high-class storage ring capable of reliable operation, and it must accommodate all the conditions imposed by the stochastic-cooling systems. The second set of requirements has led to the design of this ring and its somewhat unusual appearance, while those of the first set have also been incorporated. These conditions are:

(i) The momentum mixing factor must be correct.

$$|1/\gamma_t^2 - 1/\gamma^2| = 0.023$$

where γ_t is the transition gamma of the ring and γ is the relativistic factor of the particle. Thus for 8-GeV kinetic energy the ring must have

$$\gamma_t = 5.41$$

ii) There must be several long straight sections, some 16 m long, with very small transverse beam sizes. Some of these must have zero dispersion, and the rest dispersion of approximately 9 m. This requirement leads to the choice of transition gamma below rather than above the γ of the particles.

(iii) Betatron-cooling straight sections must be an odd multiple of $\pi/2$ apart in betatron phase. Pickup and kicker straight sections must be far enough apart physically so that a chord will be at least 75 nsec shorter than the arc for signal-transfer purpose.

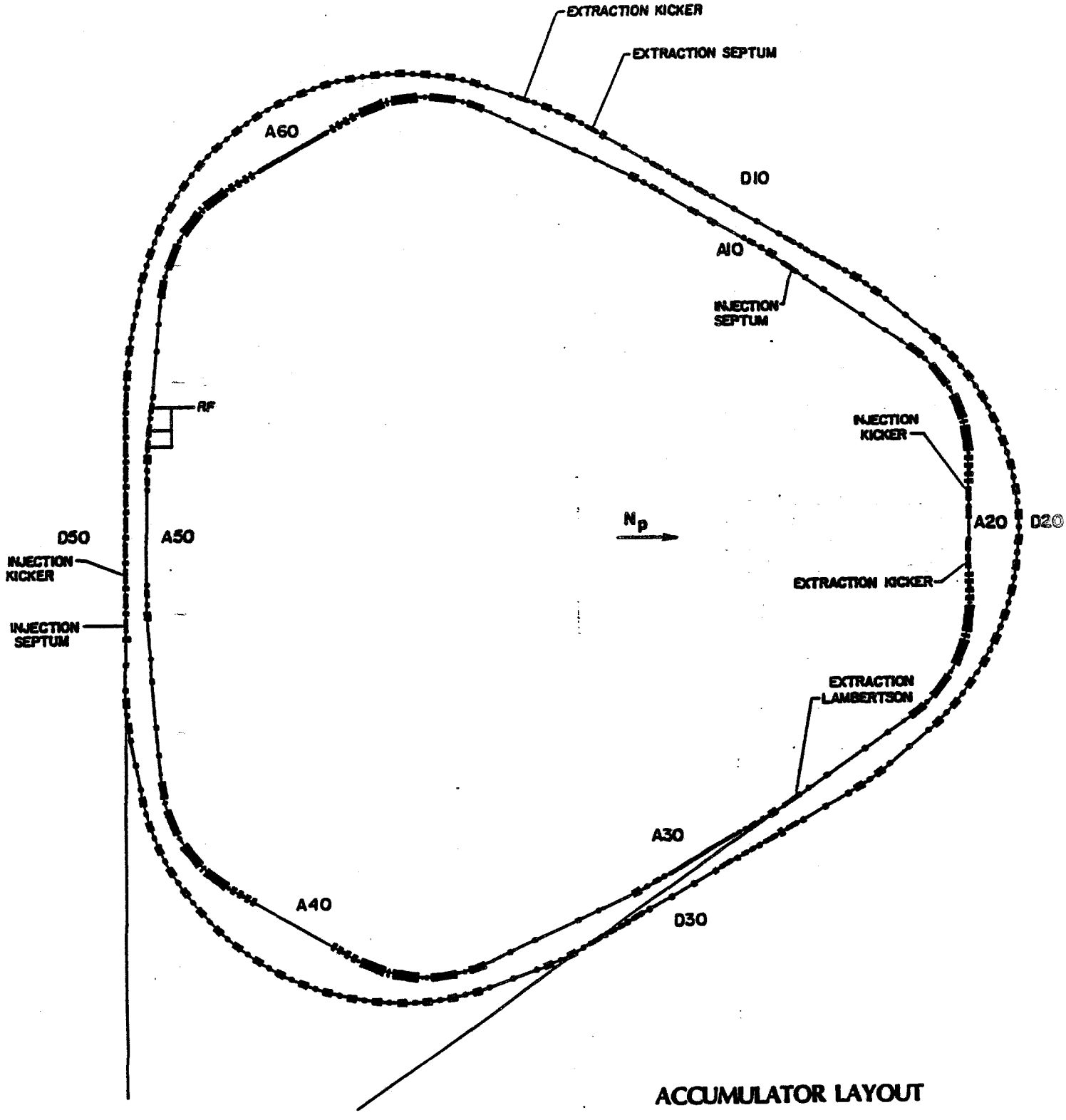
EXTRACTION KICKER
EXTRACTION SEPTUM
A60
D10
A10
INJECTION SEPTUM
RF
INJECTION KICKER
A20
D20
N_p
D50
A50
INJECTION KICKER
EXTRACTION KICKER
INJECTION SEPTUM
EXTRACTION LAMBERTSON
A30
A40
D30
ACCUMULATOR LAYOUT

Figure 5-1

(iv) The β values of the lattice should be about the same for the horizontal and vertical planes in the straight sections.

(v) The ring should match the Booster circumference.

(vi) There should be easy injection and extraction schemes.

(vii) The beam everywhere should be as small as possible, consistent with the large-dispersion straight sections.

(viii) The ring must have very good chromaticity corrections, be situated far from any resonances, have tuning flexibility, and generally be a good storage ring.

5.3 Accumulator Lattice

The lattice chosen is a six-sided ring with six 16-m long straight sections placed between optical triplets. The dispersions of the straight sections alternate between zero and 9 meters. The lattice has mirror symmetry about the straight sections and periodicity three. The middle quadrupole of the triplets near the high dispersion straight sections has been split in order to allow space for orthogonal chromaticity correction and to reduce the required sextupole fields. A plan view of the ring is shown in Fig. 5-1. The triangular shape was chosen as the most efficient in terms of the stochastic-cooling requirements. A ring with four straight sections and periodicity two will not allow a signal to be propagated from a high-dispersion to a zero-dispersion region fast enough relative to the beam. Lattices with eight and ten straight sections were considered, but had several drawbacks, including the fact that they severely limited the amount of non-straight section free space in which to put trim and correction elements.

Table 5-III lists the lattice structure and parameters for the Accumulator. The lattice functions for one sixth of the ring are plotted in Fig. 5-2.

TABLE 5-III DETAILED ACCUMULATOR PARAMETERS

1. General

Kinetic Energy (central orbit)	7.94779 GeV
Bend field	16.84 kG
Magnetic bend radius (ρ)	17.46 m
Circumference	474.07 m
Revolution time	1.59 μsec
Superperiodicity	3
Focusing structure	Separated function FODO normal cell
Nominal working point	

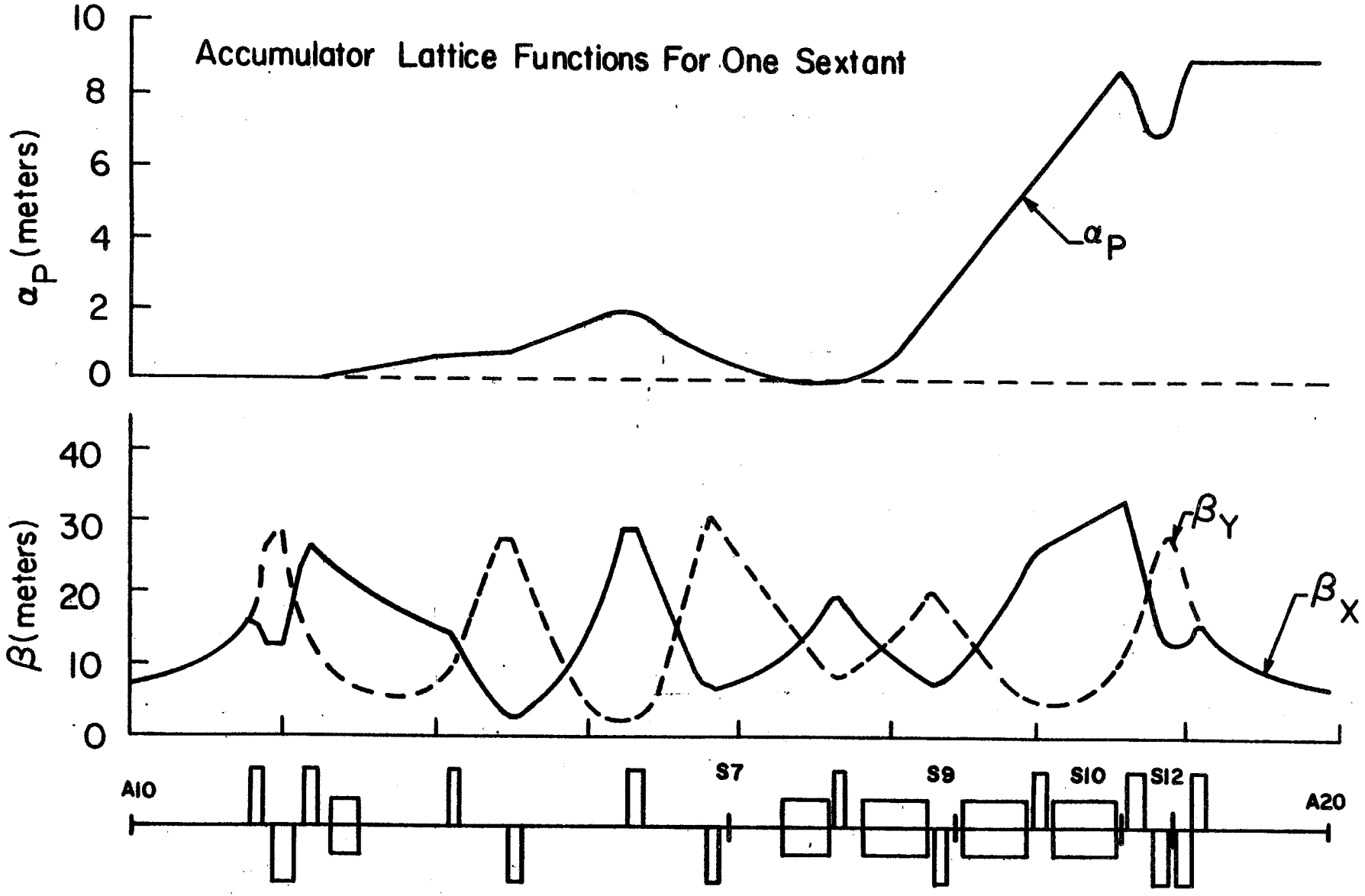
Accumulator Lattice Functions For One Sextant
10
8
6
4
2
0
α_P (meters)
α_P
40
30
20
10
0
β(meters)
β_Y
β_X
A10
S7
S9
S10
S12
A20

Figure 5-2

ν_x	6.61
ν_y	8.61

Nominal chromaticity

ξ_x	-8.52
ξ_y	-12.93

Chromaticity-Corrected Parameters

	Injection Orbit	Stacking Orbit	Core Orbit	Central Orbit
Kinetic Energy (GeV)	8.02951	7.96229	7.89068	7.94779
$\Delta p/p$ (%)	+0.930	+0.165	-0.690	
ν_x	6.616	6.611	6.614	
ν_y	8.611	8.611	8.611	
ξ_x	2.05	1.13	-0.22	
ξ_y	0.21	0.32	0.33	
γ_t	5.37	5.42	5.50	
$1/\gamma_t^2 - 1/\gamma^2$	0.023	0.023	0.022	

2. Magnets

Number of dipoles 30
Number of quadrupoles 84
Number of sextupoles 24

A. Small-aperture dipoles

	Length	Field	Number
(B3)	5.0 ft.	16.84 kG	6
(B7)	10.0 ft.	16.84 kG	6
(B8)	15.0 ft	16.84 kG	6

B. Large-aperture dipoles

(B9)	15.0 ft.	16.84 kG	6
(B10)	15.0 ft.	16.84 kG	6

C. Small-aperture quadrupoles

(Q1)	25.2 in	103.81 kG/m	6
(Q2)	51.6 in	-103.81 kG/m	6

(Q3)	27.6 in	103.81 kG/m	6
(Q4)	18.0 in	96.63 kG/m	6
(Q5)	32.6 in	-97.41 kG/m	6
(Q6)	27.6 in	96.63 kG/m	6
(Q7)	27.6 in	-97.41 kG/m	6
(Q8)	18.0 in	96.63 kG/m	6
(Q9)	18.0 in	-97.41 kG/m	6

D. Large-aperture quadrupole

(Q10)	18.0 in	40.88 kG/m*	6
(Q11)	34.4 in	89.40	6
(Q12)	30.4	-89.40	6
(Q13)	30.4 in.	-89.40	6
(Q14)	25.3 in.	89.40	6

*Q10 will be built with missing turns to run in series with the other large aperture quadrupoles.

E. Sextupoles

(S7)	8.0 in.	53.58 kG/m^2
(S9)	8.0 in.	-329.28
(S10)	10.0 in.	162.16
(S12)	10.0 in.	-205.01

F. Octupoles

(O10)	10.0 in.	-390.33 kG/m^3
(O12)	10.0 in.	325.12 kG/m^3

3. Structure

A. Drift Lengths

LS	7.9465 m
LS*	7.8449
01	0.5124
02	0.9606
03	0.9042
0B3	6.4237
04	3.2610
05	7.3478
06	4.1872
07	0.3556
0S7	3.8866
0B7	0.5080
08	1.2192
0B8	0.5080
09	0.3556
0S9	0.6604

0B9	0.5080
010	0.5080
0B10	0.3173
0S10	0.3173
011	0.5210
012	0.2432
0S12	0.2432
013	0.4972

B. Sextant Structure (S)

LS (Q1)	01 (Q2)	02 (Q3)	03 (B3)	
0B3 (Q4)	04 (Q5)	05 (Q6)	06 (Q7)	
07 (S7)	0S7 (B7)	0B7 (Q8)	08 (B8)	
0B8 (Q9)	09 (S9)	09 (B9)	0B9 (Q10)	
010 (B10)	0B10	(S10)	0S10 (Q11)	011 (Q12)
012 (S12)	0S12	(Q13)	013 (Q14)	LS*

C. Ring Structure

$\bar{S}(\bar{S})\bar{S}(\bar{S})\bar{S}(\bar{S})$

Length of central orbit 474.0702 m
1555.348 ft

4. Aperture and Acceptance

Maximum Lattice functions (central orbit)

	β_x	β_y	α_p
Center of LS1	7.565 m	7.268 m	0.000 m
End of LS1	15.912	15.956	0.000
Center of LS2	7.577	7.520	8.946
End of LS2	15.699	15.704	8.946

Required beam
Emittance $\varepsilon_x = \varepsilon_y < 10\pi$ mm-mrad
Momentum aperture $\Delta p/p = \pm 1.25\%$

Beam Size	A_x	A_y
Small-aperture dipole	52.4 mm	29.2 mm
Large-aperture dipole	219.6	17.3
Small-aperture quadrupole	68.3	36.9
Large-aperture quadrupole	246.3	33.1
Small-aperture sextupole	54.9	34.1
Large-aperture sextupole	245.4	33.2

Injection into and extraction from this ring are done in a similar manner. The injection orbit is displaced radially outward by approximately 0.9% in $\Delta p/p$. The shuttered kicker in the high-dispersion straight section is closed just before the $\bar{p}$'s are injected. The momentum displacement is enough to allow the injected beam to clear the shutter. Beam is transferred from the Debuncher ring via two 2 m long, 6-kG current septum magnets located near the upstream end of a zero-dispersion straight section. It arrives at the kicker and is kicked onto the injection orbit. The kicker is 2 m long and has a field of 500 G. The shutter is then opened and the beam is rf stacked. A drawing of the injected, stacked and accumulated beams at the position of the shuttered kicker is shown in Fig. 5-3. The injection and extraction positions are shown on Fig. 5-4.

The beam envelope for one half of a superperiod is shown in Fig. 5-5. Four orbits have been superposed, corresponding to the rf-displaced injection orbit, the stacking orbit, the accumulated antiprotons, and the very dense core.

5.4 Tuning

The Accelerator ring is designed to have a nominal tune of 6.61 horizontally and 8.61 vertically for the central orbit. This puts the working point in a region clear of all resonances up to 15th order. It is easily tunable over a large range using the four existing quadrupole buses - QF, QD in the "regular" part of the lattice and QT, QL, the triplet buses for the zero and high dispersion straight sections, respectively. the tuning properties of the Accumulator are totally linear over a large range of values. While the beta and dispersion values vary as a function of tune in the straight sections, the variation is very small and causes no problems up unitil the structural stop band $\nu_y = 9.0$. A list of the tuning parameters is given in Table 5-III and is plotted in Fig. 5-6. The natural chromaticity vs. tune is shown in Fig. 5-7 and the zero-dispersion straight section lattice functions vs. tune are plotted in Fig. 5-8.

5.5 Chromaticity Corrections

The Accumulator has a momentum aperture of about 2%, 1% for stochastic accumulation and 1% for rf stacking. The largest part of the beam stays near the edge of the aperture for several hours. It must be noted that the equilbrium orbit for an off-momentum beam is changed so drastically in the curved section that the octupole tune shift coming from edge effects of the quadrupole magnets becomes very signficiant in the vertical plane. In principle, we can reduce this octupole tune shift by a suitable configuration of sextupoles, which gives large second-order sextupole fields. We avoid such a configuration for the stability of betatron oscillations. We take care to minimize the distortion of transverse emittance coming from nonlinear kicks in sextupoles, because the geometry of the pickups and kickers is very tight. We use four families of sextupoles and two families of octupoles, where each two families of sextupoles and octupoles correct the chromaticity and the additional two

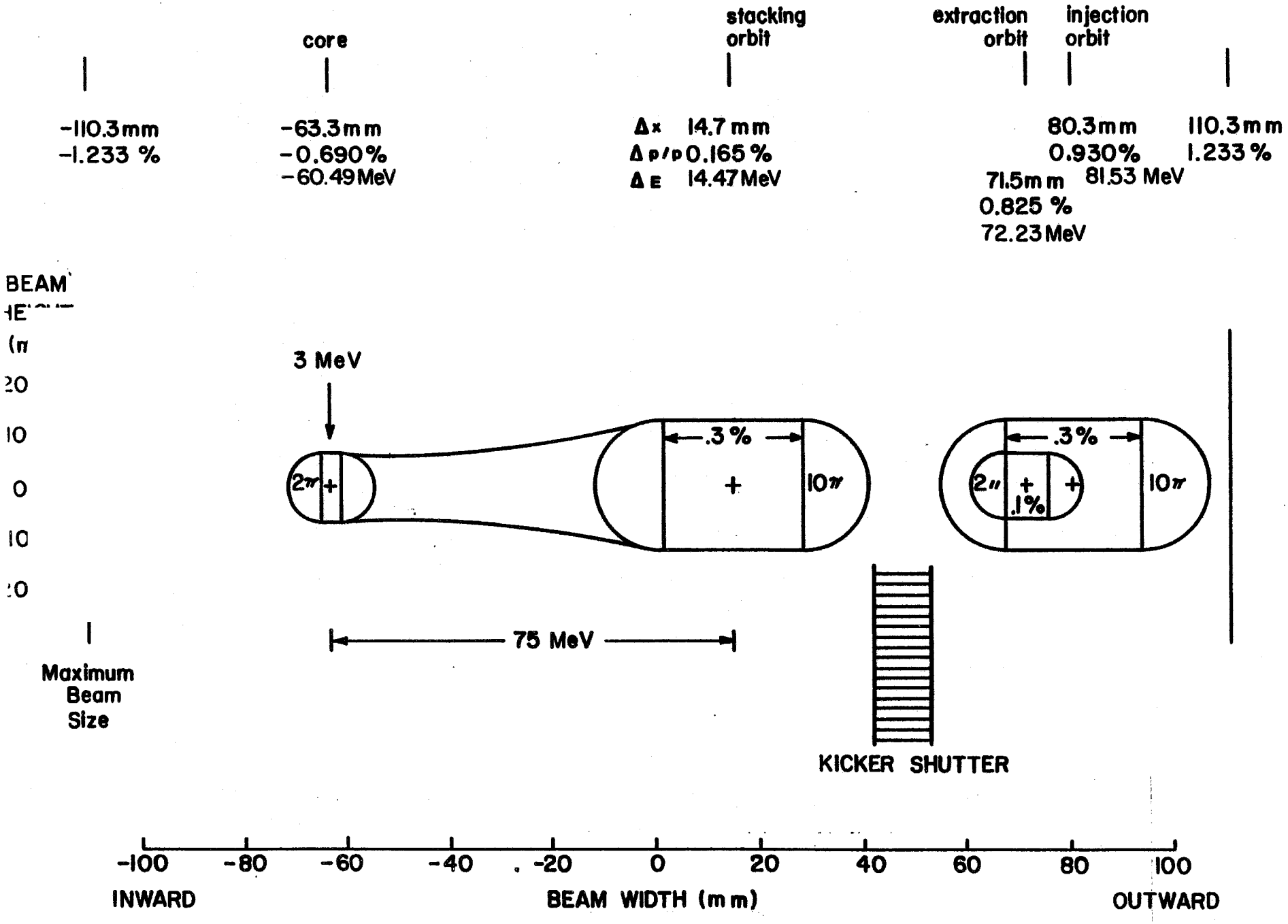
ACCUMULATOR BEAM AT END OF HIGH DISPERSION STRAIGHT (at kicker)
core
stacking orbit
extraction orbit
injection orbit
-110.3mm
-1.233 %
-63.3mm
-0.690%
-60.49MeV
Δx 14.7mm
Δp/p 0.165%
ΔE 14.47MeV
80.3mm
0.930%
110.3mm
1.233%
71.5mm
0.825 %
72.23MeV
81.53 MeV
BEAM
3 MeV
.3%
2π
10π
.1%
75 MeV
Maximum Beam Size
KICKER SHUTTER
-100
-80
-60
-40
-20
0
20
40
60
80
100
INWARD
BEAM WIDTH (mm)
OUTWARD

Figure 5-3

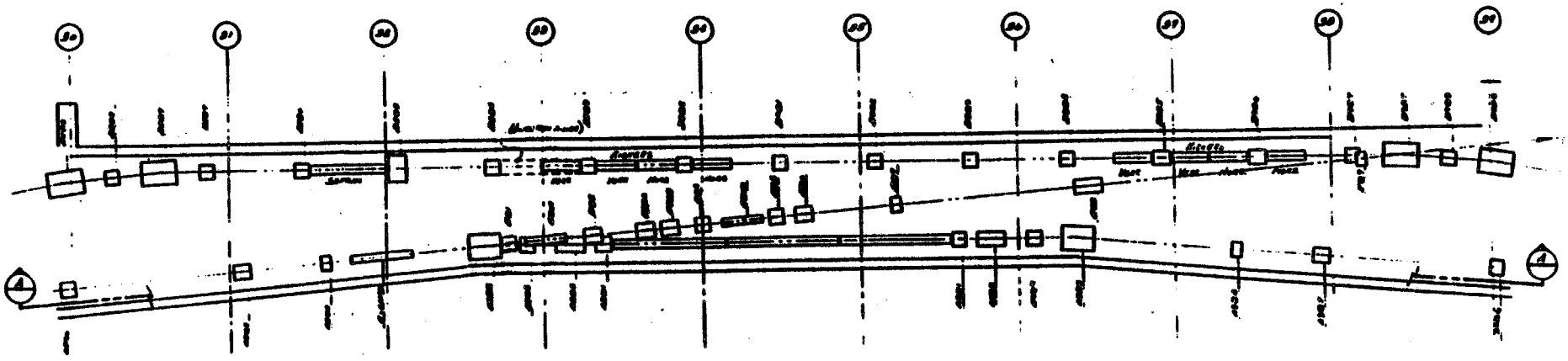

Extraction Straight Section
Plan View

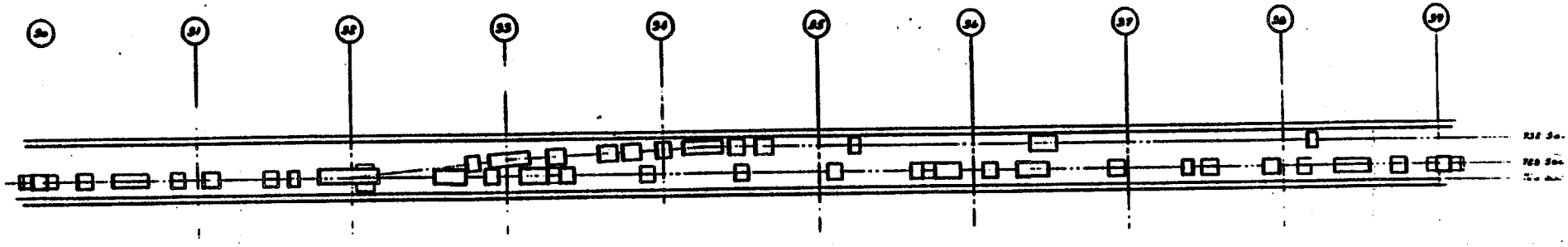

Extraction Straight Section
Elevation View

Figure 5-4

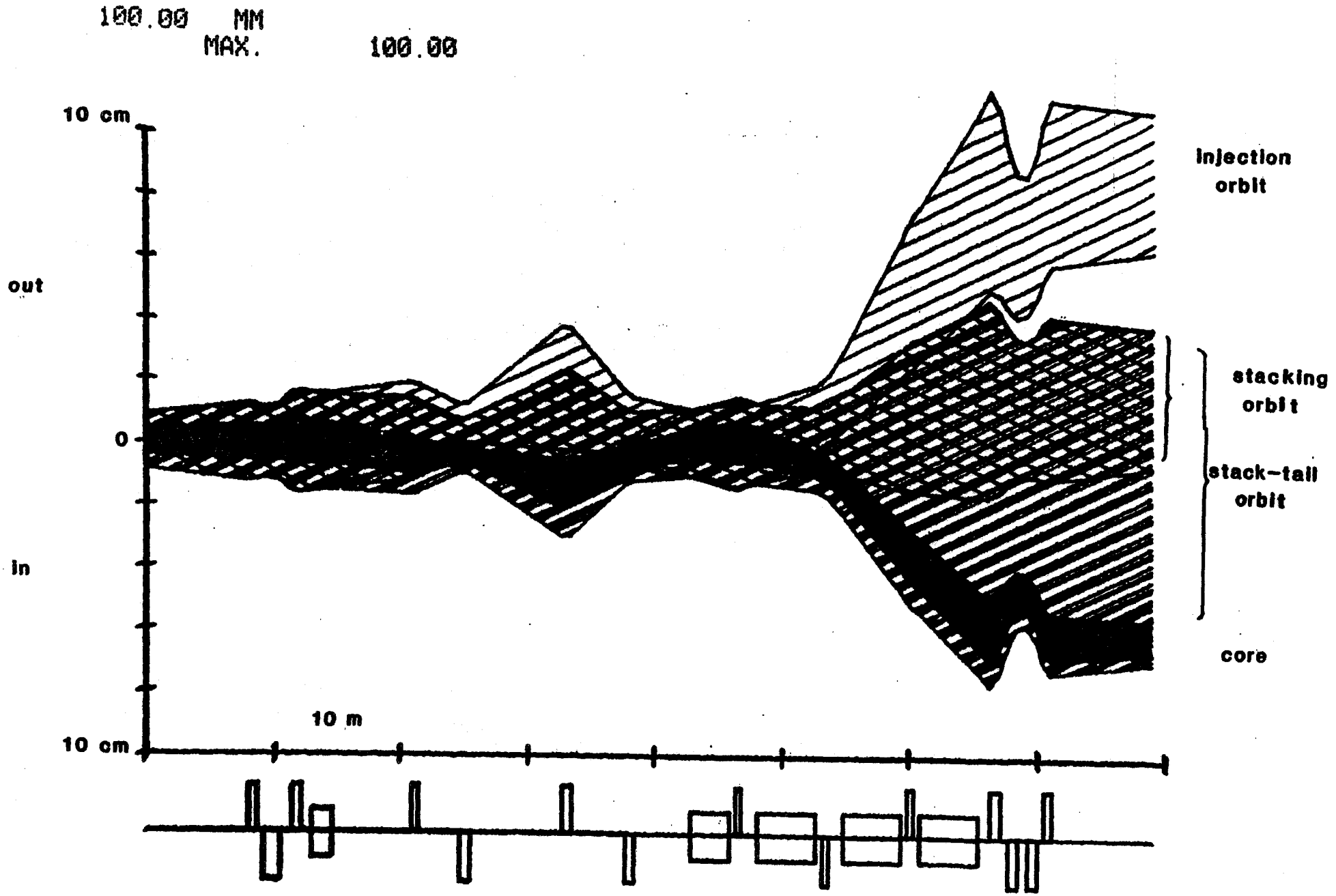
100.00 MM
MAX. 100.00
10 cm
out
0
in
10 cm
10 m
injection orbit
stacking orbit
stack-tail orbit
core

Figure 5-5

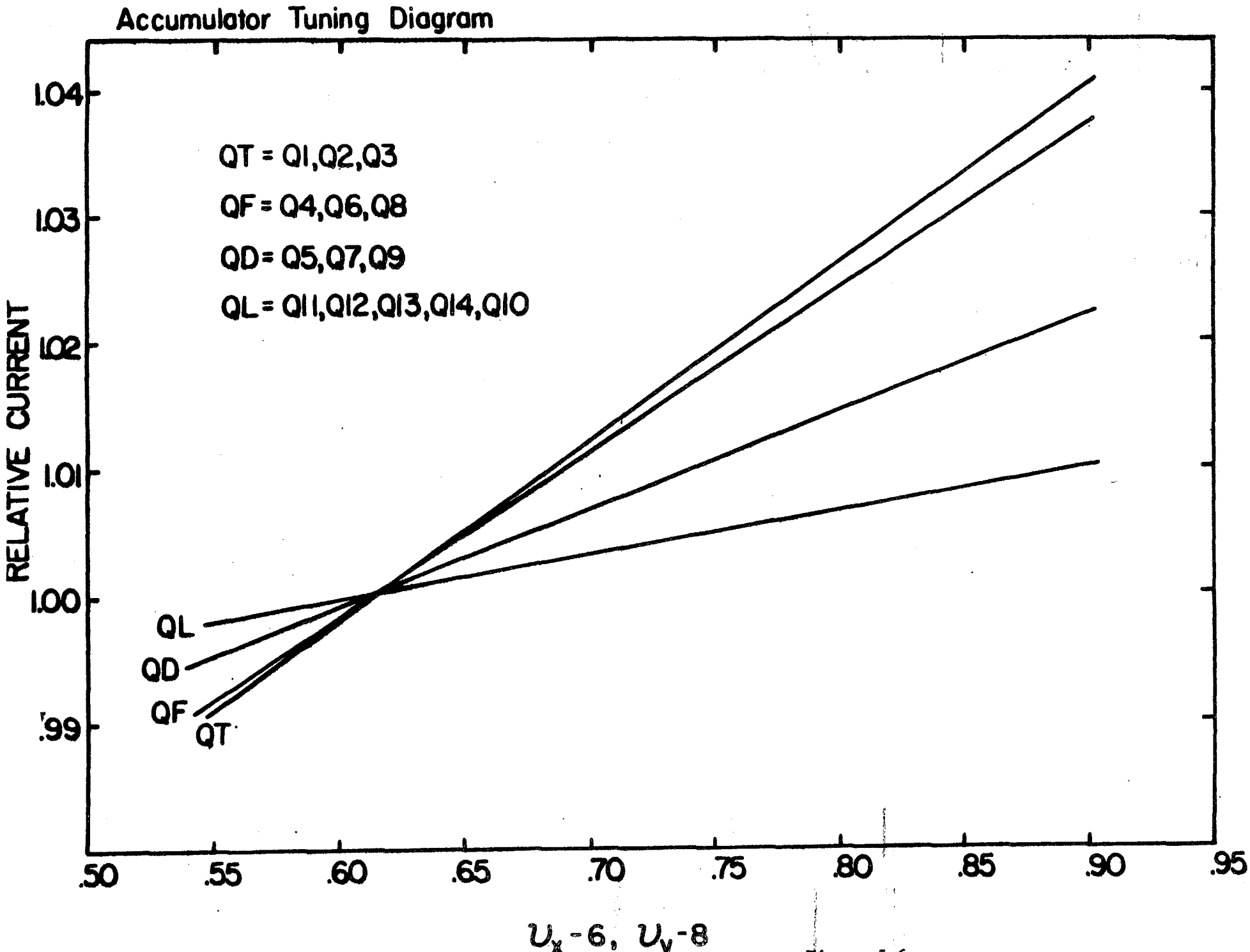
Accumulator Tuning Diagram
QT = Q1,Q2,Q3
QF = Q4,Q6,Q8
QD = Q5,Q7,Q9
QL = Q11,Q12,Q13,Q14,Q10
RELATIVE CURRENT
1.04
1.03
1.02
1.01
1.00
.99
QL
QD
QF
QT
.50
.55
.60
.65
.70
.75
.80
.85
.90
.95
ν_x-6, ν_y-8

Figure 5-6

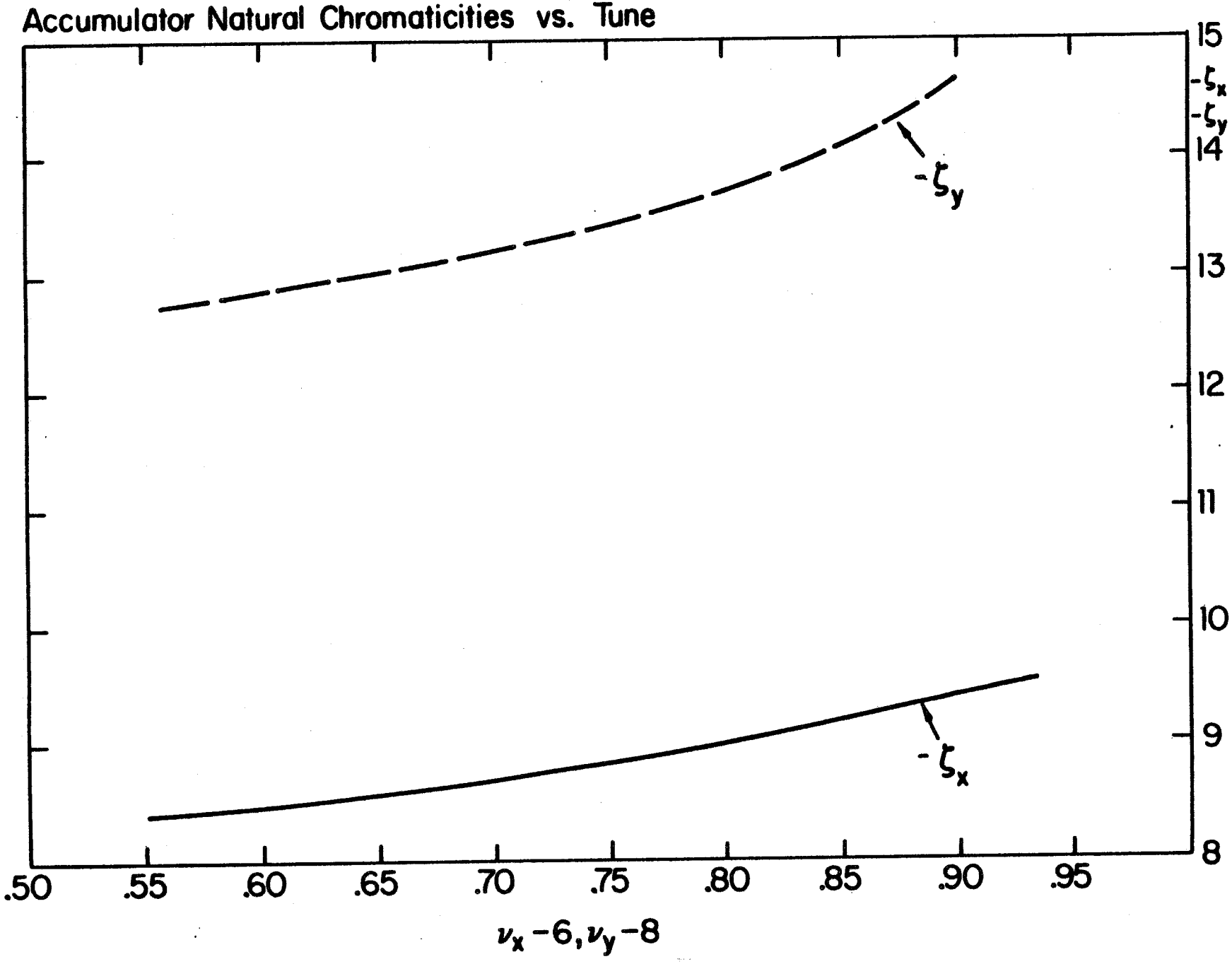
Accumulator Natural Chromaticities vs. Tune
15
-ζx
-ζy
14
13
12
11
10
9
8
-ζy
-ζx
.50
.55
.60
.65
.70
.75
.80
.85
.90
.95
νx -6, νy -8

Figure 5-7

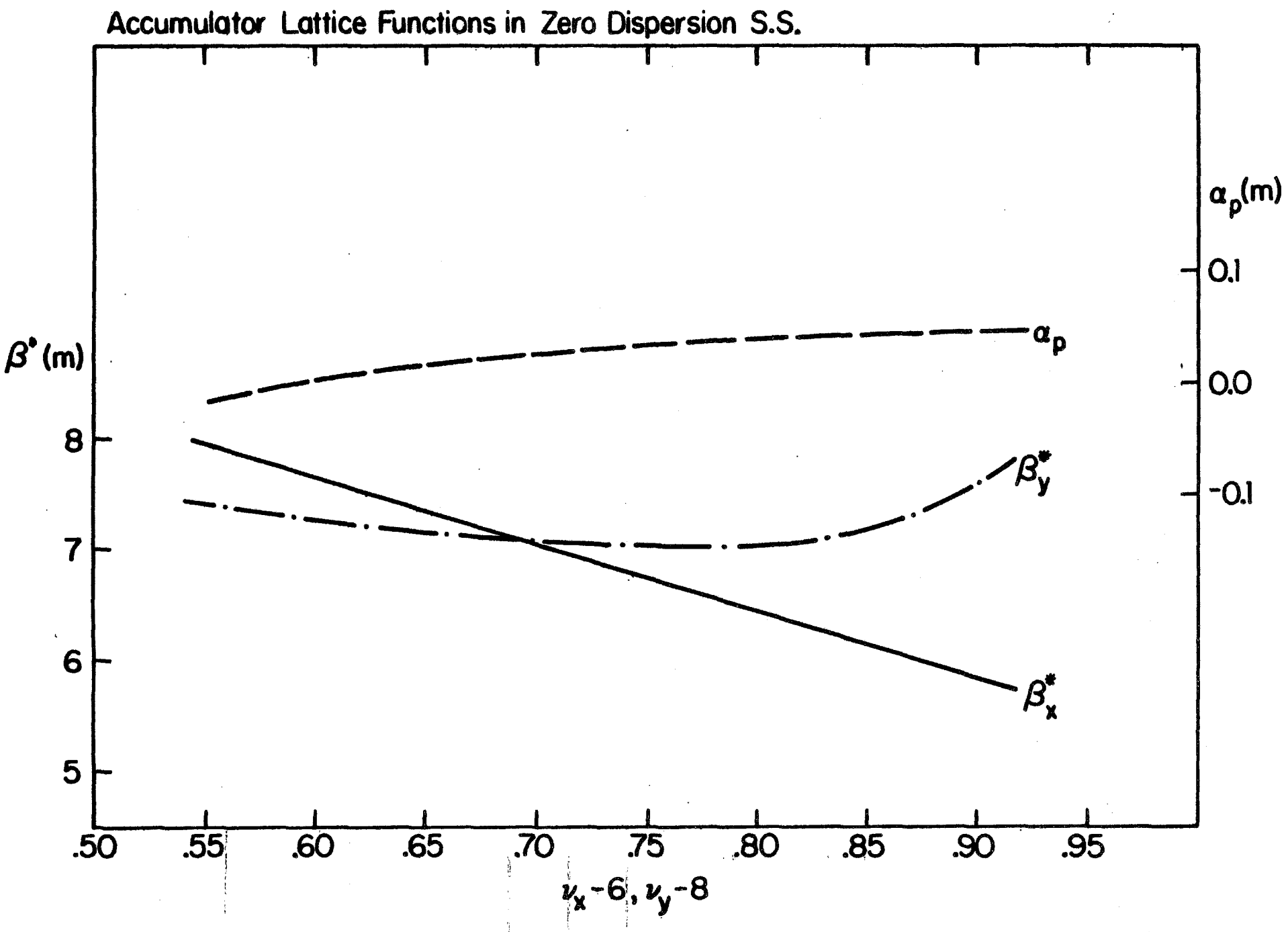
Accumulator Lattice Functions in Zero Dispersion S.S.
β*(m)
8
7
6
5
.50
.55
.60
.65
.70
.75
.80
.85
.90
.95
ν_x-6, ν_y-8
α_p(m)
0.1
0.0
-0.1
α_p
β^*_y
β^*_x

Figure 5-8

families of sextupoles compensate the emittance distortion. The locations and strengths of these multipoles are given in Table 5-III. The lattice also has enough space to install more sextupoles or any multiples if they are necessary for more correction.

5.6 RF Stacking System

With the injection shutter closed, antiprotons are injected from the Debuncher with a total momentum spread of about 0.2%. The energy spread (18 MeV) and Accumulator revolution period (1.5 μsec) result in an injected longitudinal emittance of about 29 eV-sec. This beam is bunched adiabatically and then decelerated by 0.7% to the edge of the stack of previously injected antiprotons by an h = 84 (53 MHz) rf system. Finally the beam is released and debunched by reducing the rf voltage adiabatically.

The phase-oscillation period is 0.9 msec; the capture can be accomplished in about 5 msec. The deceleration time at $\phi_s = -2°$ is 30 msec. Thus, about 40 msec is required for the entire stacking operation.

At frequencies well below the GHz cooling band, the cooled core may be subject to longitudinal instabilities induced by the shunt impedance of the stacking rf cavity. Additional 53 MHz rf at nearly the required voltage will be installed for bunching of the antiprotons for extraction (see Sec. 6.1). It appears that this system should be used for stacking to economize on the number of high-impedance gaps in the ring. A criterion $Z_n/n < 500\ \Omega$ requires a shunt impedance $\leq 42\ k\Omega$. The rf power required during the deceleration is about 135 kW. The parameters for the stacking system are summarized in Table 5-IV.

TABLE 5-IV RF STACKING PARAMETERS

Injected Longitudinal Emittance	30 eV-sec
Stacking rf Total Bucket Area	32.3 eV-sec
Stationary Bucket RF Voltage	91 kV
Stationary Bucket Phase Oscillation Period	0.88 msec
$\Delta p/p$ Required for Stacking	0.77%
Δ (cp)	69.2 MeV
Deceleration Synchronous Phase Angle	2 degrees
$\Gamma = \sin \phi_s =$	0.035
Moving Bucket Factor $\alpha(\Gamma)$	0.918
RF Voltage During Deceleration	106 kV
Time Required for Deceleration	29.4 msec
Number of Cavities (similar to Debuncher cavity with ceramic gap in beam tube and broad-band swamping applied to reduce shunt impedance)	2
Cavity Small-Signal Shunt Impedance	42 kΩ
Peak RF Power Requirement	135 kW
Average RF Power Requirement	2.7 kW

Harmonic Number (h)	84
RF Starting Frequency	52.8104 MHz
$\eta = \gamma_t^{-2} - \gamma^{-2}$	0.023
$\beta = v/c$	0.99447
Injection Orbit Circumference	474.202 m
Stacking Efficiency*	98%

*Based on computer simulation

5.7 Accumulator Magnets

The main magnet system consists of 30 dipoles and 84 quadrupoles. In Table 5-III is shown a list of magnets, lengths, strengths and required apertures. The required apertures were calculated assuming construction tolerances of 2.5×10^{-4} (relative standard deviation) for dipole strengths, dipole level angles (radians), and quadrupole random position errors (meters). Sufficient space is allowed for at least 4σ, where σ is the standard deviation of the expected orbit position error, or the beam emittance plus momentum spread plus 10 mm whichever is larger. In addition, space is left for 4-mm (thickness plus deflection) vacuum chamber thickness and 5-mm insulation thickness. Several mm must be included also for heating tapes to bake the chamber (dipoles). The specification of these magnets are listed in the tables of Chapter 12.

There are three lengths of dipoles, all with field strengths of 1.689 T. There are 2 different apertures, 3 different lengths in the smaller aperture, in the larger. Because of the large sagitta, these magnets will be curved. The coils will be made of four pancakes plus two single-layer saddle coils.

There are 13 different quadrupoles, of two different profiles. Q1-Q9 have poletip radii of 1.75 mm and 5 different lengths. Q10-Q14 have poletip radii of 3.312 in and four different lengths. Each quadrupole will have a shunt with capability of about 10% of the quadrupole strength. The coils are fabricated in individual layers and assembled on the quad half cores, which are then assembled as a complete magnet.

There are 24 sextupoles of two types. S7 and S9 have a poletip radius of 71.4 mm and a length of 20.3 cm. The (maximum required strength is $33.0 T/m^2$. These sextupoles will be the same as those used in the Debuncher and will be constructed with parallel-sided poles and a single-layer 6-turn winding. S10 and S12 are located in the high dispersion region and require an aperture of 96.5 mm x 300.0 mm (vertical and horizontal). These magnets will have a rectangular aperture with a variable current density across the upper and lower poles to produce the desired field. Octupole and vertical (correction) dipole windings will also be incorporated. The maximum required strengths are 20.5 T/m^2 (s), 39.0 T/m^3 (O), and .064 T (D). The

sextupoles are divided into four families each with its own power bus. There are two families of octupoles. These magnets are described in Tables 5-V and 5-VI.

TABLE 5-V ACCUMULATOR SEXTUPOLES

Max. B"	205	330 T/m^2
ℓ eff	0.25	0.20 m
poletip radius	96.5x300.	71.4 mm
NI	6420	1550 AT/pole
Max. I.	430	2560 A
N	15	6 Turns/pole
Conductor		
Current density	5.2	5.0 A/mm^2
R	8.6	5.6 mΩ
Max. voltage drop	3.7	1.5 V
Max. ohmic loss	1575	375 W
Weight, cu	63	16 lbs
Fe	590	200 lbs

TABLE 5-VI ACCUMULATOR OCTUPOLES

Max. B"	39.0	T/m^3
Length	0.25	m
Aperture	96.5x300	mm
Current	15	A
Current Density	2.3	A/mm^2
Turns	120	
R	0.22	Ω
Voltage	3.2	V
Power	47.0	W
Number of magnets	12	

5.8 Accumulator Vacuum System

5.8.1 Vacuum Requirements. The base pressure is determined by the effects of the residual gas on the accumulated antiproton beam. These effects include particle loss by single Coulomb scattering and nuclear interactions, beam heating by multiple Coulomb scattering, energy loss by ionization, and effects of neutralization by positive ions attracted to the negative beam.

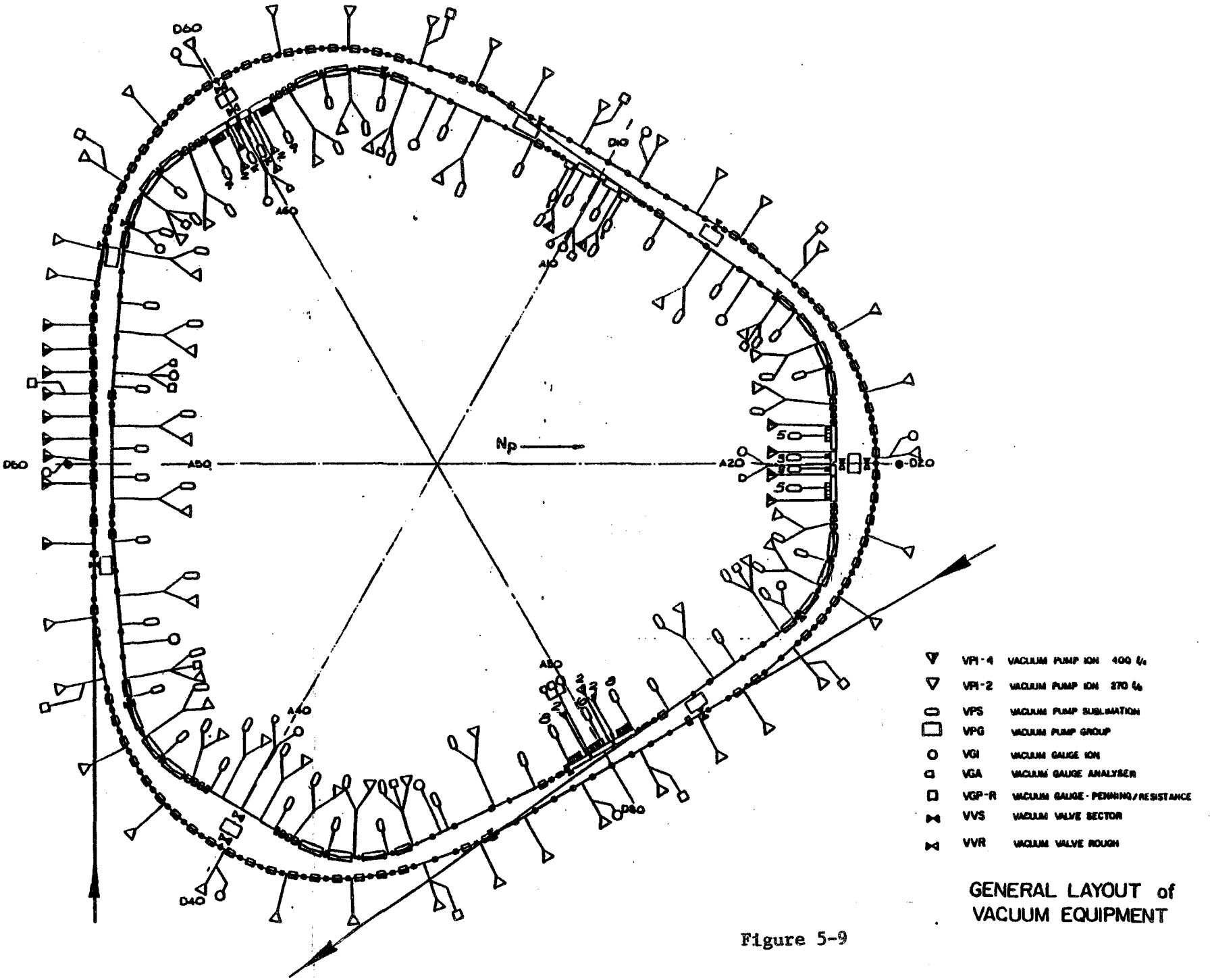

GENERAL LAYOUT of VACUUM EQUIPMENT

Figure 5-9

A detailed analysis has been made[1] of these effects. As a result, the system is designed for a nominal pressure of 3×10^{-10} Torr (nitrogen equivalent). At this pressure, the single-scattering lifetime will be 240 hr and the nuclear-interaction lifetime will be 2000 hr. Thus these effects are negligible. The heating rate for the final stack from multiple scattering will be 2×10^{-5}/sec, 10 times less than the cooling rate. (Here a gas composition of 50% H_2, 50% N_2 or CO is assumed). The energy loss per antiproton will be 20 keV/hr. Both the heating and energy loss can be easily compensated by the stochastic-cooling systems. We will keep the nominal design value of the neutralization factor H 0.03. With this value, the scattering by positive ions trapped in the beam will be increased less than 2%. The vertical space-charge tune shift will be reduced by 10^{-3}. Thus these neutralization effects are negligible.

5.8.2 Vacuum System Layout and Characteristics. The pressure requirement can be met with a combination of sublimation sputter ion-pumps. Furthermore, vacuum-annealed austenitic high-tensile stainless steel will be used for the chambers so that specific degassing rates of better than 1×10^{-12} Torr-ℓ/cm^{-2}-sec can be attained. The maximum design bakeout temperature is 300°C.

Figure 5-9 shows the vacuum-system layout over one-sixth of the Accumulator ring. The sputter ion pumps should have a speed of 200 ℓ/sec. The stochastic-cooling pickups and kickers will be isolated with all metal valves, during the bakeout to prevent any vacuum contamination. These valves will divide the ring into approximately 5 irregular vacuum sectors.

The baking equipment (heaters, controls, thermal insulation) will be installed in a permanent fashion to allow bakeout to proceed without major preparations. Exceptions are areas that cannot tolerate the high temperature e.g. pump magnets, cable feedthrus and special devices.

Pump-down during bakeout will be carried out using mobile turbopump carts. This will allow the use of a large number of pumps in any given section being baked. These carts will be connected to metal valves distributed for that purpose throughout the system. Tests indicate that the pressure during bakeout has little effect on the success of the bake.

Vacuum gauges include 6 Pirani gauges to monitor pumpdown, 36 Bayard-Alpert ionization gauges, and 6 mass-analyzer heads, located near areas of complex equipment to monitor leaks and contamination.

The stochastic-cooling equipment will be capable of being baked at a maximum temperature of 150°C and materials compatible with the high-vacuum requirements will be used. Sublimation and ion pumping will be used to provide a pumping speed of up to 2000 ℓ/sec/m.

Clearing electrodes will be installed to remove low-energy positive ions and thus keep the neutralization factor H 0.03. There will be a pair of electrodes at the downstream end of each magnet. Ions move

longitudinally to the electrodes by E x B drifting caused by the beam electric field and the ring guide field. This kind of system has been used successfully in the ISR.

The straight sections between magnets will also need clearing electrodes to avoid trapping ions in the cool-beam potential of 5 V. We plan to apply a dc potential of more than 5 V to the clearing electrodes and to the beam-position detector electrodes whenever these are in a suitable location.

All devices and ring sections will undergo a preliminary bake and low-pressure test before being installed. Their design will conform with strict rules of choice of material and will be subject to approval by the vacuum coordinator.

The vacuum control system will be constructed along the design evolved for the Tevatron. It is highly modular and economical. Many of the required modules and device controls have already been developed, including ion-pump supplies and ion-gauge controllers. A card cage containing all control modules will interface to the host computer through a CAMAC module. Much of the necessary software can be used or adapted.

5.9 Momentum Cooling

5.9.1 Introduction to Stochastic Stacking. The stochastic stacking system consists of pickup electrodes, an amplifier system with electronic filters and phase-compensation networks, and kicker electrodes. Each particle produces an electronic signal that, when applied to the kicker, changes its momentum in the direction of the core. The signal of each given particle thus produces a kick that tends to cool the beam into a small momentum width around the core. Other particles in the beam with approximately the same revolution frequency produce random kicks on the given particles and cause diffusion or heating. The interesting systems, of course, are those in which cooling dominates over heating.

Momentum cooling is usually described in terms of the Fokker-Planck equation

$$\frac{\partial \psi}{\partial t} = \frac{\partial}{\partial E} \left[-F\psi + (D_0 + D_1 + D_2\psi) \frac{\partial \psi}{\partial E} \right] \qquad (5.1)$$

where $\psi = \partial N/\partial E$ is the particle density, F is the coefficient of the cooling term, D_0 is the coefficient of the heating term due to intrabeam scattering (described later), D_1 is the coefficient of the heating term due to thermal noise, and D_2 is the coefficient of the heating due to other particles. A derivation and discussion of this equation are given by Mohl et al.[2]

A simplified version of the Fokker-Planck equation has been used by van der Meer[3] to describe the stacking process. It is assumed that the voltage on the kicker is exactly in phase with the particles that created it, that there is no amplifier thermal noise or intrabeam scattering, the feedback gain is independent of harmonic number, and that there are no beam-feedback effects. A more general approach, including thermal noise, is possible.[4] While none of these assumptions is justified in the proposed system, the simplified discussion yields semi-quantitative results that can form the basis of a design. Following van der Meer, the flux can be written as

$$\Phi = -\frac{V}{T}\bar{\psi} - AV^2\psi\frac{\partial\psi}{\partial E} \quad , \tag{5.2}$$

cooling term — heating term

where N(E,t) is the number of particles with energy less than E and

$$\Phi = \frac{\partial N}{\partial t}$$

$$\psi = \frac{\partial N}{\partial E} \quad ,$$

from which the Fokker-Planck equation

$$\frac{\partial\psi}{\partial t} = \frac{\partial\Phi}{\partial E} \tag{5.3}$$

follows. Here V = V(E) is the average energy loss per turn and T is the revolution period. The constant A describes the strength of the heating term and is given by

$$A = \frac{\beta p \Lambda}{4T^3 W^2 |\eta|} \quad , \tag{5.4}$$

where $\beta = v/c$, p is the momentum, T is the revolution period, W is the bandwidth $= f_{max} - f_{min}$, $\Lambda = \ln (f_{max}/f_{min})$, and $\eta = \gamma_t^{-2} - \gamma^{-2}$. If the amplifier gain is not independent of frequency, Λ is modified. The ideal gain profile, in fact, rises linearly with frequency, but the exact value of Λ is not important for this discussion.

The Fokker-Planck equation is nonlinear in ψ and it is therefore usually solved numerically. Stationary solutions, $\Phi(E,t) = \Phi_0 =$ constant, can often be found by elementary methods. These solutions are useful because in the stack tail between the core region and the injection region, the actual time-dependent solution is normally very close to the steady-state solution.

Consider $\Phi_0 =$ constant and $\psi(E,t) = \psi(E)$, and ask what the shape of the voltage profile $V(E)$ should be. The answer, as given by van der Meer, is to maximize $d\psi/dE$ everywhere and thus minimize the energy aperture which is required. This choice also minimizes the total Schottky power in the amplifier. The solution is

$$V(E) = -\frac{2\Phi_0 T}{\Psi(E)} = -\frac{2\Phi_0 T}{\Psi_1} e^{-(E_1 - E)/E_d} \quad , \tag{5.5}$$

where Ψ_1 is the initial stack-tail density at E_1 and E_d is the characteristic energy

$$E_d = -4A\Phi_0 T^2 = -\frac{4p\Lambda\Phi_0}{TW^2|\eta|} \quad . \tag{5.6}$$

This equation exhibits the major design consideration. We know that $d\psi/dE$ is maximized by a gain profile $V(E)$ that is exponential in energy. The exponential slope $d\psi/dE$ is maximized by minimizing E_d. In the stack tail, we want a density increase of 1000, so we require a minimum momentum aperture of $\Delta p/p = \ln(1000)\ E_d/p = 6.9\ E_d/p$. If we want to limit the aperture $(\Delta p/p)$ required for the stack tail to 0.75%, then $E_d\ 0.001\ p = 10$ MeV for $p = 8.9$ GeV/c. Since we want to have Φ_0 as large as possible, we must make E_d small by choosing $TW^2|\eta|$ to be as large as possible. The density profile is shown in Fig. 5-10.

We have chosen to work with a maximum frequency of 4 GHz for the purposes of this report, but we intend to use frequencies up to 8 GHz for core cooling if our research program indicates that 8 GHz cooling systems are practical. The stack-tail system was chosen to have a maximum frequency of 2 GHz. As described below, the choice of frequency dictates the choice of η. By limiting the stack-tail system to 2 GHz, we are able to use a relatively high η ($\eta = 0.02$). The high value of η is useful for the core-cooling systems, where the core cooling times are inversely proportional to η.

The maximum value of η is limited once we choose f_{max}. For a number of reasons, it is required that $\eta(\Delta p/p) f_{max} T < \delta$, where δ is some number of order unity. The reasons that determine the value of δ are:

(i) The Schottky bands must not overlap in a system that uses electronic filters for gain shaping. In such a system, the particle energy is sensed in the electronics by the connection between energy and the harmonics of the revolution frequency. If the relationship is not unique, it is difficult and probably impossible to design appropriate filters. In this case, $\delta = 1$ and $\Delta p/p = 1\%$ so η 0.03 with $T = 1.6$ μsec.

(ii) The phase shift between PU and kicker must not vary across the momentum band more than about ±45°. If PU and kicker are exactly opposite in the Accumulator Ring, then $\delta = 0.5$. If the stack-tail system is divided into subsystems with $\Delta p/p = 1/3\%$, then this constraint applies to each system individually, so η 0.05.

(iii) For reasons described below, the filters must have the peak of their response at the tail end and a notch in the core. Between Schottky bands, of course, the response must rise from the notch in the core back to the peak value. Since the rise back to the peak value cannot be done infinitely sharply, at least without undesirable phase characteristics, this requirement is more severe than 1) above. We have found that $\eta = 0.02$ is a suitable value for a maximum frequency of 2 GHz.

We have chosen a Booster-sized ring ($T = 1.6$ μsec) because it is large enough to accommodate the cooling-system hardware and can run at 8 GeV, a good energy for production of $\bar{p}$'s and their injection into the Main Ring.

5.9.2 Summary of Design Considerations. We have chosen $E_d = 0.001p = 10$ MeV to keep the required momentum aperture sufficiently small. The product $Tf_{max}\eta$ is fixed by the requirement of a minimum spacing between Schottky bands. We have chosen $W = 1$ GHz with $f_{max} = 2$ GHz to yield a somewhat higher value of η (0.02) than would be the case if we chose a higher frequency. Higher frequencies also have the disadvantage that it is somewhat more difficult to build the quality of hardware that is required.

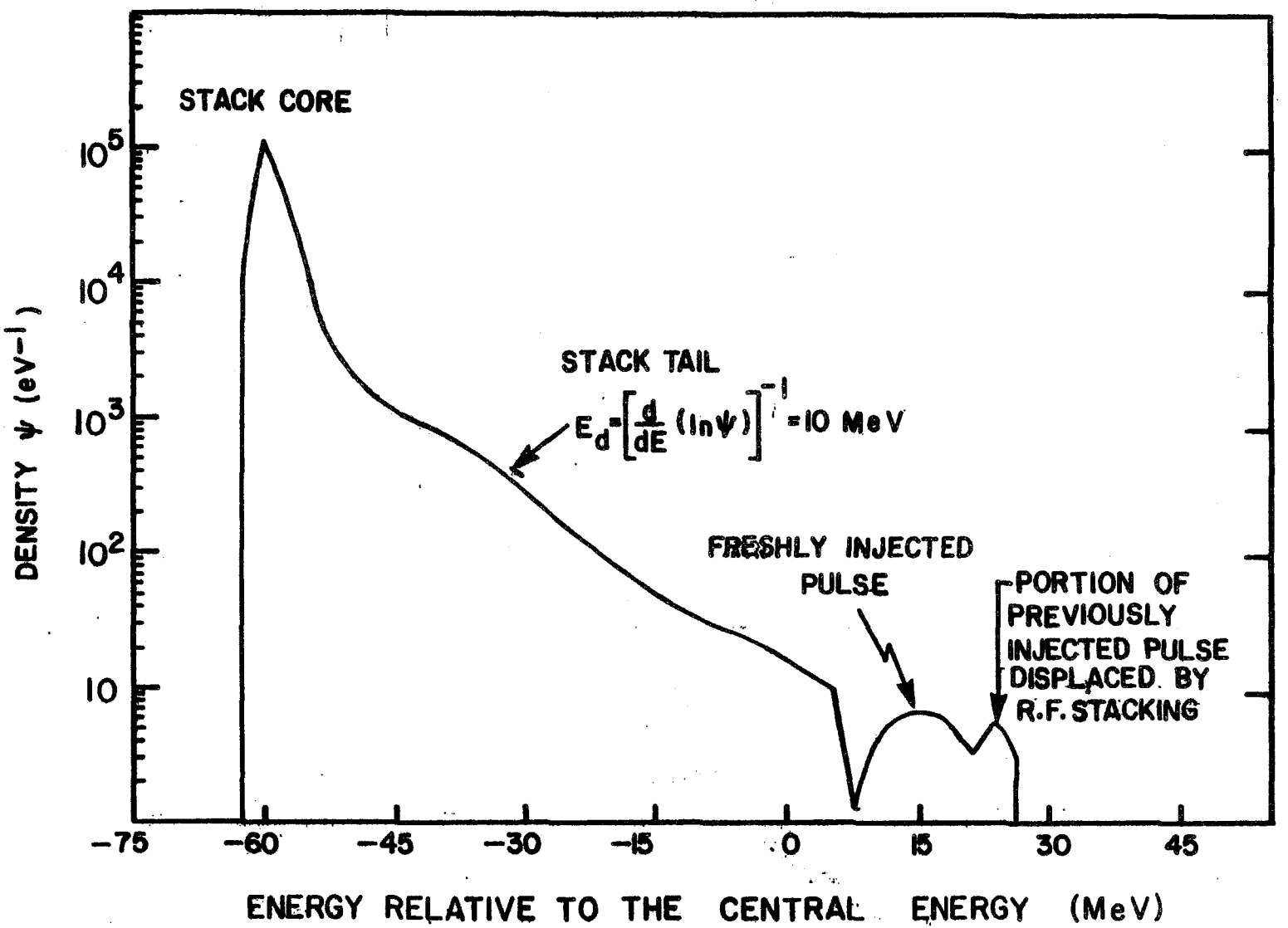
STACK CORE
STACK TAIL
$E_d = \left[\frac{d}{dE}(\ln\psi)\right]^{-1} = 10$ MeV
FRESHLY INJECTED PULSE
PORTION OF PREVIOUSLY INJECTED PULSE DISPLACED BY R.F. STACKING
DENSITY ψ (eV^{-1})
10^5
10^4
10^3
10^2
10
−75
−60
−45
−30
−15
0
15
30
45
ENERGY RELATIVE TO THE CENTRAL ENERGY (MeV)

Figure 5-10

5.9.3 Building the Exponential Gain Profile. Once the parameters of the stack tail have been chosen, the next step is to build the required gain profile. We use a combination of two techniques. The first technique is to sense the particle momentum by sensing its position in a region of high momentum dispersion. The position sensitivity of the strip-line pickups we plan to use is given in Section 5.11.1. For large horizontal displacement x the sensitivity of these pickups becomes

$$s(x,0) \quad e^{-\pi x/h}, \tag{5.7}$$

where h is the gap between plates. In our case, the momentum dispersion is $\alpha_p = 9$ m and we have chosen h = 3 cm. Thus for large ΔE,

$$V(E) \quad e^{-|\Delta E|/E^*}, \tag{5.8}$$

$$\text{where } E^* = \frac{\beta^2 E h}{\pi \alpha_p}$$

where V(E) is the average (coherent) particle voltage gain per second, ΔE is the difference between energy E and the energy where the pickup response is centered, and $E^* = 10$ Mev. In our system we use the pickups in the region where the falloff is not truly exponential, but the system can be characterized roughly by an E^* of approximately 15 MeV for the pickup response.

The second method of gain shaping is with filters. However, the main purpose of the filters is to reduce the thermal noise in the core. In order to maintain a flux of 3×10^7 sec^{-1} into the stack tail, an amplifier system with very high gain (150dB) is required. Even with preamplifiers with low noise temperatures (80°K), the thermal noise produces an rms voltage of approximately 1500 V/turn. This noise voltage is (perhaps surprisingly) tolerable in the tail where the average (cooling) voltage gain is about 10 V/turn. In the core region, where the cooling voltage is a few mV/turn, this noise voltage must be reduced to a tolerable level. The filter does this by making a notch at all harmonics of the revolution frequency of the particles in the core. The filter also does some gain shaping in the tail region. The filters used are composed of a series of notch filters similar in concept to those used at CERN. A schematic diagram of the individual component filters is given in Fig. 5-11. The response of these filters is given by[5]

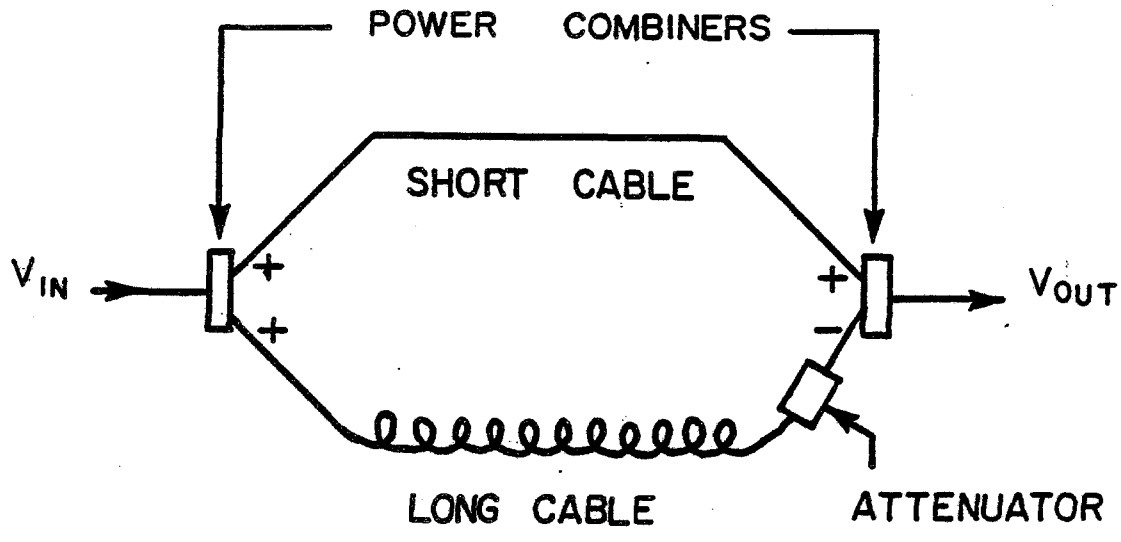
POWER COMBINERS
SHORT CABLE
V_{IN}
+
+
+
−
V_{OUT}
LONG CABLE
ATTENUATOR

Figure 5-11

$$\frac{V_{out}}{V_{in}} = (e^{-i\gamma_1 \ell_1} - \xi e^{-i\gamma_2 \ell_2})/2 \ , \qquad (5.9)$$

where γ_1, γ_2 and ℓ_1, ℓ_2 are the propagation constants and lengths of cables and ξ is a variable attenuation of order unity. To get a clearer picture of the operation of this filter, consider the approximation $\xi = 1$, $\ell_1 = 0$, $\gamma_2 = \omega T_c/\ell_2$, where ω is the applied frequency electrical length of the cable. In this case,

$$\left|\frac{V_{out}}{V_{in}}\right|^2 = (1 - \cos \omega T_c)/2 \ , \qquad (5.10)$$

and the phase changes linearly with frequency except at the transmission zero, where it takes a discontinuous jump of 180°.

The absence of amplifier noise would not necessarily eliminate the need for filters. Nonlinearities in the pickups, amplifiers and other components cause frequency mixing, as is well known to rf engineers. The input power at frequencies corresponding to the stack tail, where the power density is high, will mix in a nonlinear device and produce output power at frequencies corresponding to the core where the power density must be low. The filters suppress the most dangerous part of the unwanted distortion because of the notch at the frequency of the core particles. (These particles are cooled by a separate system without filters, as will be described later.) It will be advantageous to place some of the filtering after the final amplifier to reduce the sensitivity to the nonlinear distortions from that source.

The shape of the gain curve at the injection end is purposely different from the ideal exponential curve, becoming flat in the injection region because of several practical considerations:

(i) It is desirable to keep the electronic gain between Schottky bands as low as possible. The gain between Schottky bands does not affect the cooling process, but the thermal power between Schottky bands is significant.

(ii) To maximize the ratio of Schottky signal to thermal noise, it is desirable to place the pickups so they have maximum sensitivity to the freshly injected beam, i.e., so they operate in the non-exponential region.

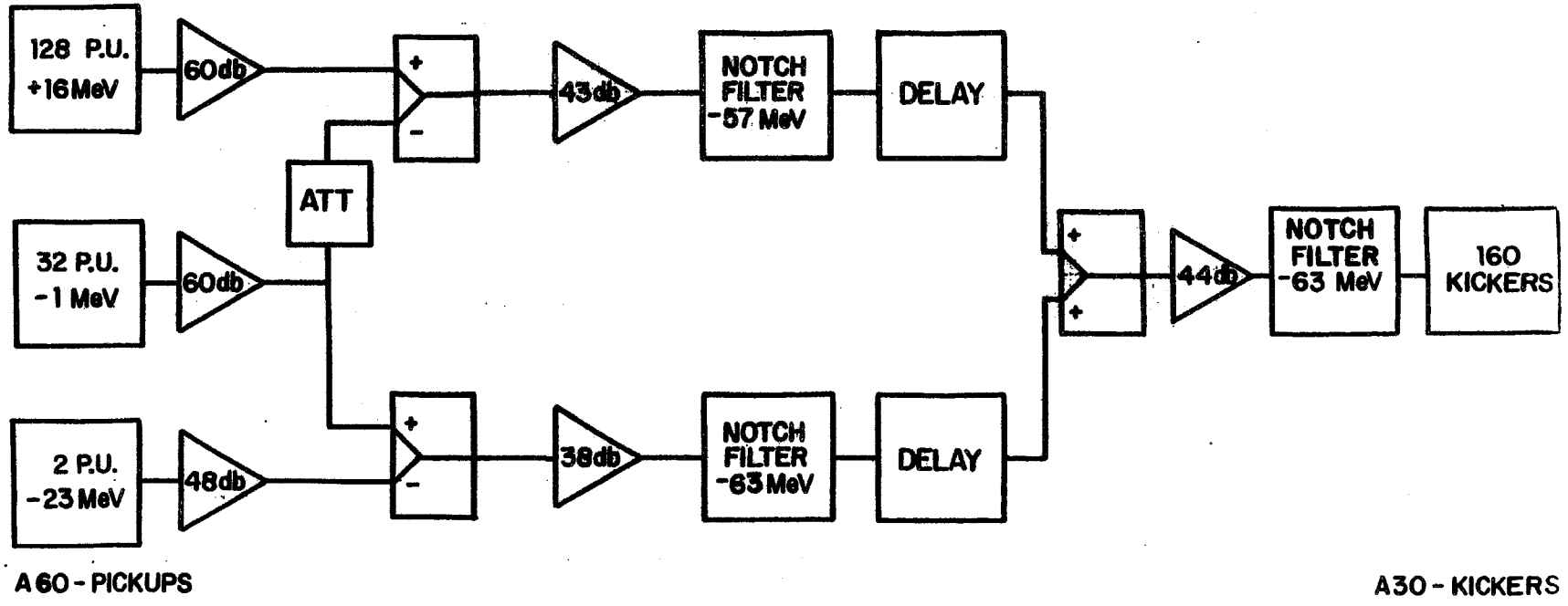

STACK TAIL MOMENTUM COOLING SYSTEM 1-2 GHz

Figure 5-12

(iii) The exponential gain profile minimizes Schottky power only in the approximation that beam is injected in a steady state manner. In fact, each newly injected pulse substantially alters this picture since the density of particles will differ by factors of 2 or 3 from the steady state situation. By making the gain profile flatter in the injection region, we can reduce the required Schottky power immediately after a new pulse is injected.

The stack-tail system we have designed consists of two sections of pickups and associated amplifiers and filters. The two sections make it possible to control undesirable phase shifts and thermal noise in the tail. A block diagram of the system is shown in Fig. 5-12. The number of pickups was chosen to be a large as possible to minimize the thermal-noise to Schottky-signal ratio and to minimize the total thermal power. In order to keep the betatron oscillations from substantially affecting the momentum cooling, the betatron amplitudes must be limited. To achieve the desired gain profile, the pickups have a plate separation of 3 cm. Calculations indicate that the beam size should be less than 2.4 cm to avoid trouble with betatron motion. For an emittance of 10π mm-mrad, the β function at the pickup must be 15 m or less. This requirement limits the pickup straight section to 15 m in length and a total of 200 pickups. The function of the subtracting pickups is discussed in the next section. The number of kickers was chosen to fill the straight section across from the pickups to minimize total power (inversely proportional to the number of kickers). The gain profile achieved with this system is shown in Fig. 5-13 abc for the Schottky bands at 1.1, 1.5 and 1.9 GHz.

5.9.4 Signal Suppression and Stability. An important aspect of the cooling process, when using high-gain cooling systems, is signal feedback via the beam. A signal of frequency ω will modulate the beam at frequency ω, and this modulation will be sensed at the pickup. Thus the cooling system forms a closed-loop feedback system. This feedback system is analogous to amplifier systems with conventional electronic feedback. An expression for the beam feedback has been given by van der Meer[6] and independently by Ruggiero.[7] An approximate expression is

$$F = \frac{I_p}{V} = jef_0^2 \bar{p} \int \frac{CP}{nk(E-E')} \frac{d\psi}{dE'} dE' - \frac{\pi ef_0^2}{n|k|} CP \frac{d\psi}{dE} , \qquad (5.11)$$

where $\bar{p}$ denotes the principal value of the integral, I_p = induced current at the frequency $f = nf_0$ in the pickup due to modulation caused by voltage V on the kicker, f_0 is the revolution frequency corresponding to energy E, n is the harmonic number, e is the unit charge, $j = \sqrt{-1}$, $k = 2\pi\, df_0/dE$, C is the phase factor due to transit time differences between pickup and

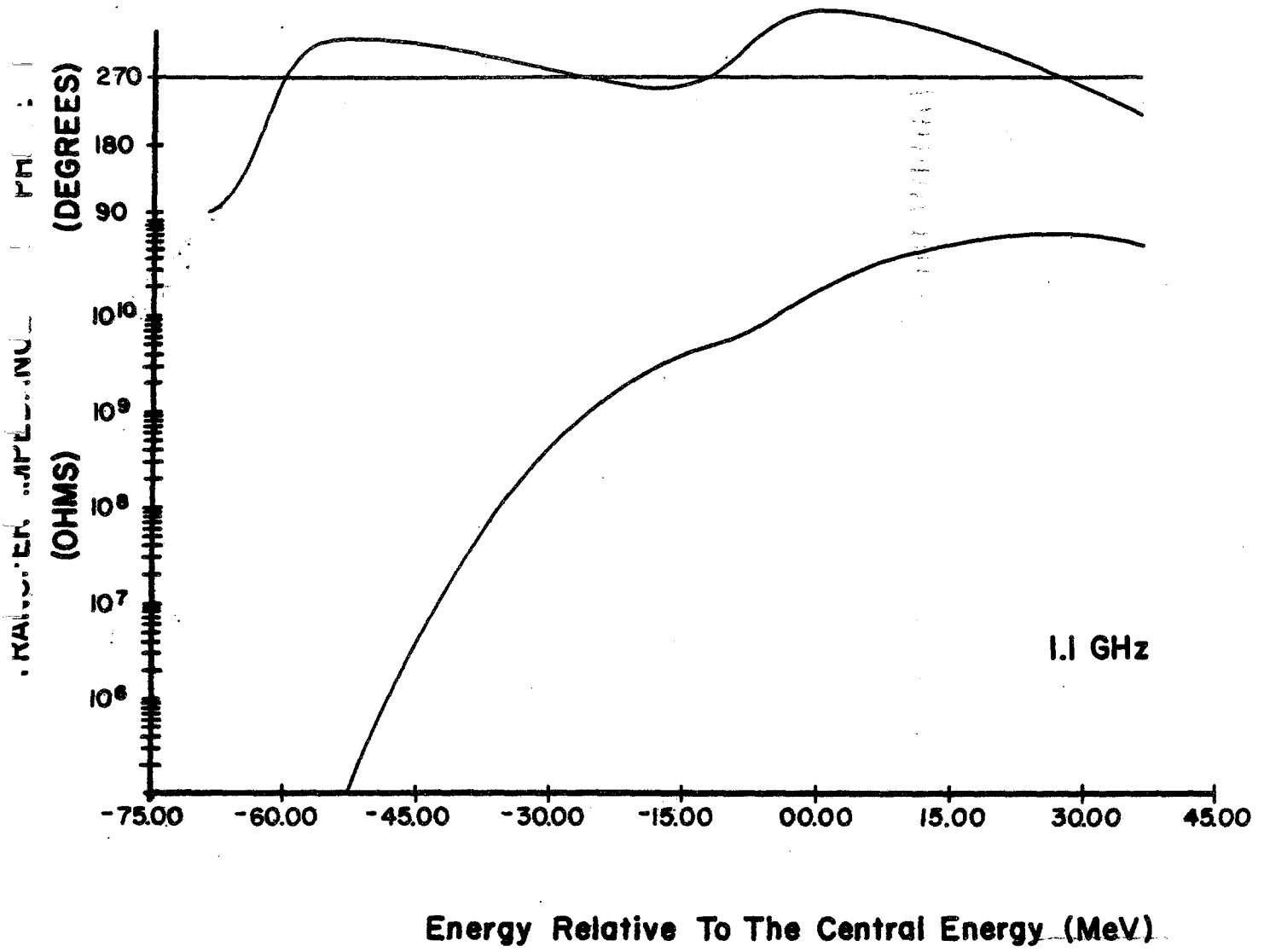
(DEGREES)
270
180
90
(OHMS)
10^{10}
10^{9}
10^{8}
10^{7}
10^{6}
1.1 GHz
-75.00
-60.00
-45.00
-30.00
-15.00
00.00
15.00
30.00
45.00
Energy Relative To The Central Energy (MeV)

Figure 5-13a

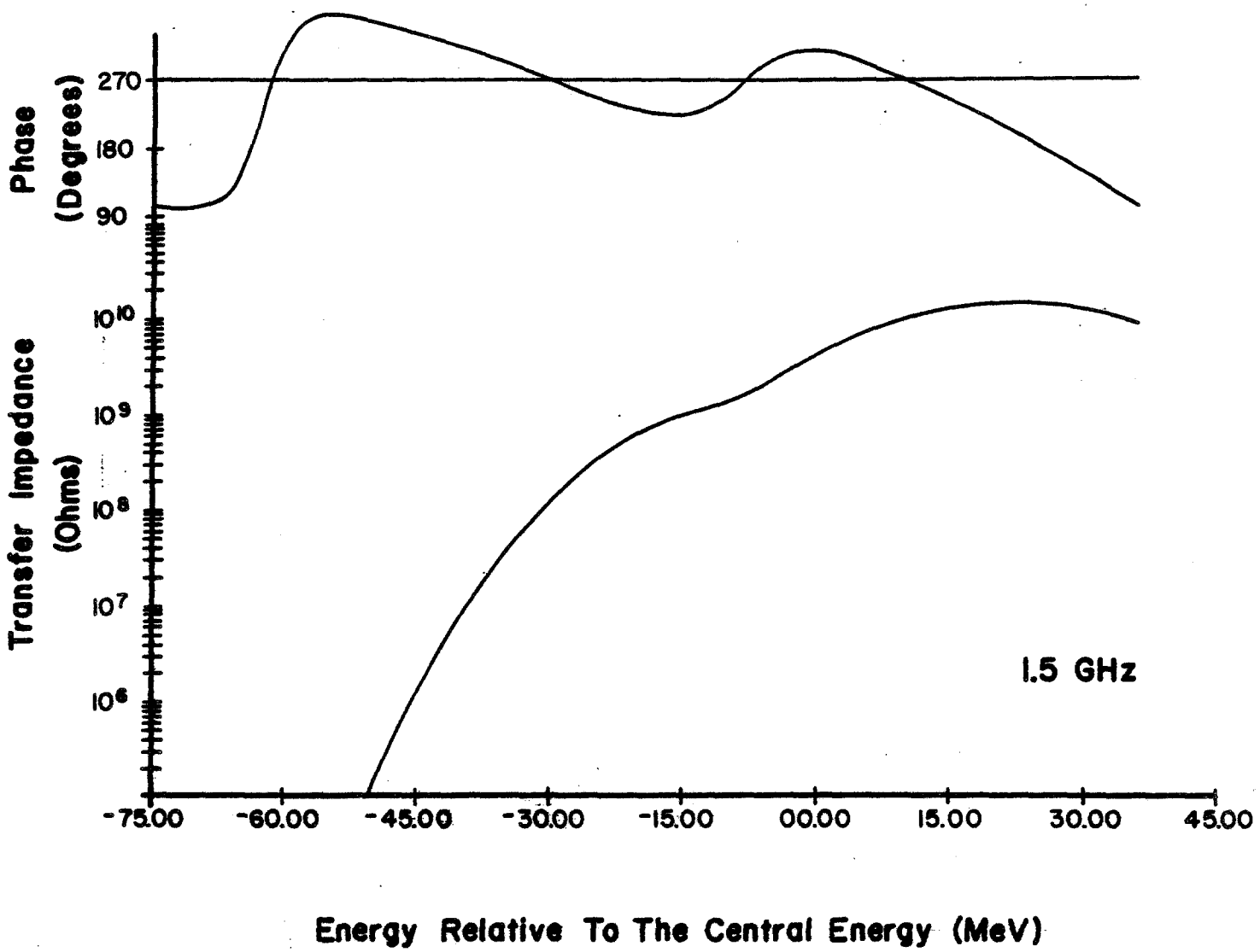
Phase
(Degrees)
270
180
90
Transfer Impedance
(Ohms)
10^{10}
10^{9}
10^{8}
10^{7}
10^{6}
1.5 GHz
-75.00
-60.00
-45.00
-30.00
-15.00
00.00
15.00
30.00
45.00
Energy Relative To The Central Energy (MeV)

Figure 5-13b

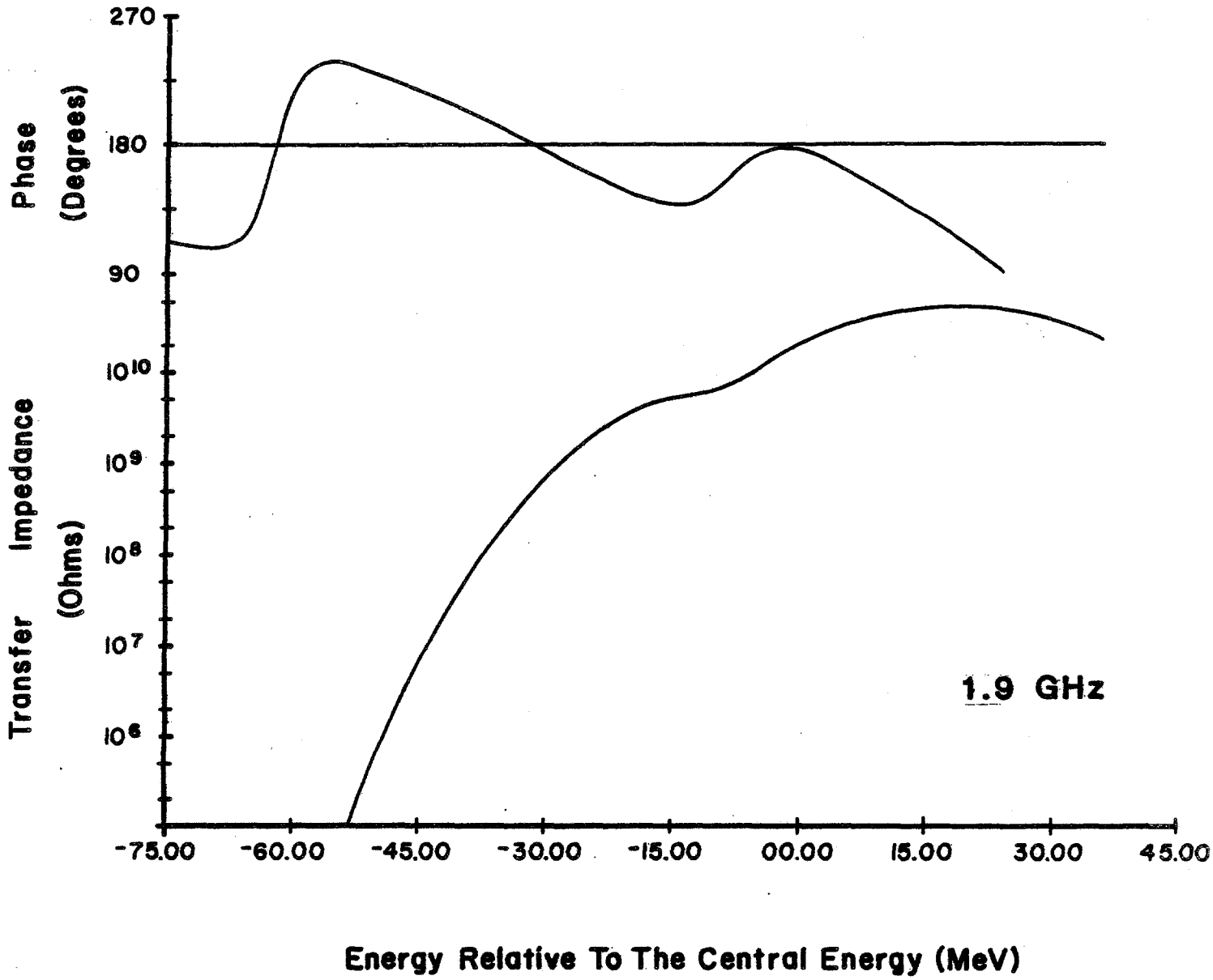
270
180
90
Phase (Degrees)
10^{10}
10^{9}
10^{8}
10^{7}
10^{6}
Transfer Impedance (Ohms)
1.9 GHz
-75.00
-60.00
-45.00
-30.00
-15.00
00.00
15.00
30.00
45.00
Energy Relative To The Central Energy (MeV)

Figure 5-13c

kicker, and P = P(f,E') is the pickup sensitivity. P depends on E' because P depends on particle position, which depends on E' (usually exponentially). The dependence of P on f comes from electrical properties and is usually weak.

This approximation is valid when the Schottky bands are well separated, but is a poor approximation for quantitative results for the system described here. Nonetheless, it is sufficient to show the main features of the physical process.

The closed-loop gain of the system is given by G' = G/(1-FG), where G is the open-loop gain ($G = V/I_D$) of the electronics going from pickup to kicker. If the real part of FG is less than zero, then G' < G and the cooling signal is suppressed. If the real part is greater than zero, the signal may be enhanced. If the real part of FG > 1, when the imaginary part is zero, the system is unstable. (This situation is completely analogous to the case of conventional electronic circuits with feedback).

In the approximate expression for F, one sees that there is a resistive (energy-absorbing) component of the beam response proportional to the gradient of the density at the driving frequency and a reactive component that depends on the asymmetry of the gradient about the driving frequency. It would be wrong to conclude, however, that the resistive term is the more important when looking at system stability. Both terms must be considered because the open-loop gain function G is a complex quantity; it unavoidably contains phase shifts from the filters and differences in time delays between pickup and kicker.

In fact, in the stack tail, the feedback can be dominated by the contribution from the particles in the core where $d\psi/dE$ is very large - 10^4 times larger than in the tail. Fortunately, $d\psi/dE$, which is increasing exponentially, is multiplied by the pickup response, which is decreasing exponentially. The rate of exponential increase of $d\psi/dE$ depends on the total gain profile, i.e., the product of pickup and filter response. The damping of $d\psi/dE$ in the feedback integral, however, depends only on the pickup response. Thus, it is important that the filter gain profile not be too sharp compared with the pickup in order to avoid severe problems with stability and signal suppression. The importance of the relative amounts of the gain profile derived from filters and pickups has been pointed out previously by Sacherer.[8]

An additional suppression of signal from particles in the core is provided by the subtracting pickups in each section. These pickups are placed closer to the core and normalized so that their sensitivity to the core region is equal and opposite to the sensitivity of the main pickups. In the stack tail, however, they subtract less than 10% of the signal. Several subtracting pickups followed by substantial attenuation are required to avoid having the subtracting pickups appreciably affect the amount of thermal noise in the pickups. Immediately after injection, the signal suppression is substantially larger because of the large values of

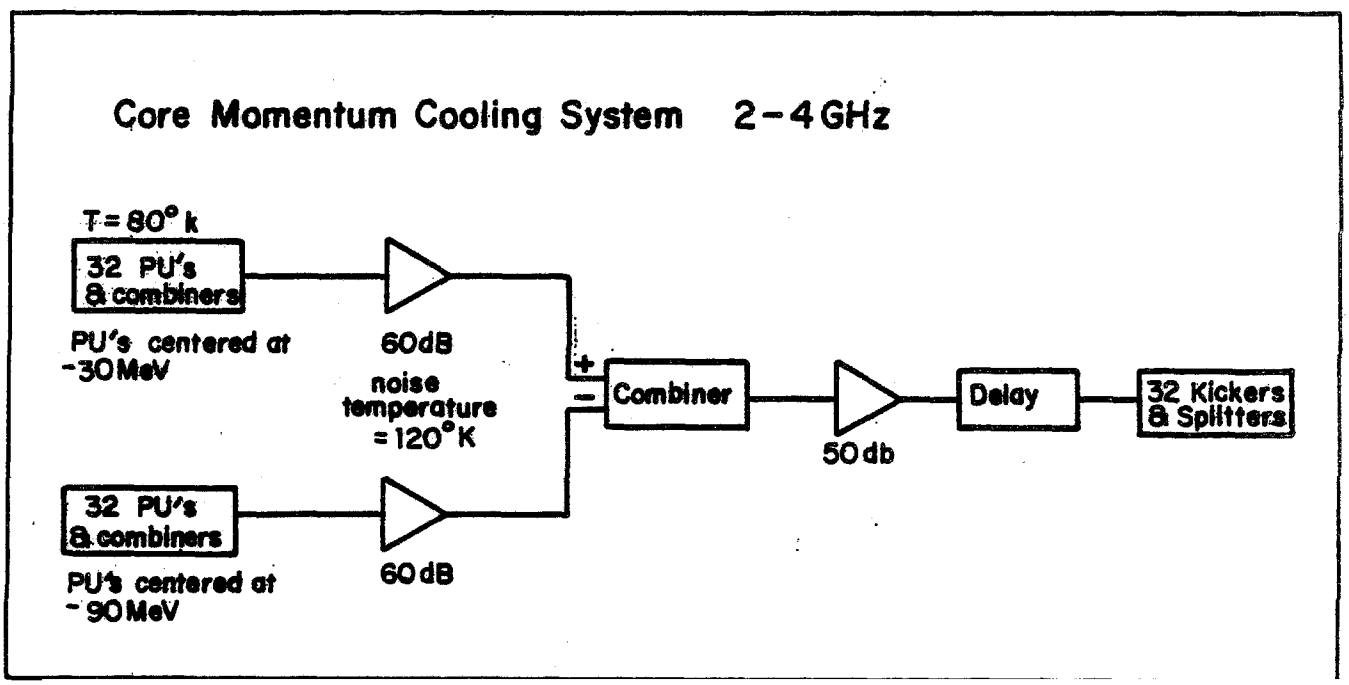
Core Momentum Cooling System 2-4 GHz
T = 80° k
32 PU's & combiners
PU's centered at -30 MeV
60dB
noise temperature = 120° K
+
−
Combiner
50 db
Delay
32 Kickers & Splitters
32 PU's & combiners
PU's centered at -90 MeV
60 dB

Figure 5-14

$d\psi/dE$ created by the RF stacking process. The gradients quickly (after 200 msec) smooth out because of the diffusion terms in the Fokker-Planck equation. It appears that during the first 200 msec of the injection cycle, it may be necessary to reduce the amplifier gain in order to maintain beam stability. This gain reduction has been taken into account in computer simulations and, in any event, is only of minor importance.

5.9.5 Core Cooling. The same Fokker-Planck equation that describes the stack-tail system also describes the core system. In fact, the distinction between core and tail cooling systems is somewhat arbitrary. The asymptotic distribution is given by

$$\Phi = F\Psi + (D_0 + D_1 + D_2\Psi)\ \frac{\partial \Psi}{\partial E} = 0 \qquad (5.12)$$

The cooling coefficient F has a zero at the peak of the core and a slope proportional to $g^2(E-E_c)$ where g is the electronic gain and E_c is the energy at the peak of the core. The other terms are heating terms. D_0 is the contribution of intrabeam scattering (via the Coulomb force) to the diffusion and has been calculated by Ruggiero[9] to be $D_0 = 0.0015\ N_{\bar{p}}$ $(eV)^2/sec$, where $N_{\bar{p}}$ is the total number of antiprotons in the Accumulator. This value of D_0 corresponds to a momentum heating time of 2 hr. D_0 is independent of both g and E. D_1 is the contribution of thermal noise and is proportional to g^2. D_2 is the Schottky heating term and is proportional to $g^2\ (E-E_c)^2$. In our system D_1 is small compared with D_0. Optimum performance occurs when g is adjusted so that intrabeam scattering dominates in the central part of the core and the Schottky heating term dominates at the edges of the core. Smaller values of g leave the cooling term F less than optimum (g = 0 means no cooling) and larger values of g mean that Schottky heating is larger than the cooling. Computer calculations show that densities in excess of $1 \times 10^5/eV$ can be reached.

The choice of 1 - 2 GHz bandwidth (and $\eta = 0.02$) for the tail system was made because of the desire to optimize core cooling. Since D_2 is proportional to $1/\eta$, a larger gain can be used to counteract intrabeam scattering in the core. Choosing a higher maximum frequency and the same momentum width for the stack tail system would have required a lower η for the lattice. This would have reduced the core cooling effectiveness.

A block diagram of the core cooling system is shown in Fig. 5-14. The zero in gain is obtained by subtracting the signals from two sets of pickups placed in a region of high momentum dispersion. One set of pickups is centered above the core energy and one is centered below. The signal is then applied to a kicker placed in a region of zero momentum dispersion. The gain profile for the core system Schottky bands at 2.2, 3.0, and 3.8 GHz is shown in Fig. 5-15 abc.

5.9.6 Numerical Calculations of Momentum Cooling. A computer simulation of the combined core and stack-tail momentum cooling systems has been made. These calculations use the full theory developed by van der Meer et al and not the simplified models given here. It has been found that a core density of 1×10^5/eV can be obtained after 4 hours of stacking with an average flux of 4×10^7 sec^{-1}. Figure 5-16 shows the stack profile as a function of time. Figure 5-17 shows the cooling term (F) including the effects of beam feedback after 3 hours. Figures 5-18 and 5-19 show the heating term coefficients $D_0 + D_1$ and D_2. Figures 5-20 and 5-21 are stability plots: the real versus the imaginary part of the cooling system gain G times the beam feedback F. In this plot the system is stable if the curve does not enclose the point (1,0).

5.10 Betatron Cooling

5.10.1 Introduction. Betatron cooling is accomplished by using a pickup sensitive to the transverse displacement of the particles. In going from pickup to kicker the particle oscillates in betatron phase by an odd multiple of $\pi/2$, converting the position displacement to an angle displacement. Each given particle creates a signal in the pickup which, when applied to the kicker, decreases the angle displacement. Other particles with similar revolution frequencies contribute noise that tends to increase the betatron amplitude. This situation is similar to the momentum-cooling discussed earlier.

Betatron cooling is conventionally described in terms of the time decrease of the betatron emittance[10]

$$\frac{d\bar{\varepsilon}}{dt} = \frac{W}{N}\left(2g - g^2(M+U)\right)\bar{\varepsilon} \quad , \tag{5.13}$$

where W is the system bandWidth, N is the number of particles being cooled, g is the system gain, M is the mixing factor, and U is the ratio of noise to signal power. The rms beam size is the square root of the beta function times $\bar{\varepsilon}$. Equation (5.13) can be an exact result if the definition of g is given by a sum over Schottky bands of a gain function including signal suppression. Some algebraic license is also required to define g^2 as something different than g times g. However, the approach taken here will be that the gain function is constant, independent of frequency. The sum over Schottky bands is therefore trivial.

For the loop pickups and kickers that we plan to use, g is defined by

$$g = N \beta_p \beta_k n_p n_k \left(\frac{d}{h}\right)^2 \frac{e f_o Z_{pu}}{(\beta^2 E/e)} \frac{g_A}{k} \quad , \tag{5.14}$$

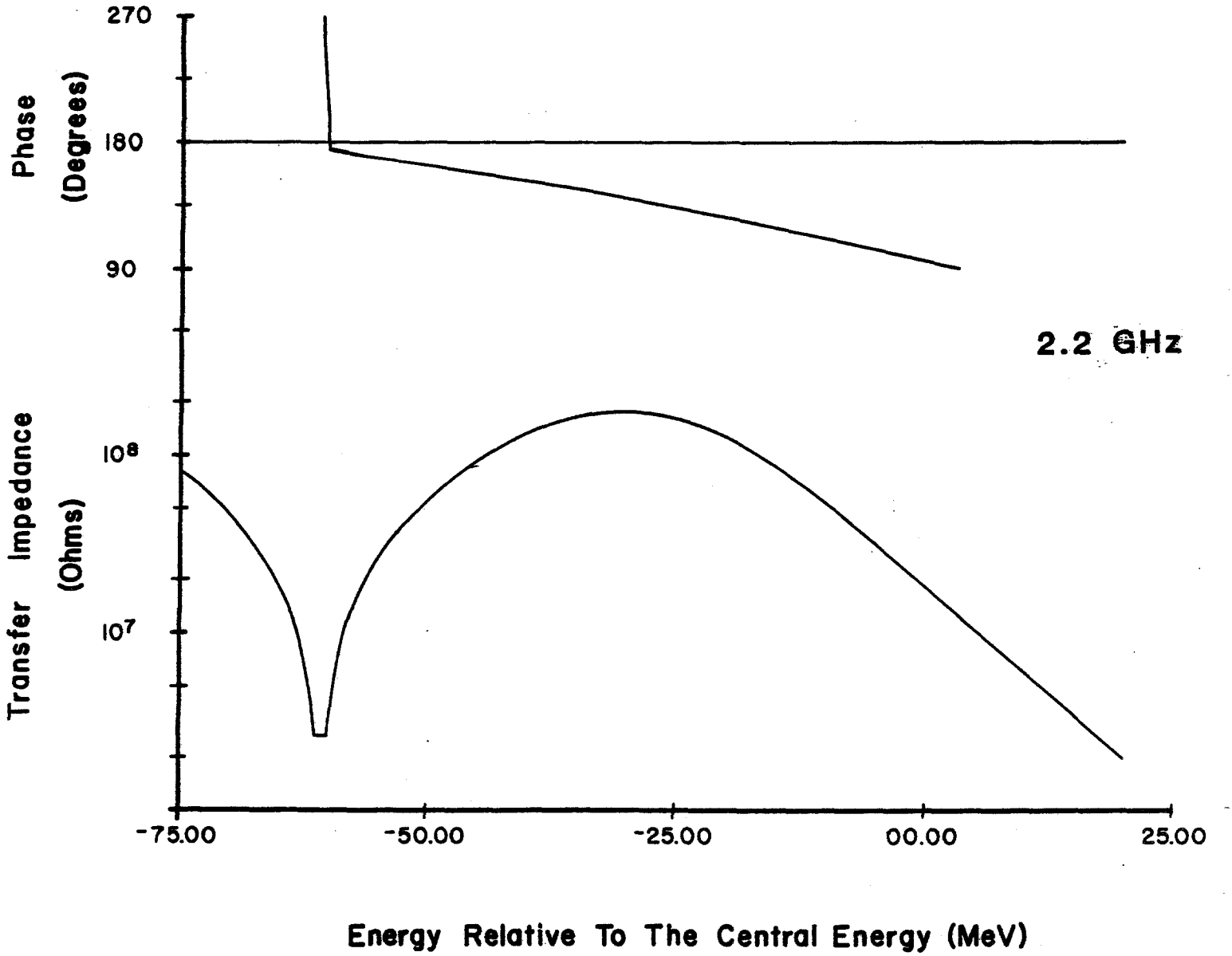
270
180
90
Phase
(Degrees)
2.2 GHz
10^8
10^7
Transfer Impedance
(Ohms)
-75.00
-50.00
-25.00
00.00
25.00
Energy Relative To The Central Energy (MeV)

Figure 5-15a

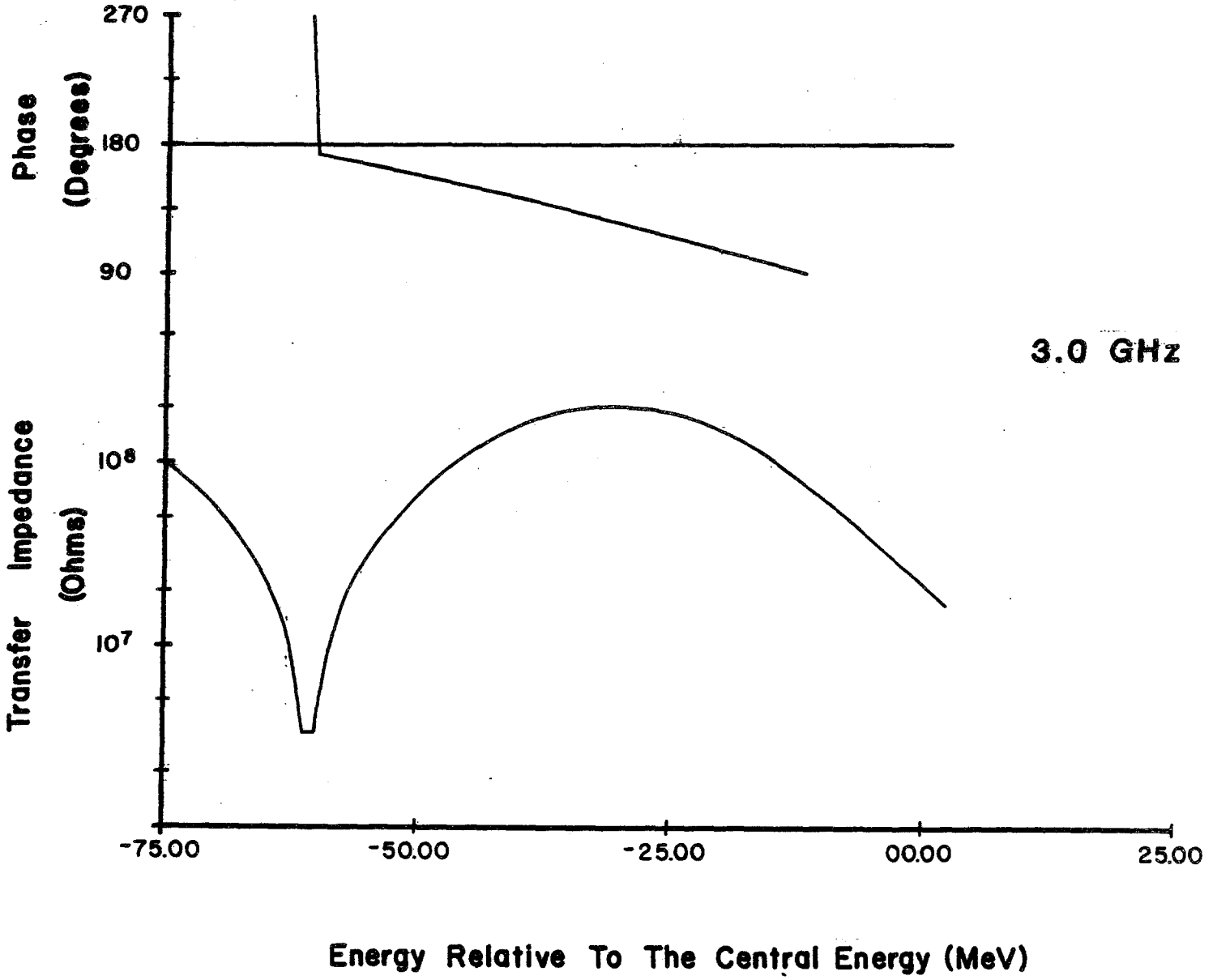
270
180
90
Phase
(Degrees)
3.0 GHz
10^8
10^7
Transfer Impedance
(Ohms)
-75.00
-50.00
-25.00
00.00
25.00
Energy Relative To The Central Energy (MeV)

Figure 5-15b

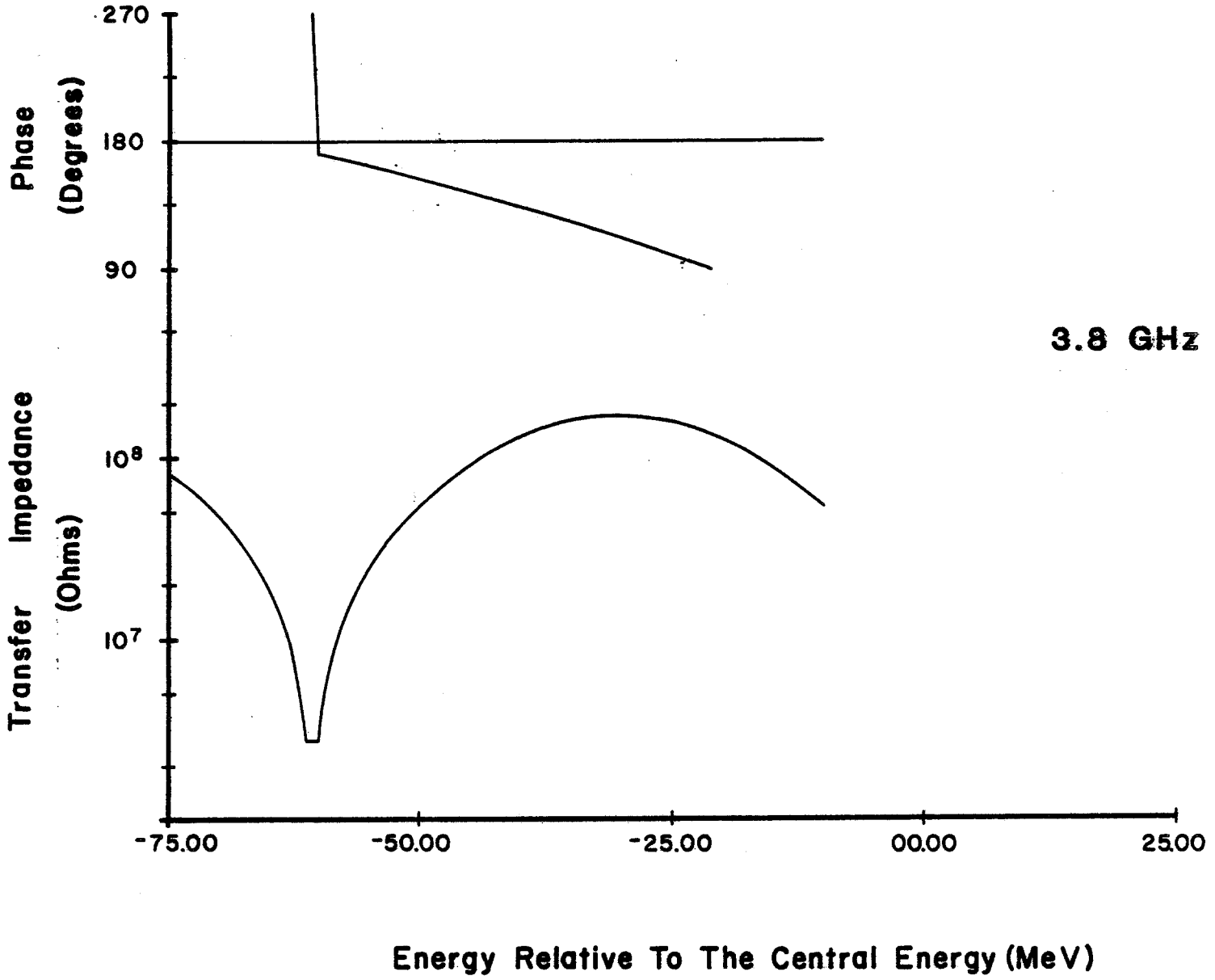
270
180
90
Phase
(Degrees)
3.8 GHz
10^8
10^7
Transfer Impedance
(Ohms)
-75.00
-50.00
-25.00
00.00
25.00
Energy Relative To The Central Energy (MeV)

Figure 5-15c

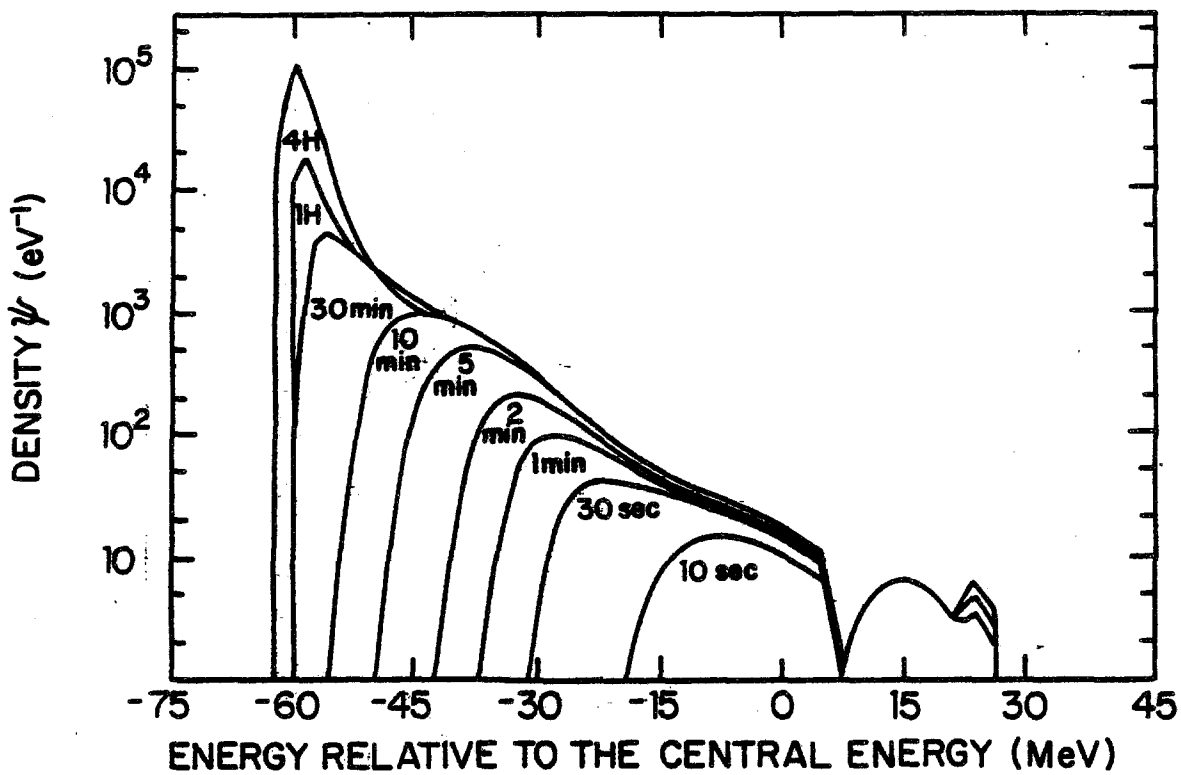
DENSITY ψ (eV⁻¹)
10⁵
10⁴
10³
10²
10
4H
1H
30min
10 min
5 min
2 min
1min
30 sec
10 sec
-75
-60
-45
-30
-15
0
15
30
45
ENERGY RELATIVE TO THE CENTRAL ENERGY (MeV)

Figure 5-16

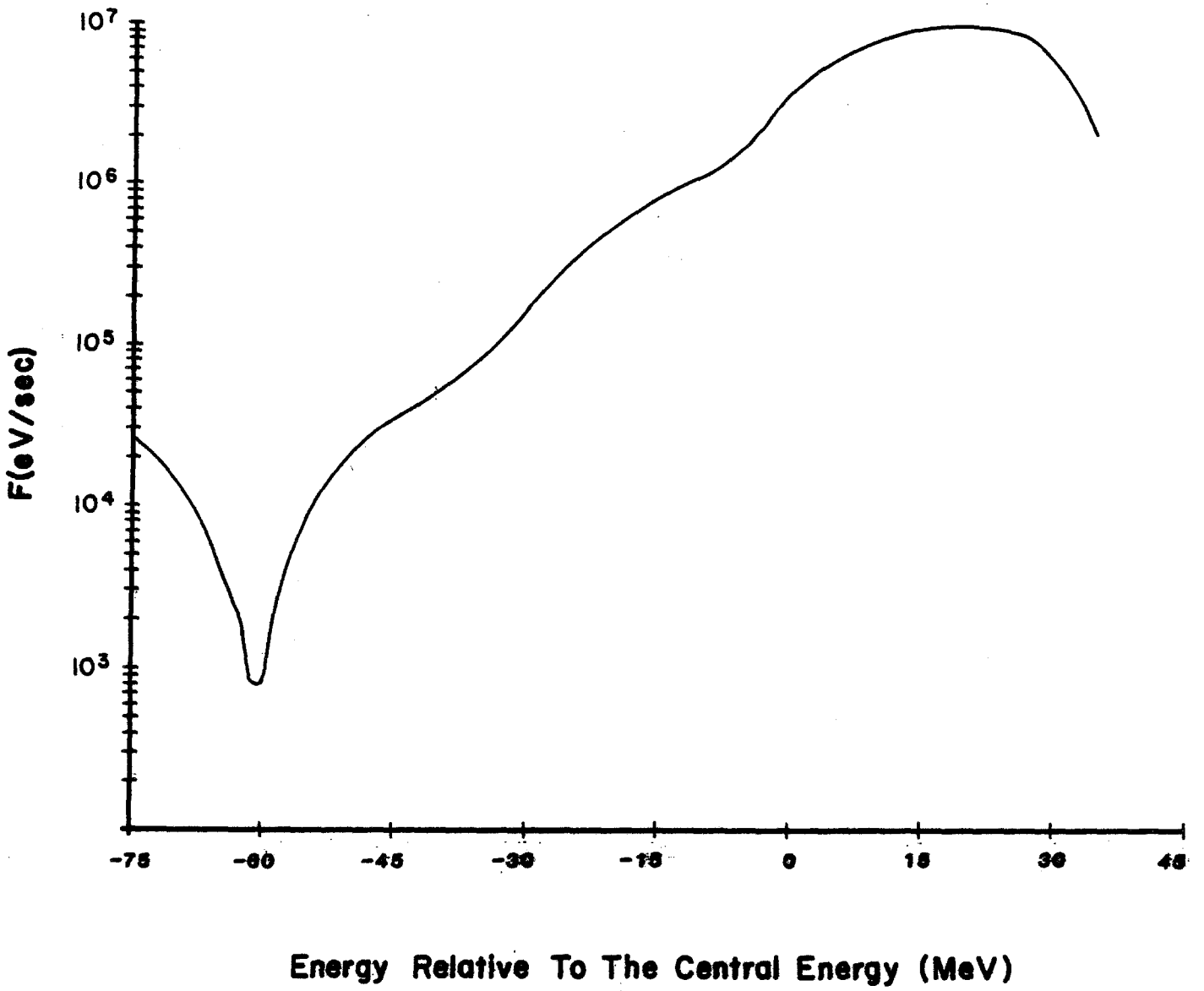
10^7
10^6
10^5
10^4
10^3
F(eV/sec)
-75
-60
-45
-30
-15
0
15
30
45
Energy Relative To The Central Energy (MeV)

Figure 5-17

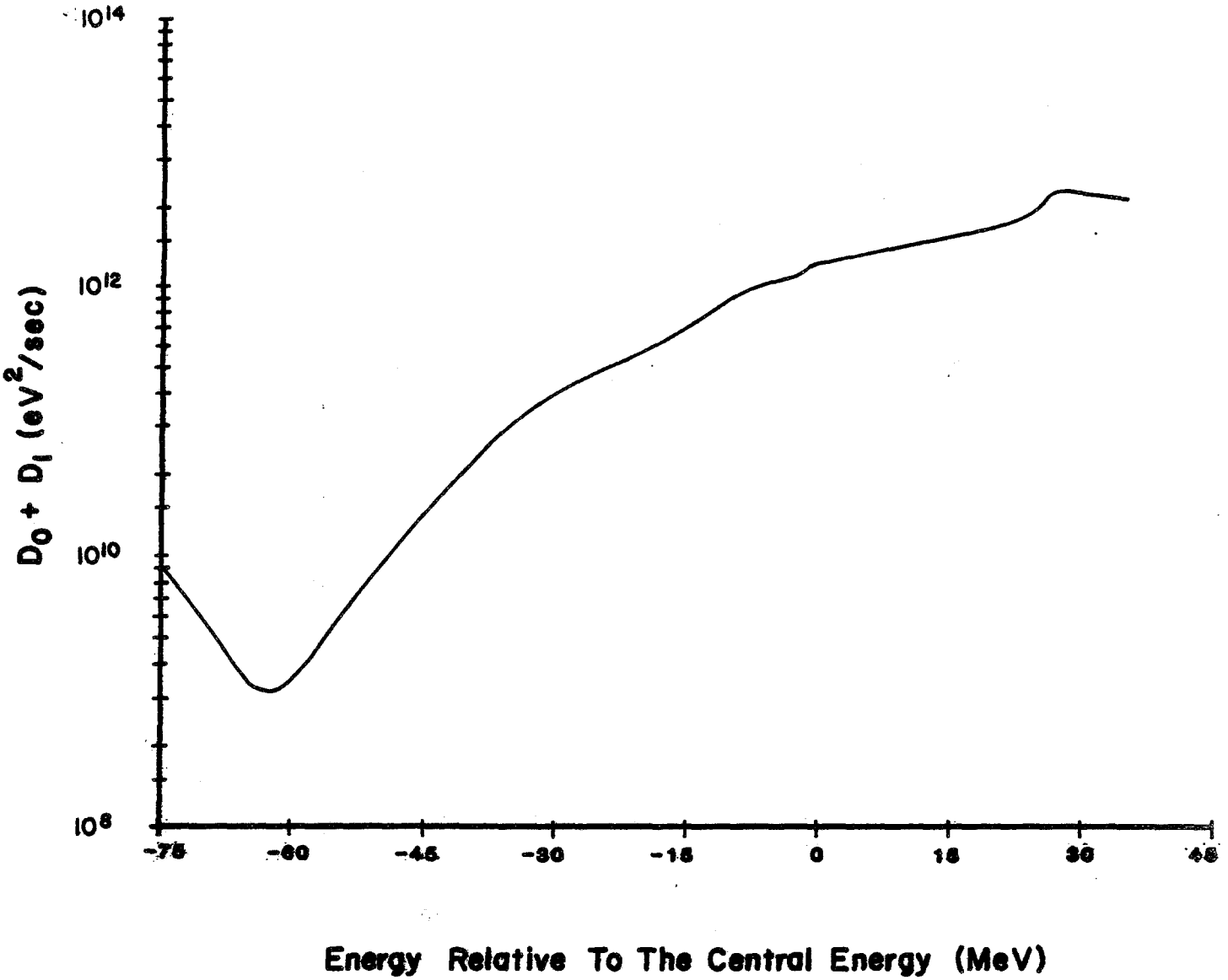
10^{14}
10^{12}
10^{10}
10^{8}
$D_0 + D_1$ (eV^2/sec)
-75
-60
-45
-30
-15
0
15
30
45
Energy Relative To The Central Energy (MeV)

Figure 5-18

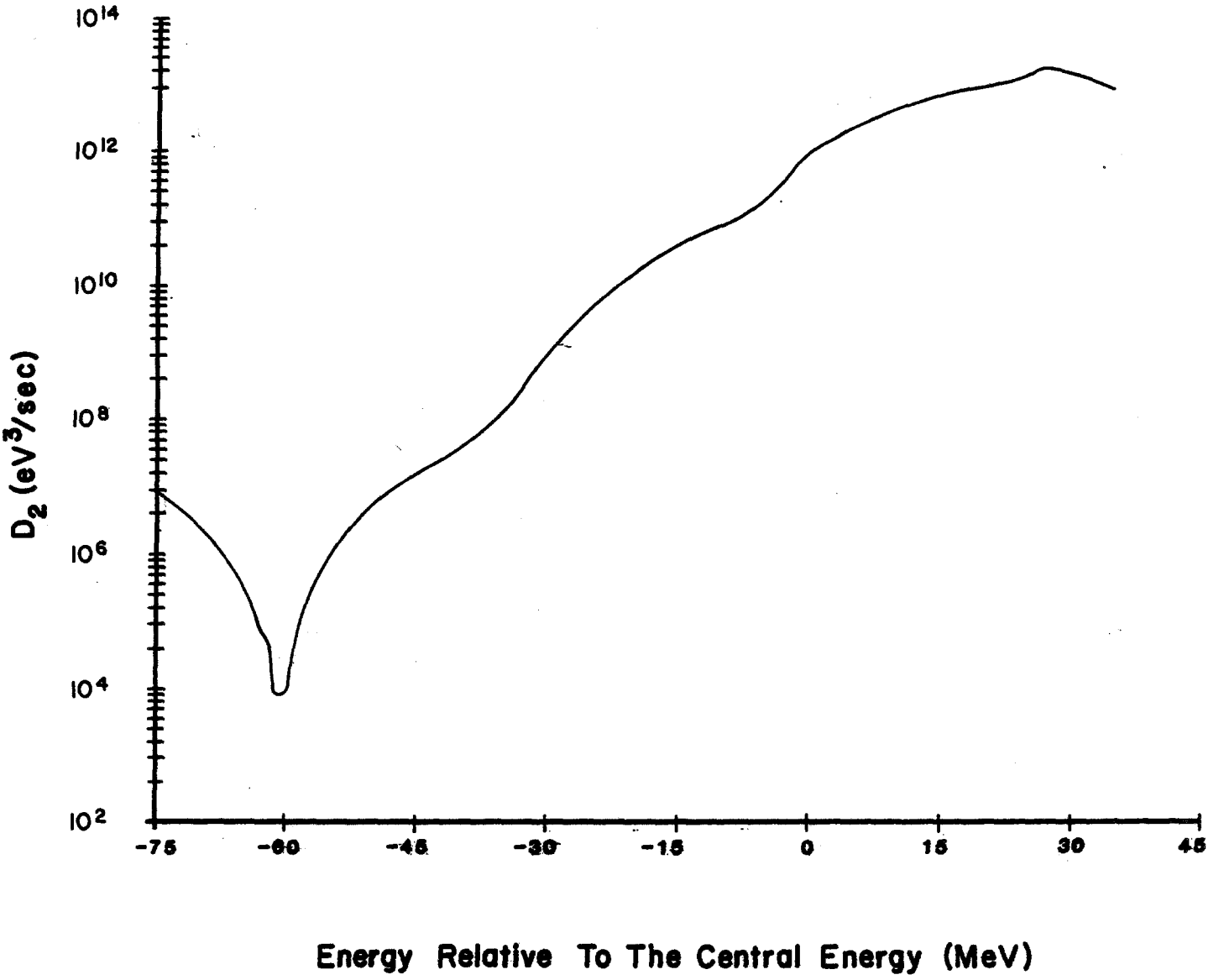
10^{14}
10^{12}
10^{10}
10^{8}
10^{6}
10^{4}
10^{2}
D_2 (eV^3/sec)
-75
-60
-45
-30
-15
0
15
30
45
Energy Relative To The Central Energy (MeV)

Figure 5-19

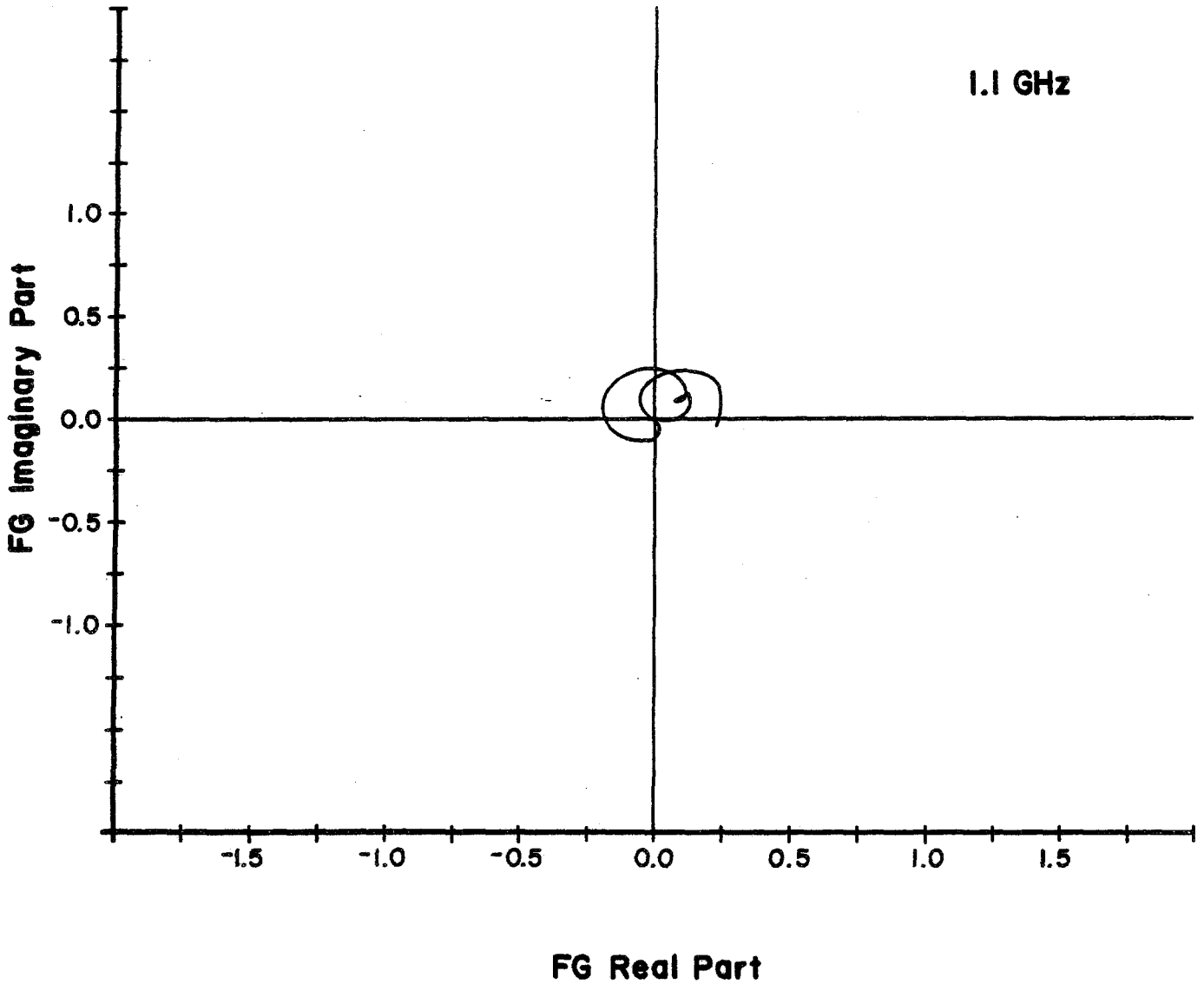
1.1 GHz
FG Imaginary Part
1.0
0.5
0.0
-0.5
-1.0
-1.5
-1.0
-0.5
0.0
0.5
1.0
1.5
FG Real Part

Figure 5-20a

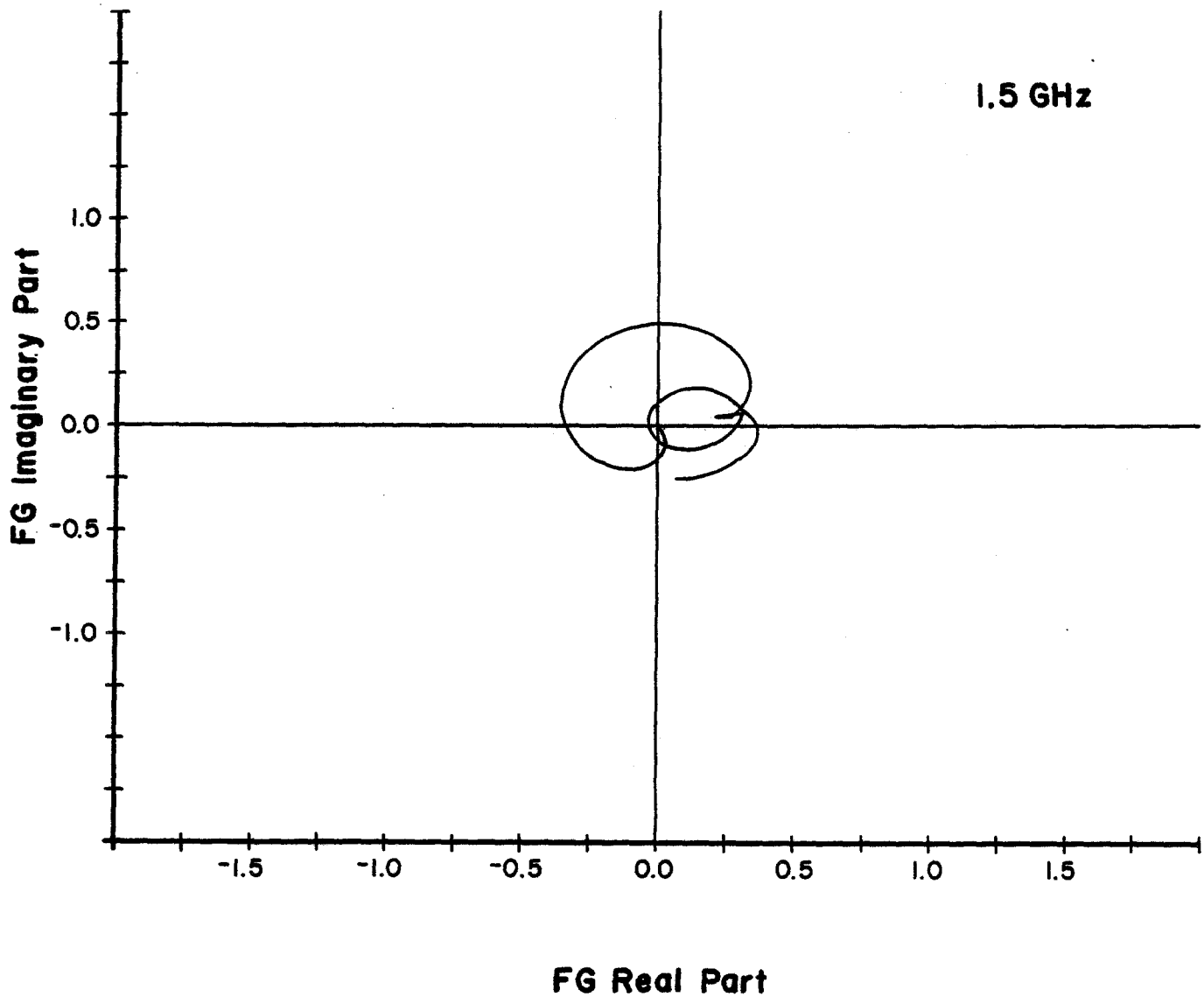
1.5 GHz
FG Imaginary Part
1.0
0.5
0.0
-0.5
-1.0
-1.5
-1.0
-0.5
0.0
0.5
1.0
1.5
FG Real Part

Figure 5-20b

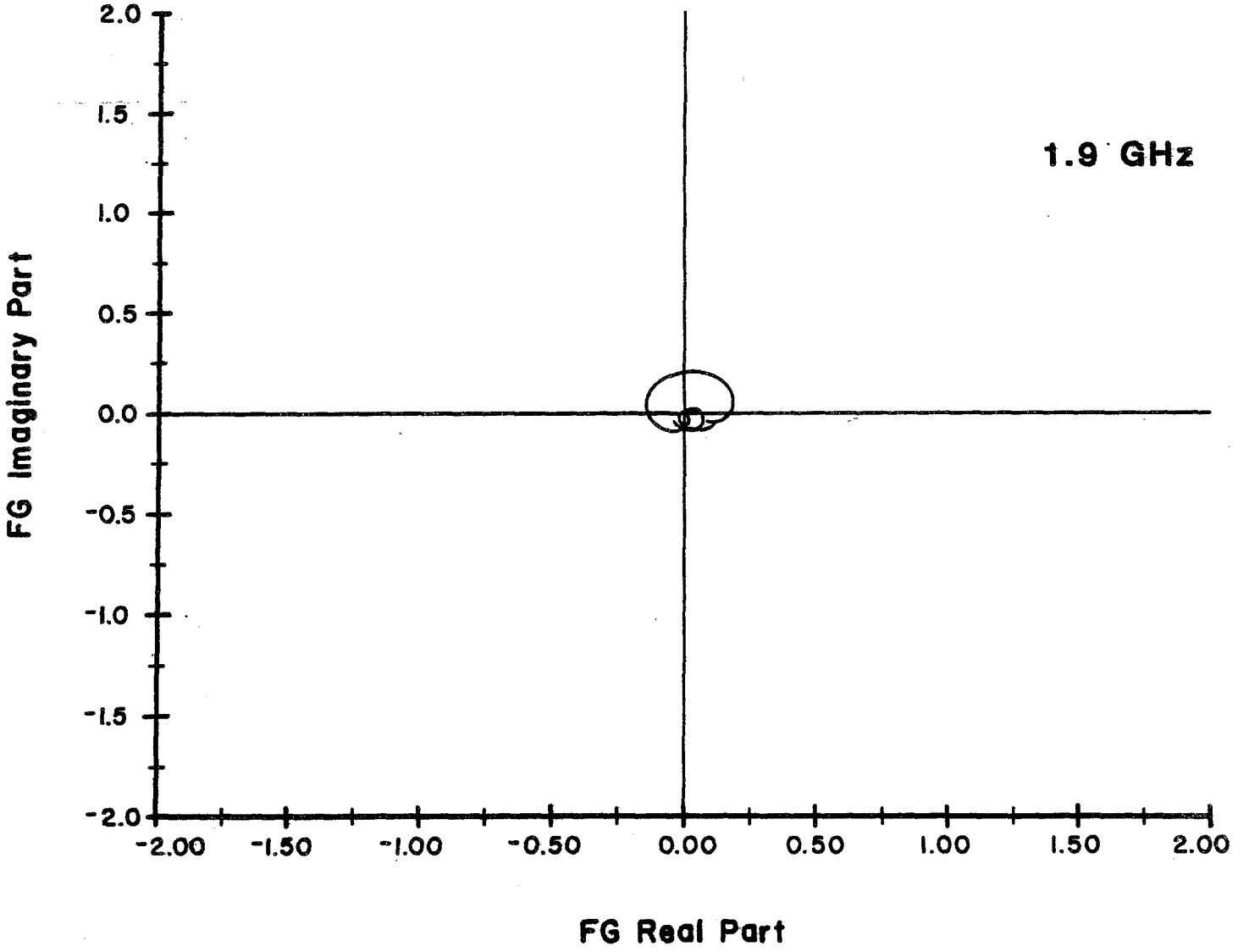
1.9 GHz
FG Imaginary Part
FG Real Part
2.0
1.5
1.0
0.5
0.0
-0.5
-1.0
-1.5
-2.0
-2.00
-1.50
-1.00
-0.50
0.00
0.50
1.00
1.50
2.00

Figure 5-20c

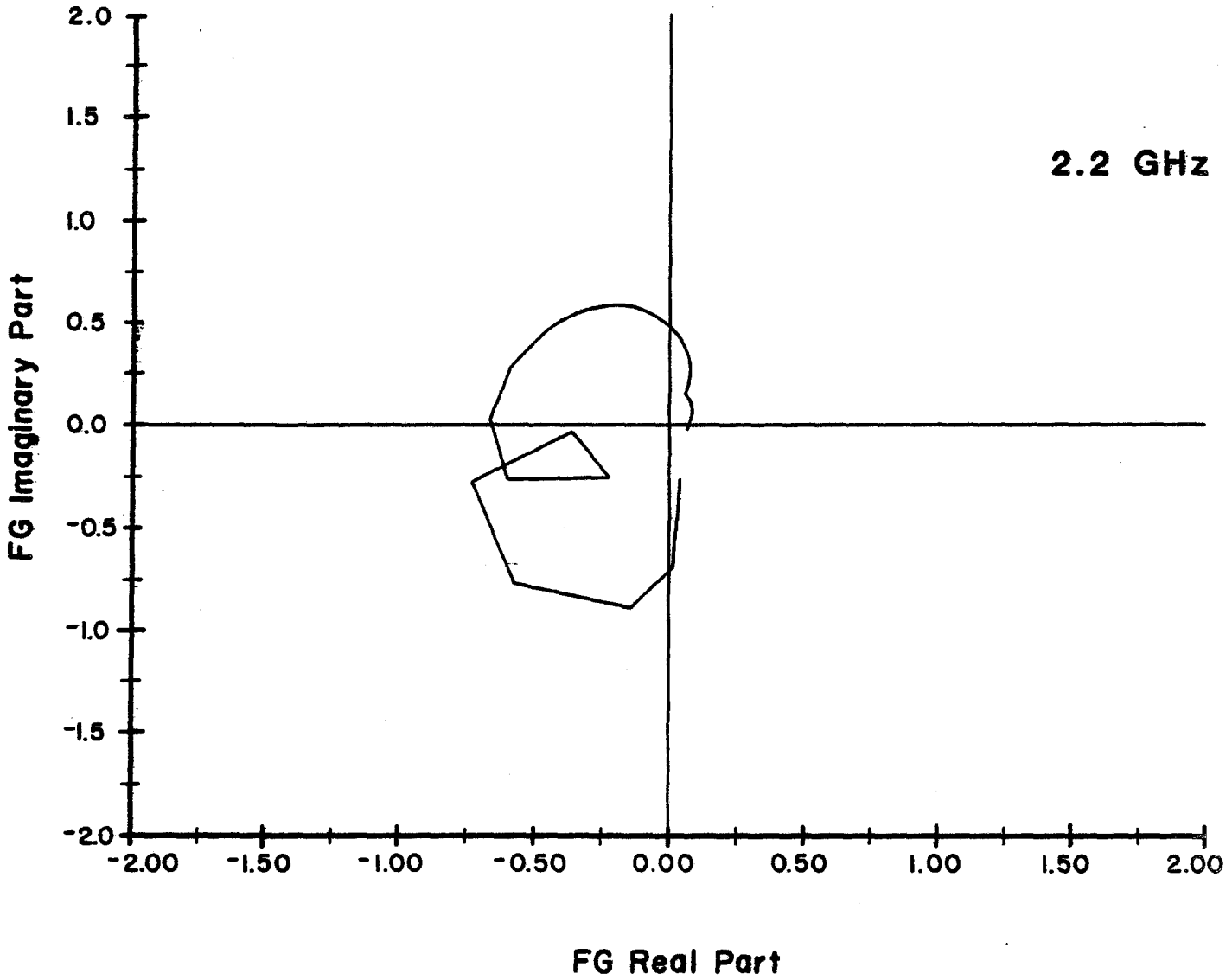
2.2 GHz
FG Imaginary Part
FG Real Part
2.0
1.5
1.0
0.5
0.0
-0.5
-1.0
-1.5
-2.0
-2.00
-1.50
-1.00
-0.50
0.00
0.50
1.00
1.50
2.00

Figure 5-21a

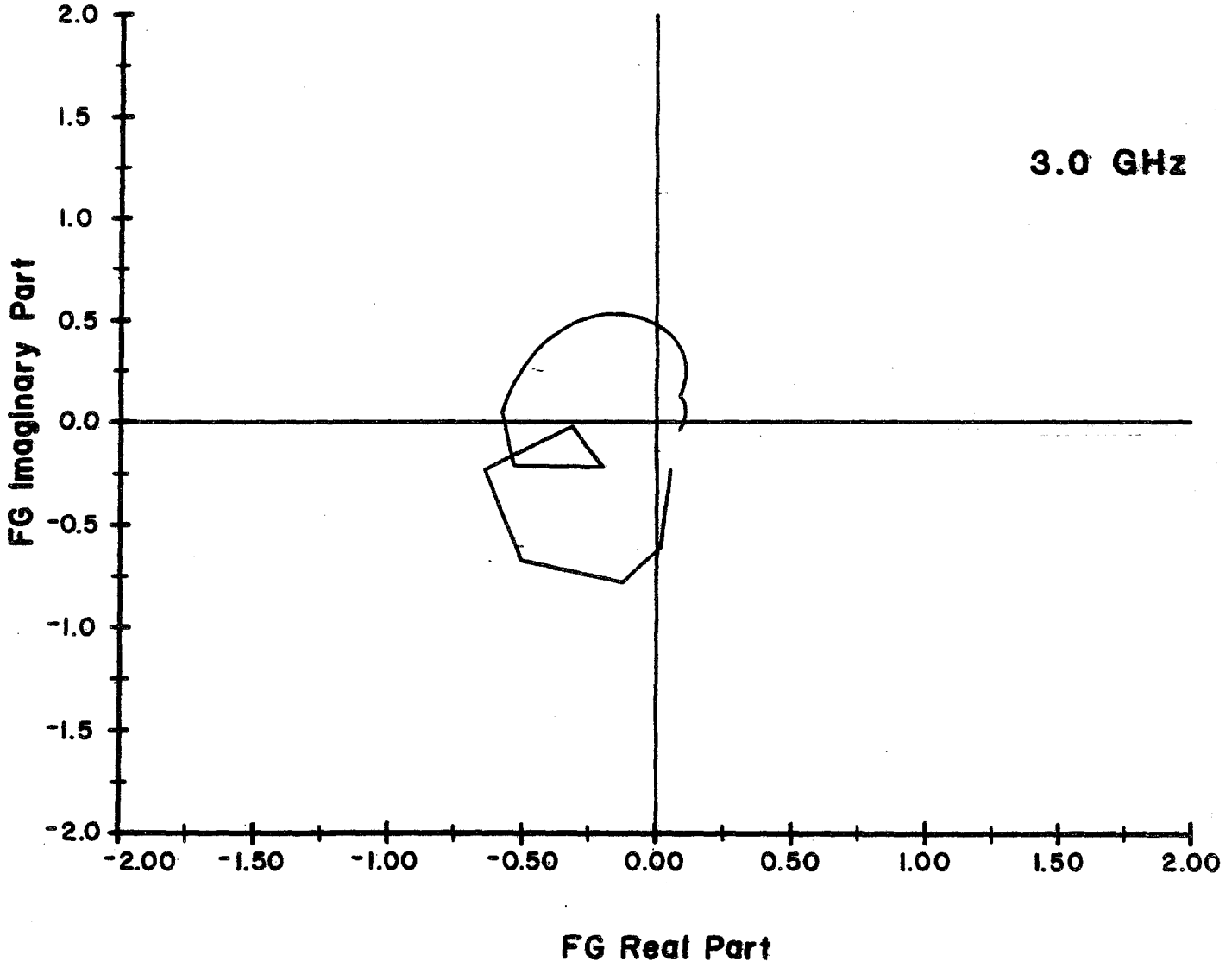
3.0 GHz
FG Imaginary Part
FG Real Part
2.0
1.5
1.0
0.5
0.0
-0.5
-1.0
-1.5
-2.0
-2.00
-1.50
-1.00
-0.50
0.00
0.50
1.00
1.50
2.00

Figure 5-21b

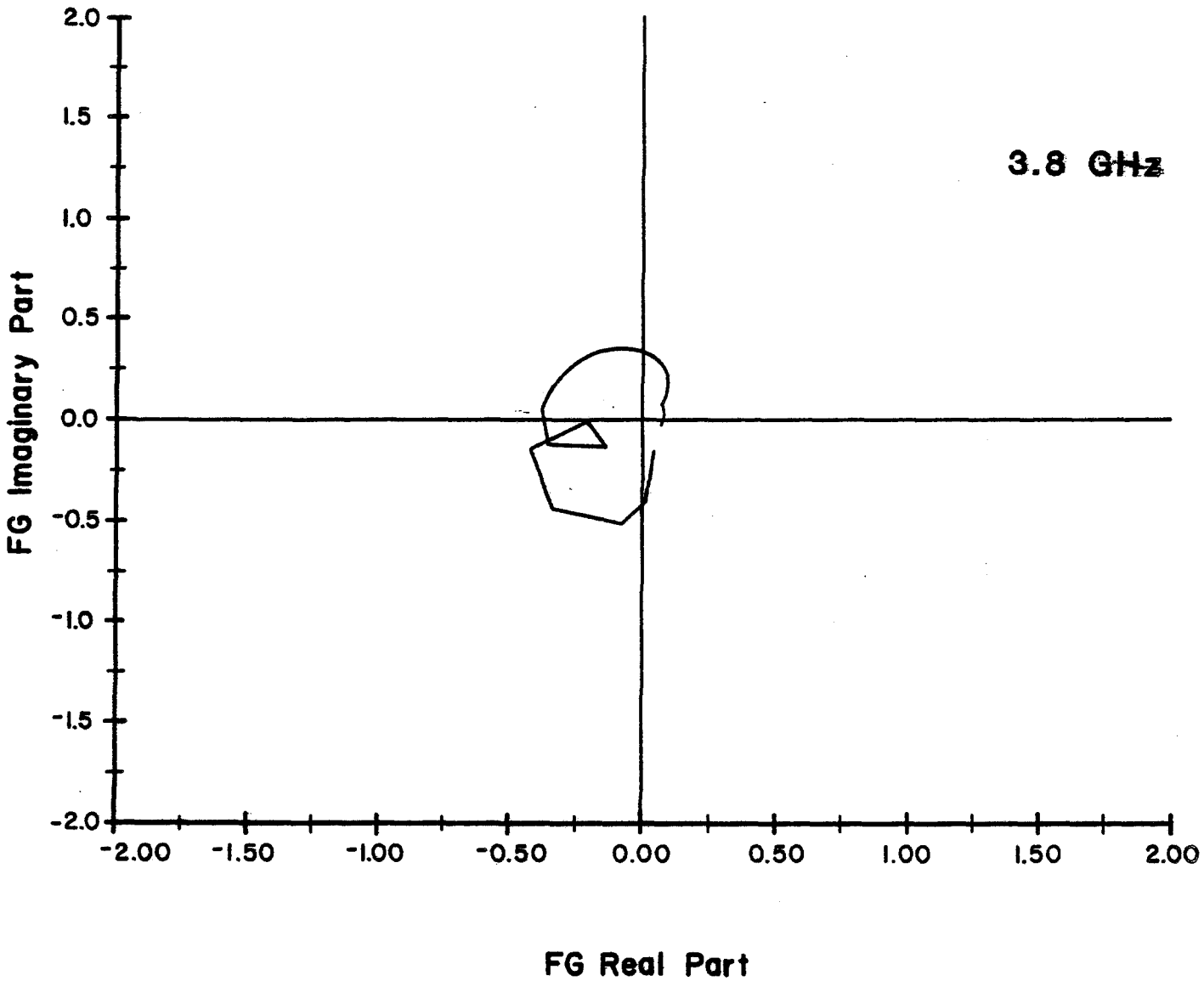
3.8 GHz
FG Imaginary Part
FG Real Part
2.0
1.5
1.0
0.5
0.0
-0.5
-1.0
-1.5
-2.0
-2.00
-1.50
-1.00
-0.50
0.00
0.50
1.00
1.50
2.00

Figure 5-21c

where $\beta_p(\beta_k)$ is the function at the pickup (kicker), $n_p(n_k)$ is the number of pickups (kickers), d is the pickup and kicker sensitivity defined in section 5.11.1, h is the pickup and kicker gap, g_A is the amplifier gain, and $k=\omega/\beta c$. In order for g to be independent of frequency, g_A must increase linearly with frequency. The optimum gain profile would be for g to increase with frequency and therefore for g_A to increase with frequency squared. The effect of signal suppression is to modify 5.2. At small values of amplifier gain, such as exist in the stack tail betatron cooling system, the signal suppression is small and can be ignored. As the gain is increased to obtain the optimum cooling the beam feedback reduces the effective gain of the system by a factor of 2 at the center of a symmetric distribution that is peaked at the center. Off center, the value of the suppression factor depends on the shape of the distribution, but it is generally true that the cooling is slowest at the peak of the distribution. For a system like the core betatron cooling system, it is sufficient to perform calculations ignoring signal suppression, remembering that the actual amplifier gain required is 2 g_A.

The mixing factor M is the ratio of the peak power density in the Schottky band to a uniform power density of the same power. For a system with constant gain g,

$$M = \frac{f^2\psi(f)\Lambda}{2WN} = \frac{f\beta^2 E\psi(E)\Lambda}{2WN\,\eta} \quad , \tag{5.15}$$

where f is the revolution frequency, $\psi(f)$ is the particle density (number/Hz), $\psi(E)$ is the particle density (number/eV), $\Lambda=\ln 2$, and $\eta=1/\gamma_t^2 - 1/\gamma^2$.

The total thermal power in the system is

$$P_T = k_B(\theta_R+\theta_A)g_A^2 W \quad , \tag{5.16}$$

where k_B is Boltzman's constant (1.38×10^{-23} Joules/K), θ_R is the temperature of the pickup terminating resistor, θ_A is the equivalent noise temperature of the amplifier. Strictly speaking, g_A^2 should be averaged over the system bandwidth, but it suffices to take the value at midband. The Schottky power is

$$P_S = \frac{1}{2} N e^2 f_o Z_{pu} \left(\frac{d}{h}\right)^2 \beta_p n_p \bar{\varepsilon} g_A^2 W; \tag{5.17}$$

U is the ratio of noise to signal power

$$U = \frac{P_T}{P_S} \tag{5.18}$$

5.10.2 Betatron Cooling in the Core. Betatron cooling in the core is limited by the relatively large density of particles. The cooling is therefore necessarily a slow one, accomplished with low power and a large signal to noise ratio. The core betatron cooling is accomplished with two identical systems. A schematic of one system is given in Fig. 5-22. Both pickups and kickers are located in zero dispersion straight sections. The betatron phase advance between pickup and kicker is $2\text{-}3/4\times 2\pi$ in the horizontal and $2\text{-}3/4\times 2\pi$ in the vertical. After 4 hours of stacking there are 5×10^{11} particles in the core, with a peak density of 10^{5}/eV. For W=2 GHz and η=0.02 the mixing factor M is equal to 10. Other relevant parameters are $\beta_D=\beta_K=6$, $n_D=n_K=8$, h=3 cm, d=1.73, $Z_{PU}=75\,\Omega$, $\theta_A=\theta_R=373$ K. With these parameters U=0.5 for the final emittance $\bar{\varepsilon}=0.5\,\pi$ mm-mrad. From Eq. (5.13) it can be seen that the maximum cooling rate is obtained when

$$g = \frac{1}{M+U} \quad , \tag{5.19}$$

For this value of g the amplifier gain at midband according to Eq. (5.16) is g_A=100 dB. If the signal suppression effect is included the required gain will become 106 dB. The Schottky power is given approximately by Eq. (5.3) with g_A=100 dB and is about 1 watt. The thermal power is given approximately by Eq. (5.16) with g_A=106 dB (most of the thermal power is between Schottky bands and not greatly affected by the suppression). The thermal power is also about 1 watt.

5.10.3 Stack-Tail Betatron Cooling. The stack tail betatron cooling system uses the same pickups as the second section of the tail momentum-cooling system. The pickup plates are centered at -1 MeV relative to the central energy. For horizontal signals the pickup is most sensitive at its edges at +21 MeV and -19 MeV. Most of the cooling takes place at the -19 MeV edge because the momentum cooling system is pushing particles much more slowly past the -19 MeV edge than the +21 MeV edge. The pickup is most sensitive at its center (-1 MeV) for signals in the vertical direction. The kickers are also placed at -1 MeV in a region with high dispersion. A block diagram of the system is shown in Fig. 5-23.

Approximate calculations of the system performance have been made with Eq. (5.13) except that the time variable has been replaced with the energy variable, using the relationship

$$\frac{dE}{dt} = \frac{\Phi}{\psi(E)} \quad ,$$

where Φ is the flux of particles and $\psi(E)$ is the density of particles. This approximation ignores fluctuations in energy gain in the stacking process. With this approximation, Eq. (5.13) is easily integrated numerically. Figure 5-24 shows the emittance reduction as a function of energy. The thermal power in each system is 10W and the Schottky betatron

CORE BETATRON COOLING SYSTEM 2-4 GHz

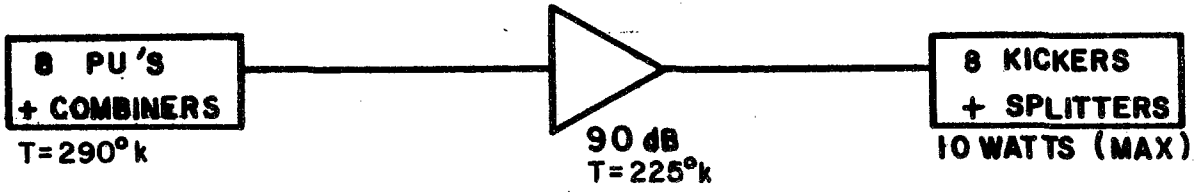

Figure 5-22

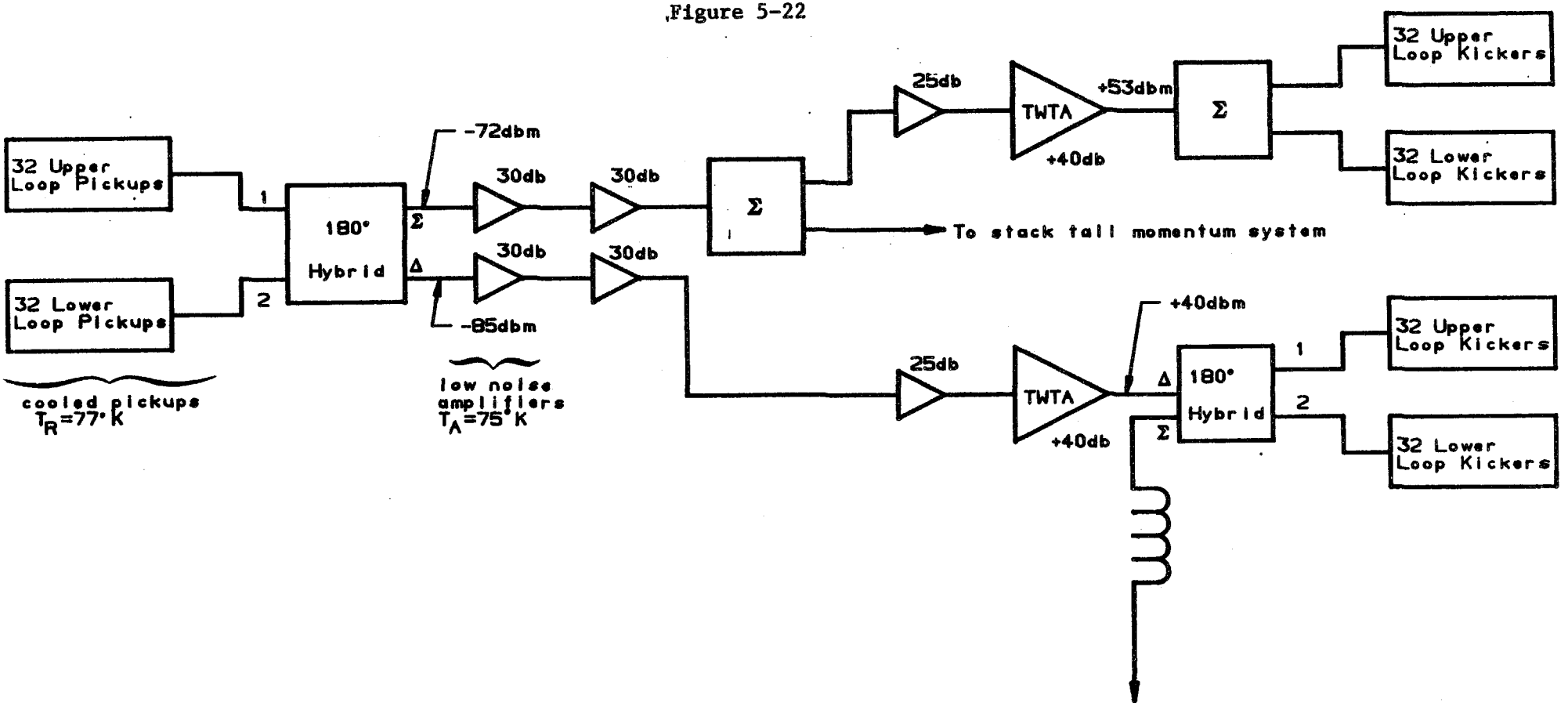

Stack Tail Betatron Cooling System

Figure 5-23

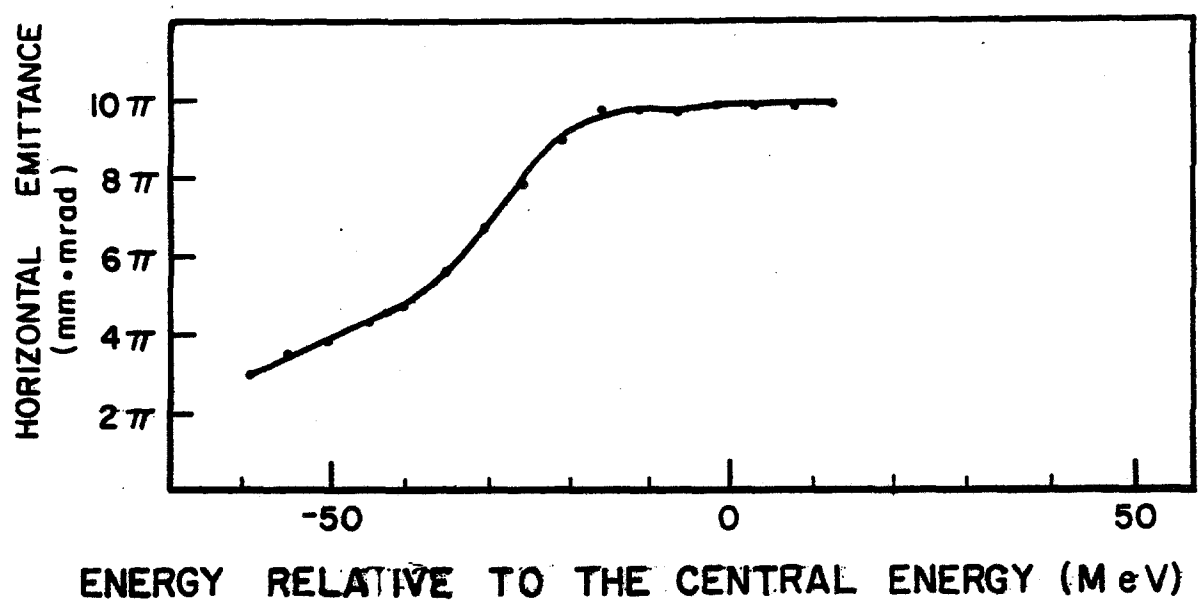
HORIZONTAL EMITTANCE
(mm • mrad)
10π
8π
6π
4π
2π
-50
0
50
ENERGY RELATIVE TO THE CENTRAL ENERGY (MeV)

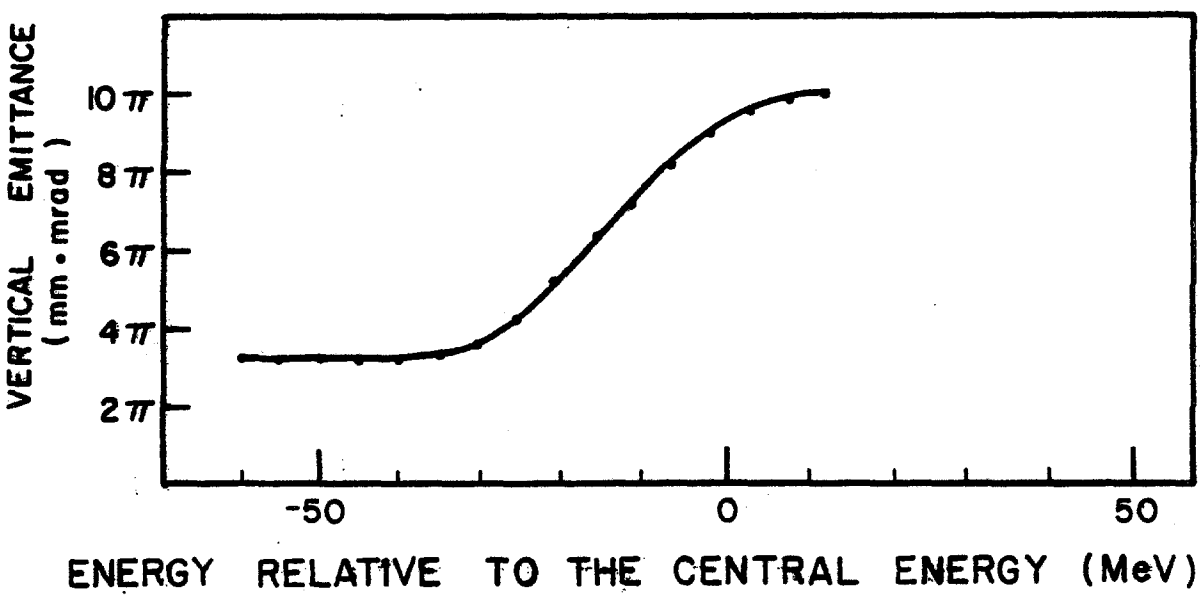
VERTICAL EMITTANCE
(mm • mrad)
10π
8π
6π
4π
2π
-50
0
50
ENERGY RELATIVE TO THE CENTRAL ENERGY (MeV)

Figure 5-24

sideband power is 10W. The horizontal system has a large momentum Schottky signal as well-about 200W.

5.10.4 Operation of Betatron Cooling Systems. In the Accumulator we have available two betatron cooling systems, either of which is capable, or nearly capable, of cooling the beam emittance from 10 to 2π mm-mrad. The core system is clearly required so that a core of $\bar{p}$'s may be held for several hours without diffusion. The tail system serves two functions: 1) to cool the betatron amplitudes in a system with a low particle density (it is not necessary to wait one half to one hour for the core cooling system to do its work) and 2) to counteract possible betatron heating by the momentum-cooling system. The size of the latter effect is difficult to estimate; it depends on how well we are able to build the momentum kickers for the stack-tail system. If the effect is larger than expected, the gain of the stack-tail system can be raised to achieve better cooling, but, of course, the power requirements will be greater. Tentatively, however, we would plan to use the stack-tail system to reduce the beam emittance by about a factor of e and use the core system to reduce it below 2π mm-mrad.

5.11 Stochastic-Cooling Hardware

The purpose of this section is to outline the hardware and techniques we expect to use in order to meet the design requirements presented above. Although the design is not complete, it has been carried out in sufficient detail to make reliable cost estimates. In several instances alternative designs are possible. We present here the design that is most sound technically. Research and development are presently in progress to investigate alternatives that could lead to better system performance, reliability, or cost reduction.

Each stochastic cooling system is composed of 5 basic parts: beam pickup electrodes, low-level electronics (including preamplifiers), medium level electronics (including gain and phase correction circuits, filters etc.), high-level electronics (including traveling-wave tubes), and kicker electrodes. As several of the cooling systems share common elements in their design, and the performance of these elements effects for the proper functioning of the cooling system, they are discussed below.

5.11.1 Pickup Electrodes. The design of the 1 to 2 GHz and the 2 to 4 GHz stochastic cooling systems is based on the known[5,11] and measured[12] performance of quarter-wave loop (directional-coupler) pickups. The loop pickup is a segment of transmission line of well-defined characteristic impedance on which beam-wall (image) currents can be induced. The magnitude of the voltage induced on it depends on its characteristic impedance Z_{pu}, its effective length ℓ, its geometrical coupling $e(x,y)$ (which depends on the transverse beam location as well as the height of the vacuum chamber, and the amplitude of the beam current $i_b(\omega)$.

$$V_{pu}(\omega), = e(x,y)\ Z_{pu}\ \sin(\frac{\ell\omega}{c})\ e^{i\pi/2}\ i_b(\omega), \tag{5.20}$$

where the 90° phase shift at the reference plane (the center of the loop) is due to the inductive nature of the coupling. The geometry of a typical pickup pair is shown in Fig. 5-25. Here h is the full height of the gap between the electrodes and w is their effective width. If the signals are added in a microwave power combiner circuit and the output signal is referenced to a transmission line of impedance Z_o, the output voltage is

$$V_{out}(\omega), = s(x,y)\sqrt{\frac{Z_{pu}Z_o}{2}}\ \sin(\frac{\ell\omega}{c})\ e^{i\pi/2}\ i_b(\omega), \tag{5.21}$$

where $s(x,y) = e(x,y) + e(x,-y)$

$$= \frac{1}{\pi}\left[\tan^{-1}\left(\frac{\sinh\frac{\pi}{h}(x+w/2)}{\cos(\pi y/h)}\right) - \tan^{-1}\left(\frac{\sinh\frac{\pi}{h}(x-w/2)}{\cos(\pi y/h)}\right)\right] \tag{5.22}$$

For $x = y = 0$,

$$s(0,0) = \frac{2}{\pi}\tan^{-1}\{\sinh(\pi w/2h)\}. \tag{5.22a}$$

Transfer impedances of pickup pairs in sum mode are defined with a centered beam at center frequency ($\omega = \pi c/2\ell$) and in a $Z_o = 50$ ohm transmission line,

$$Z_s = s(0,0)\sqrt{25\ Z_{pu}}\ .$$

At large x, $\quad s(x,0) \to \frac{4}{\pi}\ e^{-\pi x/h}\ \sinh(\pi w/2h)$

A plot $s(x,0)$ vs x is given in Fig. 5-26(a).

If the differences of the signals in the pickup electrode pair are combined into a transmission line of impedance Z_o, the output voltage is

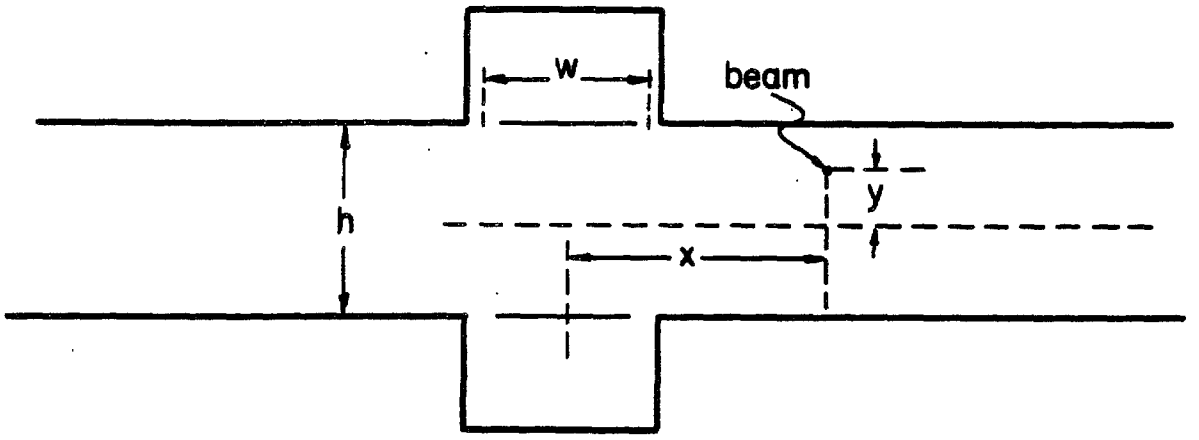

PICKUP - PAIR GEOMETRY

Figure 5-25

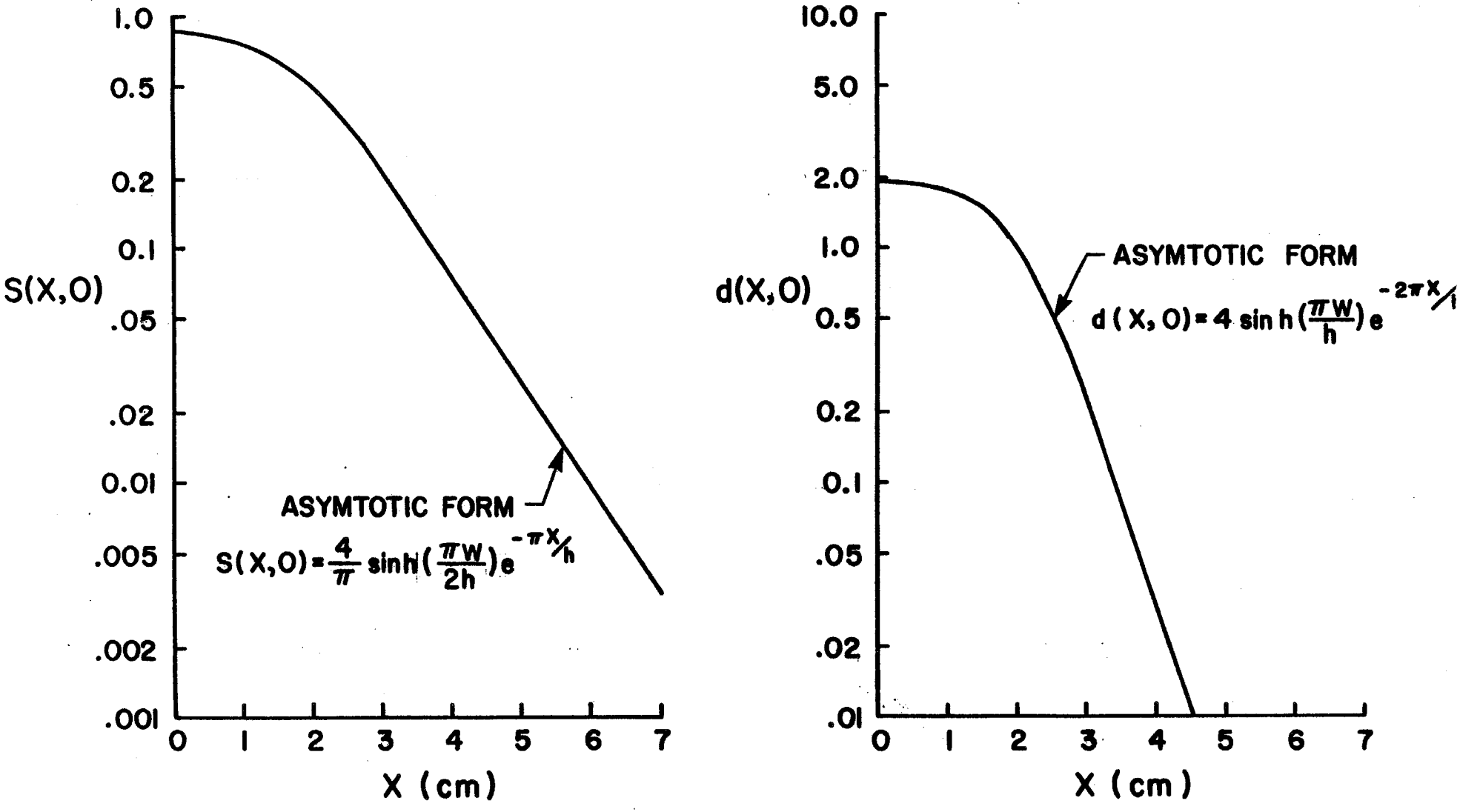

Plots of S(X,0) and d(X,0) us x for h=3cm and w=4cm

Figure 5-26

$$V_{out}(\omega) = d(x,y)\ \frac{y}{h}\sqrt{\frac{Z_{pu}Z_o}{2}}\ \sin(\frac{\ell\omega}{c})\ e^{i\pi/2}\ i_b(\omega). \qquad (5.23)$$

$$\text{where } d(x,y) = \{e(x,y) - e(x,-y)\}\ \frac{h}{y},$$

and the difference mode transfer impedance at x = 0 is

$$Z_d(0,y) = d(0,y)\frac{y}{h}\ \sqrt{25\ Z_{pu}}, \qquad (5.24)$$

where $d(0,y) = 2\tanh(\pi w/2h) = \pi\ s(0,0)[1-1/3\ s^3(0,0)]$

and at large x, $d(x,0) \to 4\sinh(\pi w/h)e^{-2\pi x/h}$.

A plot of d(x,0) vs x is presented in Fig. 5-26(b).

Microwave power combiners add power of coherent signals, and the coupling impedance of n_p loop-coupler pairs is $\sqrt{n_p}$ times the impedance for a single pair, in both Sum and difference modes. Figures 5-27 and 5-28 show a typical electrode assembly.

Based on calculations, as well as measurements with both wires and electron beams, the loop coupler characteristics shown in Table 5-VII are the values we use in this Design Report.

TABLE 5-VII LOOP COUPLER CHARACTERISTICS

Characteristic		1-2 GHz band	2-4 GHz band
characteristic impedance	Z_{pu}	100	75 Ω
height (gap) typical	h^{pu}	3.0	3.0 cm
effective width	w	4.0	2.5 cm
pairs per meter		15	25 per m
Sum Mode			
s(0,0)		0.843	0.664
transfer impedance	Z_s	42.2	28.8 Ω

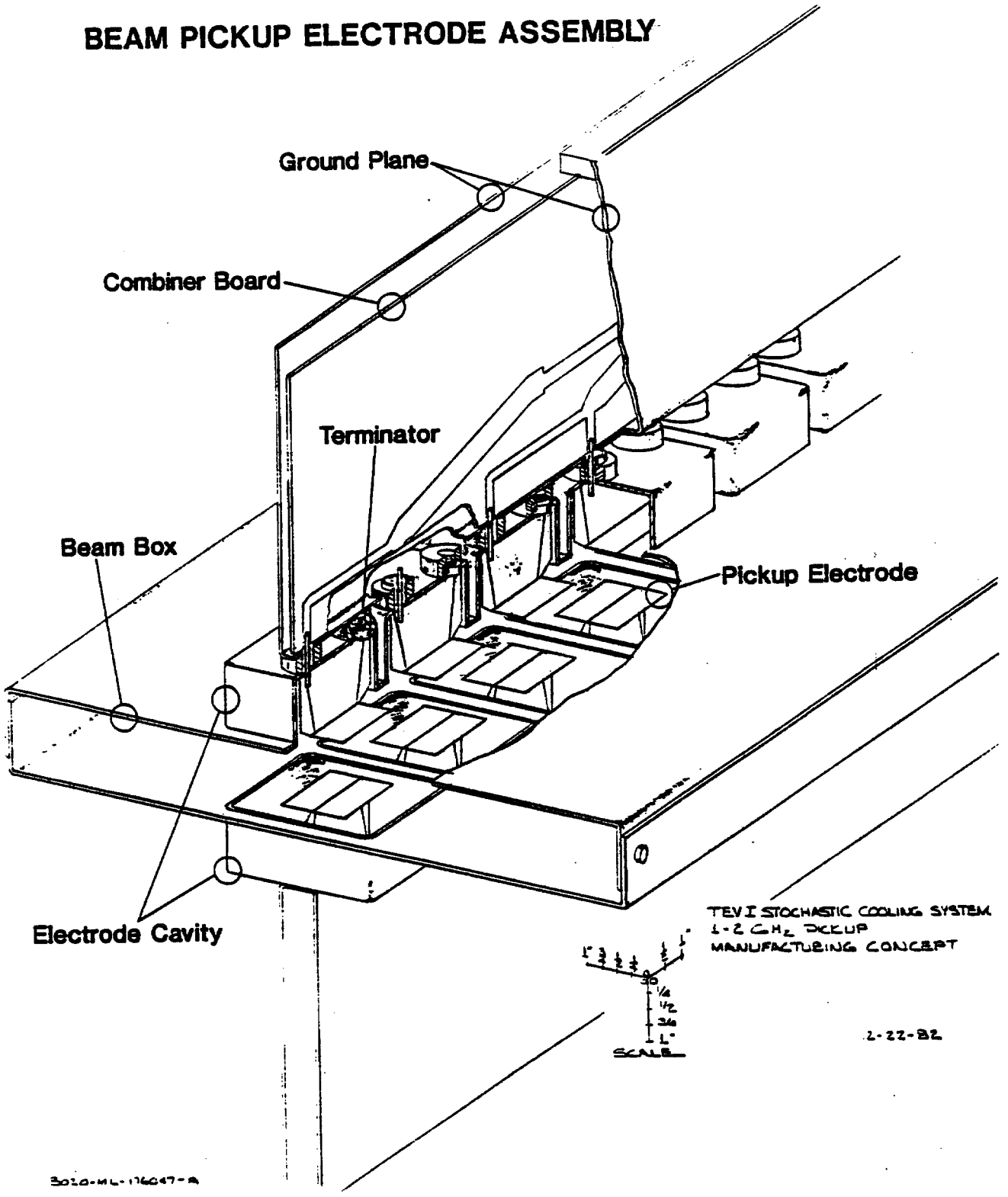
BEAM PICKUP ELECTRODE ASSEMBLY
Ground Plane
Combiner Board
Terminator
Beam Box
Pickup Electrode
Electrode Cavity
TEV I STOCHASTIC COOLING SYSTEM
1-2 GHz PICKUP
MANUFACTURING CONCEPT
2-22-82
SCALE
3010-ML-176047-A

Figure 5-27

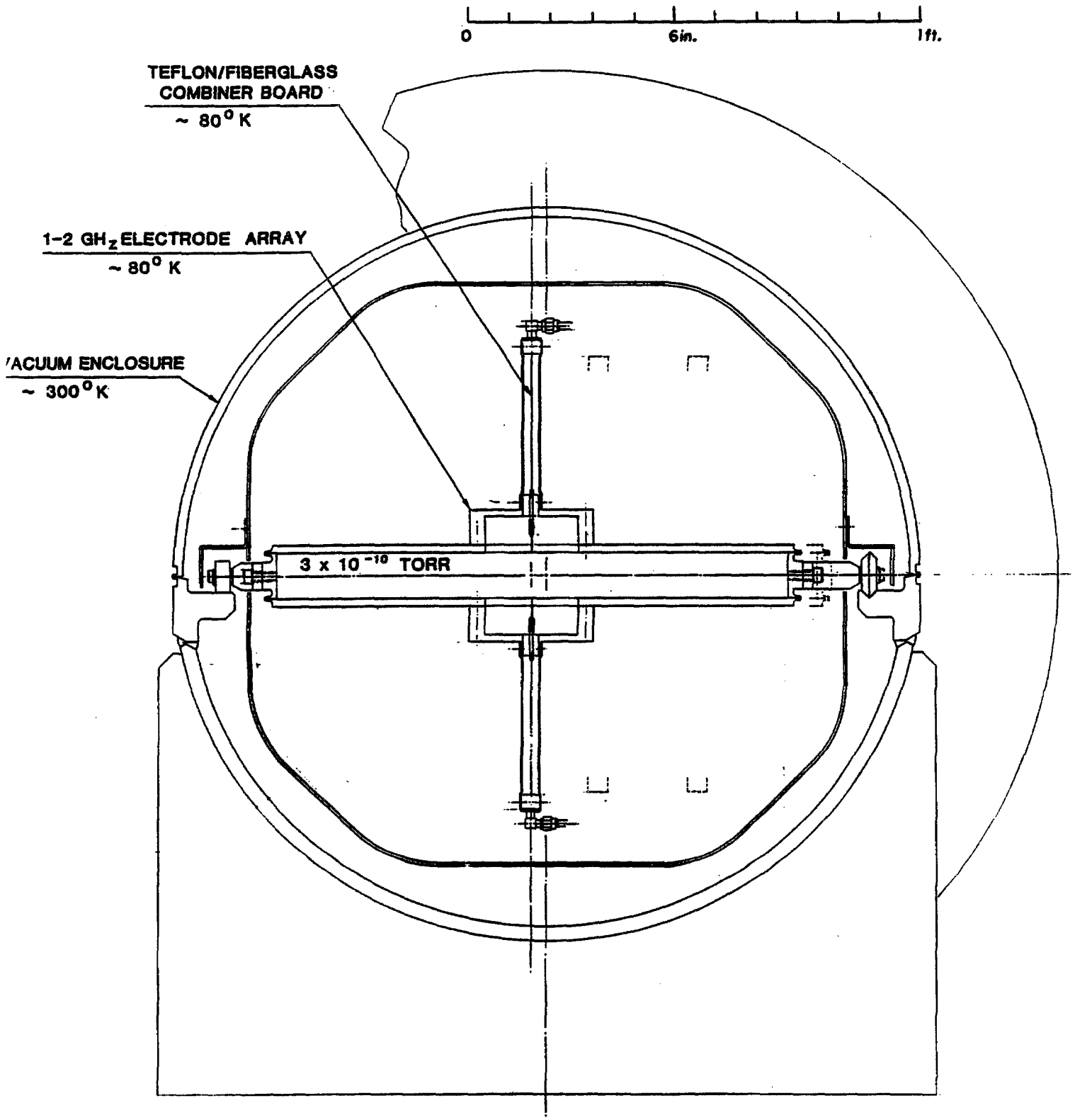

TYPICAL PICK-UP CROSS SECTION

Figure 5-28

Difference Mode			
d(0,y)		1.94	1.73
transfer impedance	Z_d	3230	2500 Ω/m

The electrode assemblies shown in Figs. 5-27 and 5-28 are approximately 1.2 meters long (for the 1-2 GHz band) and contain 16 pickup pairs. The signals are combined separately for top and bottom electrodes using a double-sided Teflon printed circuit board. The air-spaced ground plane yields a group velocity of about 0.98c. The electrodes are back-terminated in their characteristic impedance, and the whole assembly is cooled to liquid-nitrogen temperature to reduce the thermal noise power from the back termination, the skin effect losses in the circuit board, and teflon outgassing. In the 2-4 GHz band, it is quite possible that slot couplers will have a higher coupling impedance per unit length than loop couplers. A research and development program is underway in this area.

Tests on 16 pair 1-2 GHz electrode arrays connected in sum mode have been carried out at Argonne National Laboratory using a 20 MeV pulsed electron linear accelerator. Fast Fourier transforms of the electrode array output signal yield transfer-impedance measurements in the frequency domain. Transfer impedances at centerband of about 140 ohms have been measured in this manner (the calculated value is 168 ohms). The tests have also confirmed the $e^{-\pi x/h}$ spatial sensitivity, which is an important parameter in matching the electrode response to the expected antiproton spatial density in the Accumulator high-dispersion straight section. At large x, there is an indication that the beam excites resonances in the beam box which in turn are picked up by the electrodes. As the spatial sensitivity of the electrodes to these resonances is much flatter than the desired signal, they could dominate the electrode transfer impedance at large x. More beam tests are required to understand the magnitude of this effect, and to develop ways of attenuating these modes (e.g., use of ferrites in the beam box).

5.11.2 Preamplifiers. Commercial gallium-arsenide field-effect transistor (GaAsFet) amplifiers are available in the microwave frequency bands required for stochastic cooling. Although their thermal noise characteristics are relatively low (a 2.0 db noise figure amplifier, available in the 1-2 GHz band[13], has an equivalent noise temperature of 170 K) it would still contribute nearly 70% of the total thermal noise power. The design therefore includes preamplifiers cooled to liquid nitrogen temperatures. We expect equivalent noise temperatures of 75 K (NF = 1.0 db) and 120 K (NF = 1.5 db) for 1-2 GHz and 2-4 GHz amplifiers respectively. Minimization of thermal noise is not only important in relation to beam heating, but also in relation to the cost of extra traveling wave tube installed power required to amplify it.

Commercially available GaAsFet amplifiers designed to operate in the Mil spec temperature range (-55 C to 70 C) have been successfully operated as low as 77 K[14]. In this case a 1-2 GHz amplifier achieved an equivalent

noise temperature of 120 K (NF = 1.5db). GaAsFet amplifiers have been specially designed for operation at liquid-helium temperatures, and equivalent noise temperatures of 20 K (NF = 0.2 db) have been achieved in narrow band operation[15] (0.5 GHz bandwidth at 1.5 GHz).

We are presently pursuing parallel research and development efforts in this area. At Lawrence Berkeley Laboratory, a prototype GaAsFet amplifier has been built which has the following properties in the 1-2 GHz band:

Gain Average	33 db
Gain Flatness	±1.5 db
Phase Linearity	±15°
Noise Temperature Peak (NF=0.5)	40 K
Average (NF=0.35)	30 K
Input VSWR Peak	2.5:1
Average	1.75:1

Only slight improvements are seen when the amplifier is cooled to 14 K.

At Fermilab, measurements are being made on cooled commercially available amplifierss. This includes amplifiers with integrated bipolar biasing circuits which can only be cooled to -50°C, and amplifiers with separated biasing circuits, which can be cooled to 77°K. We have achieved average noise temperatures of 80 K and 110 K for amplifiers cooled to -50°C and 77 K respectively. Input VSWR has typically been better than 1.4:1.

Research and development is continuing in the 1-2 GHz band in both the above efforts. In addition, work is beginning in the 2-4 GHz band.

5.11.3 Notch Filters. Notch filters are needed in our design of the stochastic cooling system for several reasons. In one system, the stack tail momentum cooling system, notch filters are used both for reducing the microwave power at frequencies corresponding to particles in the core, and to assist in shaping the gain vs momentum (frequency) in the stack tail. In systems with poor signal to thermal noise ratio, notch filters are useful in reducing the extra traveling-wave tube installed power required to amplify it. If momentum cooling is implemented in the debuncher, a notch filter would be used to produce a phase inversion of the pickup sum signal at the harmonics of the central revolution frequency. The tolerance on the frequency deviation of the notch centers at each harmonic of the revolution frequency ω_0 in the frequency bandwidth is of the order of (for the Accumulator)

$$\left|\frac{\omega_n - n\omega_0}{n\omega_0}\right| < \eta\frac{\delta p}{p} \approx 10^{-5},$$

Where $\eta = 0.02$, p is 8.9 GeV/c and δp is about 2 MeV/c.

Filter designs include both shorted stubs, which use reflections from the shorted end of a long transmission line (nominally half the circumference of the Accumulator), and correlator types, which use the constructive and destructive interference of the same signal transmitted over two transmission lines (whose lengths differ by about the circumference of the Accumulator).

In our application, the large circumference of the Accumulator, in combination with the very high frequencies used in the electronics, imposes severe restrictions on the selection of transmission lines. In room-temperature transmission lines, the skin effect conductor resistance causes dispersion as well as attenuation. This is reduced by using larger diameter transmission lines. However, the maximum size of the transmission line is limited, since higher order modes are excited and affect the dispersion. In particular, in a 7.5-cm diameter 50-ohm transmission line, the TE_{11} mode propagates at frequencies above 2.0 GHz. These effects are only marginally better at 76.6 ohms, the impedance at which skin effect losses are minimized.

Our present notch filter is based on a correlator circuit using a 1.6 mm diameter 50 ohm superconducting transmission line. In such a line the major attenuation (power loss) is due to the loss tangent in the dielectric, and results in an attenuation of about 1.0 db per km in the 1-2 GHz band. Early measurements showed that shorted-stub filters typically had much higher dispersion than the same cable when used as a correlator filter. This due to the fact that power reflected by a single discontinuity in a correlator-filter is absorbed by the isolated port on the input hybrid splitter, and can only reach the output hybrid if it is re-reflected by another discontinuity. Recent measurements have been made on a 330 m line in a cryostat as shown in Fig. 5-29. Dispersion and notch depth measurements in the 1-2 GHz band are shown in Fig. 5-30. This performance is believed to be adequate for the stack tail system. Shorted-stub filters do offer some advantages over correlator filters, however, as they allow greater flexibility in gain and phase shaping within each Schottky band. Present measurements indicate that the present superconducting line does indeed provide adequate performance in terms of dispersion and notch depth when used as a shorted stub. Research is still proceeding in this area. Research is also going on in the area of TWT correlator filters, to help control the TWT intermodulation (IM) distortion. This is discussed in the next section.

5.11.4 Traveling Wave Tubes (TWT's). The power amplifier stages in all our cooling systems are traveling wave tube amplifiers. Several commercial units are available in the 1-2 and 2-4 GHz bands with saturated output power ratings up to 200 watts. Traveling wave tubes are also available with power ratings above 1 kW.

Numerical studies show that in the stack tail momentum cooling system, the depth of the notches between the Schottky bands must be at least 40 db deep in order not to excessively heat the core. Even though notches of

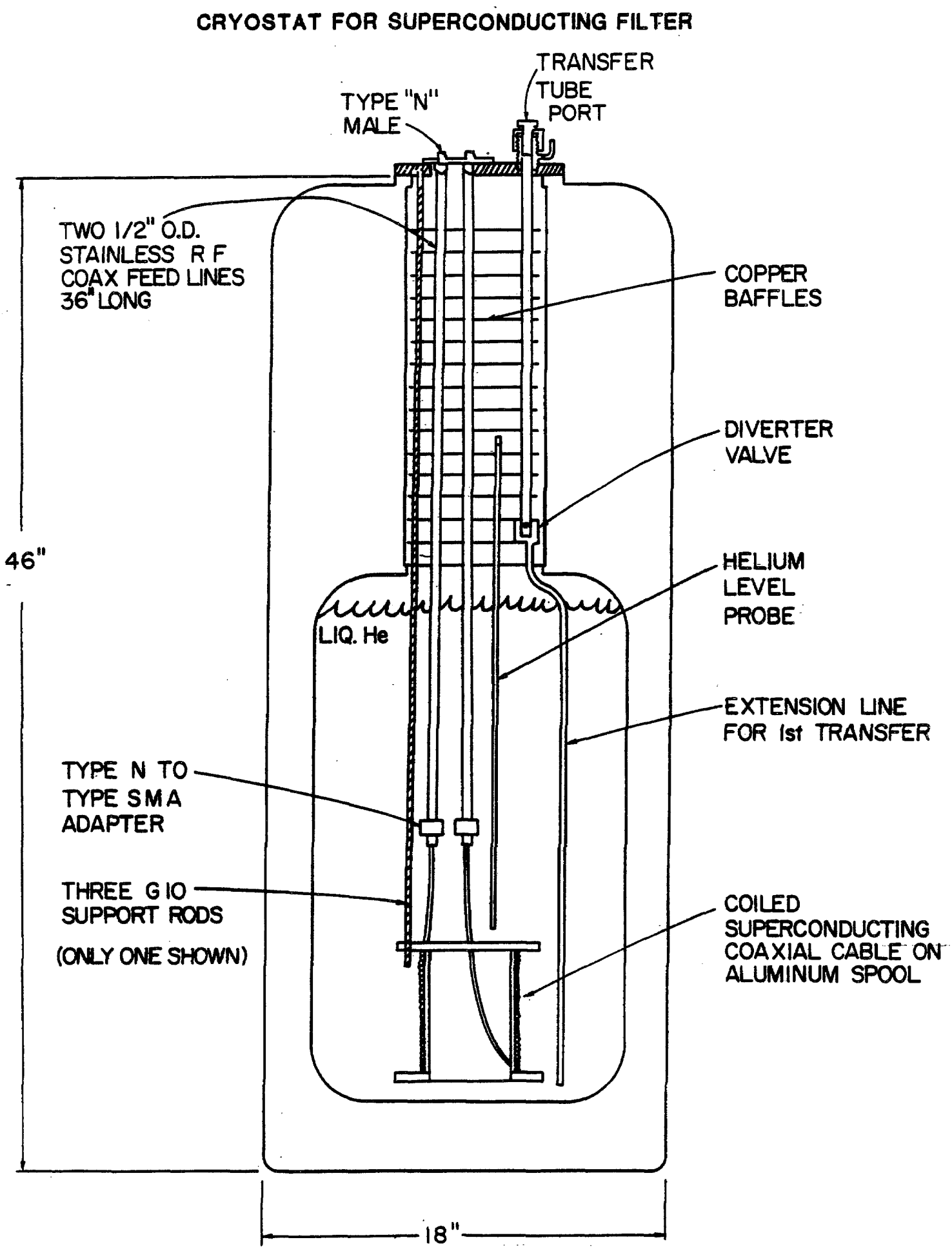
CRYOSTAT FOR SUPERCONDUCTING FILTER
TRANSFER TUBE PORT
TYPE "N" MALE
TWO 1/2" O.D. STAINLESS R F COAX FEED LINES 36" LONG
COPPER BAFFLES
DIVERTER VALVE
46"
HELIUM LEVEL PROBE
LIQ. He
EXTENSION LINE FOR 1st TRANSFER
TYPE N TO TYPE SMA ADAPTER
THREE G10 SUPPORT RODS
(ONLY ONE SHOWN)
COILED SUPERCONDUCTING COAXIAL CABLE ON ALUMINUM SPOOL
18"

Figure 5-29

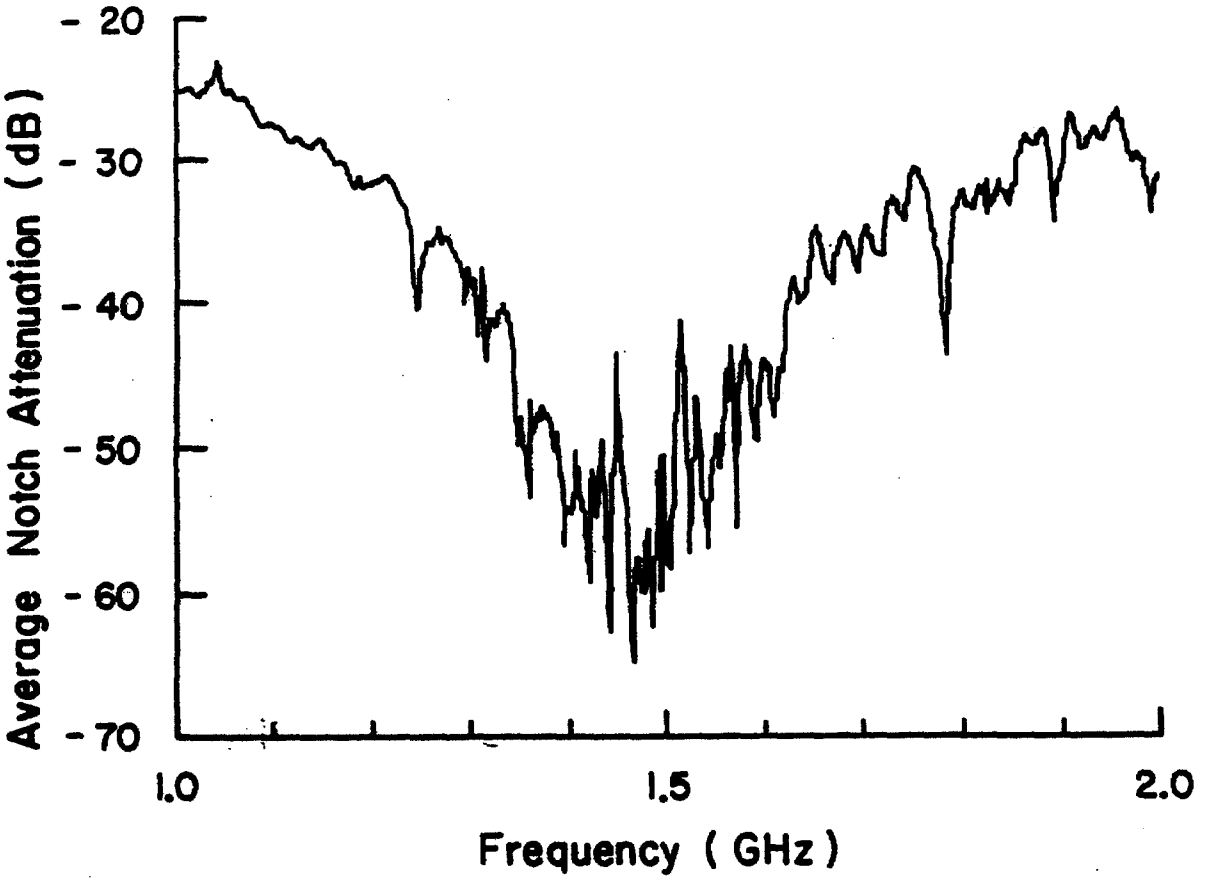
- 20
- 30
- 40
- 50
- 60
- 70
Average Notch Attenuation (dB)
1.0
1.5
2.0
Frequency (GHz)

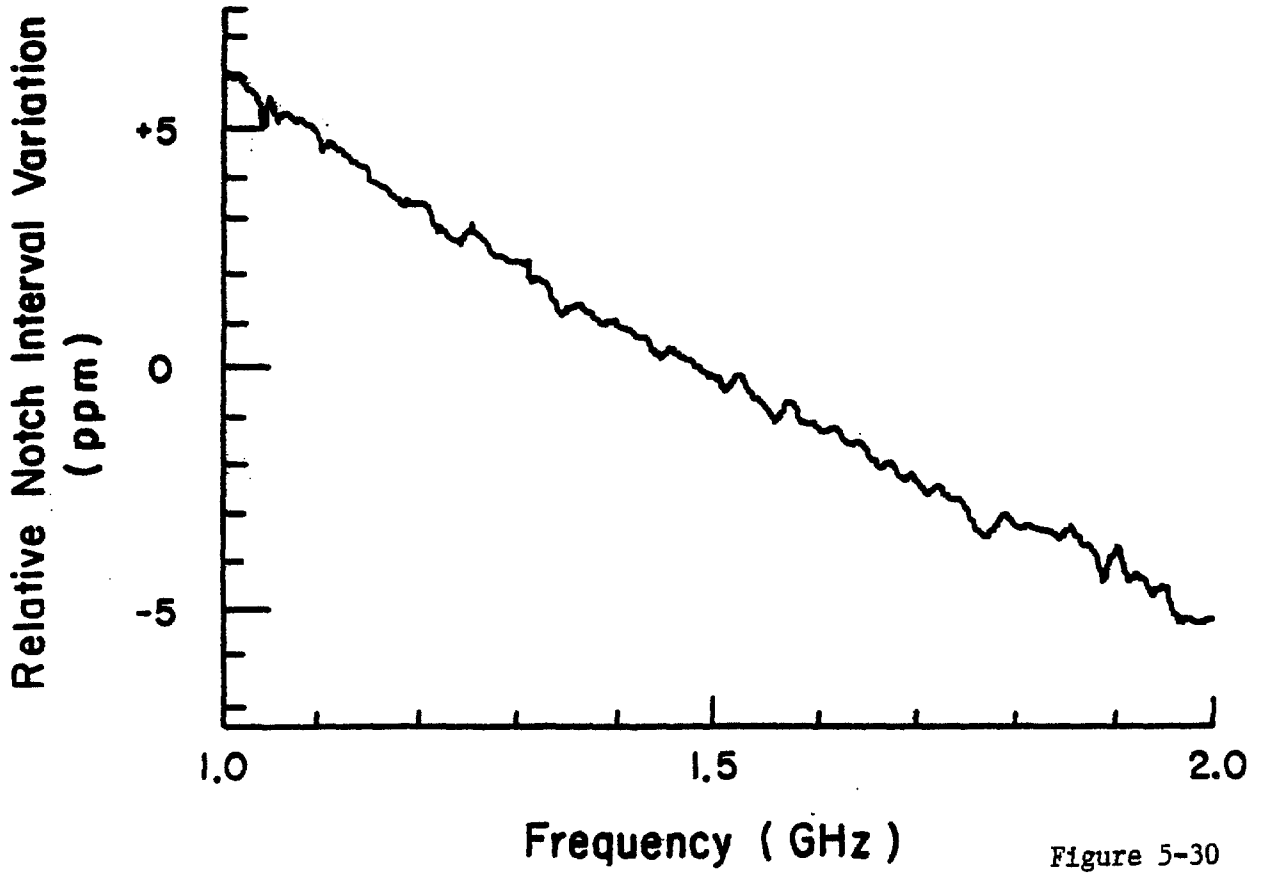
+5
0
-5
Relative Notch Interval Variation (ppm)
1.0
1.5
2.0
Frequency (GHz)

Figure 5-30

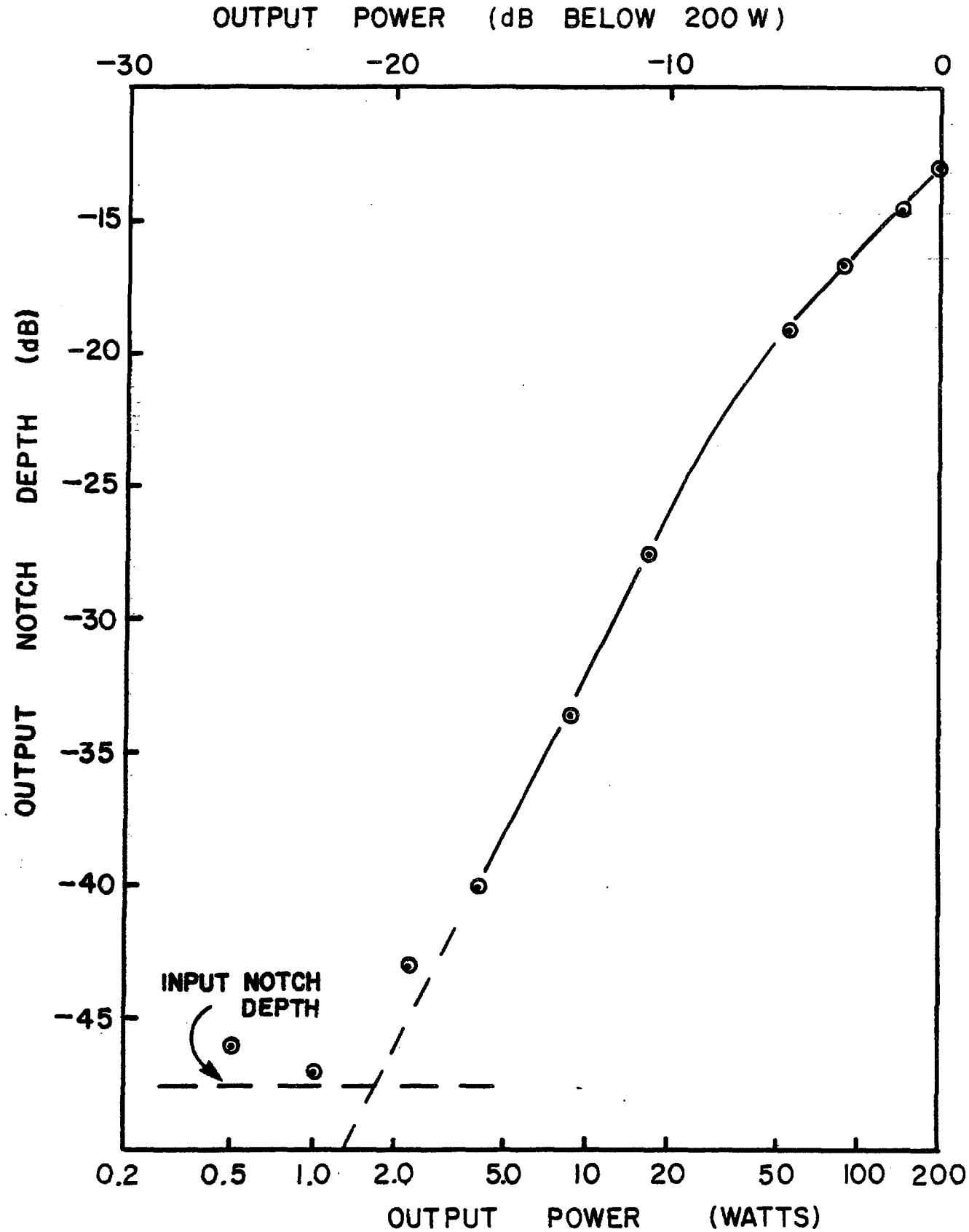
OUTPUT POWER (dB BELOW 200 W)
-30
-20
-10
0
-15
-20
-25
-30
-35
-40
-45
OUTPUT NOTCH DEPTH (dB)
INPUT NOTCH DEPTH
0.2
0.5
1.0
2.0
5.0
10
20
50
100
200
OUTPUT POWER (WATTS)

Figure 5-31

this depth can be obtained with the filters discussed above, the intermodulation distortion that occurs at higher power levels in TWT's can rapidly fill these in. Second-order intermodulation distortion can occur at the edges of the operating band of octave-bandwidth TWT's. Operation of the TWT's in a push-pull mode can reduce the second order IM products effectively, but, third-order IM distortion can occur at midband frequencies and is not reduced by operating the TWT's in push-pull mode. Measurements using a single TWT and a notched white-noise source show that the remaining notch depth at the TWT is only 13 dbc at full power (200 watts), but improves to about -30 dbc at 10 watts per TWT. This result is shown in Fig. 5-31. Since this measurement was made, tests on another design TWT with a higher bandwidth indicated a somewhat lower level of IM distortion at the same power levels. Specifically, the IM distortion improved to about -23 dbc from -20 dbc at 40 watts output power. The highly peaked Schottky spectrum produces a third-order intermodulation distortion which is naturally peaked in, rather than between, the Schottky bands, providing another 12 db of notch depth at core frequencies. To obtain 1600 watts of output power and notch depths of 40 db would require roughly 160 TWTs, each operating at about 10 watts.

The potential cost saving of being able to run the TWT's at 40 W rather than 10 has stimulated interest in using superconducting correlator filters on the output of the TWT's. In principle, the filter need only provide a notch depth of the order of 20 db, the remainder being provided by the TWT IM distortion of -20 dbc, and the IM form factor of the Schottky bands of 12 db. As a correlator filter using a superconducting transmission line is nearly lossless, we are investigating the possibility that such a filter could be used on the TWT outputs. Calculations show that the superconducting line could dissipate about 0.7 W/meter without quenching. In principle a superconducting correlator filter could carry several hundred watts of microwave power if the attenuation were 1 db per km. Such a power-correlator filter could be used on the output of a push-pull TWT pair to reduce the output power between the Schottky bands caused by IM distortion.

A research and development program has been directed toward building a power correlator filter capable of handling 80 watts of microwave power in the 1-2 GHz band (this corresponds to 40 watts per TWT, and 40 watts in the superconducting line). Tests thus far have only achieved 50% of this power level, and the present belief is that the thermal coupling between the Teflon and the outer conductor is less than optimal, causing an additional temperature rise. Pulsed-power tests with more than 100 watts being transmitted through the superconducting cable indicate that the attenuation is about as expected (around 1 db per km) even at these high power levels, hence the present limit is not due to anomalous attenuation at high power levels.

If further research in this area is unsuccessful in achieving reliable operation at 40 watts in the superconducting line, then an alternative circuit in which the superconducting line and the TWTs are combined in the

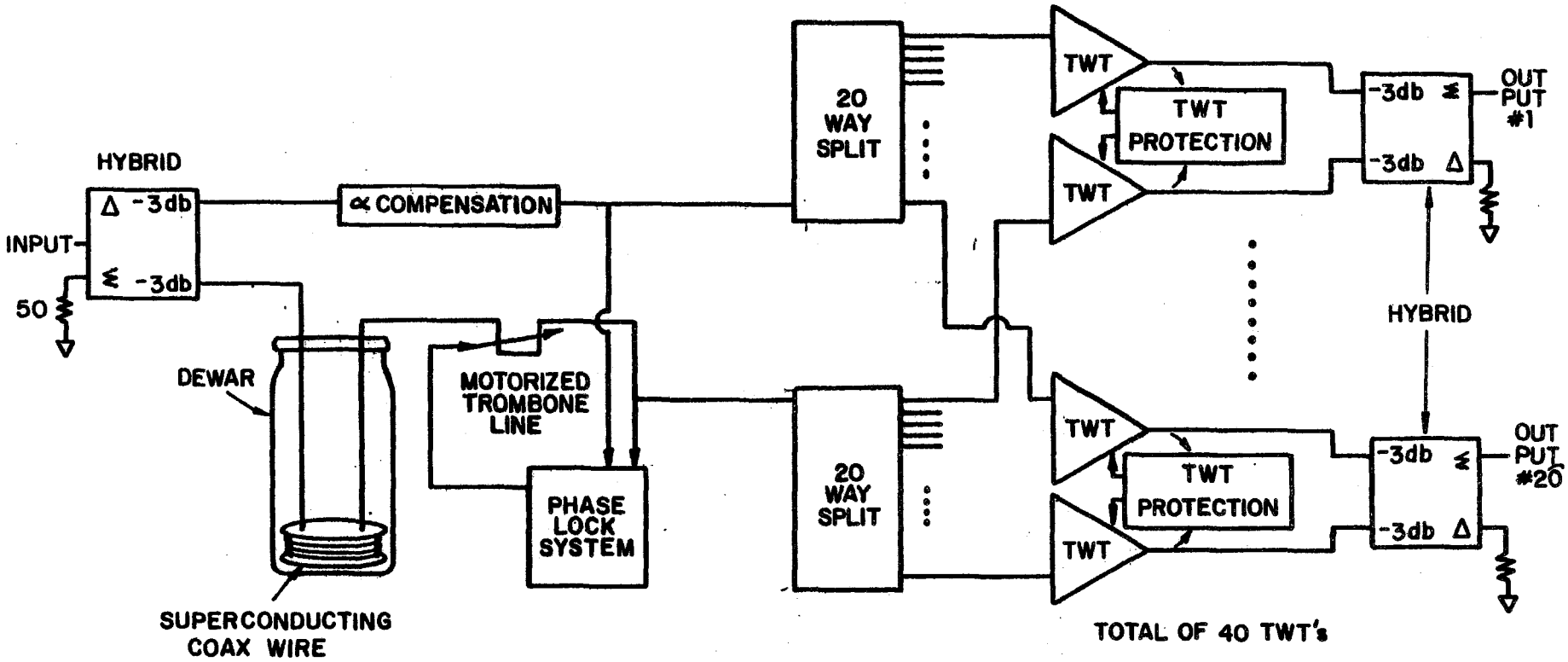

POWER CORRELATOR FILTER FOR STACKTAIL MOMENTUM COOLING

Figure 5-32

same correlator type loop circuit will be used. It is shown in Fig. 5-32. Such a circuit is more demanding on the TWT performance in the areas of gain and phase matching, phase linearity and IM distortion. It is believed that such a circuit could yield IM distortion reduction of the order of 6 db more than the same circuit without the filter. Hence present calculations show that IM distortion levels are marginal at 40 watts per TWT.

5.11.5 Kicker Electrode Assemblies. The kicker electrode assemblies are conceptually similar to the pickup electrode assemblies by virtue of the reciprocity theorem, which states that transfer impedances between pairs of terminals are unchanged when inputs and outputs are exchanged. The major differences are of a hardware nature: the combiner board is now a power splitter and some power dissipation and heating should be anticipated. The terminating resistor now must absorb microwave power, and means must be provided for heat removal. There is no thermal-noise problem as there was in the pickup case, so cryogenic cooling is only needed if adequate vacuum cannot be obtained otherwise, or if the terminating resistors cannot operate at 7 watts/resistor at room temperature. Tests on outgassing of materials are continuing in order to better understand their compatibility with the kicker electrode array design.

There is some concern that kicker electrodes will generate evanescent and propagating modes in the beam pipe. This is especially true of betatron cooling kickers, but can also be a problem in the momentum-cooling systems. Evanescent modes, even though highly damped, have phase velocities considerably different than the beam, and could lead to stochastic heating effects. The propagating modes, besides being able to heat the beam, can also propagate through the beam pipe back to pickup arrays and interfere with the pickup operation. The TE_{11} cutoff in a 35 mm diameter beam pipe is about 5 GHz, so such insertions would have to be placed in low-dispersion areas of the ring.

5.11.6 Other Considerations. Most of the components in the stochastic-cooling electronics have a limited bandwidth of about an octave, and this normally causes the frequency derivative of the phase delay to be frequency dependent. This leads to two parameters that need to be known for each element. The group delay (the slope of a straight-line fit to the phase delay vs frequency data in the operating band) and the phase intercept (the zero frequency intercept of the above straight line) need to be measured for each component and accounted for the final system. Deviations from the average group delay at particular frequencies, as well as gain nonuniformity may have to be corrected. Special circuits to cause gain shaping and constant phase offset will need to be designed and built. In brief, the group delay is adjusted using cables so that the information signal arrives at the kicker at the correct time. The phase intercept correction assures that it arrives with the correct phase angle. The gain correction assures that the signal power is properly apportioned to each Schottky band.

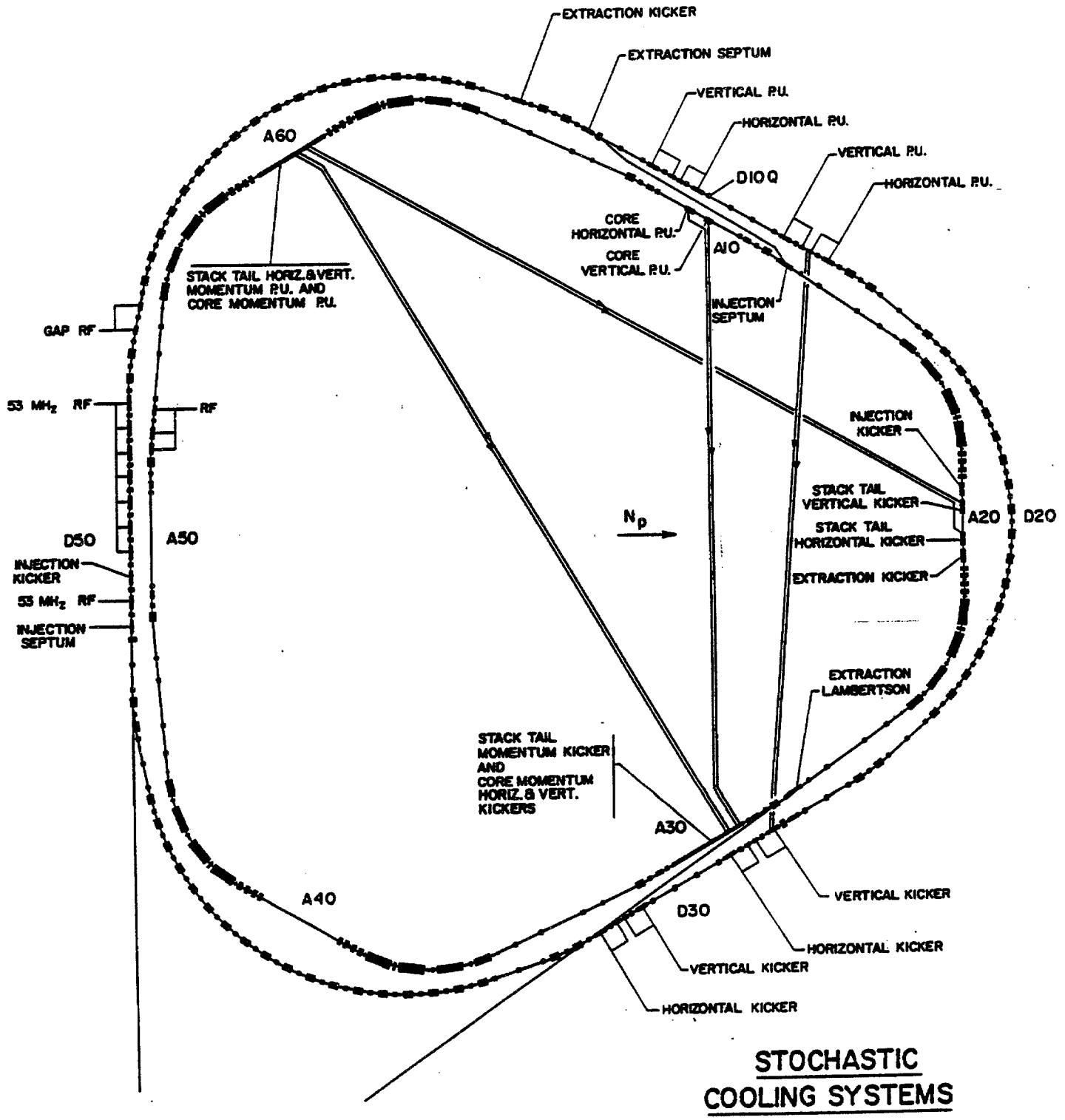
EXTRACTION KICKER
EXTRACTION SEPTUM
VERTICAL P.U.
HORIZONTAL P.U.
VERTICAL P.U.
HORIZONTAL P.U.
A60
D10Q
CORE HORIZONTAL P.U.
CORE VERTICAL P.U.
A10
STACK TAIL HORIZ.&VERT. MOMENTUM P.U. AND CORE MOMENTUM P.U.
INJECTION SEPTUM
GAP RF
53 MHz RF
RF
INJECTION KICKER
STACK TAIL VERTICAL KICKER
A20
D20
STACK TAIL HORIZONTAL KICKER
EXTRACTION KICKER
D50
A50
N_p
INJECTION KICKER
53 MHz RF
INJECTION SEPTUM
EXTRACTION LAMBERTSON
STACK TAIL MOMENTUM KICKER AND CORE MOMENTUM HORIZ.& VERT. KICKERS
A30
A40
D30
VERTICAL KICKER
HORIZONTAL KICKER
VERTICAL KICKER
HORIZONTAL KICKER
STOCHASTIC COOLING SYSTEMS

Figure 5-33

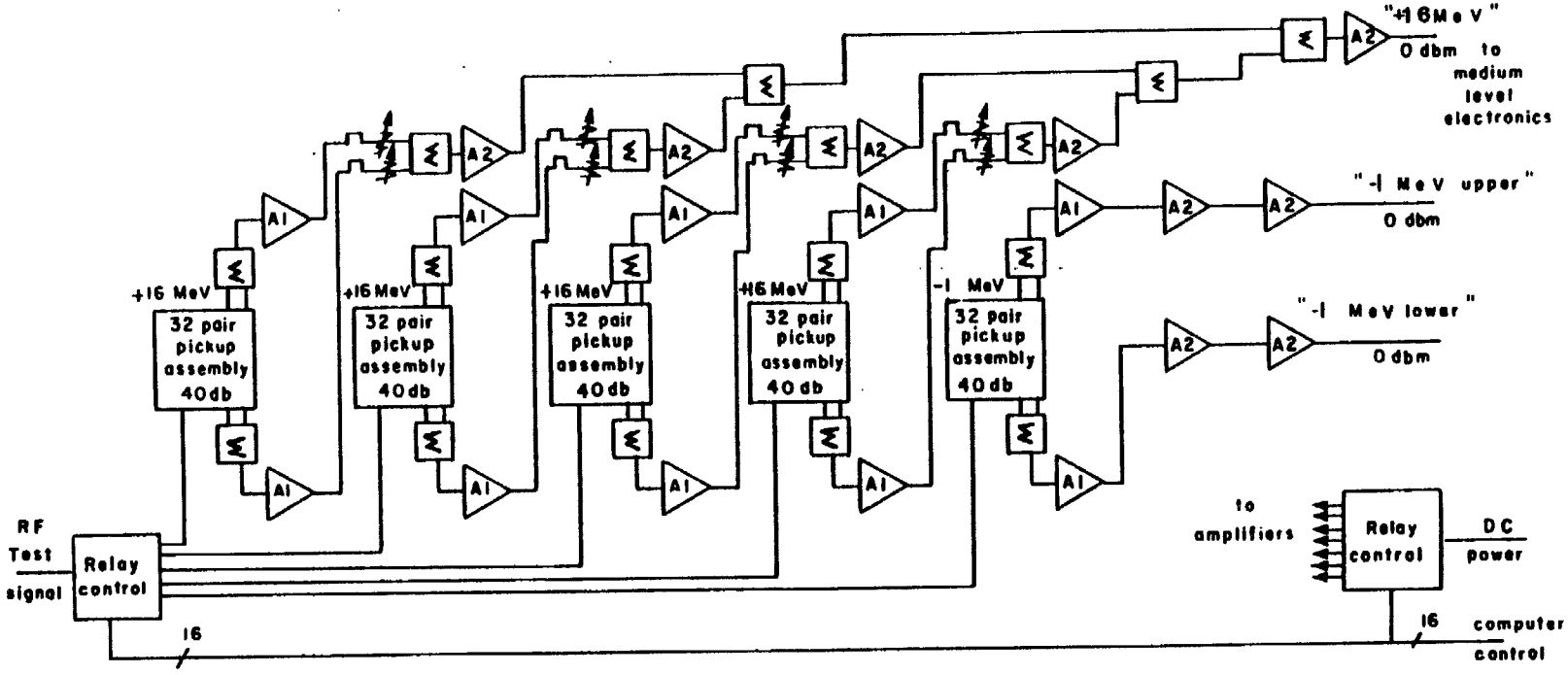

32 pair pickup assembly = 2.4m long module containing 32 pair of 1-2 GHz loop couplers cooled to 77°K. Upper and lower electrode signals are separately brought to cooled GaAsFet amplifiers through vacuum chamber wall. A 40 db coupler built into assembly allows insertion of test signal.

A1 = Low noise GaAsFet amplifier cooled to 77°K. Gain about 30 db. Equivalent noise temperature about 75°K.

A2 = Commercial bipolar 1-2 GHz amplifier, Avantek #UTC-20-104 or equivalent (gain = 23 db; equiv. noise temp. = 500°K).

= 2:1 power/inphase power combiner/splitter.

= Manually adjusted liner delay pad.

= Manually adjusted attenuator pad.

Figure 5-34a

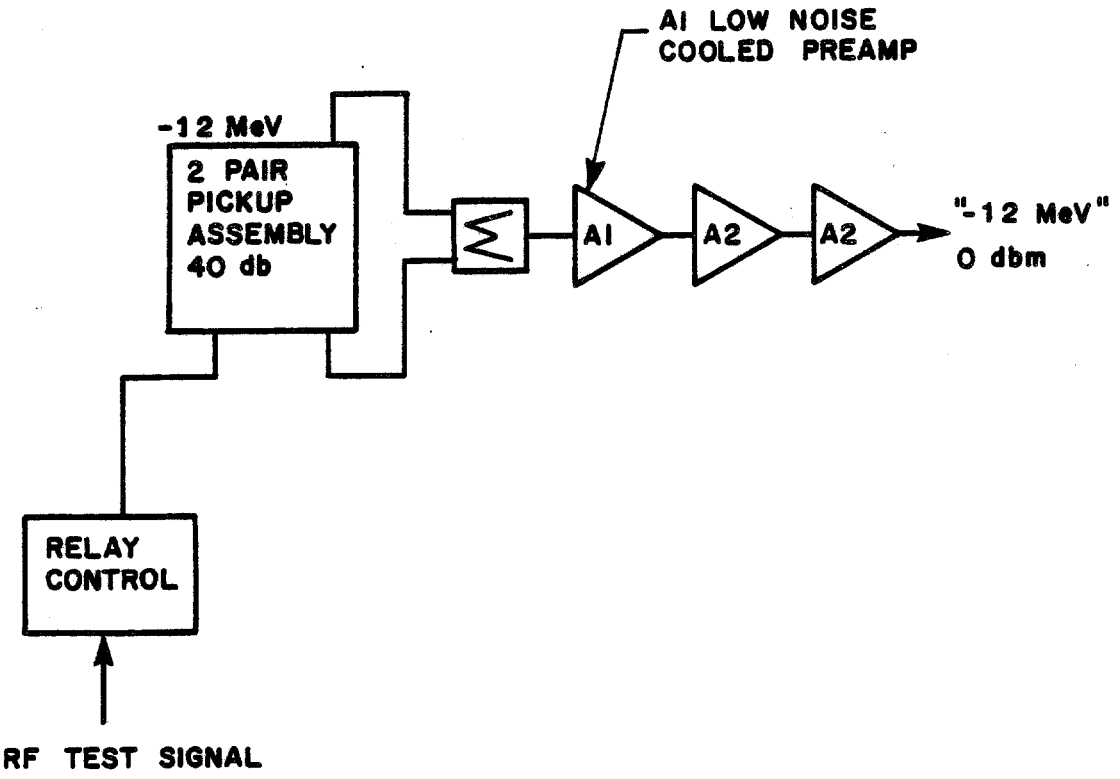

Stack Tail Momentum Low Level Electronics

Figure 5-34b

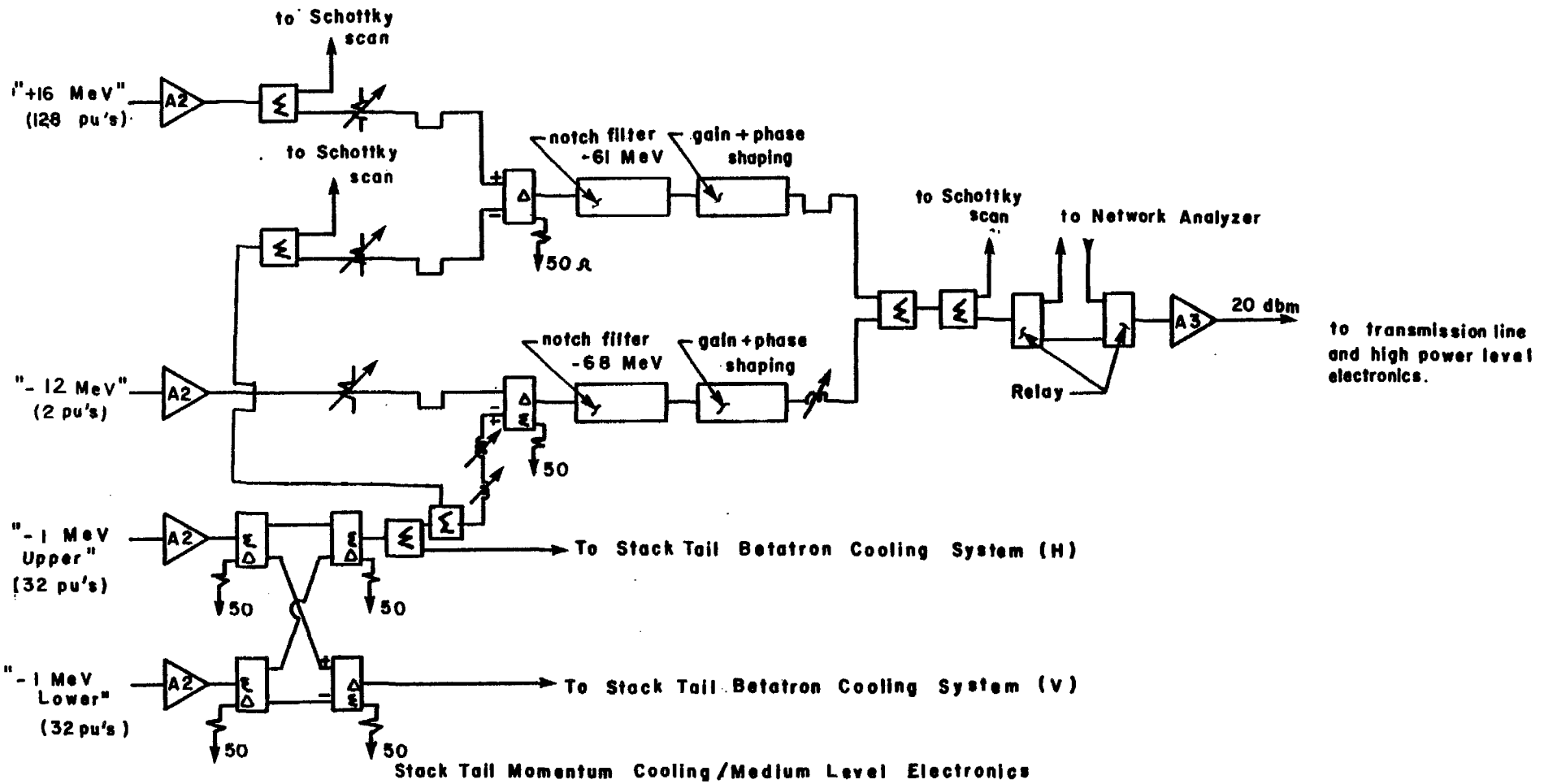
to Schottky scan
"+16 MeV" (128 pu's)
A2
to Schottky scan
notch filter -61 MeV
gain + phase shaping
to Schottky scan
to Network Analyzer
50 Ω
20 dbm
to transmission line and high power level electronics.
notch filter -68 MeV
gain + phase shaping
"- 12 MeV" (2 pu's)
Relay
50
"- 1 MeV Upper" (32 pu's)
To Stack Tail Betatron Cooling System (H)
50
50
"- 1 MeV Lower" (32 pu's)
To Stack Tail Betatron Cooling System (V)
50
50
Stack Tail Momentum Cooling/Medium Level Electronics

Figure 5-35

The dispersion in the transmission lines carrying the signals across the ring also needs to be considered. In the 1-2 GHz stack tail systems, the largest diameter coaxial line which we can use is 1-5/8-in. diameter rigid line (air dielectric) as the TE_{11} mode propagates above 3.5 GHz. Calculations show that the expected dispersion is about 8° over the 1-2 GHz band for 150 m of line, based on the known skin effect losses. Preliminary measurements indicate that it may actually be somewhat larger, possibly due to excitation of evanescent modes at 2 GHz. In the 2-4 GHz range, the transmission line diameter would have to be limited to about 7/8", and the calculated dispersion would be about 18°. This line will probably be of the foam dielectric type, because the time-delay requirements are not overly restrictive.

5.11.7 Accumulator Stochastic Cooling System Layout. There are 6 specific cooling systems in the Accumulator. Their location is shown in Fig. 5-33. Their basic operating parameters are outlined in Table 5-VIII. All 3 stack tail systems operate in the 1-2 GHz band, while the 3 core systems operate in the 2-4 GHz band. All kicker assemblies have been located remotely from the pickup electrodes to minimize coupling and feedback.

The largest system is the stack-tail momentum-cooling system, requiring about 1600 W of microwave power. The pickup electrodes are located in the 9 m dispersion short straight section A60, and the kickers in the zero dispersion long straight section A30. A block diagram of the low-level electronics is shown in Fig. 5-34a and b. Groups of 16 pickup electrodes are summed on an internal edge-supported teflon printed circuit board into low noise preamps. Signals are separately amplified for the upper and lower electrodes to allow for gain and phase correction, as well as for forming both sum and difference signals. Signal processing is done in the medium level of electronics as shown in Fig. 5-35. This includes 3 notch filters (superconducting correlators) with notch minima set at +4, -2, and -3 MeV relative to the core. After gain and phase corrections, the signals are amplified to about +20 dbm and transmitted across the ring to the high level electronics (TWT's). At present we estimate that 40 TWT's are needed if we can operate them at 40 W each and maintain a 40 db notch depth at the core frequency (this number includes the Schottky form factor of about 12 db).

The stack-tail betatron cooling systems derive their pickup signals from the stack-tail momentum system as shown in Fig. 5-36. The kickers, however, are in straight Section A20, where the dispersion is about 9 m. The vertical and horizontal betatron systems require about 20 and 200 watts of output power respectively. As was pointed out earlier, the horizontal betatron signal is derived from beam in the asymptotic region of sum-mode pickups where the response is $e^{-\pi x/h}$, and hence there is a momentum Schottky signal as well as the normal betatron sidebands. It is expected that 1 TWT will be sufficient for the vertical and 2 for the horizontal system. It is possible that a notch filter could be used to reduce the momentum Schottky signal.

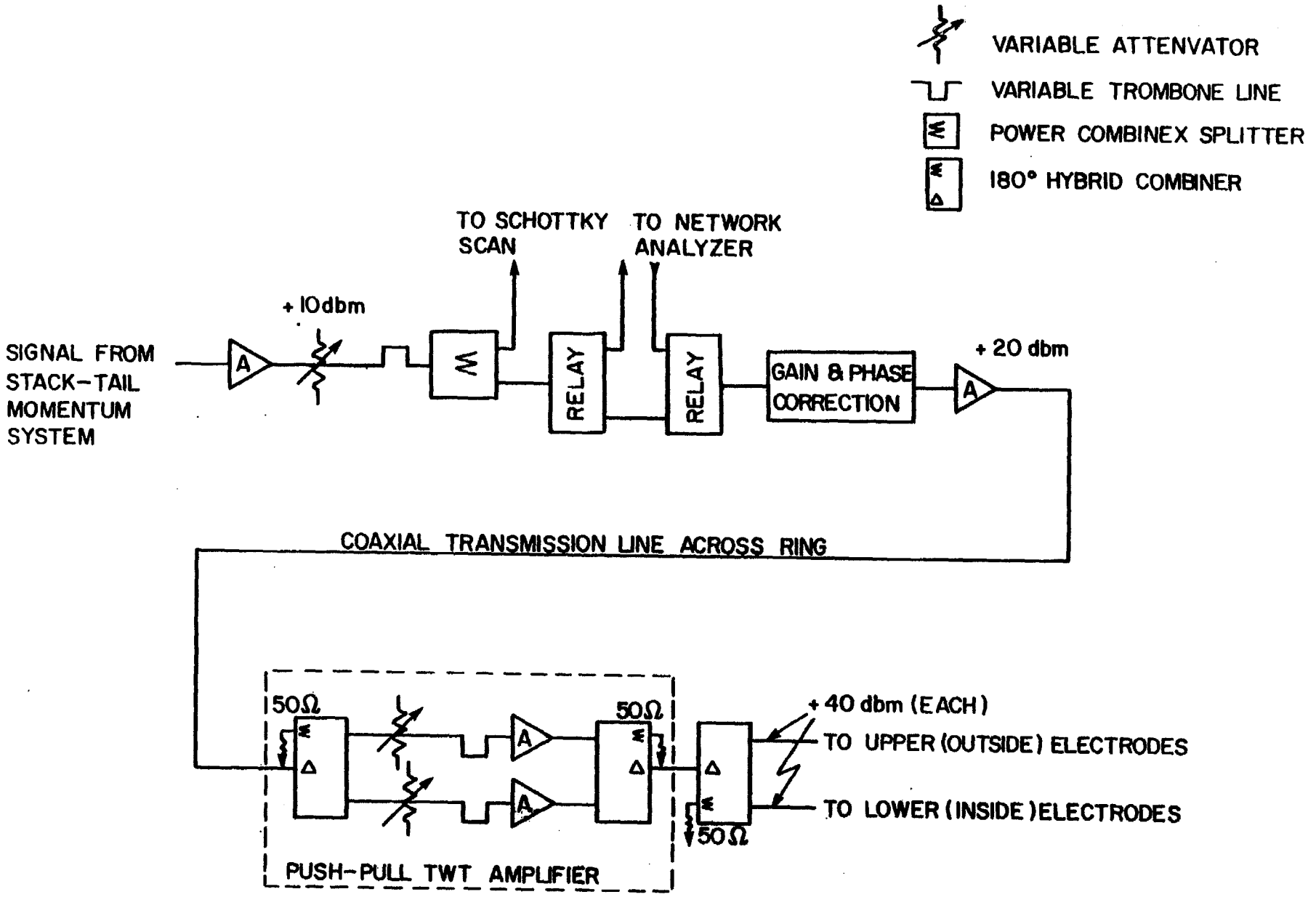

STACK-TAIL BETATRON COOLING SYSTEM (2 REQUIRED)

Figure 5-36

The core momentum system pickups are located in the high-dispersion straight Section A60 along with the stack-tail pickups. As indicated in Section 5.9.5 and Fig. 5-37, the core momentum pickups are double rows of pairs, each pair in sum mode. The difference signal of the two rows is then formed. These signals are processed as shown in Fig. 5-38 and also sent to kickers in the zero-dispersion straight section shared with the stack tail momentum kickers. This system requires about 30 W.

The core betatron system pickups are located in the zero-dispersion straight section A10. The signals are processed as per Fig. 5-38 and also sent to kickers in zero-dispersion straight section A30. Each system requires about 2 W.

TABLE 5-VIII ACCUMULATOR STOCHASTIC COOLING SYSTEMS

	Stack tail Momentum	Stack tail Betatron	Core Momentum	Core Betatron
Frequency band	1-2GHz	1-2GHz	2-4GHz	2-4GHz
Number of pickup pairs (loops)	128+32+8+2	(32)(H,V)	32 + 32	8(x2)
Pickup characteristic impedance	108 Ω	108,70 Ω	97 Ω	83 Ω
Pickup sensitivity s(0,0) or d(0,0)	0.85(s)	1.93(d)	0.59(ds)	1.59(d)
Back termination thermal noise temperature	80 K	80 K	80 K	293 K
Amplifier equivalent thermal noise temperature	25 K	25 K	200 K	293K
Amplifier gain (net)	150db	125db	110db	106db
Number of filters (superconducting correlators)	3	0	0	0
Output power		V+H		
-Schottky	1400W	10W+200W	30W	10W(x2)
-thermal	200W	10W+10W	0	0
-total	1600W	20W+210W	30W	10W(x2)
Number of TWT's (200 watt saturated power)	40	1+2	1	1(x2)
Number of kicker pairs (loops)	160	32(x2)	32	8(x2)
Kicker characteristic impedance	108[1] Ω	108[1],70[2] Ω	97[1] Ω	83[2] Ω
Kicker sensitivity s(0,0) or d(0,0)	0.85(s)	1.93(d)	0.59(s)	1.59(d)
Spare time delay with air dielectric line (β=.998)	205 nsec	23 nsec	230 nsec	110 nsec
Spare time delay with heliax (β=0.819)	197 nsec	-34 nsec	166 nsec	63 nsec

[1] even mode
[2] odd mode

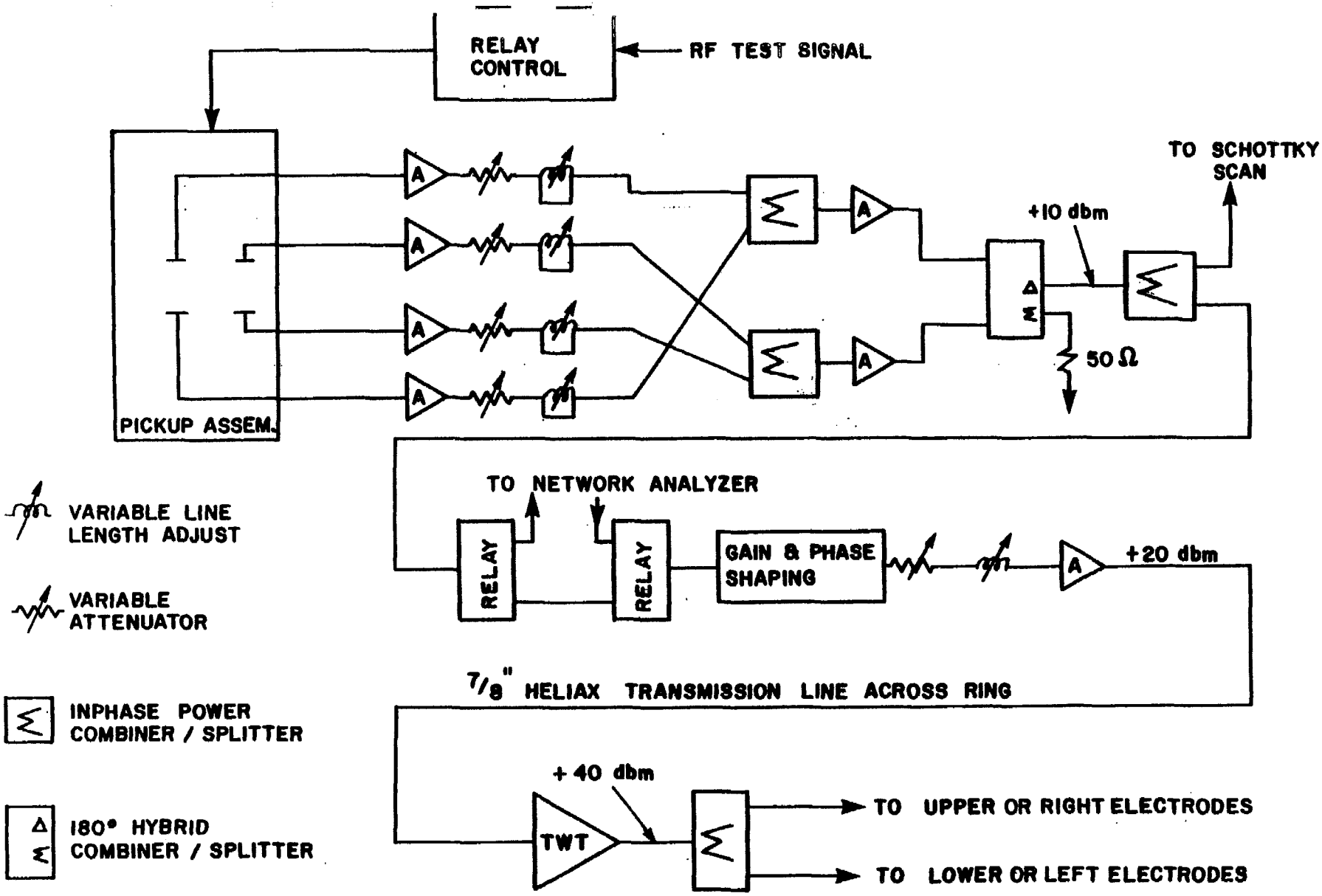

2-4 GHz Core Momentum Cooling System

Figure 5-37

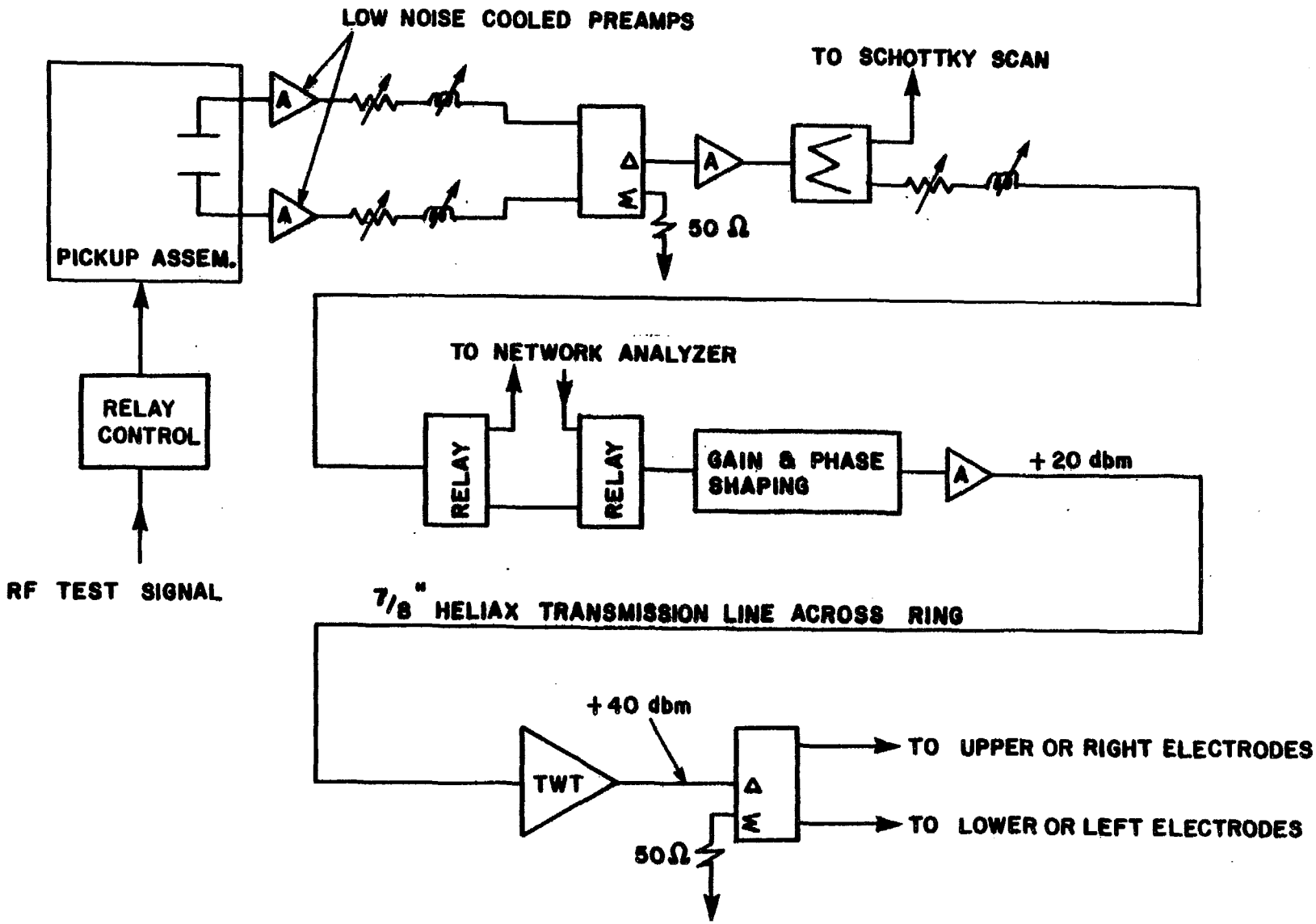

2-4 GHz Core Betatron Cooling System (2 Systems Required)

Figure 5-38

References

1. A.G. Ruggiero, "Vacuum Considerations for the Accumulator Ring," Fermilab $\bar{p}$ Note 194 (1982), unpublished.

2. D. Möhl, G. Petrucci, L. Thorndahl, and S. van der Meer, Physics Reports C, 58 (1980) 73-119.

3. S. van der Meer, "Stochastic Stacking in the Antiproton Accumulator," CERN/PS/AA/78-22 (1978); unpublished.

4. A.G. Ruggiero, "Stochastic Cooling - A Comparison with Bandwidth and Lattice Functions," Fermilab $\bar{p}$ note 171 (1981), unpublished.

5. A.G. Ruggiero, "Pickup Loop Analysis" $\bar{p}$ note 148 (1981), unpublished.

6. S. van der Meer, "A Different Formulation of the Longitudinal and Transverse Beam Response," CERN/PS/AA/80-4 (1980), unpublished.

7. A.G. Ruggiero, "Theory of Signal Suppression for Stochastic Cooling with Multiple Systems," Fermilab $\bar{p}$ note 193 (1982), unpublished.

8. F. Sacherer, "Stochastic Cooling Theory," CERN/ISR/TH/78-11 (1978), unpublished.

9. A.G. Ruggiero, "Revised Intrabeam Scattering Calculation," Fermilab $\bar{p}$ note 192 (1982), unpublished.

10. This discussion follows the discussion of C. Kim, "Design Options for the Fast Betatron Precooling Systems in the Debuncher or in the Injection Orbit," LBL Note BECON-25, unpublished.

11. Unslatter (CERN) unpublished; D. Neuffer, $\bar{p}$ note 199; A. Ruggiero, $\bar{p}$ Note 201.

12. F. Voelker (LBL) unpublished; J. Simpson (ANL) unpublished.

13. Avantek model ABG-2015 for example.

14. J. Shanley, Honeywell Inc., private communication (1982).

15. W. Weinreb et al; IEEE Trans. on Microwave Theory and Techniques 30, pg. 849 (1982).

CHAPTER 6

EXTRACTION OF ANTIPROTONS FROM THE ACCUMULATOR AND TRANSFER TO THE MAIN RING

6.1 Accumulator Beam Manipulation and Extraction

Prior to extraction of the first $\bar{p}$ bunch, a nearly Gaussian distribution of $\bar{p}$'s will exist in the core. The density can be characterized by two numbers, the total number of $\bar{p}$'s in the core, N_o, and the rms energy spread, σ. If ε represents the energy difference between the particle energy and the most probable energy of the particles in the core, then the density function $\psi(\varepsilon)$ can be written as

$$\psi(\varepsilon) = \frac{N_o}{(2\pi)^{1/2}\,\sigma} \exp\left(-\frac{\varepsilon^2}{2\sigma^2}\right) \qquad (6.1)$$

The example presented here uses the following values for these parameters: $\sigma = 2.0$ MeV, $N_o = 4.5 \times 10^{11}$ and $\psi(0) = 10^{5}\text{eV}^{-1}$. Because we want to extract an assembly with the smallest longitudinal emittance, we begin the adiabatic capture with a bucket centered at the peak of the distribution. We plan to extract a single bunch containing 8×10^{10} $\bar{p}$'s. These $\bar{p}$'s exist within a range of ± 452.5 keV. The revolution period of the ring is 1.59 μsec, so the longitudinal emittance of the core region selected is 1.44 eV-sec. The Accumulator parameters which are used in this calculation are $\bar{R} = 75.4716$ m, $\eta = 0.02$, $E_s = 8.938$ GeV, and $\Delta p/p = 1.6\%$ ($\Delta p = 142$ MeV/c) from core to extraction orbit. Because η (i.e. $\gamma_t^{-2}-\gamma^{-2}$) varies over the aperture, the rf parameters determining bucket areas must be varied accordingly.

The rf voltage required to develop a single bucket of area 1.44 eV-sec at harmonic h is $V = 2.44\ h^3$. At $h = 1$, only 2.44 V is required and it may be difficult to establish such a low voltage with sufficient precision to control accurately the number of $\bar{p}$'s extracted. We propose to extract using a single $h = 2$ bucket with the remaining bucket suppressed. The required rf voltage is 19.5 V. Following adiabatic capture, a moving bucket will be established for deceleration to the extraction orbit.

The time required for this unstacking process depends upon the choice of rf voltage and synchronous phase angle. In order to minimize both the disturbance of the stacked $\bar{p}$'s and the particle loss from the moving bucket, the bucket will be moved very slowly, with a small phase angle. After the first $\bar{p}$ bunch has been extracted and placed in the Tevatron at 150 GeV, the duration that this bunch is required to reside in the Tevatron at low field depends upon the time required to extract the remaining

bunches from the core. If the lifetime at 150 GeV is not long enough, it may be necessary to accelerate the process. Optimization of this time can only be accomplished after the Energy Saver and the Antiproton Source are operational. The rf voltage required to maintain the specified bucket area, the deceleration rate, and the time required for deceleration to the extraction orbit are shown in Table 6-I for several synchronous phase angles.

TABLE 6-I RF PARAMETERS FOR DECELERATION TO THE EXTRACTION ORBIT (CONSTANT BUCKET AREA 1.44 EV-SEC.)

ϕ_s (deg)	$\Gamma=\sin\phi_s$	$\alpha(\Gamma)$	V_{rf}(volts)	Decel.Rate (MeV/sec)	Decel.Time (sec)
10	0.1736	0.696	36.2	3.33	43
20	0.3420	0.4918	72	12.93	11
30	0.500	0.3334	157	41.1	3.5

Frequency and phase control of the rf system during unstacking may be improved by a phase-lock system that partially locks the system to the coherent component of beam current. Since this component of current is of order 10 mA, detection and phase locking should not be technically difficult. The bunch length during the unstacking process will be about 500 nsec.

A bunch of 1.44 eV-sec area is too large to accelerate in the Main Ring without large loss and dilution. It is therefore necessary to subdivide the bunch into smaller ones. This subdivision is accomplished by adiabatically capturing the h = 2 bunch into h = 84 (53 MHz) buckets supplied by the same rf system used for the injection stacking. The resulting bunches can be synchronously transferred into standard Main Ring buckets. The optimum number of bunches, which depends on the longitudinal emittance to be transferred and details of a later recombination process, lies in the range of 11 to 13. On the other hand, the bunch produced by the 100-V suppressed-bucket cavity spans many more 53-MHz buckets; between 500 V and 1 kV is required to shorten the bunch. The additional 900 V is generated by a fixed-frequency h = 2 system. Although this system forms two adjacent buckets, only one will contain antiprotons because of the prebunching provided by the suppressed-bucket cavity. The 1-kV bucket height is about 12 MeV or ±0.13%, so these buckets have negligible effect on the remaining cooled core. The momentum spread of the shortened h = 2 bunch is $\Delta p/p = 5.2 \times 10^{-4}$, easily accepted by the Main Ring.

After the eleven to thirteen 53-MHz bunches have been established on the extraction orbit, the extraction kicker shutter is closed, isolating the bunches from the accumulated beam. The bunches are then extracted and delivered to synchronized Main Ring buckets.

Movement of the isolated extraction bucket through part of the stack results in partial replacement of the antiproton density in the core by displacement deceleration from the stack above. Moreover, the cooling system quickly fills the depleted region left by the extracted bunch. During the acceleration of the extracted beam to 150 GeV and prior to the next extraction, core cooling systems will re-establish adequate core density.

The single bucket rf wave consists of one complete sinusoidal wave with a period of one half the rotation period. Because the fundamental frequency is 0.632 MHz, such a wave can easily be generated with Fourier components below 100 MHz. The accelerating structure may consist of an insulating gap in the beam pipe in parallel with a 50 Ω resistance of sufficient power-dissipating capability. This structure will be contained within a shielded enclosure with sufficiently high shunt inductance (introduced by high-permeability ferrite) so that the load presented to a broad-band amplifier will be essentially real over the operating range. The power requirements will be less than 100 W. The 50 Ω real impedance presented to the beam by this structure is well within the longitudinal-stability impedance limit.

The additional 900 V at h=2 is required only at a single frequency at the extraction momentum. It will be developed by a single ferrite-loaded resonant accelerating cavity with a shunt impedance of 1 kΩ. This shunt impedance meets the beam-stability requirement and the required voltage can be developed with an excitation power of 400 W.

After the single antiproton bunch has been narrowed to span the desired number of 53-MHz buckets, the $h = 84$ system is turned on adiabatically over 30 msec to 120 kV. The initial 1.5 eV-sec bunch, 244 nsec wide, shown in its $h = 2$ bucket in Fig. 6-2, is subdivided into thirteen $h = 84$ bunches. An intermediate stage in this operation is shown in Fig. 6-3 with the central $h = 84$ bucket indicated. The $h = 2$ voltage can be left unchanged. At this stage, the distribution lies just within a "ruffled" separatrix, the bucket arising from the sum of the two voltages. The final emittances of the five central bunches are approximately 0.15 eV-second and the outermost bunches are approximately 0.05 eV-sec. At the end of this process, the bunches are matched to 500-kV Main Ring buckets.

Extraction from the Accumulator occurs using a 2.1336 m long shuttered kicker and a 2.921 m long Lambertson magnet. The extraction orbit is rf displaced radially outward by 0.825% in $\Delta p/p$. At station A20 in the high dispersion straight section (See Fig. 5-1), the extraction closed orbit is displaced 71.5 mm outward. The orbit parameters are β_x=7.06 m, β_y=6.63 m, and $\alpha_x=\alpha_y=0$. A shuttered kicker centered 6.32 m downstream of station A20 gives the extracted beam an inward kick of 2.5 mrad and moves the extraction orbit to a position of x=37.19 mm, x_0=-0.002 mrad at the entrance to the Lambertson magnet. Figure 6-1 shows the extraction orbit. The Lambertson then bends the beam up by 100 mrad.

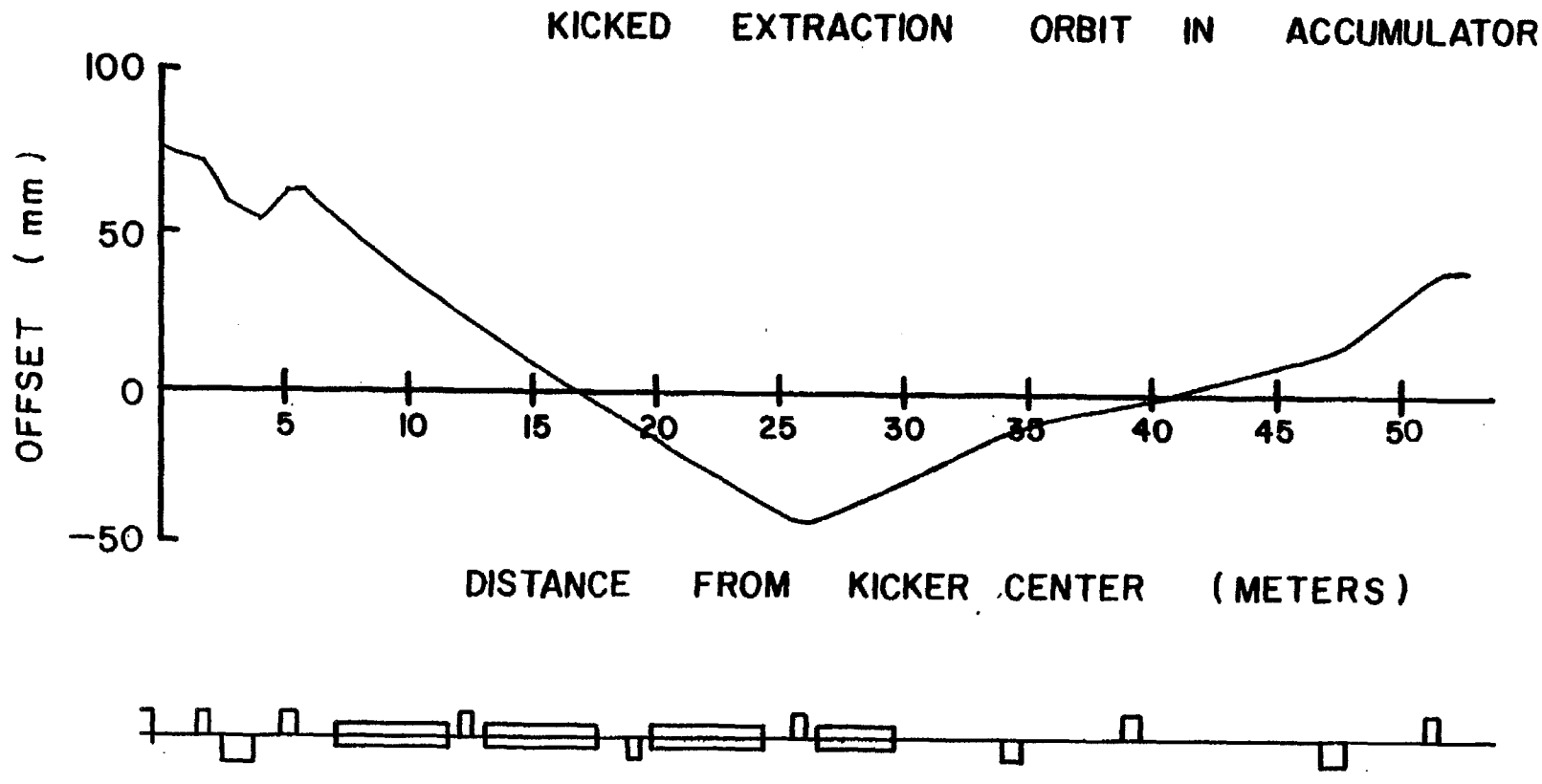
KICKED EXTRACTION ORBIT IN ACCUMULATOR
100
50
0
-50
OFFSET (mm)
5
10
15
20
25
30
35
40
45
50
DISTANCE FROM KICKER CENTER (METERS)

Figure 6-1

6.2 Main Ring Acceleration and Bunch Recombination

6.2.1 Introduction. We describe here the acceleration in the Main Ring of the several contiguous antiproton bunches that will constitute a single bunch in the Tevatron and the process whereby that single bunch is formed before extraction. Statements containing numerical values refer to the same illustrative example used in the preceding section, that is, 11 to 13 bunches with a total emittance of about 1.5 eV-sec.

6.2.2 Injection and Acceleration. The injection process is similar to injection from the Booster except that the Main Ring RF is phase-locked to the Accumulator. The injected intensity is lower by a factor of 20, and the batch is about 1/7 as long as a Booster batch. These differences require that the Main Ring be tuned differently from the $\bar{p}$-production mode, but do not represent unreasonable requirements for the same rf system. In addition, the Main Ring voltage should be about 500 kV to match the bucket produced by the h = 84 system in the Accumulator.

The longitudinal emittance is expected to increase by a factor of about 1.5 during acceleration. Recent studies in the Main Ring and careful simulation of transition crossing both indicate that bunches with initial longitudinal emittance in the range 0.2 to 0.3 eV-sec are diluted by a factor of about 1.25 between injection and γ=21, above transition. This dilution is accompanied by a slight bunch-to-bucket shape mismatch so that further dilution resulting from coherent bunch motion within the bucket results in the total dilution during acceleration of a factor of approximately 1.5.

6.2.3 Bunch Recombination at 150 GeV. At 150 GeV, the Main Ring field is held on flat top while the 13 adjacent bunches are coalesced into a single bunch. The h=1113 rf voltage is reduced slowly over a period of 0.1 seconds to about 12 kV by counterphasing equal numbers of rf cavities. At this voltage, the bucket containing the center bunch is nearly full. Adjacent buckets are not quite full and the total longitudinal emittance of all the bunches is about 2.2 eV-sec. At this time, the h=53 rf system is turned on at a voltage level (700 V) such that the h=53 bucket is matched to a 2.2 eV-sec distribution extending over the filled h=1113 buckets, 245 nsec. At the same time the counterphased Main Ring rf voltage is turned off and replaced by a single small h=1113 rf cavity at 12 kV. The voltage of this cavity is then lowered slowly to (nominally) zero so that the adjacent bunches are adiabatically debunched into matched orbits in the h=53 bucket. A simulation of this process, starting with bunch distributions derived from previously simulated acceleration is shown in Figs. 6-5 and 6-6. The result is a uniform bunch of about 2.4 eV-sec matched to the h=53 bucket and spanning a range $\pm 2\pi/3$ radians.

The next step in the bunch-coalescence procedure is to rotate the extended low momentum spread distribution into a vertical strip with sufficiently short time duration so that it can be contained within a single 53-Mhz (h = 1113) bucket. Because the bunch initially spans a range

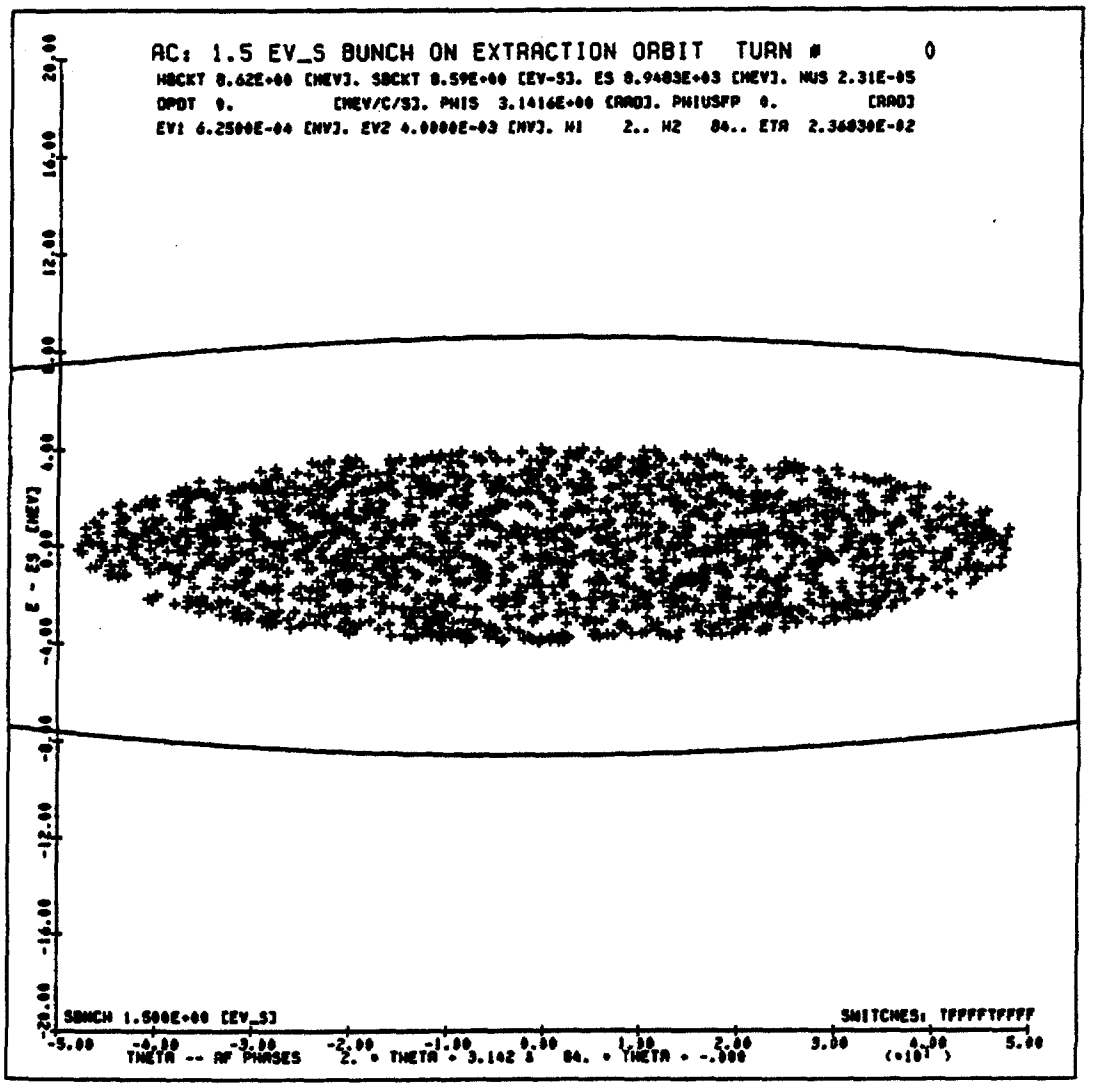
AC: 1.5 EV_S BUNCH ON EXTRACTION ORBIT TURN # 0
HBCKT 8.62E+00 [MEV]. SBCKT 8.59E+00 [EV-S]. ES 8.9403E+03 [MEV]. NUS 2.31E-05
DPDT 0. [MEV/C/S]. PHIS 3.1416E+00 [RAD]. PHIUSFP 0. [RAD]
EV1 6.2500E-04 [MV]. EV2 4.0000E-03 [MV]. H1 2.. H2 84.. ETA 2.36830E-02
E - ES [MEV]
SBUCH 1.500E+00 [EV_S]
SWITCHES: TFFFFTFFFF
THETA -- RF PHASES
2. * THETA + 3.142 & 84. * THETA + -.000
(*10^1)

Figure 6-2

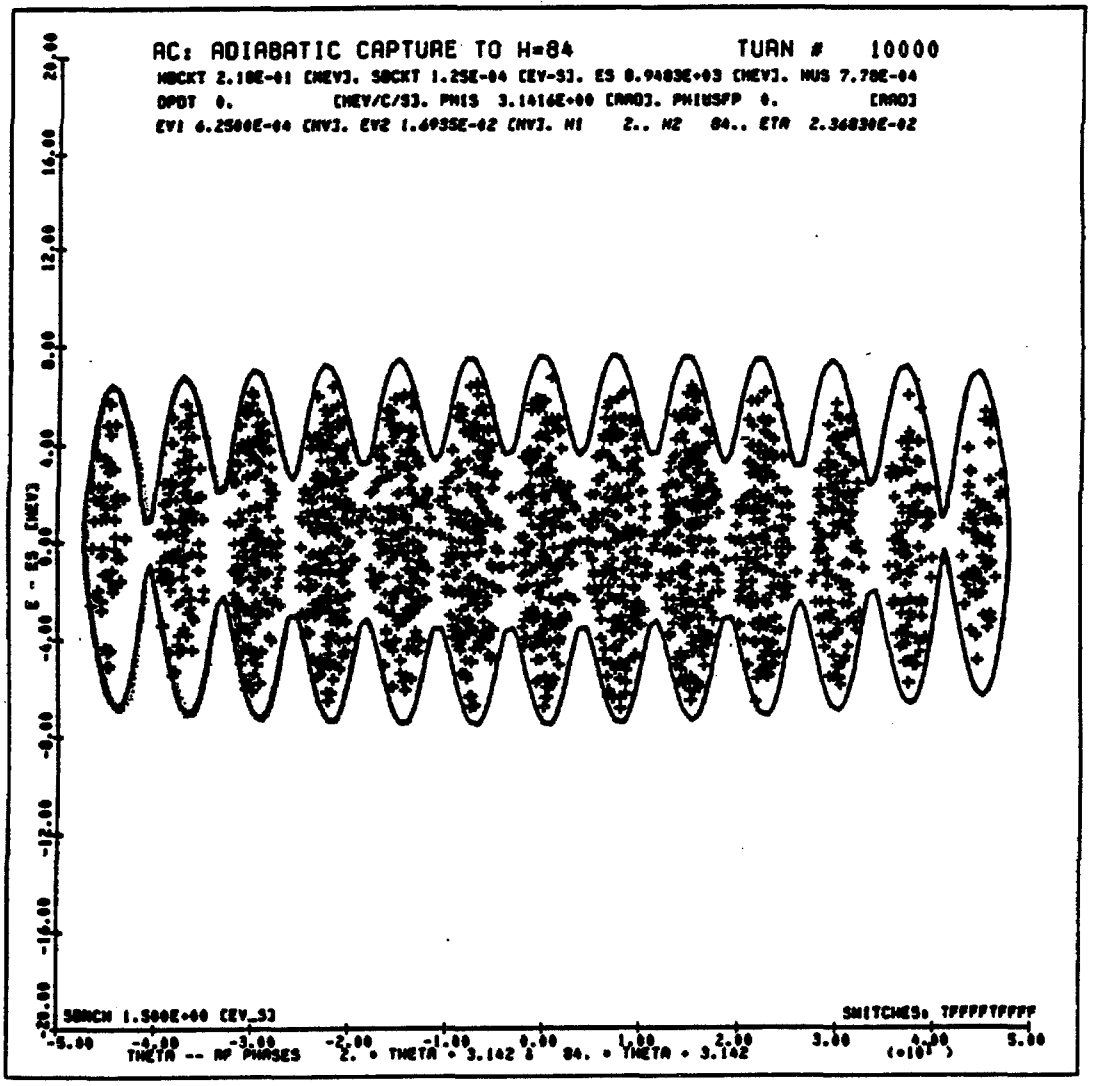
AC: ADIABATIC CAPTURE TO H=84
TURN # 10000
MBCKT 2.18E-01 [MEV]. SBCKT 1.25E-04 [EV-S]. ES 0.9483E+03 [MEV]. NUS 7.78E-04
DPDT 0. [MEV/C/S]. PHIS 3.1416E+00 [RAD]. PHIUSFP 0. [RAD]
EV1 6.2500E-04 [MV]. EV2 1.6935E-02 [MV]. H1 2.. H2 84.. ETA 2.36830E-02
E - ES [MEV]
SBNCH 1.500E+00 [EV_S]
SWITCHES: TFFFFTFFFF
THETA -- RF PHASES
2. * THETA * 3.142 &
84. * THETA * 3.142
(*10^)

Figure 6-3

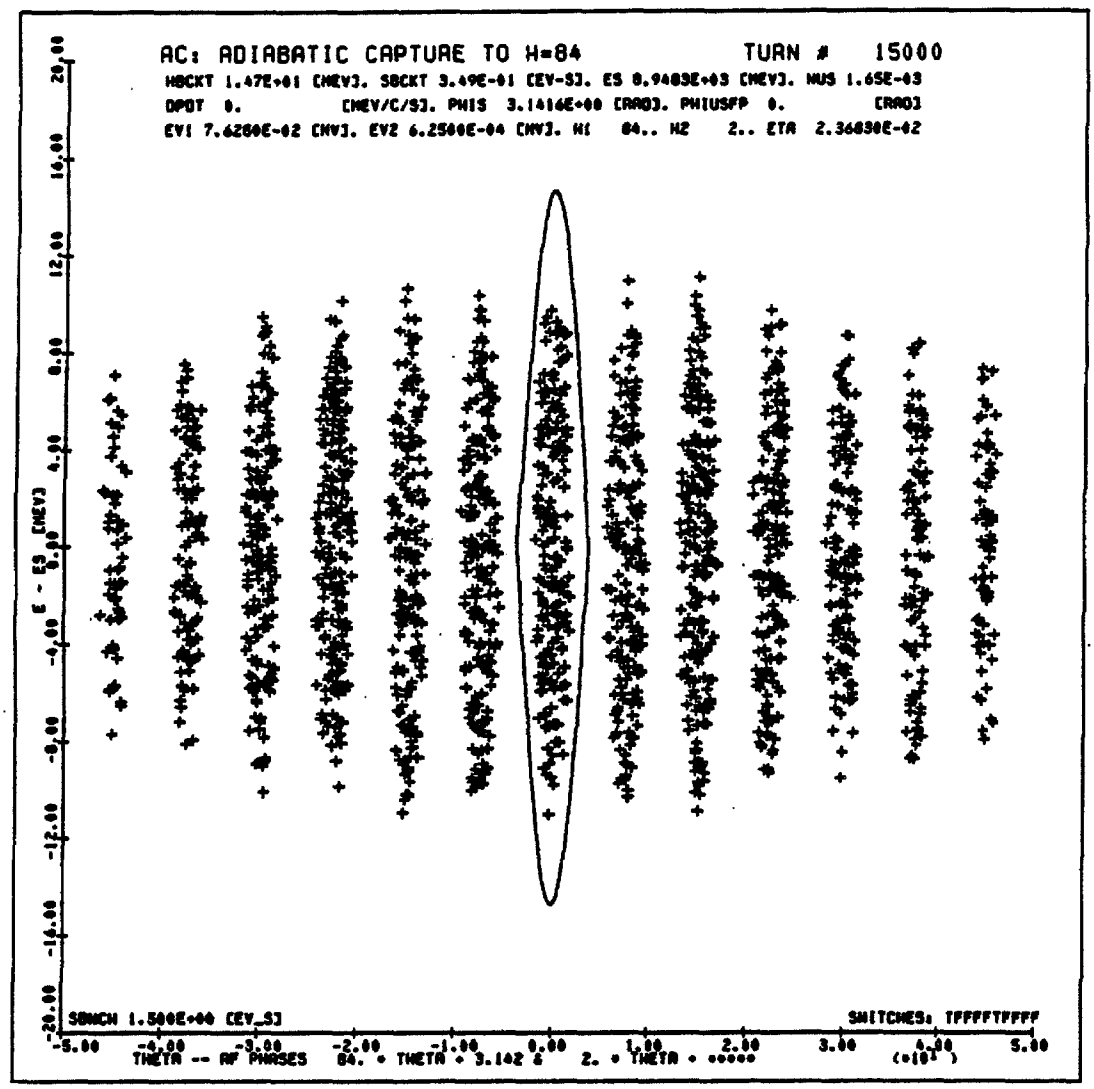
AC: ADIABATIC CAPTURE TO H=84
TURN # 15000
HBCKT 1.47E+01 [MEV]. SBCKT 3.49E-01 [EV-S]. ES 0.9483E+03 [MEV]. MUS 1.65E-03
DPDT 0. [MEV/C/S]. PHIS 3.1416E+00 [RAD]. PHIUSFP 0. [RAD]
EV1 7.6280E-02 [MV]. EV2 6.2500E-04 [MV]. H1 84.. H2 2.. ETA 2.36830E-02
E - ES [MEV]
SBUNCH 1.500E+00 [EV_S]
SWITCHES: TFFFFTFFFF
THETA -- RF PHASES 84. * THETA + 3.142 & 2. * THETA + ...
(*10³)

Figure 6-4

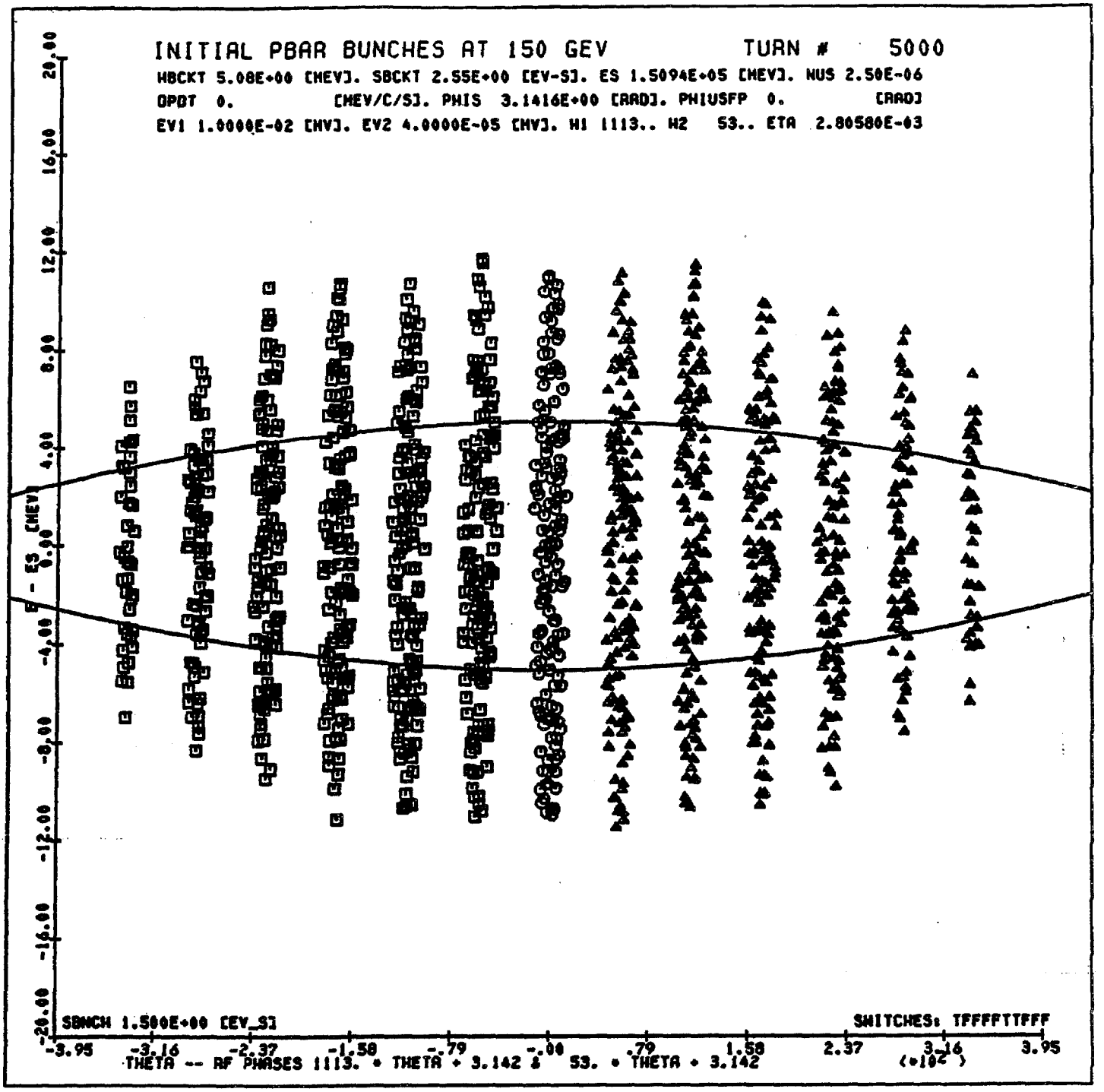

Figure 6-5 Adjacent antiproton bunches prior to final h=1113 debunching. The bucket outline shown is an h=53 bucket which will match the distribution of the coalesced bunches. The particles in the lefthand bunches have been indicated by squares, those in the center bunch by octogons, and those in the righthand bunches by triangles to aid in interpretation of the coalesced distribution shown in the following figere

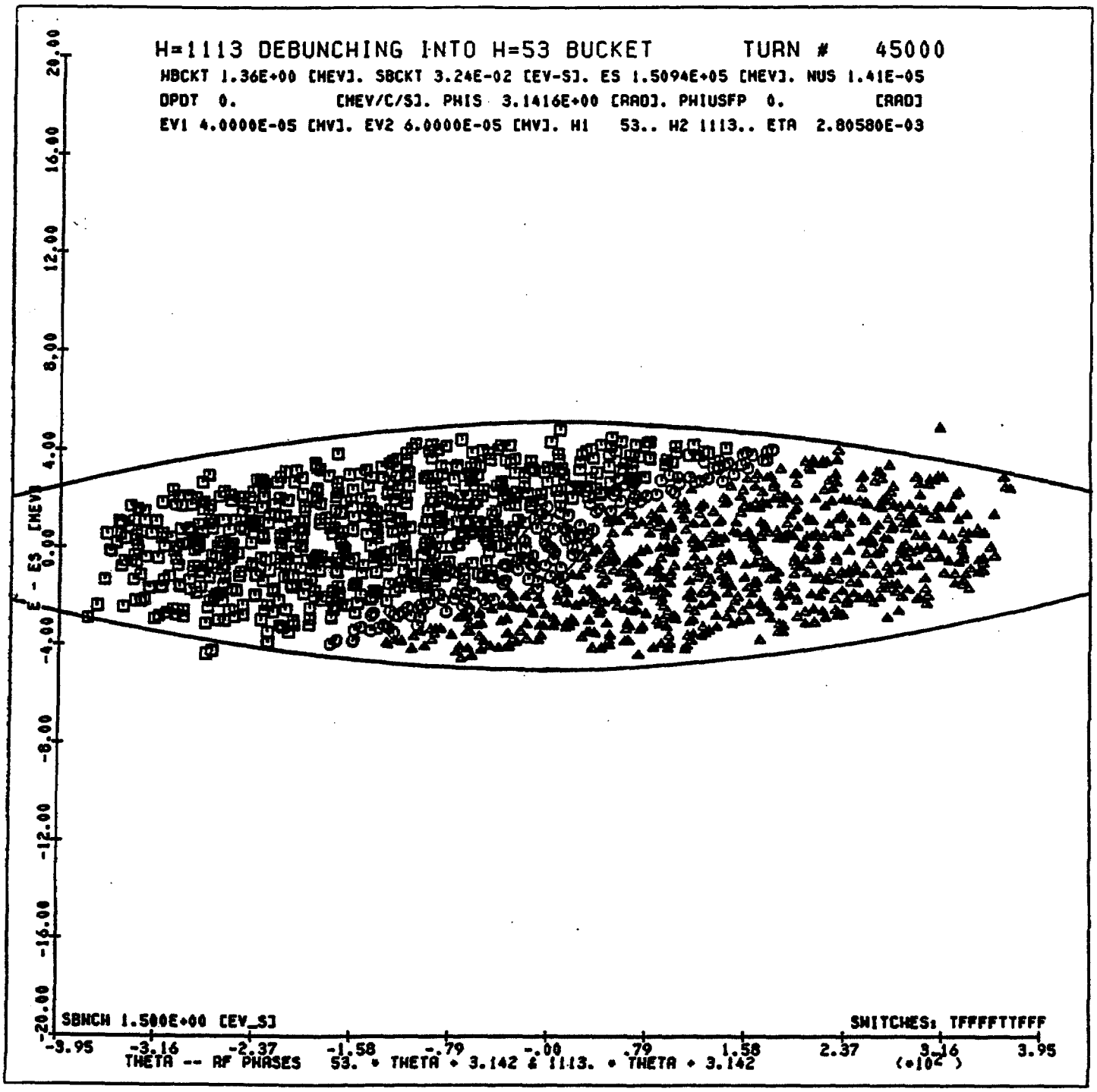

Figure 6-6 The antiproton distribution within the h=53 bucket following slow removal of the h=1113 rf voltage. The bunch extends over ± 13/21 π radians within within the bucket and the longitudinal emittance (95%) is about 2 eV-sec. Particles originating from h-1113 bunch left of the central bunch are indicated by squares, those from the central bunch by octagons, and those from the right-hand bunches by triangles.

of $\pm 2\pi/3$ radians in the h = 53 bucket, rotation within a h = 53 bucket created by a sinusoidal rf voltage at 2.53 MHz would not be satisfactory because of the spread in phase-oscillation period. Antiprotons on the outer edges of the distribution would lag behind those nearer the center and the vertical strip would be decidedly S-shaped. In order to "linearize" the synchrotron motion, the rf cavity wave-shape has been augmented with appropriate amounts of second, third, and fourth harmonics so that the rf gap voltage is linear to within about 10 percent between $\pm 0.63\pi$ radians. In this circumstance, particles within the linear portion of the wave move with harmonic motion of nearly constant period so that the entire distribution reaches maximum momentum spread and minimum time spread at approximately the same time.

In Fig. 6-7, a simulated result of such a rotation is shown. The rf voltage used for this simulation was composed of a fundamental h = 53 voltage of 22.8 kV and a second-harmonic component of 4.9 kV at the correct phase angle for optimum linearization.

In Fig. 6-8, we show the results of a preliminary experiment in bunch coalescing. The experiment is done at h = 159 using four adjacent proton bunches. The successive oscilloscope traces starting at the bottom of the pictures show two or four proton bunches merging into a single bunch of larger intensity and emittance, as expected. Since the bucket covered only seven h = 1113 bucket lengths, the four bunches extended farther into the bucket than is proposed. This results in a more nonlinear process than will occur in the proposed scheme.

Following recapture, the rf voltage is raised to 1 MV. As a result, the bunch length shrinks to 12 nsec full width, and the bunch height grows to ± 166 MeV, corresponding to a momentum spread $\Delta p/p$ of $\pm 1.1 \times 10^{-3}$. The bunch parameters are ideal for injection into pre-established matching buckets in the Tevatron.

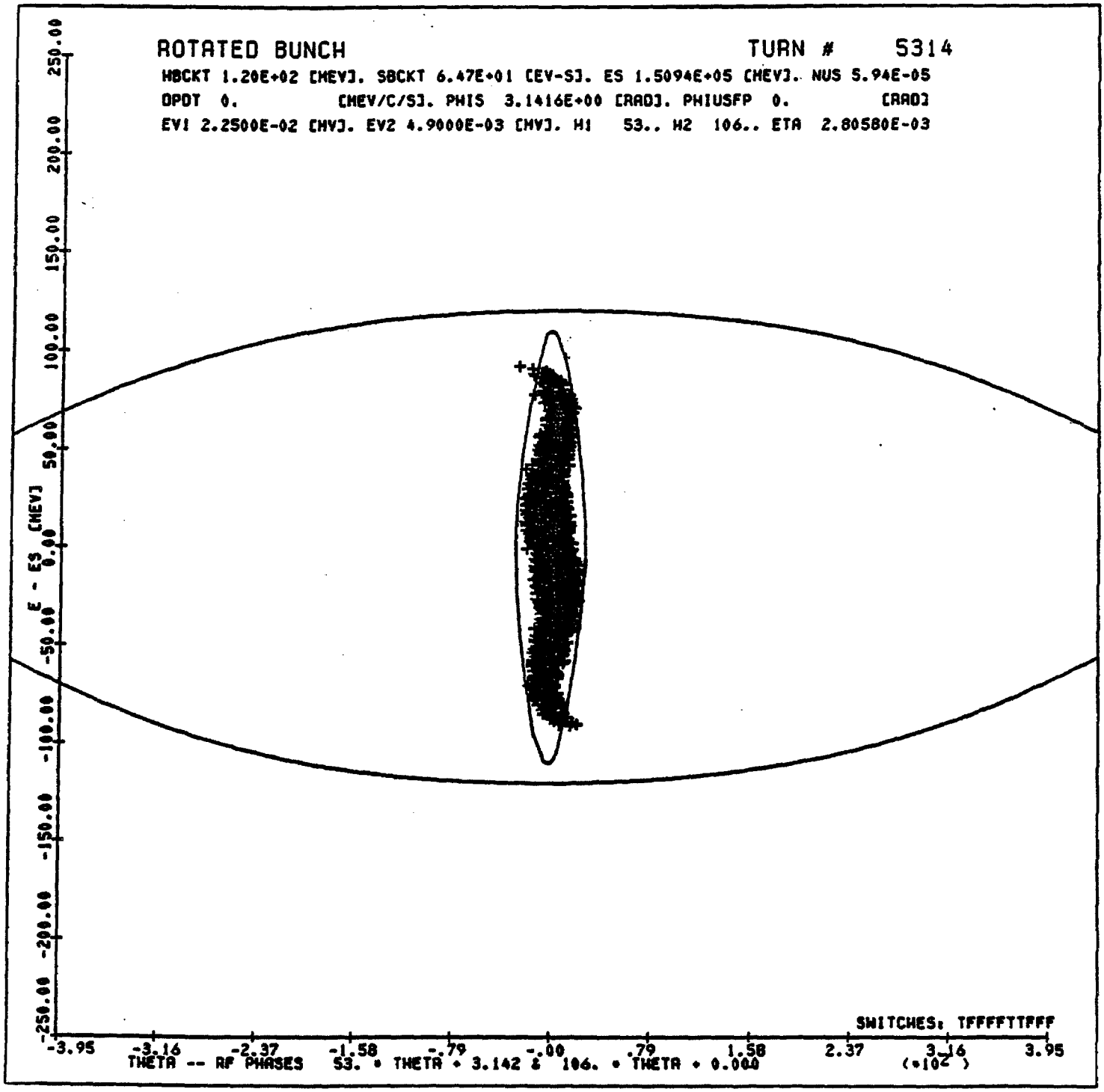

Figure 6-7 Antiproton distribution following bunch rotation in h=53 bucket. The rotated distribution has a full length of about 16 nsec and spans an energy range of ±100 MeV.

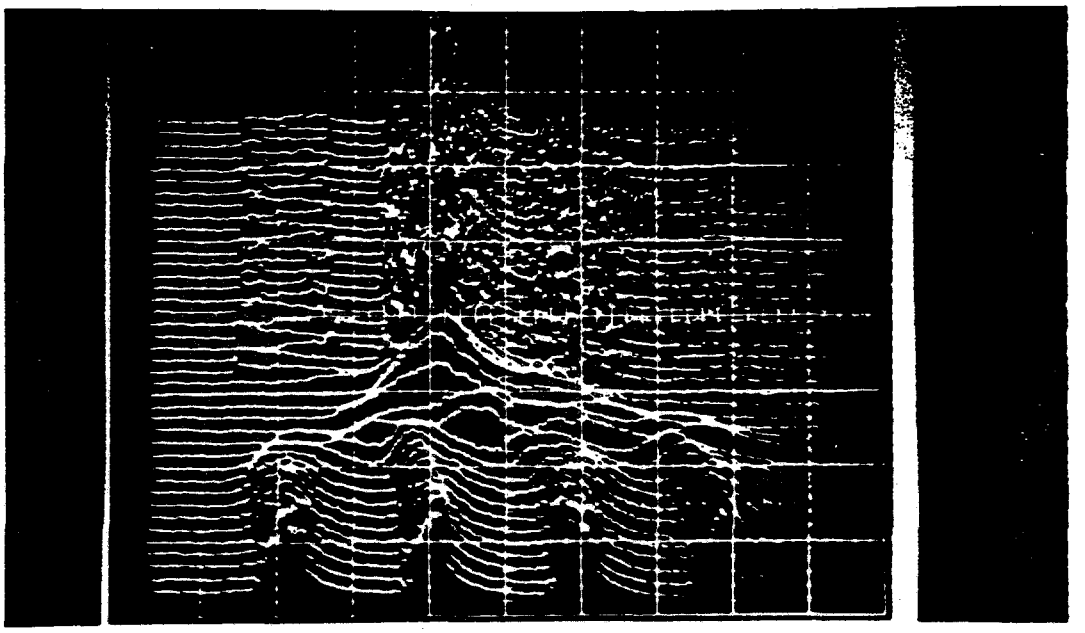

Figure 6-8a

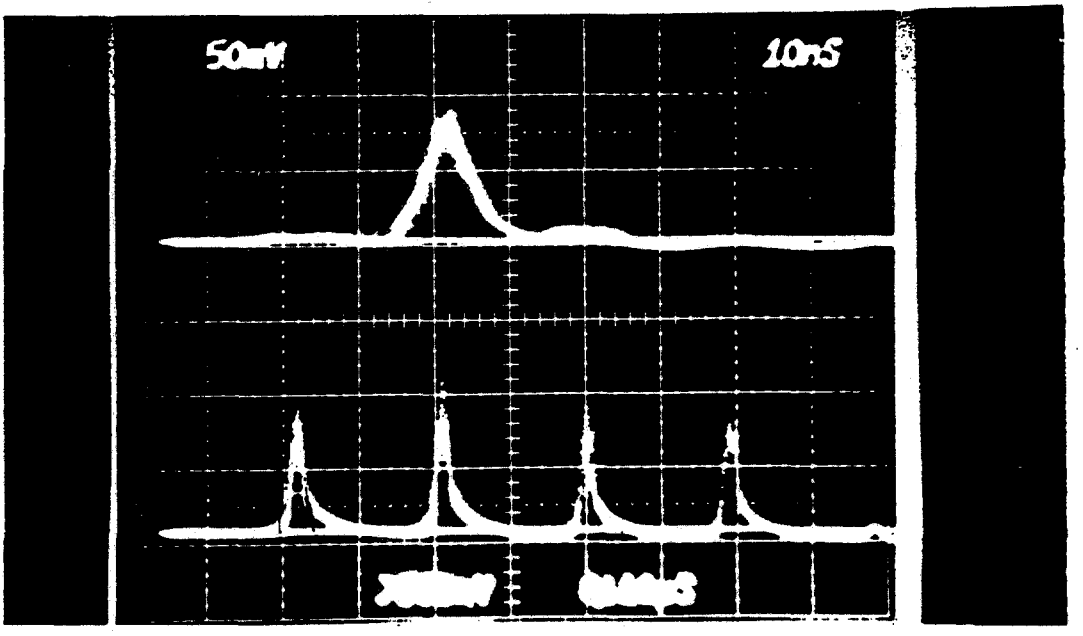

Figure 6-8b

Figure 6-8 Results of an early experiment in coalescing adjacent 53 MHz bunches in a lower harmonic bucket. The experiment was done at h=159 (7.5 MHz) where the lower harmonic bucket spans seven 53 MHz buckets. (a) The evolution of the coalescing process, time progressing upwards in 5ms steps. (b) The four bunches .1s before and .1s after coalescing. The coalescing efficiency (ratio of areas under the peaks) is about 90%. The time base is 10ns per major division in both pictures.

CHAPTER 7

THE MAIN RING IN TEVATRON I

7.1 Functions of the Main Ring in Tevatron I

The Main Ring is required to perform five separate functions in the Tevatron I mode:

1. Acceleration of protons for antiproton production. During antiproton production and accumulation, the Main Ring will be required to accelerate single batches of protons (approx. 82 bunches) of intensity greater than 2×10^{12} protons per batch to 120 GeV. This will be done routinely on a 2-sec cycle. Each of these acceleration cycles must include the bunch-narrowing technique and extraction at F17 described in Chapter 2.

During this mode of operation, a special low-level rf system must be used. This system will contain provision for transient beam-loading compensation. In addition, the technique for phase-locking the Main Ring to the Booster will be slightly different from that used during fixed-target operation.

2. Injection of $\bar{p}$'s from the Accumulator into the Main Ring. Bunches of antiprotons containing 10^{11} $\bar{p}$'s must be transported to the Main Ring and injected.

3. Acceleration of antiprotons to 150 GeV. After a sufficient number and density of antiprotons have been established in the Accumulator, the Main Ring must be used to accelerate groups of antiproton bunches to 150 GeV. This acceleration cycle must include the bunch manipulations at 150 GeV described in Sections 6.1 and 6.2. Special additions to the rf systems will be required to accomplish these manipulations. Following these acceleration cycles, the single antiproton bunches must be extracted at E0 for injection into the Tevatron.

4. Acceleration of protons to 150 GeV. The Main Ring will be required to accelerate a few bunches of protons to 150 GeV, where they will be combined to form single proton bunches containing 10^{11} protons. This operation will be similar in many respects to the antiproton acceleration described above and the same special additions to the rf systems will be utilized.

5. Transfer of particles from the Main Ring into the Energy Saver. Transfers of 150 GeV protons and antiprotons are both described in Chapter 8.

7.2 Antiproton Injection

The antiproton bunches from the Accumulator are matched into the proton extraction line at EB5. They are then transported back down the 120-GeV extraction line and injected into the Main Ring at the F17 Lambertson. Special low-current power supplies are used to power the 120-GeV extraction line to ease regulation problems caused by running large power supplies at 5% levels.

The orbit excursions of the injected beam between F17 and E48 are limited by a 4-bump centered at F0 (produced by the horizontal correction dipoles at E48, E49, F11 and F13.) An additional orbit bump centered at F17 (produced by the correction dipoles at F15, F17, F19 and F22) may be used to steer the beam up to 14 mm away from the Lambertson septum on the first turn, if this is necessary. These bumps will be on at pbar injection time, and will probably be left on throughout the acceleration cycle.

The kicker will be a copy of one module (40 in.) of the Main Ring C48-style magnet. The necessary kick angle of approximately 450 μrad requires approximately 500 A. The pulser will be a simple SCR-switched capacitive discharge type, producing a half-sine-wave of falltime approximately 15 μsec. Flat top uniformity of approximately ±.01% for approximately 350 msec is expected.

The following calculations have been done for a momentum of 8.89 GeV/c, emittance (at that energy) of 2 pi mm-mrad, and a momentum spread of ±0.09%.

Figures 7-1, 7-2 and 7-3 show the injected beam spot at the C-magnet, Lambertsons, and the F17-1 quad. In the figures, the dotted line indicates the beam spot for the circulating beam with the F17 steering bump on at maximum (14 mm). For the injected beam, the closest clearance in the Lambertson aperture is 3 mm (on both sides,) and also 3 mm at the F17-1 quad.

Figure 7-4 shows the orbit produced by the kicker at E48 alone; Fig. 7-5 shows the kicker plus the kick-offsetting bump at F0; and Fig. 7-6 shows the injected orbit and the F17 bump which may be used to steer the beam away from the septum on the first turn after injection.

Figure 7-7 shows the region near F17 in detail, indicating both the circulating and injected beam envelopes. Nearly the full inner limits of the physical aperture of the quad at F17-1 and the dipoles at F16-7 are explored.

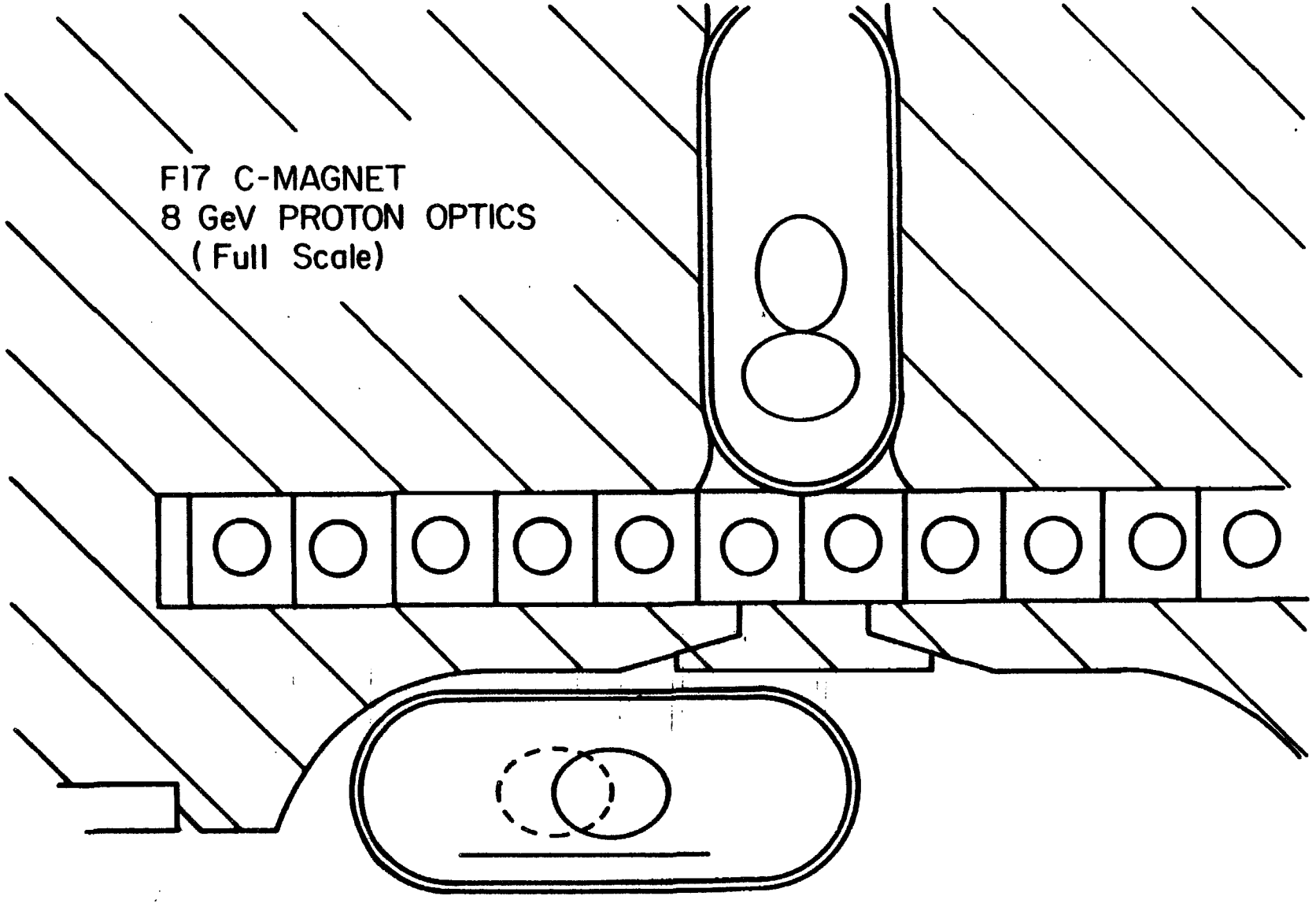

Figure 7-1

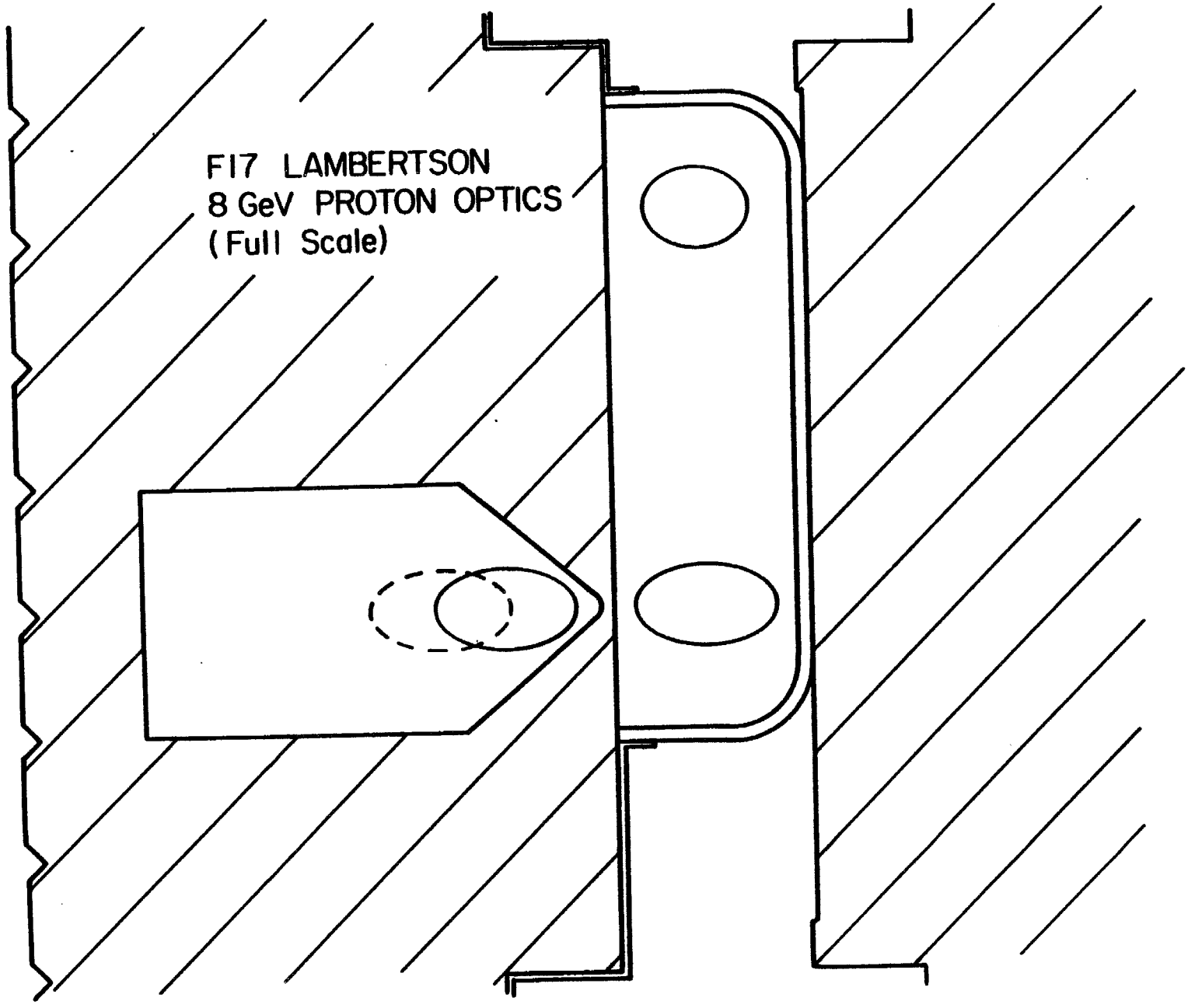

Figure 7-2

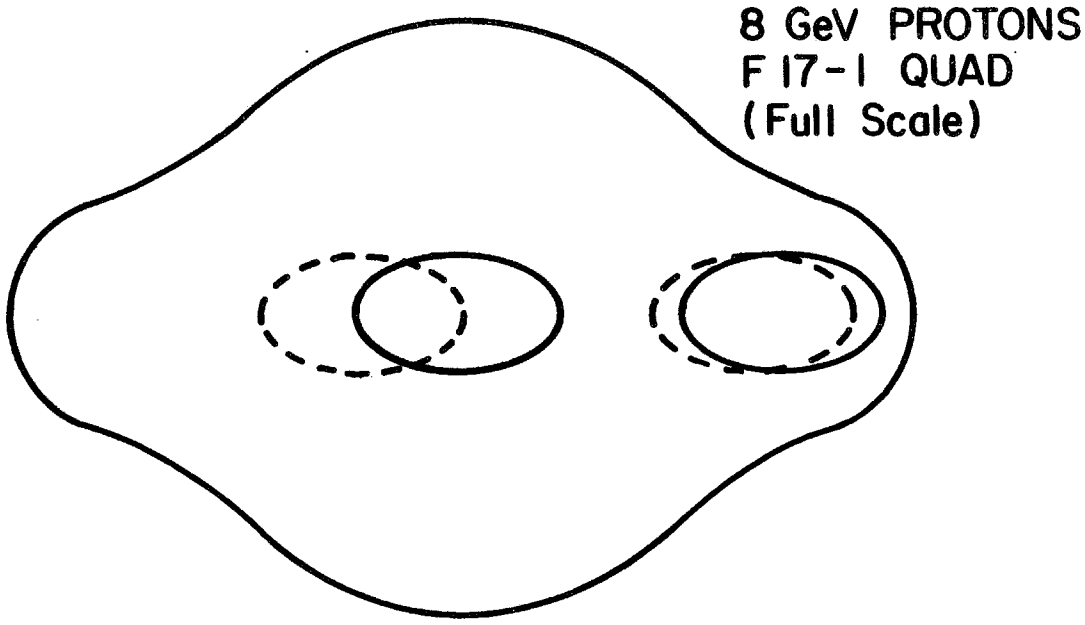

Figure 7-3

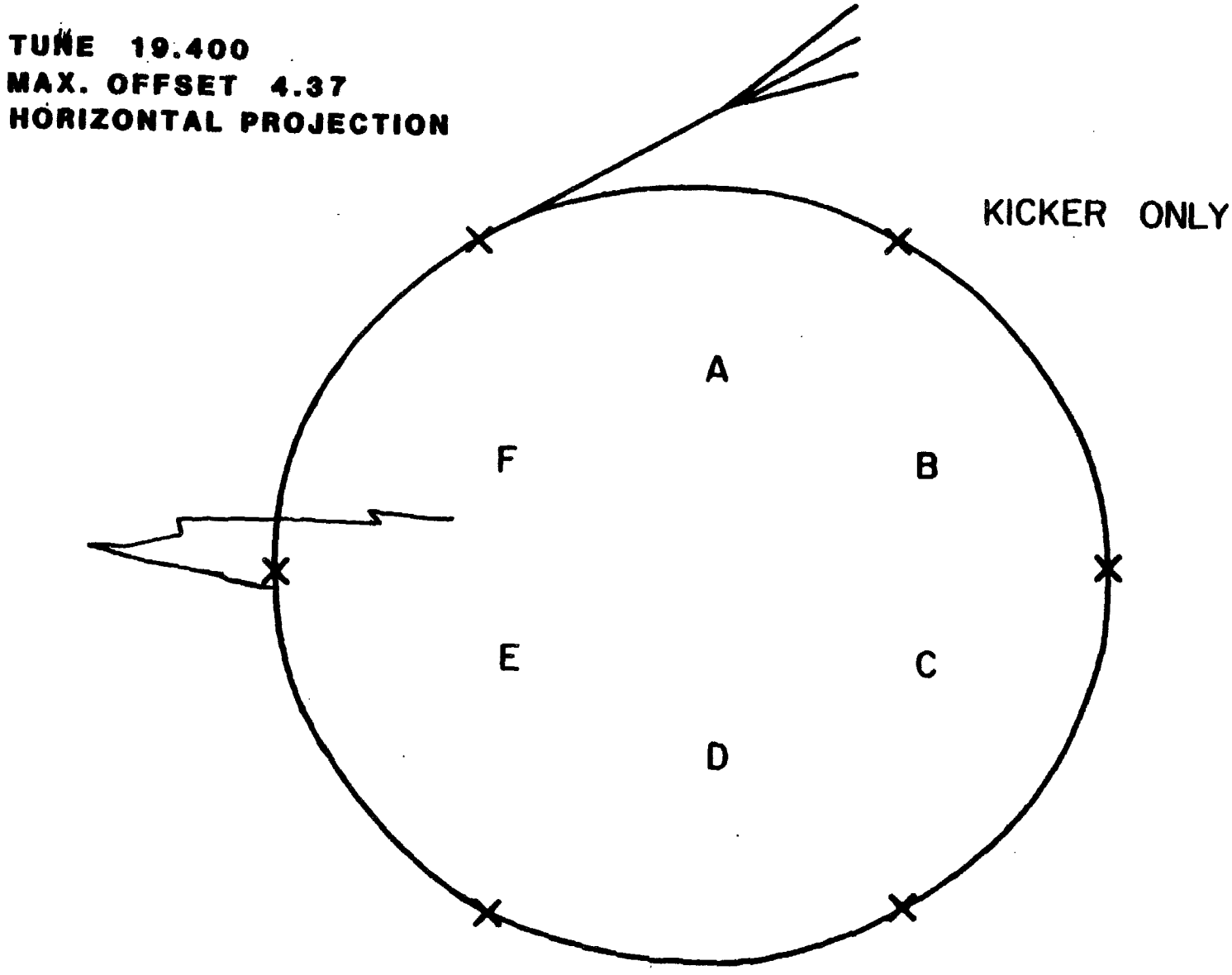
TUNE 19.400
MAX. OFFSET 4.37
HORIZONTAL PROJECTION
KICKER ONLY
A
B
C
D
E
F

Figure 7-4

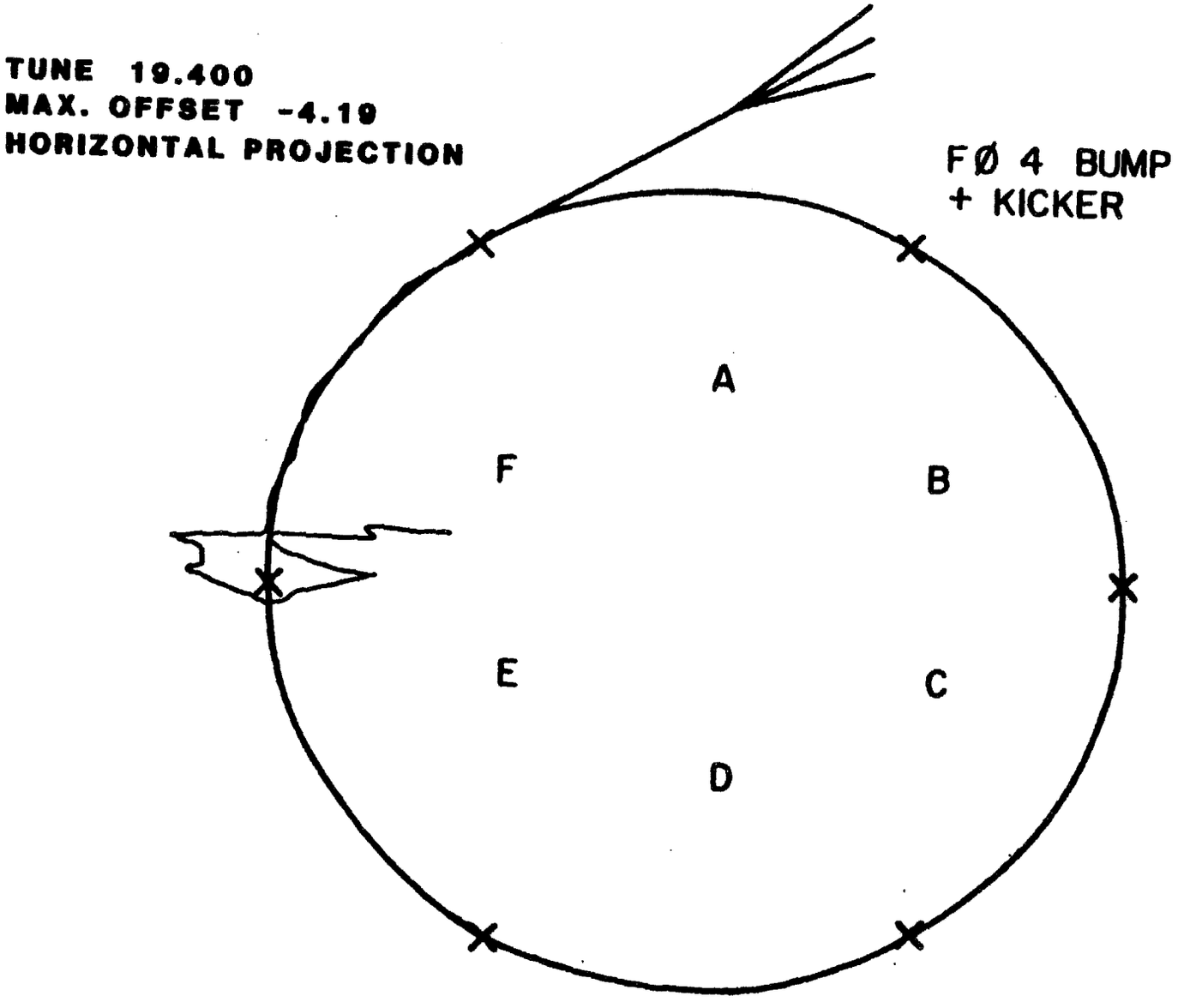
TUNE 19.400
MAX. OFFSET -4.19
HORIZONTAL PROJECTION
FØ 4 BUMP
+ KICKER
A
B
C
D
E
F

Figure 7-5

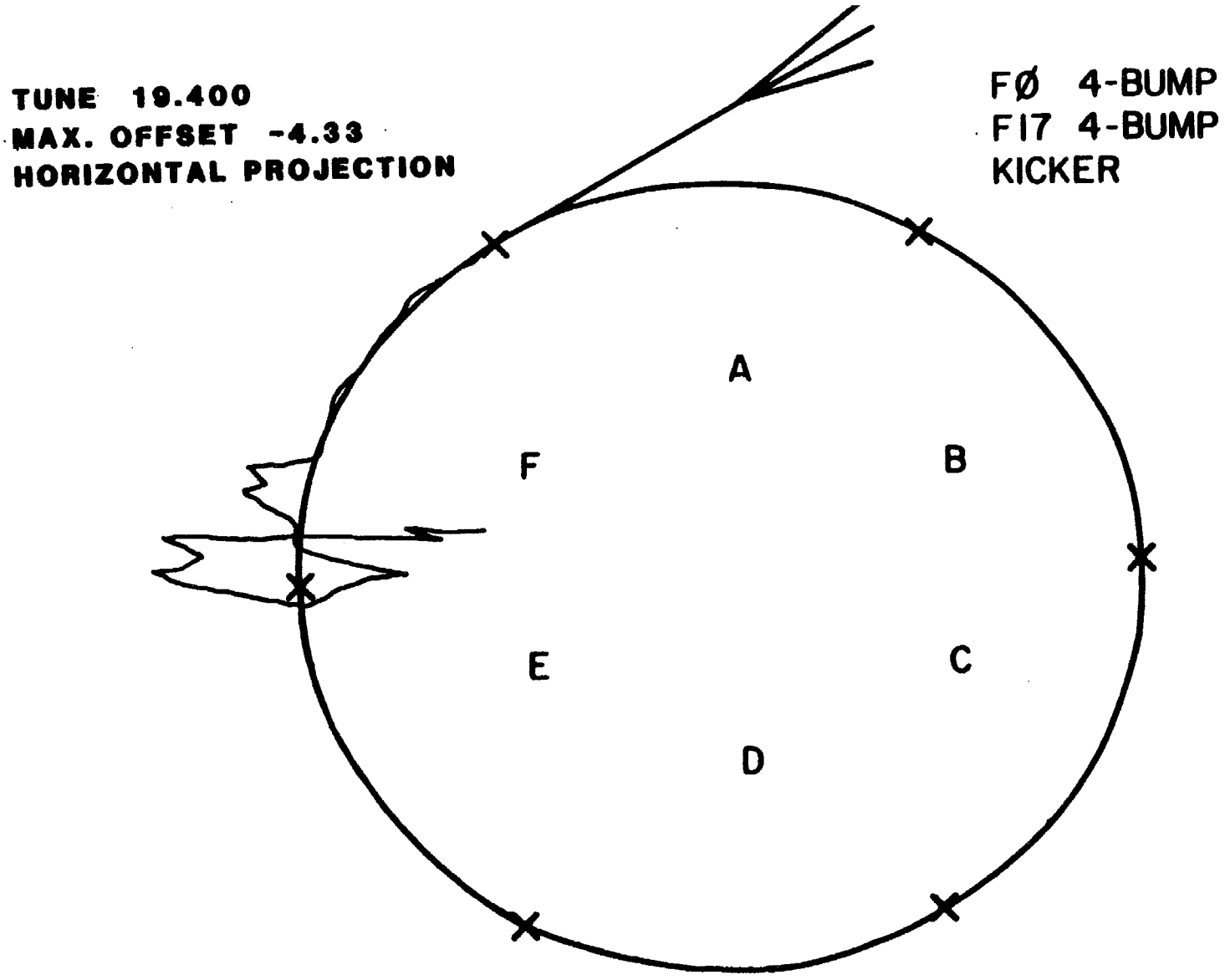
TUNE 19.400
MAX. OFFSET -4.33
HORIZONTAL PROJECTION
FØ 4-BUMP
F17 4-BUMP
KICKER
A
B
C
D
E
F

Figure 7-6

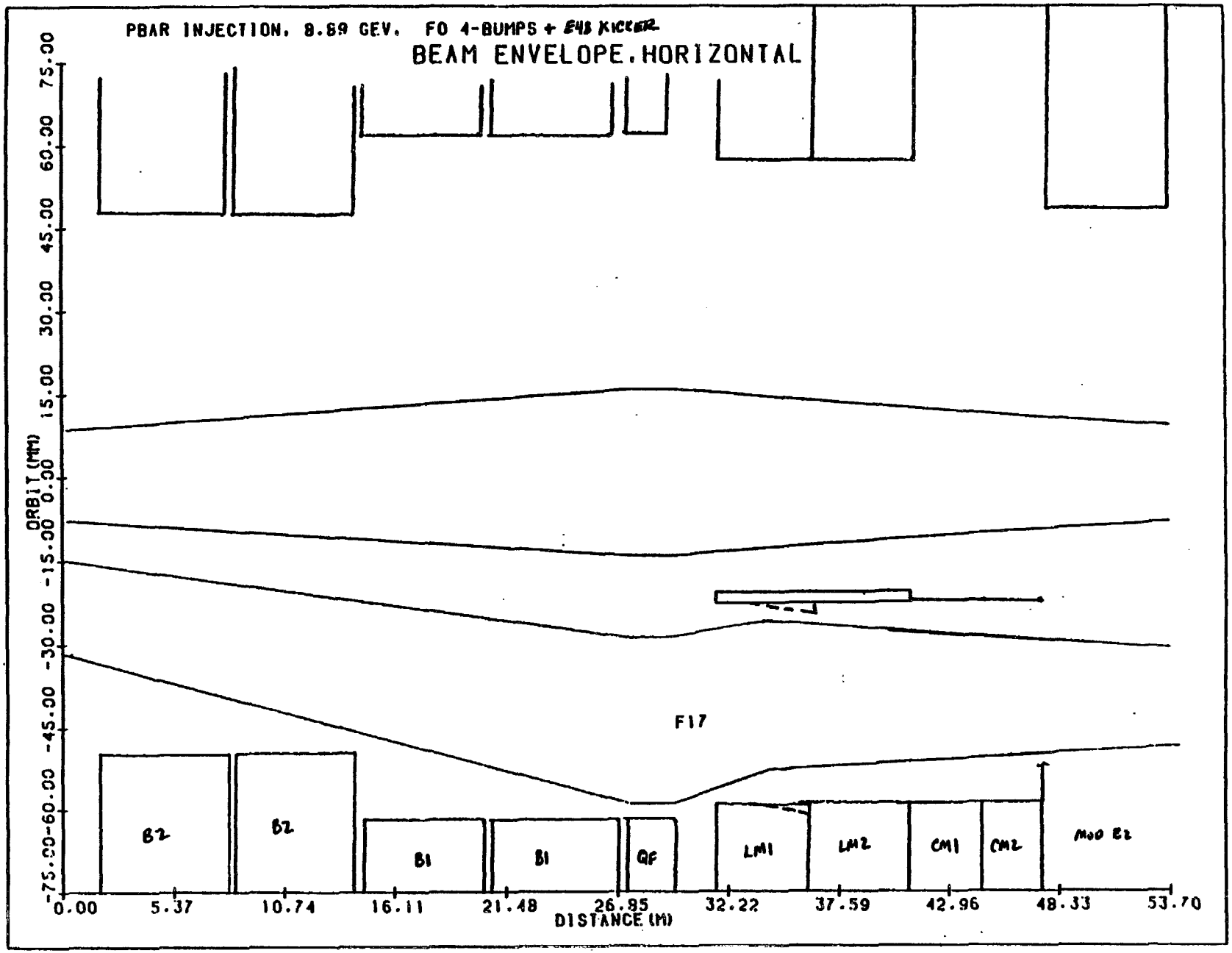
PBAR INJECTION, 8.89 GEV. FO 4-BUMPS + E48 KICKER
BEAM ENVELOPE, HORIZONTAL
ORBIT (MM)
75.00
60.00
45.00
30.00
15.00
0.00
-15.00
-30.00
-45.00
-60.00
-75.00
F17
B2
B2
B1
B1
QF
LM1
LM2
CM1
CM2
MOD E2
0.00
5.37
10.74
16.11
21.48
26.85
32.22
37.59
42.96
48.33
53.70
DISTANCE (M)

Figure 7-7

The injection angle required at F17 is 0.95 to 1.05 mrad (depending on the size of the F17 steering bump required.) The difference between this angle and the 0.8 mrad introduced by the rolled Lambertson can be achieved using the trim dipole in the AP1 line. In the worst case, this produces a 4 mm beam offset from the C-magnet center line, which is tolerable (see Fig. 7-1.)

7.3 Main Ring Acceleration and Rebunching Hardware

The processes of accelerating small groups of proton bunches and cooled antiprotons to 150 GeV has been described previously in Chapter 6. In those descriptions reference was made to an rf system in the Main Ring providing 22kV at h = 53 (2.529 MHz) and 3.7 kV at h = 106. This requirement will be met by installing two heavily ferrite-loaded rf cavities, each operating at the 20-kW level. These cavities will be refurbished and slightly modified cavities from the Princeton Pennsylvania Accelerator (PPA). Operation of these cavities in the Main Ring will require installation of an anode power supply of about 8 kV, 15 A (120 kW). Small additions to the low-level rf system will also be required to provide appropriate rf driving signals phase-locked to the integrally related h=1113 53 MHz rf.

Small additions to the control system will also be required for remote operation of these systems.

7.4 Main Ring Overpass

The performance of both the Antiproton Source and the Collider Detector can be significantly improved by bypassing the Main Ring beam around the Collider Detector at B0. This bypassing - called here the "Overpass" - has at least two advantages:

(i) It allows elimination of the asymmetric hole for the Main Ring through the Collider Detector;

(ii) It allows accumulation of antiprotons to proceed simultaneously with colliding-beam operation. This will increase the average luminosity of the entire system by eliminating the pause of several hours while the antiproton beam is being refreshed.

The design of an overpass for the Main Ring, called TCB21, has been worked out in detail by T.L. Collins and is presented here. There are a number of constraints that such a design must satisfy:

(a) Space must be generated for additional bending elements;

(b) The new path must close smoothly on to the old path to high precision in both horizontal and vertical dimensions and at all energies with a minimum of programmed external control.

(c) The path lengths must be the same in old and new paths, or differ by an integral number of rf wavelengths;

(d) the betatron functions must match, as in any insertion;and

(e) Any residual dispersion introduced outside the overpass must be small.

The overpass design limits Main Ring operation to 200 GeV or less. Some magnets are operated at twice the normal field. Consider a set of four bending magnets. The outer two magnets will be unchanged to provide the normal horizontal bend. The inner magnets will be rolled about the beam axis to produce a vertical bend of 32.3 mrad. Such four-magnet sets placed symmetrically around the long straight section (for example, at A41 and B12) will produce a 19 ft vertical separation, enough to miss the entire detector. The new orbit connects smoothly on both ends. A total of four sets (16 magnets) is in the additional circuit. The additional excitation of this circuit will be provided by a separate power supply.

Of sixteen special dipoles excited by a common power supply, eight for the vertical bending have (3"x3") aperture, while the remaining eight for the horizontal bending are essentially the same as the main ring B2 dipole with (2"x4") aperture but are modified to provide a field twice as large as the main bend field at the same excitation current.

The overpass has approximately 8 in. of extra orbit length. This undesired length is cancelled by combining the vertical bends with a slight inward bend to "cut across" the arc. The inward bend can be accomplished easily by rolling the vertical dipoles by 6.3°.

The betatron functions are easily matched across the insertion. The vertical dispersion introduced in the remainder of the ring must be balanced with some care. Its maximum value has been reduced by this balancing to approximately 0.5 m, which is noticeable, but tolerable. Coordinates of the overpass insertion magnets are given in Table 7-I and the maximum values of vertical dispersion around the ring are listed in Table 7-II. The locations of elements are shown in Fig. 7-8.

TABLE 7-I OVERPASS COORDINATES FOR TCB21

Numbers in parentheses are for the original Main Ring ($Z=\theta_v=0$).

Station	x(feet)	y(feet)	θ_h(rad)	Z(inches)	θ_v(rad)
A39	962.531 (962.531)	2,285.083 (2,285.083)	.8175454 (.8175454)	0.000	0.00000
A42	1,034.911 (1,034.808)	2,350.493 (2,350.639)	.8535781 (.850017)	19.286	.0322656
A43	1,109.464 (1,109.175)	2,413.368 (2,413.813)	.8860663 (.882488)	57.063	.0322656
A44	1,186.021 (1,185.554)	2,473.789 (2,474.539)	.9185544 (.914959)	94.840	.0322656
A45	1,264.500 (1,263.864)	2,531.691 (2,532.754)	.9510426 (.947430)	132.617	.0322656
A46	1,344.818 (1,344.023)	2,587.013 (2,588.396)	.9835307 (.979902)	170.393	.0322656
A47	1,426.890 (1,425.946)	2,639.697 (2,641.406)	1.0160189 (1.012373)	208.180	.0322656
A48	1,510.566 (1,509.547)	2,689.860 (2,691.728)	1.00448499 (1.044844)	226.656	.0000000
B0	1,686.376 (1,685.357)	2,787.887 (2,789.756)	1.0692033 (1.069198)	226.656	.0000000
B11	1,772.743 (1,771.723)	2,835.248 (2,837.117)	1.0692033 (1.069198)	226.656	.0000000
B12	1,870.616 (1,869.596)	2,887.172 (2,889.042)	1.1016746 (1.101669)	226.656	.0000000
B13	1,958.274 (1,957.352)	2,929.994 (2,931.709)	1.1304914 (1.134140)	207.364	-.0322641
B14	2,047.177 (2,046.446)	2,970.092 (2,971.504)	1.1629795 (1.166611)	169.589	-.0322641
B15	2,137.335 (2,136.786)	3,007.281 (3,008.386)	1.1954677 (1.199083)	131.815	-.0322641
B16	2,228.654 (2,228.275)	3,041.523 (3,042.315)	1.2279558 (1.231554)	94.040	-.0322641

B17	2,321.037 (2,320.818)	3,072.779 (3,073.256)	1.2604440 (1.264025)	56.625	-.0322641
B18	2,414.047 (2,413.981)	3,102.116 (3,102.275)	1.2766880 (1.280261)	18.491	-.0322641
B19	2,507.920 (2,507.920)	3,128.673 (3,128.673)	1.3127319 (1.312732)	.000	.0000000

TABLE 7-II. VERTICAL DISPERSION AT β_v = 100m WITH THE B0 OVERPASS TCB21

	ν = 19.40	ν = 19.60*
outside	0.51m	0.34m
A39 - A47	2.58	2.30
A47 - B12	4.68	4.39
B12 - B19	2.55	2.25

*The tune of 19.40 is the standard value for the fixed-target run while 19.60 might be preferable for the storage mode of operation.

7.5 Main Ring Diagnostics

7.5.1 Main Ring Position Detectors. The electronics used to read out the position of the Main Ring beam will be improved to have capabilities similar to the Energy Saver position detectors described in Sec. 8.6.1. This improvement is needed for commissioning the $\bar{p}$ system. Orbit information is necessary at both h=53 and h=1113 for both protons and antiprotons in the Main Ring.

7.6 D0 Overpass

A second Main Ring overpass will be built at D0 for the same purpose as the B0 overpass: to bypass the Main Ring beam around the detector or detectors. The D0 overpass is planned to minimize tunnel modifications. The maximum possible height under this restriction is 63.7 in. from the present Main Ring beamline or a clearance of 63.7 in. + 25.5 in. = 89.2 in. over the Tevatron center line.

One vertical dipole (instead of two for the B0 overpass) and two special horizontal dipoles are needed at each of two outer bend locations. At two inner bend locations, we need only vertical dipoles, one at each location. In order to achieve te maximum possible separation of 89.2 in., two outer bends should be at C46-2 and D13-5. Two inner bends are within the D0 longstraight and the clear space at D0 along the beamline for the detector is 32 ft upstream and 37.8 ft downstream from D0. This design is called WD89. Unlike TCB21 at B0, the D0 overpass has been designed without any attempt to localize the vertical dispersion within the overpass. As a

consequence, the maximum vertical dispersion outside the overpass can be as large as 2m at β_v = 100m when the B0 overpass is also installed. In order to find out how much the momentum and transverse acceptances are affected with such a large vertical dispersion around the ring, we will install a test overpass, called WD51, during the shutdown in July, 1984. The beam height of this overpass is 51.15 in. from the present Main Ring beamline and the outer bends are at C46-4 and D13-3, while the inner vertical bends are in the D0 long straight section. They are as far apart as possible in order to prevent the overpass line from penetrating the tunnel ceiling. Although the height is not as much as in WD89, the maximum vertical dispersion is approximately 1.7m around the ring. Later, by simply moving two inner vertical dipoles to the location specified in WD89, we can increase the beam height to 81.3 in. from the Tevatron beamline. This version, called WD81, keeps all other magnets in the same positions as in WD51. At present, the design of detectors at D0 is still in progress and the final choice between WD81 and WD89 cannot be made. For WD89, most magnets inside the overpass must be moved from the position specified for the test overpass WD51. The maximum vertical dispersions at β_v = 100m for various cases are listed in Table 7-III. The locations of all the elements of the two bypasses are shown in Fig. 7-8.

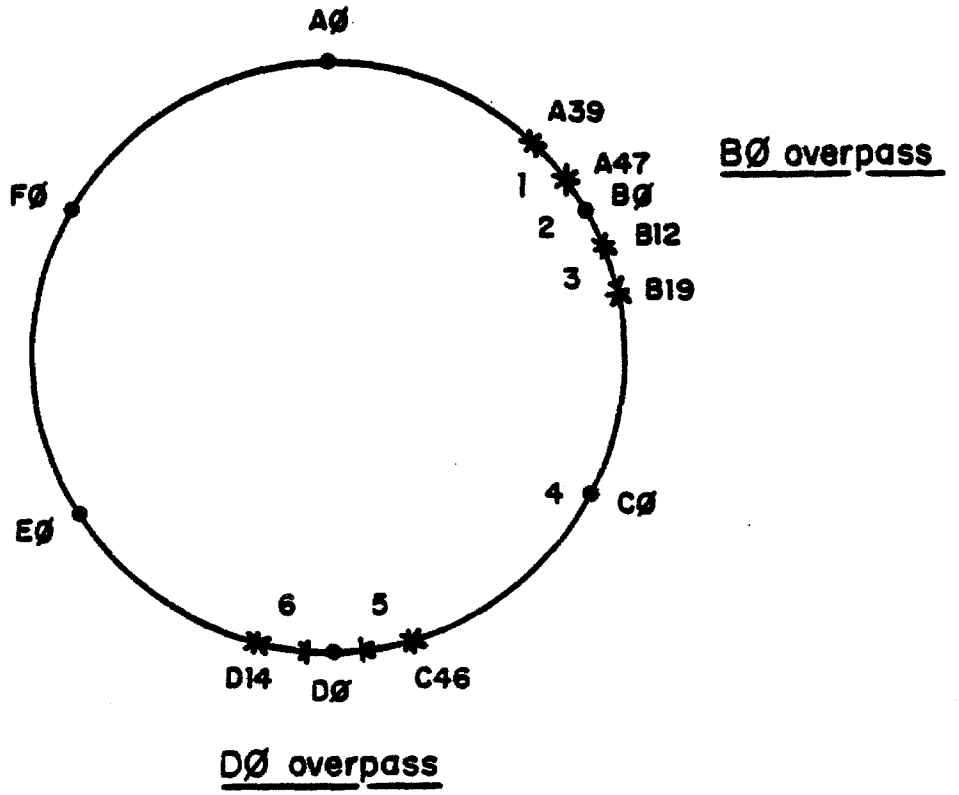

Overpass Elements

Figure 7-8

TABLE 7-III VERTICAL DISPERSIONS IN EACH REGION (normalized at β_v = 100m)

		outside	"1"	"2"	"3"	"4"	"5"	"6"
fract. length	=	60.4%	2.8%	2.5%	3.3%	27.1%	1.9%	1.9%
	tune							
(A)	19.40	<------	------	1.67m	------	--->	1.42m	1.52m
(B)	19.40	1.16	2.12	4.43	2.97	2.12	1.91	1.15
	19.60	1.38	2.20	4.48	3.02	2.03	2.34	1.91
(C)	19.40	1.46	2.50	4.79	3.38	2.43	2.04	0.90
	19.60	1.65	2.61	4.88	3.45	2.29	2.34	1.92
(D)	19.40	0.51	2.58	4.68	2.55	<-----	0.51 -	--->
	19.60	0.34	2.30	4.39	2.25	<-----	0.34 -	--->

(A) WD51 alone (B) TCB21 and WD81 (C) TCB21 and WD89 (D) alone.

CHAPTER 8

THE ENERGY SAVER IN TEVATRON I

8.1 Functions of the Energy Saver in Tevatron I

The Tevatron I project uses the Energy Saver Ring as a 1-TeV storage ring for bunched-beam collisions. The construction of this ring was a separate project undertaken for the purpose of operating the Fermilab fixed-target program at 500 GeV. It was recognized that the Energy Saver could be used as a 1-TeV storage ring if proper attention was given to a number of details such as position monitors and beam-transfer systems.[1] Since the field quality for slow extraction was at least as stringent as the requirement for colliding beams, the Energy Saver is inherently a useful storage ring. For that reason, the Energy Saver was designed so that it could be modified in the future to operate as a 1-TeV collider. These modifications are part of the Tevatron I project.

The Energy Saver will perform the following functions in the Tevatron I project:

1. Injection. It will sequentially accept bunches of 150-GeV protons and antiprotons from the Main Ring, one bunch at a time.

2. Acceleration. After the appropriate number of bunches has been stored, it will simultaneously accelerate the proton and antiproton bunches to the collision energy.

3. Collision. After acceleration, the beams will be stored and the low-beta sections described in Chapter 9 will be turned on to increase the luminosity.

The material presented in Sections 8.2 and 8.3 is based on the Superconducting Accelerator Design Report, May, 1979. Since 1979, there have been a number of changes in the design. The changes that are important to the use of the Energy Saver as a collider are described in this chapter. The most notable of these are: the correction coils are separate from the quadrupole windings, the rf system has been expanded to handle the larger longitudinal emittance of the antiprotons, and the beam transfer at E0 has been simplified substantially after it was decided to make the circumference of the Energy Saver exactly the same as the Main Ring.

8.2 Energy Saver Lattice

8.2.1 Ring Location and Normal Lattice. The lattice of the Energy Saver ring is constrained by the requirement that it fit beneath the Main Ring magnets. Therefore, it has the same basic configuration as the Main Ring,

which has 6 superperiods with 6 long straight sections and normal cells with 8 dipoles and 2 quadrupoles. Because the Energy Saver dipole ends could not be placed directly under the Main Ring ends, the Energy Saver dipoles are displaced 15.5 in. upstream of their Main Ring counterparts.[2] Figures 8-1 and 8-2 sketch the position of the quadrupole in the lattice and the position of a normal cell relative to the Main Ring lattice. The beam center line is 25.5 inches below Main Ring center line. The circumference of the two rings is identical. At the time the Superconducting Accelerator Design Report was prepared, it was proposed to make the two rings differ in circumference by 4.4 cm, as a way of providing for pp collisions with the Main Ring and Saver. That option has been dropped because it compromised the beam transfer between the Main Ring and the Saver.[3]

Like the Main Ring, the present lattice has a medium straight section at location 17 formed by omitting two dipoles. Its layout is shown in Fig. 8-3. There are long straight sections of "normal" configuration, ones with high beta for extraction, and ones with low beta for colliding-beam interactions. These are discussed separately in subsequent sections. Table 8-I summarizes the warm straight-section lengths available in the lattice. It gives the drift lengths between "effective" magnetic ends of the elements, the available warm length and the space allotted for the cryogenic bypasses of cold-to-warm transitions and vacuum isolation.

TABLE 8-I WARM STRAIGHT-SECTION LENGTHS

Location of Warm Regions (In.)	Drift Length[a] (In.)	Available Warm Length (In.)	Hot-Cold Transition Upstream	Hot-Cold Transition Downstream
Median location 17 (standard quadrupole with corrections)	566.2	493.2	39	34
Normal-β median location 48	310.9	238.9	36	36
High-β median location 48	308.7	236.7	36	36
Normal-β doublet space 49,11	150.36	78.36	36	36
High-β doublet space 49,11	151.65	79.65	36	36
Long straight section	2094.2	2022.2	36	36
Low-β long straight section	600.24	528.24	36	36

[a]Magnetic lengths used throughout to define drift lengths.

All medium straight sections at 17 and 48 locations, and all long straight sections are warm. The space between the long straight-section doublets is warm only where necessary.

8.2.2 Normal and High-Beta Long Straight Sections. Figure 8-4 shows the geometry of the normal long straight section together with amplitude

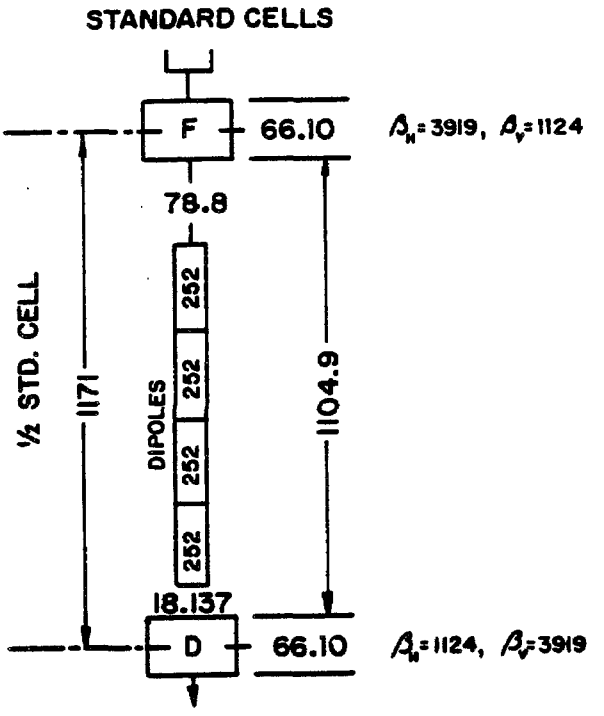

All dimensions in inches, slot length for dipoles, effective magnetic length for quads except for focussing, D-F 1/2-cell is similar.

Phase advance 1/2-cell = 33.903°

Figure 8-1 Locations of elements in standard cell.

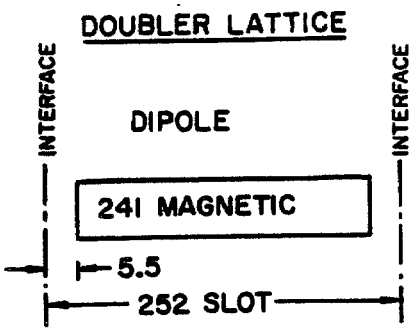

Dipoles are 252" flange to flange. Assume effective magnetic length $\ell = \frac{1}{B_0}\int B d\ell = 241"$. Each Dipole bends $\theta = 2\pi/774$ Rad. Quads are in series with bends. At a current (nom. 4527A) when dipole $B_0\ell$ = 245 kG x 241", I assume a quad grad. G_0 =19.627 kG/in or $k = (G_0\theta/B_0\ell)^{\frac{1}{2}}$ = .003833/in.

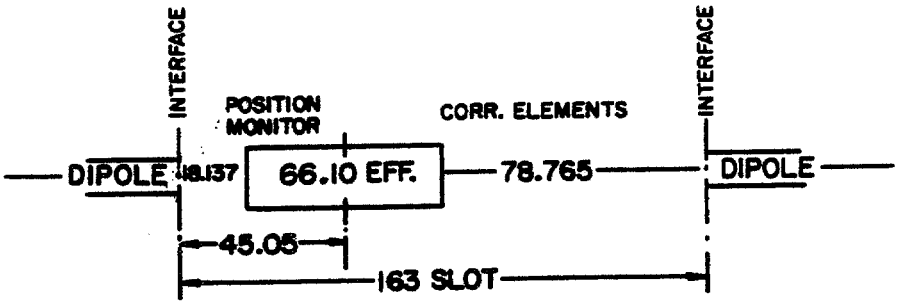

Standard quad. Showing effective length $\frac{1}{G_0}\int G d\ell$ and its position in cryostat. There are many non standard quads

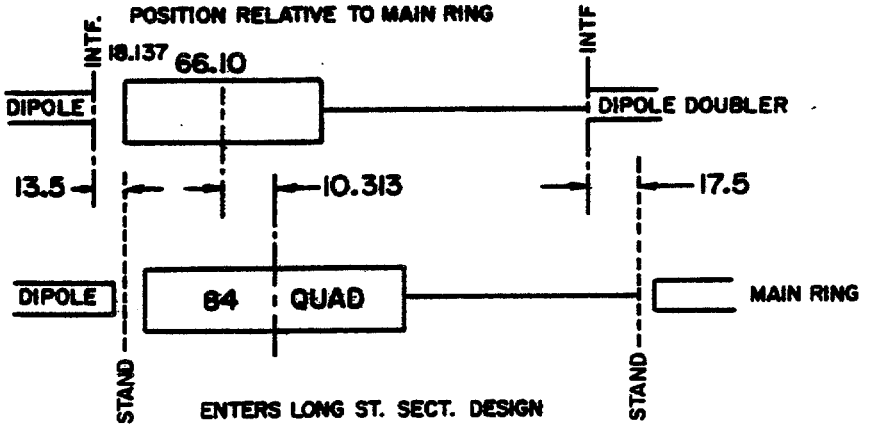

Figure 8-2 Locations of superconducting magnets relative to Main Ring.

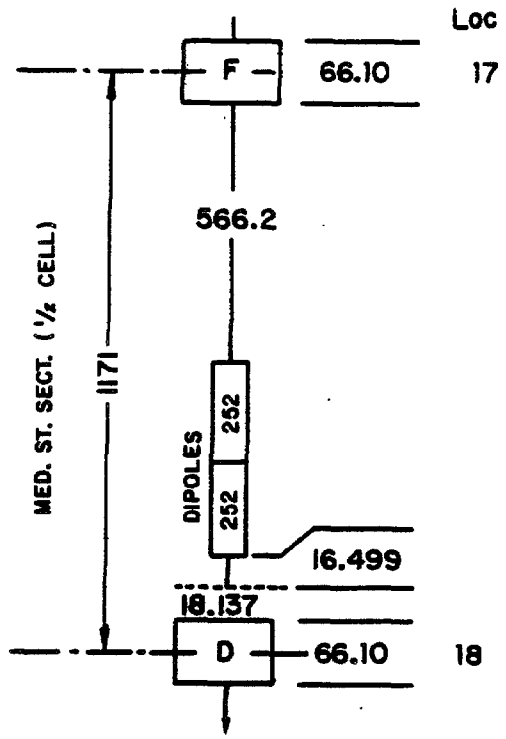

Figure 8-3 Medium straight section. A standard 1/2-cell with two dipoles omitted. A space of 16-1/2 inches must be inserted at downstream end to close the geometric orbit in the shifted Doubler.

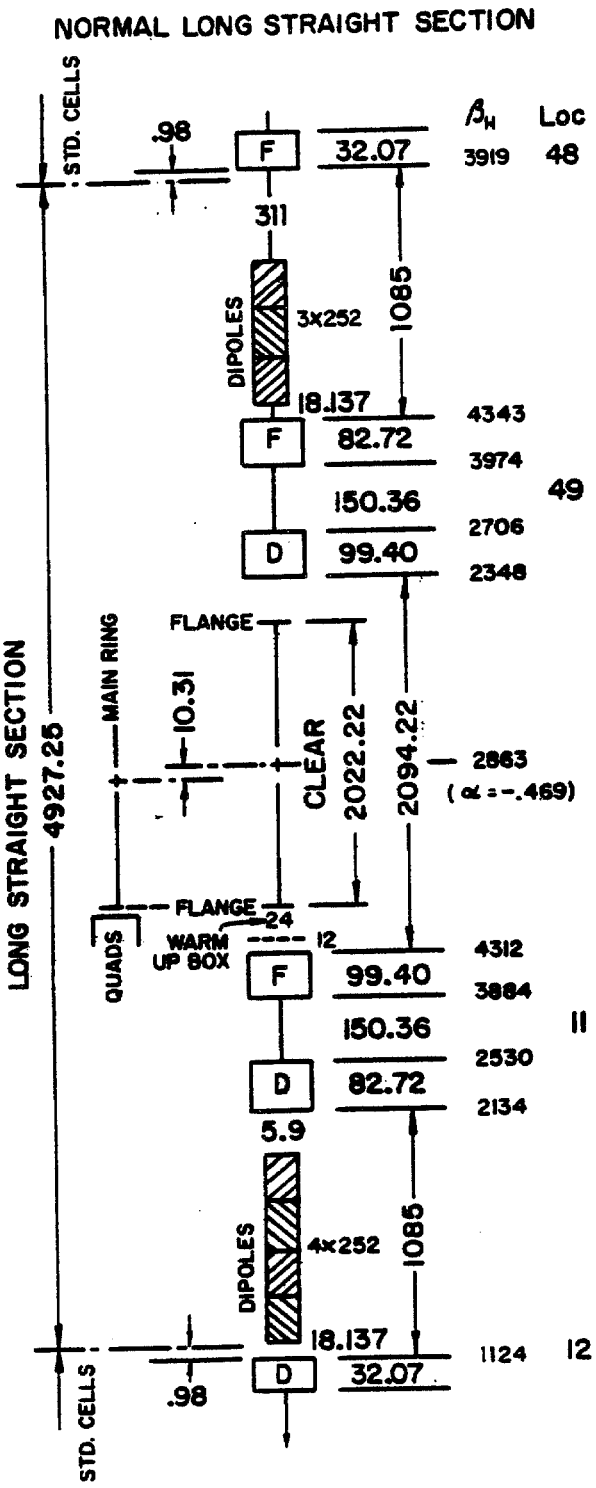

All dimensions in inches

Dipoles in slot length
Quads in eff. gradient length

Note: end quads are shorter than 1/2 standard quad so first "element" of long st. section removes .98" of quad from last standard cell

Main Ring at st. section center has $\beta = 2863$, $\alpha = -.725$
injection matching requires weak F quad at center of transfer line

17.6 kG @ 150 GeV/c

Effective phase advance for long st. section 113.04° (84.02° for sector)

For β_v read backwards

Figure 8-4 Normal long straight section.

functions. The design is very similar to normal Main Ring straight sections with the exception that two, rather than four, quadrupoles are used at either end of the straight section. CO, EO, FO are normal long straight sections. With this choice for EO, the lattice functions of the Main Ring and Energy Saver are matched nicely for the purpose of beam transfer.

The high-beta long straight section is illustrated in Fig. 8-5. Here the order of focusing in the doublets is reversed and lengths of all six quadrupoles are slightly changed. A large horizontal beta is produced at the upstream end of the straight section. High-beta straight sections were chosen for AO and DO because they facilitated resonant extraction, which places the most severe demands on the size of the good-field aperture. Since the good-field aperture of the superconducting magnets is not large, the use of high-beta at this location of the extraction electrostatic and magnetic septa reduces the aperture required for extraction in the rest of the magnet ring. This choice, which was made for fixed-target operation, will not affect the collider performance.

8.2.3 Lattice Elements. Table 8-II lists the various elements required for a ring incorporating two high-beta long straight sections and four normal long straight sections. The lengths shown are magnetic lengths in inches.

TABLE 8-II LATTICE ELEMENTS

Element	Magnetic Length (In.)	Number
Dipole	241.0	774
Standard quadrupole	66.1	180
Long straight inner quadrupole	99.4	12
Normal long straight short quadrupole (48,12 location)	32.07	8
Outer quadrupole	82.72	8
High beta long straight short quadrupole (48,12 location)	25.5	4
Outer quadrupole	90.19	4

8.2.4 Low-Beta Long Straight Section. The low-beta straight section at BO is made by replacing the 32.07 in. quadrupoles at each end of the normal straight section with stronger, separately powered 66.10 in. quadrupoles and adding eight additional quadrupoles within the 2054 in.clear space around BO. During injection these eight quadrupoles are turned off and the two 66.10 in. quadrupoles are excited to a lower current than those in the rest of the ring. After injection and acceleration, the inner eight quadrupoles are turned on, and all ten quadrupoles are slowly adjusted until the final beta-value of 1 m is reached. This process is described in detail in Chapter 9. It is noted that these eight quadrupoles will be turned off during fixed-target operation. The additional elements required

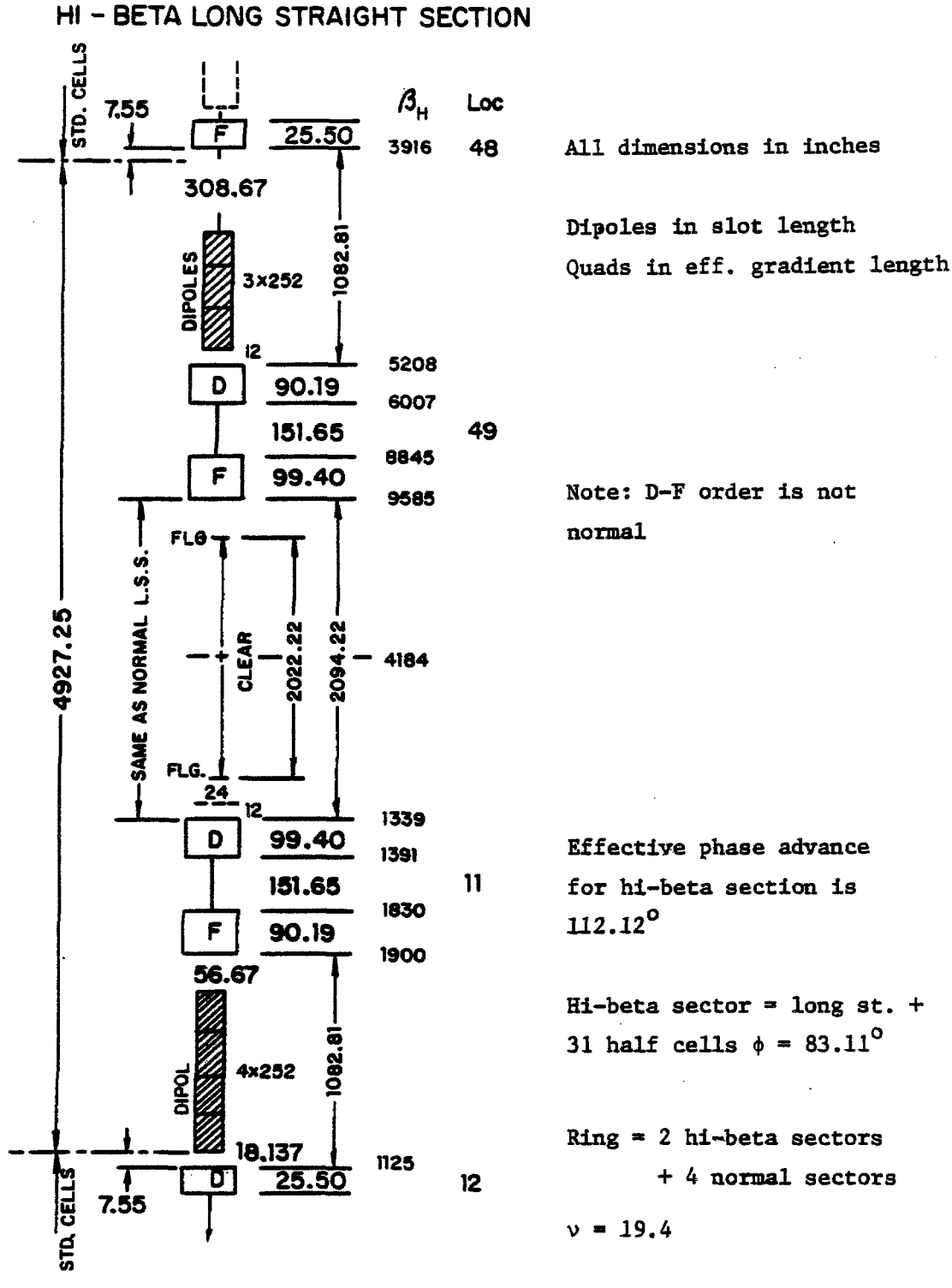

Figure 8-5 High-beta long straight section.

for the low-beta are listed in Table 8-III. A layout of the magnet elements of the low-beta straight section is shown in Fig. 9-1.

TABLE 8-III LOW-BETA QUADRUPOLES

Element	Magnetic Length (In.)	Number
Outer quadrupole(48,12 location)	66.1	2
	144.0	6
Inner quadrupole	180.0	2

8.3 Correction Systems

8.3.1 Types of Correction Elements. The correction magnets are built as a cluster of three functionally different superconducting coils concentric with one another and with beam-tube center line.[4] Since it was chosen to mount the coils on the cold beam pipe, or spool piece, between the quadrupole and the adjacent dipole in each cell, the correction magnet package is now called a spool piece. There are two basic types of spool pieces, the regular spool piece associated with each regular cell quadrupole, and the others. The distinction arises from the fact that each regular spool piece has two clusters of magnets, while the others have only one cluster of magnets. The upstream cluster of regular spool pieces contains dipole, sextupole, and quadrupole windings and the downstream cluster contains octupole, sextupole, and quadrupole windings. The orientations of the dipole winding and the downstream sextupole and quadrupole windings provide further differentation of the types of spool piece. The shorter spool pieces also contain three coils. Altogether there are seven types of spool pieces. The types of coils on each spool piece are given in Table 8-IV. The designations for the type of coils are as follows; horizontal dipole (H), vertical dipole (V), sextupole (S), quadrupole (Q), skew quadrupole (SQ), skew sextupole (SS), and octupole (E). Table 8-IV lists the types of spool pieces and Tables 8-IVa and 8-IVb give coil dimensions and parameters.

TABLE 8-IV ENERGY SAVER SPOOL PIECES

Spool piece Type (Code)	Upstream (DSQ coils)	Downstream (OSQ coils)	Length (in.)
"A"	H, S, Q,	None	43
"B"	V, S, Q	None	43
"C"	H, S, Q	E, SS, SQ	72
"D"	V, S, Q	E, SS, SQ	72
"E"	H, S, Q	E, S, Q	72
"F"	V, S, Q	E, S, Q	72
"G"	H, S, Q	E, S, SQ	72
"H"	H, V, SQ	None	50

TABLE 8-IVa DC MAGNETIC PARAMETERS OF CORRECTION ELEMENT COIL ASSEMBLIES

Package	Coil	T(bare) (G) (a)	Iron Factor	T(iron) (G) (a)	Effective Length (in.)(b)	$\int$Bdl at 50A and 1" (kG-in.)	Inductance (mH) warm	cold	
							bare(c)	iron(d)	iron(e)
DSQ	Dipole	89.20	1.466	130.80	27.69	181.10	475	696	686
	Sext	32.25	1.259	40.60	28.31	57.46	462	582	556
	Quad	31.67	1.662	52.63	28.56	75.16	293	487	479
OSQ	Octu	21.76	1.054	22.94	28.88	33.12	198	209	198
	Sext	24.51	1.281	31.39	28.32	44.45	300	384	370
	Octu	31.76	1.662	52.63	28.56	75.16	293	487	479

(a) Gauss at 1"/amp.

(b) Average of outer and inner coil lengths.

(c) Based on inductance-bridge measurements before installation of Al pipe.

(d) Base value x iron factor.

(e) Allowance for screening effect of superconductor.

TABLE 8-IVb PHYSICAL PARAMETERS OF CORRECTION ELEMENT COIL ASSEMBLIES

Package (a)	Coil	Coil inner radius (in.)	Coil outer radius (in.)	Iron inner radius (in.)	θ_{min} (b)	θ_{max} (b)	Coil inner length (in.)	Coil outer length (in.)	Iron length (in.)	Total turns	Coil-end geometry N-end
DSQ	Dipole	1.602	1.814	2.504	0°	60°	25-3/8	30	30	1170 (2x585)	0
	Sext	1.854	2.142	2.504	0°	20°	26-5/8	30	30	1965 (3x655)	2
	Quad	2.182	2.335	2.504	0°	30°	27-1/8	30	30	1240 (4x310)	0
OSQ	Octu	1.602	1.870	2.504	0°	15°	27-3/4	30	30	1500 (4x375)	2
	Sext	1.910	2.142	2.504	0°	20°	26-5/8	30	30	1560 (3x520)	2
	Quad	2.182	2.335	2.504	0°	30°	27-1/8	30	30	1240 (4x310)	0

(a) Packages include either normal or skew coils depending on subclass spec.

(b) Half angles given for normal coil-angles chosen to concel 3^{rd} harmonic.

(c) Using coil-end geometry ω per Snowdon's definition (memo dated 10/24/80).

8.3.2 Correction Magnet Circuits. The current leads of each coil are separately brought out of the spool piece cryostat, thereby making it possible to excite each coil independently. As will be discussed later, the dipoles are individually excited in order to correct orbit dislocations locally. The sextupoles, quadrupoles, and octupoles are series connected in functional groups in order to adjust global properties such as the tune and chromaticity.

Tables 8-V, 8-VI, and 8-VII show the type of spool piece at each quadrupole location, by pairs of sectors. Superscripts designate the arrangement of the coils into global circuits. Coil windings that are not noted in those tables are not connected to power supplies, although this could be done if a need arose.

TABLE 8-V COIL CIRCUITS IN SPOOL PIECES IN SECTORS A AND D

Quad Loc.	Spool Type	Upstream Coils	Downstream Coils	Quad Loc.	Spool Type	Upstream Coils	Downstream Coils
11	"H"	H, V, SQ^4	----------	12	"D"	V	SS^3
13	"G"	H, S^f, Q	SQ^0	14	"D"	V, S^d, Q	SS^3
15	"A"	H, S^f, Q	--------	16	"D"	V, S^d, Q	SS^3
17	"C"	H, S^f, Q	SQ^0	18	"D"	V, S^d, Q	SS^3
19	"C"	H, S^f, Q	SQ^1	21	"B"	V, S^d, Q	--------
22	"C"	H, S^f, Q	SS^2, SQ^0	23	"D"	V, S^d, Q	E^4, SS^4
24	"C"	H, S^f, Q	SS^2, SQ^2	25	"B"	V, S^d, Q	--------
26	"C"	H, S^f, Q	SS^2, SQ^0	27	"D"	V, S^d, Q	E^4, SS^4
28	"C"	H, S^f, Q	SS^2, SQ^1	29	"B"	V, S^d, Q	--------
32	"C"	H, S^f, Q	SS^1, SQ^0	33	"D"	V, S^d, Q	E^4
34	"C"	H, S^f, Q	SS^1, SQ^2	35	"B"	V, S^d, Q	--------
36	"C"	H, S^f, Q	E^3, SS^1, SQ^0	37	"D"	V, S^d, Q	E^4, SS^4
38	"C"	H, S^f, Q	SS^1	39	"B"	V, S^d, Q	--------
42	"C"	H, S^f, Q	E^3, SQ^0	43	"D"	V, S^d, Q	SS^4
44	"C"	H, S^f, Q		45	"B"	V, S^d, Q	--------
46	"C"	H, S^f, Q	SQ^0	47	"D"	V, S^d, Q	
48	"A"	H	--------	49	"H"	H, S^d, V, SQ^4	

TABLE 8-VI COIL CIRCUITS IN SPOOL PIECES IN SECTORS B AND E

Quad Loc.	Spool Type	Upstream Coils	Downstream Coils	Quad Loc.	Spool Type	Upstream Coils	Downstream Coils
11	"H"	H, V, SQ^4	--------	12	"D"	V	
13	"C"	H, S^f, Q	SQ^0	14	"D"	V, S^d, Q	
15	"A"	H, S^f, Q	--------	16	"D"	V, S^d, Q	
17	"C"	H, S^f, Q	E^1, SQ^0	18	"D"	V, S^d, Q	
19	"E"	H, S^f, Q	E^1, Q^1	21	"B"	V, S^d, Q	--------
22	"C"	H, S^f, Q	E^2, SQ^0	23	"F"	V, S^d, Q	E^4, Q^2
24	"E"	H, S^f, Q	E^2, Q^3	25	"B"	V, S^d, Q	--------

26	"C"	H, S^f, Q	E^1, SQ^0	27	"F"	V, S^d, Q,	E^4, Q^4
28	"E"	H, S^f, Q	E^1, Q^1	29	"B"	V, S^d, Q	--------
32	"C"	H, S^f, Q	E^2, SQ^0	33	"F"	V, S^d, Q	E^4, Q^2
34	"E"	H, S^f, Q	E^2, Q^3	35	"B"	V, S^d, Q	--------
36	"C"	H, S^f, Q	E^3, SQ^0	37	"F"	V, S^d, Q	E^4, Q^4
38	"C"	H, S^f, Q		39	"B"	V, S^d, Q	--------
42	"C"	H, S^f, Q	E^3, SQ^0	43	(D)	V, S^d, Q	
44	"C"	H, S^f, Q		45	"B"	V, S^d, Q	--------
46	"C"	H, S^f, Q	SQ^0	47	(D)	V, S^d, Q	
48	"A"	H	--------	49	"H"	H, V, SQ^4	

TABLE 8-VII COIL CIRCUITS IN SPOOL PIECES IN SECTORS C AND F

Quad Loc.	Spool Type	Upstream Coils	Downstream Coils	Quad Loc.	Spool Type	Upstream Coils	Downstream Coils
11	"H"	H, V, SQ^4		12	F	V	S^3
13	"C"	H, S, Q	SQ^0	14	"F"	V, S, Q	S^3
15	"A"	H, S, Q	--------	16	"F"	V, S, Q	S^3
17	"C"	H, S, Q	E^1, SQ^0	18	"F"	V, S, Q	S^3
19	"E"	H, S, Q	E^1, Q^1	21	"B"	V, S, Q	--------
22	"C"	H, S, Q	E^2,S^2,SQ^0	23	"F"	V, S, Q	E^4,S^4,Q^4
24	"E"	H, S, Q	E^2,S^2,Q^3	25	"B"	V, S, Q	--------
26	"G"	H, S, Q	E^1,S^2,Q!0	27	"F"	V, S, Q	E^4,S^4,Q^4
28	"E"	H, S, Q	E^1,S^2,Q^1	29	"B"	V, S, Q	--------
32	"G"	H, S, Q	E^2,S^1,SQ^0	33	"F"	V, S, Q	E^4,Q^2
34	"E"	H, S, Q	E^2,S^1,Q^3	35	"B"	V, S, Q	--------
36	"G"	H, S, Q	E^3,S^1,SQ^0	37	"F"	V, S, Q	E^4,S^4,Q^4
38	"E"	H, S, Q	S^1	39	"B"	V, S, Q	--------
42	"C"	H, S, Q	E^3,SQ^0	43	"F"	V, S, Q	S^4
44	"C"	H, S, Q		45	"B"	V, S, Q	--------
46	"C"	SQ^0		47	"D"	V, S, Q	
48	"A"	H	--------	49	"H"	H, V, SQ^4	

8.3.3 Coil Strength Requirements. The Q^f and Q^d quadrupoles are used to adjust the machine tune. There is a Q^f quadrupole adjacent to every regular horizontally focusing main quadrupole and a Q^d quadrupole next to every vertically focusing main quadrupole. The Q^f quadrupoles are connected in one series circuit, and the Q^d quadrupoles are connected in another. The S^f and S^d sextupoles are also designated in the same way by the adjacent main quadrupole. The S^1 and S^d circuits are used to adjust the chromaticity.

The remaining correction magnets can be used initially for half-integer resonant extraction. The Q^1 and Q^3 circuits can be used for half-integer extraction, the Q^2 and Q^4 circuits can be used in conjunction with the Q^1 and Q^3 circuits to correct the $2\nu_x = 39$ and $2\nu_y = 39$ resonances. The 48 skew quadrupoles located in standard cells, SQ^0, are

connected in series. These are used to compensate the difference resonance, $\nu_x - \nu_y = 0$. If needed, skew quadrupoles at the ends of the long straight sectors, SQ^3, can also be excited to provide additional compensation of the $\nu_x - \nu_y = 0$ resonance.

The circuits SQ^1 and SQ^2, when powered, can be used to manipulate the half-integer sum resonance $\nu_x + \nu_y = 39$. The circuits S^1, S^2, S^3, and S^4, when powered, can affect the driving terms of the $3\nu_x$ and $\nu_x + \nu_y$ resonance should the need arise. Similarly, the skew sextupoles SS^1, SS^2 SS^3, and SS^4 are installed at the locations given in the tables for driving the $2\nu_x + \nu_y$ and $3\nu_y$ resonances.

Octupoles are arranged in four circuits. Circuits E^1 and E^2 provide the two phases of the 39th harmonic for resonant extraction. Circuits E^3 and E^4 produce the zero-harmonic nonlinearity for control of tune versus betatron-oscillation amplitude. The strengths of the coils appropriate for 1 TeV are expressed as field integrals at 1 in. radius.

Steering Dipoles. The primary function of the steering dipoles is the correction of the closed orbit at all energies. The rigidity of the superconducting-magnet system and the tight tolerance on orbit centering imposed by extraction rules out the movement of magnets for orbit correction. In order to make efficient use of the available magnet aperture, it was specified that the closed-orbit excursions be limited to ±0.1 in. during extraction. This requirement is met by using the steering dipoles. The steering-dipole strength was determined to be 170 kG-in. on the basis of the following analysis:

At points in the normal cells where the amplitude function is a maximum, the rms orbit distortion due to dipole field errors and quadrupole misalignments can be written as

$$< x^2 > 1/2 = \frac{1}{4}(a^2 + \frac{5}{9}b^2) > 1/2 \text{ in.}, \qquad (8.1)$$

Here a denotes the rms dipole field error in units of 0.1%, and b the rms quadrupole misalignment in units of 0.01 in. In the horizontal plane, a arises from the fluctuation in the field-length product from dipole to dipole. In the vertical plane, a receives contributions from both rotational alignment error and any uncertainty or instability in the dipole field direction. It was assumed that the typical misalignment error introduced into the orientation of the dipole vertical plane during installation was 1 mrad and the stability of that of the vertical plane also had an error of 1 mrad. It was assumed that the quad placement accuracy was 0.02 in. This leads to an rms closed-orbit distortion of 0.5 in. The dipole strength required to compensate the deflection generated locally by the quadrupole misalignment and by the 8 neighboring main dipoles, is, for uncorrelated dipole errors

$$(\int Bd\ell)_{rms} = 23(a^2 + 0.31b^2)^{1/2}\ \text{kG/in.}, \qquad (8.2)$$

where a and b have the same significance as in the previous expression. The assumptions made for alignment in the previous paragraph require a 41 kG/in. field integral to correct the rms error. For Gaussian errors, a steering strength of about 130 kG/in. is needed to have 90% probability of successful correction at 100 locations. The steering dipole was designed for a strength of 170 kG/in. This was considered adequate to meet the concerns of the preceding paragraphs.

Trim quadrupoles. Since the main dipoles and quadrupoles are connected in series, trim quadrupoles assume the burden of tune correction and adjustment. Appropriate quadrupole harmonic terms are needed for half-integer extraction.

One of the main functions of the trim quadrupoles is to compensate for the large incremental increase in tune caused by the low-beta interaction regions used in colliding beams. A typical interaction-region introduces an added betatron phase advance of close to 180° in both planes of oscillation. The trim quadrupoles must, in effect, lower both tunes by approximately 0.5 to restore the operating point. The B0 design described in Chapter 9 produces a shift in tune of 200°. The required trim-quadrupole strength at 1000-GeV may be inferred from

$$\begin{aligned} \Delta\nu_H &= 0.0214(B'\ell)_F - 0.0062(B'\ell)_D \\ \Delta\nu_V &= -0.0062(B'\ell)_F + 0.0214(B'\ell)_D \end{aligned} \qquad (8.3)$$

The subscripts indicate the focusing character in the horizontal plane of the adjacent quadrupole. A reduction of both tunes by 0.5 requires a contribution to trim quadrupole strength of 33 kG/in.

Tune corrections that must be made to compensate for magnet errors require considerably smaller strengths. A systematic quadrupole term b_1 in the dipoles would produce tune shifts $\pm 1.1\times 10^{3} b_1$ in the two planes of motion. On the basis of the production of 764 dipoles, the average value of b_1 is less than 10^{-5}/inch. This b_1 makes an inconsequential demand on the trim-quad strengths.

The trim-quadrupole strength was specified at 60 kG/in., safely above the requirement imposed by a single interaction region after allowance for tune correction. In order to operate two interaction regions, somewhat greater strength is required. The quad can be excited to higher currents if necessary, although a special supply is required. Alternatively, the operating point of the collider can be shifted from 19.4 to 19.6 to allow a greater tuning range.

Sextupoles. The principal role of the sextupoles is control of the chromaticity. At the time of the Superconducting Acceleration Design

Report, May 1979, high-field sextupole moments were cause for concern because b_2 was large. On the basis of the production of 764 magnets, the average value of b_2 is measured to be $10^{-4}/in^2$. As the following analysis shows b_2 is no longer a cause for concern.

The contributions to the chromaticity from systematic sextupole terms in the dipoles and from chromatic aberration in the quadrupoles can be written as

$$\xi_H = 2.64\times10^5 < b_2 > -22$$
$$\xi_V = -2.45\times10^5 < b_2 > -22, \qquad b_2 \text{ in } (\text{in.})^{-2} \tag{8.4}$$

The constant value of -22 is due to the natural chromaticity of the basic lattice exclusive of enhancements from colliding-beam interaction regions. The magnet-selection criteria imposed a bound of 6.0×10^{-4} in.^{-2} on the magnitude of b_2. The measured average value of b_2 leads to a chromaticity in one plane or the other of about 50. Compensation of this effect requires sextupole strengths of 4.5 and 1.5 kG/in. at horizontally focussing and defocussing quadrupoles respectively.

A colliding-beam interaction region can be expected to increase the natural chromaticity. For example: the design presented in Chapter 9 increases the magnitude of the chromaticity by 9 units, to -31. The sextupole associated with the standard-cell quadrupole was designed to have a strength of 50 kG/in., a value which is conservatively beyond the minimum requirements.

Octupoles. The major purpose of the octupoles is to facilitate resonant extraction. They provide the nonlinearity that divides the phase plane into stable and unstable regions for the case of half-integer extraction. On the basis of the requirements for resonant extraction, the individual octupole strength has been specified as 30 kG/in.

Skew quadrupoles. At an early stage of the operation of the Main Accelerator at high energy, it was observed that a large horizontal oscillation would couple over into the vertical in a single turn. On the basis of magnet measurements, the same thing occurs in the Energy Saver. For that reason, skew quadrupoles were incorporated into the spool pieces as noted in Tables 8-V, 8-VI, and 8-VII. The skew quadrupole is similar in all respects to the trim quadrupole except that it is rotated by 45°. It has the same strength of 60 kG/in.

8.3.4 Excitation. In this section, the tolerances on the currents delivered to the correction and adjustment magnets and their arrangement in circuits are discussed. The coils were specified to achieve their nominal design strengths at a current of 50 A. The coils can be separately powered at much higher currents. As noted earlier the circuits for exciting the coils are given in Tables 8-V, 8-VI, and 8-VII.

Current Tolerances. Because of their role in orbit correction, the steering dipoles inherently require independent bipolar power supplies. Stability and ripple suppression at 0.1% of full scale are sufficient to satisfy the demands of injection and extraction. Each of the global circuits, defined in 8.3.2, is powered by a precision supply which provides a current stability in the range of 0.1% to .005%. The most severe requirement these supplies must satisfy is to provide a relatively unmodulated resonant extraction over 10 seconds.

8.3.5 Power Supplies. Two distinct types of power supplies have been built, one with an accuracy of 0.1% in regulation for the steering dipoles, and a high precision supply for the other elements. There are 180 steering dipoles in the standard cells of the lattice, and at least 4 dipoles are installed at each long straight section.

The design value is ±50A. The supplies are designed with load compensation and a conventional roll-off characteristic of 20 db/decade.

Steering-Dipole Supplies. The current stability and ripple limit for these supplies is ±0.1% of full scale. To complete the specifications, the bandwidth and voltage must be determined. It is reasonable to have a bandwidth that allows the power supply output to follow a constant ramp input within ±0.1% of full scale. The error between programmed input and supply output for a constant ramp is

$$\varepsilon = \frac{AB}{2\pi f_0} , \qquad (8.5)$$

where ε is the lag error (amps), A is the power supply DC gain (amps/volt), B is the input voltage ramp rate (volts/s), and f_0 is the power supply bandwidth or corner frequency (Hz)

For an error of 0.1% (0.05A) and a ramp from 0 to 50 A in 10 s, a power supply bandwidth of 20 Hz is adequate. With this 20 Hz bandwidth, the equation above then yields a maximum output ramp rate for 0.1% accuracy of 6.3 A/s.

The supplies are installed in the existing Main-Ring service buildings. The longest lead from the supply to dipole and back is 1200 ft. At 50A and 35°C, the voltage drop in that length of No. 1 wire is 8.1 V. The load inductance is approximately 0.7 H; at the maximum ramp rate, for 0.1% accuracy, the drop across the magnet would be 4.4 V. A maximum power-supply output of 15 V satisfies these requirements and provides a higher slewing capability for current changes under conditions where the accuracy specification can be relaxed.

A block diagram of such a supply is shown in Fig. 8-6. The control system provides a bipolar analog reference waveform from a generator with

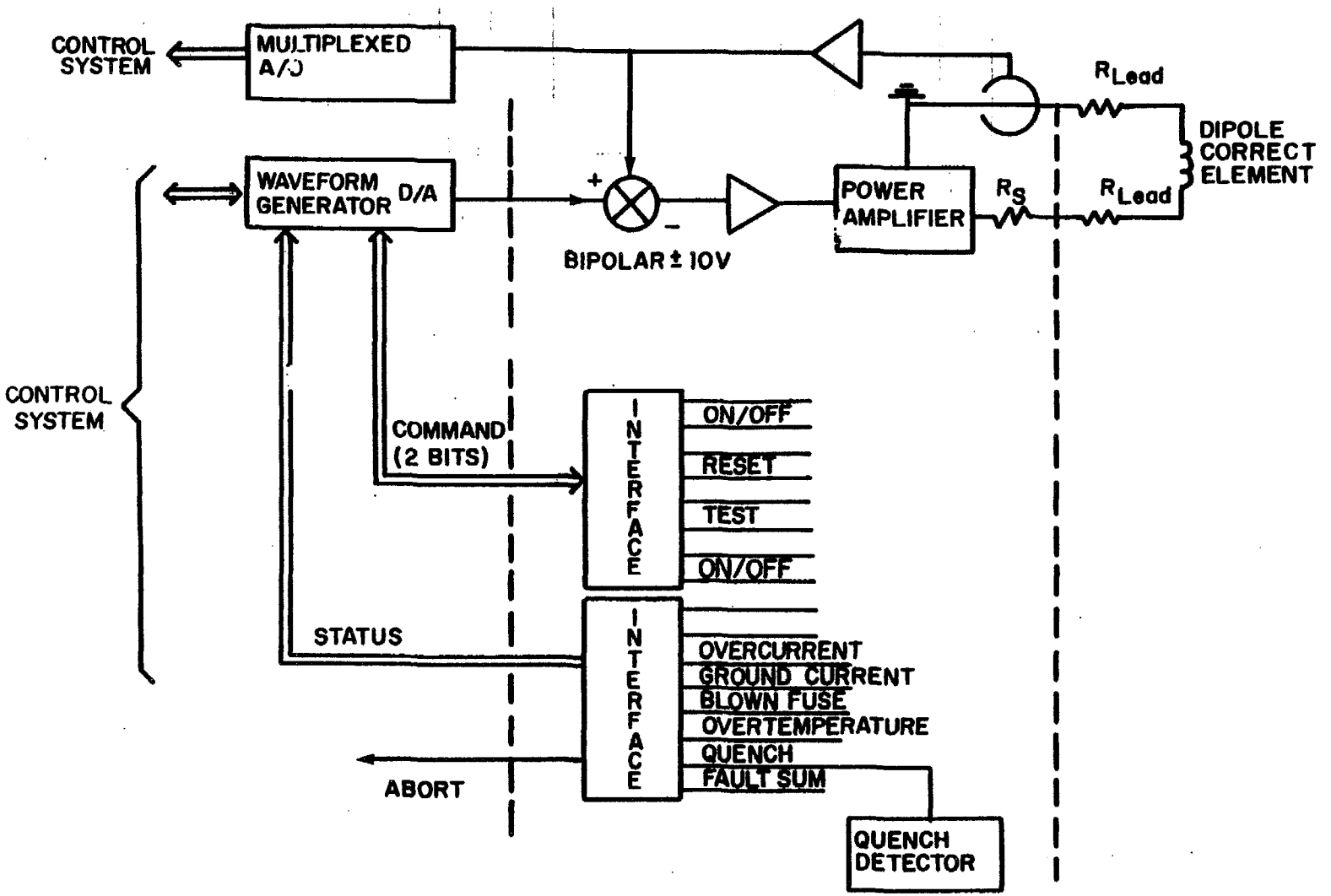
CONTROL SYSTEM
MULTIPLEXED A/D
WAVEFORM GENERATOR D/A
+
−
BIPOLAR ± 10V
POWER AMPLIFIER
R_S
R_{Lead}
R_{Lead}
DIPOLE CORRECT ELEMENT
CONTROL SYSTEM
COMMAND (2 BITS)
INTERFACE
ON/OFF
RESET
TEST
ON/OFF
STATUS
INTERFACE
OVERCURRENT
GROUND CURRENT
BLOWN FUSE
OVERTEMPERATURE
QUENCH
FAULT SUM
ABORT
QUENCH DETECTOR

Figure 8-6

12 bit resolution and 2 bits for commands to operate. The current reading is returned to the control system via a multiplexed A/D along with 8 status and fault bits. Isolation is provided between the control system and the power supply for command, status, and faults by means of optical couplers. Isolation of the analog signals is accomplished through differential drivers and receivers.

High-Precision Supplies. These supplies have a stability and ripple limit in the range 0.005% to 0.01% of full scale current. They are rated at ±50A, ±600V. The low ripple current is achieved with a bipolar transistorized output regulator.

It is noted that certain of these supplies have a relatively high output voltage. To reduce transistor-bank dissipation, these supplies use a bipolar SCR preregulator to provide variable voltage to the output transistor regulator. The preregulators are adjusted to keep a nearly constant voltage across the output transistor banks and thus reduce the transistor-bank requirements. The transistor-bank regulators for the various high-precision supplies are essentially the same. The same is true of the preregulator.

The reference voltage is provided by a high precision 16 bit D/A and the current sensor is a high-quality current transductor with a stability of 1 ppm/°C. The waveform generator is located within the supply to minimize noise pickup. Quench detection is also provided by comparing the voltage across one half the series regulators to the other half.

8.4 Main Ring Extraction and Energy Saver Injection and Abort

The design of the antiproton beam transfer was simplified considerably once the circumference of the Energy Saver was made equal to the Main Ring. Fig. 8-7 is a schematic representation of the E0 straight section, which shows both the proton and antiproton transfer lines.

Proton injection for colliding beams will proceed with the transfer of a single bunch from the Main Ring to the Tevatron. The bunch will be kicked horizontally across a magnetic septum (Lambertson magnets) in the Main Ring at the upstream end of E0 using the existing extraction kicker magnet at C48. This initiates a downward bend (16.6 mrad) towards the superconducting string at E11, 25.5 in. below the Main Ring. The vertical dog-leg is completed by two more Lambertson magnets at the downstream end of the long straight section, which brings the beam back on to the horizontal plane. The beam is then placed on the closed orbit by another fast rise-time kicker magnet located at the warm E17 medium straight in the Tevatron. Although the basic lattice structures of the Main Ring and the Tevatron are similar, a transverse-emittance dilution of approximately 30% would occur if no attempt were made to match the beam shape. A quadrupole in the injection line will be used to provide both horizontal and vertical matching. Horizontal beam steering is accomplished in the Main Ring and the injection line by a series of bump magnets; the correction dipoles accomplish the corresponding function in the Tevatron.

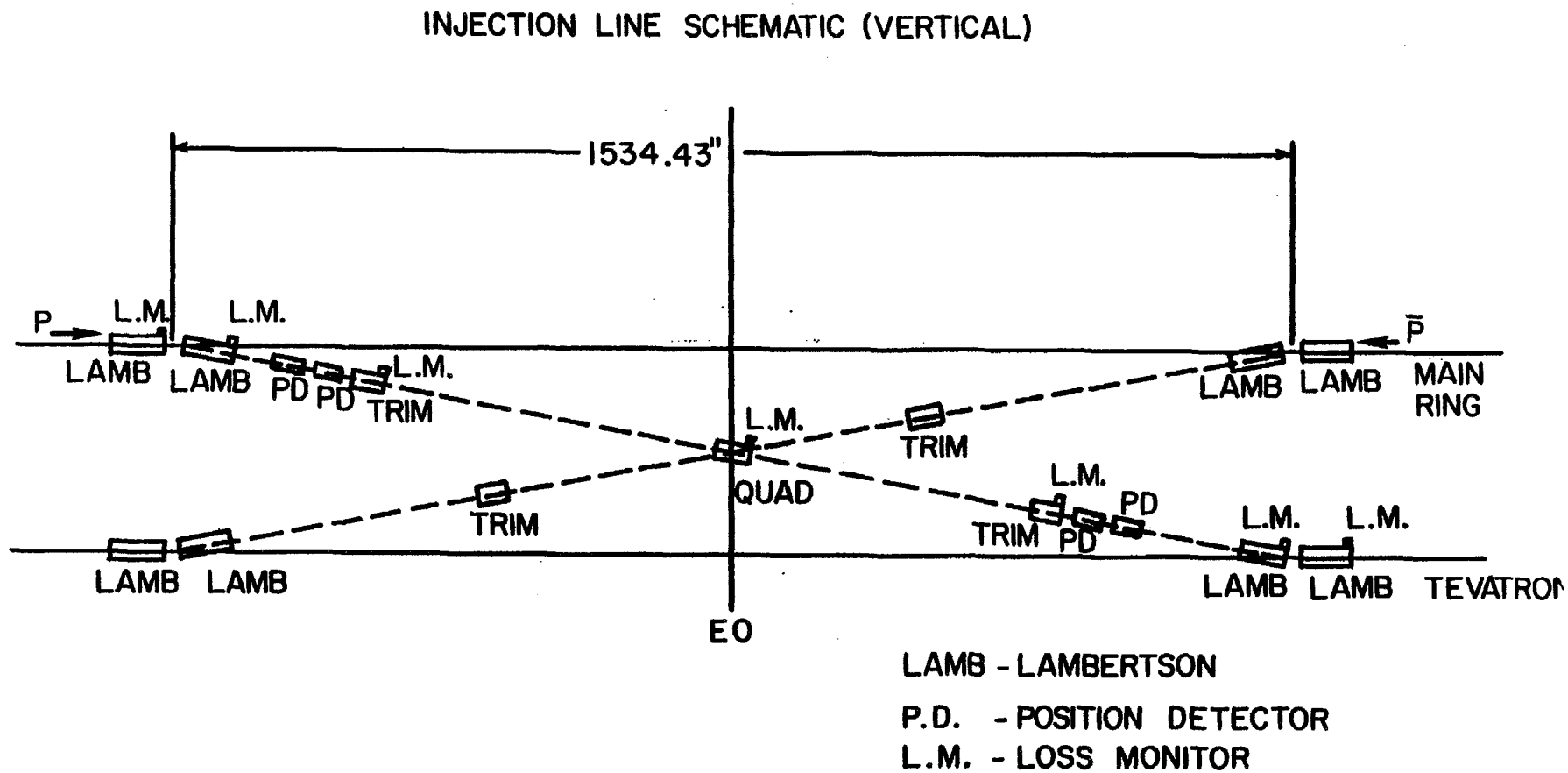
INJECTION LINE SCHEMATIC (VERTICAL)
1534.43"
P
L.M.
L.M.
LAMB
LAMB
PD
PD
TRIM
L.M.
LAMB
LAMB
MAIN
RING
L.M.
TRIM
QUAD
TRIM
L.M.
PD
TRIM
PD
L.M.
L.M.
LAMB
LAMB
LAMB
LAMB
TEVATRON
EO
LAMB - LAMBERTSON
P.D. - POSITION DETECTOR
L.M. - LOSS MONITOR

Figure 8-7

Antiproton injection uses four additional Lambertsons and two trims, as shown in Fig. 8-7. The matching quad is common to both lines. The $\bar{p}$ transfer is accomplished in a similar manner as for protons with the Main Ring extraction kicker located at E17 and the saver injection kicker located at D48.

Table 8-VIII lists the kicker requirements for six bunches of protons and six bunches of antiprotons, all equally spaced. This establishes the maximum number of bunches that can be injected. Nevertheless, it is not planned to exceed 3 bunches of protons and 3 bunches of antiprotons at this time. The specifications for the proton transfer kickers were set by the requirements for fixed-target operations.

The specifications listed in Table 8-VIII allow injection of either protons or antiprotons first. If the protons are injected first, either a single bunch at a time may be injected, or all three (or six) bunches may be injected together. The antiprotons are then interspersed among the proton bunches, one bunch at a time. However, the resulting collision points are then approximately 200 m from the 0 stations. Subsequent to injection, the collision points may be moved to the 0 stations using the orthogonal RF systems in the Tevatron. This operation involves non-head-on collisions (e.g., ΔR-0.1 mm) but is completed in such a short period of time (7 secs), that, on the basis of both, computer simulations and operational experience at CERN, no significant phase-space dilution due to the enhanced beam-beam interaction is expected.

Table 8-IX lists the requirements of the proton and antiproton abort kickers. The requirements for the proton abort kicker are met in the existing design for fixed-target application.

The $\bar{p}$ abort kicker requirements can be met by three 1.9 m long modules of the Main Ring abort style (tape-wound core). These kickers produce a -25 mm displacement at the downstream end of the C0 straight section. A 10 feet long steel dump located at this point serves as the abort dump. This simple abort system suffices because of the low beam intensity in the $\bar{p}$ beam. The more complicated abort system for the protons has been designed for the two orders of magnitude more intense proton beams that is required for fixed-target operation.

The use of the C48 kicker to inject protons at E0 creates the possibility of introducing uncomfortably large amplitude oscillations through D sector of the Main Ring. In order to reduce the size of these oscillations where possible, three bump magnets have been installed in the Main Ring at C22, C32 and D38. These three magnets can be excited to produce a closed orbit 180° out of phase with the kicked beam and thus reduce the effective orbit excursions by a factor of 2 throughout most of the sector. Precise control of the beam position in the Main Ring across the long straight section, essential to ensure loss-free injection, is provided by another set of bump magnets at D46 and E17. Powered in series, these magnets generate an orbit bump similar to that currently used in the

MAIN RING CLOSED ORBIT
PRIOR TO INJECTION

HORIZONTAL PROJECTION
TUNE: 19.420
MAX. OFFSET: 2.34 cm

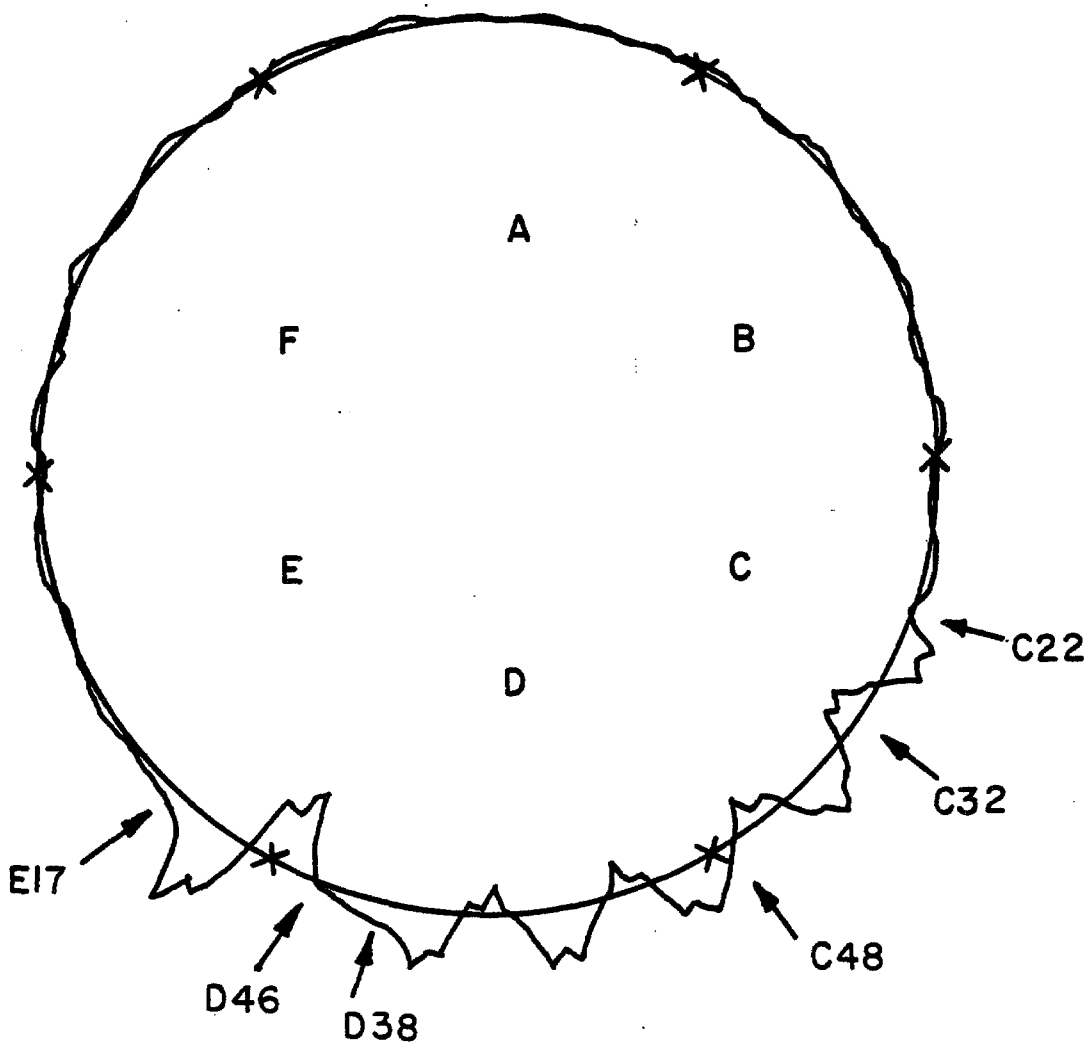

Figure 8-8

Main Ring for extraction. A hypothetical closed orbit suitable for injection is shown in Fig. 8-8. The orbit excursions between C22 and D38, D46 and E17 are apparent. Figure 8-9 shows the same closed orbit modified by firing the kicker that produces the orbit cusp at C48. The orbit amplitude remains approximately constant up to D38, after which the amplitude increases to a maximum offset of 48 mms at D48. The horizontal orbits across the long straight section are shown in more detail in Fig. 8-10a, where the error bars on the Main Ring orbits give the expected beam size (±4 mm) at the Lambertson septum. With these injection parameters, one can see an intrabeam separation of 7 mm with the septum offset at 25 mm. The corresponding Tevatron orbits are shown in Fig. 8-10b. The closed orbit bump between E11 and E17 is generated by the correction coil dipoles at E11, E13, E15, and E17 and serves to reduce orbit excursions within the restricted aperture of the Tevatron as well as decrease the integrated field strength required from the kicker magnet at E17.

For $\bar{p}$ reverse transfer, the 046-E17 Main Ring bump magnets will be used for position control of the $\bar{p}$ beam at the reverse injection Lambertsons. Figure 8-11 shows the $\bar{p}$ extraction orbit in the Main Ring. The maximum expansion from the Main Ring center line is 35 mm at E15.

Figure 8-12 shows the $\bar{p}$ transfer line trajectory. The Main Ring Lambertson septa are at approximately 15 mm (relative to the Main Ring center line); the Tevatron Lambertson septa are at approximately 16 mm and approximately 8 mm (relative to the Tevatron center line). The relatively large injection angle shown in the figure is necessary because of the small phase advance between the injection point and the D48 kicker.

Horizontal correction dipoles at D48, D49, E11 and E13 will be used to control the beam position at the Lambertsons after injection.

The injection Lambertson magnets are similar in design to the present Main Ring extraction devices. The magnets have 12 turns of water-cooled 0.46"-square copper giving a useful dipole field aperture of 3.5" x 0.9". The nominal operation current of 1575 A produces a 9 kG field. The maximum useable field is defined by the saturation of the steel (Republic Steel LoCore 'B') and is 12 kG. The septum is 2 in. thick and is formed with a half angle of 45°.

TABLE 8-VIII EXTRACTION AND INJECTION MAGNET PARAMETERS

	p Extraction	p Injection	$\bar{p}$ Extraction	$\bar{p}$ Injection
B-ℓ	1.97 kG-m	1.5 kG-m	2.25 kG-m	5.2 kG-m
Rise time	20 μsec	1.39 μsec	11 μsec	1.5 μsec
Fall time	--	2.0 μsec	--	1.5 μsec
Magnets	6	2	1	2
Magnet impedance	25Ω	12.5Ω	5.5 Ω	5Ω
Magnet length (m)	1	2.1	1.9	2.1
No. of				

MAIN RING INJECTION ORBIT

HORIZONTAL PROJECTION
TUNE: 19.420
MAX. OFFSET: -4.82 cm

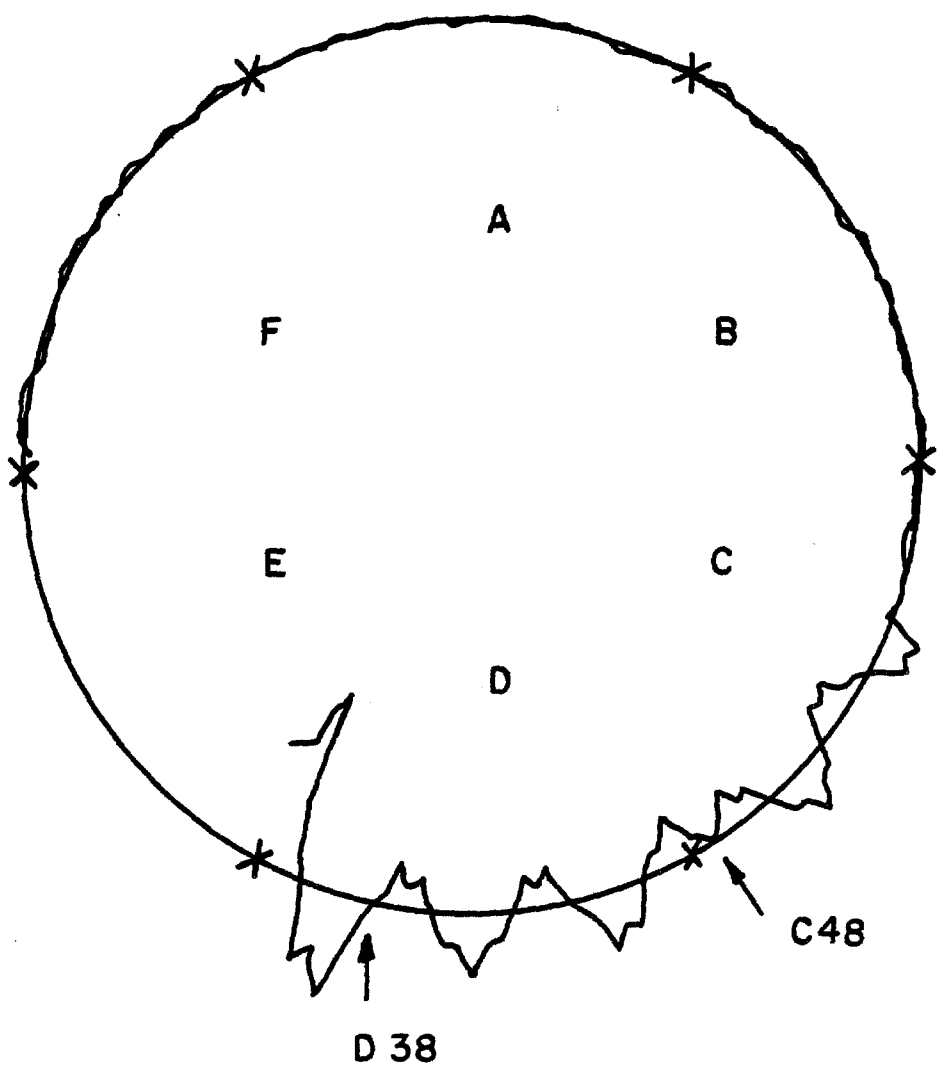

Figure 8-9

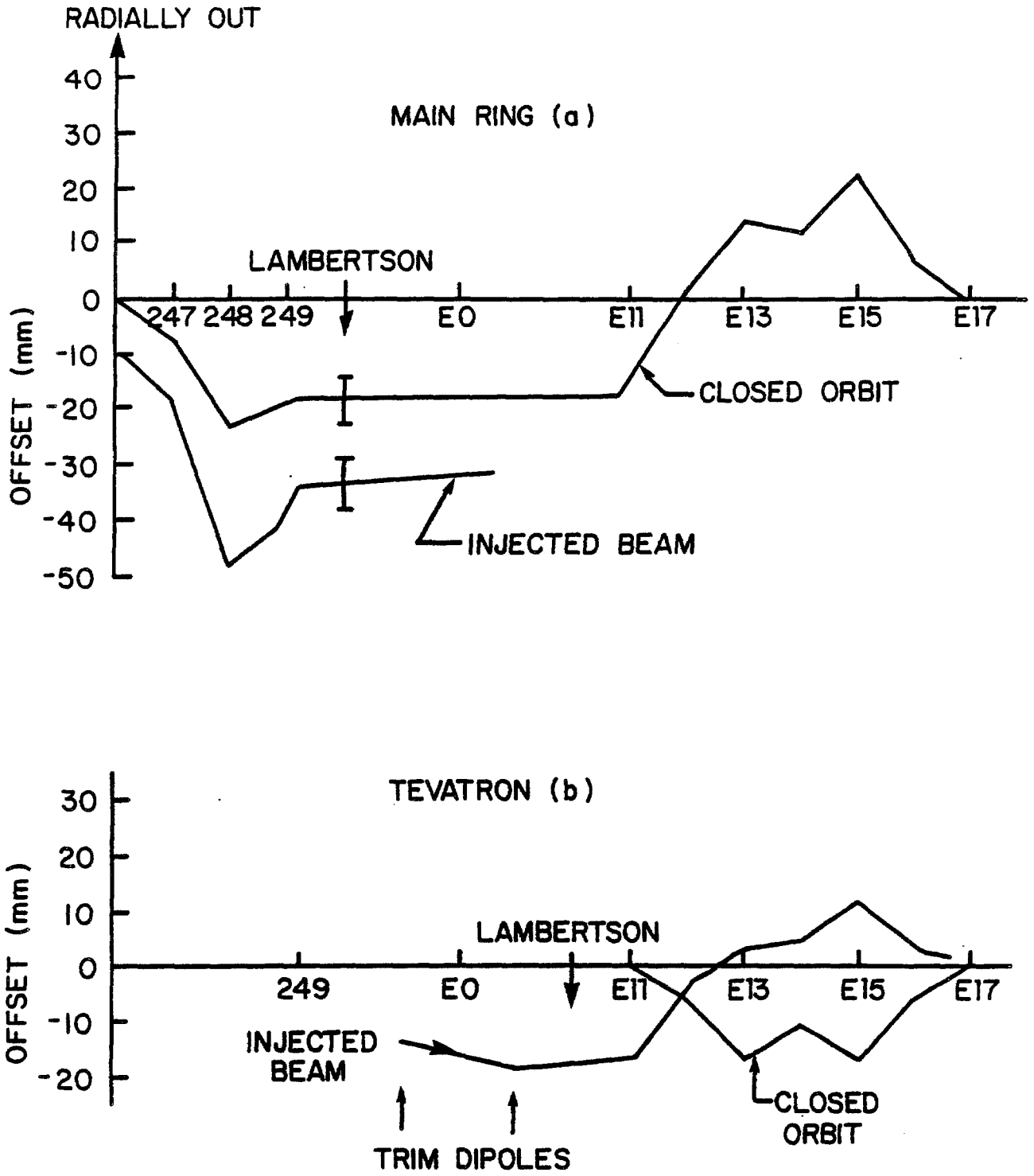
RADIALLY OUT
MAIN RING (a)
40
30
20
10
0
-10
-20
-30
-40
-50
OFFSET (mm)
LAMBERTSON
247 248 249
E0
E11
E13
E15
E17
CLOSED ORBIT
INJECTED BEAM
TEVATRON (b)
30
20
10
0
-10
-20
OFFSET (mm)
LAMBERTSON
249
E0
E11
E13
E15
E17
INJECTED BEAM
CLOSED ORBIT
TRIM DIPOLES

Figure 8-10

TUNE 19.400
MAX. OFFSET 3.5
HORIZONTAL PROJECTION

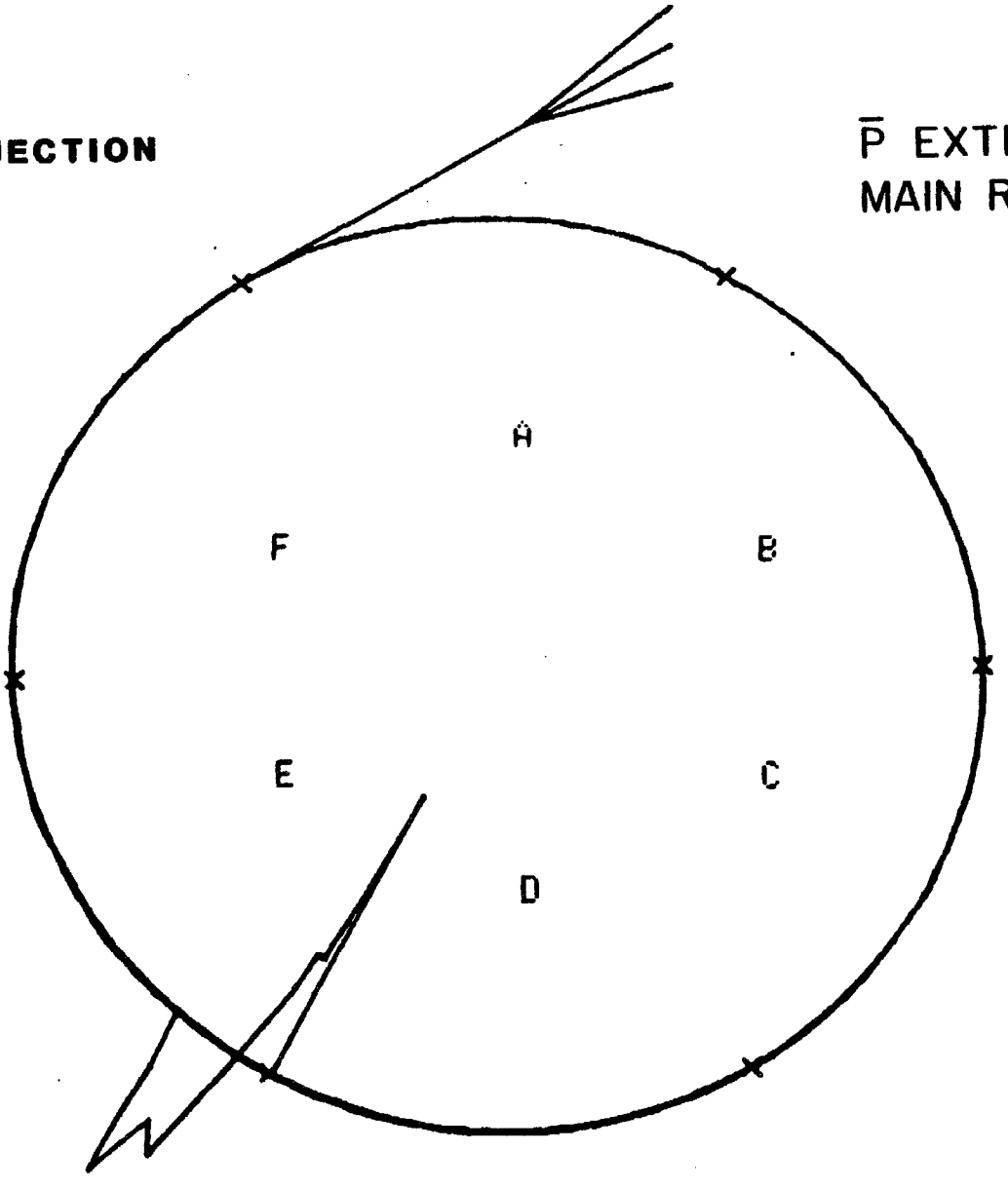

Figure 8-11

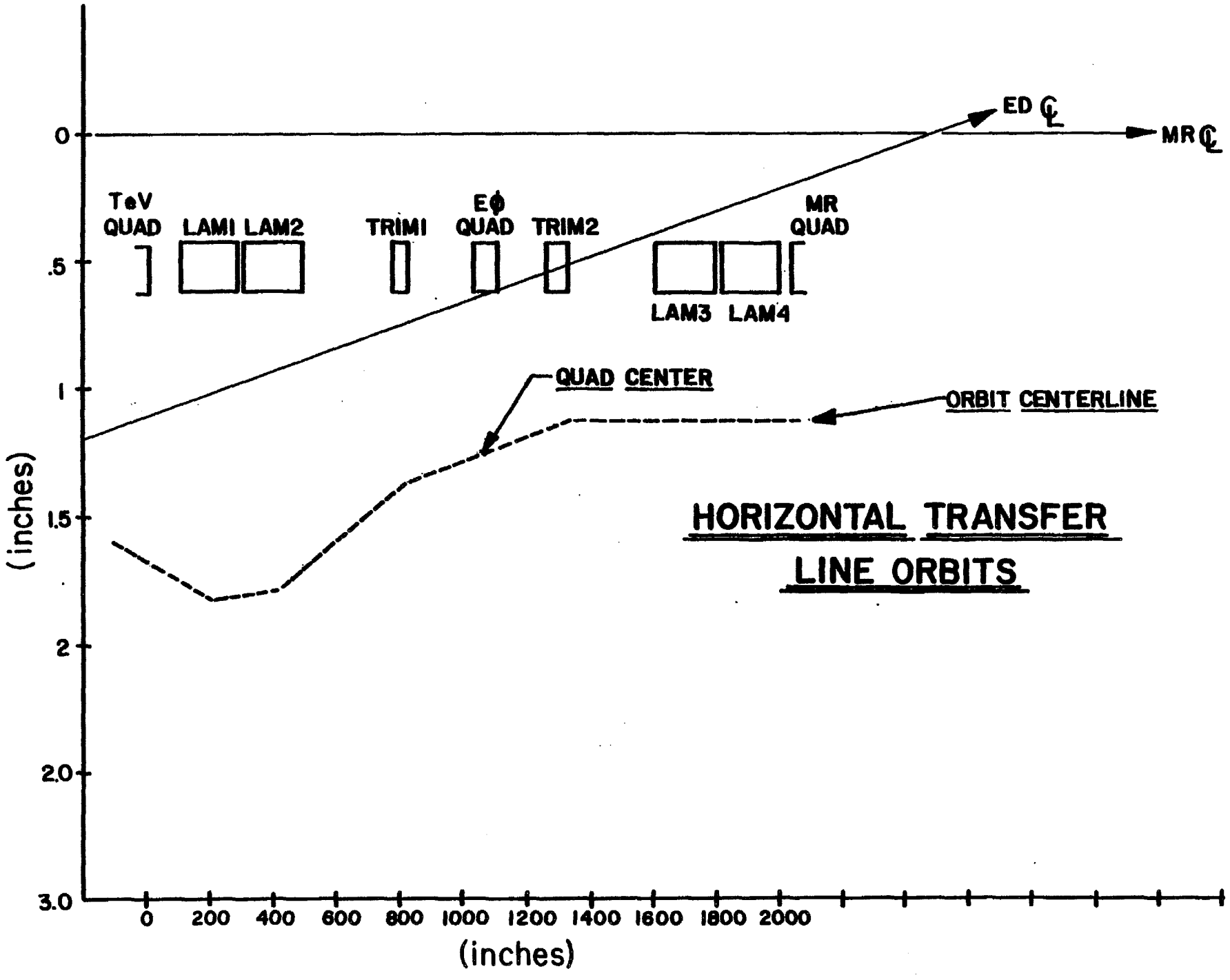
ED ℄
MR ℄
TeV QUAD
LAM1 LAM2
TRIM1
Eϕ QUAD
TRIM2
MR QUAD
LAM3 LAM4
QUAD CENTER
ORBIT CENTERLINE
HORIZONTAL TRANSFER LINE ORBITS
(inches)
0
.5
1
1.5
2
2.0
3.0
0 200 400 600 800 1000 1200 1400 1600 1800 2000
(inches)

Figure 8-12

pulse-forming networks	1	1	1	1
PFN impedance	12.5Ω	6.25Ω	1 Ω	2.5Ω
Gap (inches)				
HxV	6x2	2x2	3.4x1.5	2x2
Voltage	56 kV	43 kV	4 kV	50 kV

TABLE 8-IX ABORT MAGNET PARAMETERS

	P Abort	$\bar{p}$ Abort
B-ℓ	24 kG-m	15 kG-m
Rise time	1.6 μsec	2.0 μsec
Location	B-48	C-17
No. module	4	3
Length	2 m	2 m
I_{max}	19 kA	11 kA

8.5 Acceleration of Protons and Antiprotons

8.5.1 Energy Saver RF Requirements for Colliding Beams. When the Energy Saver is used for colliding beams, the rf system must be able to accelerate protons and antiprotons simultaneously from 150 to 1000-GeV. Because the longitudinal emittances of proton and antiproton bunches may be slightly different, it may be necessary to provide different bucket areas for each in order to minimize dilution during acceleration and storage. Dynamic phase adjustment of proton and antiproton buckets will be necessary in order to damp coherent dipole oscillations of the separate bunches. The rf system should also have the capability of moving the azimuthal location of the $\bar{p}p$ collision point. These functions can be satisfied if the rf system allows independent control of the amplitude and phase of the proton and antiproton buckets.

Independent control can be achieved by arranging the cavities in pairs with appropriate spacing and phasing. Consider a pair of cavities separated in space by $3/4\lambda$ ($\lambda=2\pi R/h$, the rf wavelength at $\beta=1$). If the phase of the rf voltage on the downstream cavity is advanced by $\pi/2$ radians the rf fields encountered by a particle moving downstream through the two cavities will be exactly in phase. These same fields are exactly out of phase for a particle moving from the downstream cavity to the upstream cavity.

There are eight Energy Saver rf accelerating cavities, each of which is capable of sustaining 35-GeV/sec accelerating voltage for colliding beam

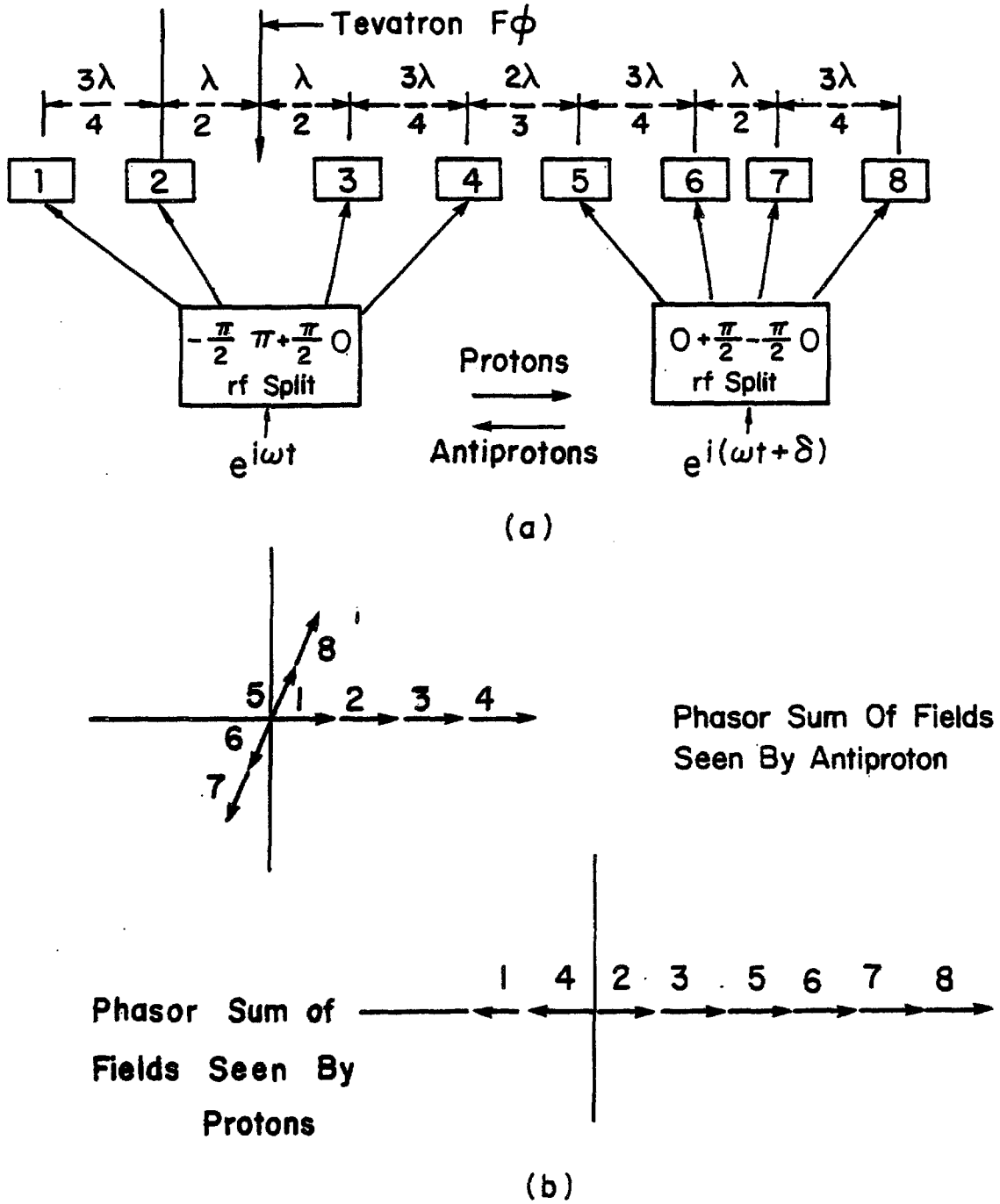
Tevatron Fϕ
3λ/4
λ/2
λ/2
3λ/4
2λ/3
3λ/4
λ/2
3λ/4
1
2
3
4
5
6
7
8
-π/2 π +π/2 0
rf Split
0 +π/2 -π/2 0
rf Split
Protons
Antiprotons
e^iωt
e^i(ωt+δ)
(a)
8
5
1
2
3
4
6
7
Phasor Sum Of Fields
Seen By Antiproton
Phasor Sum of
Fields Seen By
Protons
1
4
2
3
5
6
7
8
(b)

Figure 8-13

operations. Five of these cavities were built as part of Tevatron I. Four cavities are arranged in two pairs with a spacing of $3/4\lambda$ to accelerate protons and the remaining four will be arranged in two pairs with the same spacing to accelerate antiprotons as shown in Fig. 8-13a. Cavities 1, 2, 3, 4 are phased so that they couple to antiprotons, which move to the left. Cavities 5, 6, 7, 8 couple to protons, which move to the right. The center of cavity number 2 is located at the Tevatron F0 location. Since this location is symmetrically located with respect to the design collision points at D0 and B0, bunches that collide at those points must arrive at the F0 point at the same time (i.e., they collide there also, in the case where there are three bunches each of protons and antiprotons in the Collider). The arbitrary angle δ is adjusted to establish the correct collision pont. For the spacing shown the required value of δ is $\pi/6$ radians.

These cavities are adequate for an acceleration rate of 34 GeV/sec at a synchronous phase of 30°. The acceleration time to 1000 GeV is then 25 sec. The bucket size is ample. The relative phase between the two sets of cavities is adjustable, so that the $\bar{p}$ and p bunches can be rotated relative to each other to move the collision point to any desired azimuth.

8.5.2 Failure Modes. The requirement of orthogonal control of the two sets of cavities establishes uniquely the spacing between pairs of cavities. However, the precise location of the cavities and the selection of which set to assign to protons or antiprotons is arbitrary. The collision point can be adjusted by selection of arbitrary phase angles δ, as illustrated. The effect of the failure of a single cavity on beam size, luminosity and stability of the collision point is determined by cavity location and deployment. Failure of any rf cavity will always result in some beam deterioration, but the damage can be minimized by optimum cavity placement and selection.

The placement of cavities is partially limited by the location of penetrations and equipment in the RF Building and the F0 Straight Section. The cost of rearranging equipment did not always justify the gains that the optimum arrangement provided. The distribution described here is a partial optimization consistent with existing constraints.

In Fig. 8-13b the instantaneous fields seen by protons and antiprotons are shown. A failure of any one of the proton cavities, 5-8, would result in a sudden change in the phase and amplitude of the rf field seen by antiprotons. The antiproton bunches would immediately start a coherent dipole oscillation about the new phase angle, together with higher-order oscillations resulting from a change in bucket size. This would appear as an oscillation of the collision point and ultimately a dilution of the antiproton bunch length to cover the entire oscillation range. This dipole motion can be prevented by automatically turning off a second proton cavity so that the balance is restored. Removal of two proton cavities results in a reduction in bucket height by a factor of 0.707. This will cause a bunch

quadrupole oscillation with attendant dilution and bunch lengthening, but no dipole motion of the bunch or collision point.

On the other hand, failure of one of the antiproton cavities, 1-4, does not cause a phase displacement of the proton field, so no additional cavity need be removed from the system. Such a failure results in a decrease in the antiproton bucket height by a factor of 0.866 with a small attendant quadrupole oscillation and bunch lengthening. The effect on the proton bucket height and bunch length is to increase or decrease it by an even smaller factor. In summary, the cavity locations and assignments are such as to minimize the effect of failure of any cavity on the quality of the antiproton bunches at the expense in some cases, of proton bunch quality.

It is conceivable that if many faults occur, resulting in unacceptable dilution of proton bunches, both beams could be decelerated to 150 GeV and the proton bunches replaced with fresh ones while keeping the old antiproton bunches.

8.6 Energy Saver Diagnostics

At the time the Energy Saver components were fabricated, it was recognized that it would be used as a collider. For that reason the beam position detectors were designed so that the proton and antiproton beam could be detected simultaneously. Since the decision to build this type of monitor was made after the preparation of the Superconducting Accelerator Design Report, a description of them is given in Section 8.6.1. The beam-loss monitors of the Energy Saver are described in 8.6.2. Following the first year of operation of the SPS collider, the requirements for diagnostics in the Energy Saver were reviewed. The additional diagnostic equipment to be added to the Energy Saver for colliding beams is given in Section 8.6.3.

8.6.1 Energy Saver Position Detectors. The position detectors in the Tevatron are of the directional-coupler type[5]. There are 216 detectors in all, 108 each for vertical-position measurement (in vertical focusing quadrupoles) and for horizontal-position measurement (in horizontally focusing quadrupoles). The pickups have about 24 db of directivity (i.e. rejection of signals from beam traveling in the unwanted direction) so that the pickups can be used to detect $\bar{p}$'s in the presence of p's and vice versa.

The fast electronics for extracting the position signal from the pickup signal uses amplitude-to-phase (AM to PM) conversion to provide a large dynamic range of beam intensity[6]. The electronics was specifically designed to detect single isolated bunches of p's or $\bar{p}$'s (collider mode) as well as contiguous filled buckets (batch mode) for fixed-target operation. The lower limit of sensitivity for operation in these modes is about 3×10^9 p's per bucket (collider mode) or 1×10^8 p's per bucket (batch mode). The

position-signal rise time is about 70 nsec due to the presence of a half-wavelength resonant filter which rings when hit by a signal from isolated p or $\bar{p}$ buckets. The estimated precision of position measurement is about ±0.5 mm at the lowest intensities. Precision of ±30 microns has been obtained with high intensities in a detector installed in the Main Ring.

The microprocessor-controlled digitizing electronics allows simultaneously digitizing the position signal from all 216 detectors with about 100 nsec (least significant bit) resolution on the timing for each detector. This "FLASH" picture of a single turn of beam can be used to examine the beam orbit for any complete revolution including injection. Other operating modes include measurements of beam position averaged over many turns to average out the contributions of betatron oscillations. These latter measurements have large RAM memories associated with them to store many measurements without requiring readout by the Host control computer. These data are used to determine closed orbits for correction-coil programming and for orbit reconstruction in case of a beam-induced quench. The microprocessor circuits can initiate beam aborts if the beam exceeds preset position limits.

The electronics has been designed and built to detect beams in either direction. In order to fully implement these features, coaxial relays are installed in the tunnel to select the proper pair of ports from the directional coupler pickups. A signal to control them is provided in the Service Buildings. In addition, a Saver Clock signal (a signal with diphase encoded timing signals on a 10 MHz carrier) is installed in the $\bar{p}$ direction around the ring. The electronics is equipped to receive this at the same time it controls the coaxial relays. A control cable for the coaxial relays will also be installed.

8.6.2 Beam Loss Monitors. The Tevatron beam-loss monitor system, like the beam-position system has detectors at every quadrupole (a total of 216 around the ring). They are argon filled chambers designed to have a very large dynamic range and fast response. Their signals are amplified in a fast-risetime integrating 4-decade logarithmic readout. Real-time analog output signals are also available for fast time plots. The 60 msec integration time of the electronics corresponds to the response time of the Doubler magnets to beam-induced heating, and therefore is a good monitor of the likelihood of inducing quenches. The beam-loss monitor system, like the beam-position system, can initiate a beam abort if the radiation level exceeds preset limits.

8.6.3 Diagnostics for the Energy Saver Collider Operation. Initial experience from the CERN SPS collider has shown the importance of adequate beam diagnostics. In the Fermilab Collider, much of the tuning of the transfers, acceleration, and storage parameters will necessarily be done with antiprotons, which are relatively rare even if the $\bar{p}$ accumulation works well. Thus, diagnostic devices should work at low beam intensities.

Furthermore, since the time to improve transfer and storage efficiency of the Collider will be in competition with other uses of the Tevatron, there must be a complete set of diagnostic devices with well developed software at the onset of Collider commissioning.

The obvious requirement is to be able to measure the beam intensity, position and emittance as a function of time as the particles make their way to a successful store at 1 TeV.

Beam-transfer lines will be equipped with sensitive intensity and profile monitors. The Main Ring and Tevatron have position and intensity measuring devices that will be well developed by the time collider commissioning begins.

In order to measure the profile of circulating p's and $\bar{p}$'s in the Tevatron, we are constructing several flying wire scanners[7]. These devices flip a thin-wire filament through the circulating beam at about 5 m/sec, and the resultant scattered flux is monitored by several scintillator telescopes placed both upstream and downstream of the flying wire. Such a device will be placed near (and in) the B0 Colliding Detector Facility to measure beam position as well as profile. Each flying wire can measure only one coordinate, so several are needed. Such a device has been implemented at the CERN SPS and is recognized as an important diagnostic tool[8].

Motion of the wire through the beam is about 0.1 mm per turn, which results in about 10 points across a beam 1 mm in diameter. The scattered flux from p's and $\bar{p}$'s are quite directional, and hence the p and $\bar{p}$ beam profiles are recorded simultaneously in the two sets of scintillators. The emittance blowup per scan is about 6×10^{-6} mm-mrad, hence for the SPS about 200 scans per hour is equivalent to multiple scattering by the residual gas. The heating of the wire (a low-Z material such as beryllium or carbon) is not excessive. The particle flux lost is less than 0.02% per scan.

Longitudinal emittances will be monitored by the devices associated with the Main Ring and Tevatron low-level rf systems.

Schottky scans should be adequate for tune measurements. An active tune measurement is also under consideration.

The intensity and position devices in the Tevatron can give information on individual bunches of protons or antiprotons. In addition, the flying-wire scanner gives bunch-by-bunch information.

References

1. Superconducting Accelerator Design Report, May 1979, Fermilab, Chapter 14.
Fermilab Report UPC 73, F.E. Mills and D.E. Young, November 11, 1978.
Fermilab Report UPC 129, F.T. Cole, April 24, 1980
Fermilab Report UPC 132, S. Ohnuma, June 26, 1980

2. Fermilab Report UPC 96, T.L. Collins, April 1979.

3. Fermilab Report UPC 17, L.C. Teng, December 1, 1978

4. D. Ciazynski and P. Mantsch, "Correction Magnet Packages for the Energy Saver" IEEE Trans. on Nuclear Science, Vol. NS-28 , No. 3, 3275 (1981).
D. Ciazynski and P. Mantsch, "Typical Problems of Correction Magnets for Fermilab", IEEE Trans. on Magnets, Mag-17, 165 (1980).

5. R. Shafer et al., IEEE Trans. Nucl. Sci. 28 , No. 3, page 2290 (1981).

6. Ibid, page 2323.

7. L.R. Evans and R.E. Shafer, Proc. Workshop on Intensity Limitations in Storage Rings, BNL 57236, page 68 (1979).

8. A. Barisy et al., IEEE Trans. on Nucl. Sci. 28 , page 2180 (1981).

CHAPTER 9

INTERACTION REGIONS AND EXPERIMENTAL FACILITIES

9.1 EXPERIMENTAL AREAS

9.1.1 B0 Experimental Area. A general-purpose detector is being designed and constructed by the Colliding Detector Facility Department, CDF. The desire to measure antiproton-proton collisions and available technology both demand a large, massive and complicated apparatus. The B0 Colliding Beam Experimental Area has been designed to handle the assembly, installation, operation and maintenance of such a detector.

The project includes the following:

B0 Collision Hall an underground structure that will replace approximately 100 ft of the Main Accelerator enclosure, and will contain the experimental physics detectors and both the accelerator and Energy Saver beam components. On the outside wall (away from the accelerator center) will be a large door and movable shield wall that will provide acess to the Assembly Hall.

B0 Transition and Equipment Bypass Enclosure an underground structure that connects the Collision Hall to the existing Main Accelerator enclosures, and provides a passage for personnel, utilities, and magnet-moving vehicles around the B0 Collision Hall.

B0 Assembly Hall a large pit at the elevation of the Collision Hall and adjoining to the shield door passage, with a service floor at grade level, all covered by a highbay building with an overhead crane. The various experimental physics detectors will be assembled, tested and serviced in this hall prior to placement in the B0 Collision Hall.

B0 Site Development hardstands, access roads, drainage facilities, relocation of utilities, extension of services and temporary earth retaining structures for construction sequencing and adjacent road and building protection.

B0 Primary Power 13.8 kV feeders, substations and switchgear for extending primary power to the B0 Experimental Area and into the B0 Assembly Hall.

The B0 Collision Hall connects with and becomes a part of the Main Accelerator and Energy Saver enclosures. All systems, services and utilities are designed for compatibility with these systems. Access to the B0 Assembly Hall will be from the adjacent Road D near the Industrial Buildings.

At the time of writing, construction of the B0 area is almost complete.

9.1.2 D0 Experimental Area. This experimental area is still in the process of definition and conceptual design.

9.2 B0 Low Beta Design[1]

9.2.1 Lattice Design. As discussed in Chapter 6, the $\bar{p}$ and p bunches are placed at equal spacings around the circumference of the Tevatron, arranged so that one of their crossings occurs in the B0 long straight section, the location of the Collider Detector Facility. There will also be crossings in the D0 long straight section, the second colliding-beam experimental area, at present in a primordial state of design.

The luminosity can be enhanced for given beam currents by focusing the beams down to narrow waists at the collision point, using extra quadrupoles on either side of the collision point. These quadrupoles give a decrease in the amplitude function β and the low β gives the narrow waist.

It is desirable for our purposes to achieve a minimum β value of 1 meter. Given the Tevatron lattice and dimensions, it is possible to achieve this minimum with a design that utilizes quadrupoles having gradients of 25 kG/in. and requires replacement of a single normal-cell quadrupole on either side of B0, at A48 and B12, by longer quadrupoles. The design uses four separately powered quadrupole buses and either can be adiabatically varied from the normal $\beta^* = 72$ m configuration to $\beta^* = 1$ m, while causing very little betatron mismatch or manipulation outside the interaction region except for correction-quadrupole changes to preserve the overall tunes and sextupole changes to maintain the desired chromaticity.

A layout of the 25 kG/in. low-beta insertion is shown in Fig. 9-1. It requires the replacement of the 32 in. quadrupoles at A48 and B12 with separately powered 66 in. quadrupoles and the addition of two 180 in. quadrupoles and 6 144 in. quadrupoles within the long straight section. These ten quadrupoles are powered anti-symmetrically on four separate circuits and must reach a maximum gradient of 25.5 kG/in. at 1 TeV. In order to keep maximum luminosity point close to the Tevatron B0 location, the quadrupoles at A48 and B12 must be pushed as far upstream as possible. To do this, the normal dipole interface-to-quadrupole magnetic length has been reduced from 18.137 in. to 7.137 in. by changing the upstream bellows and moving the beam detector to the downstream end of the quadrupoles. This motion puts the maximum luminosity point 0.9 in. downstream of the Tevatron B0 for the final low beta of 1 m.

9.2.2 Transition to Low Beta. For normal fixed-target operation, Q1 must run at approximately 10 kG/in. and Q2, Q3, and Q4 must all be off. By contrast, in the low-beta configuration, all the quadrupoles must be on and running quite hard. The problem is to find a method of connecting these

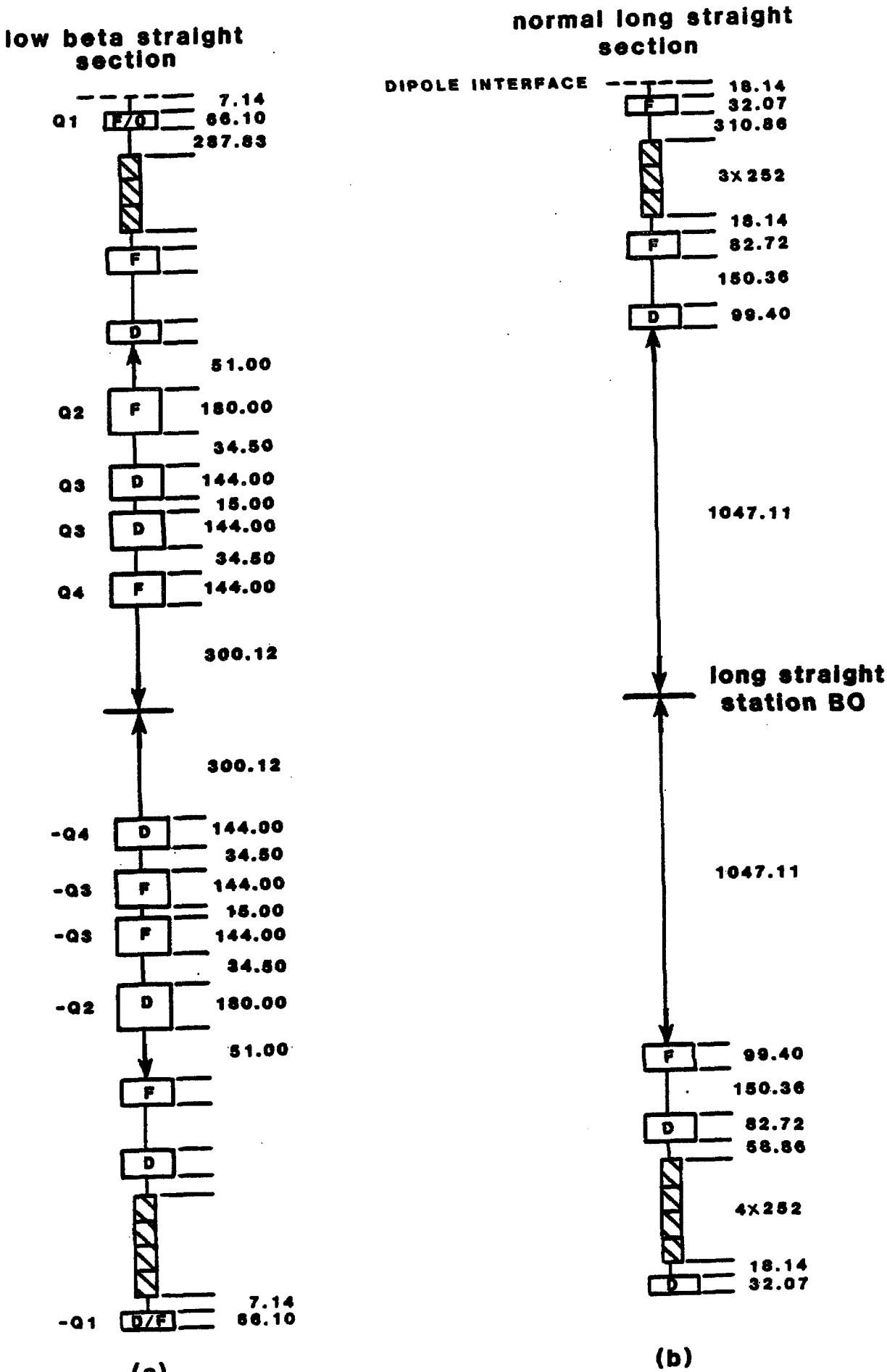
low beta straight section
7.14
Q1 F/D 66.10
287.83
F
D
51.00
Q2 F 180.00
34.50
Q3 D 144.00
15.00
Q3 D 144.00
34.50
Q4 F 144.00
300.12
300.12
-Q4 D 144.00
34.50
-Q3 F 144.00
15.00
-Q3 F 144.00
34.50
-Q2 D 180.00
51.00
F
D
7.14
-Q1 D/F 66.10
(a)
normal long straight section
DIPOLE INTERFACE
18.14
F 32.07
310.86
3x252
18.14
F 82.72
150.36
D 99.40
1047.11
long straight station BO
1047.11
F 99.40
150.36
D 82.72
58.86
4x252
18.14
D 32.07
(b)

Figure 9-1

two solutions in a stepwise continuous manner while maintaining the overall tune of the Tevatron. This is by no means a simple straightforward process. The two solutions are in fact quite different and probably cannot be connected without disturbing the normal lattice functions outside the insertion region. A method has been found, however, that does not greatly disturb the rest of the ring. This sequence takes the lattice from a retuned fixed mode to a low beta of 1 m.

In all this sequence, the Tevatron has been retuned to 19.585 in each plane. For particle-antiparticle collisions it is desirable to be above the half integer and the value of 0.585 centers the tune in a region free of all resonances of order lower than 11th. The correction quadrupoles consist of two families, QFC and QDC, located next to the correponding quadrupoles, QF or QD, at all stations 13 through 47. These corrections have a range of approximately ±2 kG/in. at 50 amps. QFC has ranges from +0.4 kG/in. to -0.9 kG/in. QDC is given by

$$QDC = 0.0457 - QFC \text{ (kG/in.)}$$

In this turn-on sequence, there is some disturbance to the lattice functions outside the insertion region, for three distinct reasons:

1. The "off" solution and the "low-beta" solution are, in fact, quite different. It is doubtful that they can be connected without allowing some mismatch.

2. The initial sequence, in steps of less than 1/3 kG/in., was not a very smooth curve. Some amount of mismatch was allowed in order to produce smoother curves.

3. It was found that a higher luminosity can be achieved in the "1 meter low-beta" by introducing some mismatch. This is because the long straight sections are not exactly antisymmetric; one side has more dipole edge focusing than the other, while the low beta quads of necessity are symmetric.

The amount of disturbance to the normal lattice, however, is quite small and should cause no problem since this turn-on will not start until high energy where the beam is very small.

9.3 Hardware Modifications

9.3.1 Magnets. Special quadrupoles have been designed and are being built for the B0 interaction region. These magnets use special cable with 20 micron filaments and a copper-to-superconductor ratio of 1.3 (as opposed to 8 microns and a ratio of 1.8). This cable has a short sample limit of 5250A at 6.5T. The new quadrupole has added turns to reach higher fields.

There are many new features of the new design. The strength of the coil collars has been carefully considered, as has quench protection. A

smaller cross section is being considered to give less interference with the Collider Detector. Because the special quads are powered separately from the regular Superconducting Ring magnets, the regular excitation currents are bypassed through the quads in a notch at the outside of the coil collar.

The beam monitor and correction magnet at B12 have been redesigned in a special package and relocated downstream of the special quad. Dipole fields will arise from quad misalignment. Even though shimming will be done, misalignments in the high-β regions adjacent to the low-β interaction region can give large orbit distortions and trim dipoles are being designed for correction.

9.3.2 Power Supplies and Bus. Four separate power supplies and associated circuits will be needed for the 1-m β^* design. The supplies will be modified Tevatron holding supplies capable of providing up to 6000 A. The supplies will be located in an annex to the B0 service building and the power will be transported to the magnets via water-cooled copper bus (total length of 4 circuits is 2700 ft). For a current of 6000 A, the power consumed by the bus is 770 kW. Power will enter the magnets through lead boxes constructed especially to fit the 15 in. space provided for them.

9.3.3 Refrigeration. Liquid-He refrigeration needs are as follows: quadrupoles (50 W), four pairs of 5-kA leads at 10 W each (40 W + 56 l/hr), two turnaround boxes at 10 W each (20 W), two feed boxes (45 W) and U tubes (5 W), for a total of 160 W plus 60 liters per hour. This refrigeration need can be met initially by the A4(C4) and B1(D1) satellite refrigeration systems. Later, it may be desirable to provide stand-alone refrigeration, and it would certainly be needed if operation at 1.8 K is desired. The 60 liters per hour of liquid He will come from the Central Helium Liquifier through the A4 and B1 refrigerator and magnet systems. The estimated LN_2 requirement is 250 W. Refrigeration estimates for the interaction-region detector magnets are not included here, because it is expected that those needs will be satisfied by separate refrigeration.

9.3.4 Vacuum. Pressure in the interaction region straight section should not exceed 10^{-9} Torr. This means the warm vacuum pipe through the detector plus a transition piece on either side will require special preparation (possible bakeout). The transition pieces will contain isolation valves and ion pumps, as well as the connections to turbomolecular and roughing pumps.

9.4 D0 Low-Beta Design

At this time, the D0 low-beta region is still being designed.

References

1. D.E. Johnson, Tevatron B0 Low Beta Tuning Report, Fermilab Report TM-1106, May 1982 (unpublished).

CHAPTER 10

PERFORMANCE AND LUMINOSITY

In this chapter we describe colliding-beam performance at 1000 GeV in the Energy Saver. For this purpose, we assume that beams of protons and antiprotons have been accelerated and are circulating in opposite directions so they collide in the center of the low-beta insertions at B0 and D0.

We assume the populations for the two beams are those required for a luminosity of 10^{30} $cm^{-2}s^{-1}$. Larger luminosity figures are also possible (see Table 1-I).

10.1 Beam Geometry

As an example, it is possible to create three bunches of antiprotons, each with 6×10^{10} particles and each with a longitudinal phase area of 3 eV-sec, which we define as the area including 95% of the population with a biGaussian distribution. To prepare the necessary number of antiprotons in the Accumulator will take a little more than 2 hours.

Similarly, we can assume that three proton bunches, each with 6×10^{10} particles and a longitudinal area of 3 eV-sec, coexist with the antiproton beam. Both beams have equally spaced bunches since the harmonic number 1113 can be divided by 3. In principle, there are therefore 6 equally spaced collision regions. We assume here that beams are not kept separated by electrostatic deflectors. We also assume that two sets of four rf cavities exist, giving orthogonal control of the two beams, as discussed in Sec. 8.5. In this mode of operation, there will be a total of 1.4 MV/turn for each beam.

Using the equations of Chapter 2, which apply to the Tevatron as well as to the Main Ring, we obtain the rms bunch length $\sigma_\ell = 40$ cm and the rms momentum spread $\sigma_p/p = 1.2 \times 10^{-4}$. The area of the stationary bucket is 12.7 eV-sec, four times larger than the bunch area. Finally, the phase-oscillation period is $T_s = 27$ msec.

10.2 Beam Cross Section at the Collision Point

As a result of the transverse stochastic cooling in the Debuncher and Accumulator Rings, and because the two beams have roughly the same number of particles, the two beams have the same emittance in both horizontal and vertical planes. The normalized emittance is assumed to be 24 π mm-mrad. That is, $\varepsilon_V = \varepsilon_H = 0.0225$ π mm-mrad at 1000 GeV (this includes 95% of the beam) distributions.

A low-beta figure of approximately 1 m is expected in both planes and therefore the rms beam radius is

$$\sigma = 0.06 \text{ mm}$$

or

$$\sigma^2 = 3.5 \times 10^{-5} \text{ cm}^2 .$$

Since the low-beta insertion has very small dispersion, there will be negligible contribution to the beam size from momentum spread. In Fig. 10-1 we show the variation of beta and the dispersion in the interaction region. Observe that the beta minima are about 10 cm apart. The dispersion is approximately 18 cm. For comparison in Fig. 10-1, we also show the longitudinal distribution of a bunch.

10.3 Luminosity

Because the low-beta value of 1 m is larger than the rms bunch length (0.4 m), a formula for luminosity valid for varying beam sizes is

$$L = \frac{N_p N_{\bar{p}} B f_0}{4\pi\sigma^2} K \quad , \qquad K = \int G(s)ds$$

where $N_p = 6 \times 10^{10}$ is the number of protons per bunch, $N_{\bar{p}} = 6 \times 10^{10}$ is the number of antiprotons per bunch, $B = 3$ is the number of bunches per beam, and $f_0 = 4.77 \times 10^4$ Hz is the revolution frequency. This gives

$$L = 1.0 \times 10^{30} \text{ cm}^{-2} \text{ sec}^{-1} .$$

The distribution G(s) of luminosity in the interaction region is shown in Fig. 10-2. It is approximately Gaussian with an rms value of 26 cm. This figure has already been adjusted by a factor 0.92 because of the variation of beta with bunch length[14]. This luminosity figure is clearly within reach with the methods and the techniques described in this report. Several alternative luminosity scenarios can be invented. For instance, it would be possible to replenish the Collider every hour with only one single bunch of protons and antiprotons with 10^{11} particles each, for the same luminosity of 10^{30} cm^{-2} sec^{-1}. This takes less filling time but requires an understanding of the bunch combination that we can achieve only with the collider at hand.

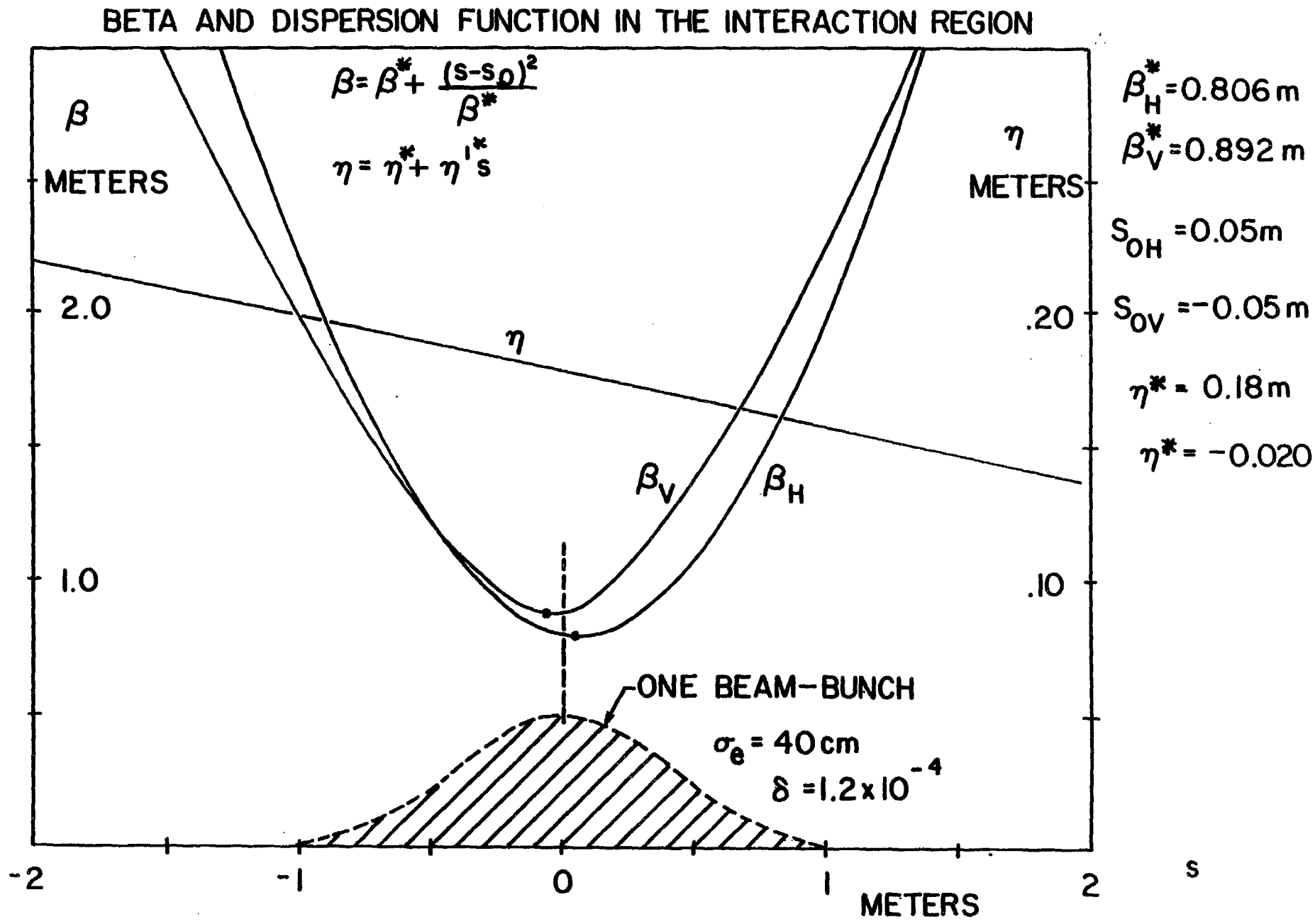
BETA AND DISPERSION FUNCTION IN THE INTERACTION REGION
$\beta = \beta^* + \frac{(s-s_0)^2}{\beta^*}$
$\eta = \eta^* + \eta'^* s$
β
METERS
η
METERS
2.0
1.0
.20
.10
η
β_V
β_H
ONE BEAM-BUNCH
$\sigma_e = 40\,cm$
$\delta = 1.2 \times 10^{-4}$
-2
-1
0
1
2
METERS
s
$\beta_H^* = 0.806\,m$
$\beta_V^* = 0.892\,m$
$S_{OH} = 0.05m$
$S_{OV} = -0.05\,m$
$\eta^* = 0.18\,m$
$\eta^* = -0.020$

Figure 10-1

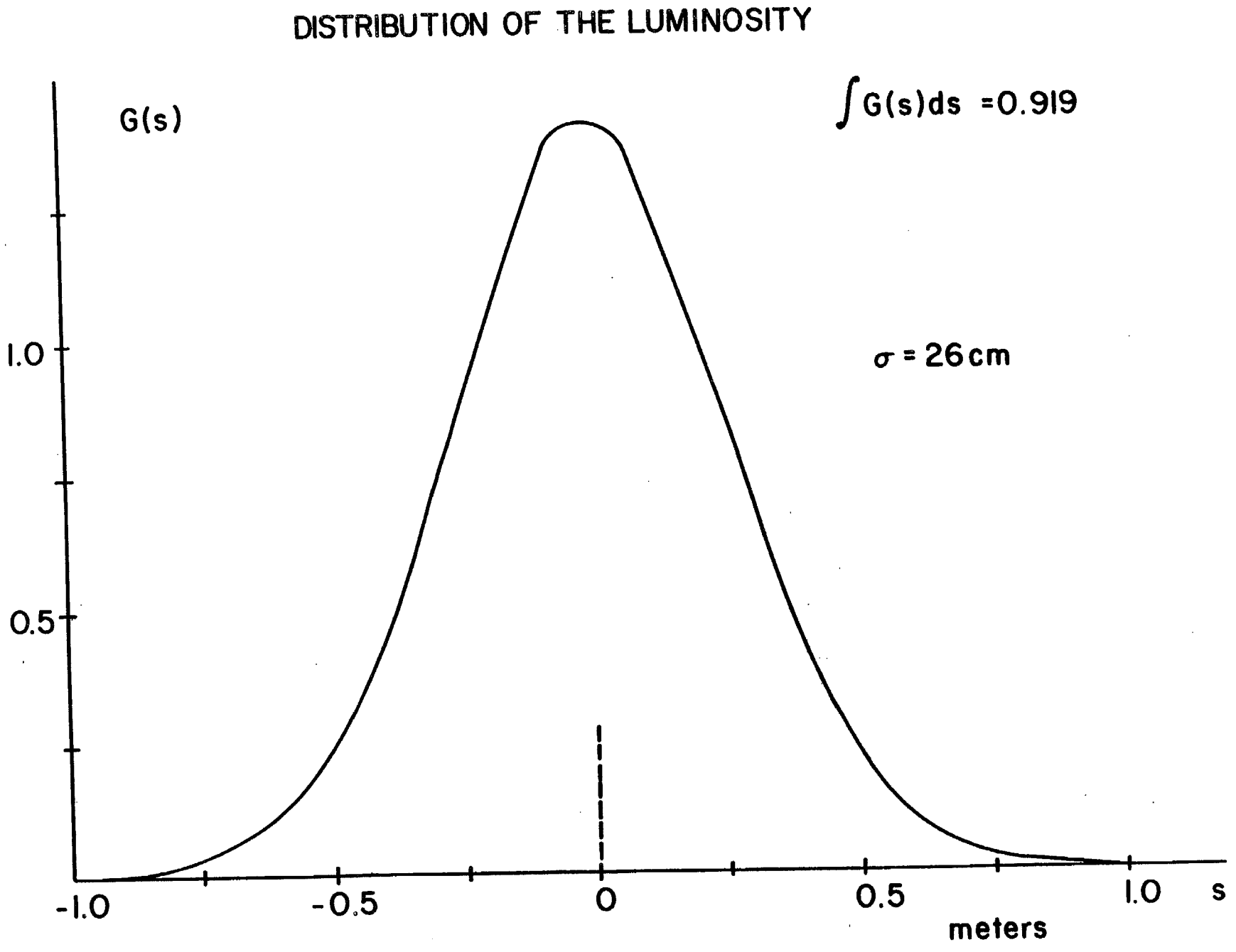
DISTRIBUTION OF THE LUMINOSITY
G(s)
∫G(s)ds =0.919
σ = 26cm
1.0
0.5
-1.0
-0.5
0
0.5
1.0
s
meters

Figure 10-2

Higher luminosity figures can also be expected, as high as 6×10^{30} $cm^{-2}sec^{-1}$ (see Table 1-I), by improving either the stochastic cooling (a factor of two), or the beam intensity in the Main Ring and Tevatron (also possibly by a factor of two) or with 6 bunches per beam instead of the 3 assumed here.

10.4 Beam-Beam Tune Shift

Collisions are head on, the emittances of both beams in both planes are all equal, and the lattice functions are approximately the same in both planes. The beam-beam tune shift is therefore the same for both beams, is independent of the beam energy, and does not depend on the lattice functions. The linear beam-beam tune shift is given by

$$\xi = \frac{3\, N r_o}{2\varepsilon_N},$$

where $N = 6 \times 10^{10}$ is the number of particles per bunch, $\varepsilon_N = 24\pi$ mm-mrad is the normalized emittance and $r_o = 1.535 \times 10^{-18}$m is the classical proton radius. We have

$$\xi = 0.0017/\text{crossing}$$

Even with a low-beta insertion, the beam cross-section in the other five collision regions with normal β values is round and the contribution to the beam size from the momentum spread is negligible. The tune shift per crossing is therefore the same at each crossing so long as the collision is head-on, or at least at an angle $\theta \ll \sigma/\sigma_e$. If there is a total of 6 crossings, the total tune-shift per turn

$$\xi_{tot} = 6\, \xi = 6 \times 0.0017 = 0.01.$$

10.5 Single-Beam and Luminosity Lifetime

We have investigated four possible sources of lifetime deterioration in the Tevatron: scattering by the residual gas, intrabeam scattering, beam-beam effects and beam-beam cross sections. An analysis of periodic or random crossings of nonlinear resonances has also been carried out[15]. This will help to determine not only possible limits on the nonlinearities in the Energy Saver superconducting magnets, but also on the amount of coherent and incoherent noise amplitude allowable.

10.5.1 Effects of Residual Gas[1]. The following effects have been investigated:

(i) Multiple Coulomb Scattering

(ii) Single Coulomb Scattering

(iii) Nuclear Scattering

The first effect causes a beam-emittance growth, which leads both to a luminosity decay and a single-beam lifetime in a finite aperture. The single-beam lifetime due to multiple Coulomb scattering is very long and this effect is quite negligible. The second and third effects cause an intensity decay, but the third effect is more important than the second[1].

The average vacuum pressure expected in the Tevatron is 10^{-8} Torr in the warm regions and 5×10^{-9} Torr in the cold regions with the gas composition:

warm region: 60% H_2 and 40% CO
cold region: 75% H_2 and 25% He.

The intensity decay per beam due to single Coulomb and nuclear scattering is

$$\frac{1}{I}\frac{dI}{dt} = -1.07 \times 10^{-6}/\text{sec} . \qquad (10.1)$$

The emittance growth due to multiple Coulomb scattering is

$$\frac{1}{\varepsilon}\frac{d\varepsilon}{dt} = 1.3 \times 10^{-6}/\text{sec} . \qquad (10.2)$$

These effects combined lead to a luminosity decay of

$$\frac{1}{L}\frac{dL}{dt} = -3.44 \times 10^{-6}/\text{sec} ,$$

giving a loss of 23% of the luminosity in 20 hours.

10.5.2 Intrabeam Scattering[2] To estimate intrabeam scattering diffusion

rates for the colliding-beam mode, we have used the same computer code we used to estimate intrabeam scattering for the Accumulator. For our estimate, we have used the actual Tevatron lattice with the low-beta insertion. From this calculation, we have found empirical formulas for diffusion rates, which apply to a bunched beam at 1000-GeV. Define

$$\Delta\delta = \sigma_p/\sigma_{p_o}$$

$$\Delta\varepsilon = \varepsilon/\varepsilon_o ,$$

where σ_p is the rms momentum spread and $\varepsilon = 2\sigma^2/\beta$ is the rms betatron emittance; σ_{p_o} and ε_o are the initial values. Then

$$\frac{d\Delta\delta}{dt} = \frac{\tau_p^{-1}}{(\Delta\delta)^{m_p-1}\,(\Delta\varepsilon)^{r_p}} \tag{10.3}$$

$$\frac{d\Delta\varepsilon}{dt} = \frac{2\tau_x^{-1}}{(\Delta\delta)^{m_x}\,(\Delta\varepsilon)^{r_x-1}} \tag{10.4}$$

Here r_p, r_x, m_p and m_x are empirically determined exponents. There is actually damping of the vertical betatron emittance.
For $\sigma_{e_o} = 40$ cm, $N_o = 6 \times 10^{10}$, $\varepsilon_o = 0.0077$ mm-mrad and $\sigma_{p_o}/p = 1.2 \times 10^{-4}$,

$$m_p = 2.2 \qquad r_p = 1.4$$

$$m_x = 0.7 \qquad r_x = 2.0 .$$

We obtain as initial diffusion times

$$\tau_p = (63.5 \text{ hours}) \frac{N_o\,\sigma_e}{N\,\sigma_{e_o}}$$

$$\tau_x = (24.0 \text{ hours}) \frac{N_o\,\sigma_e}{N\,\sigma_{e_o}}$$

There is a loss of luminosity caused by intrabeam scattering diffusion in

the horizontal betatron oscillation. We assume that there is also diffusion of the vertical emittance at the same rate caused by nonlinear coupling of the type induced by beam-beam effects and chromatic/sextupole effects. It has been found[8] that the CERN-SPS-Collider performance is limited to a luminosity lifetime of about 16 hours mostly because of intrabeam scattering. The calculations made to explain the experiment are very similar to the ones here.

10.5.3 Beam - Beam Effects. Beam-beam effects have been extensively simulated on the computer. Several issues have been discussed, studied, and, we hope, resolved.

A systematic search for Arnol'd diffusion for the Tevatron parameters has given negative results.[3,4] We have been able to simulate in some cases up to 20 minutes real time of collisions. From our data, we can extrapolate beam-beam lifetimes of several days. We believe the stability of the system arises from the "roundness" of the beam geometry and of the lattice functions.[5]

We found that the addition of the nonlinear beam-beam interaction to a system already affected by external random noise (such as gas scattering) causes an enhancement of the diffusion rates.[6] The largest enhancement encountered was a factor 6 for a beam-beam tune shift of 0.06 in proximity to a fourth-order resonance. This is well above the tune shift we can expect, as shown in section 10.4.

We have investigated beam-beam interactions with the beam centers offset or oscillating around each other.[7] This could be caused by either a dipole oscillation or a finite dispersion in the collision region coupled to the momentum oscillation. We have not found any effect of significance.

Of more serious concern are the effects created by betatron tune oscillations. If proper care is not taken, it is possible to cause an emittance growth of a factor two in a few minutes.[8] Fortunately, we have found a threshold and the growth can be tuned out by either adjusting the betatron tunes or by improving the power-supply regulation to better than 10^{-4} and flattening the lattice chromaticity.

This latter effect has been clearly observed in the CERN Collider[17]. But, once a better tune of the machine was available, this effect, even for a tune-shift of 0.004_5 did not cause a significant effect compared with intrabeam scattering[17].

We have also investigated multiple crossings per revolution, 2 or 6 instead of 1, with similar results. The emittance growth due to the beam-beam effect has been modeled by the equation

$$\frac{1}{\varepsilon_0}\frac{d\varepsilon}{dt} = \frac{\sqrt{n_c}}{\tau_{BB}}\frac{N/N_0}{\varepsilon/\varepsilon_0} \tag{10.5}$$

with n_c the number of crossings and τ_{BB} = 100 hours for $\Delta\nu = 0.0017$, which fits observations in the CERN SPS.[18]

10.5.4 Total Cross Section. As the two bunched beams interact with each other, there is a continuous loss of luminosity due to particles being removed by single events or as the beam size grows under the effect of multiple scattering. The total cross section is built from four pieces,[19] diagramaticlly shown in Fig. 10-3. If σ is the cross section in mb and p the momentum in GeV, the following equations apply, where x' is the transverse momentum transfer normalized to the longitudinal momentum:

for elastic:

$$\frac{d\sigma}{dx'^2} = 18p^2\sigma\, e^{-18p^2x'^2} \tag{10.6}$$

for single-diffraction and a given beam particle:

$$\frac{d\sigma_{SD}}{d\delta dx'^2} = \frac{6.1p^2}{\delta} e^{-9p^2x'^2} \tag{10.7}$$

for double-diffraction

$$\frac{d\sigma_{DD}}{d\delta dx'^2} = \frac{5.3p^2}{\delta} e^{-9p^2x'^2} \tag{10.8}$$

and for the core:

$$\sigma_{CORE} = 26.3 \text{ mb} . \tag{10.9}$$

10.5.5 Luminosity Lifetime[13,14]. All the effects discussed before have been taken into account to estimate the luminosity lifetime. In Fig. 10-4 we show the variation of the emittance and the momentum spread with time. The luminosity variation with time is shown in Fig.10-5 for an initial value of $10^{30}cm^{-2}sec^{-1}$, which corresponds to the case discussed in the previous sections. The luminosity lifetime is about 20 hours. As we have

CROSS SECTIONS

THE TOTAL CROSS–SECTION IS BUILT FROM FOUR PIECES:

ELASTIC

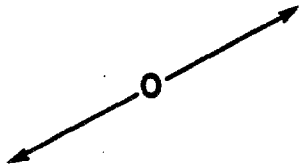

CORE

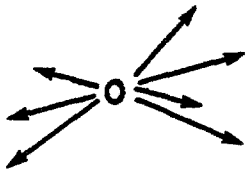

SINGLE DIFFRACTIVE

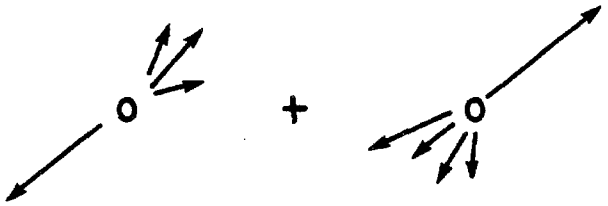

DOUBLE DIFFRACTIVE

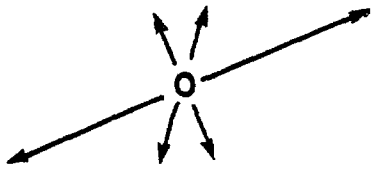

Figure 10-3

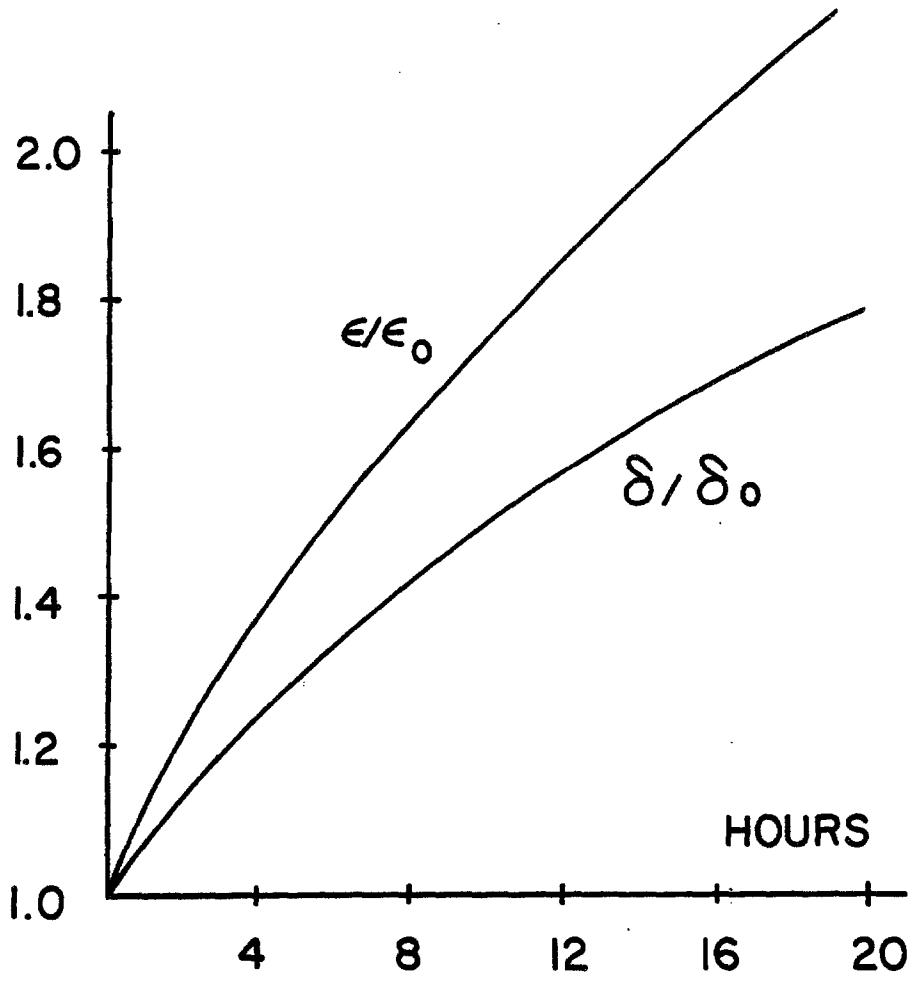

STANDARD

$$\frac{1}{\epsilon_0}\frac{d\epsilon}{dt} \sim \frac{1}{9.2h}$$

FROM INITIAL SLOPES

$$\frac{1}{\delta_0}\frac{d\delta}{dt} \sim \frac{1}{13.6h}$$

Figure 10-4

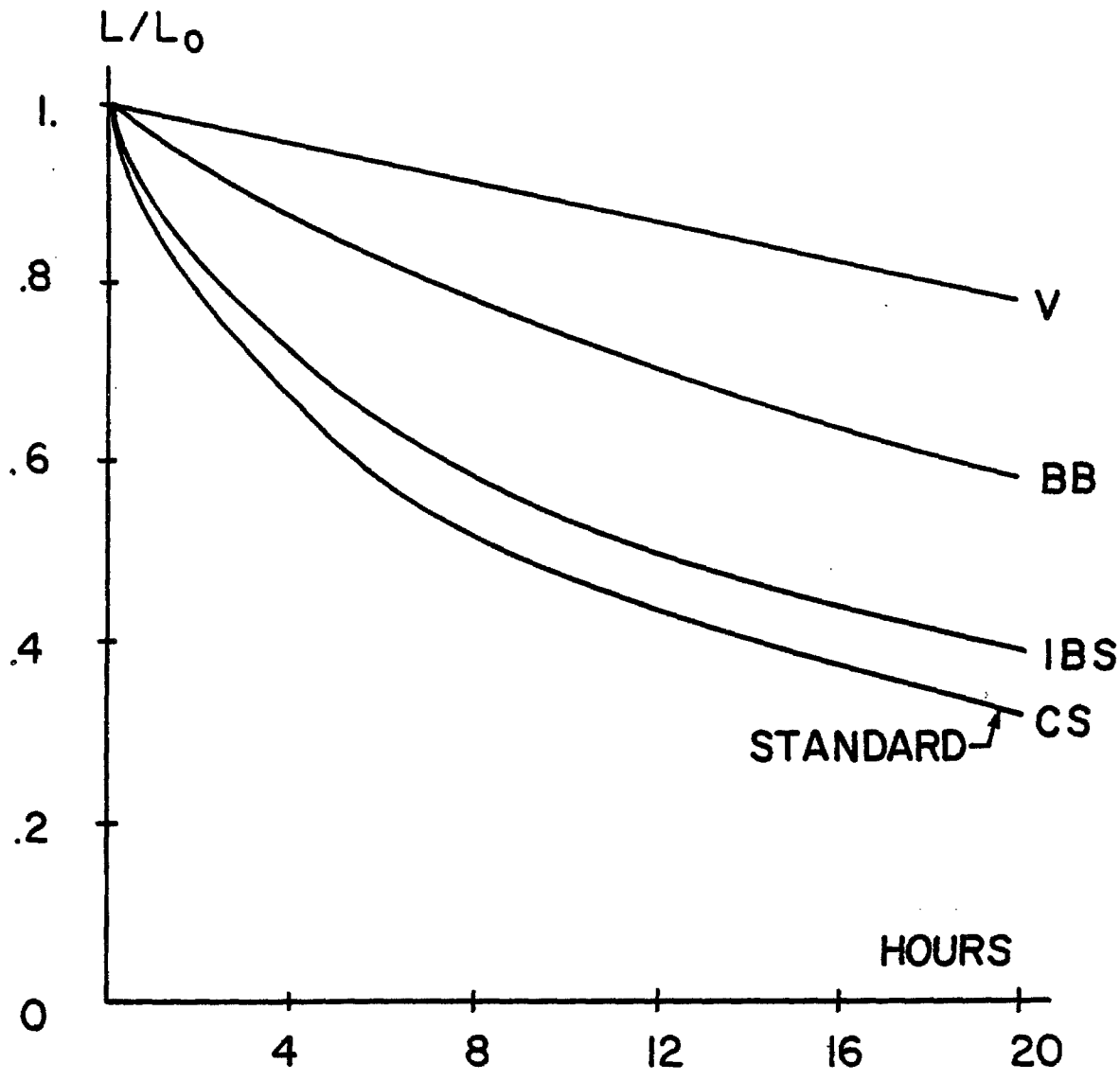

V	VACUUM EFFECTS ONLY.
BB	BEAM-BEAM EFFECTS ADDED TO ABOVE.
IBS	INTRA BEAM SCATTERING ADDED TO ABOVE.
CS	CROSS-SECTIONS ADDED TO ABOVE.

Figure 10-5

seen, each beam is made of three bunches, each with 6×10^{10} particles and a longitudinal area of 3 eV-sec. The beam intensities, both average and peak, are very modest. A considerable effort has been made in the recent past to estimate the longitudinal stability of each beam for both individual bunch and bunch-to-bunch modes.[9,10] The beam-wall impedance expected in the Tevatron was estimated[11] to be $|Z_n|/n \sim 1$ ohm. In Fig. 10-7 we give an estimate of the longitudinal-coupling impedance verses the harmonic number. Every contribution from the vacuum-chamber equipment has been included except for the major rf system. Because of the small longitudinal beam density, we believe the beams are quite stable. Moreover, a longitudinal damper operating on each individual bunch is planned.

Fewer calculations have been done for the case of transverse instabilities. But again we do not foresee major problems. In addition, a transverse active damper has been proposed[12] that will be fast enough to operate on individual bunches in both radial and vertical modes of oscillation.

10.6 Collider Filling Strategy.[13,14]

Because of the luminosity deterioration as a function of time, the refilling of the Tevatron I Collider with fresh beams of protons and antiprotons can be thought of as follows.

Let T_1 be the running time, that is, the period when colliding beam experiments are usefully done, and let T_2 be the period without beams in the storage ring. One can also include in T_2 the average failure time. The useful average luminosity L_{av} normalized to the initial luminosity L_o is

$$\frac{L_{av}}{L_o} = \frac{1}{T_1+T_2}\int_0^{T_1}\frac{L(t)}{L_o}\,dt\,, \qquad (10.10)$$

where $L(t)$ is the actual luminosity as a function of time as given in Fig. 10-5.

For a given ratio L_{av}/L_o one can derive from Eq. (10.10) the pause T_2 as a function of the running period T_1. This is shown in Fig. 10-6. For instance, with the present accumulation scheme, except at the first filling, one can produce enough antiprotons for the goal luminosity of $10^{30}cm^{-2}sec^{-1}$ in less than 2 hours. It is therefore conceivable to run for a period of 2 hours and rest, for refilling and other interruptions, for 6 minutes. This would correspond to an average luminosity of 80% of the initial value. To do better than this would require a larger production of antiprotons.

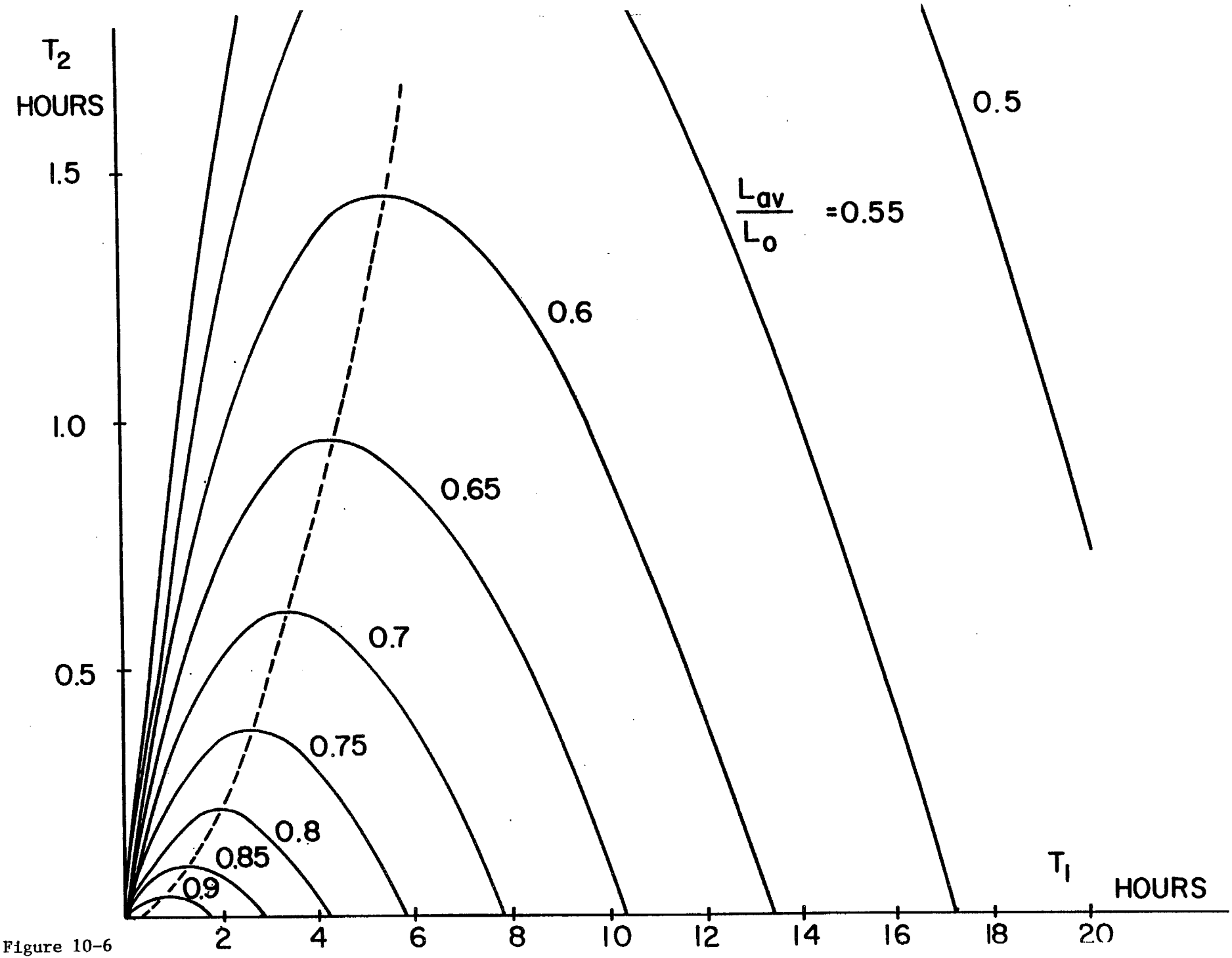
T_2
HOURS
1.5
1.0
0.5
$\frac{L_{av}}{L_o}$ =0.55
0.5
0.6
0.65
0.7
0.75
0.8
0.85
0.9
T_1
HOURS
2
4
6
8
10
12
14
16
18
20

Figure 10-6

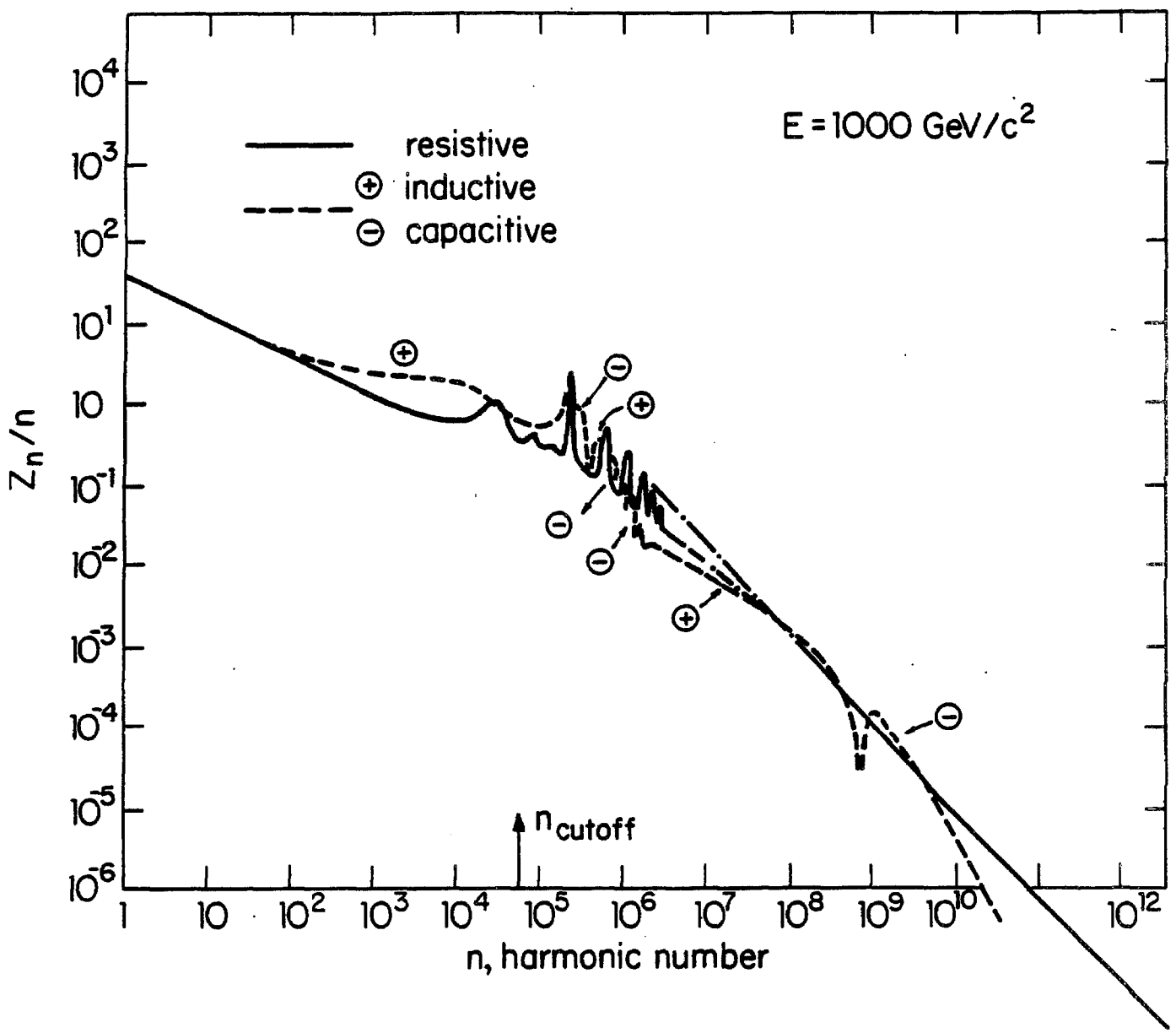
E = 1000 GeV/c²
resistive
⊕ inductive
⊖ capacitive
Z_n/n
10^4
10^3
10^2
10^1
10
10^{-1}
10^{-2}
10^{-3}
10^{-4}
10^{-5}
10^{-6}
n_{cutoff}
1
10
10^2
10^3
10^4
10^5
10^6
10^7
10^8
10^9
10^{10}
10^{12}
n, harmonic number

Figure 10-7

References

1. H. Mizuno, S. Ohnuma, A. G. Ruggiero, "Vacuum and Beam Lifetime in the Doubler," UPC No. 119, Fermilab 21, 1979.

2. A.G. Ruggiero, "Revised Intrabeam Scattering Calculations," Fermilab $\bar{p}$-note 192 (1982), unpublished. .

3. D. Neuffer, A. Riddiford, A. Ruggiero, "Searches for Arnol'd Diffusion and Chaotic Motion in the Beam-Beam Interaction," 1983 Particle Accelerator Conference IEEE Trans. NS-30, p. 2427 (1983).

4. D. Neuffer, A. Riddiford, A. Ruggiero, "Long Time Simulation of the Beam-Beam Interaction," FN-343, Fermilab, July 1981.

5. A.G. Ruggiero, Particle Accelerators, 12, 45 (1982).

6. D. Neuffer, A. Riddiford, A. Ruggiero, "A Theoretical Model and Computer Simulations to Describe Diffusion Enhancement by the Beam-Beam Interaction," 1983 Particle Accelerator Conference IEEE Trans. NS-30, p. 2430 (1983).

7. D. Neuffer, A. Riddiford, A. Ruggiero, "Effects of Transient and Modulation of Beam Displacement on Long-time Stability with the Beam-Beam Interaction," FN-358, Fermilab, March 1982.

8. D. Neuffer, A. Riddiford, A. Ruggiero, "Study of Periodic Tune Modulation with the Beam-Beam Effect," 1983 Particle Accelerator Conference IEEE Trans. NS-30, p. 2433 (1983).

9. A.G. Ruggiero, "Individual Bunch Longitudinal Instabilities," Fermilab, UPC-72, Jan. 1979.

10. A.G. Ruggiero, "Bunch-to-Bunch Longitudinal Instabilities," Fermilab, UPC-81, Jan. 1979.

11. King-Yuen Ng, "An Estimate of the Longitudinal Coupling Impedance of the Energy Doubler," Fermilab, UPC-150, May 1981.

12. H.W. Miller, "Transverse Active Dampers for the Tevatron," Fermilab, UPC-36, Jan. 1979.

13. A.G. Ruggiero, "Average Luminosity Performance for Tevatron I , Fermilab, $\bar{p}$ note 224, September 1982.

14. A.G. Ruggiero, "Tevatron I Collider Performance", Fermilab, $\bar{p}$ note 240, October 1982.

15. A.G. Ruggiero, "Crossing a Single Weak Non Linear Resonance," Fermilab, $\bar{p}$ note 62, April 1980.

16. L.R. Evans, Proceedings of the 12th International Conference on High Energy Accelerators, Fermilab Aug. 1983, p. 229.

17. L.R. Evans, J. Gareyte, IEEE Trans. on Nucl. Sci., NS-30, p. 2347 (1983).

18. J. Gareyte, Proceed. of the 12th International Confer. on High Energy Accelerators, Fermilab Aug. 1983, P. 17.

19. J.D. Bjorken, Private Communication, Fermilab 1982.

CHAPTER 11

BEAM - TRANSPORT LINES

11.1 120-GeV Proton Transport From F17 to Target (Line AP-1)

The extraction energy for the protons to be used for antiproton production was 80 GeV in an earlier design. It was decided to raise this energy to 120 GeV in order to increase antiproton production. The earliest choice for a 120-GeV extracted beam was to upgrade the then-existing 80-GeV line, which extended 1000 ft from F17 to F25 within the Main Ring tunnel. Although this design satisfied most of the project requirements, it possessed a number of undesireable features. Its estimated power consumption of 2 MW would place a heavy burden on the operating cost of the Antiproton Source. The elements of the 80-GeV line were placed immediately above the Main Ring magnets, below which the Energy Saver magnets have now been installed. As a consequence, difficult operational problems would be encountered wherever work had to be performed on the Main Ring or the Energy Saver. It was necessary to dismantle the 80-GeV beam in many locations in order to install the Energy Saver. The location of the original $\bar{p}$ hall, which is very close to F25, limited the ability to vary the proton targeting. The 80-GeV line had been put in the Main Ring tunnel because the 400-GeV operating schedule in 1977 and 1978 did not allow the several-month interruption that was believed to be needed to modify the Main Ring tunnel at F18 in order to build a more flexible beam. This constraint is no longer relevant. For these reasons, a more efficient and flexible beam design was developed.

The design of the 120-GeV proton transport line was based on the following requirements:

(i) It must leave the Main Ring tunnel as close as possible to location F18.

(ii) The target elevation is to be 7.0 ft above Main Ring beam height.

(iii) It must transport a 120-GeV proton beam with a momentum spread of $\pm 0.2\%$.

(iv) It must be possible to bypass the target and collection system in the reverse direction.

(v) It must transport the 8.9-GeV/c cooled antiproton beam with an emittance of 2.0π mm-mrad.

(vi) It must produce a round proton beam spot at the target which can be varied from 0.2 mm to 0.8 mm rms.

(vii) It must have zero dispersion at the target.

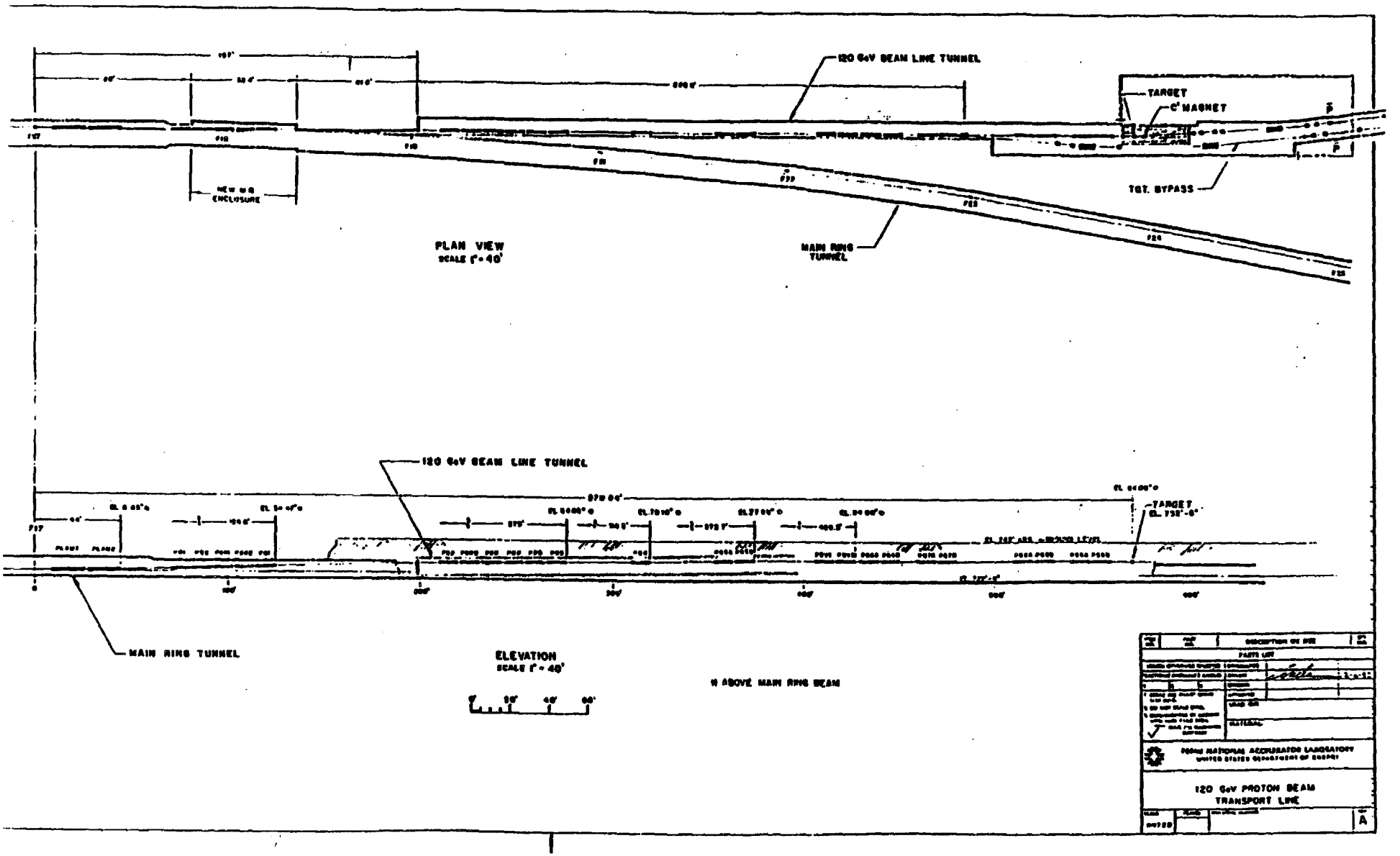
120 GeV BEAM LINE TUNNEL
TARGET
C' MAGNET
TGT. BYPASS
MAIN RING TUNNEL
PLAN VIEW
SCALE 1" = 40'
120 GeV BEAM LINE TUNNEL
TARGET
MAIN RING TUNNEL
ELEVATION
SCALE 1" = 40'
ABOVE MAIN RING BEAM
120 GeV PROTON BEAM TRANSPORT LINE

Figure 11-1

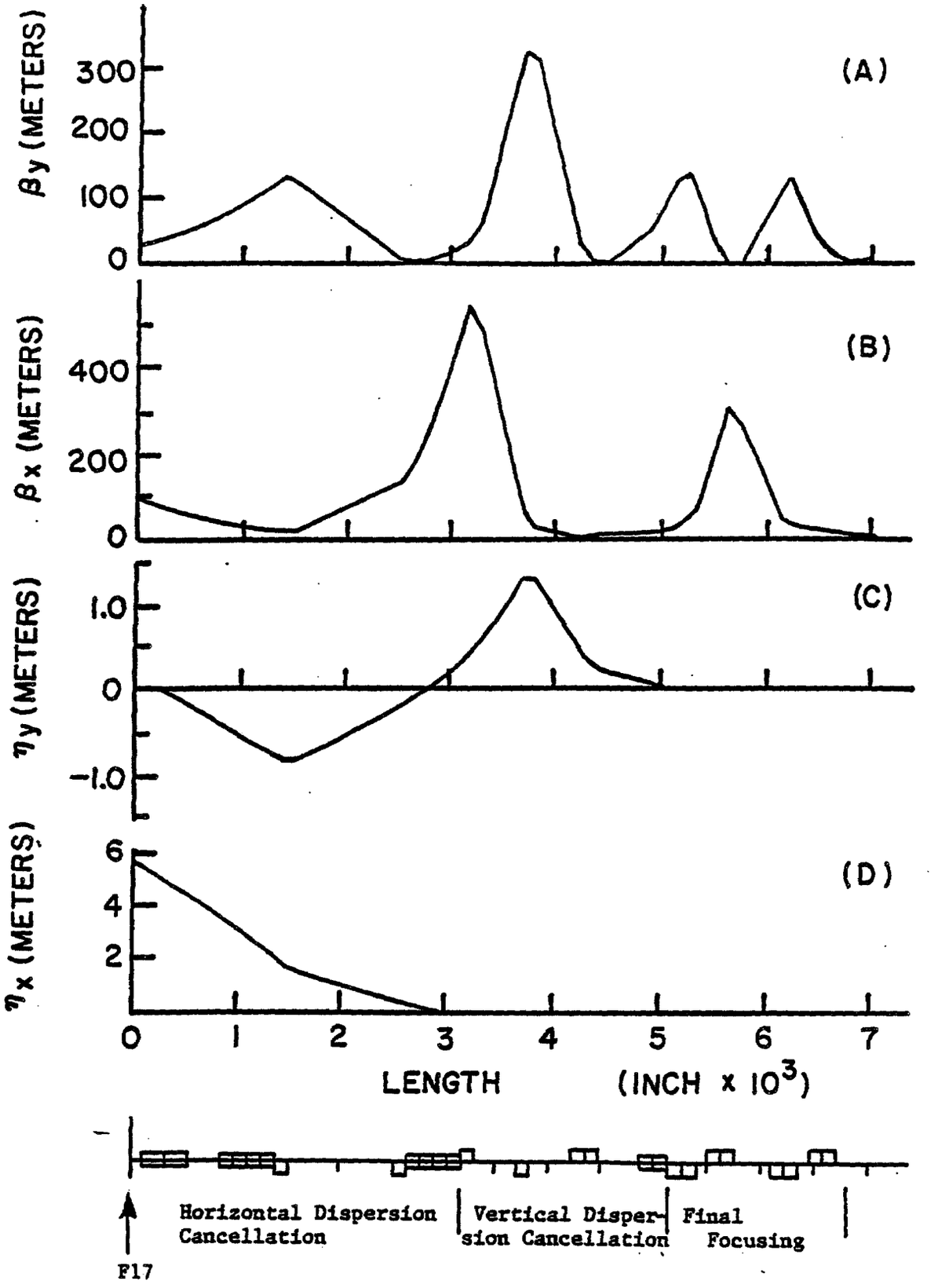

Figure 11-2 Twiss parameters β_y, β_x and dispersion functions η_y, η_x through the 120 GeV beam transport system.

(viii) The power consumption must remain below 500 kW.

A layout of the beam is shown in Fig. 11-1 and its parameters are tabulated in Table 11-I. In Fig. 11-2 we show the behavior of the monoenergetic β_y, β_x, η_y, and η_x through the system from extraction to the target. The beam consists of 10 EPB dipoles excited to a field of 13 kG or less and 14-3Q120 quadrupoles excited to a field gradient of 4.75 kG/in. or less. Three of the dipoles, indicated by (R), are rotated by 45° to achieve the necessary vertical and horizontal bends with the minimum number of magnets. The Main Ring tunnel must be widened over a distance of roughly 18 m in order to accommodate the four EPB dipoles and one 3Q120. The length of the beam is 174 m, of which 41 m is located in the Main Ring tunnel. The remainder of the beam elements are located in a new 115-m long enclosure. The new enclosure and the Main Ring tunnel are connected by an 18-m long pipe.

A 4.5° bending magnet, which bends the reverse antiproton beam to the left, is placed within the final focus section between PQ7B and PQ8A in order to allow the target and antiproton collection lens to be bypassed whenever cooled antiprotons are transported back to F17. The total power consumption of the beam is estimated to be less than 390 kW. In Table 11-II the gradients of the four final focusing quadrupoles, which obtain the required range of beam sizes, are listed.

TABLE 11-I 120-GEV TRANSPORT ELEMENTS

NEW BEAM TRANSPORT MAIN RING TO TARGET
AP-1-NEW

3 APRIL 84. DE JOHNSON

120 GEV PROTONS KINETIC

X,Y,Z SITE COORDINATES
COORDINATES GIVEN AT EACH END OF ELEMENT
MAIN RING STATION A0 AT X=0.0, Y=0.0

NAME	EFF.	LENGTH (IN)	FIELD (KG-KG/M)	X (FT)	Y (FT)	Z (FT)
MAIN RING				1010.527	-2444.090	725.300
drift		74.70		1008.807	-2441.782	725.300
P-LAMBERTSON 1		142.00	8.48	998.839	-2432.679	725.359
drift		13.00		994.916	-2431.835	725.371
P-LAMBERTSON 2		142.00	8.48	984.932	-2422.729	725.749
drift		18.00		983.844	-2421.717	725.776
P-CMAG 1		118.40	10.31	974.363	-2415.063	725.988
drift		21.00		973.272	-2413.883	726.033
P-CMAG 2		118.40	10.31	967.991	-2407.229	726.321
drift		142.00		958.031	-2398.127	726.767
PB1		120.00	13.11	950.620	-2391.421	727.097
drift		12.00		949.876	-2390.754	727.131
PB2		120.00	13.11	942.399	-2384.122	727.461
drift		12.00		941.648	-2383.463	727.494
PBR1		120.00	13.11	934.114	-2376.893	727.789
drift		12.00		933.358	-2376.239	727.816
PBR2		120.00	13.11	925.778	-2369.722	728.041
drift		12.00		925.017	-2369.073	728.060
PQ1		120.00	-43.87	917.413	-2362.581	728.250
drift		1012.20		833.271	-2307.823	729.856

NAME	EFF. LENGTH (IN)	FIELD (KG-KG/M)	X (FT)	Y (FT)	Z (FT)
PQ2	120.00	-48.90	845.467	-2301.333	730.046
drift	12.00		844.906	-2300.684	730.065
PBR3	120.00	12.72	837.324	-2294.166	730.221
drift	12.00		836.568	-2293.512	730.234
PB3	120.00	12.72	829.039	-2286.932	730.396
drift	16.17		828.028	-2286.040	730.372
PB4	120.00	12.72	820.563	-2279.389	730.495
drift	16.17		819.561	-2278.487	730.512
PB5	120.00	12.72	812.160	-2271.764	730.634
drift	16.17		811.167	-2270.853	730.651
PQ3	120.00	120.93	803.798	-2264.094	730.773
drift	400.00		779.235	-2241.563	731.182
PQ4	120.00	-159.61	771.866	-2234.804	731.305
drift	400.00		747.304	-2212.274	731.714
PQ5A	120.00	183.05	739.935	-2205.515	731.836
drift	12.00		739.198	-2204.839	731.848
PQ5B	120.00	183.05	731.829	-2198.080	731.971
drift	391.43		707.780	-2176.022	732.371
PBV1	120.00	8.12	700.411	-2169.262	732.463
drift	12.00		699.674	-2168.586	732.470
PBV2	120.00	8.12	692.304	-2161.827	732.500
drift	24.00		690.831	-2160.475	732.500
PQ6A	120.00	-114.28	683.462	-2153.715	
drift	12.00		682.725	-2153.039	
PQ6B	120.00	-114.28	675.355	-2146.280	
drift	100.00		649.214	-2140.647	
PQ7A	120.00	102.73	641.845	-2133.887	
drift	12.00		641.108	-2133.211	
PQ7B	120.00	102.73	633.738	-2126.451	
drift	350.00		632.244	-2106.736	
PQ8A	120.00	-123.78	624.875	-2099.976	
drift	12.00		624.138	-2099.300	
PQ8B	120.00	-123.78	616.769	-2092.541	
drift	100.00		610.628	-2086.908	
PQ9A	120.00	92.66	603.258	-2080.148	
drift	12.00		602.521	-2079.472	
PQ9B	120.00	92.66	595.152	-2072.713	
drift	150.00		585.940	-2064.263	
TARGET			585.940	-2064.263	732.500

** END OF LISTING **

TABLE 11-II GRADIENT OF FINAL FOCUSING QUADRUPOLES AS A FUNCTION OF BEAM SIZE AT THE TARGET, IN T/m. (MAXIMUM GRADIENT 18T/m)

		QUADRUPOLES			
β*(m)	σ(mm)	PQ6A/B	PQ7A/B	PQ8A/B	PQ9A/B
1.17	0.20	-13.2	+10.3	-12.1	+13.2
4.69	0.40	-11.4	+10.3	-12.4	+ 9.3
18.75	0.79	-10.3	+ 9.7	- 9.8	+ 2.0

11.2 8-GeV Antiproton Transport to Debuncher (Line AP-2)

The antiproton transport line is shown symbolically in Fig. 11-3. This beam line can transport an 8-GeV beam with 20π mm-mrad transverse emittance and $|\Delta p/p| > 4.0\%$. The match to the Debuncher is accomplished with an integrated efficiency of 80% over the 4.0% passband in $\Delta p/p$.

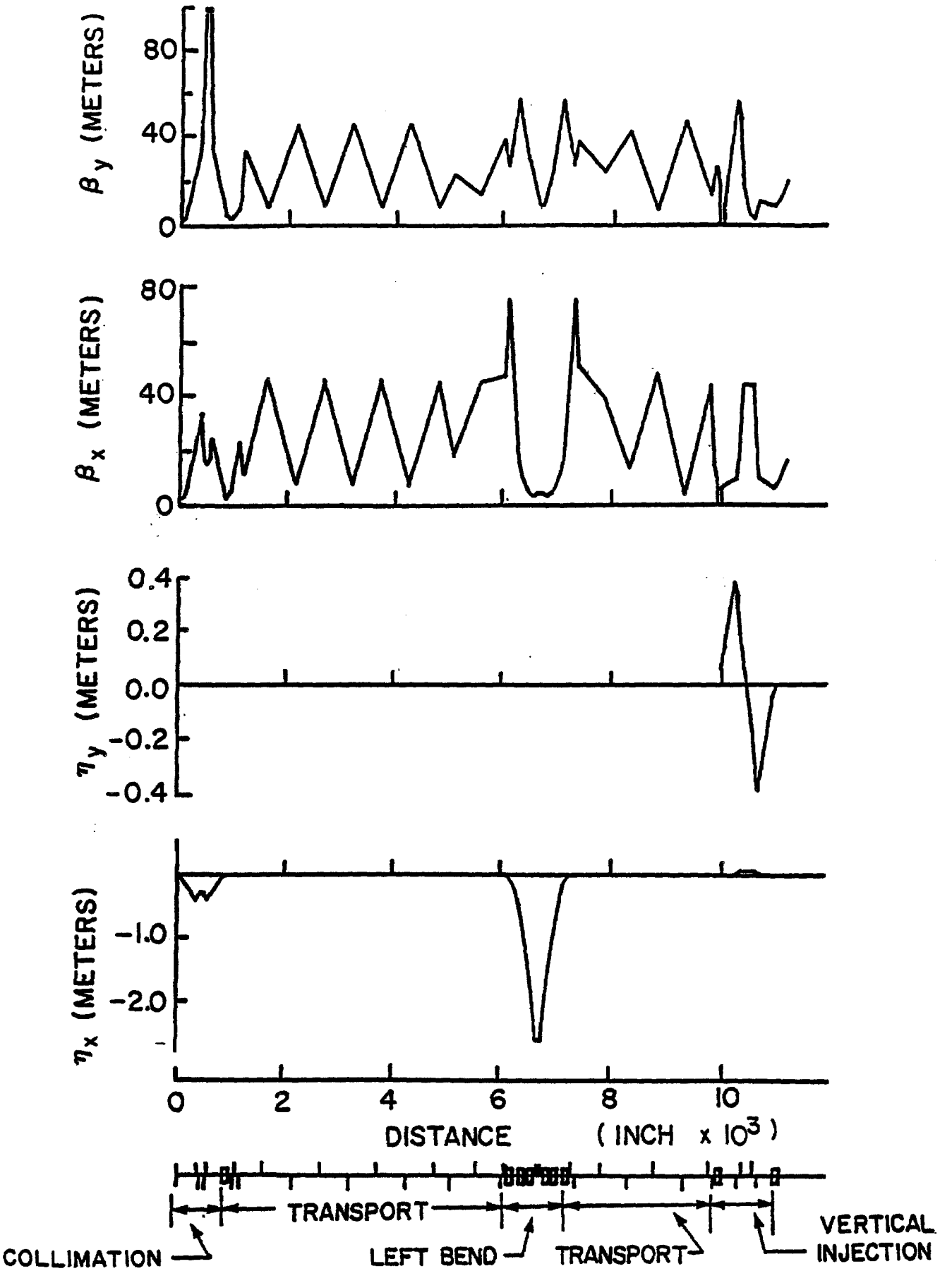

Figure 11-3 The antiproton transport line to the Debuncher monoenergetic envelope functions β_y, β_x and dispersion functions η_y, η_x.

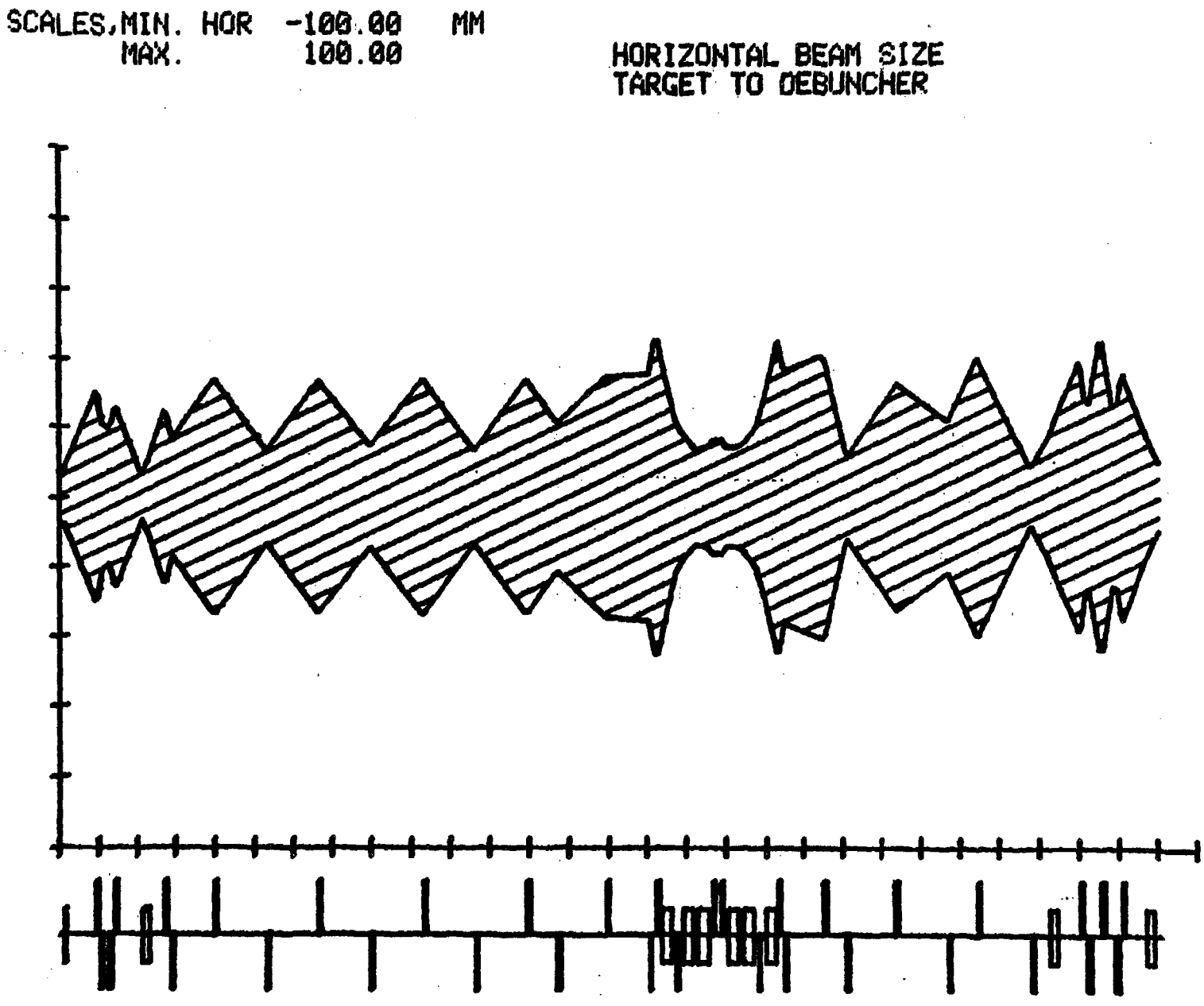
SCALES,MIN. HOR -100.00 MM
MAX. 100.00
HORIZONTAL BEAM SIZE
TARGET TO DEBUNCHER

Figure 11-4a

Independent controls for emittance definition in both x and y planes and $\Delta p/p$ selection are possible using collimators. The detailed design can be found in Reference 9.

The "source" for the beam line is the center of the 5.0 cm $\bar{p}$ production target. For the purpose of the transport calculations we have assumed a circular spot and a β^* of 2.25 cm. The lithium lens collector then performs point to parallel optics for negatives with a momentum of 8.9-GeV/c (8-GeV $\bar{p}$). The beam line consists of five basic sections: (i) cleanup, (ii) long transport, (iii) left bend, (iv) long transport, and (v) injector. Section (i) uses a pulsed C magnet to bend the 8-GeV $\bar{p}$ 3° left, and two quadrupole doublets and another 3° bend left in order to complete the achromatic transformation. Charge, central momentum and vertical emittance ε_y are selected within this section using collimators. The long transport sections (ii) and (iv) consist of 90° FODO quadrupole cells and matching quadrupole lenses. The periodic structure has a cell length of 88.81 ft. with β_{max}/β_{min}=45.93m/7.98m. The left bend (iii) which deflects the antiproton by 36.53°, consists using of six dipoles. Horizontal emittance (ε_x) selection is performed at the entrance and exit of this section where β_x is nearly 80 m. The fine $\Delta p/p$ selection is performed in the center of the left bend section where β_x = 5.0 m and a maximum in the dispersion η_x^* = 2.62 m is obtained. The first-order momentum resolving power is 1.31 for $\varepsilon_x = 20\pi$ mm-mrad and $\Delta p/p$ = 1.0% and 2.62 for $\varepsilon_x = 5\pi$ mm-mrad. The injector (v) is an achromatic vertical translation ending at the downstream end of the 2.1 m long current septum. The beam is deflected downward by 48 inches using 3.62° bends.

The components for the beam line are listed in Table 11-V.

TABLE 11-III BEAM TRANSPORT TARGET TO DEBUNCHER

BEND AND QUAD CENTERS FOR AP2 INJECTION LINE
IN FEET WITH AO AT (0.,0.)

A. J. LENNOX 7-17-84

CALCULATED FROM D JOHNSON'S TRANSPORT OUTPUT WHICH GIVES COORDINATES DEFINING INCOMING AND OUTGOING RAYS FOR EACH MAGNET. FOR BENDS CALCULATED THE INTERSECTION OF THE RAYS. ALSO PROJECTED TO THE BENDPOINT FROM BOTH UPSTREAM AND DOWNSTREAM ENDS. ANSWER GIVEN HERE IS THE AVERAGE OF THE PROJECTIONS. WHICH GENERALLY AGREES WITH THE INTERSECTION CALCULATION TO WITHIN ONE MIL.

FOR QUADS FOUND THE MIDPOINT BETWEEN THE POINTS DEFINING THE MAGNETIC EDGES OF THE MAGNET.

DEVICE	X(FEET)	Y(FEET)	ELEVATION(FEET)
LITH	585.3961	-2063.7639	732.5000
CMAG	582.3137	-2060.9358	732.5000
IQ1	562.0705	-2044.2266	732.5000
IQ2	558.7672	-2041.4999	732.5000
IQ3	553.1373	-2036.8529	732.5000
IQ4	549.8339	-2034.1263	732.5000
IB1	529.5908	-2017.4171	732.5000

DEVICE	X(FEET)	Y(FEET)	ELEVATION(FEET)
IG5	515.9906	-2007.3399	732.5000
IG6	511.5648	-2004.0605	732.5000
IG7	482.3402	-1982.4062	732.5000
IG8	447.1932	-1956.3636	732.5000
IG9	412.0462	-1930.3211	732.5000
IG10	376.8991	-1904.2785	732.5000
IG11	341.7521	-1878.2359	732.5000
IG12	306.6051	-1852.1933	732.5000
IG13	271.4581	-1826.1507	732.5000
IG14	251.4719	-1811.3417	732.5000
IG15	199.9270	-1773.1489	732.5000
IG16	186.9132	-1763.5062	732.5000
IG17	184.0553	-1761.3886	732.5000
IB2	178.0788	-1756.9602	732.5000
IG18	170.3371	-1752.4074	732.5000
IB3	162.5955	-1747.8590	732.5000
IB4	151.4725	-1742.8232	732.5000
IG19	142.9373	-1740.0056	732.5000
IG20	136.5429	-1737.8947	732.5000
IB5	128.0077	-1735.0771	732.5000
IB6	116.0727	-1732.5012	732.5000
IG21	107.1433	-1731.5486	732.5000
IB7	98.2139	-1730.5959	732.5000
IG22	90.7756	-1730.5958	732.5000
IG23	84.5753	-1730.5958	732.5000
IG24	53.4534	-1730.5956	732.5000
IG25	23.9291	-1730.5955	732.5000
IG26	-17.3335	-1730.5952	732.5000
IG27	-60.7370	-1730.5950	732.5000
IG28	-90.6750	-1730.5948	732.5000
IG29	-145.0596	-1730.5945	732.5000
IG30	-148.7762	-1730.5945	732.5000
IBV1	-159.0362	-1730.5944	732.5000
IG31	-181.0839	-1730.5943	731.0734
IG32	-189.8568	-1730.5942	730.5057
IG33	-195.9009	-1730.5942	730.1144
D4QS	-214.7902	-1730.5941	728.8924
SEPT	-222.6742	-1730.5940	728.3822

15.09.34. UCLP, 00, TS10, 0.115KLNS. ** END OF LISTING **

Fig. 11-3 shows the evolution of the monoenergetic β_y and β_x envelope functions and the beam dispersions η_y and η_x through the transport line from the target to the downstream end of the injection kicker. Figure 11-4 shows beam envelopes through the line.

11.3 Debuncher to Accumulator Transfer (Line D to A)

The beam transfer between the Debuncher and the Accumulator is a horizontal transfer taking place in the 10 straight section. Extraction

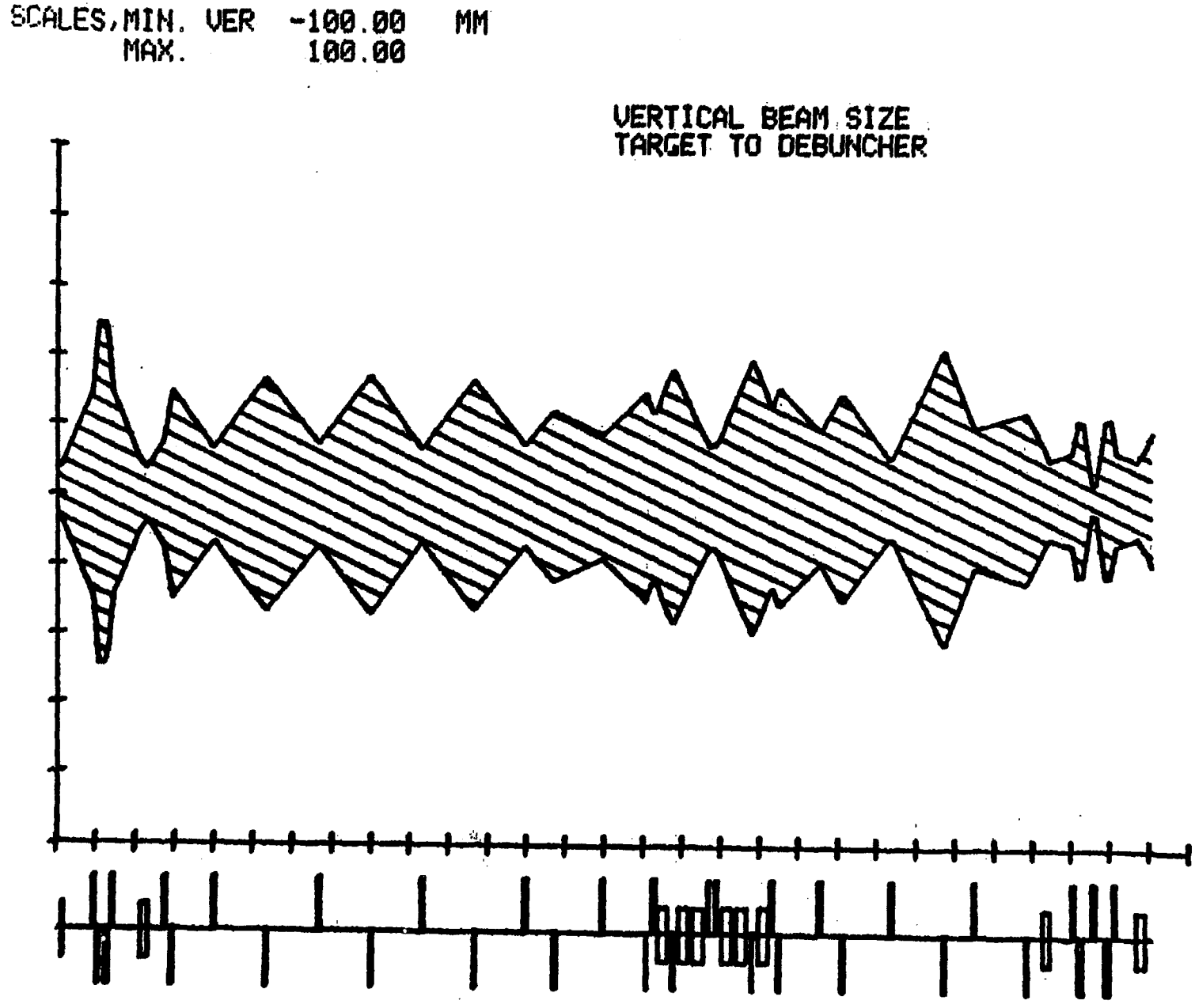
SCALES, MIN. VER -100.00 MM
MAX. 100.00
VERTICAL BEAM SIZE
TARGET TO DEBUNCHER

Figure 11-4b

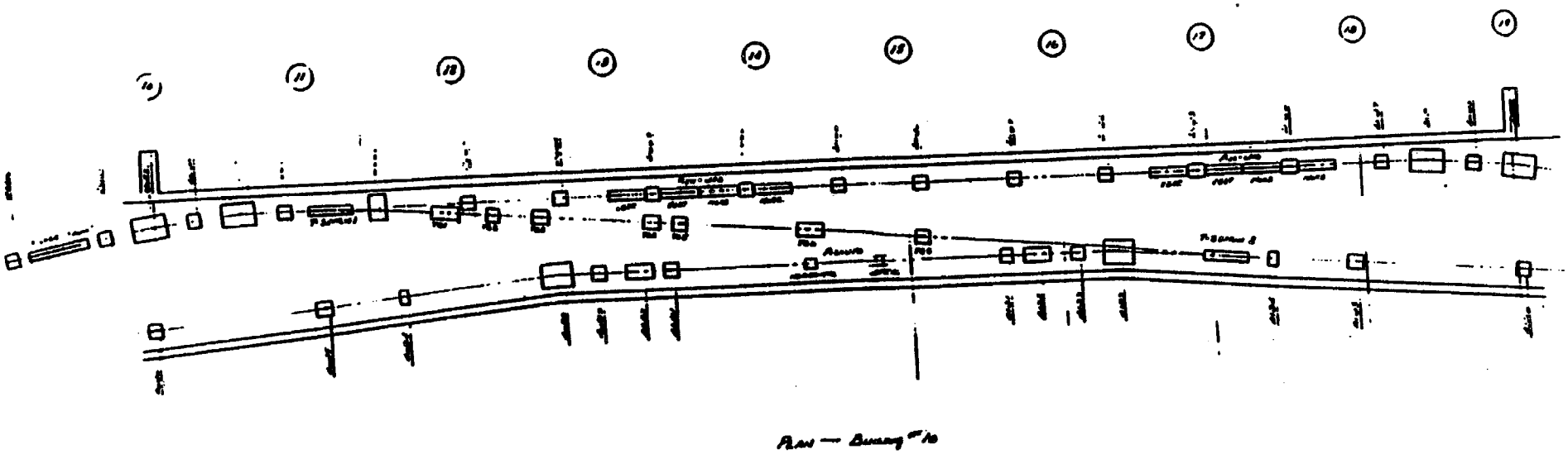

Beam Transfer From Debuncher To Accumulator

Figure 11-5

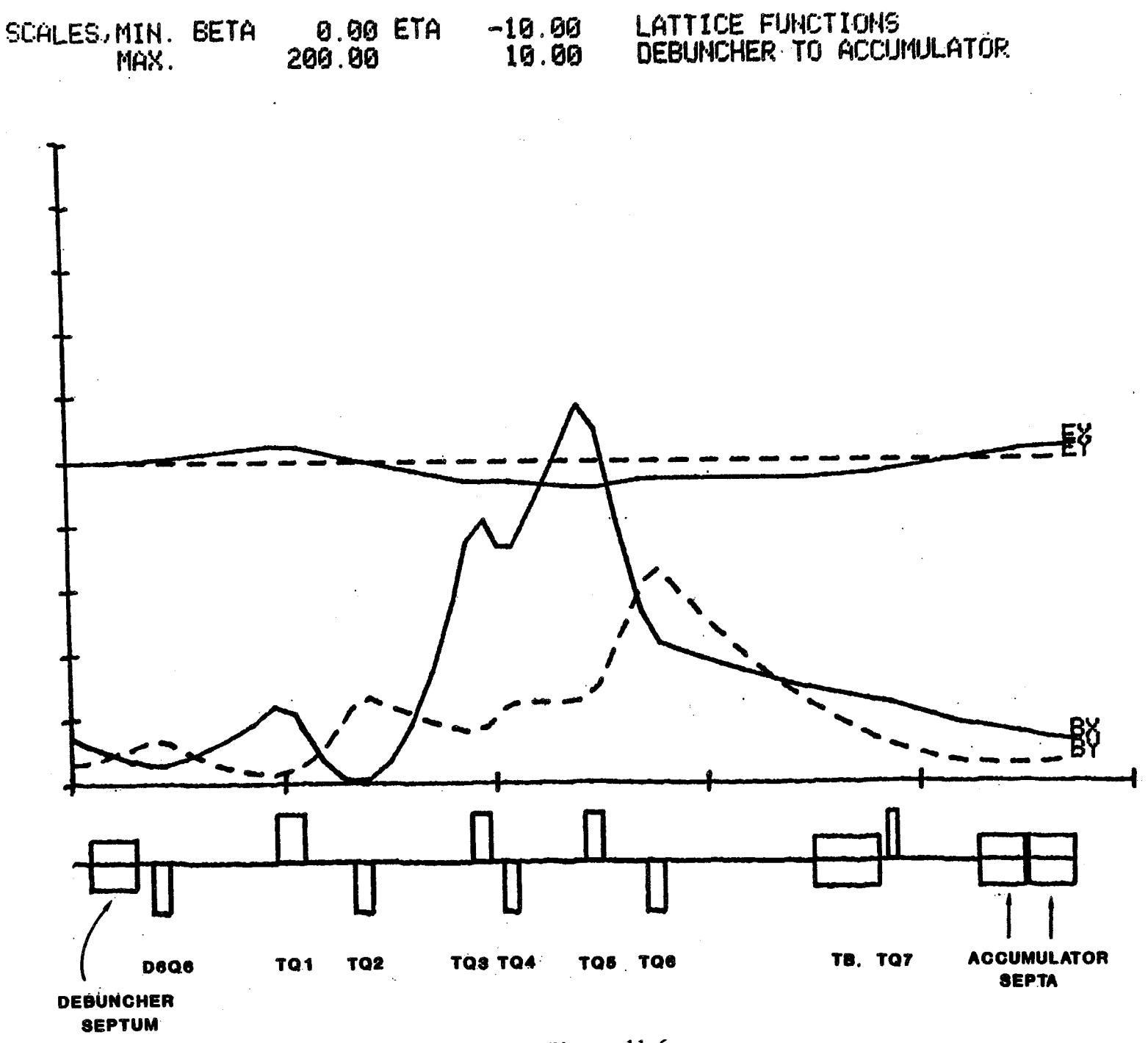
SCALES, MIN. BETA 0.00 ETA -10.00
MAX. 200.00 10.00
LATTICE FUNCTIONS
DEBUNCHER TO ACCUMULATOR
EY
EY
BX
BY
D6Q6
TQ1
TQ2
TQ3 TQ4
TQ5 TQ6
TB. TQ7
ACCUMULATOR SEPTA
DEBUNCHER SEPTUM

Figure 11-6

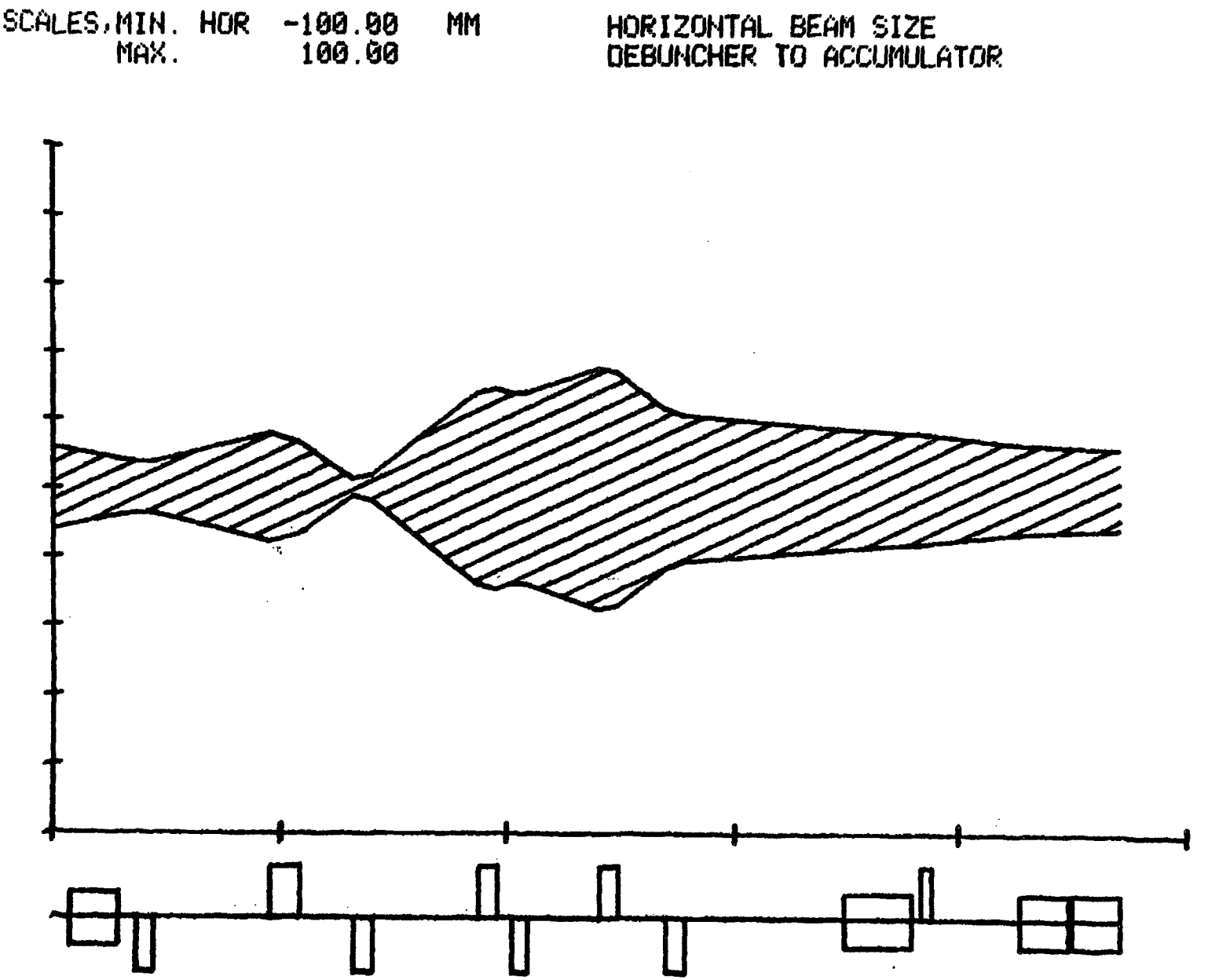
SCALES,MIN. HOR -100.00 MM
MAX. 100.00
HORIZONTAL BEAM SIZE
DEBUNCHER TO ACCUMULATOR

Figure 11-7a

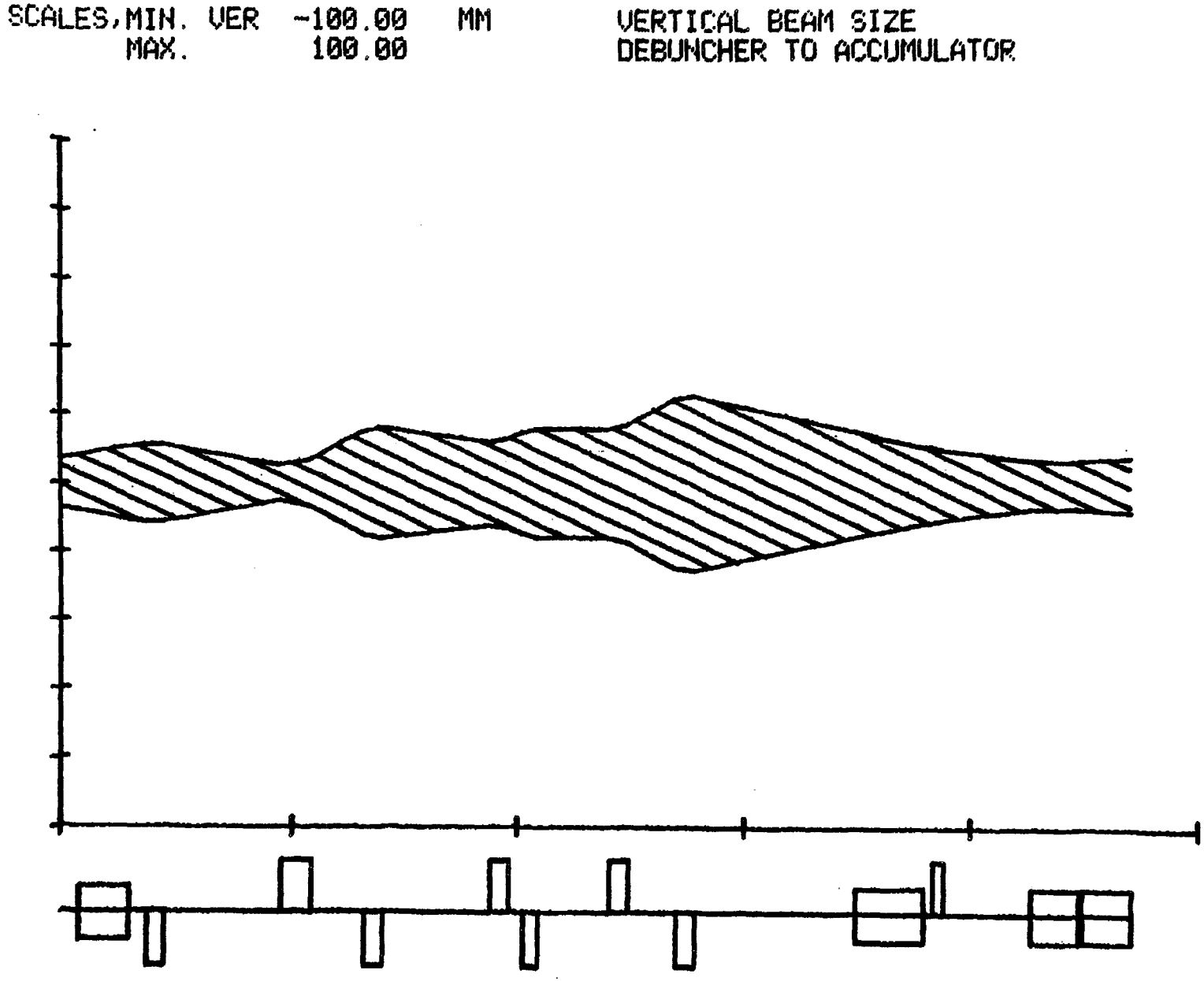
SCALES, MIN. VER -100.00 MM
MAX. 100.00
VERTICAL BEAM SIZE
DEBUNCHER TO ACCUMULATOR

Figure 11-7b

from the Debuncher is accomplished with a kicker and a septum magnet, as shown in Fig. 11-5. The quadrupole after the septum magnet, QD3, has a large aperture to accommodate both the circulating and the extracted beam. This quad kicks the beam further to the inside of the ring toward the Accumulator. The horizontal displacement of the extracted beam from the magnet axis is 5 in. After extraction, the beam is transported to the Accumulator with no further bending through a string of 6 quadrupoles. At the Accumulator, the beam is injected onto a path displaced from the central momentum by $\Delta p/p=+0.775\%$ with a 12-kG 7 ft long pulsed septum placed between A1B3 and A1S3. Finally the beam is kicked onto the proper orbit in the Accumulator with a 500-G, 7 ft long shutter kicker placed in the A20 straight section. A plot of the lattice functions of the transfer line is shown in Fig. 11-6 and the elements are listed in Table 11-IV. Figure 11-7 shows beam envelopes through the line.

TABLE 11-IV BEAM TRANSFER, DEBUNCHER TO ACCUMULATOR

Element	Name	Length (m)	Field
Debuncher kicker		3.0480	459.32 G
Septum	TS1	2.1336	7.03 kG
Drift		0.3099	
Debuncher Quad	D6Q6	0.4140	-96.24 kG/m
Drift		5.1272	
Quad	TQ1	1.3120	70.12 kG/m
Drift		2.1527	
Quad	TQ2	0.8280	-90.68 kG/m
Drift		4.4904	
Quad	TQ3	0.8280	90.68 kG/m
Drift		0.5818	
Quad	TQ4	0.7010	-90.68 kG/m
Drift		5.2097	
Quad	TQ5	1.3120	70.12 kG/m
Drift		3.5860	
Quad	TQ6	0.8280	-90.68 kG/m
Drift		4.8706	
Quad	TQ7	0.7010	94.22 kG/m
Drift		5.8240	
Septum	TS2	2.1336	11.72 kG
Accumulator Kicker		2.1336	515.56 G

11.4 Accumulator to Main Ring Transport (Line AP-3)

Two separate downward bends of 50 mrad each eventually restores the extracted beam to target height (Δz=48.0 in.). Then the beam is taken through four modules consisting of: (i) long transport, (ii) left bend, (iii) long transport, and (iv) target bypass. Following this, the beam rejoins the 120-GeV proton line just downstream of quadrupole PQ7B and is reverse-injected into the Main Ring at F17. The orbit parameters are identical for 120-GeV protons and 8-GeV antiprotons at this point.

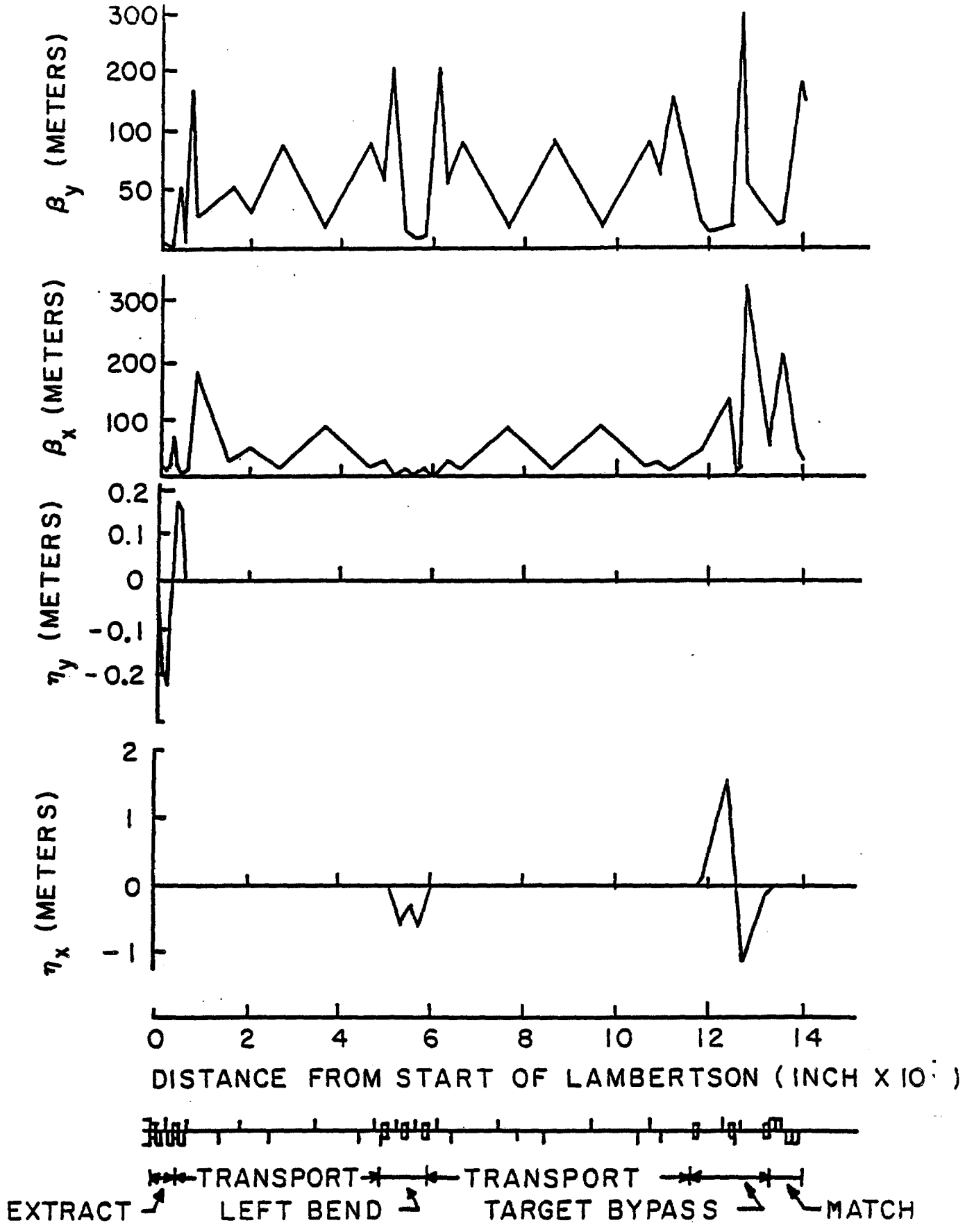

Figure 11-8 Beam functions β_y, β_x and dispersion functions η_y, η_x for the antiproton beam transport from the Accumulator to the 120 GeV proton transport line.

The long transport (iii) parallels the long transport carrying the hot $\bar{p}$ to the Debuncher. The target bypass is an achromatic transport using three dipoles and three quadrupoles. Figure 11-8 shows the behavior of the monoenergetic β_x, β_y, η_x, and η_y functions through the extraction system, starting at the Lambertson and ending at the downstream end of EB6. Figure 11-9 shows beam envelopes through the line.

Table 11-V lists the antiproton transport line elements from the Accumulator to the match point in the proton extraction line (EB6).

TABLE 11-V BEAM TRANSPORT ACCUMULATOR TO TARGET BYPASS

BEND AND QUAD CENTERS FOR AP3 EXTRACTION LINE
IN FEET WITH AO AT (0.,0.)

A LENNOX 7-17-84

CALCULATED FROM D JOHNSON'S TRANSPORT OUTPUT WHICH GIVES COORDINATES DEFINING INCOMING AND OUTGOING RAYS FOR EACH MAGNET. FOR BENDS CALCULATED THE INTERSECTION OF THE RAYS. ALSO PROJECTED TO BENDPOINT FROM BOTH UPSTREAM AND DOWNSTREAM ENDS. BENDPOINTS GIVEN HERE ARE THE AVERAGES OF THE PROJECTIONS WHICH NORMALLY AGREE WITH THE INTERSECTION CALCULATION WITHIN 1 MIL.
FOR QUADS FOUND THE MIDPOINT BETWEEN THE POINTS DELIMITING THE EFFECTIVE LENGTHS.

DEVICE	X(FEET)	Y(FEET)	ELEVATION(FEET)
LAMB	-121.6827	-1344.1093	728.5000
CMAG	-116.7765	-1351.1117	729.1230
EQ1	-109.1432	-1362.0059	730.4588
EBV1	-105.9929	-1366.5021	731.0101
EQ2	-101.8382	-1372.4317	731.3727
EQ3A	-97.3078	-1378.8976	731.7681
EQ3B	-95.1778	-1381.9376	731.9541
EQ4	-92.3343	-1385.9959	732.2022
EBV2	-88.9229	-1390.8647	732.5000
EQ5	-85.2979	-1396.0383	732.5000
EQ6	-82.9022	-1399.4575	732.5000
TRIM	-80.4490	-1402.9586	732.5000
EQ7	-57.9644	-1435.1434	732.5000
EQ8	-33.9041	-1469.5837	732.5000
EQ9	-.4771	-1517.4316	732.5000
EQ10	16.9957	-1542.4423	732.5000
EQ11	54.8459	-1596.6217	732.5000
EQ12	82.2884	-1635.9033	732.5000
EQ13	110.7951	-1676.7082	732.5000
EQ14	122.4967	-1693.4580	732.5000
EB1	126.2317	-1698.8043	732.5000
EQ15	135.2586	-1709.1464	732.5000
EB2	149.5821	-1725.5569	732.5000
EQ16	162.8483	-1737.8019	732.5000
EB3	173.4980	-1747.6318	732.5000
EQ17	178.7384	-1751.5139	732.5000
EQ18	191.0764	-1760.6539	732.5000
EQ19	218.5475	-1781.0044	732.5000

SCALES, MIN. HOR -100.00 MM
MAX. 100.00

HORIZONTAL BEAM SIZE
ACCUMULATOR TO TARGET BYPASS

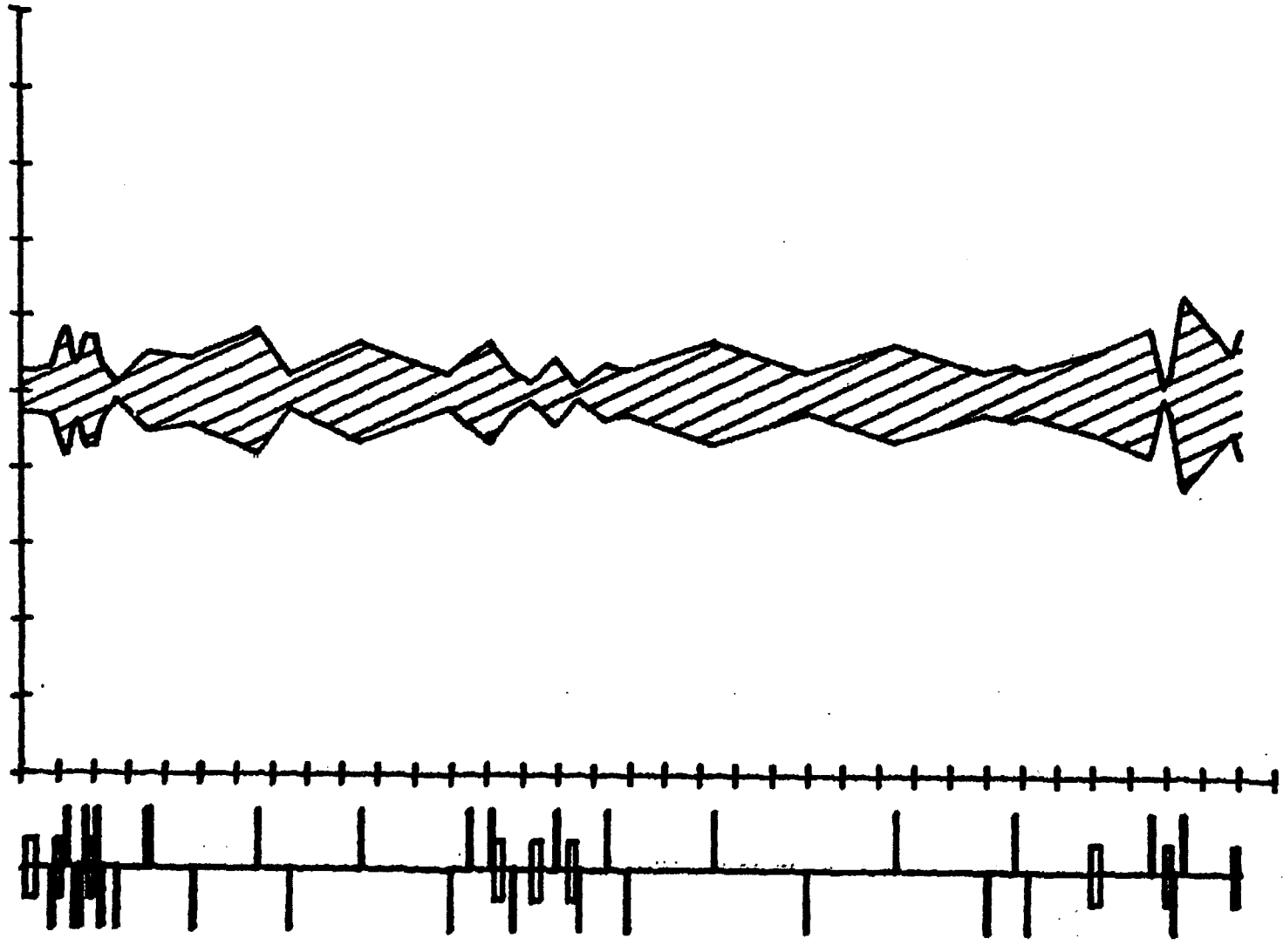

Figure 11-9a

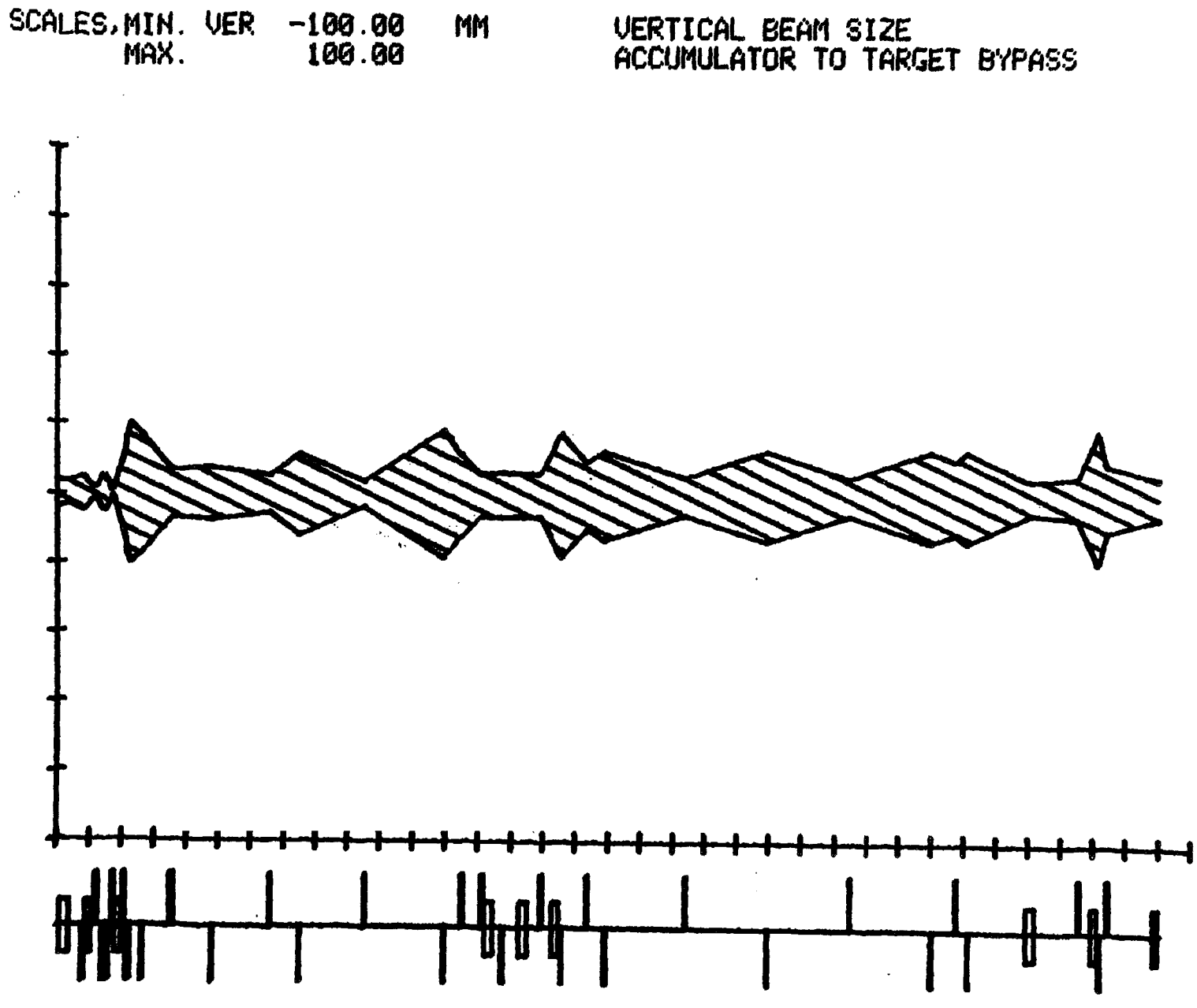
SCALES, MIN. VER -100.00 MM
MAX. 100.00
VERTICAL BEAM SIZE
ACCUMULATOR TO TARGET BYPASS

Figure 11-9b

DEVICE	X(FEET)	Y(FEET)	ELEVATION(FEET)
EQ20	279.6268	-1826.2518	732.5000
EQ21	346.6145	-1875.8761	732.5000
EQ22	413.6021	-1925.5003	732.5000
EQ23	480.5898	-1975.1246	732.5000
EQ24	500.7278	-1990.0427	732.5000
EQ25	510.0000	-1996.9116	732.5000
EB4	560.4502	-2034.2850	732.5000
EQ26	597.1626	-2067.9670	732.5000
EB5	607.9111	-2077.8283	732.5000
EQ27	612.0593	-2082.2827	732.5000
EQ28	617.3697	-2087.9850	732.5000
EB6	650.1344	-2123.1679	732.5000
PQ7B	657.4153	-2129.8478	732.5000
PQ7A	665.5208	-2137.2843	732.5000
PQ6B	679.0300	-2149.6784	732.5000
PQ6A	687.1355	-2157.1149	732.5000

15.09.55. UCLP, QQ, TB10, 0.113KLNS. ** END OF LISTING **

11.5 Booster Test Beam Line (Line AP-4)

This section describes the beam line connecting the Booster to the Debuncher Ring. The 8-GeV kinetic energy beam is extracted vertically from the Booster with a kicker and a pulsed septum at Booster long straight 3. At 1.5 ft above the Booster beam height, the extracted beam is bent down by 10 mrad to level, taken out of the Booster enclosure and focused down to a 6 mm spot on a Be target. With a set of vertical dipoles, the targeting angle is varied from 10 mrad to 50 mrad down. The target is followed by a dump and collimator set at a level that collects secondary 8-GeV protons. The variable targeting angle allows the intensity of the secondary to vary from 10^7 to 10^{11} per Booster batch. The beam is bent up and transported to the Debuncher at the same elevation as the other beam lines. Finally, the beam is bent down and injected vertically into the Debuncher with a Lambertson magnet at station D23 in a manner similar to the antiproton injection line.

Lattice functions for this line are shown in Figs. 11-9 and 11-10 and the line is described in Table 11-VI.

TABLE 11-VI XYZ COORDINATES OF BOOSTER TO DEBUNCHER LINE

(Coordinates given at end of element (toward Debuncher) Main Ring Station A0 at X=0.0, Y=0.0)

NAME	LENGTH (IN)	FIELD (KG-KG/M)	X (FT)	Y (FT)	Z (FT)
BOOSTER LONG STRAIGHT 3			-488.791	-689.897	726.500
B-SEPTUM	84.00	7.28	-485.293	-695.956	726.683
BQ1	32.60	-142.28	-474.283	-715.026	727.836

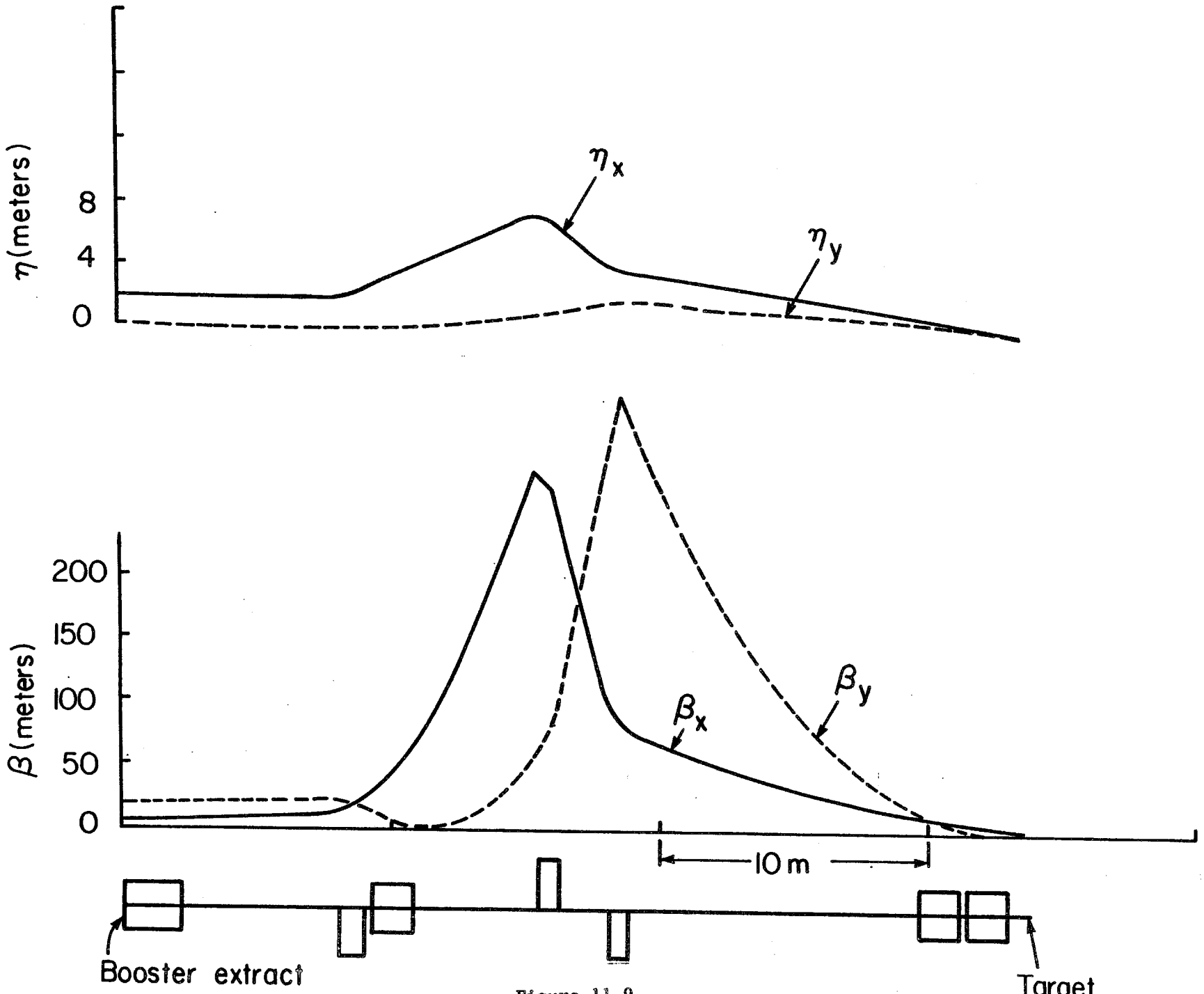
η(meters)
8
4
0
η_x
η_y
β(meters)
200
150
100
50
0
β_x
β_y
10 m
Booster extract
Target

Figure 11-9

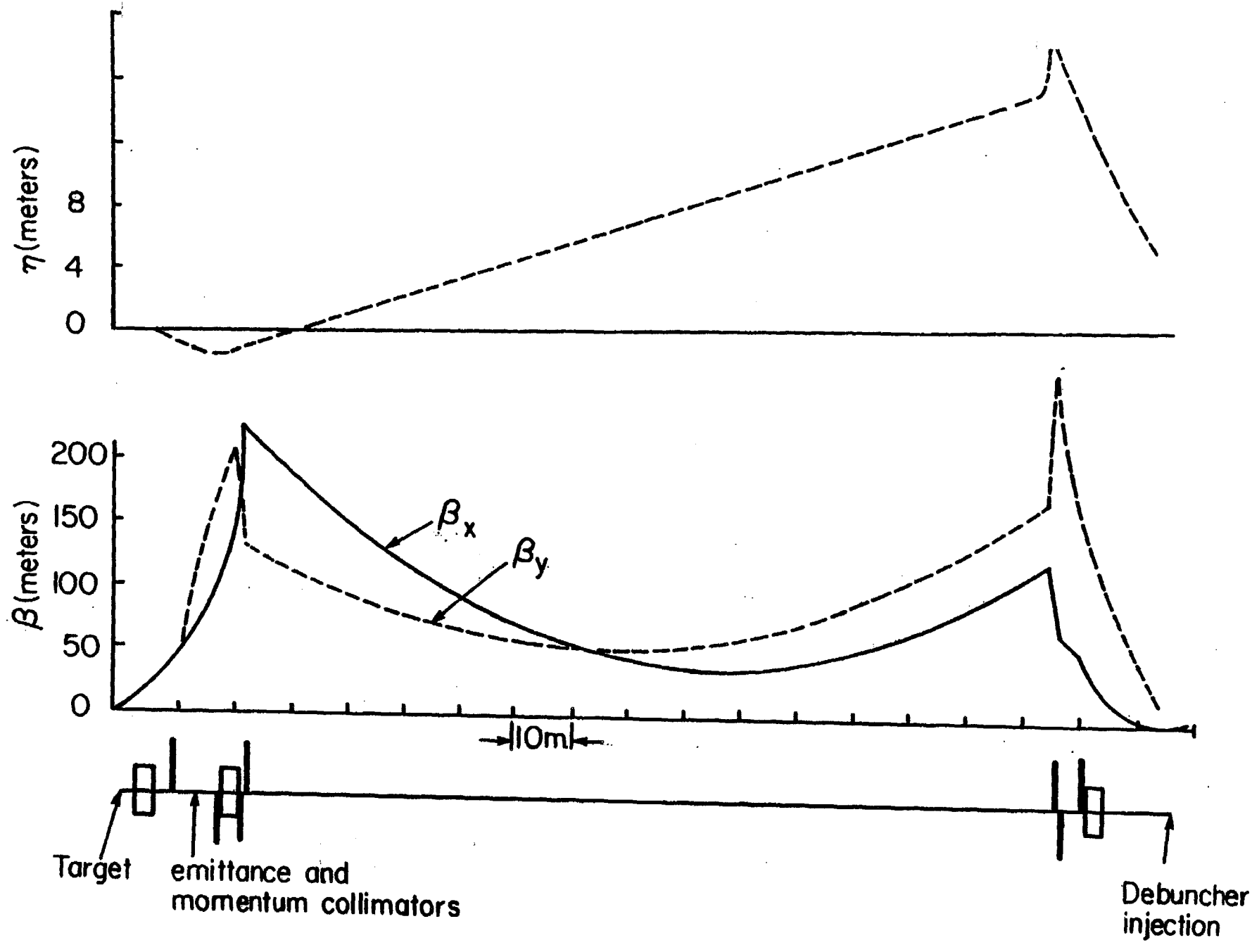
η(meters)
8
4
0
β(meters)
200
150
100
50
0
β_x
β_y
10m
Target
emittance and
momentum collimators
Debuncher
injection

Figure 11-10

BB1	60.00	-12.14	-471.284	-720.220	728.000
BQ2	25.20	142.28	-462.365	-735.669	727.818
BQ3	25.20	-142.28	-458.148	-742.972	727.734
BB2	60.00	10.00	-437.700	-778.389	727.326
BB3	60.00	-10.00	-434.784	-783.440	727.267
TARGET			-433.534	-785.605	727.242
COLLIMATOR					
BEND UP .573 DEG; BEND LEFT .363 DEG.					
DUMP					
BB4	120.00	10.49	-411.872	-822.582	727.781
BQ4	18.00	25.84	-405.669	-833.169	729.110
BQ5	18.00	-20.53	-392.859	-855.035	731.854
BB5	120.00	-10.49	-387.312	-864.504	732.500
BQ6	18.00	-152.02	-386.048	-866.661	732.500
BQ7	18.00	154.12	-384.279	-869.681	732.500
BEAM PIPE					
BQ8	27.60	118.61	-146.351	-1275.813	732.500
BQ9	27.60	-129.92	-144.683	-1278.660	732.500
BQ10	18.00	24.91	-139.302	-1287.844	732.500
BB6	120.00	-6.31	-133.075	-1298.473	732.176
MID D2Q5		90.60	-107.183	-1342.670	728.847
DEBUNCHER RING					728.500

11.6 Beam-Line Vacuum Systems

The vacuum in the 5 beam lines is required to be comparable in quality to that of the Debuncher (1×10^{-8}). It is planned to use SEM grid profile monitors in the beam lines. There are 3 lines that connect directly with the Accumulator ring: AP-4, D to A, and AP-3. The first two lines have thin windows to isolate their vacuum system from the Accumulator vacuum system. The AP-3 line uses differential pumping to isolate the Accumulator vacuum from the almost 1000 times worse vacuum in the Main Ring.

CHAPTER 12

MAGNETS

12.1 Magnets

The main magnet systems of the Debuncher and Accumulator rings and all five beam lines will with few exceptions utilize four magnet cross-section types, a small and a large dipole and a small and large quadrupole. These magnets will each come in a number of different lengths, but will retain the advantages of common laminations and coil designs. In addition, many of the correction elements in the ring and beam lines will be of the same design. Table 12-I shows the magnet types and lengths to be used and their disposition around the project.

The parameters of the major dipole and quadrupole types are given in Tables 12-II and 12-III.

In these designs, higher multipole content has been minimized by empirical chamfering of the poles of the end packs. These end packs are made of standard laminations glued to make a rigid assembly.

These magnets are rich in copper in order to lower the excitation and therefore to decrease operating cost.

Figures 12-1 through 12-4 show the four types of magnet cross sections.

Measured field data are now available on a number of the magnet types listed in Tables 12-I, 12-II, and 12-III. One result of the measurements is that the excitation currents for the magnets have changed. The magnet currents expected at this time are as follows:

I. Debuncher

SDD: 1,176A

SQC: design tunes 277A, top tunes 290A

SQD: " 232A, " 244A

LQE: " 1500A, " close to 1700A

II. Accumulator

SDA, SDB, SDC, LDA: not measured

SQA: design tunes	234A, top tunes	241A
SQB:	250	260
SQC:	250	260
SQD:	234	240

TABLE 12-I TEVATRON I MAGNETS

Magnet	Length (in.)	Debuncher	Accum	AP1	AP2	DA	AP3	AP4	Refer
Small Quadrupole									
SQA	18		18		5	1	16	5	1
SQB	25.2		6		6		3	2	1
SQC	27.6	102	18		14	1	5	2	2
SQD	32.6	9	6		5	4	5	1	1
SQE	51.6		6		3	1	1		1
Large Quadrupole									
LQA	17.2		6						1
LQB	25.3		6						1
LQC	30.4		12						1
LQD	32.6	3							1
LQE	34.4		6						1
Large Dipole									
LDA	180		12						1
Small Dipole									
SDA	180		6						1
SDB	120		6						1
SDC	60		4						1
SDD	65.2	66			1		2		1
SDE	98.4				6		4		1
Modifed Main Ring Bl's									
MWGB1	60		2		1		2	1	1
MWGB2	120					1			1
Existing Dipoles									
EPB	120			10				3	
AVB	60							2	1
Existing Quadrupoles									
3Q120A	120			14					15
Lambertsons									
Lamb	204			2					1
Lamb	115						1		
Septum Magnets									
Sept	84					4		1	1
Booster Septum								1	
Correction Elements									
RSex	8	138	12						1
SSex	12		12						1
BL Trim Dipole		28	30	3	7	3	7	5	1

TABLE 12-II DIPOLE MAGNET PARAMETERS

MAGNET DATA LATEST REVISION 8/10/83

INPUT PARAMETERS AND COMPUTED FIELDS

DIPOLES * INPUT DATA

MAGNET TYPE		SDA	SDB	SDC	SDD	SDE	SDP	LDA	LDP
GAP *	IN	2.375	2.375	2.375	2.375	2.375	2.375	2.375	2.375
GOOD FIELD WIDTH *	IN	4	4	4	4	4	4	10	10
ARC LENGTH *	IN	180	120	60	65.3702	98.4252	48	180	48
RADIUS OF CURVATURE *	IN	687.549	687.549	687.549	687.549	926.083	687.549	687.549	687.549
BEND ANGLE	RAD	.2617995	.1745330	.0872665	.0950772	.1062812	.0698132	.2617995	.0698132
FE LENGTH	IN	176.9364	117.2977	57.43096	62.79558	95.82888	45.44025	176.9364	45.44025
FE SAGITTA	IN	5.715439	2.505982	.5999127	.7172840	1.240349	.3754970	5.715439	.3754970
FE WIDTH *	IN	45.25	45.25	45.25	45.25	45.25	45.25	57	57
FE HEIGHT *	IN	29	29	29	29	29	29	35	35
COIL PROTRUSION *	IN	11	11	11	11	11	11	11	11
PANCAKE TURNS *		56	56	56	56	56	56	56	56
SADDLE TURNS *		16	16	16	16	16	16	16	16
PANCAKE H2O PATHS *		4	4	4	4	4	4	4	4
SADDLE H2O PATHS *		1	1	1	1	1	1	1	1
WATER FLOW	GAL/MIN	6.517570	7.728468	10.04321	9.746194	8.364456	10.82087	6.428168	10.41549
FIELD	KG	16.98848	16.98848	16.98848	16.98848	12.41268	16.98848	17.01224	17.01224
CURRENT *	AMP	1178.61	1178.61	1178.61	1178.61	875.03	1178.61	1179.44	1179.44
AMPFAC *		1.04	1.04	1.04	1.04	1.04	1.04	1.04	1.04
MAGNET RESISTANCE	OHM	.0197479	.0141110	.0084727	.0089774	.0120845	.0073449	.0202802	.0078773
VOLTAGE	VOLT	23.27503	16.63136	9.986047	10.58091	10.57431	8.656817	23.91932	9.290813
POWER	WATT	27432.18	19601.88	11769.68	12470.76	9252.836	10203.01	28211.40	10957.96
H2O TEMP RISE	DEG C	15.99404	9.638024	4.453234	4.862299	4.203594	3.583025	16.67712	3.997914
STORED ENERGY	JOULE	113569.1	75833.05	37952.65	41347.08	34311.22	30365.59	163040.8	43593.12
INDUCTANCE	HENRY	.1635121	.1091813	.0546427	.0595298	.0896232	.0437191	.2344092	.0626753
L/R TIME	SEC	8.279991	7.737322	6.449224	6.631042	7.416368	5.952279	11.55851	7.956432
CAPACITANCE *	MF								
TOTAL MAGNET WT	LB	58372.03	39286.32	20150.44	21864.57	32418.56	16319.44	90766.62	16843.74

MAGNET DATA LATEST REVISION 8/10/83

INPUT PARAMETERS AND COMPUTED FIELDS

DIPOLES * INPUT DATA

MAGNET TYPE		SDA	SDB	SDC	SDD	SDE	SDP	LDA	LDP
LENGTH EXTENSION *	IN	2.55	2.55	2.55	2.55	2.55	2.55	2.55	2.55
THICKNESS LAMS **	IN	.0598	.0598	.0598	.0598	.0598	.0598	.0598	.0598
NUMBER LAMS		5918	3923	1921	2100	3205	1520	5918	1520
CHAMFER *	IN	2.5	2.5	2.5	2.5	2.5	2.5	2.5	2.5
REDUCED ANGLE	RAD	.2507277	.1635126	.0762763	.0840851	.0981179	.0588265	.2507277	.0588265
PANCAKE END *	IN	30.1	30.1	30.1	30.1	30.1	30.1	36.31	36.31
SADDLE END *	IN	64.25	64.25	64.25	64.25	64.25	64.25	68	68
TOTAL PANCAKE LENGTH	IN	22678.61	15962.57	9244.892	9846.212	13548.12	7901.161	23374.13	8596.681
TOTAL SADDLE LENGTH	IN	7572.403	5653.534	3734.198	3906.004	4963.690	3330.275	7692.403	3470.275
TOTAL CU LENGTH	IN	30251.01	21616.10	12979.09	13752.22	18511.81	11251.44	31066.53	12066.96
WT/IN CU *	LB/IN	.36632	.36632	.36632	.36632	.36632	.36632	.36632	.36632
TOTAL CU WT.	LB	11081.55	7918.411	4754.500	5037.712	6781.245	4121.626	11380.29	4420.367
WATER HOLE DIAM *	IN	.375	.375	.375	.375	.375	.375	.375	.375
H2O PRESSURE **	PSI	70	70	70	70	70	70	70	70
TURB FLOW PARM **	ENGLISH	19600	19600	19600	19600	19600	19600	19600	19600
LAM FLOW PARM **	ENGLISH	31900	31900	31900	31900	31900	31900	31900	31900
TURB PANCAKE FLOW	GAL/MIN	5.358423	6.386934	8.392557	8.132248	6.932753	9.078200	5.278098	8.703217
LAM PANCAKE FLOW	GAL/MIN	31.15425	44.26199	76.42438	71.75705	52.15006	89.42168	30.22723	82.18696
TURB SADDLE FLOW	GAL/MIN	1.159147	1.341314	1.450656	1.413946	1.431703	1.742669	1.150070	1.712274
LAM SADDLE FLOW	GAL/MIN	5.831497	7.810768	11.82542	11.30528	8.896294	13.18055	5.740527	12.72477
LAMINATION AREA *	SQ IN	447.51	447.51	447.51	447.51	447.51	447.51	759.44	447.51
IRON DENSITY **	LB/CU IN	.284	.284	.284	.284	.284	.284	.284	.284
LAM WT.	LB	7.600152	7.600152	7.600152	7.600152	7.600152	7.600152	12.89772	7.600152
TOTAL LAM WT.	LB	44974.70	29815.41	14598.13	15961.74	24338.33	11550.26	76323.62	11550.26
STRUCTURE AREA *	SQ IN	44	44	44	44	44	44	57.75	57.75
UNIT STRUCT VOL *	CU IN	279	279	279	279	279	279	448	448
STRUCTURE WT.	LB	2315.785	1552.497	797.8151	865.1251	1278.986	647.5254	3062.703	873.1118
RESIST/LENGTH *	OHM/IN	6.528E-7	6.528E-7	6.528E-7	6.528E-7	6.528E-7	6.528E-7	6.528E-7	6.528E-7
INDUCT/LENGTH *	HENRY/IN	.000911	.000911	.000911	.000911	.000911	.000911	.001306	.001306
H2O SP HT * GAL/MIN	WATT OC	.0038	.0038	.0038	.0038	.0038	.0038	.0038	.0038
TRANSFER CONST *	KG/IN AMP	.014414	.014414	.014414	.014414	.014414	.014414	.014424	.014424

TABLE 12-III QUADRUPOLE MAGNET PARAMETERS

MAGNET DATA LATEST REVISION 8/10/83

INPUT PARAMETERS AND COMPUTED FIELDS

QUADS * INPUT DATA

MAGNET TYPE		SQA	SQB	SQC	SQD	SQE	SQP	LQA	LQB	LQC	LQE	LQ
POLE TIP DIAMETER*	IN	3.5	3.5	3.5	3.5	3.5	3.5	6.625	6.625	6.625	6.625	6.625
GOOD FIELD WIDTH *	IN	5	5	5	5	5	5	10	10	10	10	
EFFECTIVE LENGTH *	IN	18	25.2	27.6	32.6	51.64	49.42	17.284	25.3	30.4	34.4	32.
FE LENGTH	IN	16.58	23.78	26.18	31.18	50.22	48	14.604	22.62	27.72	31.72	
COIL PROTRUSION *	IN	4	4	4	4	4	4	6	6	6	6	6
FE WIDTH *	IN	30.5	30.5	30.5	30.5	30.5	30.5	54.75	54.75	54.75	54.75	54.75
FE HEIGHT *	IN	29	29	29	29	29	29	51.75	51.75	51.75	51.75	51.75
NUMBER TURNS *		132	132	132	132	132	132	40	84	84	84	
NUMBER H2O PATHS *		4	4	4	4	4	4	1	2	2	2	
WATER FLOW	GAL/MIN	1.512802	1.373134	1.334519	1.263527	1.070031	1.088122	1.763305	3.147041	2.994803	2.889726	2.9335
GRADIENT *	KG/IN	2.499471	2.499471	2.499471	2.499471	2.499471	2.499471	2.250133	2.250133	2.250133	2.250133	2.250133
CURRENT *	AMP	234.45	234.45	234.45	234.45	234.45	234.45	1206.7	1206.7	1206.7	1206.7	1206.7
AMPFAC *		1	1	1	1	1	1	1.015	1.015	1.015	1.015	1.0
MAGNET RESISTANCE	OHM	.0323385	.0392517	.0413561	.0463569	.0646385	.0625069	.0029507	.0074107	.0081833	.0087892	.00852
VOLTAGE	VOLT	7.581752	9.202554	9.742821	10.86838	15.15450	14.65475	3.560550	8.942462	9.874730	10.60592	10.291
POWER	WATT	1777.542	2157.539	2284.204	2548.091	3552.972	3435.806	4296.516	10790.87	11915.84	12798.16	12418.76
H2O TEMP RISE	DEG C	4.464997	5.970757	6.504200	7.663267	12.61767	11.99871	9.259194	13.02980	15.11958	16.82963	16.08683
STORED ENERGY	JOULE	1182.336	1655.270	1812.915	2141.342	3391.990	3246.169	12583.83	18419.98	22133.10	25045.35	23793.08
INDUCTANCE	HENRY	.04302	.060228	.065964	.077914	.1234196	.1181138	.017284	.0253	.0304	.0344	.032
L/R TIME	SEC	1.330305	1.534406	1.587349	1.680742	1.909382	1.889611	5.857690	3.413994	3.714904	3.913897	3.8317
CAPACITANCE *	MF											
TOTAL MAGNET WT	LB	2927.012	4069.174	4449.895	5243.063	8263.446	7911.280	7703.009	12766.49	15380.70	17431.06	16549.40

MAGNET DATA LATEST REVISION 8/10/83

INPUT PARAMETERS AND COMPUTED FIELDS

QUADS * INPUT DATA

MAGNET TYPE		SQA	SQB	SQC	SQD	SQE	SQP	LQA	LQB	LQC	LQE	LQ
LENGTH EXTENSION *	IN	1.42	1.42	1.42	1.42	1.42	1.42	2.68	2.68	2.68	2.68	2.68
THICKNESS LAMS **	IN	.0598	.0598	.0598	.0598	.0598	.0598	.0598	.0598	.0598	.0598	.0598
NUMBER LAMS		595	795	876	1043	1680	1605	488	757	927	1061	100
END LENGTH *	IN	17.1	17.1	17.1	17.1	17.1	17.1	26.3	26.3	26.3	26.3	26.
TOTAL CU LENGTH	IN	8891.52	10792.32	11425.92	12745.92	17772.48	17186.4	3272.32	8218.56	9075.36	9747.36	9458.
WT/IN CU *	LB/IN	.06576	.06576	.06576	.06576	.06576	.06576	.26519	.26519	.26519	.26519	.2651
WATER HOLE DIAM *	IN	.1875	.1875	.1875	.1875	.1875	.1875	.375	.375	.375	.375	.375
H2O PRESSURE **	PSI	70	70	70	70	70	70	70	70	70	70	70
TURB FLOW PARM **	ENGLISH	19600	19600	19600	19600	19600	19600	19600	19600	19600	19600	1960
LAM FLOW PARM **	ENGLISH	31900	31900	31900	31900	31900	31900	31900	31900	31900	31900	3190
TURB WATER FLOW	GAL/MIN	1.512802	1.373134	1.334519	1.263527	1.070031	1.088122	1.763305	3.147041	2.994803	2.889726	2.93353
LAM WATER FLOW	GAL/MIN	4.966355	4.091655	3.864761	3.464516	2.484653	2.569383	13.49454	21.49206	19.46301	18.12119	18.67481
LAMINATION AREA *	SQ IN	239.72	239.72	239.72	239.72	239.72	239.72	801.01	801.01	801.01	801.01	801.01
IRON DENSITY **	LB/CU IN	.284	.284	.284	.284	.284	.284	.284	.284	.284	.284	.284
LAM WT.	LB	4.071213	4.071213	4.071213	4.071213	4.071213	4.071213	13.60371	13.60371	13.60371	13.60371	13.6037
TOTAL LAM WT.	LB	2257.549	3237.908	3564.694	4245.499	6838.003	6535.726	6644.436	10291.50	12611.87	14431.77	13649.2
STRUCTURE AREA *	SQ IN	18	18	18	18	18	18	46	46	46	46	4
UNIT STRUCT VOL *	CU IN	0										
STRUCTURE WT.	LB	84.75696	121.5634	133.8322	159.3922	256.7246	245.376	190.7867	295.5077	362.1341	414.3901	391.92
TOTAL CU WT.	LB	584.7064	709.7030	751.3685	838.1717	1168.718	1130.178	867.7865	2179.480	2406.695	2584.902	2508.27
RESIST/LENGTH *	OHM/IN	3.637E-6	3.637E-6	3.637E-6	3.637E-6	3.637E-6	3.637E-6	9.017E-7	9.017E-7	9.017E-7	9.017E-7	9.017E-7
INDUCT/LENGTH *	HENRY/IN	.00239	.00239	.00239	.00239	.00239	.00239	.001	.001	.001	.001	.001
H2O SP HT * GAL/MIN	WATT OC	.0038	.0038	.0038	.0038	.0038	.0038	.0038	.0038	.0038	.0038	.0038
TRANSFER CONST *	KG/IN AMP	.010661	.010661	.010661	.010661	.010661	.010661	.0018647	.0018647	.0018647	.0018647	.0018647

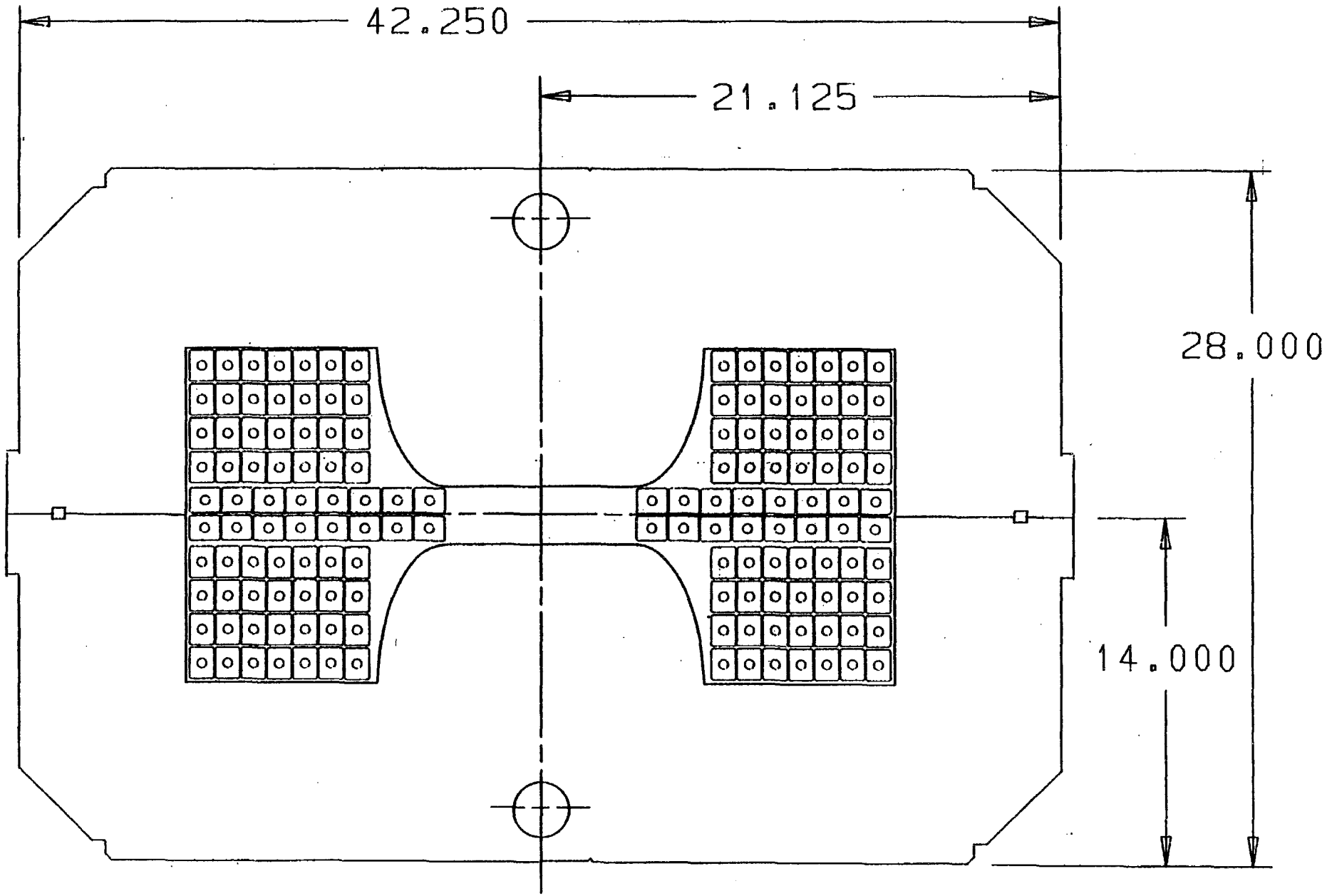

SMALL DIPOLE

units are in inches

Figure 12-1

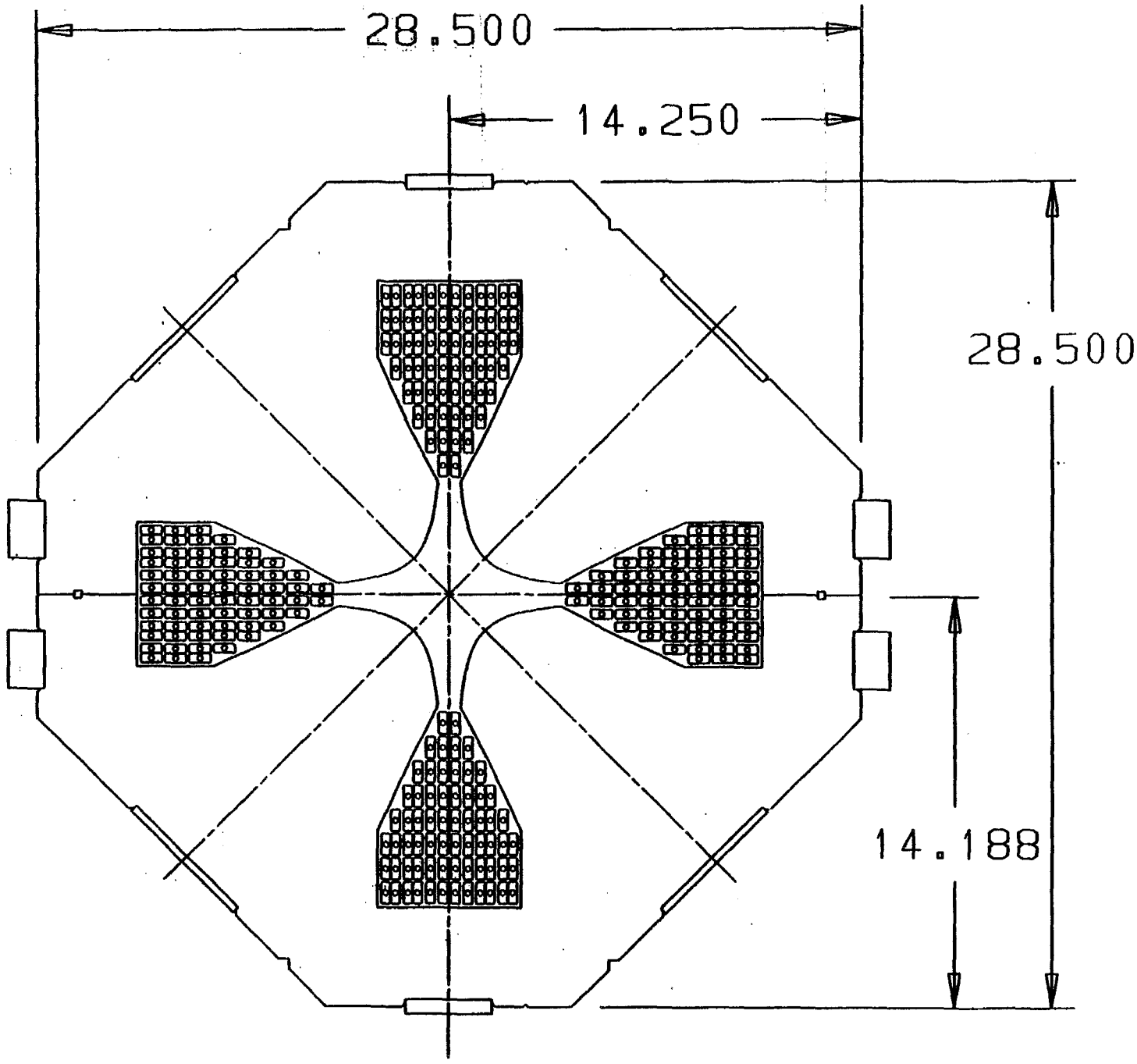

Figure 12-2 SMALL APERTURE QUAD (SQ) units are in inches

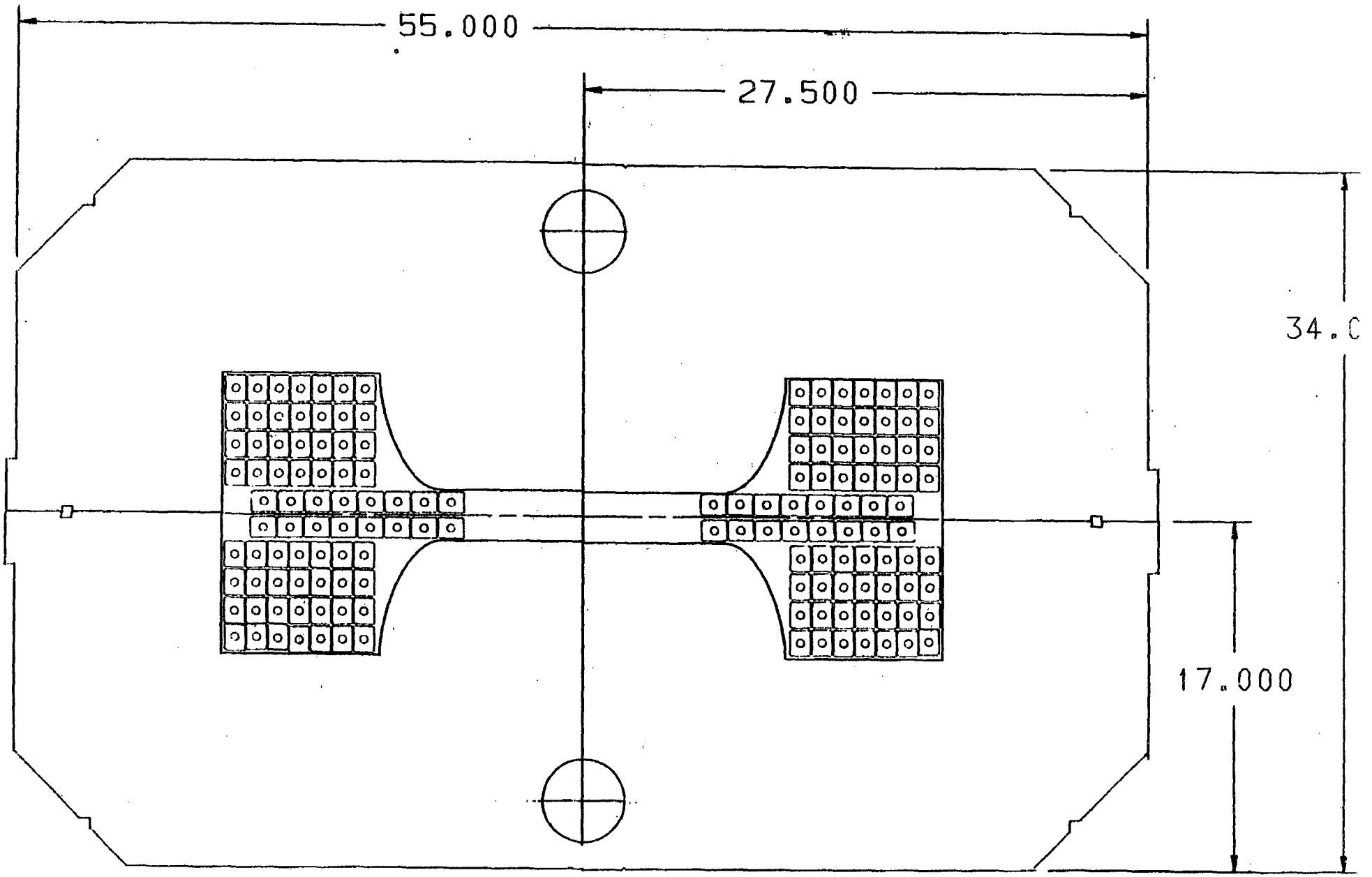

Figure 12-3

units are in inches

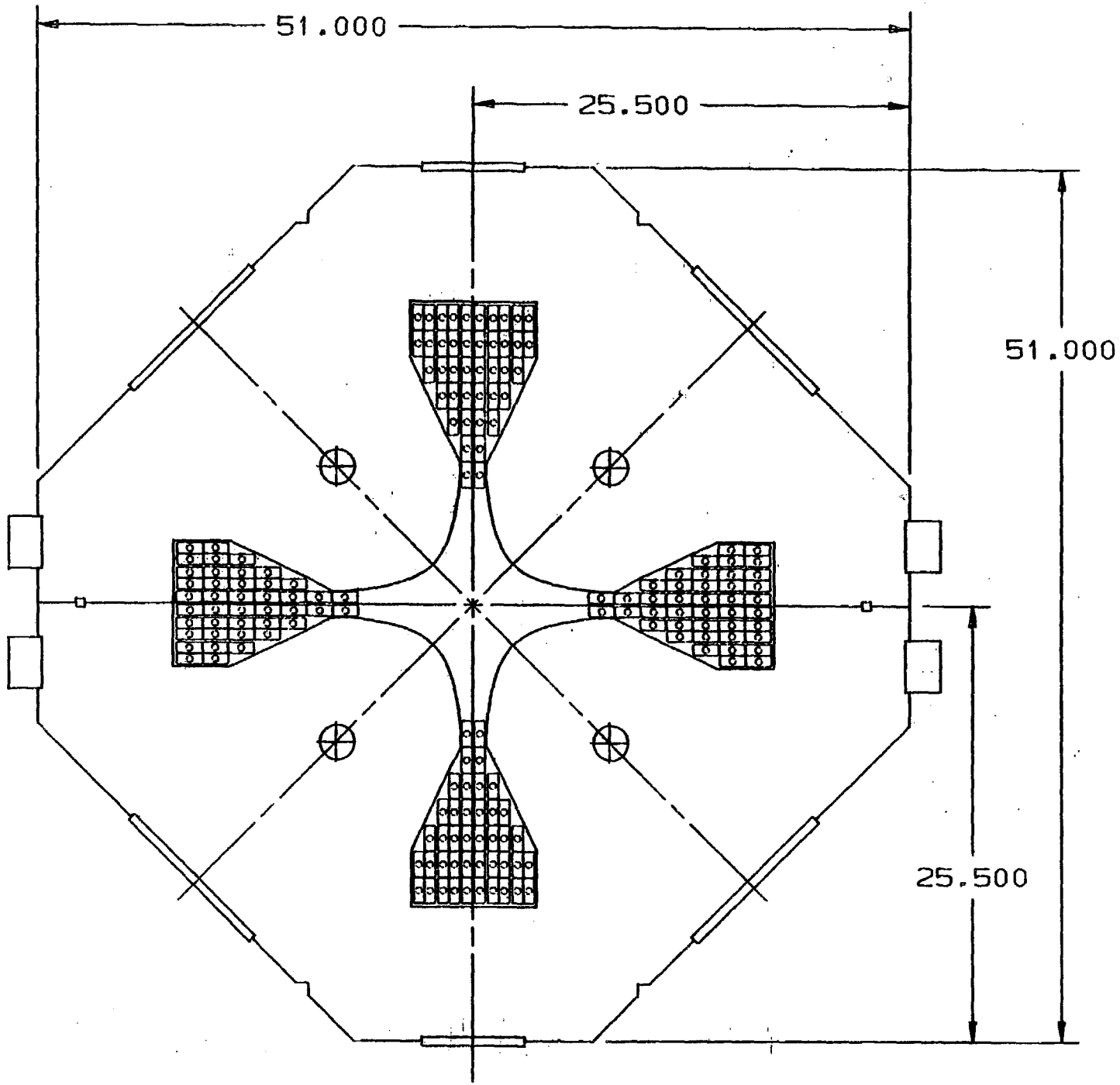

Figure 12-4 LARGE QUAD (LQ) units are in inches

SQE: 250 260

LQA: not measured

LQB: design tunes 1325A, top tunes 1345A
LQC: 1305A, 1330A
LQD: 1305A, 1330A

In addition, extensive measurements of field quality have been made. These are depicted in Figs. 12-5 through 12-10. Figures 12-5 and 12-6 show the change of field shape (all well within the acceptance area) with current (for the small quadrupole SQC). The remaining graphs show measured field shapes for the small dipole SD and several lengths of large quadrupole.

12.2 Magnet Power Supplies

12.2.1 Debuncher. The Debuncher ring has 111 small quadrupoles, 3 larger quadrupoles, and 66 small dipoles. The small dipoles and large quadrupoles are in series and fed by one ring bus using a 1200-A power supply. Three 300-A supplies run the SQ elements (QF, QD, and QSS buses). The total tunnel equipment consists of the 180 major magnetic elements, 33 shunts, and 186 correction magnets, dipoles and sextupoles. These elements are operated from 57 power supplies and 33 shunt controllers placed in the service buildings. The table below shows the relationship of tunnel and service building equipment.

TABLE 12-IV DEBUNCHER POWER SUPPLIES

Magnetic Element	Type	Power Supply (A)
B	66 SD	1200
D2Q5, D4Q5, D6Q6	3 LQ	
QF	42 SQ-27.6	300
D1Q5, D3Q5, D5Q5, D6Q5	4 SQ-32.6	
QD	39 SQ-27.6	300
DnQ6, (n=1,5)	5 SQ-32.6	
DnQ0, (n=1,3,5)	21 SQ-27.6	300
DnQ2, Q3, Q4, (n=1,6)		
D2Q5, D4Q5, D6Q6	3 LQ-32.6	3-50 (shunt)
D2Q5, D4Q5, D6Q6	3 LQ-32.6	3-200 (trim)
D1Q5, D3Q5, D5Q5, D6Q5	9 SQ-32.6	30-40 (shunt)
DnQ6, (n=1,5)		
DnQ0, (n=1,3,5)	21 SQ-27.6	

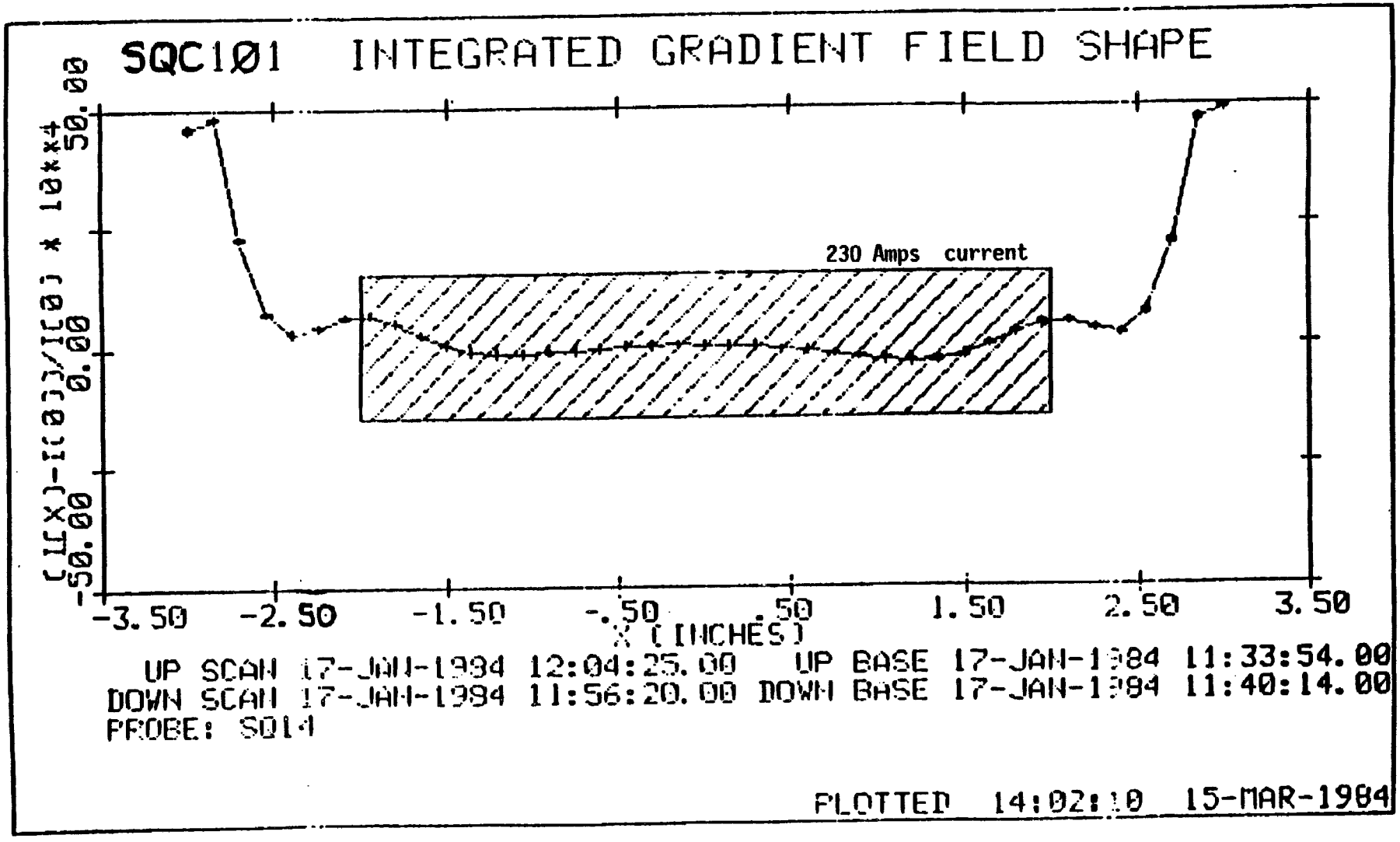
SQC101 INTEGRATED GRADIENT FIELD SHAPE
50.00
0.00
-50.00
(I(X)-I(0))/I(0) * 10**4
230 Amps current
-3.50
-2.50
-1.50
-.50
.50
1.50
2.50
3.50
X (INCHES)
UP SCAN 17-JAN-1984 12:04:25.00 UP BASE 17-JAN-1984 11:33:54.00
DOWN SCAN 17-JAN-1984 11:56:20.00 DOWN BASE 17-JAN-1984 11:40:14.00
PROBE: SQ14
PLOTTED 14:02:10 15-MAR-1984

Figure 12-5

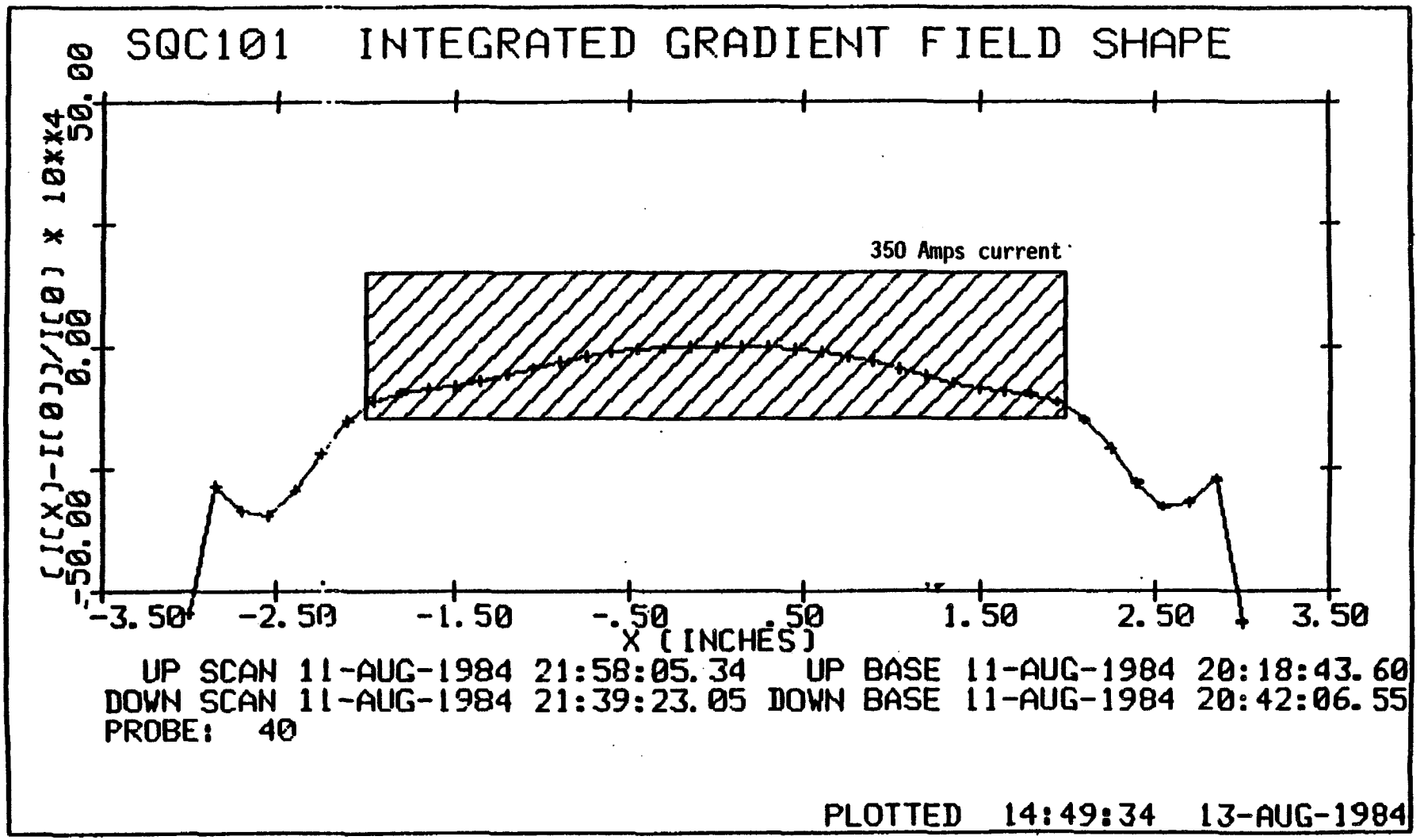
SQC101 INTEGRATED GRADIENT FIELD SHAPE
[I(X)-I(0)]/I(0) * 10xx4
50.00
0.00
-50.00
350 Amps current
-3.50
-2.50
-1.50
-.50
.50
1.50
2.50
3.50
X (INCHES)
UP SCAN 11-AUG-1984 21:58:05.34 UP BASE 11-AUG-1984 20:18:43.60
DOWN SCAN 11-AUG-1984 21:39:23.05 DOWN BASE 11-AUG-1984 20:42:06.55
PROBE: 40
PLOTTED 14:49:34 13-AUG-1984

Figure 12-6

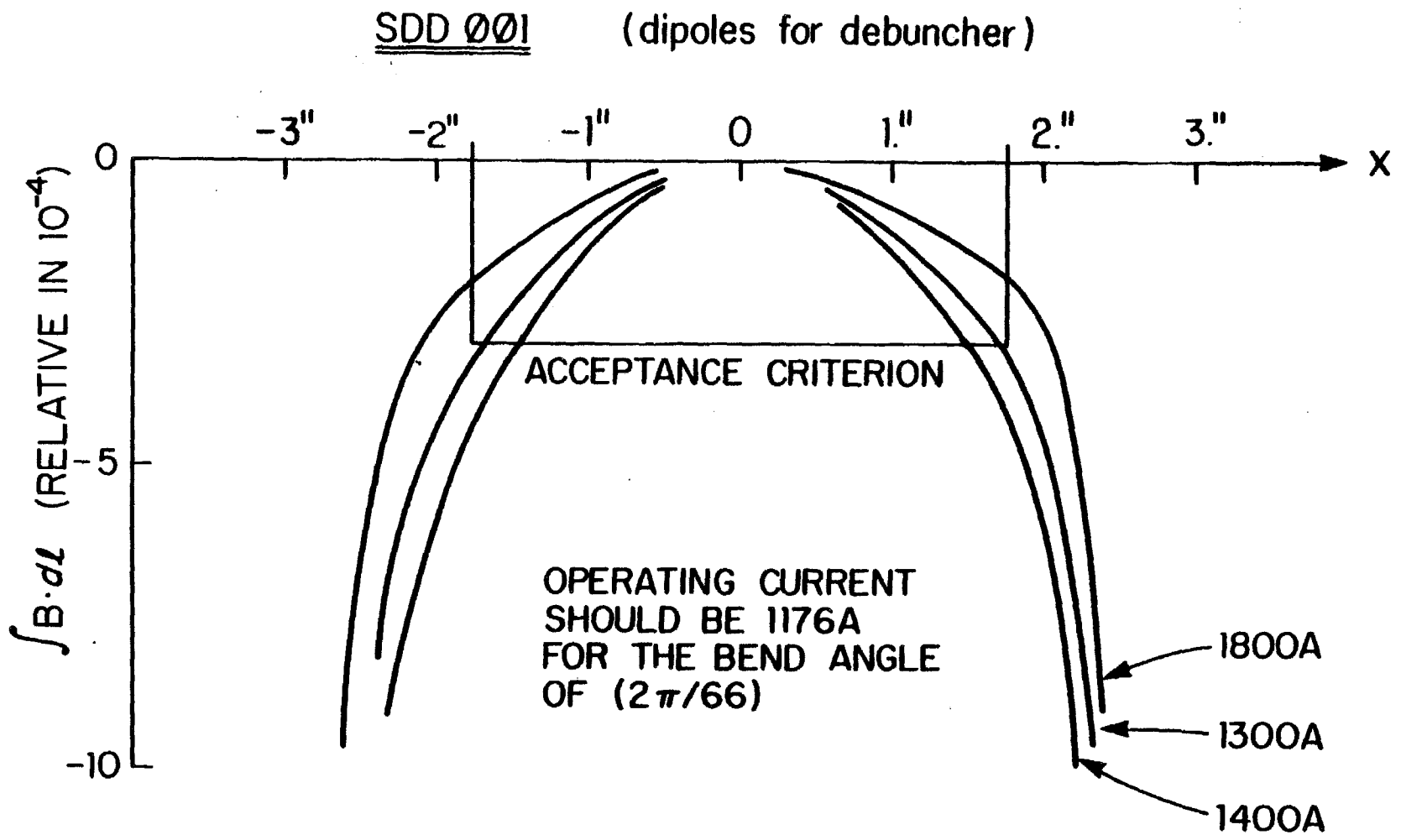
SDD ØØ1
(dipoles for debuncher)
-3"
-2"
-1"
0
1."
2."
3."
X
0
-5
-10
$\int B \cdot dl$ (RELATIVE IN 10^{-4})
ACCEPTANCE CRITERION
OPERATING CURRENT
SHOULD BE 1176A
FOR THE BEND ANGLE
OF $(2\pi/66)$
1800A
1300A
1400A

Figure 12-7

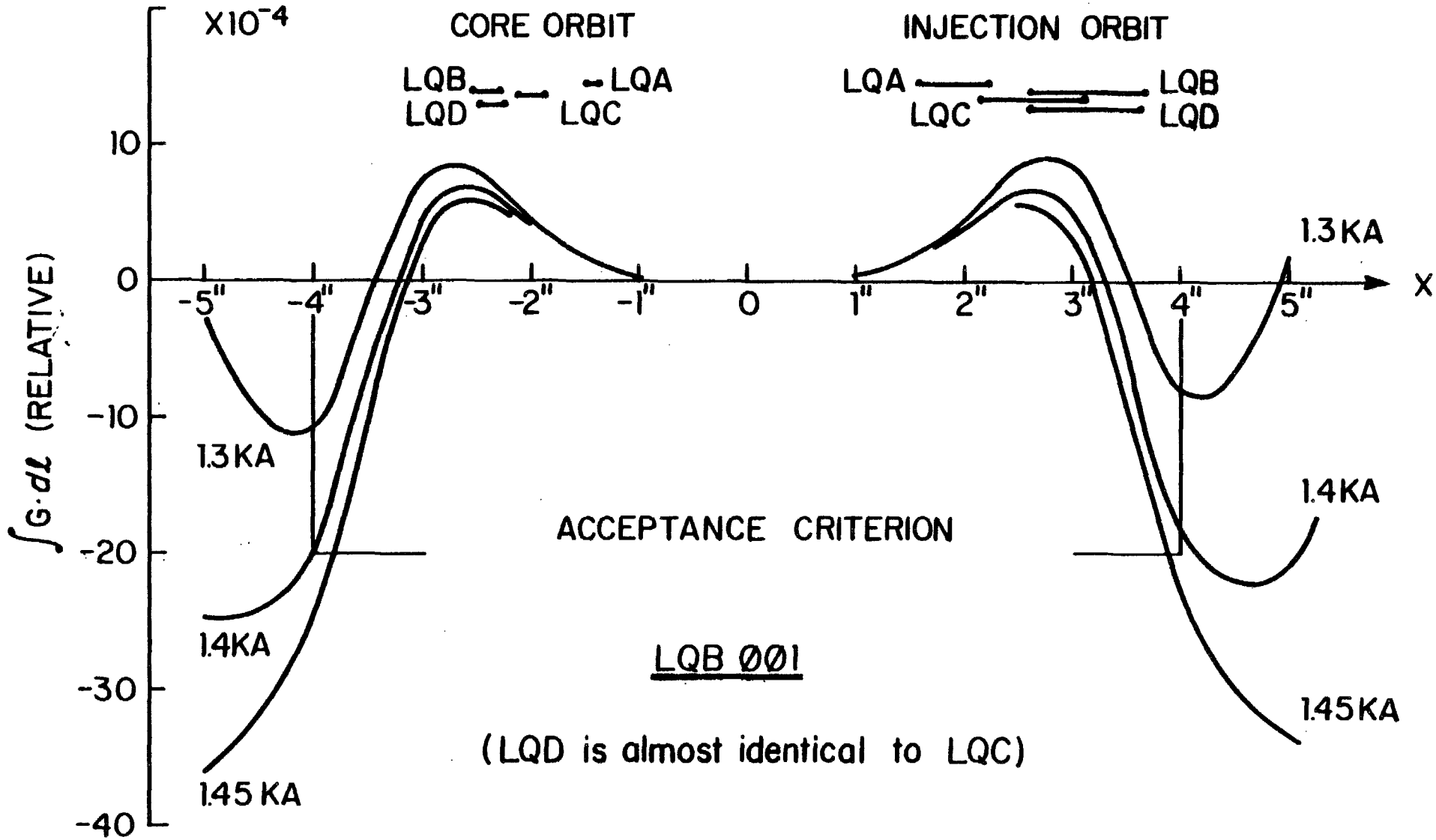
X10⁻⁴
CORE ORBIT
INJECTION ORBIT
LQB
LQD
LQA
LQC
LQA
LQC
LQB
LQD
10
0
-10
-20
-30
-40
∫G·dℓ (RELATIVE)
-5"
-4"
-3"
-2"
-1"
0
1"
2"
3"
4"
5"
X
1.3KA
1.3KA
1.4KA
1.4KA
1.45KA
1.45 KA
ACCEPTANCE CRITERION
LQB 001
(LQD is almost identical to LQC)

Figure 12-8

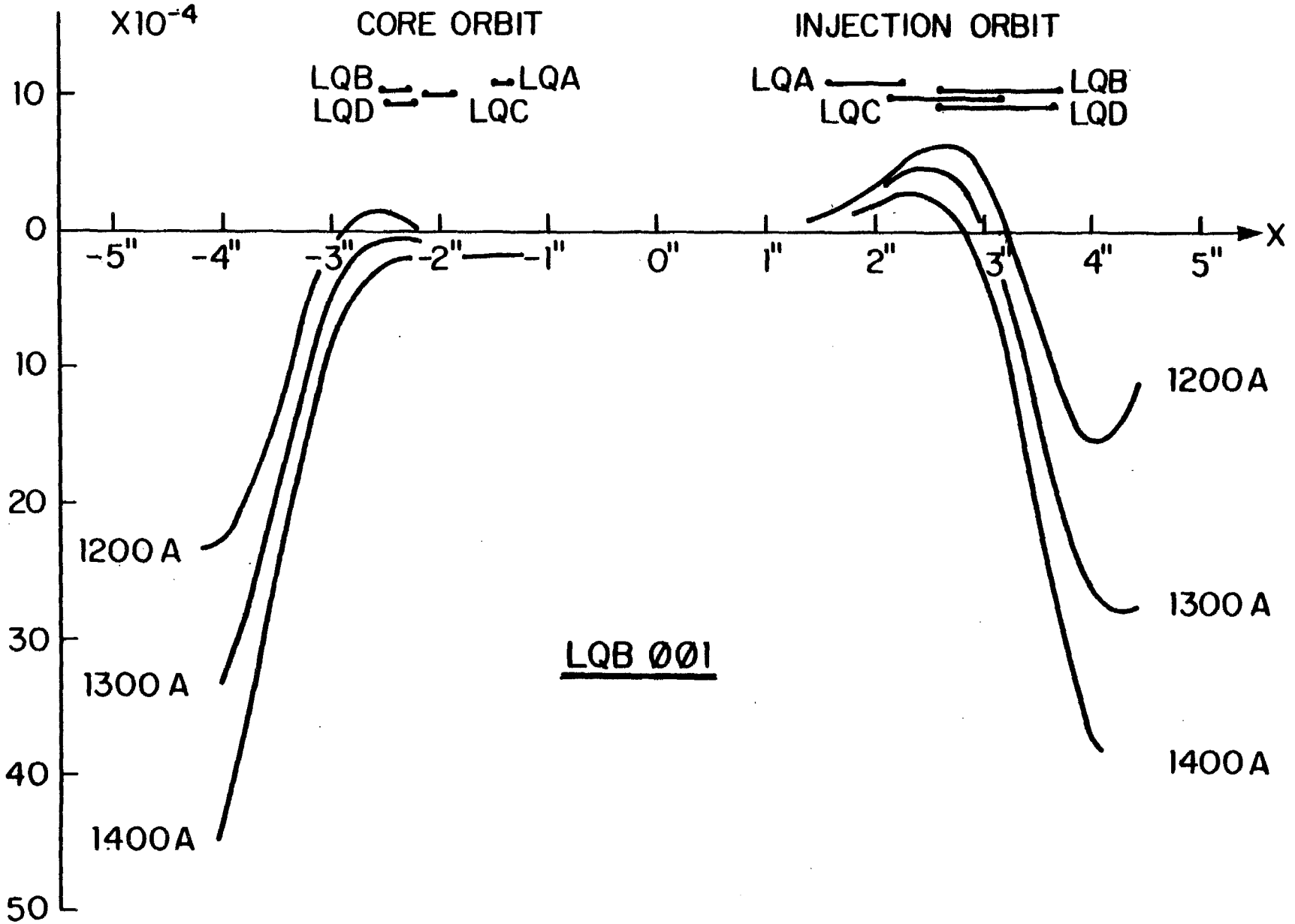
X10⁻⁴
CORE ORBIT
INJECTION ORBIT
LQB
LQD
LQA
LQC
LQA
LQC
LQB
LQD
10
0
10
20
30
40
50
-5"
-4"
-3"
-2"
-1"
0"
1"
2"
3"
4"
5"
X
1200 A
1300 A
1400 A
1200 A
1300 A
1400 A
LQB 001

Figure 12-9

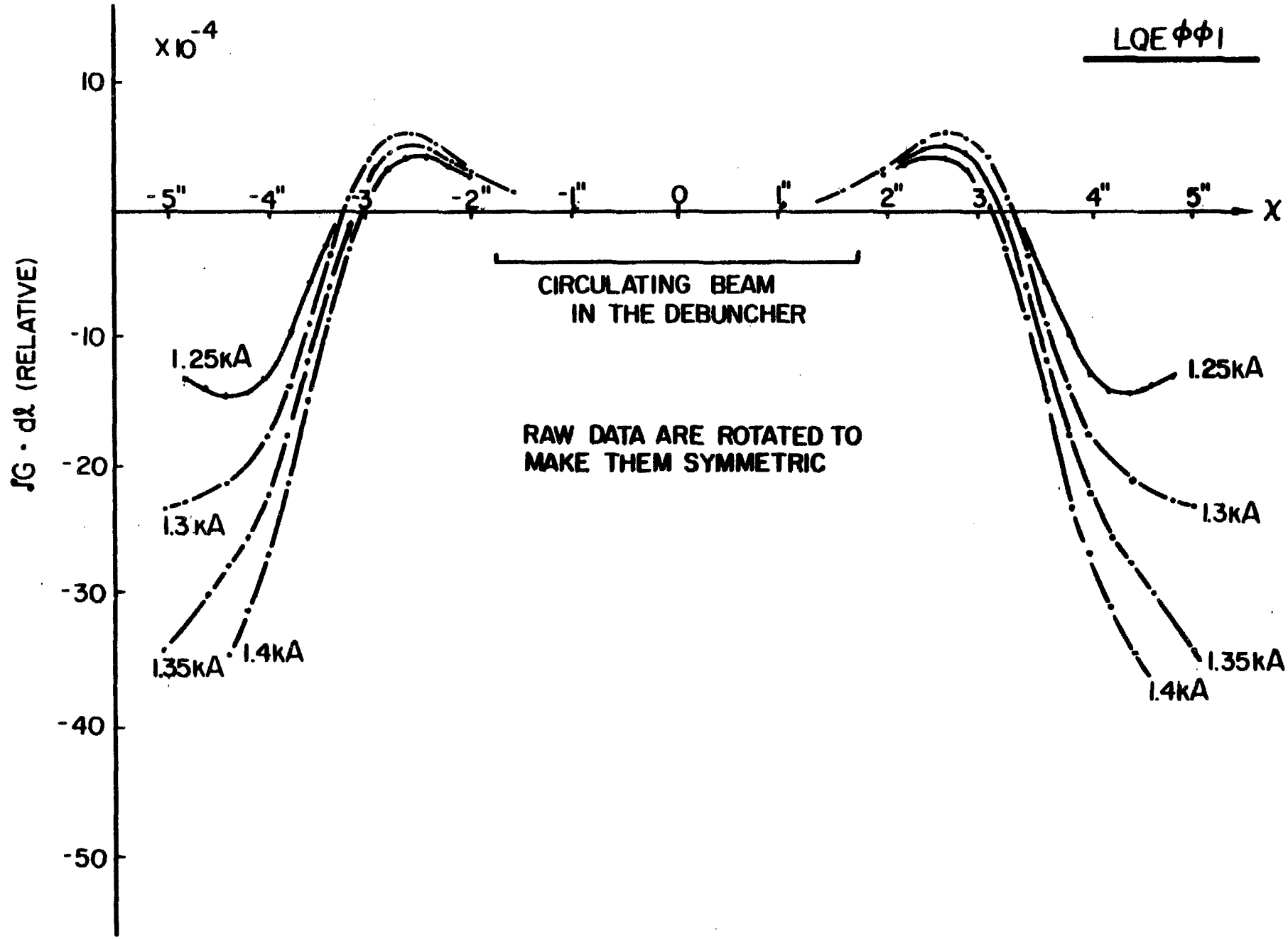
X10^-4
LQEΦΦ1
10
-10
-20
-30
-40
-50
-5"
-4"
-3
-2"
-1"
0
1"
2"
3
4"
5"
X
∫G · dℓ (RELATIVE)
CIRCULATING BEAM
IN THE DEBUNCHER
RAW DATA ARE ROTATED TO
MAKE THEM SYMMETRIC
1.25kA
1.3kA
1.35kA
1.4kA
1.25kA
1.3kA
1.35kA
1.4kA

Figure 12-10

DnQ2, Q3, Q4, (n=1,6)

Hor Corr Dipoles	24	24-10 (bipolar)
Ver Corr Dipoles	24	24-10 (bipolar)
SF Sextupoles	72 - S	200
SD Sextupoles	66 - S	200

12.2.2 Accumulator. The Accumulator has 54 small quadrupoles, 30 large quadrupoles, 12 large dipoles, and 18 small dipoles. There are two 1200-A supplies, one feeding all the dipoles, and the other feeding the LQ. There are two 300-A supplies feeding the SQ. Each of the 30 dipoles in the Accumulator has a shunt. These supply horizontal corrections.

In addition, there are 24 standard vertical-correction magnets. Besides the dipole shunts there are shunts on the quadrupoles. In the Accumulator there are also 4 kinds of sextupoles. There are 2 families of "regular" sextupoles, 6 of each and two systems of combination sextupole-octupole correction magnets. In the tunnel are 114 major magnetic elements, 114 shunts, and 48 correction elements. These connect to 34 power supplies and 114 shunt controllers. The table below summarizes these requirements.

TABLE 12-V ACCUMULATOR POWER SUPPLIES

Magnetic Element	Type	Power Supply
B	2 MOD-B1-60 4 SD-60 6 SD-120 6 SD-180 12 LD	1200
Q10 F Q14 F Q12, Q13 D Q11 F	6 LQ-18 6 LQ-25.3 12 LQ-30.4 6 LQ-34.4	1200
QF: Q1 Q3, 6 Q4, 8	6 SQ-25.2 12 SQ-27.6 12 SQ-18	300
QD: Q2 Q5 Q7 Q9	6 SQ-51.64 6 SQ-32.6 6 SQ-27.6 6 SQ-18	300
B (Hor corr)	18 SD 12 LD	30-10 (shunt)

Q10 - Q14	30 LQ	30-60 (shunt)
Q1 - Q9	54 SQ	54-25 (shunt)
Vert Corr Dipoles	24	24-10 (bipolar)
S7 - Sextupoles	6	200
S9 - Sextupoles	6	200
S-O-10 Sext-Oct	6	200 Sext winding 200 Oct winding
S-O-12 Sext-Oct	6	200 Sext winding 200 Oct winding

12.2.3 Beam Lines. Next we consider the five beam lines in the Tevatron I project. AP-1 has 26 major elements powered by 13 power supplies.

In addition there are 3 correction magnets. AP-1 contains the only ramped supplies in the project. These power the Lambertsons, the 45 degree horizontal bend, and the bend in a plane rotated 45 degrees relative to horizontal. In addition to three standard correction trim magnets, there are 13 additional AP-1 supplies that power the main elements during reverse injection.

During operation of AP-1, there are three systems in the Main Ring that have to be controlled and their effect on the beam monitored: (1) C48 kicker, (2) four-magnet orbit bump at F17 consisting of standard 35-in. long bump magnets at F15, F17, F18, and F22. Two ramped power supplies are used for this bump. The F17 Lambertson is included in the list below.

TABLE 12-VI AP-1, 120-GEV MR TO TARGET

Magnetic Element	Type Power Supply
PLAM1, PLAM2	2 LAM-204 500 KW Blue Tr
PB1,2 2 EPB-120 PBR1, 2 2 EPB-120	500 KW Blue Tr
PQ1,2 2 3Q120A PBR3, PB3-5	2 200 4 EPB-120 500 KW Blue Tr
PQ3,4 2 3Q120A PQnA,B (n=5,9) PBV1,2 2 EPB-120	2 500 10 3Q120A 5 500 1200
F17 Kicker	
PLAM1, PLAM2 rev	2 LAM-204 100

PB1,2 rev	2 EPB-120 100
PBR1, 2 rev	2 EPB-120
PQ1,2 rev	2 3Q120A 2 30
PB3, PB3-5 rev	4 EPB-120 100
PQ3,4 rev	2 3Q120A 2 30
PQnA,B (n=5,9) rev	10 3Q120A 5 30
PBV1,2 rev	2 EPB-120 100
3 Trim Dipoles	3 New Trim 3 100 (Bipolar)

AP-2 transports antiprotons from the target to the Debuncher. The first two elements in this line are the Li-lens and the C-magnet. The transport consists of 33 standard Tevatron I quadrupoles, IQ1 - IQ33, and 8 bending magnets, IB1 - IB7, and IBV1. The first 7 bending magnets in the line are standard Tevatron I SD's. The vertical bend, IBV1 is a rotated 5 ft modified B1.

Tentatively, 7 correction elements have been placed in this line. Finally, there are 12 shunts.

From an operational point of view the I-line also includes D4Q5. The lithium lens is discussed in Section 3.2.2.

TABLE 12-VII AP-2, 8-GEV TARGET TO DEBUNCHER

Magnetic Element	Type Power Supply (A)
Li-Lens	
C - Magnet	
IQ1, 4-6 5 SQ-27.6	500
IQ2, 3 2 SQ-27.6	500
IB1 SD-65.37	1200
IQ7 - 14 7 SQ-27.6	200
IQ15 SQ-18	
IQ16, 23 2 SQ-25.2	500
IQ17, 22 2 SQ-32.6	
IQ18 -21 4 SQ-25.2	200
IQ24, 26 - 28	4 SQ-18
IQ25 SQ-32.6	
IB 2 - 7 6 SD-98.4	1200
IQ 29 - 30	2 SQ-32.6 500
IQ 31 - 33	3 SQ-51.64 500
IBV1 MOD-B1-60	1200

IQ1, 4	2 SQ	2 10 (shunt)
IQ15	SQ	20 (shunt)
IQ16, 17, 22		3 SQ 3 20 (shunt)
IQ24, 25	2 SQ	2 20 (shunt)
IQ26, 27, 28, 30		4 SQ 4 20 (shunt)
ISEPT	SEPT-84	
IKICK	3 Kickers	1-PS
7 Trims	7 New Trim	7 50 (bipolar)

The line transfering antiprotons from the Debuncher to the Accumulator is relatively simple. It consists of 2 kickers and 2 septa, one of each in each ring, a series of 7 quadrupoles requiring 3 supplies and 1 shunt, a modified B1 and 5 trim magnets.

TABLE 12-VIII DA 8-GEV D TO A

Magnetic	Element	Type Power Supply (A)
DKICK	3 500 g-3 m	1-PS
TDSEP	SEPT-84	
TB1	MOD-B1-120	1200
TQ1	SQ-51.64	500
TQ2, 3	2 SQ-32.6	
TQ4	SQ-27.6	200
TQ5	SQ-51.64	
TQ6	SQ-32.6	
TQ7	SQ-27.6	100
TQ2, 3, 4, 6		4 SQ 4 20 (shunt)
TASEP	SEPT-84	
AKICK	3 Kickers	1-PS
5 Trim Magnets		5 New Trim 5 50 (bipolar)

AP-3 has 30 quads, EQ1-EQ29 (EQ3A and EQ3B are run as a pair), 1 Lambertson, and 8 dipoles, EBV1 - EBV2, and EB1 - EB6. The E-line shares PQ7B with the P-line. There are 15 large power supplies, 7 trim magnet supplies, and 8 shunts.

TABLE 12-IX AP-3, IX-GV A TO MR

Magnetic Element		Type Power Supply (A)
EKICK	1 Kicker	1-PS
E-LAM	LAM-115	1200
EQ1, 5	2 SQ-27.6	500
EQ2, 6	2 SQ-22.6	
EQ4	SQ-25.2	
EQ3A, B	2 SQ-32.6	500
EQ7	SQ-18	30
EQ8	SQ-51.64	100
EQ9	SQ-18	
EQ10-13	4 SQ-18	200
EQ14	SQ-18	200
EQ16	SQ-27.6	200
EQ15	SQ-18	500
EQ17	SQ-27.6	
EQ18, 19	2 SQ-18	
EQ20	SQ-25.2	200
EQ21 - 24		4 SQ-18
EQ25, 26	2 SQ-18	200
EQ27	SQ-25.2	500
EQ28	SQ-27.6	
EQ29	SQ-32.6	
EBV1, 2	2 MOD-B1-60	1200
EB1 - 4	4 SD-98.42	1200
EB5, 6	2 SD-65.37	1200
EQ15	SQ-18	40 (shunt)
EQ17	SQ-27.6	20 (shunt)
EQ18	SQ-18	40 (shunt)
EQ10	SQ-18	10 (shunt)
EQ27	SQ-25.2	40 (shunt)
EQ29	SQ-32.6	10 (shunt)
EQ26	SQ-18	20 (shunt)
EB4	SD-98.42	40 (shunt)
7 Trim Magnets		7 New Trim 7 50 (bipolar)

AP- 4 has 10 quads, BQ1 - BQ10, and 6 vertical dipoles, BBV1 - BBV6. They require 10 power supplies. In addition are BSEPT (at Booster), and BDSEP (at Debuncher) and kickers in each ring.

From an operational point of view the B-line also includes D4Q5.

TABLE 12-X AP-4, 8 GEV BOOSTER TO DEBUNCHER

Magnetic Element		Type Power Supply (A)
BKICK		
BSEPT	SEPT-84	
BQ1	SQ-32.6	500
BQ2,3	2 SQ-25.2	
BBV1	MOD-B1-60	1200
BB2, 3	2 AVB-60	1200
BB4, 5	2 EPB-120	1200
BQ4	SQ-18	100
BQ5	SQ-18	100
BQ6, 7	2 SQ-18	500
BQ8, 9	2 SQ-27.6	500
BQ10	SQ-18	100
BQ8	SQ-27.6	40 (shunt)
BB6	EPB-120	1200
BDSEP	SEPT-84	
DKICK (same as IKICK?)		1 Kicker 1-PS K
5 Trim magnets		5 New Trim 5 50 (bipolar)

CHAPTER 13

CONTROLS

13.1 General Requirements and Architecture

The requirements of the Tevatron I control system go beyond those customary in many accelerators because of the long cycle time for antiproton collection. The system must monitor and control the repetitive sequence of antiproton production, transport, injection, debunching, cooling, and extracting over this entire cycle without significant loss of antiprotons. This will require extensive automatic control and feedback.

In addition, the Tevatron I control system must interface with the existing Energy Saver control system at several stages of the process. Their functions are so intertwined that it is efficient to build the Tevatron I control system as an extension of the Energy Saver control architecture and the description given in this chapter will follow that architecture.

In this note unless otherwise stated, a cycle means a standard Tevatron I 2-sec Debuncher cycle.

13.2 Computer Configuration

The complete Tevatron computer configuration is shown in Fig. 13-1. Four PDP-11's will be used for the Tevatron I control system. Three of these will run the three control consoles, and one will be the $\bar{p}$ front end called "DEC-P", a PDP 11/44. There are 3 Programmed Control Links (PCL) in the full system. As indicated, 5 console PDP-11/34's communicate directly with the Linac, Booster and DEC-P front ends through a PCL. Of course, the number of consoles available for Tev I operation is not fixed since, in principle, any console in the system can communicate with Tev I devices.

A CAMAC System similar to the Energy Saver system will be used. This system adheres to the IEEE 583 standard. Most modules will be those types developed by the controls group, but commercially available CAMAC modules will also be used for some applications.

Fifteen-Hz data rates are supported in the standard way, i.e. using the console-front end combination. Success with the Energy Saver is proof that this approach will work. CAMAC-190 modules, or other modules containing local buffer memories mandate the need for block-transfer facilities.

Each console supports the following devices: a color monitor, a storage scope, a color-graphics monitor, an alarm-message display monitor, a keyboard, a track ball, and a touch panel.

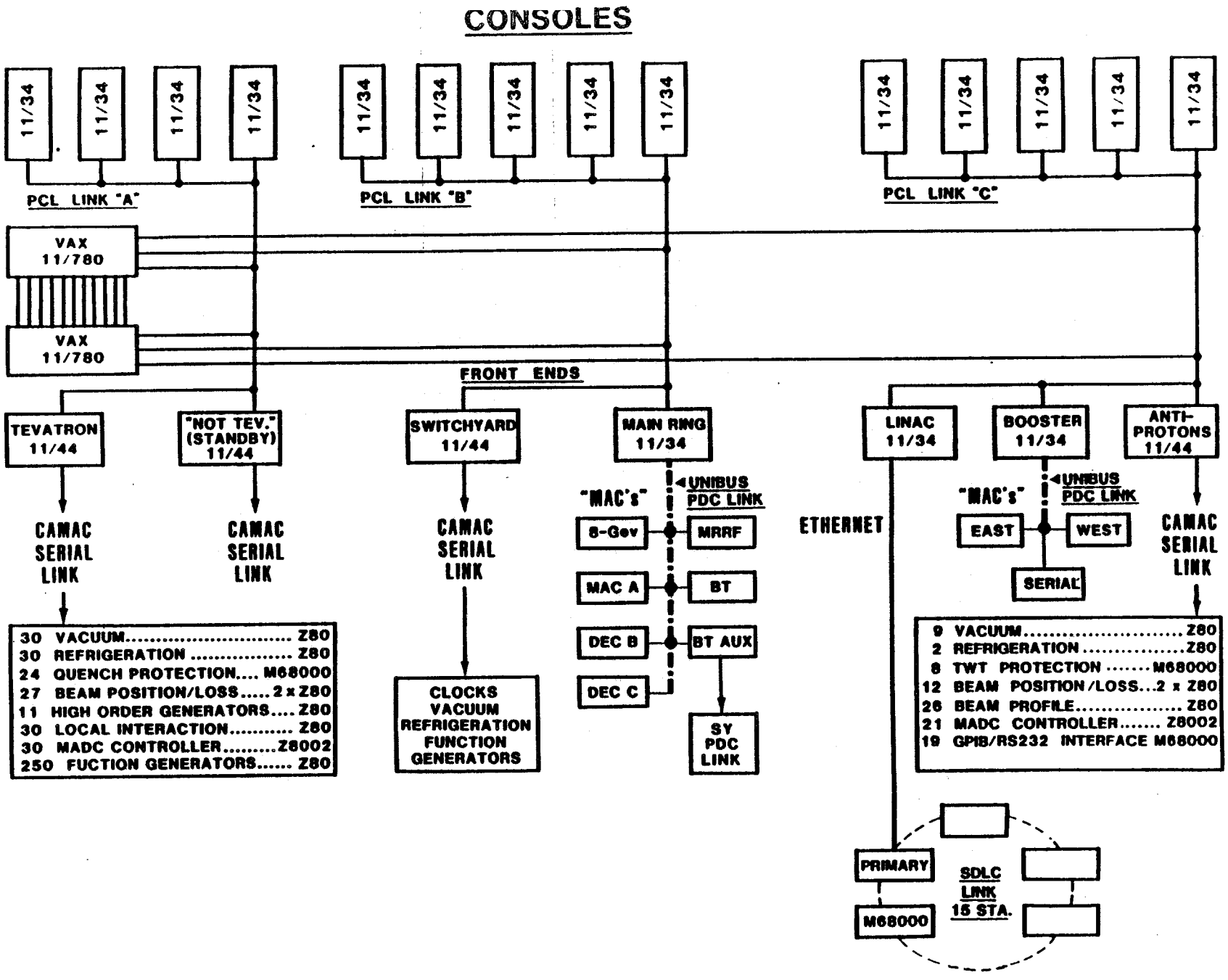
CONSOLES
11/34
PCL LINK "A"
PCL LINK "B"
PCL LINK "C"
VAX 11/780
VAX 11/780
FRONT ENDS
TEVATRON 11/44
"NOT TEV." (STANDBY) 11/44
SWITCHYARD 11/44
MAIN RING 11/34
LINAC 11/34
BOOSTER 11/34
ANTI-PROTONS 11/44
CAMAC SERIAL LINK
"MAC's"
UNIBUS PDC LINK
8-Gev
MRRF
MAC A
BT
DEC B
BT AUX
DEC C
SY PDC LINK
ETHERNET
EAST
WEST
SERIAL
30 VACUUM..... Z80
30 REFRIGERATION Z80
24 QUENCH PROTECTION.... M68000
27 BEAM POSITION/LOSS..... 2 x Z80
11 HIGH ORDER GENERATORS.... Z80
30 LOCAL INTERACTION..... Z80
30 MADC CONTROLLER.....Z8002
250 FUCTION GENERATORS..... Z80
CLOCKS
VACUUM
REFRIGERATION
FUNCTION
GENERATORS
9 VACUUM..... Z80
2 REFRIGERATION Z80
8 TWT PROTECTION M68000
12 BEAM POSITION/LOSS...2 x Z80
26 BEAM PROFILE..... Z80
21 MADC CONTROLLER..... Z8002
19 GPIB/RS232 INTERFACE M68000
PRIMARY
M68000
SDLC LINK 15 STA.

Figure 13-1

Devices in the Main Ring will be controlled from the "old" system. This includes F17 extraction. By late fall 1984, the Main Ring (MR) system will be accessible from a standard console. One will therefore be able to combine parameter pages and displays for MR parameters and Tevatron I devices. No problems are expected from having MR and Tevatron I devices related to extraction on two different PCL links.

13.3 Software

The required Tev I software effort falls into several categories:

1. Modification of existing microprocessor programs: CAMAC-170-Z80 (vacuum), CAMAC 080-Z80 (refrigerator for stochastic cooling), slow loop controls for stochastic cooling and RF, and Beam Position Monitors (BPM) similar to those in the ED.

2. New microprocessor programs: e.g. M68000 GPIB/RS-232 interface, M68000 TWT protection monitors.

3. DEC-Programs. The software philosophy followed is to keep the front-end programs in DEC-T, DEC-S, and DEC-P identical. Changes required to drive special devices are incorporated into all the front-end programs.

4. Applications programs. Some of these are adaptations of existing Energy Doubler (ED) programs; others will be specially written for Tev I.

13.4 Communications

The $\bar{p}$ link system is shown schematically in Fig. 13-2. Separate networks are required for DEC-P and consoles. Twelve 1/2-in. Heliax 50-ohm cables run from the Main Control Room to Service Bldg 10. From there six 3/8-in. Heliax 50-ohm cables branch to the Tevatron I locations: buildings 30, 50, target building, F23 and F27. Two 1/2-in. Heliax 50-ohm cables run from the Main Control Room to 30-2 and to TB-1 to support mini-consoles. Also two 3/8-in. Heliax 50-ohm cables run from service building 10 to 50-2 to support a mini-console in building 50. A mini-console is a semiportable 1 or 2 rack version of the standard 3 rack console.

An additional location is the power-supply building next to the Booster, called the Booster Stair Enclosure. Equipment there will tie in through the Booster front-end computer. It is assumed that Tevatron I devices in the Booster to Debuncher-line (AP-4) requiring equipment in the Booster West Gallery will be installed in existing CAMAC crates.

Buildings 10, 30, and 50 are each 216 ft long; there will be 3 control points in each of them. The target building is 144 ft long; two control nodes are planned there. In addition are F23, F27, and the Booster Stair

LINK SYSTEM - P BAR

RF LINKS: PIOX, PIOR, BTR, & TCLK (4)
TWO CONSOLES AT BLDG 10 (4)

MISC.: BEAM PERMIT LOOP (HIGH LEVEL D/C) SPARE

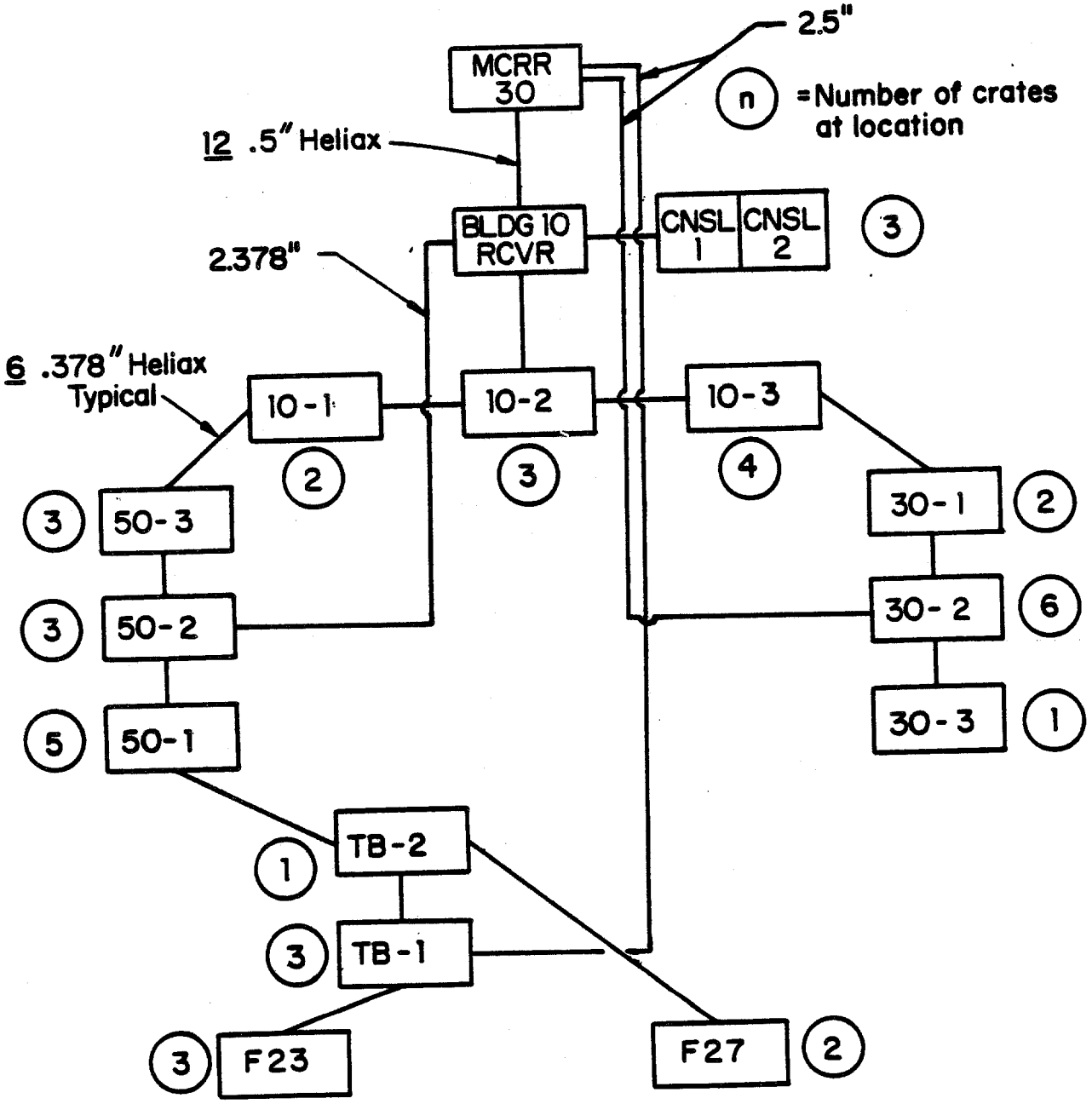

Figure 13-2

Enclosure, making a total of 14 nodes. The 13 repeaters that tie in through DEC-P are shown in fig. 13-2. In the same figure is shown the approximate number of crates controlled at each point. This is still being refined, as is the exact location within the buildings of the control clusters.

13.5 Magnet Controls

None of the main magnet power supplies require microprocessor control or function generators. Magnet protection (thermal interlocks, etc.) is read out in status bits. For magnet elements in series, the protective devices will be hardwired to the power supply for those elements. This will require several hardwire loops around the rings. Reversing ring polarities will be done manually by reversing cables of all appropriate elements.

The five main buses will be driven by 5 supplies, 3 delivering 1200 amps, 2 delivering 300 amps. Each will be regulated to 16-bit accuracy. Each supply will have an internal, commercially availabe 0-10 volt DAC (Analogic). 16 parallel lines will go from the CAMAC crate to opto-isolators at the power supply. One CAMAC-182 and one CAMAC-119 provide the 16 drivers plus the necessary status and control bits. Each supply will contain a commercial Racal-Dana DVM connected to the control system using a CAMAC-488 GPIB interface. In addition, measurement of the current ripple is needed. An internal comparator in each power supply will generate a difference signal which will be sent to a 12-bit MADC/190 channel.

Of the 78 DC power supplies (mostly for beam lines) requiring 14 bit control, 75 will use CAMAC-119's. A 16-bit DAC is built into a CAMAC-119. In the three 300-A Debuncher quad supplies, the DAC will be in the power supply cabinet. The 14-bit readback is accomplished with a new system that places the 14 bit ADC locally in the power supply and reads it back serially using a 1553 bus.

Correction elements are bipolar, 11 bits plus sign. They use a CAMAC-053 (quad unit) and standard MADC/190 channel.

Shunts need 12-bit accuracy but do not require control or status bits. Shunts will be controlled by a new DAC system, a CAMAC-054 designed for this application. The 054 is a single-width CAMAC module having 6 channels.

Ramped supplies and kickers require 14-bit accuracy and will use a CAMAC-165, a new module which also has applications in the switchyard.

13.6 Transfer Marker Timing System (XMR)

The main purpose of the XMR system is to synchronize and distribute timing pulses to pulsed septa, kickers, lithium lens, C-magnet, and SWIC

scanners. These devices are used in ring-to-ring transfers of protons and antiprotons.

Timing of pulsed devices requires two programmable timers: (1) a programmable predet that counts revolutions, (2) a programmable 15-bit delay to set the time relative to the desired revolution to 1 ns resolution (using Lecroy 4222). The gap in the beam is used to trigger the revolution counter. This has to be done very stably (to 1 ns). It is necessary to measure and readback these time delays. This can be done with a commercial (Lecroy 4208) TDC with 1 ns resolution.

The XMR system consists of the following 4 sub-systems:

XMR#1 Transfers from Main Ring to Debuncher or Accumulator

A) Standard antiproton production
(MR to P-line to Target to I-line to D)
B) Proton forward injection to Debuncher
(MR to P-line to I-line to D)
C) Proton reverse injection to Accumulator
(MR to P-line to E-line to A)

XMR#2 Transfers between Debuncher and Accumulator

A) Antiprotons from Debuncher to Accumulator
(D to T-line to A)
B) Protons from Debuncher to Accumulator
(D to T-line to A)
C) Protons from Accumulator to Debuncher
(A to T-line to D)

XMR#3 Antiproton extraction
(A to E-line to P-line to MR)

XMR#4 Protons from Booster to Debuncher

XMR1 is the most complicated system. A clock is phase locked to the Main Ring revolution frequency (47713 Hz) and operated at the 209th harmonic (9.972 MHz). The signal is distributed with standard repeater hardware. An event to signal extraction time would be encoded on to this clock, and be decoded at all other repeater locations by standard CAMAC-177 octal timers. 177 modules provide 1 μsec resolution, while Lecroy 4222 modules provide 1 nsec resolution. Lecroy 4222 modules will be started from a 177 module trigger.

XMR#2 will use a coincidence signal generated by a pulse from a Tevatron clock driven 177 module, and the signal from either the gap in the Debuncher beam or the gap in the Accumulator beam. The coincidence signal will be distributed around the Debuncher and Accumulator rings on a dedicated cable. Devices requiring high resolution (better than 1 μsec) will use signals from Lecroy 4222 modules delayed from the coincidence signal. Other devices will use Tevatron clock driven 177 module pulses.

XMR#3 and XMR#4 use similar hardware but are not yet completely defined.

13.7 Vacuum Controls

At each of 7 locations is a CAMAC-170 module and a Controls Interface Adapter (CIA). An eighth unit will be purchased and can serve as a spare or be hooked up to the control system and used in a vacuum development laboratory. Locations are 2 each in service buildings 10, 30, 50, (one for the D and one for the A), and one in the target building. Sector valve control is done by a hard wire system. The devices controlled and/or monitored by these 7 CIA crates are: 133 ion pumps, 21 Pirani gauges, 21 cold-cathode gauges, 26 ionization gauges, 16 sector valves, and 134 sublimation pumps.

Additional vacuum systems to be controlled are roughing (23 each roughing pumps, turbo pumps and roughing valves), Accumulator bake-out and Accumulator residual gas analysis (3 units).

13.8 RF Control Systems

The location of equipment to be controlled or monitored is in buildings 10 and 50. There are 2 main systems in the Debuncher: (1) the 53 MHz system which uses inversion of the drive phase and counter phasing to reduce voltage to a low value, and (2) the gap preserving system. In the Accumulator are (1) a stacking system, h=10, 6.289 MHz, (2) an unstacking system and (3) a 53 MHz rebunching system.

The controls use standard modules. Local microprocessors will be used for slow loop control. A precision frequency meter will require a GPIB interface.

There are additional RF controls needed for the MR $\bar{p}$ production cycle:

1. Main Ring phase lock to Booster for single batch acceleration
2. Low level RF system for single batch acceleration and bunch rotation

There are controls needed for MR and ED p and $\bar{p}$ acceleration:

1. 53 MHz RF system

2. 2.5 MHz RF system including second harmonic

3. Phase locking of the Main Ring to the Energy Saver

4. Colliding region position control.

All of the above controls are being implemented with Standard Tevatron Controls hardware.

13.9 Stochastic Cooling Controls and Monitoring

Stochastic Cooling Controls and Monitoring are centralized in building 30. For control and monitoring purposes the following classification may be useful: (1) beam pickup electrodes, (2) low level electronics (including preamplifiers), (3) medium level electronics (including gain and phase correction, circuits, filters, etc), (4) high level electronics (including TWT), (5) kicker electrodes.

1. TWT power supplies. There are 62 travelling wave tube power supplies distributed as follows: A20 tunnel or stub room, 3; A30 tunnel or stub room, 18; A30 service building, 41. Each supply requires the following monitoring and controls:

    1. 5 status bits: timeout state off/on, standby state off/on, beam on/off, local/remote, fault.

    2. Analog helix voltage remote monitor output, 1 mV per volt. 1% accuracy implies 7 bits + sign is adequate.

    3. 3 control bits: AC power on/off, fault reset, beam voltage on/off.

    4. DAC to control the helix voltage.

    5. Turn on permit signal.

2. TWT protection monitor. All 33 systems are located in Service building 30. Each monitor measures forward and reverse TWT power as well as power delivered to the kickers. Each monitor will contain an M68000 microprocessor. The output from the microprocessor to the control system will be values of powers and status bits.

3. Trombones. There are 74 located as follows: 17 of these are in service building 30 and the remaining 57 are in the tunnel or stub rooms: A60, 11; A10, 10; A20, 8; A30, 28. Trombones are delay lines whose length is changed by a stepping motor actuator. Readback of the position can be done either with a linear pot with a local voltage reference or by a shaft position encoder.

4. Microwave Amplifier power supply regulators. There are a total of 96. 44 of them are in service building 30; the remaining 52 are in the tunnel or adjoining stub rooms distributed as follows: A60, 23; A10, 26; A20, 3. A raw power source feeds a tightly regulated supply to a microwave amplifier. The regulator requires a single control signal for on/off and provides 5 bits of status readback on the microwave amplifier.

5. PIN diode switch. There are 9 distributed as follows: A60 tunnel or stub room, 2; A10 tunnel or stub room, 4; service building 30, 3. The switch is a 1 bit device to pass or block a single RF signal. The input is TTL compatible; switch is "on" at logic "0" and "off" at logic "1". The switch does not provide any status information. Power requirements are 5 volts, 60 mamp and -5 volts, 20 mamp.

6. PIN diode attenuators. There are 13 distributed as follows: A60, 5; A10, 4; service building 30, 4. The attenuator is an 8 bit device producing 256 levels of attenuation for RF signals. Inputs are TTL compatible. The attenuator does not provide any status information. Power requirements are 12 volts, 128 mamp and -12 volts, 35 mamp.

7. Coaxial relays. These will be used for a variety of functions. Test signals can be inserted into amplifiers. Multiplexed coaxial relays switch the spectrum analyzers and the network analyzer to different places. Coaxial relays in trunk lines (medium level electronics) are used to inject and extract signals, and also used while beam is on. The total number is 100, but provision will be made in the control system to add more later. They are all in the tunnel or adjacent stub rooms distributed as follows: A60, 15; A10, 20; A20, 9; A30, 56. Each relay requires a control bit and a status bit.

8. 3 spectrum analyzers, 2 in bldg 10 and 1 in bldg 30 require GPIB interfaces.

9. The network analyzer in building 10 requires a special interface to the HP-9826 computer. This will consist of two separate parts: (1) an interface between an 080 module and one of the GPIB buses in the HP computer for block data transfer. Data rates expected are 100-200 Kbytes every 20 minutes or so during startup of the system. Data will be passed through DEC-P to the VAX without any work done on it by DEC-P. (2) an interface using GPIB to another bus of the HP computer for "chit-chat," a short list of commands that load already written programs from the Winchester Disk into the HP computer and make inquiries as to whether or not the processing is done or how far along it is. A command will also allow termination of the program in the HP.

10. Refrigeration and compressor control and monitoring will be done in a way similiar to the Energy Saver and use multibus REF crates connected to the CAMAC system by 080 modules.

11. Thermocouple refrigeration monitoring points (A10: 10, A20: 10, A30: 15, and A60: 30) will go to ADC channels.

12. There will be a small number of devices to control cryogenics valves, and monitor flows. These will use Standard CAMAC modules. Dewars each have a He level controller. A status bit indicates that the level is high enough to cover the filter.

The system being developed to control and monitor the microwave amplifiers, pin diode switches and alternators, and coaxial relays (items 4-7 in above list) is shown schematically in fig 13-3. The motivating design criterion has been to remove CAMAC equipment from the tunnel enclosure for purposes of reliability and access for repairs.

The CAMAC crate with the associated Crate Controller and connections to the Link are all standard Tevatron components. The Interface Box and the Patch Box are new designs. The Power Supplies are to provide power to the pin attenuators, pin switches, and microwave regulators. The cables terminate at the Patch Box in the tunnel. With this arrangement it is possible to include the power lines in a single cable which runs from the Patch Box to a particular attenuator, regulator, etc.

It is proposed that each location be served with the equipment shown in the block diagram. An exception is the CAMAC crate which has sufficient slots to accommodate more than one system.

The system provides 3 key features:

1. Signal conditioning, amplification, optical coupling, etc. are accomodated in one location, the Interface Box.

2. Provision is made for future expansion. Sufficient cables are proposed to support additional devices if they become necessary. This additional capacity is also incorporated in the Interface and Patch Boxes.

3. The Patch Box provides a central point from which individual cables are run to the various pieces of equipment. All necessary signals for that equipment are included in that one cable.

The CAMAC 180 is well suited for status readback. This module has provision for storing 16 sixteen-bit words giving a total of 256 input channels. The module provides 4 output lines to control a multiplexor which selects one of the 16 words. This word is latched in the 180 and the module scans ahead to read the next word at a 500 kHz rate. Any of the 16 words are easily accessed through the CAMAC system. Output signals for

STOCHASTIC COOLING CONTROLS BLOCK DIAGRAM

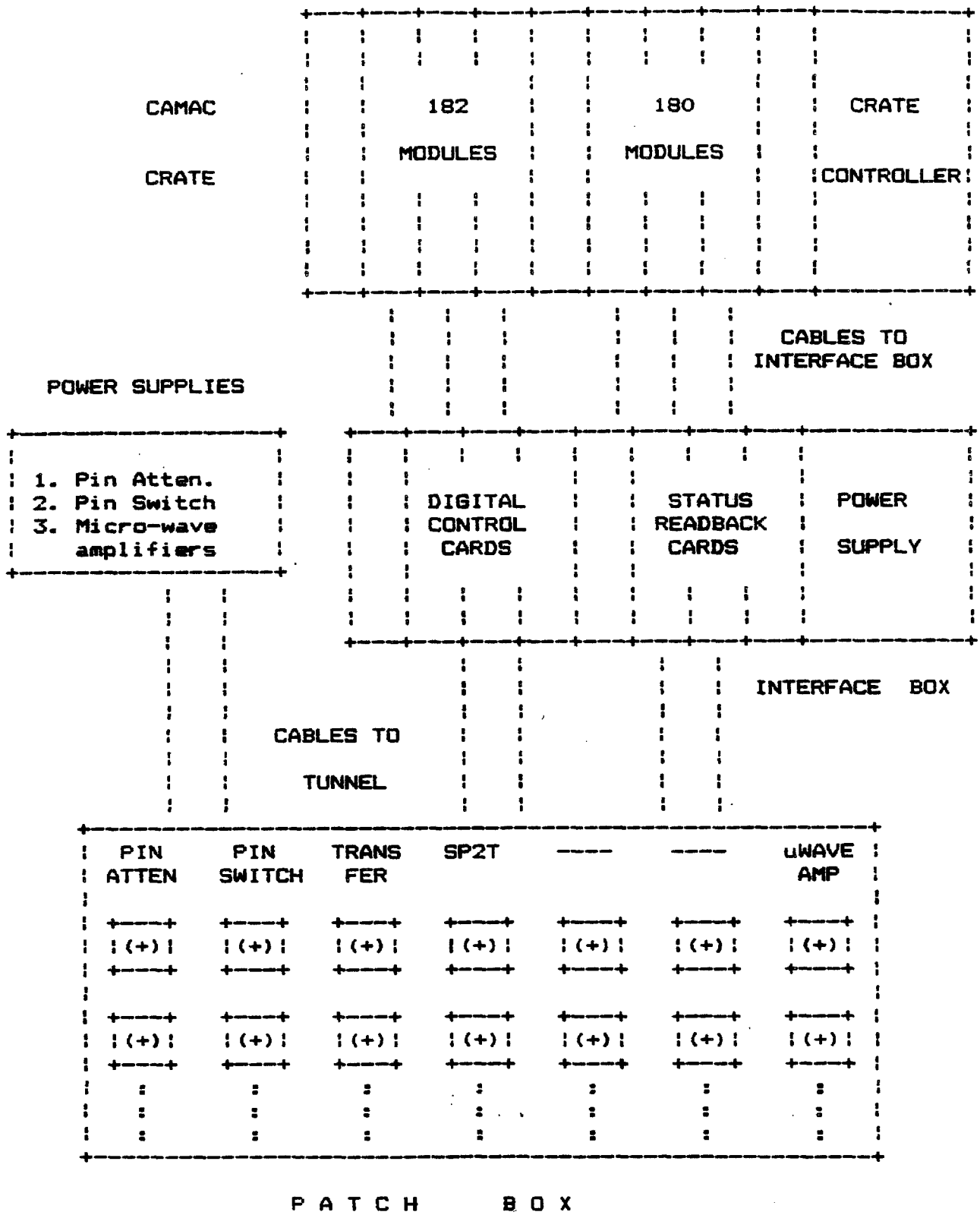

Figure 13-3

controlling switches, setting attenuators, etc., are provided by the CAMAC 182 module. It consists of 32 output channels and can be configured to control individual output channels or to operate at the word (16 bits) level.

The Interface Box has several major functions: (1) provide multiplexing for the CAMAC 180 module; (2) provide optical coupling and filtering of incoming status signals; (3) provide contact closure monitoring for the various coaxial relays; (4) provide high voltage (28 V), high current (60 mA) signals for the coaxial switches; and (5) provide a convenient and reliable means of grouping and terminating the cables which go to the tunnel. The Interface Box is built around a 21-slot double-high Eurocard cage and accommodates Eurocards of 233 x 220 mm. This card size has an area of approximately 80 square inches. A typical CAMAC card has an area of about 84 square inches. Appropriate power supplies are housed in the Interface Box. Two types of cards are used with the Interface Box: an input card called the Status Readback Card and an output card called the Digital Control Card.

The Status Readback Card has 32 channels for input signals. Depending on jumper position a channel monitors TTL signals received optically or a channel monitors relay contacts. Current through the contacts when they close is 5 mA. The interface Box contains up to 8 Status Readback Cards providing 256 input channels. The 8 cards are multiplexed and supply data to a single CAMAC 180 module. One-shots provide 100 msec outputs with either a positive or negative edge acting as the trigger. A transistor driver is used to drive a relay coil.

The Patch Box is simply a means for terminating the multiconductor signal cables and power cables which run from the service buildings to the tunnel areas and distributing these signals to the appropriate Burndy style connectors. The Patch Box is wall mounted with a hinged front door for easy access inside. The box is of the style presently used in the Booster as a fan-in box for analog signals. Cables from the service building enter the Patch Box from the top while the sides are used for the various Burndy connectors. Various connector blocks are mounted inside the Patch Box for the distribution of the power signals to the attenuators, pin switches, and microwave amplifiers.

The digital Control Card contains 32 channels of output with several options available for each channel. The Interface Box contains up to 8 Digital Control Cards which are driven by 8 CAMAC 182 modules.

13.10 Tev I Beam Diagnostics Interface to the Controls System

13.10.1 Beam Position Monitors. This section is condensed from TM-1254 (T. Bagwell, S. Holmes, J. McCarthy, R. Webber, "Anti-proton Source Beam Position System") and mainly emphasizes the controls aspect of that system.

The Tev I Beam Position Monitor (BPM) system is designed to provide a useful diagnostic tool during both the commissioning and operational phases of the antiproton source. The design goal is to provide single-turn-beam position information for intensities of greater than $1x10^9$ particles, and multi-turn (closed orbit) information for beam intensities of greater than $1x10^7$ particles, both with sub-millimeter resolution. The system will be used during commissioning for establishing the first turn through the Debuncher and Accumulator, for aligning injection orbits, for providing information necessary to correct closed orbits, and for measuring various machine parameters (e.g. tunes, dispersion, aperture, chromaticity.) During normal antiproton operation the system will be used to monitor the beam position throughout the accumulation process.

There are 210 beam pickups in the system--120 in the Debuncher and 90 in the Accumulator. Usually there is one pickup at each quadrupole (with horizontal pickups at F quadrupoles and vertical pickups at D quadrupoles.) This results in more than five position measurements per view per betatron wavelength in each ring, and provides more than sufficient information for precision alignment of closed, injection, and extraction orbits. The pickups themselves are either cut cylinders or rectangles, depending on location, with signals capacitively coupled from the beam. To maximize signal levels the pickups cover the full azimuth and every effort has gone into minimizing their capacitance to ground. The pickups are bidirectional to accommodate beams circulating in either direction and in the Accumulator also function as clearing electrodes.

During the commissioning period approximately $1x10^{10}$ protons will be injected into the Debuncher and Accumulator rings. These protons will be delivered from the Booster in 80 bunches at 52.8 MHz, either directly (via the Booster-Debuncher line), or by way of the Main Ring to the Debuncher (forward injected via the Target-Debuncher line) or to the Accumulator (reverse injected through the Accumulator-Target line.) For these modes to operation there is capability to measure orbits both over a single turn and averaged over multiple turns.

During the normal accumulation cycle approximately $7x10^7$ antiprotons are injected into the Debuncher once every 2 seconds. These antiprotons arrive in a train of 80 bunches with a spacing of 53.1 MHz. In the Debuncher they are rotated one quarter of a turn in longitudinal phase and allowed to debunch. A low level wideband system is provided to preserve the 200 nsec gap which is present at injection. After approximately 2 seconds in the Debuncher the beam is extracted and sent to the Accumulator. The $7x10^7$ antiprotons are placed orbit with an average momentum 0.93% above the central orbit of the Accumulator. They are then quickly moved to the tail of the accumulated antiproton stack by a 6.3 MHz RF system and subsequently cooled by the stochastic cooling systems. Eventually a core of up to $5x10^{11}$ antiprotons is collected at an average momentum lying 0.69% below the central orbit value. Following accumulation approximately $1x10^{11}$ antiprotons, in thirteen 52.8 MHz bunches, are moved onto a momentum displaced extraction orbit and kicked out the extraction line in a single

turn. The BPM system has been designed with the capability of observing the (single turn) injection orbit and circulating closed orbit in the Debuncher, and the (multi-turn) injection orbit, core orbit, and extraction orbit in the Accumulator.

Parallel systems are used for the signal processing of single turn and multiple turn measurements. Single turn-by-turn measurements are processed by a high frequency (53 MHz), wide bandwidth (5 MHz) system which relies on 53 MHz signals produced by the bunched beam. This system is very similar to the present Energy Saver detection system. Multiple turn (closed orbit) measurements are processed through lower frequency (2.4 MHz in the Debuncher and 6.3 MHz in the Accumulator), narrow bandwidth (100-1000 Hz) systems which rely on naturally occurring gaps in the circulating beam, Schottky noise, and/or modulation produced by low frequency RF for signal generation. The bandwidth of these systems is chosen simply to cover the momentum spread in the beam. The narrow bandwidth produces an analog average which typically extends over several hundred turns and is necessary to reduce the contribution to position resolution from noise in the system. In addition to analog averaging there is digital averaging up to 256 measurements at any particular pickup to obtain sub-millimeter resolution even at very low signal levels. Twelve systems of each type exist in each ring. Signals from the pickups are multiplexed so that each system services between 7 and 10 pickups.

The digital signal processing is done through a multibus based system which is very similar to that used in the Energy Saver. This allows a large amount of hardware and software to be directly copied from the Energy Saver system. Provisions are made for testing and monitoring of the entire system.

Sum and difference signals from each position monitor are processed through gain switchable amplifiers within the tunnel and are then received in the service buildings through a modified version of the Main Ring multiplexor. Twelve service stations exist in the total system--six each in the Debuncher and Accumulator. Each station handles both the horizontal and vertical position monitors for one sixth of one ring. This implies ten BPM's per multiplexor in the Debuncher and seven/eight per vertical/horizontal multiplexor in the Accumulator system. Following, the multiplexor, position and intensity signals are generated through both the high and low frequency systems. The fast (53 MHz) position and intensity signals are then sent to a fast A/D converter which communicates with the Turn By Turn card in a multibus crate. Multiturn orbit measurements are digitized through the Saver Analog Box operating in Flash Mode. Only two of a possible twelve daughter cards are actually present in the Analog Box. Input to the Analog Box is selected from either the high or low frequency detector. Provisions are made for both magnifying and offsetting the position signal in order to utilize more effectively the eight bit resolution provided by the digitizers.

The multiplexors need to be able to switch inputs at speeds measured in milliseconds. This is because for multiple turn measurements in which bandwidths of 1 KHz are used one must wait up to tens of milliseconds for the input levels to the analog box to stabilize once a change is made. For measurements which utilize digital averaging to improve resolution it will be necessary to cycle through the multiplexor 100-200 times during the course of a measurement. For a measurement of the antiproton core for example, a bandwidth of 70 Hz is chosen. If 256 measurements are taken at each of eight multiplexor positions the entire measurement period lasts 60 seconds. For the Debuncher coasting beam it should be possible to make approximately 100 measurements at each pickup during the 2 seconds the beam is present on each cycle.

Special provisions have to be made for triggering the Analog Box in flash mode since the narrow bandwidth of the multiple turn system precludes any rapidly changing intensity signals entering the box. Flash mode will be initiated by a software generated lowering of the preset intensity threshold within the box at a specific time. The fast A/D will be self triggering on the intensity signal. The bandwidth of the high frequency system is about 5 MHz. This means that the associated time constant is 32 nsec, or 1.7 bunches. In order for the trigger circuit to be able to recognize a gap in the beam, and hence distinguish subsequent turns, approximately eight empty bunches are needed.

A great deal of flexibility is built into the system as a consequence of the need to detect and measure circulating beams with vastly different characteristics. Among the parameters of the system which are variable are,

1. Pickup Signal Level: Switchable between either 0 db (normal) or 40 db attenuation through a capacitive divider at the preamp input.

2. Tunnel Switched Gain Amplifier: Variable gain between 0-60 db in 20 db steps.

3. Multiplexor Cycle Pattern.

4. Oscillator Frequency: In the low frequency detector. Variable over ±.05%.

5. Position Gain and Offset: Gain x 1,2,4 and seven offset positions.

6. Filter Bandwidth: Variable 75 Hz to 1000 Hz in four steps.

7. Test Signal Generator: Generates difference and sum signals for monitoring scale of offset of position measurement.

All control of variable parameters is through the multibus External Device Bus.

Each multibus crate is controlled by an 8004 microprocessor and an associated M080 processor which handles communications to the host computer through CAMAC. The multibus crate used is identical to what is used in the Energy Saver system except for the addition of a Fast Access Board needed to control the fast A/D. As mentioned earlier, existing software will be used to the fullest extent possible.

13.10.2 Beam Loss Monitors. No clear plan has been developed for beam loss monitoring except in the AP-1 line. There standard Energy Saver loss monitors and controls hardware to read them will be installed. Some use will be made of standard high energy physics detectors and electronics, initially without an interface to the accelerator control system.

13.10.3 Beam Current Monitors. There needs to be one in each ring and one in each beam line. In the D one needs to measure pulse to pulse variations to accuracy of about 1% for optimizing targeting. Sensitivity desired is 0.1 μA or 10^7 $\bar{p}$'s. The precision current monitors will use GPIB interfaces to the control system. The use of a "SQUID" (Superconducting Quantum Interference Device) is under consideration.

13.10.4 Beam Profile Measurements. There are several possibilities: flying wire scanners, SWIC's, segmented or grid SEM's, gas jets with collection of ions. SEM grids appear to be the best solution for the beam lines and gas jets for the Debuncher and Accumulator rings and these are the devices currently under construction.

Each SEM grid will use the microprocessor system used in the FNAL secondary beam line SWIC scanners. This generates a digitized profile, calculates the mean and sigma of the distribution, and has snapshot capability. This information can be viewed on the TV system. It will also be interfaced into the control system using a CAMAC-032. Once done, graphical displays, emittance measurements, etc. are possible using the VAX. The numbers needed are approximately AP-1, 8 (including 3 special high resolution SEM-grids near the target); AP-2, 7; AP-3, 7; T-line, 4; for a total of 26.

Some of the characteristics of the SEM grid system are the following:

1. All are remotely retractable by the Control System from the beam.

2. The number of channels/monitor is 32x, 32y.

3. The grids are made of 10μ. titanium and are of three types: 1 mm wide strips, 1.5 mm apart; 2 mm wide strips, 3 mm apart; and special high resolution target region grids.

4. The goal is to achieve a least count of 5×10^{-15} coulombs.

13.11 Utility Monitoring for the Antiproton Source

The FIRUS System is the standard Fermilab fire protection system. It can also serve to monitor utilities whose failure can hamper operations or endanger equipment. There is no connection between the *FIRUS* and *ACNET* systems envisioned.

The purpose of the utility portion of the FIRUS system is to alert people in the main control room, at the fire station, and in the building 10 control room when either environmental conditions are unhealthy for antiproton source devices, or electrical or mechanical equipment is malfunctioning. The FIRUS system consists of the following equipment:

1. FIRUS mini-computers for Tev I (wall mounted--one for fire, others for utility)
2. Emergency power supply (also wall mounted)
3. Coax hardline communication cable
4. Junction boxes
5. Contact points and analog transducers
6. Three-pair 18 gauge shielded cable
7. Silent printer

Each mini can monitor 16 contact points or 15 analog points or a combination of contact and analog points. Each contact point can be more than one physical point if the points are wired in series. An alarm then indicates any one of a group of points has opened.

The following devices/quantities will be monitored by the utility portion of the FIRUS system:

1. sump pumps
2. LCW (Low Conductivity Water)
3. auxiliary generator
4. service building temperatures
5. stub room/tunnel temperature
6. stub room/tunnel humidity

Two contact sets per sump pump would be used. The first opens when a controlling float reaches a high water position, and the second opens upon loss of 120 VAC power to the pump.

The LCW cooling system for the rings enclosure will be derived from new equipment in the Central Utility Building (CUB). One transducer for water pressure and one transducer for water temperature will be located just downstream of the 1000 gpm, 150 psi pump in CUB. The LCW cooling system for the Antiproton Target Hall and Pretarget Enclosure will be extended from the Main Ring LCW system at Service Building F-23. Since the Main Ring LCW system is already monitored by FIRUS, no additional monitoring is necessary, as is true of the hot water (HTW) and chilled water (CHW) systems used for heating and airconditioning.

The auxiliary power generator (to be located outside Service Building 50) has a panel (to be located inside Service Building 50) with 8 monitors of contacts. A FIRUS contact will be wired such that if any one of these 8 monitors trips, the FIRUS contact will open, indicating trouble with the auxiliary power system.

Service Building temperatures will be monitored with either one to three distributed contacts that open upon a high temperature limit and one contact that opens upon a low temperature limit or two distributed analog temperature sensors with FIRUS software set limits. The Service Buildings are heated and airconditioned, so temperature monitoring provides a check on the correct operation of the air handling units. The high temperature limit will insure a healthy environment for the electronic equipment, and the low temperature limit will protect water pipes from freezing in winter.

An analog temperature sensor with FIRUS software set limits will be used for the stub rooms. Human access to the Antiproton Rings Enclosure will be prohibited if a beam is present. Remote monitoring of environmental temperature allows an operator to comfortably assess any long term danger to electronic equipment and decide if and when an access should be performed to investigate a high temperature indication. Also, during bakeout of the Accumulator, access to the rings enclosure will be possible, but not comfortable. The high temperature limit for electronics is higher when electronics are not operating, and the analog temperature sensor will be useful.

The rings enclosure is heated and indirectly air-conditioned by Service Building forced air ventilation. The possibility of electrical equipment damage due to condensation exists in the summer when warm, humid air could be cooled in the nearly constant temperature, below-ground rings enclosure. An analog humidity sensor, with a FIRUS software set limit in selected stub rooms provides a check on the ventilation system.

Lighting and power for the new F18 Extraction Hall will be extended from the adjoining Main Ring sections. Similarly, the ventilation for the new hall will be the same as for the present F18 enclosure.

14.1.2 Pretarget Enclosure.

The Pretarget Enclosure is an underground structure approximately 325 ft long and links the F18 Extraction Hall to the Target Hall. Throughout most of this length, a rectangular cross section 7'-0" wide and 8'-0" high is used and contains the beam transport magnets for the 120-GeV proton beam. It is also shown in Fig. 14-2.

The floor slab of the Pretarget Enclosure rises in elevation from 724'-0" to 726'-0", approximately paralleling the rise in beam line. Near the south end of the enclosure is a personnel exit stairway, and at the north end the enclosure joins into the Target Hall.

A 65 ft long steel beam pipe connects the F18 Extraction Hall and the Pretarget Enclosure. In the length of this beam pipe, the extraction line has moved away from the Main Ring sufficient distance that the new Pretarget Enclosure may be constructed without interference to the existing Main Ring sections.

A soldier beam, wood lagging and earth tieback system is planned to retain uniform earth pressures around the adjacent Main Ring arch sections, and to minimize the excavation size. These soldier beams also are part of the helium pipe truss abutments used for the F18 construction.

Lighting and power will be extended from the Target Hall. Ventilation through the Pretarget Enclosure is done with an exhaust fan at the south personnel exit and make-up air from the Target Hall. Power communication conduits will join the Pretarget Enclosure to the Main Ring at the south end, and to the F23 Ancillary Service Building at the north end.

An earth shielding berm is placed above the entire length of the Pretarget Enclosure merging into the Main Ring berm at the south end and abutting to the Target Hall at the north end.

14.1.3 Antiproton Target Hall and 120 GeV Target Station. The 120-GeV Target Station is housed in a 144 ft long underground structure that is contiguous with the Pretarget Enclosure and the Antiproton Transport Enclosure. This structure is 8'-6" high and varies in width from 11'-6" to 16'-0". A large shaft 11'-6" wide and 37'-0" long contains the target vault steel core and provides access from the Target Hall above. Figure 14-3 shows plan views of the Target Hall.

The Target Hall is a large, high crane-bay building 57'-6" wide, 144'-0" long and 27'-0" above grade. A 20 ton bridge crane provides 17'-0" clear lift above the Target Hall floor at Elevation 747 ft.

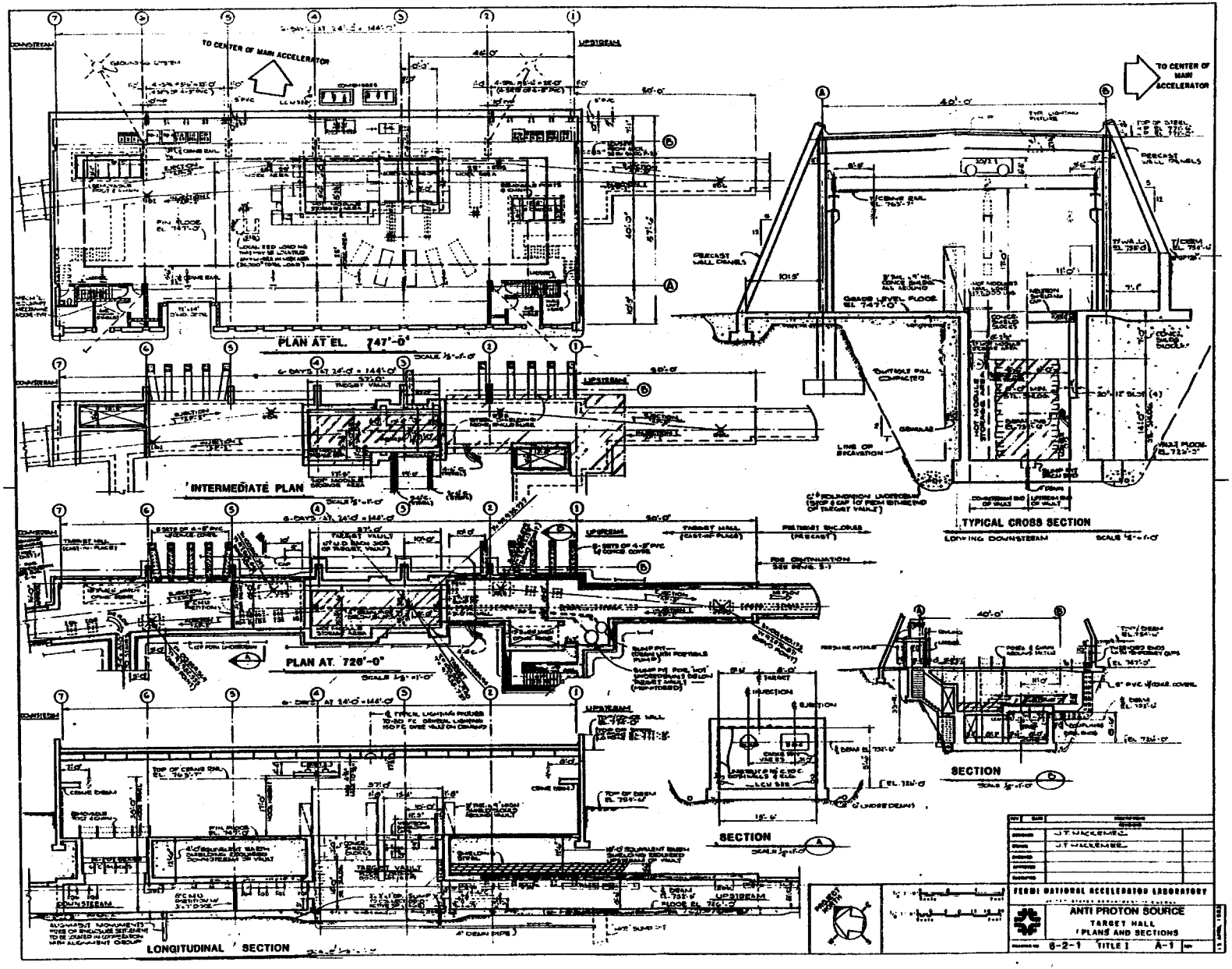
PLAN AT EL. 747'-0"
INTERMEDIATE PLAN
PLAN AT 726'-0"
LONGITUDINAL SECTION
TYPICAL CROSS SECTION
SECTION
SECTION
TO CENTER OF MAIN ACCELERATOR
FERMI NATIONAL ACCELERATOR LABORATORY
ANTI PROTON SOURCE
TARGET HALL
PLANS AND SECTIONS
8-2-1 TITLE 1 A-1

Figure 14-3

The exterior appearance of the Target Hall is akin to the Antiproton Service Buildings and reflects the construction of the Linac, Transfer Gallery and Cross Gallery. Sloping textured concrete walls along the long dimensions meet into massive end walls that retain the earth berm. Window, door and louver openings and contrasting wall panels interrupt the sloping walls in a symmetric pattern.

Access to the Target Hall is via existing and improved Kautz Road, which swings south of the Rings Enclosure and leads north to the Wilson Hall west parking areas. A large equipment door and two personnel doors open from the Target Hall to the parking area by Kautz Road.

A number of functions are served in the Target Hall. Access to the target vault and to the thirteen target modules is provided both for initial installation and subsequent maintenance and changeover. In addition, weather protection is afforded during the changeover times when target modules are being placed in shield caskets. The Target Hall also provides space for the power supplies and support equipment associated with the target-station and beam-transport magents. Access to the Pretarget Enclosure and to the Antiproton Transport Enclosure is allowed through shielded vertical hatches. The Target Hall also provides physical security to the equipment within.

The Target Station is constructed within a concrete vault resting on undisturbed glacial till. This stratum is firm and dense with very low permeability. Along the sides of the target vault, underdrains will be placed and connected to a sump for ground water monitoring. Five ft of granular material adjacent to the concrete vault walls will assure drainage to the underdrains below.

Several closed-loop cooling water systems will be used for cooling target modules. Within the target vault, concrete floor curbs will limit spread of any accidental water leak in target modules. A separate sump will connect to this curbed area and the piping will be cast into the base slab. Similarly, at the floor above the vault opening, curbing will prevent water spills at grade from dropping into the vault.

Above the Target Vault, shield blocks will be placed and securely anchored to the floor. These shield walls will provide both physical and radiation protection during the time target modules are removed from the vault and placed in shielding caskets. At no time will repair work be done on radioactive modules components within the Target Hall.

Equipment access to the Pretarget Enclosure and Antiproton Transport Enclosure will be through two vertical hatches. At the upstream hatch, three ft of steel and nine ft of concrete will be used for the 120-GeV proton beam requirement. At the downstream hatch, 12 ft of concrete will provide the 8-GeV antiproton-beam requirement.

Personnel access is through two stairway/labyrinths. Interlocked doors will limit access during power-on and beam-on conditions.

Ventilation in the Target Hall will be maintained with positive pressure to assure no outflow of possible air contamination from the vault below. High efficiency particulate filters will be used at the upstream end of the target vault for the air system circulating through target modules.

Fire protection in the Target Hall will be served by a fire hydrant at the road, two hose cabinets within the building, portable Metal-X extinguishers throughout the area and ionization type smoke detectors. No sprinklers will be used in the Target Hall.

Secondary power enters the Target Hall from a substation along Kautz Road and serves the switchboard for the building. A small service of emergency power from the diesel generator at Service Building 50 will be extended to the Target Hall for crane and sump pump operation.

LCW cooling water will be extended from the F23 Main Ring Service Building. ICW water will be available for a primary heat exchange for the small closed loop water systems for the target modules.

14.1.4 Antiproton Transport Enclosure. The Antiproton Transport Enclosure is an underground structure approximately 680 ft long and links the Target Hall to the Rings Enclosure. The first 400 ft of enclosure joins to a "Y" section 80 ft long, which divides into two enclosures, each 200 ft long, each connecting to Sector 50 and 30. It is shown in Fig. 14-4.

Through the long straight lengths of this enclosure, a rectangular cross section 8'-0" wide and 8'-0" high is used and contains the beam transport magnets for both the 8-GeV antiproton beam injected into the Debuncher Ring at Sector 50 and the antiproton beam extracted from the Accumulator Ring at Sector 30. A 9'-0" high enclosure and in width varying from 9'-0" to 30'-0" contains the larger dipole magnets that bend the beams through the legs of the "Y" section.

The magnets are suspended from the special inserts cast into the enclosure ceiling. Magnets and other equipment are rolled beneath the suspended magnets to install or replace such items without removing other magnets for access. Cable trays, piping and utilities are mounted on the ceiling or tightly against the walls.

In the section containing both the injected and extracted beam lines, only small quadrupoles are used and a reasonable personnel aisle is maintained. No hatches open directly into the Antiproton Transport Enclosure. Equipment access is made from both ends through the hatch in the Target Hall and Hatch 40 in the Rings Enclosure.

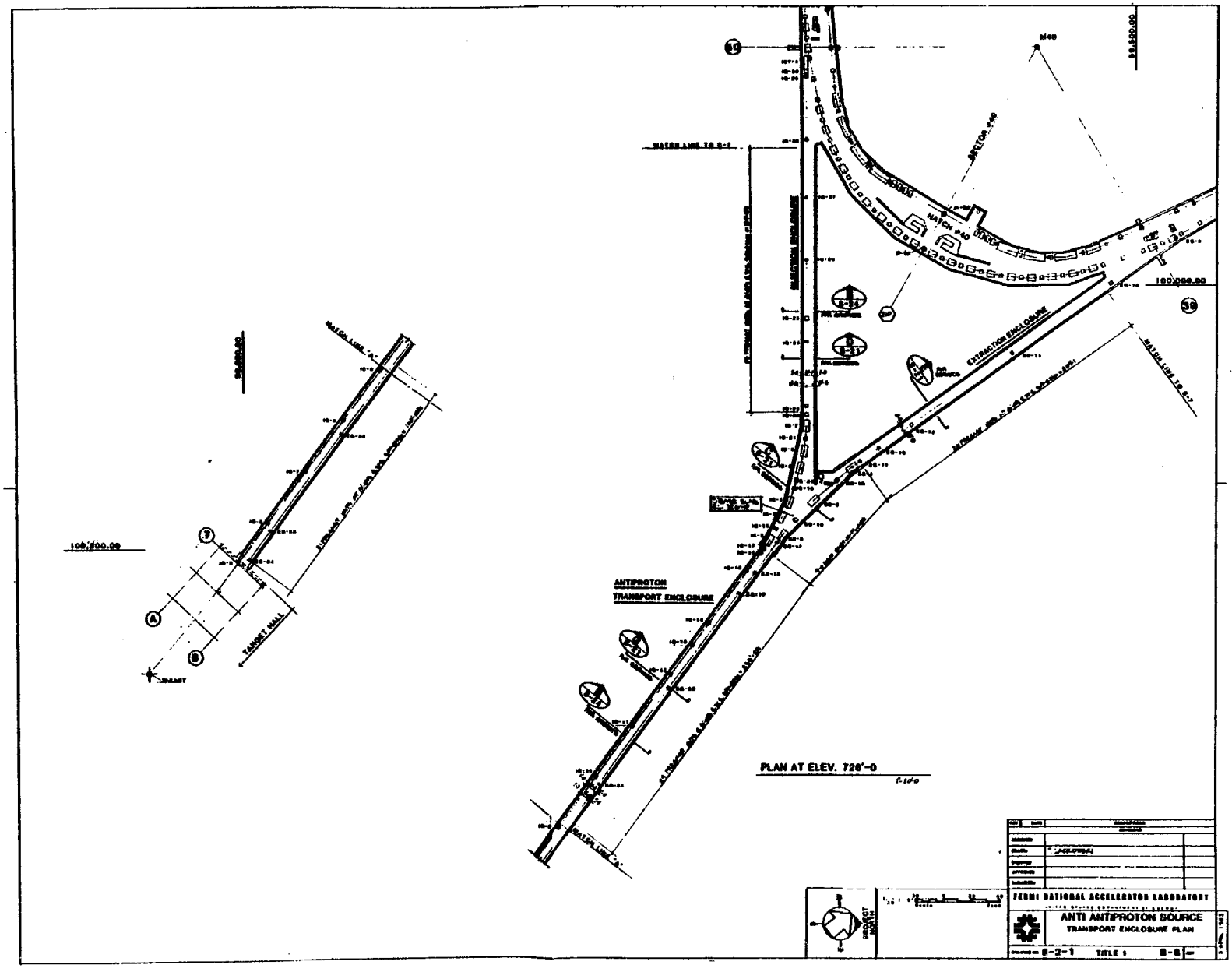
ANTIPROTON TRANSPORT ENCLOSURE
EXTRACTION ENCLOSURE
TARGET HALL
PLAN AT ELEV. 720'-0
FERMI NATIONAL ACCELERATOR LABORATORY
ANTI ANTIPROTON SOURCE
TRANSPORT ENCLOSURE PLAN

Figure 14-4

Precast inverted "U" sections placed on a poured slab are used for the straight sections and cast-in-place concrete is used at the "Y" section.

A low earth shielding berm above the entire length of the Antiproton Transport Enclosure defines the location of the enclosure. Design has shown that no additional steel shielding is required between the enclosure and the Indian Road crossing near Sector 40.

14.1.5 Debuncher-Accumulator Rings Enclosure. The Rings Enclosure is a doughnut-shaped underground structure approximately 1650 ft in perimeter. The doughnut is flattened in three places, and these straight sections are termed Sectors 10, 30 and 50. The intervening curved sections are Sectors 20, 40 and 60. There is basic three-fold symmetry throughout. This is shown in Fig. 14-5.

Antiprotons are injected into the Debuncher Ring at Sector 50; they are transferred from the Debuncher Ring to the Accumulator Ring at Sector 10 and are extracted from the Accumulator Ring at Sector 30. Tune-up protons from the Booster Enclosure are also injected into the Debuncher Ring at Sector 30.

The Rings Enclosure has a constant level floor throughout and at the same Elevation 726 ft. as the Target Hall and Antiproton Transport Enclosures. The Rings Enclosure is 8'-0" high and of width varying between 17'-8" to 35'-0". Most of the enclosure is clear span; only at Sectors 20, 40 and 60 are walls placed to reduce the very wide roof spans.

The Debuncher Ring is installed at Elevation 728'-6", or 30" above the floor along the outer wall of the enclosure. The Accumulator Ring is at the same height along the inside wall and the Sector 10 Beam Transfer is also at this height. Both Rings and Beam Transfer components are floor mounted. The Extracted Beam and both Injected Beams enter the Rings Enclosure at Elevation 732'-6", or 18" below the ceiling, and all these components are suspended from the ceiling.

Cable trays, power bus, piping and other utilities are ceiling-mounted or wall-mounted on both inner and outer walls. Numerous penetrations connect to the Service Buildings above Sector 10, 30 and 50.

Six stairway-labyrinths provide personnel access to and emergency egress from the Rings Enclosure. These stairways are located near the ends of the straight Sectors 10, 30 and 50 and connect to the Service Buildings above. There is also personnel access through the Antiproton Transport Enclosure that leads into and out of the Target Hall.

Three heavy equipment hatches are located at the curved Sectors 20, 40 and 60. These hatches are fitted for removable concrete shield blocks so that the shielding integrity of the entire Rings Enclosure is maintained. Equipment also may be rolled into the Rings Enclosure through the

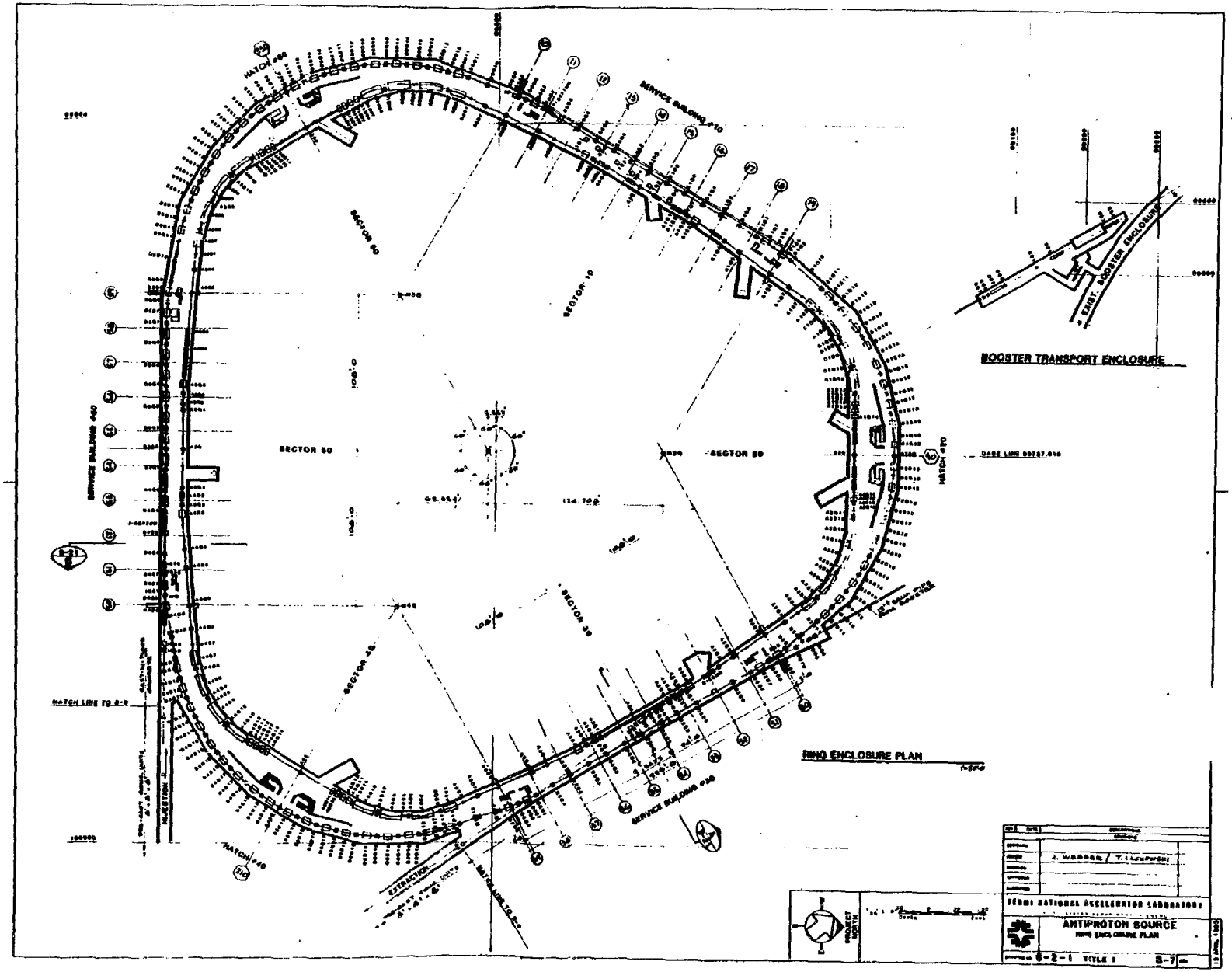
BOOSTER TRANSPORT ENCLOSURE
RING ENCLOSURE PLAN
SECTOR 50
SECTOR 10
SECTOR 20
SECTOR 30
SECTOR 40
SECTOR 60
SERVICE BUILDING #10
SERVICE BUILDING #20
SERVICE BUILDING #30
SERVICE BUILDING #40
SERVICE BUILDING #50
HATCH #10
HATCH #20
HATCH #40
HATCH #50
EXTRACTION
MATCH LINE TO B-9
FERMI NATIONAL ACCELERATOR LABORATORY
ANTIPROTON SOURCE
RING ENCLOSURE PLAN
B-2-1
B-7

Figure 14-5

Antiproton Transport Enclosures. Lightweight and compact equipment may be lowered into the Rings Enclosure via a 500 pound equipment lift that connects to the Service Buildings at Sector 10, 30 and 50. During construction and prior to final backfilling, an open wall panel and earth ramp will temporarily provide access into Sector 30 where the Booster beam pipe eventually will be installed.

Ventilation of the Rings Enclosure will be accomplished with three air intakes in the Sector 10, 30 and 50 and three exhaust fans at the Sectors 20, 40 and 60. A portion of this ventilation system will provide the air supply for the Antiproton Transport Enclosures.

Earth berm defines the location of the Rings Enclosure below. The berm is interrupted by the Service Buildings and by the Hatches. Berms from the beam transport lines join into the Rings berm.

14.1.6 Antiproton Service Buildings. The three Antiproton Service Buildings 10, 30 and 50 derive their numbers from the Rings Enclosure Sectors over which the buildings are sited. These service buildings interrupt the Rings Enclosure Berm and, with the berm, emphasize the shape and location of the Debuncher/Accumulator Rings below.

The three service buildings are identical in exterior appearance and nearly identical in interior construction and function. Each building is 35 ft wide and 220 ft long and approximately 14 ft high. Sloping textured concrete walls along the long dimension are interrupted with window, door and louver openings and contrasting texture panels. The end walls are vertical with a massive appearance abutting into the earth berm. The architecture reflects the construction of the Linac, Transfer Gallery and Cross Gallery.

Access to the three service buildings is from a loop road comprised of Kautz Road, Giese Road and Indian Road. A personnel door and an equipment door is near each end of a service building and opens out on the front parking area.

The principal function of each service building is to provide space for the power supplies, control equipment, detection electronics and cryogenic equipment that relate to the accelerator components in the Rings Enclosure below. Much of this equipment is audibly and electronically noisy and requires both water and air cooling systems.

Several special areas are partitioned off in the service buildings. In Service Building 10, a control room requires special air conditioning. In Service Building 30, a cryogenics room separates the machinery noise as well as special ventilation requirements from the balance of the building. Service Building 50 has no partitions, but rather wire cages around certain power supply systems.

Personnel access from the service buildings down to the Rings Enclosure below is through a stairway/labyrinth at each end of the building. Doors at the top of each stair provide radiation interlock, ventilation separation, entrance to the service building and emergency egress. Earth shielding is placed around the stair/labyrinths selectively to maintain the radiation shielding integrity.

The 500-pound equipment lifts are not personnel lifts, but are located, enclosed and shielded for both radiation and personnel safety requirements.

Ventilation equipment for both the Rings Enclosure and service building is contained in the service building. No external ventilation units are used. The air supply for the Rings Enclosure is brought into the left end of each building and fed down the stairway/labyrinth opening. Within each service building, approximately 5 to 7 air conditioning units will be installed under the sloping outside walls. Chilled water and heating water will connect to fan coils in these units.

Secondary power enters each service building at the left end. Process water systems enter each service building from headers in the Rings Enclosure below. Cryogenic piping from F3 enters Service Building 30 through a shielded below-floor trench. Conduits connect the Rings Enclosure to each service building.

14.1.7 Booster Beam Enclosure and 8 GeV Target Station. The Booster Beam Enclosure is an underground structure approximately 120 ft long and, together with beam pipe, links the Booster Accelerator to the Rings Enclosure at Sector 30. The first 25 ft of existing beam pipe connects the Beam Enclosure to the Booster Accelerator Enclosure. New beam pipe, 460 ft long, connects the Beam Enclosure to Sector 30.

The Booster Beam Enclosure is a rectangular cross section, 8'-0" wide by 8'-0" to 12'-0" high, and contains the Target Station equipment and beam transport magnets. The upstream group of magnets are floor mounted, and the downstream magnets are suspended from the ceiling as the beam pitches up and bends level to run to injection magnets in the Debuncher Ring at Sector 30.

Three types of access are provided into the Booster Beam Enclosure. For placing the Target Station steel plate and drawer modules, a removable roof slab is used above the Target Station. Steel is placed during the construction phase, and the roof slab replaced and backfilled over.

Magnets and other equipment are lowered into the enclosure through a new hatch that will be filled with concrete shield blocks during beam operations. Small items may be also rolled in from the adjacent Booster Accelerator enclosure at a common floor elevation.

Personnel access and emergency exit from both the Booster Accelerator Enclosure and the Beam Enclosure will be by a new stair structure which replaces the existing stairs that are demolished by the new construction.

Adjoining the stair structure and hatch opening at grade is a small power supply room, 13 ft x 20 ft. Conduits will run from this room down to the enclosure below and other conduits will connect the Booster Accelerator Enclosure to the Beam Enclosure. Ventilation fan and air supply equipment will also be contained in the power supply room.

A new parking area southwest of the Booster Berm will provide access to the equipment hatch. A low shielding berm will define the beam line and enclosure running from the Booster Berm to the Rings Enclosure Berm. Additional steel will be placed where required above the beam pipe that passes below the South Booster, Well Pond and Indian Roads.

14.1.8 Radiation Shielding. The Antiproton Source Enclosures will provide adequate personnel shielding. Consideration will be given to various operational conditions of the program and to the major components in the target halls, transport lines, and Debuncher/Accumulator Rings. Four conditions are of interest:

a. Tune up with 8-GeV protons from Booster.

b. Antiproton production and accumulation.

c. Debuncher/Accumulator Enclosure access during tune up on the antiproton target.

d. Work on the antiproton target station.

The sources of radiation considered are:

a. During tune up with 8-GeV protons from the Booster:

    1. Targeting losses in the Booster area.

    2. Accidental loss of transferred beam in the 8-GeV line between Booster and the Debuncher Ring.

    3. Accidental loss of 8-GeV proton beam in the Debuncher/Accumulator Ring Enclosure.

    4. Residual activity of Booster target.

b. During antiproton operation:

    1. Targeting losses in the antiproton target hall.

2. Accidental loss of beam in 120-GeV transport line between the Main Ring and the Debuncher Ring.

3. Accidental loss of stored 8-GeV beam in Accumulator Ring.

4. Residual activity of target.

Expected radiation levels under normal operations in all areas with the exception of the antiproton target station will be minimal in any accessible area. The area adjacent to the antiproton target station will be a designated radiation area with posting and authorized access only. Normal operation will be equivalent to the worst case for both the antiproton and Booster target stations. In other areas, accidental loss of the entire beam is the worst case. The following assumptions are being used in designing the shielding:

a. Tune up of the Debuncher/Accumulator Rings:

   1. Targeting in the Booster area to reduce the 8-GeV intensity from 3E12 protons per 2 sec to a maximum of 1E11 protons per 2 sec transmitted to the Debuncher Ring.

   2. Injection of 1E11 8-GeV protons per 2 sec into the Debuncher and Accumulator Rings.

b. Antiproton operation:

   1. Proton targeting for antiproton production with 3E12 protons per 2 seconds at 120-GeV.

   2. Stored beam in Accumulator Ring of E12 at 8-GeV.

Antiproton production operation is the worst case for the 120-GeV transfer line and target station, and proton tune up is the worst case for the Accumulator Ring and the 8-GeV transfer line and Booster target station. Calculated dose rates assume these conditions.

Shielding materials to be used include compacted earth, regular density concrete and steel plate. Various combinations and thicknesses of these materials will be proportioned according to the limitations of economic design and space. Areas of special shielding design are described below:

Tune Up Booster Targeting: The Booster target area will be an exclusion area with no personnel access while the beam is on. All areas accessible to personnel while the beam is on will have adequate shielding to bring the radiation levels to 2.5 mrem/hr or less. Sufficient shielding of the target will be provided to allow beam off personnel access to the target area.

Outdoor Area Over 8 GeV Transfer Line: A combination of shielding and interlocked devices will be used to insure that the above ground loss rate under accident conditions will not exceed 10 mrem per hour.

Area Above Antiproton Target: This area will be an exclusion area. No personnel will be allowed to work in this area during normal operation. When not operating, personnel will be allowed access. Signs and concrete block walls with interlocked gates will be used to prevent access during beam on conditions.

Area Adjacent to Antiproton Target: Precast regular density 150 pcf concrete blocks will be placed on the floor to separate this from the area above the target and to provide shielding. This barrier will be 3 ft thick and 9 ft tall. Normally personnel will have access to the exterior side of this barrier. This indoor area will require access restricted to authorized personnel only.

Access Labyrinths: There will be several labyrinths throughout this project to permit access to areas of 8-GeV up to 120-GeV beam energy. They will provide a shielding effect equivalent to the adjacent shields. The labyrinths will be consistent with Fermilab experience.

Road Crossings: Access roads over beam enclosures and transfer lines will be shielded to conform with uncontrolled outdoor areas with minimal occupancy.

Air Activation: Air sampling equipment will be installed to monitor activation of air from targeting operations. Ventilation systems will be designed to protect occupied areas and to purge target areas prior to access.

Soil Activation: Sufficient shielding will be included around the targets to insure that calculated soil activation will be below release limits and Fermilab guidelines. Underdrain sumps for the target station will be available to monitor soil activation.

14.1.9 Survey and Alignment Control. A coordinated system of monuments, benchmarks and working points is planned for complete geometric control of the project construction from initial site work to final machine component alignment.

Two principal base lines, the Extraction Base and the Booster Base, relate the Main Ring, Booster and Antiproton geometries. Other monuments tie in the three-fold symmetry of the Antiproton Ring, the Target Hall and the Booster Beam Enclosure. Additional monuments are used for the road alignment and utility location

For component alignment, a series of offset lines and monuments will form a closed traverse through the Debuncher and Accumulator Rings

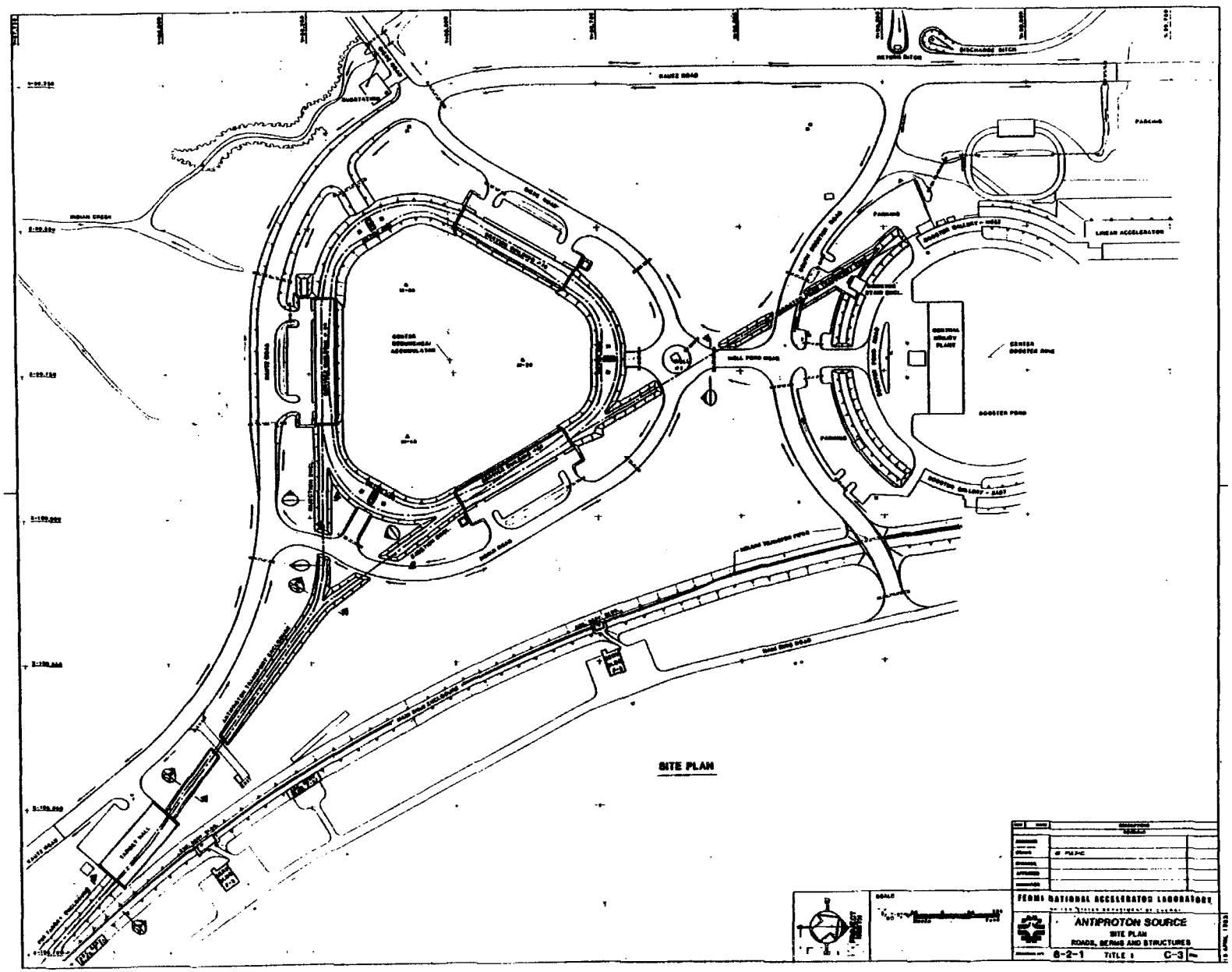
SITE PLAN
FERMI NATIONAL ACCELERATOR LABORATORY
ANTIPROTON SOURCE
SITE PLAN
ROADS, BERMS AND STRUCTURES
8-2-1
C-3

Figure 14-6

Enclosure. Reference to the internal offset traverse and the external monuments will be provided by sight lines through the equipment hatches and vertical sight tubes up through the berms. Other offset lines will extend the geometry through the Target Hall, Pretarget Enclosure, Antiproton Transport Enclosure and Booster Target Enclosure.

Elevation control benchmarks will be referenced to the Main Ring and Booster Systems. In strategic locations with the Target Hall and Debuncher Ring, concentrically sleeved deep concrete piers will be installed for long term stability of primary benches.

14.1.10 Roads, Hardstands and Parking. Access to the Antiproton Source site by Fermilab personnel is from relocated Kautz Road that runs along the west parking lot by Wilson Hall and the Booster Gallery Enclosures. The Subcontractor's construction traffic will be entering the site via the south Kautz Road entrance off Illinois Highway 56. The roads of the project are shown in Fig. 14-6.

Portions of three roads will surround the Antiproton Ring Enclosures. Relocated Kautz and Giese Roads provide access to Service Buildings 10 and 50 and to Hatch 60. The new Indian Road provides access to Service Building 30 and to Hatch 20 and 40. A short connector, Well Pond Road, joins Indian and Giese Roads to the present Booster area.

The new South Booster Road joins the relocated Kautz Road with the existing Main Ring Road. The existing berm crossing point is preserved to maintain the present Helium Transfer Line underpass. The South Booster Road intersects the new Well Pond Road and provides access to the new Booster Beam Enclosure as well as parking areas south of the Booster Berm. The present Kautz Road provides convenient access to the Target Hall and to the Pretarget Enclosure.

Parking areas are provided at each of the Antiproton Service Buildings, at the Target Hall and at the Booster Beam Enclosure. Additional parking is also provided between the South Booster Road and the existing Booster Berm.

Hardstand Areas adjacent to the Target Hall, Hatches and Service Buildings are provided. In addition, the adjacent road shoulders and designated parking areas may be used when an occasional large rigging job demands.

A portion of Kautz Road and Giese Road near Service Building 10, Hatch 60 and Service Building 50 will be constructed on a geotextile mat. Due to the considerable depth of unsuitable material at this location, it is not economic to remove such material and backfill with aggregate in the conventional manner. Instead, only the organically filled topsoil and clay layers will be removed, a heavy geotextile mat will be laid and a graded aggregate road subbase will be placed. The principal function of the

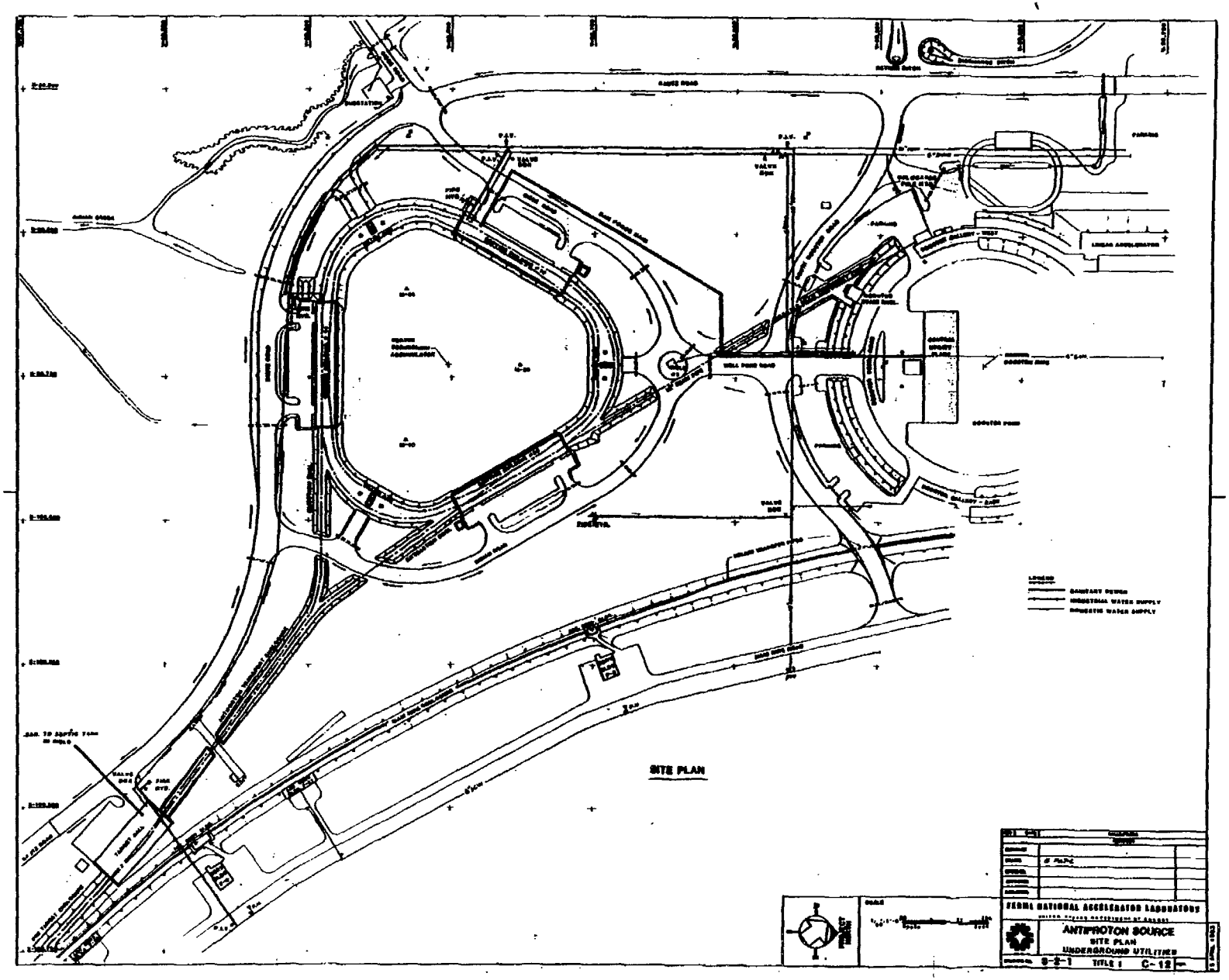
SITE PLAN
FEDERAL NATIONAL ACCELERATOR LABORATORY
ANTIPROTON SOURCE
SITE PLAN
UNDERGROUND UTILITIES
TITLE I
C-12

Figure 14-7

geotextile mat is to separate the road aggregate from the clayey-silt and fine sand lenses in the lower strata.

Concrete will be used for door aprons, sidewalks and ramps. Bituminous materials will be placed on all roads and parking areas. Coarse aggregate will surround substation pads and other mechanical equipment pads.

14.1.11 Underground Utilities. Power ducts, communication ducts, industrial cold water (ICW) piping, domestic water (DOM) piping and sanitary sewers (SAN) will be extended from existing utility corridors near the Central Utility Plant, south of the Booster Berm, and along the Main Ring Road. These are all shown in Fig. 14-7.

A new 13.8-kV power duct bank will be installed for the Antiproton Source and will run under the existing Main Ring Road. The duct bank will connect from Manhole P71 near the S & C Switches to new manholes along the Main Ring A-Sector and F-Sector Service Buildings and to the new substations at the Target Hall and the three Antiproton Service Buildings.

A new communication duct bank will also parallel the new power duct and connect Service Building 30 to the Main Ring. Other duct bank extensions will join the Pretarget Enclosure to the Service Building F23, the Antiproton Transport Enclosure to Service Building F27 and the Antiproton Ring Enclosures to the Central Utility Plant.

Another group of six communication duct banks connect various sectors of the Antiproton Ring Enclosures with minimum length, nearly straight line runs across the interior of the Ring. Sector 10 is joined with two duct banks to Sector 30; Sector 20 is joined to Sector 40, 50 and 60; and Sector 30 is joined to Sector 60.

Industrial cold water (ICW) piping will be extended from the utility corridor by the South Booster Road at two places. These lines will run along Giese Road, Indian Road and Kautz Road and will serve fire hydrants and hose cabinets at Service Buildings 10, 30 and 50. ICW piping will also be extended from the Main Ring Road corridor under the Main Ring Berm and to the Target Hall fire hydrants and hose cabinets.

Domestic water (DOM) piping will parallel portions of the new ICW piping and will connect to Service Building 10 and the Target Hall. Domestic water will not be available at Service Building 30 and 50.

Sanitary sewers (SAN) will be extended with a lift station from the Central Utility Plant along Well Pond Road and Giese Road to Service Building 10. Sanitary facilities will not be available at Service Building 30 and 50. Due to the remote location, the Target Hall sanitary lines will be connected to a septic field system south of Kautz Road.

14.1.12 Primary Power, Switchgear and Substations. The Antiproton Source will be powered from three primary feeders. Two of these feeders are existing feeders that will power the geographical extremities of the project that are near the Main Ring and the Booster Accelerators. One new dedicated feeder will power the bulk of the Antiproton Source loads.

The existing Main Ring Pulsed Feeder 21A4 will connect to the existing Service Building F23, in which are housed the power supplies for the Pretarget Enclosure.

The existing Booster Pulsed Feeder 41 will connect to the new power supplies for the Booster Beam Enclosure.

The new dedicated Feeder 49 will power the Target Hall and the existing Service Building F27 in which are power supplies for the Antiproton Transport Enclosure. However, the principal load for Feeder 49 will be the primary loop around the Antiproton Ring connecting the substations at the new Service Buildings 10, 30 and 50.

A three-way air switch will be installed to provide feeder backup at the Service Building F3 area. Both Feeder 49 and Feeder 48 will be connected to the Antiproton Source primary loop through this switchgear so that each feeder backs up the other. Local switchgear at the Service Buildings 10, 30 and 50 will not be used, but the primary feeder loop ends will be in the substation cubicle to allow manual cable disconnect for primary cable replacement in any part of the loop.

The existing Feeder 48 will be replaced by new feeder cable installed through the new duct bank from the S & C Switchgear to the Service Building F0 area. Direct buried cables will connect all present Feeder 48 loads to the nearest power manhole of the new installation.

The new dedicated Feeder 49 will be derived by freeing up one leg of Feeder 22B at the P71 manhole near the S & C Switchgear. New feeder cable will extend through the new duct bank to Manhole F23 as well as to the new three-way air switch at F3. From this switchgear, Feeder 49 extends through the duct bank that surrounds the Antiproton Rings Enclosure.

An existing 1.5-MVA substation will be used at Service Building F23, and will be connected to pulsed Feeder 21A4. At Service Building F27, a 1.5-MVA substation will be connected to the dedicated Antiproton Feeder 49. A 0.5-MVA substation will be installed at the Target Hall and will be connected to Feeder 49.

Three new 1.5-MVA substations will be installed at Service Buildings 10, 30 and 50. In addition, at Service Building 50, two 1.0-MVA special substations configured for 12-phase operation of power supplies will be installed.

14.1.13 Secondary Power and Distribution. 480-volt, 3-phase power will be brought into the three Service Buildings and the Target Hall and will be terminated into large switchboards. Branch feeders and smaller 480-volt panelboards will distribute the power through the Service Buildings, down through the Rings Enclosure, Pretarget Enclosure and Antiproton Transport Enclosure. Stepdown transformers and smaller panels will provide 120/208 volt, 1 and 3-phase power as required.

The 12-phase power from the special power-supply transformers will be brought in directly to the power-supply equipment at Service Building 50. Except for this case, all other technical power and all house power will be obtained from the same substations and switchboards.

Regulated power from static line conditioners or motor-generator equipment will not be furnished in the Service Buildings or Rings Enclosure. It may be that the dedicated Feeder 49 serving only the Antiproton Source loads, will provide sufficient isolation from other pulsed loads. An alternative that will be considered in Title II design is to reactivate the reserve 345 kV Master Substation Transformer 82 and use this equipment to supply the Feeder 49 loads.

Emergency power will be provided in limited amounts for critical equipment by a 480-volt, 3-phase diesel driven generator mounted next to the substations at Service Building 50. Automatic switch-over and start-up equipment will be provided. Connected loads will be limited to deep sump pumps, instrument air compressors and critical cryogenic equipment such as LHe pumps or vacuum pumps.

14.1.14 Process-Water Systems. The four process water systems that will be used in the various areas of the Antiproton Source include Cooling Pond Water (CPW), Low Conductivity Water (LCW), Hot Water (HTW) and Chilled Water (CHW). In addition, two small closed loop subsystems will be used for the targeting and dump components in the Target Hall. Air cooling is planned in the Booster Target Station.

Existing CPW intake and discharge piping from the Booster Pond to the existing Swan Lake and Kidney Pond ditches will be rerouted for the Kautz Road/South Booster Road construction. The intake pipe will be replaced with larger capacity pipe and the intake structure in the Booster Pond will be rebuilt. The discharge piping will be rerouted to a new bubbler on the west side of Kautz Road. Ditches will be realigned to suit.

The LCW cooling system for the Antiproton Target Hall and Pretarget Enclosure will be extended from the Main Ring LCW system at Service Building F23. Similarly, the LCW cooling systems for the Booster Enclosure will be extended from the Booster LCW system at Booster Station 3.

The LCW cooling system for the Rings Enclosure will be derived from new equipment in the Central Utility Plant and new piping that extends

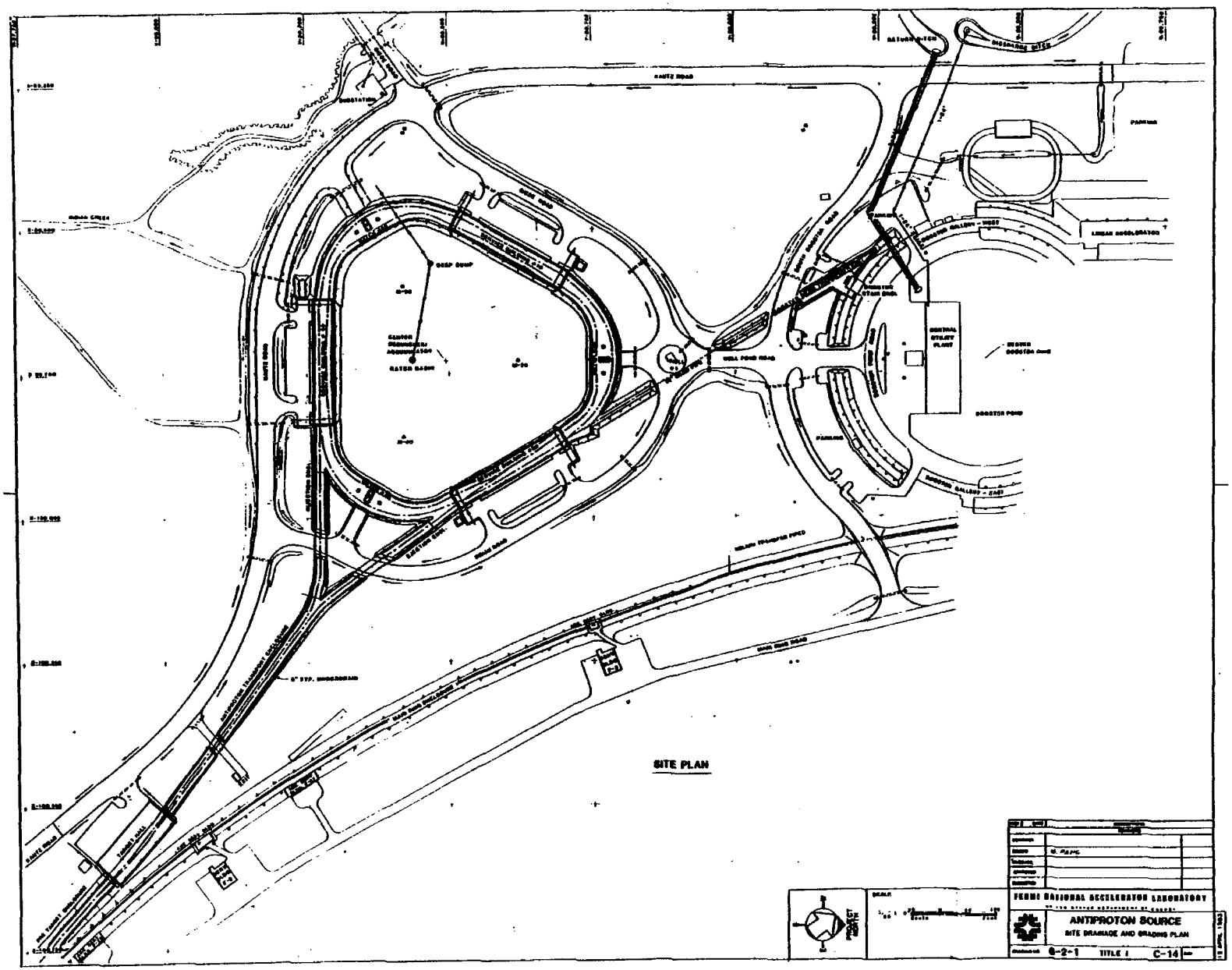
SITE PLAN
FERMI NATIONAL ACCELERATOR LABORATORY
ANTIPROTON SOURCE
SITE DRAINAGE AND GRADING PLAN
C-14

Figure 14-8

along Well Pond Road into the Hatch 20 area. Primary heat exchange for this LCW system will be to the Booster Pond, Kidney Pond and Swan Lake air-water surfaces. Except for the shared primary heat exchange, the new LCW system will be completely independent of the existing Linac, Booster and RF systems in the Central Utility Plant. New CPW/LCW heat exchanger, duplex pumps, expansion tanks, piping and controls will be installed on the upper platform in the east end of the Central Utility Plant. New LCW headers will extend out the south utility tunnel and continue as direct buried piping into the Hatch 20 area.

Hot water will be used for the fan coil units of the Service Buildings and Rings Enclosure. However, due to remote location, hot water is not economic to use in the Target Hall, Pretarget Enclosure and Booster Beam Enclosures. Electric fan coils will be used for these areas instead. There is sufficient capacity in the Central Utility Plant boilers and the HTW piping will be extended down the south utility tunnel and continue as direct buried piping into the Hatch 20 area.

The chilled water required for the fan coil units and other electronic equipment in the Service Buildings and Rings Enclosure will also be obtained from the existing chiller systems in the Central Utility Plant. Chilled water for the Booster Beam Enclosures will be obtained from the nearby existing Booster Gallery. For the Target Hall and Pretarget Enclosure, raw chilled water will be obtained from the systems in the RF Building near Ring Service Building F2.

Piping for the LCW, CHW and HTW systems will be direct buried from the Central Utility Plant into the Rings Enclosure. Within the enclosure, the piping will be wall or ceiling mounted. Headers will be extended from the enclosure up to the Service Buildings.

14.1.15 Finished Site Drainage. Site drainage after all construction is complete will be accomplished with surface grading to open ditches that will drain south and west into Indian Creek. Only the area enclosed by the Rings Enclosure Berm will be drained through catch basins and a pumped deep sump. The drainage plan is shown in Fig. 14-8.

Roof drainage will be collected within the buildings and will be routed out the buildings, under the roads and parking areas and into the adjacent road ditches. Discharge piping from the underdrains deep sumps will also be run to these road ditches. Roads and parking areas are crowned and sloped toward ditches as well. Swales and slopes along the Main Ring Berm and the new Antiproton Source Berms will divert surface drainage away from the buildings and to the road ditches. A small dike along the eastern bank of the Indian Creek contains a high water overflow.

14.1.16 Landscaping. Special precautions will be observed during construction work to protect and preserve the large specimen oak trees within the meadow area bounded by the Antiproton Ring Berm. Trees will be fenced at the drip line where possible; temporary sheeting will be used where deep conduit trenches run near the trees and regrading around these trees will be avoided.

The meadow area within the ring will be graded only where needed for drainage to the catch basins. Topsoil will be replaced and the natural field grasses will be allowed to reappear. The meadow will not be mowed in the future.

Topsoil will be replaced on all other new or disturbed earthwork. Grass seed will be planted on flat areas, a limited amount of sod will be placed at ditch bottoms, and crown vetch cover will be sown on berm slopes and crests.

14.2 B0 COLLIDING BEAM AREA

The construction includes:

B0 Collision Hall consisting of an underground structure that will replace approximately 100 ft of the Main-Accelerator enclosure, and will contain the experimental physics detectors and both the accelerator and Energy Saver beam components. On the outside wall (away from the accelerator center) will be a large door and moveable shield wall that will provide access to the Assembly Hall.

B0 Transition and Equipment By-pass Enclosure consisting of an underground structure that connects the Collision Hall to the existing main accelerator enclosures, and provides a passage for personnel, utilities and magnet moving vehicle around the B0 Collision Hall.

B0 Assembly Hall consisting of a large pit at the elevation of the Collision Hall and adjoining to the shield-door passage, with a service floor at grade level, all covered by a high-bay building with an overhead crane. The various experimental physics detectors will be assembled, tested, and serviced in this hall prior to placement in the B0 Collision Hall.

B0 Site Development consisting of hardstands, access roads, drainage facilities, relocation of utilities, extension of services, and temporary earth retaining structures for construction sequencing and adjacent road and building protection.

B0 Primary Power consisting of 13.8-kV feeders, substations and switchgear for extending primary power to the B0 Experimental Area and into the B0 Assembly Hall.

More detailed descriptions of these individual packages follows below. A general plan of the building is shown in Fig. 14-9.

14.2.1 B0 Colliding Beam Experimental Area. The B0 Experimental Area has two completely underground structures, the Collision Hall and the Transition and Equipment Bypass Enclosure, and has a third above-ground structure, the Assembly Hall. All these structures connect with each other and to the main ring enclosure at the B0 straight section.

The Collision Hall is a large cast-in-place concrete structure which will replace approximately 100 ft of the main ring enclosure. The central region portion of the Collision Hall, 50 ft long, 50 ft wide and 35 ft high with a pit 4 ft deep, will contain the 2400-ton Central Detector. The backward and forward regions, which adjoin the central region, are 25 ft long, 36 ft wide and 30 ft high. Various toroidal magnets and detectors, ranging in weight from 400 to 600 tons will occupy the backward/forward regions.

The Transition and Equipment Bypass Enclosure is at both ends of and along the south wall of the Collision Hall. The transition portion, 15 ft wide, 10 ft high, and 40-50 ft long abuts up to the precast arch elements of the main ring enclosure. The Equipment Bypass, 7 ft wide, 9 ft high and approximately 160 ft long, joins into the transition portion. A stair shaft connect the forward region to the forward end of the bypass. All structures are cast-in-place concrete.

The Major Access Passage, approximately 34 ft wide, 37 ft high and 37 ft long connects the Collision Hall to the Assembly Hall. To the west end of the Major Access is a personnel labyrinth and the Minor Access Passage, 5 ft wide and 9 ft high. Moveable concrete shield doors block the Major and Minor Access Passages during accelerator operations. All structures are cast-in-place concrete.

The Assembly Hall is a steel structure at grade level, approximately 98 ft wide, 175 ft long and 31 ft high. The floor level inside the Hall is depressed 4 ft below the outside grade and reached by the ramp at the west end. A lower floor level, approximately 72 ft wide and 100 ft long, matches the floor and pit of the Collision Hall central region and Major Access passage. All below grade portions of the Assembly Hall are cast-in-place concrete.

Within the Assembly Hall is a crane bay, 75 ft wide and 175 ft long. A top-riding bridge crane with a 50-ton main hook and 10-ton auxiliary hook, traverses this area and serves both the grade level floor as well as the lower level. At the east end of the Assembly Hall, a portion of the foundation extends beyond the wall to form a drop hatch, 16 ft wide and 20 ft long.

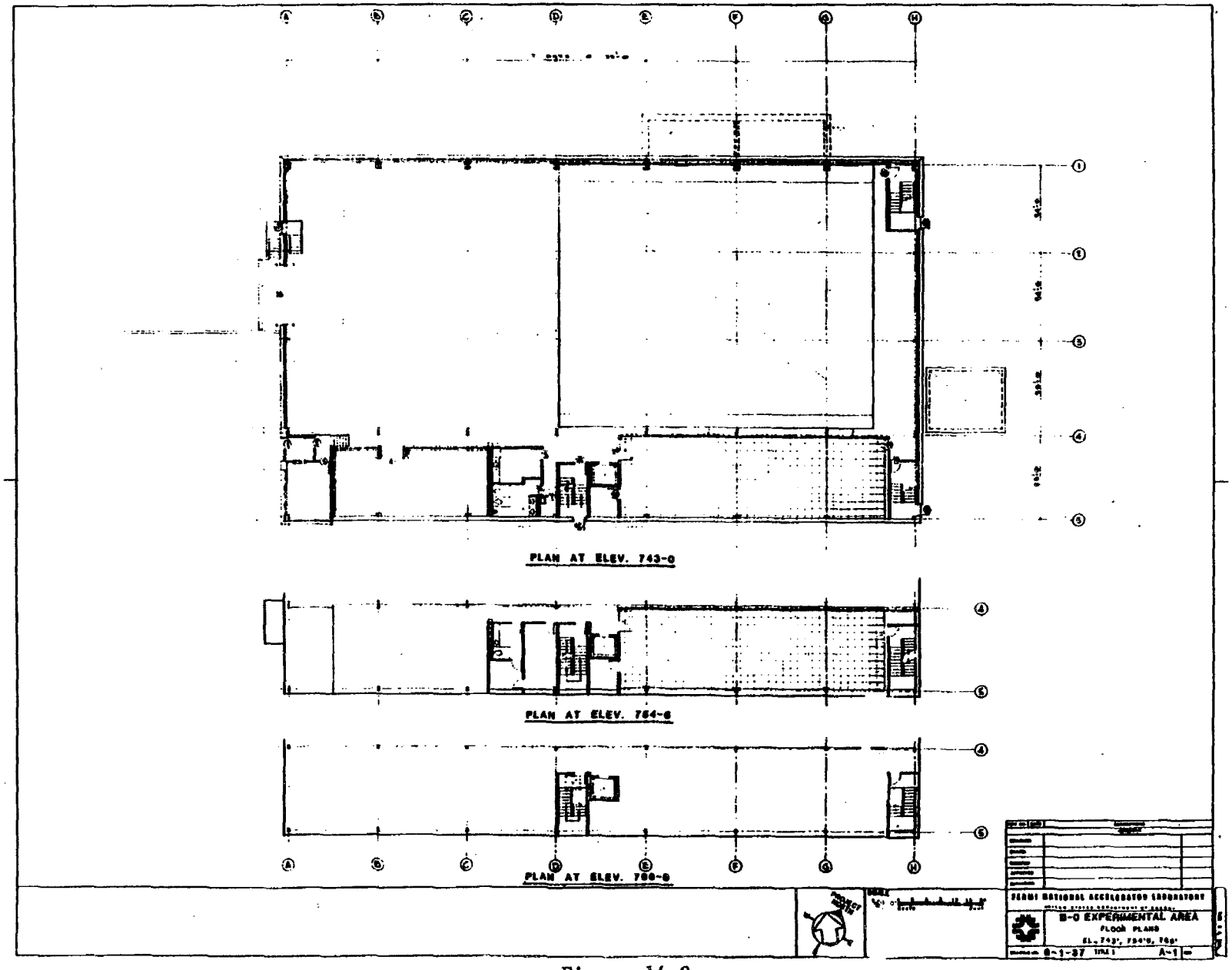
PLAN AT ELEV. 743-0
PLAN AT ELEV. 764-6
PLAN AT ELEV. 786-6
FERMI NATIONAL ACCELERATOR LABORATORY
B-0 EXPERIMENTAL AREA
FLOOR PLANS

Figure 14-9

The south bays of the Assembly Hall contain three floors. At the grade level is a Counting Room directly above the Major Access Passage, an Equipment Room, a Reception Office, a Kitchenette and a Men's Toilet. On the middle level is another Counting Room, a Women's Toilet, an Electronics Shop Area and an Electrical Equipment Area. The upper level will be used for mechanical equipment, storage and a Shop Area.

Three stairways and an elevator facilitate personnel access to the various floor levels in the Assembly Hall. Near the center of the south wall is a 2000 lb. elevator and stairway that serves all four levels in the Assembly Hall. In the northeast corner is another stairway serving the lower level and the grade level, while in the southeast corner is the third stairway that serves the grade, middle and upper levels. All stairways exist to the outside at grade level.

The main entrance to the Assembly Hall is on the west wall near the south corner. A small canopy is above a double door which leads into the Hall past a small reception office. Two other doors are on the east wall, another door is on the south wall, and no doors are on the north wall which is along side of Road D. An equipment door, 16 ft wide and 16 ft high, is on the west wall at the ramp.

The exterior of the Assembly Hall resembles that of the four industrial buildings to the north of Road D. A precast concrete wall 5 ft high capped with a ribbon of windows surround the Assembly Hall on the east, north and west elevations. Solid concrete walls that match the abutting earth shield berms are used on the south elevation. Vertical steel siding in a colored enamel finish is used above the concrete and window ribbon. The roof has the same slight slope as the industrial building roofs.

Embedded floor tracks and steel floor plates facilitate the movement of the large detector and shield-door loads on the lower operating floor levels in the Collision Hall and the Assembly Hall. The track system under the central detector will have indexing holes for the hydraulic lateral-moving systems. Other pull anchors will be provided for moving the shield doors and equipment transporters. Within the Collision Hall over the backward/forward regions, the roof will be designed for a future 5 ton underhung bridge crane.

The heating, ventilating, and air-conditioning systems in the Collision Hall will provide a variable rate of air exchange dependent on the operating mode and the season. To accommodate the wide spread of equipment head load, the air changes will vary between 1 to 12 per hour. The temperature wll range between 60° and 80°F and the relative humidity will not exceed 60%.

A large air-handling unit, with chilled-water cooling coils, electric heating coils and filters will be mounted at grade between the Assembly Hall and the berm at the west end of the Collision Hall. Intake air will

be distributed through underground ducts to four louvers on the west end wall of the Backward Region of the Collision Hall. A purge fan mounted at grade at the east end of the Collision Hall will exhaust air through underground ducts and four louvers on the east end wall of the Forward Region of the Collision Hall. Bypass and mixing dampers on both the air intake and exhaust systems will allow the maximum use of outside air for economic temperature control in the Collision Hall.

During short periods after beam shutdown in the Collision Hall, or in the event of accidental helium or other gas release, the air systems will operate on 100% outside air to rapidly purge the area. The intake and exhaust ducts are located on both sides of the beam lines as well as at floor level and ceiling level.

The Transition and Equipment Bypass enclosures will be ventilated by the systems in the main ring enclosure. Shielding walls may be used at either end of the Collision Hall during collider operations and partitions will isolate the air systems of the Collision Hall and main ring enclosure.

In the Assembly Hall, high-bay and other open areas, the seasonal temperature range will be 60° to 95°F, with no humidity control. Roof exhaust fans will ventilate at the rate of 1 to 2 air changes per hour. An air handling unit located on the upper level, with electric heating coils and intake and bypass dampers will provide make-up air. Additional heating along the outside walls, at doors and in the lower level pit will be provided by electric wall-hung heaters.

The Counting Rooms on the grade and middle levels will be air conditioned the year round. Temperature will range from 70° to 80°F, relative humidity will vary between 40% to 50% and ventilation will be between 4 to 8 changes per hour.

Two air-conditioning systems will be used in each of the Counting Rooms. For the electronic racks, a pair of air-conditioning units will distribute air into the underfloor cable space plenum, up through floor cut-outs and out the top of the racks. The second system will include an air-handling unit with both heating and cooling coils, ceiling diffusers and ductwork above the suspended ceiling. Heating will be provided by electric coils and chilled water coils will be used for cooling.

The reception office, toilets and kitchenette will be air conditioned from the same air-conditioning unit that serves the Counting Room ceilings.

The plumbing systems for the Assembly Hall include toilet facilities for the specified occupancy, electric water coolers, hot and cold domestic-water supply and connection to the site sewer system. Floor drains at the ramp, equipment door, the hatch and in the pits will connect to adjacent underdrain piping.

Underdrains at a level below the structural concrete mats will connect to two deep sumps. Granular backfill material will be placed around all outside walls to insure complete drainage and avoid buildup of hydrostatic pressure on the walls.

Fire protection systems will vary according to the occupancy, location and size of the area. In the Assembly Hall high bay and other open areas, wet sprinklers sized for "ordinary hazard" are provided. Dry pipe sprinklers with pre-action valving in combination with Halon systems are used for the Counting Rooms and the associated ceiling and floor spaces. Hose cabinets are placed at strategic locations about the Assembly Floors and the various levels. A wet standpipe with valving, alarms, siamese connection is located in the northwest corner of the Assembly Hall.

In the Collision Hall and Transition and Equipment Bypass Enclosure, the scientific equipment will serve as fire detectors similar to the operation of the main accelerator and other high radiation areas at Fermilab. Gas detectors will be installed and interlocked with the purge system where the possibility of flammable gas leaks may exist.

Electrical power will be distributed to local power panels from switchboards in the Assembly Hall. High intensity vapor lighting will be used in the high bays and fluorescent lighting will be used in rooms with normal height. Lighting levels will vary between 50 to 150 ft candles depending on the location. Exit lights and exterior lighting will be provided.

14.2.2 200-GeV Vertical Beam Bypass. See Sec. 7.3.

14.2.3 Experimental Equipment Foundations. The physical size and weight of the experimental detectors require massive and relatively stable foundations at approximately 18 ft below the colliding beams. A program of soil exploration down to bedrock has been run to better delineate the subsoil conditions and define foundation alternates.

Three foundation types have been studied; driven H-piling, drilled cast-in-place concrete caissons, and cast-in-place concrete mats. The H-piling technique has proved impractical due to extreme driving resistance indicated by the tough clays and scattered boulders at the depths required. Similarly, the drilled concrete caisson technique has installation difficulties and high cost disadvantages as well.

The massive concrete mat that serves as both an equipment foundation and a base for the underground structures has been investigated in considerable detail. Long term settlement has been computed to be on the order of 1/2". Of this amount, only 3/16" to 1/4" change is expected with the moving detector and shield door loads. The time for this settlement is short (several hours) since the design soil bearing pressure (6000 psf) is less than the creep pressure, indicating soil behavior as a linearly elastic material. No progressive long term settlement is expected since

the design soil bearing pressure is lower than the original in-situ earth pressure and preconsolidation stress.

14.2.4 Radiation Shielding. The B0 Colliding Beam Experimental Area will be designed to provide adequate personnel shielding. Consideration will be given to various operational conditions of the experimental program and to the location of the major detectors in the Collision Hall. Three conditions are of interest:

1. Detectors in place with Colliding Beams.
2. Detectors in place with Fixed Target Operations.
3. Detectors removed with Fixed Target Operations.

The sources of radiation that are considered are:

1. Accidental loss of beam on magnets in the vicinity of the B0 Collision Hall during acceleration
2. Accidental loss of beam during antiproton production
3. Accidental loss of stored beam
4. Higher intensities of these losses during fixed-target operations

Expected radiation levels under normal operations in all these cases are minimal in any accessible area. Accidental loss of the entire beam is the worst case for all three operating conditions and shielding has been designed for this worst case under the following assumptions:

1. Fixed-target operation has beam of 1×10^{14} at 1000-GeV with a 50 second cycle.
2. Colliding-beam operation has two beams each of 2×10^{12} @ 1000 GeV going in opposite directions. Antiproton production takes place using a proton beam of 2.5×10^{13} protons at 100-GeV with a 2 second cycle.

With these assumptions for accelerator operations, fixed target operations is the worst case and all calculated dose rates assume fixed target operations.

Shielding materials to be used include compacted earth, regular density concrete, high density concrete and steel plate. Various combinations and thicknesses of these materials will be proportioned according to the limitations of economic design and space. Areas of special shielding design are described below.

Berm above Collision Hall: Compacted earth at 130 pcf will be placed above the poured concrete roof slab for a total thickness combination of 11 ft. No personnel are normally required to work in or near this berm area. Calculated dose rate for an accidental loss at this location is 100 mrem/10^{14} 1000-GeV protons. This

outdoor area will require a radiation detector set to trip the beam after one such loss. In addition, signs and fences with interlocked gates that permit no access during beam on conditions will be used.

Shield Door at Collision Hall: Precast regular-density 150 pcf concrete blocks will be placed on a concrete-filled structural base frame. The door will be 12 ft thick with 1/4" staggered cracks in the block stack. Top and bottom clearances on the door will be 3" nominal, and a lapped side joint will provide 3" overlap for 6 ft thickness. Normally personnel will be working on the Assembly Hall side of the door. Calculated dose rate for an accidental loss at this location is 50 mrem/10^{14} 1000-GeV protons. This indoor area will require restricted to authorized personnel only.

Counting Room at Grade Level: Shielding for this area is provided by the aforementioned shielding door and the 12 ft of structural concrete and earth backfill of the Collision Hall major access passageway. Similar dose rates and access restrictions will apply.

Labyrinth between Collision Hall and Assembly Hall: This labyrinth will be sized with three legs and two cul-de-sacs, on the basis of Fermilab experience in previous construction. Calculated dose rate at this labyrinth for an accidental loss is 40 mrem/10^{14} 1000 GeV protons. This labyrinth is located in the same physical area as the Shield Door and will be subject to the same access restrictions.

CHAPTER 15

OPTIONS FOR FUTURE IMPROVEMENTS

The Antiproton Source design must include not only the best system for antiproton production utilizing presently known techniques, but also provisions for improvements either from new inventions or from operational experience. In this chapter, we discuss a number of possible improvements that could increase the peak luminosity or decrease the accumulation time, thus increasing the average luminosity. It is to be emphasized that these improvements are not part of the construction project.

15.1 Momentum Cooling in the Debuncher

As was pointed out in Chapter 4, there is time during the 2-sec Debuncher cycle for cooling after the initial debunching. It is planned to do transverse cooling as part of the initial design. But it is also possible to cool in momentum by a factor 2 during the same time. This will reduce the cooling power needed in the Accumulator or increase the initial cooling speed for the same power.

The momentum cooling will utilize a notch filter (Thorndahl method). The gain shaping is obtained with a long shorted cable that resonates at harmonics of the revolution frequency. This method is preferred to the Palmer method, where the gain variation is obtained with two pairs of pickups in difference mode in a large dispersion region. Because of the large electronic gain needed to obtain the desired cooling rate, thermal noise is a potential problem. Cooling would actually be impossible for our case with the Palmer method, since in it noise is not effectively filtered and would cause the equilibrium beam width to be larger than the initial beam spread. With the filter method, the thermal noise still predominates, but its effect is greatly reduced. The method is very similar to the one used for the precooling step in the CERN AA Ring.

At the start, the beam has a very small energy spread, between 25 and 30 MeV. To get a significant signal, large bandwidth and a large value of η are required. We assume a bandwidth from 2 GHz to 4 GHz and $\eta = -0.004$. An even larger value of η would be desirable, but then extremely high rf voltages would be needed for debunching.

To sharpen the depth of the notches and to cut down thermal noise in the frequency region where there is no beam, the filter will use a cable whose delay matches the revolution period and whose far end is shorted. This filter creates notches not only at harmonics of the revolution frequency, but also at frequencies halfway between. The overlap factor, the ratio of the beam Schottky band width to the separation of neighboring notches, ranges from 0.1 at the lower end to 0.2 at the upper end of the bandwidth.

The signal loss caused by beam dispersion and the cable delay between pickups and kickers is not a problem. If the distance between pickups and kickers is 0.35 times the circumference length, the fraction of signal lost is only 0.5% at the lower end of the bandwidth and 2% at the upper end.

The signal cable is approximately 125 m long. There is a time difference of about 150 nsec between the beam path length and the cable delay. Power amplifiers have electronic delays around 60 nsec.

The room-temperature performance of a copper cable seems to be adequate for the signal cable, where with a 4.45 in. outer diameter, we expect fractional losses between 18% at 2 GHz to 25% at 4 GHz. These losses can be compensated by raising the electronic gain. The phase variation is also reasonably small; from 3% at 2 GHz to 4% at 4 GHz.

To make cooling possible, differentiation of the signal in the network is required. This is accomplished with a short cable, one or two inches long, shorted at the far end.

Pickups and kickers will be made of strip-lines. They will be used for both momentum and betatron cooling. Pickups and kickers have the same configuration. They are grouped in four tanks. Each tank is 4.5 m long and accommodates 4 x 128 plates. The plates are shorted to ground at the upstream ends and their downstream ends are combined together. The combination is done under vacuum, and there are only two leads coming out at the downstream end of each tank.

15.2 Target Development

In order to achieve targets that would survive smaller beam spots (larger energy density deposited) the following approaches to target design are under study:

(i) Laminated targets with the plane of the laminations perpendicular to the proton beam would decrease the amount of material flow within the plastic zone.

(ii) Filamented targets would allow the introduction of slip planes across large temperature gradients, resulting in a lowering of the stresses.

(iii) Powder targets produced by embedding high-density particles in graphite by powder metallurgy would incorporate the excellent shock and high-temperature properties of graphite, allowing enough energy deposition to melt the metal particles. The lower antiproton yield resulting from the lower average target density could be overcome by a much smaller beam spot.

A research and development program to test these ideas will be underway before the $\bar{p}$ source becomes operational.

15.3 Improvements in Stochastic Cooling

The pace of electronic development is strikingly rapid and we expect that high-power, large-bandwidth systems will be significantly improved in the next decade. In particular, we expect that bandwidth will be increased by raising the high-frequency end of amplifier systems and that electronic noise will be lowered. Either of these developments could aid the cooling in the Accumulator. If we could predict what these advances might be, we could design them into the system. Failing that, we can make the design as flexible as possible, leaving aperture and straight-section space for testing and installation of these systems. We plan to utilize the shorter 4 ft and 10 ft straight sections for development tests of new cooling systems.

15.4 Electron Cooling of the Core

It would be possible at some later time to add an electron core-cooling system to the Accumulator. This system could be used in several different ways:

(i) to counteract intrabeam scattering of a stochastically cooled antiproton beam and to increase its density beyond what stochastic cooling can achieve;

(ii) to use the electron beam directly as the accumulating cooling system. This would require that the transverse emittance of the antiproton beam be reduced stochastically to approximately 0.5π mm-mrad before electron cooling. This stochastic cooling could be done with large momentum spread to get good mixing. Use of electron cooling would then give very high accumulation rates.

We can expect to do this core cooling at full energy, 8-GeV. Electron beams based on electrostatic generators are now being developed for free-electron laser studies with electron energies of 3 to 6 MeV and beam currents of 5 to 10A. The cooling region would be unmagnetized and could be installed in one long straight section of the Accumulator.

For this application, an electron beam of good emittance, good reliability, and very good collection efficiency would be required. We are now engaged in a program in collaboration with National Electrostatics Corporation to measure emittance and collection efficiency and to investigate long-pulse operation.

APPENDIX A

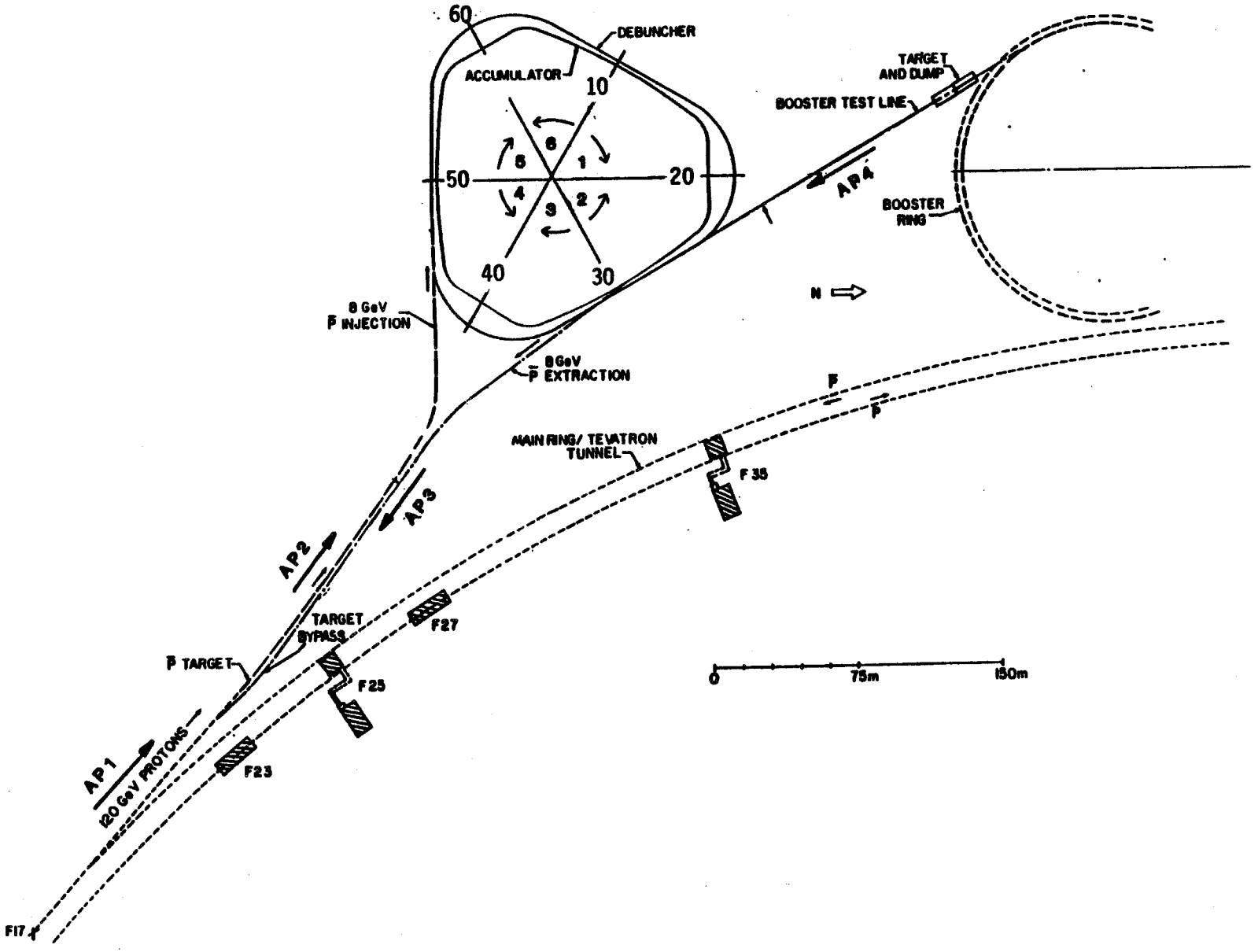
60
DEBUNCHER
ACCUMULATOR
10
50
20
40
30
6
1
5
4
3
2
TARGET AND DUMP
BOOSTER TEST LINE
AP4
BOOSTER RING
N
8 GeV P INJECTION
8 GeV P EXTRACTION
P
P
MAIN RING/ TEVATRON TUNNEL
F 35
AP3
AP2
TARGET BYPASS
F27
P TARGET
F25
AP1
120 GeV PROTONS
F23
F17
0
75m
150m

Figure A-1

APPENDIX A. BEAM LINE, ACCUMULATOR, AND DEBUNCHER MAGNET NOTATION

The Tevatron I Antiproton Source consists, in part, of five beam transfer lines and the two rings. Lists of element names for each of these are given below.

1. BEAM TRANSFER LINES

Each transfer line is numbered along the beam direction. (See Fig. A-1) Each element is designated by a three to five character label consisting of a line label, magnet label, and magnet number. The following magnet codes are used:

B	horizontal	dipole
BV	vertical	dipole
BR	rotated	dipole (45°)
Q	quadrupole	
S	sextupole, when used.	

A. 120-GeV proton line, MR to Target Line AP-1 (Antiproton 1, similar to N1, M1, M2, etc.)

All elements in this line start with "P" for proton. the elements in this line, in sequential order are:

NAME	DESCRIPTION
Main Ring F17	Extraction Location
PLAM1	Extraction Lambertsons
PLAM2	
PB1	Horizontal Dipoles
PB2	
PBR1	Rotated Dipoles
PBR2	
PQ1	Quadrupoles
PQ2	
PBR3	
PB3	
PB4	
PB5	
PQ3	
PQ4	
PQ5A	Pair of quadrupoles run as one
PQ5B	
PBV1	Vertical Dipoles
PBV2	
PQ6A	
PQ6B	
PQ7A	
PQ7B	
PQ8A	

PQ8B	
PQ9A	
PQ9B	
Target	End of this line

B. 8-GeV antiproton line, target to Debuncher Line AP-2.

All elements in this line begin with "I" for injection. The elements in this line, in order are:

NAME	DESCRIPTION
Target	Beginning of line
Lithium Lens	Special
C-Magnet	
IQ1-IQ4	Four separate quadrupoles*
IB1	
IQ5-IQ17	
IB2	
IQ18	
IB3, IB4	Two separate dipoles
IQ19, IQ20	
IB5, IB6	
IQ21	
IB7	
IQ22-IQ30	
IBV1	
IQ31-IQ33	
D4Q5	Large aperture quadrupole in Debuncher lattice
ISEPT	Injection septum
Debuncher	End of line

(*)Note: From here on I will list a series of similar magnets on one line. Thus

IQ1-IQ4	is really
IQ1	Different quadrupoles
IQ2	in different locations
IQ3	
IQ4	

C. 8-GeV antiproton line, Accumulator back to and around target Line AP-3.

All elements in this line begin with "E" for extraction. The elements in this line, in order, are:

NAME	DESCRIPTION
Accumulator	Beginning of line

ELamb	Extraction lambertson
EQ1	
EBV1	Vertical dipole
EQ2	
EQ3A, EQ3B	Pair of quadrupoles run as one
EQ4	
EBV2	Second vertical dipole
EQ5-EQ15	String of quadrupoles
EB1	
EQ16	
EB2	
EQ17	
EB3	
EQ18-EQ26	
EB4	Horizontal dipole to bypass target
EQ27	
EB5	
EQ28, EQ29	
EB6	Last element in this line
PQ7B	Quadrupole in line AP-1 into which this line merges

D. 8-GeV proton test line, Booster to Debuncher. Line AP-4

All elements in this line begin with "B" for Booster. The elements in this line, in order, are:

NAME	DESCRIPTION
Booster LS3	Extraction station, beginning of line
BSEPT	Extraction septum
BQ1	Dipoles
BBV1	All dipoles in this line are vertical
BQ2, BQ3	
BBV2, BBV3	Angle varying dipoles
Target	Target to produce secondary protons
BBV4	
BQ4, BQ5	
BBV5	
BQ6, BQ7	
BQ8-BQ10	
BBV6	
D2Q5	Large aperture quadrupole in Debuncher lattice
BDSEP	Injection septum in Debuncher
Debuncher	End of line

E. Transfer line from Debuncher to Accumulator. Line D-to-A.

All elements in this line begin with "T" for transfer. The elements in this line, in order, are:

NAME	DESCRIPTION
Debuncher	Beginning of line
TDSEP	Extraction septum in Debuncher
D6Q6	Large aperture quadrupole in Debuncher lattice
TQ1-TQ7	
TASEP	Injection septum in Accumulator

2. ACCUMULATOR AND DEBUNCHER RINGS

The Accumulator and Debuncher ring elements are designated by a four to five character name, determined by ring stations. There are six primary stations in each machine, defined by the symmetry points. These sectors are:

Accumulator: A10, A20, A30, A40, A50, A60
Debuncher: D10, D20, D30, D40, D50, D60

The meaning of A10, for example is

Accumulator, sector 1, station zero, etc.

See Fig. A-1 for the primary stations and sector numbers.

In the Accumulator, all elements begin with "A" and similarly "D" in the Debuncher. In both machines, a station goes from the station marker to the leading edge of a quadrupole, and from the leading edge of a quadrupole to the leading edge of the next quadrupole. All elements downstream of the quadrupole are labeled by the station designation of that quadrupole. Thus a typical position in the Accumulator might be "A1Q4", meaning Accumulator, sector one, quadrupole at station 4. Everything between A1Q4 and the next station, A1Q5 is in station A1Q4.

The elements and stations in the Accumulator start at A10 and go toward A20. They are:

NAME	DESCRIPTION
A10	Station marker for sector 1
A1Q1	Quadrupole beginning station 1
A1Q2	Quadrupole beginning station 2
A1Q3	Quadrupole beginning station 3
A1B3	Dipole after station 3
A1Q4	Quadrupole beginning station 4
A1Q5	
A1Q6	
A1Q7	
A1S7	Sextupole after station 7
A1B7	Dipole after station 7
A1Q8	
A1B8	
A1Q9	Beginning of station 9
A1S9	

A1Q10	End of station 9, beginning of station 10
A1B10	
A1S10	
A1Q11	
A1Q12	
A1S12	
A1Q13	
A1Q14	
A20	Station marker for sector 2

Both the Accumulator and Debuncher have mirror symmetry about all zero station markers. In order to relate the magnets in one sector to their counterparts in the other sector, the magnets can not be numbered in order while moving about the rings in a clockwise manner. Rather, at each zero station the numbers reverse. Thus, the stations and elements from A20 to A30 are:

NAME	DESCRIPTION
A20	Station marker for sector 2
A2Q14	
A2Q13	
A2S12	
A2Q12	
A2Q11	
A2S10	
A2B10	
A2Q10	End of station 9, beginning of station 10
A2B9	
A2S9	
A2Q9	
A2B8	
A2Q8	
A2B7	Dipole after station 7
A2S7	Sextupole after station 7
A2Q7	
A2Q6	
A2Q5	
A2Q4	
A2B3	Dipole after station 3
A2Q3	Quadrupole beginning station 3
A2Q2	
A2Q1	
A30	Station marker for sector 3

To find all the rest of the stations, simply take the above and put in the appropriate sector numbers. (See arrows and station markers in Fig. A-1)

The magnet numbers increase in a clockwise manner in sectors 1, 3, 5, and increase in a counter-clockwise manner in sectors 2, 4, and 6.

The Debuncher is numbered in exactly the same manner, except that there is a quadrupole at the symmetry points. That is D10, D20, etc. is in the middle of a quadrupole. This special quadrupole is called D10Q, D20Q, etc. The list of stations and elements in sector 1 is:

NAME	DESCRIPTION
D10Q	Zero station marker quadrupole. This quadrupole begins station 1
D1Q2	This quadrupole ends station 1 and begins station 2. Note that there is no Q1.
D1Q3	
D1Q4	
D1Q5	
D1Q6	
D1Q7	
D1B7	
D1Q8	
D1B8	
D1Q9	
D1Q10	
D1Q11	
D1B11	
D1Q12	
D1B12	
D1Q13	
D1B13	
D1Q14	
D1B14	
D1Q15	
D1B15	
D1Q16	
D1B16	
D1Q17	
D1B17	
D1Q18	
D1B18	
D1Q19	
D1B19	
D20Q	Zero station marker quadrupole. This ends station 19.

Again, from D20Q to D30Q is the reverse of the above, substituting sector 2 for sector 1.

In the Debuncher, the sextupoles are not explicity listed, but said to be downstream of a particular magnet, for example, there is a focussing sextupole downstream of D1B8, just as well be vacuum valves, monitors, etc.

See Fig. A-2 for an almost readable diagram of all magnets.

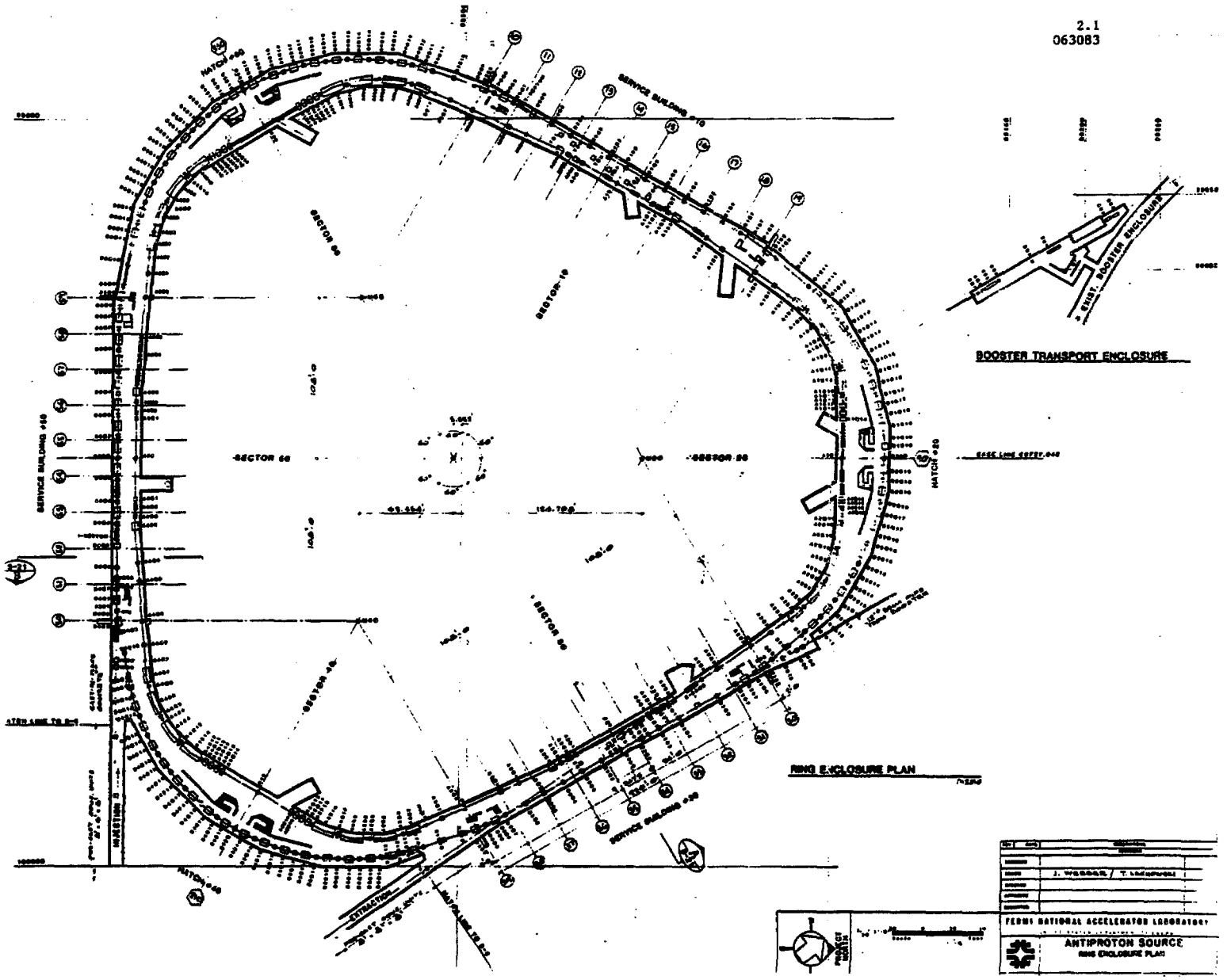
2.1
063083
BOOSTER TRANSPORT ENCLOSURE
RING ENCLOSURE PLAN
FERMI NATIONAL ACCELERATOR LABORATORY
ANTIPROTON SOURCE

Figure A-2

APPENDIX B

APPENDIX B:

TEVATRON I

PARAMETER BANK

(AR2)

(FERMILAB, JUNE 1983)

A. MAIN RING

B. TARGETRY

C. TRANSPORT LINES

D. DEBUNCHER RING

E. ACCUMULATOR RING

F. SUPERCONDUCTING RING

G. COLLIDER AT B0

H. COLLIDER AT D0

I. SYNCH FILES

TABLES OF TEVATRON I PARAMETERS

B. TARGETRY

BA. PROTON TRANSPORT TO TARGET (SEE CA)

BB. TARGET

BB.1 TARGETRY

BB.2 TARGET ENERGY DEPOSITION

BC. LITHIUM LENS
BC.1 LITHIUM LENS
BC.2 LI LENS ELECTRICAL PARAMETERS
BC.3 LI LENS OPERATING PARAMETERS

BD. ANTIPROTON TRANSPORT TO DEBUNCHER (SEE CB)

BE. DUMP

C. TRANSPORT LINES

CA. PROTONS, MAIN RING TO TARGET

CA.1 MAGNETS

CA.2 LATTICE STRUCTURE

CA.3 LATTICE FUNCTIONS

CA.4 APERTURE REQUIREMENTS

CA.5 X,Y,Z SITE COORDINATES

CB. ANTIPROTONS, TARGET TO DEBUNCHER

CB.1 MAGNETS

CB.2 LATTICE STRUCTURE

CB.3 LATTICE FUNCTIONS

CB.4 APERTURE REQUIREMENTS

CB.5 X,Y,Z SITE COORDINATES

CC. ANTIPROTONS, DEBUNCHER TO ACCUMULATOR RING

CC.1 MAGNETS

CC.2 LATTICE STRUCTURE

CC.3 LATTICE FUNCTIONS

CC.4 APERTURE REQUIREMENTS

CC.5 X,Y,Z SITE COORDINATES

CD. ANTIPROTONS, ACCUMULATOR RING TO MAIN RING

CD.1 MAGNETS

CD.2 LATTICE STRUCTURE

CD.3 LATTICE FUNCTIONS

CD.4 APERTURE REQUIREMENTS

CD.5 X,Y,Z SITE COORDINATES

CE. PROTONS, BOOSTER TO DEBUNCHER RING

CE.1 MAGNETS

CE.2 LATTICE STRUCTURE

CE.3 LATTICE FUNCTIONS

CE.4 APERTURE REQUIREMENTS

CE.5 X,Y,Z SITE COORDINATES

CF. PROTONS, MAIN RING TO SUPERCONDUCTING RING

CF.1 MAGNETS

CF.2 LATTICE STRUCTURE

CF.3 LATTICE FUNCTIONS

CF.4 APERTURE REQUIREMENTS

CF.5 X,Y,Z SITE COORDINATES

CG. ANTIPROTONS, MAIN RING TO SUPERCONDUCTING RING

CG.1 MAGNETS

CG.2 LATTICE STRUCTURE

CG.3 LATTICE FUNCTIONS

CG.4 APERTURE REQUIREMENTS

CG.5 X,Y,Z SITE COORDINATES

D. DEBUNCHER

DA. INJECTION TO DEBUNCHER RING

DA.1 LATTICE AND PARAMETERS

DA.2 MAGNETS AND DRIFTS

DA.3 LAMBERTSON MAGNET

DA.4 KICKER MAGNET

DB. LATTICE

DB.1 GENERAL

DB.2 MAGNETS

DB.3 DRIFTS (EFFECTIVE)

DB.4 LATTICE STRUCTURE

DB.5 LATTICE FUNCTIONS

DB.6 APERTURE REQUIREMENTS

DC. MAGNETS

DC.1 DIPOLES

DC.2 QUADRUPOLES

DC.3 SEXTUPOLES

DD. VACUUM

DE. RF

DF. STOCHASTIC COOLING

DG. EXTRACTION

DH. TRANSFER FROM DEBUNCHER RING TO ACCUMULATOR RING

E. ACCUMULATOR

EA. TRANSFER FROM DEBUNCHER RING TO ACCUMULATOR RING

EB. INJECTION TO ACCUMULATOR RING

EC. LATTICE

EC.1 GENERAL

EC.2 MAGNETS

EC.3 DRIFTS (EFFECTIVE)

EC.4 LATTICE STRUCTURE

EC.5 LATTICE FUNCTIONS

EC.6 APERTURE REQUIREMENTS

ED. MAGNETS

ED.1 DIPOLES

ED.2 QUADRUPOLES

ED.3 SEXTUPOLES

ED.4 OCTUPOLES

EE. VACUUM

EF. RF

EG. STOCHASTIC COOLING

EG.1 MOMENTUM TAIL COOLING SYSTEM

EG.2 MOMENTUM CORE COOLING SYSTEM

EG.3 BETATRON TAIL COOLING SYSTEMS

EG.4 BETATRON CORE COOLING SYSTEMS

EH. EXTRACTION

F. SUPERCONDUCTING RING

FA. TRANSFER FROM MAIN RING

FB. INJECTION TO SUPERCONDUCTING RING

FC. LATTICE

FD. MAGNETS

FE. VACUUM

FF. RF

FG. ABORT

G. B0 COLLIDER

GA. LOW BETA INSERTION

GB. PERFORMANCE PARAMETERS

GC. EXPERIMENTAL AREAS

H. D0 COLLIDER

HA. LOW BETA INSERTION

HB. PERFORMANCE PARAMETERS

HC. EXPERIMENTAL AREAS

I. SYNCH FILES

THE TABLES

TO SEE IF THE TABLES HAVE BEEN UPDATED SINCE THIS PRINTING:

1. LOG-ON THE CYBER ON YOUR OWN DISK AREA AT ANY TERMINAL.

2. TYPE: G,PARAM/UN=94669
   PARAM

3. FOLLOW INSTRUCTIONS APPEARING ON THE SCREEN.

AA.1 GENERAL MAIN RING PARAMETERS 10.55.34. CHANGED 5/24/83 PRINTED 5/24/83

ASSUME OVERPASS (SEE AE)

	INJECTION		MAXIMUM
KINETIC ENERGY, GEV	8.0		200
BETA	0.994475		0.999989
GAMMA	9.5262		214.16
MOMENTUM, GEV/C	8.8889		200.94
MAGNETIC RIGIDITY, TM	29.65		670.3
DIPOLE FIELD STRENGTH, T	0.0397		0.896
QUADRUPOLE FIELD GRADIENT, T/M	0.534		12.07
BETATRON TUNES (H & V)		19.4	
TRANSITION ENERGY (GAMMA/T)		18.75	
AVERAGE RADIUS, M		1000.0	
DIPOLE BENDING RADIUS, M		747.8	
HORIZONTAL BETATRON ACCEPTANCE		3.0 PI.MM.MRAD	
VERTICAL BETATRON ACCEPTANCE		2.5 PI.MM.MRAD	
MOMENTUM APERTURE, DP/P	+- 0.3 %		+- .35 %
REVOLUTION PERIOD, MICROSEC	21.075		20.959
MAX. DISPERSION, HOR. (M)		6.	
VERT. (M)		0.5	
MAX. BETA VALUE, M		120.	
PERIODICITY		NONE	
PHASE ADVANCE/REGULAR CELL		70 DEG	
STANDARD RF FREQUENCY, MHZ	52.8117		53.1045
HARMONIC NUMBER (H)		1113	
MAX. RF VOLTAGE, MV		4.0	

AB.1 INJECTION FROM THE BOOSTER

CHANGED 5/24/83
10.55.34. PRINTED 5/24/83

INJECTION KINETIC ENERGY	8.0 GEV
BETA	0.994475
GAMMA	9.5262
MOMENTUM	8.8889 GEV/C
MAGNETIC RIGIDITY	29.65 TM
NO. OF BOOSTER BATCHES INJECTED	ONE
MODE OF TRANSFER	SINGLE-TURN EXTRACTION FROM BOOSTER AND INJECTION TO MAIN RING, BUCKET-TO-BUCKET
BETATRON EMITTANCE (H & V, 95 % OF BEAM)	2.5 PI.MM.MRAD
NO. OF BUNCHES	80
NO. OF PROTONS/BUNCH	2.5E+10
NO. OF PROTONS/PULSE	2.0E+12
INDIVIDUAL BUNCH AREA (95 % OF BEAM)	0.1 - .15 EV.SEC
RF FREQUENCY	52.8117 MHZ
RF VOLTAGE	1.2 MV
BUCKET AREA, STATIONARY	0.66 EV.SEC
BUCKET HEIGHT, DP/P	+- .31 %

AB.2 PROTON ACCELERATION TO 120 GEV 10.55.34. CHANGED 5/24/83 PRINTED 5/24/83

KINETIC ENERGY, GEV	8.0		120.
TRANSITION KINETIC ENERGY, GEV		16.65	
REVOLUTION FREQUENCY, KHZ	47.451		47.712
HARMONIC NUMBER		1113	
RF FREQUENCY, MHZ	52.812		53.1035
RF VOLTAGE,MV	1.2		.75
ACCELERATION RATE, MAX, GEV/S		125	
SYNCHROTRON PHASE ANGLE	0 - 50 DEG		130 - 135 DEG
BUCKET AREA, EV.SEC	0.66		3.3
INDIVIDUAL BUNCH AREA AT 120 GEV (95 % OF BEAM) EV.SEC		0.2	
MAIN RING CYCLE PERIOD:		2.0 SEC	
FRONT PORCH		0.1 SEC	
ACCELERATION TO 120 GEV		1.2 SEC	
FLAT TOP		0.2 SEC	
FALL OFF PERIOD		0.5 SEC	

MAIN RING CYCLE PERIOD	2 SEC
KINETIC ENERGY AT FLAT-TOP	120 GEV
FLAT-TOP LENGTH	0.2 SEC
TRANSITION ENERGY (GAMMA/T)	18.75
RF FREQUENCY	53.1035 MHZ
HARMONIC NUMBER (H)	1113
(1) END OF ACCELERATION	STATIONARY BUCKET
RF VOLTAGE	.68 MV
PHASE OSCILLATION PERIOD	12.8 MSEC
BUCKET AREA	3.8 EV.SEC
BUNCH LENGTH (95 %)	79 CM
MOMENTUM SPREAD, DP/P (95 %)	4.2E-4
(2) RF VOLTAGE REDUCED SLOWLY TO	12 KV
TIME PERIOD FOR ADIABATIC REDUCTION	0.1 SEC
FINAL BUCKET AREA	0.46 EV.SEC
FINAL PHASE OSCILLATION PERIOD	105 MSEC
FINAL BUNCH LENGTH	2.82 M
FINAL MOMENTUM SPREAD, DP/P	2.5E-4
FINAL RF PHASE EXTENSION OF BUNCH	+-90 DEG
(3) FAST INCREASE OF RF VOLTAGE TO	4MV
IN A PERIOD OF TIME OF	40 MUSEC
90 DEG BUNCH ROTATION PERIOD	1.4 MSEC
EQUIVALENT TO PHASE OSCILLATION PERIOD	5.5 MSEC
BUNCH LENGTH, AT END OF ROTATION	LESS THAN 30 CM
RMS MOMENTUM SPREAD, DP/P	4.1E-3
(4) BEAM EXTRACTION	FAST: AS SOON AS BUNCHES HAVE ROTATED BY 90 DEG

EXTRACTION KINETIC ENERGY	120 GEV
MAGNETIC RIGIDITY (B-RHO)	403.27 T.M
BEAM PULSE LENGTH TO BE EXTRACTED	21 MICROSEC
REVOLUTION PERIOD	20 MICROSEC
BEAM EMITTANCE AT EXTRACTION (H & V, 95% OF BEAM)	0.2 PI.MM-MRAD
BEAM FULL MOMENTUM SPREAD AT EXTRACTION, 95% OF BEAM	0.4%

EXTRACTION MODE: (A) 4-MAGNET LOCAL HORIZ. BUMP CENTERED AT F17

(B) HORIZONTAL KICK OUTWARD

(C) LAMBERTSON MAGNETS FOR VERTICAL EXTRACTION

HORIZONTAL DISPLACEMENT AT F17 WITH 4-MAGNET BUMP	+- 37 MM
KICKER LOCATION	C48
HORIZONTAL DISPLACEMENT BY KICKER AT F17	+43 MM
ANGULAR DISPLACEMENT BY KICKER AT F17	+0.847 MRAD
LOCATION OF LAMBERTSON	F17
NUMBER OF LAMBERTSON MAGNETS	2
LAMBERTSON MAGNET LENGTH / EACH	204 INCHES
LAMBERTSON MAGNET FIELD STRENGTH	13 KG

CONTINUED

AB.4 (CONTINUED)

HORIZONTAL PLANE LATTICE FUNCTIONS:

LOCATION	BETA (M)	ALPHA	PHASE RELATIVE TO F17 (MODULO 360 DEG)	SPACE AVAILABLE (IN.)
C48 KICKER	102.414	0.46696	-90.11 DEG	(EXISTING)
F12	29.601	-0.5731	-168.30 DEG	0.0
F13	95.356	1.8584	-135.74 DEG	0.0
F14	28.383	-0.5893	-99.29 DEG	34.0
F15 (BUMP 1)	97.247	1.8396	-66.32 DEG	42.5
F16	30.093	-0.6239	-31.47 DEG	42.0
F17 (BUMP 2) (EXTRACTION)	99.648	1.9388	0.00 DEG	32.0
F18 (BUMP 3)	28.865	-0.5582	35.20 DEG	52.0
F19	94.322	1.8156	68.42 DEG	0.0
F21	28.912	-0.6177	104.71 DEG	28.0
F22 (BUMP 4)	99.541	1.8926	136.92 DEG	27.5
F23	30.073	-0.5983	171.32 DEG	35.0
F24	97.400	1.9056	203.21 DEG	0.0
F25	28.365	-0.5666	239.23 DEG	35.0
F26	95.244	1.8100	272.60 DEG	43.5

AC.1 INJECTION FROM THE BOOSTER

CHANGED 5/24/83
10.43.15. PRINTED 6/10/83

INJECTION KINETIC EVERGY	8.0 GEV
REVOLUTION FREQUENCY	47.451 KHZ
HARMONIC NUMBER	1113
RF FREQUENCY	52.813 MHZ
RF VOLTAGE	1.2 MV
RF BUCKET AREA	0.66 EV.SEC
RF BUCKET HEIGHT, DP/P	+- .31 %
NO. OF BOOSTER BATCHES INJECTED	3, EQUALLY SPACED
MODE OF TRANSFER	SINGLE-TURN EXTRACTION FROM BOOSTER AND INJECTION TO MAIN RING OF A SINGLE BATCH, BUNCH-TO-BUCKET
NO. OF BUNCHES/BATCH	7, SELECTED NEXT TO EACH OTHER, AFTER REMOVING UNWANTED BUNCHES WITH SUPERDAMPER
NO. OF PROTONS/BUNCH	1.2E+10
NO. OF PROTONS/BATCH	8E+10
INDIVIDUAL BUNCH AREA (95 % OF BEAM)	0.1 EV.SEC
BETATRON EMITTANCE (H & V, 95 % OF BEAM)	2.5 PI.MM.MRAD
MAIN RING FRONT PORCH PERIOD	0.3 SEC

AC.2 ACCELERATION TO 150 GEV

CHANGED 5/24/83
09.53.05. PRINTED 6/10/83

KINETIC ENERGY	8.0		150.	GEV
TRANSITION KINETIC ENERGY		16.65		GEV
REVOLUTION FREQUENCY	47.451		47.71	KHZ
HARMONIC NUMBER		1113		
RF FREQUENCY	52.813		53.105	MHZ
RF VOLTAGE	1.2		.68	MV
SYNCHRONOUS PHASE ANGLE	0 - 50		130 - 135	DEG
ACCELERATION RATE, MAX		125		GEV/SEC
ACCELERATION TIME		2.0		SEC
BETATRON EMITTANCE (H & V 95 % OF BEAM)	2.5		0.15	PI.MM.MRAD
INDIVIDUAL BUNCH AREA (95 % OF BEAM)	0.15		0.2	EV.SEC
STATIONARY BUCKET AREA	0.66		3.5	EV.SEC
BUCKET HEIGHT, DP/P	+- .31 %		+- .1 %	
PHASE OSCILLATION PERIOD	1.65		14	MSEC

AC.3 PROTON BUNCH RECOMBINATION FOR COLLIDER CHANGED 6/10/83

---------- 09.53.05. PRINTED 6/10/83

KINETIC ENERGY 150 GEV

RF VOLTAGE	INITIAL	FINAL
H=53	3.93E+2	3.93E+2
H=1113	6.8E+5	1.0E+2

RF FREQUENCY

H=53	2.53 MHZ
H=1113	53.105 MHZ

NUMBER OF BUNCHES

H=53	1
H=1113	7

RECOMBINATION TIME	.8 SEC
BUNCH EMITTANCE	APPROX. 1 EVS
BUNCH LENGTH	39.5 M
MOMENTUM SPREAD (APPROX. 95%)	6.7E-5

AC.4 EXTRACTION AT 150 GEV (PROTONS) 09.53.05. CHANGED 5/31/83 PRINTED 6/10/83

KINETIC ENERGY 150 GEV

RF VOLTAGE

H=53	45 KV
H=106	-9.8 KV

BUNCH ROTATION TIME	79 MS
FINAL EMITTANCE (EQUIVALENT 95% ELLIPSE)	(LESS THAN 1.5 EVS)
RF VOLTAGE AT EXTRACTION (H=1113)	1.0 MV
BUNCH WIDTH (95%)	2.3 M
BUNCH HEIGHT DP/P (95%)	1.6E-3

AD.1 ANTIPROTON INJECTION TO THE MAIN RING CHANGED 6/10/83
09.53.05. PRINTED 6/10/83

KINETIC ENERGY 8.0 GEV

RF VOLTAGE

H=53	2 KV
H=1113	3 KV

RF FREQUENCY

H=53	2.5148 MHZ
H=1113	52.8117 MHZ

MODE OF TRANSFER - SINGLE TURN EXTRACTION FROM ACCUMULATOR

- SYNCHRONOUS INJECTION INTO MAIN RING H=53 BUCKETS

NUMBER OF BUNCHES	1
BUNCH EMITTANCE	1.5 EVS (OR 1.5 - 2 EVS)
BUNCH INTENSITY	8E+10 (OR 8E+10 - E+11)
BUNCH LENGTH	73.4 M
BUNCH HEIGHT DP/P (95%)	8.710E-4
TRANSVERSE EMITTANCE (H & V)	2.5 PI MM MRAD

AD.2 BUNCH SPLITTING AT 8 GEV 10.43.15. CHANGED 5/24/83 PRINTED 6/10/83

KINETIC ENERGY 8 GEV

RF VOLTAGE	INITIAL	FINAL
H=53	2 KV	2 KV
H=1113	3 KV	500 KV

RF FREQUENCY	
H=53	2.5148 MHZ
H=1113	52.8117 MHZ

NUMBER OF BUNCHES	1	13
ANTIPROTONS/BUNCH	8E+10	8E+9
BUNCH LONG EMITTANCE	1.5	.15 MAX EVS
BUNCH LENGTH	73.4 M	2.54 M
BUNCH HEIGHT		
DP/P (95%)	8.7E-4	2.6E-3

AD.3 ACCELERATION TO 150 GEV

09.53.05.

CHANGED 5/31/83
PRINTED 6/10/83

	INITIAL		FINAL
KINECTIC ENERGY	8.0		150.00
TRANSITION ENERGY		16.65 GEV	
REVOLUTION FREQUENCY	47.451		47.71
HARMONIC NUMBER		1113	
RF FREQUENCY	52.813		53.1035
RF VOLTAGE	1.2 MV		.68 MV
SYNCHRONOUS PHASE	0-50 DEGREES		130-180 DEGREES
ACCELERATION RATE (MAX)		125 GEV	
ACCELERATION TIME		2.0 SEC	
TRANSVERSE EMITTANCE (95%)	2.5		.15 PI MM MRAD
INDIVIDUAL BUNCH AREA (MAX)	.15		.2 EVS
BUCKET HEIGHT DP/P (95%)	+.31%		+.1%
PHASE OSCILLATION PERIOD	1.5 M SEC		14 M SEC

AD.4 BUNCH RECOMBINATION FOR COLLIDER CHANGED 6/10/83
---------- 09.53.05. PRINTED 6/10/83

KINETIC ENERGY		150 GEV
ROTATION FREQUENCY		47.71 KHZ
RF FREQUENCY		
H=53		2.53 MHZ
H=1113		53.105 MHZ
RF VOLTAGE	INITIAL	FINAL
H=53	98 V	98 V
H=1113	6.8E+5 V	APPROX. 100 V
NUMBER OF BUNCHES		
H=53		1
H=1113	13	
RECOMBINATION TIME		.8 S
BUNCH EMITTANCE		APPROX. 2 EVS
BUNCH LENGTH		73.4 M
MOMENTUM SPREAD		
(95% DP/P)		6.9E-5

AD.5 EXTRACTION AT 150 GEV (ANTIPROTONS) CHANGED 6/10/83
---------- 09.53.05. PRINTED 6/10/83

KINETIC ENERGY	150 GEV
RF FREQUENCY	
H=53	2.529 MHZ
H=106	5.058 MHZ
RF VOLTAGE	
H=53	20 KV
H=106	-4.4 KV
BUNCH ROTATION TIME	115 MS
FINAL EMITTANCE	
(95% EQUIVALENT ELLIPSE)	LESS THAN APPROX. 3 EVS
RF VOLTAGE AT EXTRACTION	1.0 MV
H=1113	
BUNCH WIDTH 95%	3.93 M
BUNCH HEIGHT	
(95% DP/P)	2.2E-3

TARGET MATERIAL	TUNGSTEN-RHENIUM
LENGTH OF TARGET	6 CM
TARGET DISK	8 CM
PROTON BEAM:	
BETA.STAR, PROTON (H & V)	4.6 M
ALPHA.STAR, PROTON (H & V)	0.
ETA.STAR, PROTON (DISPERSION)	0. M
ETA.PRIME.STAR, PROTON	0.
PROTON RMS SPOT SIZE (H & V)	0.39 MM
NO. OF BOOSTER BATCHES / M R CYCLE	ONE
TIME INTERVAL BETWEEN BATCHES	2.0 SEC
MAIN RING CYCLE TIME	2.0 SEC
NUMBER OF PROTONS / BATCH	1.8E+12
NUMBER OF PROTON BUNCHES / BATCH	80
ANTIPROTON BEAM:	
ANTIPROTON PRODUCTION MOMENTUM	8.889 GEV/C
KINETIC ENERGY	8.0 GEV
BETA	0.99448 M
GAMMA	9.5264 1/M
MAGNETIC RIGIDITY (B-RHO)	29.65 T.M
MOMENTUM SPREAD ACCEPTED, FULL DELTA P/P,	3%

CONTINUED

BB.1 (CONTINUED)

EMITTANCE ACCEPTED (H & V)	20 PI.MM-MRAD
AVERAGE ANTIPROTON ANGLE	23.8MRAD
BETA.STAR, ANTIPROTON (H & V)	0.11 M
ANTIPROTON SPOT SIZE (H & V)	1.5 MM
PBAR PRODUCTION CROSS-SECTION, D3N/DPDOMEGA	=0.252 PBARS/(GEV/C) STER.INT.P
ANTIPROTON ABSORPTION LENGTH	9.29 CM
PROTON ABSORPTION LENGTH	9.86 CM
CALCULATED ANTIPROTONS/PROTONS	3.7E-5
TOTAL NUMBER OF ANTIPROTONS / M R CYCLE	6.7E+7
NUMBER OF ANTIPROTON BUNCHES / M R CYCLE	80
NUMBER OF ANTIPROTONS / BUNCH	8.4E+5
ANTIPROTON BUNCH LENGTH (AT TARGET, RMS)	5 CM
ANTIPROTON BUNCH AREA (95% OF BEAM)	0.24 EV.SEC
PROTON BUNCH TIMING	18.83115 NSEC
ANTIPROTON BUNCH TIMING	SAME
PROTON BUNCH SPACING (CENTER-TO-CENTER)	5.64527 M
ANTIPROTON BUNCH SPACING	5.61427 M
ANTIPROTON BUNCHING FREQUENCY	53.1035 MHZ

BB.2 TARGET ENERGY DEPOSITION

CHANGED 5/25/83
12.17.52. PRINTED 6/ 9/83

TARGET MATERIAL	TUNGSTEN/TUNGSTEN ALLOYS
LENGTH	6 CM
120 GEV PROTONS/PULSE	1.8+12
TOTAL BEAM ENERGY	3.46E+4 JOULES
REPETITION RATE	0.5 HZ
BEAM PULSE DURATION	1.6E-6 SEC
ENERGY DEPOSITED/PROTON GEV	1.26 GEV (1.82E-10 JOULES)
ENERGY DEPOSITED/PULSE	346 JOULES
AVERAGE ENERGY DEPOSITED	173 WATTS
AVERAGE TEMPERATURE	LESS THAN 100 DEG C
PROTON RMS BEAM SIZE (H & V)	0.39 MM
PEAK ENERGY DENSITY/PROTON	13.4 GEV/CM3
PEAK ENERGY DENSITY/PULSE	200 JOULES/GM
PEAK TEMPERATURE RISE	LESS THAN 1500 DEG C

TRANSFORMER:

OVERALL DIAMETER	42 CM
OVERALL LENGTH	24 CM
I.D. OF PRIMARY	16 CM
CORE AREA	154 SQ CM

LITHIUM LENS:

OVERALL DIAMETER	9 CM
OVERALL LENGTH	24 CM
LITHIUM CONDUCTOR	
DIAMETER	2 CM
LENGTH	15 CM
BERYLLIUM WINDOW THICKNESS	0.5 CM
TITANIUM COOLING JACKET THICKNESS	0.1 CM

TRANSFORMER (PRIMARY):	
RESISTANCE	.49 MILLIOHM
STRAY INDUCTANCE	.44 MICRO. H
NO. OF TURNS	8
LI LENS & TRANSFORMER (SECONDARY):	
RESISTANCE	.126 MILLIOHM
INDUCTANCE	31 NANO. H
REFLECTED PRIMARY CIRCUIT PARAMETERS:	
RESISTANCE	8.6 MILLIOHM
INDUCTANCE	2.4 MICRO. H
DAMPING FACTOR ALPHA = R/2L	1780 HZ

PULSED POWER SUPPLY:	
PULSE LENGTH	0.33 MSEC
VOLTAGE	2.5 KV
CAPACITANCE	4600 MICRO F
INITIAL STORED ENERGY	14.4 KJ
REPITION RATE	0.5 HZ
TRANSFORMER (PRIMARY):	
PEAK CURRENT	83 KA
DISSIPATED ENERGY/PULSE	570 J
DISSIPATED POWER	290W
NET MAGNETIC FORCE ON PRIMARY TURNS	7700 LBS
CORE BIAS	10 A
LITHIUM LENS & TRANSFORMER (SECONDARY):	
PEAK CURRENT	670 KA
DISSIPATED ENERGY/PULSE	9800 J
DISSIPATED POWER	4.9 KW
NET AXIAL MAGNETIC FORCE ON LENS	33000 LBS
TEMP RISE/PULSE	120 DEG C (MAX)
	35 DEG C (MIN)
MAGNETIC FIELD (LITHIUM):	
AC SKIN DEPTH	.45 CM
PEAK SURFACE FIELD	13.5 T
PHASE AT BEAM TIME	117 DEG
AVE. FIELD GRADIENT AT BEAM TIME	1100 T/M
PEAK MAGNETIC PRESSURE	16000 PSI
AVE. NON-LINEARITY	2.8 %

DA.1 LATTICE AND PARAMETERS

13.15.19. CHANGED 5/17/83 PRINTED 5/31/83

KINETIC ENERGY AT INJECTION	8.0 GEV
MOMENTUM	8.8889 GEV/C
MAGNETIC RIGIDITY	296.501 KG-M
EMITTANCE INJECTED (H & V)	20 PI.MM.MRAD
MOMENTUM SPREAD INJECTED,	
FULL DP/P, MAX,	4 %
METHOD:	VERTICAL INJECTION ON A HORIZONTALLY CENTERED ORBIT, FOLLOWED BY KICKING ON REFERENCE PLANE

STRING OF ELEMENTS:
FROM THE UPSTREAM END OF COMMON QUAD QF3
TO THE DOWNSTREAM END OF THE KICKER (KICK)

QF3 OS SM S1 QD2 LA QF2 O1 KICK

LOCATION OF THE LAMBERTSON (SM)	STATION D4-4
LOCATION OF THE KICKER (KICK)	STATION D4-2

DA.2 MAGNETS AND DRIFTS

CHANGED 5/17/83
13.15.19. PRINTED 5/31/83

DRIFT ELEMENTS	LENGTH
S1	1.2929 M
O1	0.4636 M
LA	3.731264 M
OS	0.3048 M

SEE ALSO TABLES DB.3 AND DB.4

QUADRUPOLES:	EFFECTIVE LENGTH	B'/(B.RHO)	BORE RADIUS
QF3	0.8280 M	0.32494 1/M**2	8.41 CM
QD2	0.7010 M	-0.38679 1/M**2	4.45 CM
QF2	0.7010 M	0.35881 1/M**2	4.45 CM

SEE ALSO TABLES DB.2 AND DC.2

DA.3 SEPTUM MAGNET

13.15.19. CHANGED 5/18/83
PRINTED 5/31/83

LOCATION			STATION D4-4
EFFECTIVE LENGTH			2.1336 M
BENDING FIELD			5.6335 KG
BENDING ANGLE			40.5384 MRAD
BENDING RADIUS			52.6316 M
BEAM HORIZONTAL DISPLACEMENT FROM REFERENCE ORBIT			CENTERED WITH REFERENCE ORBIT
BEAM VERTICAL DISPLACEMENT FROM REFERENCE ORBIT:			BEAM VERTICAL ANGLE FROM REFERENCE ORBIT:
UPSTREAM	QF3	13.4 CM	64.4 MRAD
DOWNSTREAM	QF3	9.1 CM	35.4 MRAD
UPSTREAM	SM	8.0 CM	35.4 MRAD
DOWNSTREAM	SM	4.8 CM	-5.2 MRAD
UPSTREAM	QD2	5.5 CM	-5.2 MRAD
DOWNSTREAM	QD2	5.3 CM	9.7 MRAD
MAX. FULL BEAM SIZE (H X V) IN THE SEPTUM MAGNET			35 X 26 MM**2
MIN. SEPARATION BETWEEN INJECTED AND CIRCULATING BEAMS EDGE TO EDGE			22 MM
APERTURE			5.0 CM (H) X 10.0 CM (V)

DA.4 KICKER MAGNET

13.15.19. CHANGED 5/18/83
PRINTED 5/31/83

LOCATION	STATION D4-2
EFFECTIVE LENGTH	3.048 M
BENDING ANGLE (HORIZONTAL)	6.17 MRAD
BENDING FIELD	600 G
FALL-OFF TIME	200 NSEC
BEAM VERTICAL DISPLACEMENT:	
UPSTREAM	9.4 MM
DOWNSTREAM	0.0 MM
APERTURE, FULL	4.0 CM (H) X 5.4 CM (V)

DB.1 GENERAL LATTICE PARAMETERS

CHANGED 5/17/83
13.15.19. PRINTED 5/31/83

KINETIC ENERGY	8.0 GEV
BETA	0.99448
GAMMA	9.5264
MOMENTUM (P)	8.8889 GEV/C
MAGNETIC RIGIDITY (B-RHO)	296.5 KG.M
BENDING FIELD (B)	17.0 KG
BENDING RADIUS (RHO)	17.44 M
AVERAGE RADIUS (R)	80.4182 M
REVOLUTION PERIOD	1.6948 MICROSEC
PACKING FACTOR (RHO/R)	21.7%
SUPERPERIODICITY	3
RF HARMONIC NUMBER (H)	90
FOCUSSING STRUCTURE	SEPARATED FUNCTIONS
NORMAL CELL STRUCTURE	FODO
HORIZONTAL BETATRON TUNE	9.73
VERTICAL BETATRON TUNE	9.77
TRANSITION ENERGY (GAMMA/T)	7.648
ETA = 1/(GAMMA/T)**2 - 1/GAMMA**2	0.0061
NATURAL CHROMATICITY: HORIZONTAL	-10.8
VERTICAL	-11.0

DB.2 LATTICE MAGNETS

13.15.19.

CHANGED 5/18/83
PRINTED 5/31/83

DIPOLES	EFFECTIVE LENGTH	STRENGTH	NUMBER
B	1.6604 M	17.0 KG	66

QUADRUPOLES	EFFECTIVE LENGTH	B'/(B-RHO)	NUMBER
QF	0.701 M	0.33652	42
QD	0.701	-0.32928	39
QF1	0.701	0.37747	3
QD1	0.701	-0.34714	6
QF2	0.701	0.35881	6
QD2	0.701	-0.38679	6
QF3	0.828	0.32494	6
QD3	0.828	-0.32459	6

SEXTUPOLES	EFFECTIVE LENGTH	B''/(B-RHO)(*)	NUMBER
SF	0.2 M	0.70365 1/M**2	36
SD	0.2	-1.0671	33

(*) STRENGTHS REQUIRED FOR CHROMATICITY CANCELLATION IN BOTH PLANES

DB.3 LATTICE DRIFTS (EFFECTIVE)

13.15.19.

CHANGED 5/18/83
PRINTED 5/31/83

O	0.735431 M
OO	1.035431
OS	0.300000
LA	3.731264
LB	3.667764
LC	3.131264
LZ	3.604264

REGULAR CELL (*)

```
(.C)   QF/2   .OF1   B   .OD2   QD
              .OD1   B   .OF2   QF/2
```

WHERE

```
.OF1 = OS   SF   O
.OD1 = OS   SD   O
.OF2 = O    SF   OS
.OD2 = O    SD   OS
```

HALF REGULAR CELL (*)

```
(.CH)   QF/2   .OF1   B   .OD2   QD/2
```

SPECIAL CELLS FOR DISPERSION KILLER (*)

```
(.C1)   QF/2    OO    B    OO    QD
                OO    B   .OF2   QF/2

(.CS)   QF/2   .OF1   LC  .OD2   QD
               .OD1   LC  .OF2   QF/2
```

SPECIAL CELLS FOR LONG STRAIGHT SECTIONS (*)

```
(.CS1)   QF1/2   LA   QD1   LA   QF2/2
(.CS2)   QF2/2   LA   QD2   LB   QF3/2
(.CS3)   QF3/2   LZ   QD3   LB   QF/2
```

HALF OF A SUPERPERIOD STRUCTURE:

```
.CS1   .CS2   .CS3   .C1   .CS
.C     .C     .C     .C    .CH
```

SUPERPERIOD STRUCTURE:

.CS + MIRROR REFLECTION OF .CS

(*) QX/2 DENOTES HALF OF A REGULAR QX QUAD

	BETA/H	BETA/V	ETA
MAXIMA	17.83 M	16.94 M	2.09 M
REGULAR CELL(*):			
MAX	14.97	14.88	2.09
MIN	5.24	5.23	1.28 (**)
QF1 (MAX)	17.83	5.73	-0.0009
QD1	4.79	16.94	-0.0004
QF2	11.81	5.32	-0.0003
QD2	4.44	13.64	0.0001
QF3	17.60	3.52	0.0007
QD3	5.74	13.82	0.0005

(*) INCLUDES DISPERSION KILLER

(**) EXCLUDES DISPERSION KILLER WHERE ETA/MIN = 0.0 M

BETATRON ACCEPTANCE: HORIZONTAL 20.PI MM-MRAD

VERTICAL 20.PI MM-MRAD

MOMENTUM APERTURE: +- 2%

MAXIMUM BEAM DIMENSIONS (FULL):

	HORIZ. (MM)	VERTICAL (MM)
B	101.54	32.66
QF	118.14	20.43
QD	73.36	34.50
QF1	36.88	21.96
QD1	20.23	36.82
QF2	30.73	20.64
QD2	18.86	33.04
QF3	37.54	16.78
QD3	21.44	33.24

DC.1 DEBUNCHER DIPOLES

CHANGED 5/18/83
11.40.38. PRINTED 6/ 9/83

EFFECTIVE ARC LENGTH	1.660402 M
BENDING RADIUS	17.4412353 M
IRON LENGTH	62.8 INCHES
BENDING ANGLE	95.20 MRAD
FULL GAP	60 MM
GOOD FIELD WIDTH	100 MM
SAGITTA	2.0 CM
CONDUCTOR:	
1" X 1.25" CROSS SECTION	0.375" CROSS SECTION HOLE DIAMETER
1/16" CORNER RADIUS	1.1362 SQ. IN. AREA
TURNS:	
PANCAKE COILS	56
SADDLE COILS	16
CONDUCTOR LENGTHS:	
PANCAKE COILS	9740.3"/MAGNET
SADDLE COILS	3680.45"/MAGNET
TOTAL CONDUCTOR LENGTH	13420.75"/MAGNET
COIL PROTRUSION/END	11"
CU WEIGHT/MAGNET	4906.625 LBS
TOTAL CU WEIGHT	161.92 TONS
RESISTANCE/MAGNET (43 DEG C)	8.73 MILLI-OHM
CURRENT AT 1.7T	1175.6 A
VOLTAGE AT 1.7T	10.3 V
POWER/MAGNET	12.065 KW
TOTAL POWER/DIPOLES	0.7963 MW
FULL CROSS SECTION (W X H)	45.25" X 29"
LAMINATION THICKNESS	0.0598"
IRON WEIGHT/MAGNET	16826.865 LBS
TOTAL IRON WEIGHT	555.3 TONS
COOLING WATER PRESSURE	42 PSI
WATER FLOW	2.4 GALLONS/MIN.

TYPE	REGULAR	LONG-SMALL APERTURE	LONG-LARGE APERTURE
EFFECTIVE LENGTH	27.6"	32.6"	32.6"
IRON LENGTH	26.18"	31.18"	30"
POLETIP RADIUS	44.5 MM	44.5 MM	84.1 MM
CONDUCTOR:	0.312"X 0.75" 0.1875" HOLE DIA 1/16" CORNER RADIUS AREA=0.20309 SQ IN		0.625"X 1.5" 0.375" HOLE DIA 1/16" CORNER RADIUS AREA=0.8237 SQ IN
TOTAL CONDUCTOR LENGTH/MAGNET	11069.52"	12389.52"	8804.88"
COIL PROTRUSION	4"	4"	6"
CU WEIGHT/MAGNET	722.84 PD	809.04 PD	22332.41 PD
TOTAL CU/WEIGHT	36.9 TONS	36.4 TONS	3.5 TONS
RESISTANCE/MAGNET (43 DEG C)	40.3 M OHM	45.1 M OHM	7.9 M OHM
CURRENT AT 10 T/M	250 A	230 A	1310 A
VOLTAGE AT 10 T/M	10.1 V	10.4 V	10.35 V
POWER/MAGNET	2.5 KW	2.4 KW	13.6 KW
TOTAL POWER/QUADS	0.258 MW	0.022 MW	0.041 MW
FULL CROSS SECTION (W X H)	30.5X29 SQ IN	30.5X29 SQ IN	54.75X51.75 SQ IN
LAMINATION THICKNESS	0.0598"	0.0598"	0.0598"
IRON WEIGHT	1.85 TONS	2.20 TONS	7.02 TONS
TOTAL IRON WEIGHT	188.6 TONS	19.8 TONS	21.1 TONS
COOLING WATER PRESSURE	19 PSI	26 PSI	3.1 PSI
WATER FLOW	0.8 GAL/MIN	1 GAL/MIN	2.2 GAL/MIN
NO. OF TURNS, TOTAL	4X33	4X33	4X21

MAXIMUM STRENGTH, B"L/B-RHO	0.22 M-2
BORE RADIUS	50 MM
EFFECTIVE LENGTH	0.2 M
MAXIMUM FIELD, B"	33 T/M2
AMPERE-TURNS	600 AT/POLE
CURRENT	119 A
TURNS	5 TURNS/POLE
CONDUCTOR SIZE	.3294" RECT/ 0.18" HOLE DIA/ AREA .07723 SQ IN
CURRENT DENSITY	1.55 KA/SQ IN
RESISTANCE	5 MICRO OHM/MAGNET
VOLTAGE DROP	0.65 V/MAGNET
THERMAL LOSS	77 W/MAGNET

EC.1 GENERAL LATTICE PARAMETERS

CHANGED 5/19/83
14.13.48. PRINTED 6/28/83

KINETIC ENERGY	7.9 GEV
BETA	0.99438
GAMMA	9.4492
MOMENTUM (P)	8.81616 GEV/C
MAGNETIC RIGIDITY (B-RHO)	294.1 KG-M
BENDING FIELD (B)	16.84 KG
BENDING RADIUS (RHO)	17.46375 M
AVERAGE RADIUS (R)	75.4506 M
REVOLUTION PERIOD	1.590 MICROSEC
PACKING FACTOR (RHO/R)	23.146%
SUPERPERIODICITY	3
RF HARMONIC NUMBER (H)	84
FOCUSSING STRUCTURE	SEPARATED FUNCTIONS
NORMAL CELL STRUCTURE	NONE
HORIZONTAL BETATRON TUNE	6.61082
VERTICAL BETATRON TUNE	8.61144
TRANSITION ENERGY (GAMMA/T)	5.42986
ETA = 1/(GAMMA/T)**2 - 1/GAMMA**2	0.0227
NATURAL CHROMATICITY: HORIZONTAL	-8.47593
VERTICAL	-12.88242

EC.2 LATTICE MAGNETS

CHANGED 5/19/83
11.40.38. PRINTED 6/ 9/83

DIPOLES	EFFECTIVE LENGTH	STRENGTH
B3	1.5240 M	16.839 KG
B7	3.0480 M	16.839 KG
B8, B9, B10	4.5720 M	16.839 KG
QUADRUPOLES	**EFFECTIVE LENGTH**	**STRENGTH**
Q1	0.64008 M	103.8087 KG/M
Q2	1.31166	-103.8087
Q3	0.70104	103.8087
Q4	0.45720	96.6333
Q5	0.82804	- 97.4126
Q6	0.70104	96.6333
Q7	0.70104	- 97.4126
Q8	0.45720	96.6333
Q9	0.45720	- 97.4126
Q10	0.45720	40.8765
Q11	0.87376	89.3989
Q12	0.77220	- 89.3989
Q13	0.77220	- 89.3989
Q14	0.64262	89.3989
SEXTUPOLES	**EFFECTIVE LENGTH**	**STRENGTH**
S7	0.3048 M	35.7175 KG/M2
S9	0.3048	-219.5244
S10	0.3048	134.7943
S12	0.3048	-170.5021
OCTUPOLES	**EFFECTIVE LENGTH**	**STRENGTH**
OC10	0.3048	-325.1426 KG/M3
OC12	0.3048	778.6057

EC.3 LATTICE DRIFTS (EFFECTIVE)

13.15.19.

CHANGED 5/26/83
PRINTED 5/31/83

LS	7.94650
LS*	7.84488
01	0.51241
02	0.96060
03	0.90420
0B3	6.42366
04	3.26100
05	7.33776
06	4.18716
07	0.30480
0S7	3.83584
0B7	0.50800
08	1.21920
0B8	0.50800
09	0.30480
0S9	0.60960
0B9	0.50800
010	0.50800
0B10	0.29190
0S10	0.29190
011	0.52102
012	0.21780
0S12	0.21780
013	0.49722

STRUCTURE OF HALF A SUPERPERIOD

STRING OF ELEMENTS FROM CENTER OF ZERO-DISPERSION STRAIGHT SECTION TO CENTER OF LARGE-DISPERSION STRAIGHT SECTION

.CS = LS Q1 A1 O1 Q2 Q2 O2 Q3 Q3 O3 B3
OB3 Q4 Q4 O4 Q5 Q5 O5 Q6 Q6 O6 Q7 Q7
O7 S7 OS7 B7 OB7 Q8 Q8 O8 B8 OB8 Q9 Q9
O9 S9 OS9 B9 OB9 Q10 Q10 O10 B10 OB10 S10 OS10
Q11 Q11 O11 Q12 Q12 O12 S12 OS12 Q13 Q12 O13 Q14
Q14 LS*

SUPERPERIOD STRUCTURE:

.CS + MIRROR REFLECTION OF .CS

EC.5 LATTICE FUNCTIONS

CHANGED 5/31/83
13.15.19. PRINTED 5/31/83

	BETA-H	BETA-V	ETA-H
MAXIMA	33.23 M	31.04 M	8.949 M
B3	24.59	9.40	0.067
B7	17.82	16.01	-0.088
B8	15.96	18.80	0.891
B9	23.05	15.73	4.669
B10	31.97	9.12	8.065
Q1	16.01	19.98	0.001
Q2	14.59	30.32	0.001
Q3	26.32	12.60	0.001
Q4	14.31	8.13	0.645
Q5	2.95	28.90	0.680
Q6	29.99	2.98	1.915
Q7	6.60	31.04	0.634
Q8	14.57	8.35	-0.050
Q9	7.60	20.23	1.239
Q10	26.22	4.91	5.325
Q11	31.96	15.86	8.726
Q12	16.72	27.14	6.978
Q13	13.22	27.39	7.542
Q14	15.88	16.90	8.949

	BETA-H	BETA-V	ETA-H
(*) CENTER OF ZERO-DISPERSION LONG STRAIGHT SECTION	7.764 M	7.267 M	0.002 M
(**) CENTER OF LARGE DISPERSION LONG STRAIGHT SECTION	7.580	7.514	8.949

(*) TOTAL LENGTH = 15.8930 M (**) TOTAL LENGTH = 15.6898 M

(ALPHA*-H = ALPHA*-V = ETA' = 0)

EC.6 APERTURE REQUIREMENTS

11.43.15.

CHANGED 5/31/83
PRINTED 6/ 9/83

BETATRON ACCEPTANCE: HORIZONTAL 10 PI MM-MRAD

VERTICAL 10 PI MM-MRAD

MOMENTUM APERTURE: +- 1.25%

ED.1 LATTICE MAGNETS; DIPOLES

14.13.48. CHANGED 5/31/83 PRINTED 6/28/83

TYPE	B3	B7	B8	B9 & B10
NUMBER OF MAGNETS	6	6	6	12
EFFECTIVE LENGTH (M)	1.5240	3.0480	4.5720	4.5720
BENDING FIELD (KG)	16.839	16.839	16.839	16.839
SAGITTA (CM)	1.66	6.65	14.96	14.96
DIPOLE GEOMETRY	CURVED WITH PARALLEL EDGES			
BENDING ANGLE (MRAD)	87.266	174.533	261.799	261.799
BENDING RADIUS (M)	17.464	17.464	17.464	17.464
IRON LENGTH (IN)	57.43	117.30	176.94	176.94
GAP HEIGHT (IN)	2.36	2.36	2.36	2.36
GAP WIDTH (IN)	7.68	7.68	7.68	11.22
COIL END EXTENSION (IN)	2.55	2.55	2.55	2.55
NO. OF TURNS	72	72	72	72
CURRENT EXCITATION (AMPS)	1150	1150	1150	1150
POWER / MAGNET (KW)	10.879	18.309	25.737	26.471

ED.2 LATTICE MAGNETS; QUADRUPOLES 13.15.19. CHANGED 5/31/83 PRINTED 5/31/83

TYPE	NUMBER	EFFECTIVE LENGTH	STRENGTH
Q1	6	0.64008 M	103.8087 KG/M
Q2	6	1.31166	-103.8087
Q3	6	0.7104	103.8087
Q4	6	0.45720	96.6333
Q5	6	0.82804	-97.4126
Q6	6	0.70104	96.6333
Q7	6	0.70104	-97.4126
Q8	6	0.45720	96.6333
Q9	6	0.45720	-97.4126
Q10	6	0.45720	40.8765
Q11	6	0.87376	89.3989
Q12	6	0.77220	-89.3989
Q13	6	0.77220	-89.3989
Q14	6	0.64262	89.3989

OTHER PARAMETERS:

TYPE	Q1 - Q9	Q10	Q11 - Q14
POLE TIP RADIUS	44.5 MM	85 MM	85 MM
NO. OF TURNS	132	40	84
POLE TIP FIELD (MAX)	4.5 KG	2.7 KG	7.7 KG
CURRENT EXCITATION (AMPS)	266	1150	1150
POWER / MAGNET (KW)	2.20-4.48	3.51	8.98-10.79

ED.3 LATTICE MAGNETS; SEXTUPOLES CHANGED 5/31/83
11.43.15. PRINTED 6/ 9/83

TYPE	NUMBER	EFFECTIVE LENGTH	STRENGTH
S7	6	0.3048	35.7175 KKG/M2
S9	6	0.3048	-219.5244
S10	6	0.3048	134.7943
S12	6	0.3048	-170.5021

OTHER PARAMETERS:

TYPE	S7,S9	S10,S12
POLE TIP RADIUS	?	?
NO OF TURNS	?	?
POLE TIP FIELD	?	?
CURRENT EXCITATION (AMPS)	?	?
POWER / MAGNET (KW)	?	?

ED.4 LATTICE MAGNETS; OCTUPOLES CHANGED 5/31/83
11.43.15. PRINTED 6/ 9/83

TYPE	NUMBER	EFFECTIVE LENGTH	STRENGTH
OC10	6	0.3048	-325.1426 KG/M3
OC12	6	0.3048	778.6057

OTHER PARAMETERS:

POLE TIP RADIUS	?
NO OF TURNS	?
POLE TIP FIELD	?
CURRENT EXCITATION (AMPS)	?
POWER / MAGNET (KW)	?

TYPE	NUMBER	EFFECTIVE LENGTH	STRENGTH
S7	6	8.0 "	53.57 KG/M2
S9	6	8.0	-330.1
S10	6	8.0	202.7
S12	6	8.0	-256.3

OTHER PARAMETERS:

TYPE	S7,S9
POLE TIP RADIUS	2.8125 "
NO OF TURNS	6 PER POLE
POLE TIP FIELD (KG)	0.14, 0.84
CURRENT EXCITATION (AMPS)	42.5, 262
POWER / MAGNET (KW)	.061, 0.375

TYPE	NUMBER	EFFECTIVE LENGTH	STRENGTH
OC10	6	8.0	-487.9 KG/M3
OC12	6	8.0	406.4

APPENDIX C

APPENDIX C.

FINAL SITE COORDINATES FOR ACCUMULATOR RING. COORDINATES ARE GIVEN AT BEND CENTER AND DOWNSTREAM END OF EACH MAGNET., COORDINATES ARE LISTED IN CLOCKWISE MANNER.
MAIN RING STATION IS X=0.0, Y=0.0 7/1/84 D.E. JOHNSON

NAME	LENGTH(IN)	X(FEET)	Y(FEET)	THETA(RAD)	S(METERS)
A10		-457.6270	-1398.9340	.523599	
A10	0.00	-457.6270	-1398.9340	.523599	0.0000
A1Q1		-444.0664	-1375.4464	.523599	
A1Q1	25.20	-443.5414	-1374.5370	.523599	8.5866
A1Q2		-441.6250	-1371.2177	.523599	
A1Q2	51.64	-440.5492	-1369.3543	.523599	10.4106
A1Q3		-438.3984	-1365.6291	.523599	
A1Q3	27.60	-437.8235	-1364.6333	.523599	12.0722
A1B3		-435.0894	-1359.8977	.523599	
A1B3	60.00	-433.6545	-1357.8485	.610865	14.5004
A1Q4		-421.1362	-1339.9705	.610865	
A1Q4	18.00	-420.7061	-1339.3562	.610865	21.3813
A1Q5		-413.7904	-1329.4796	.610865	
A1Q5	32.60	-413.0113	-1328.3670	.610865	25.4703
A1Q6		-398.5246	-1307.6777	.610865	
A1Q6	27.60	-397.8650	-1306.7358	.610865	33.5191
A1Q7		-389.3259	-1294.5407	.610865	
A1Q7	27.60	-388.6663	-1293.5987	.610865	38.4073
A1B7		-383.0209	-1285.5362	.610865	
A1B7	12.00	-382.7341	-1285.1266	.610865	41.5597
A1B7		-377.4257	-1277.5455	.610865	
A1B7	120.00	-373.8812	-1274.0009	.785398	45.9007
A1Q8		-372.1723	-1272.2921	.785398	
A1Q8	18.00	-371.6420	-1271.7618	.785398	46.8659
A1B8		-363.4798	-1263.5995	.785398	
A1B8	180.00	-356.9472	-1259.8280	1.047198	52.6571
A1Q9		-354.8543	-1258.6196	1.047198	
A1Q9	18.00	-354.2048	-1258.2446	1.047198	53.6223
A1B9		-352.9058	-1257.4946	1.047198	
A1B9	12.00	-352.4728	-1257.2446	1.047198	54.2319
A1B9		-344.2082	-1252.4731	1.047198	
A1B9	180.00	-336.9221	-1250.5208	1.308997	59.4135
A1Q10		-334.5878	-1249.8953	1.308997	
A1Q10	18.00	-333.8633	-1249.7012	1.308997	60.3787
A1B10		-324.9673	-1247.3175	1.308997	
A1B10	180.00	-317.4242	-1247.3175	1.570796	65.4587
A1B10		-315.9665	-1247.3175	1.570796	
A1B10	12.00	-315.4665	-1247.3175	1.570796	66.0554
A1Q11		-313.0755	-1247.3175	1.570796	
A1Q11	34.40	-311.6422	-1247.3175	1.570796	67.2211
A1Q12		-308.6662	-1247.3175	1.570796	
A1Q12	30.40	-307.3995	-1247.3175	1.570796	68.5142
A1B12		-306.1850	-1247.3175	1.570796	
A1B12	12.00	-305.6850	-1247.3175	1.570796	69.0368
A1Q13		-303.7037	-1247.3175	1.570796	
A1Q13	30.40	-302.4371	-1247.3175	1.570796	70.0268
A1Q14		-299.7517	-1247.3175	1.570796	
A1Q14	25.30	-298.6979	-1247.3175	1.570796	71.1666
A20		-272.9596	-1247.3179	1.570796	

A20	0.00	-272.9596	-1247.3175	1.570796	79.0115
A2Q14		-246.1676	-1247.3175	1.570796	
A2Q14	25.30	-245.1134	-1247.3175	1.570796	87.4990
A2Q13		-242.2155	-1247.3175	1.570796	
A2Q13	30.40	-240.9489	-1247.3175	1.570796	88.7684
A2S12		-239.7343	-1247.3175	1.570796	
A2S12	12.00	-239.2343	-1247.3175	1.570796	89.2910
A2Q12		-237.2531	-1247.3175	1.570796	
A2Q12	30.40	-235.9864	-1247.3175	1.570796	90.2809
A2Q11		-232.8438	-1247.3175	1.570796	
A2Q11	34.40	-231.4104	-1247.3175	1.570796	91.6757
A2S10		-229.9527	-1247.3175	1.570796	
A2S10	12.00	-229.4527	-1247.3175	1.570796	92.2724
A2B10		-220.9519	-1247.3175	1.570796	
A2B10	180.00	-213.6658	-1249.2698	1.832596	97.1363
A2Q10		-211.3315	-1249.8953	1.832596	
A2Q10	18.00	-210.6071	-1250.0894	1.832596	98.1015
A2B9		-201.7111	-1252.4731	1.832596	
A2B9	180.00	-195.1785	-1256.2446	2.094395	103.1815
A2S9		-193.0135	-1257.4946	2.094395	
A2S9	12.00	-192.5805	-1257.7446	2.094395	104.0959
A2Q9		-191.0649	-1258.6196	2.094395	
A2Q9	18.00	-190.4154	-1258.9946	2.094395	104.8579
A2B8		-182.4395	-1263.5995	2.094395	
A2B8	180.00	-177.1057	-1268.9333	2.356195	109.9379
A2Q8		-173.7469	-1272.2921	2.356195	
A2Q8	18.00	-173.2166	-1272.8224	2.356195	111.6143
A2S7		-168.4935	-1277.5455	2.356195	
A2S7	120.00	-165.6184	-1281.6517	2.530727	115.1703
A2S7		-162.8984	-1285.5362	2.530727	
A2S7	12.00	-162.6116	-1285.9458	2.530727	116.7681
A2Q7		-156.5934	-1294.5407	2.530727	
A2Q7	27.60	-155.9338	-1295.4826	2.530727	120.3167
A2Q6		-147.3947	-1307.6777	2.530727	
A2Q6	27.60	-146.7351	-1308.6197	2.530727	125.2049
A2Q5		-132.1289	-1329.4796	2.530727	
A2Q5	32.60	-131.3498	-1330.5922	2.530727	133.3807
A2Q4		-124.7830	-1339.9706	2.530727	
A2Q4	18.00	-124.3528	-1340.5849	2.530727	137.0989
A2B3		-110.8299	-1359.8977	2.530727	
A2B3	60.00	-109.5791	-1362.0642	2.617994	145.0466
A2Q3		-107.5208	-1365.6291	2.617994	
A2Q3	27.60	-106.9459	-1366.6250	2.617994	146.6518
A2Q2		-104.2943	-1371.2178	2.617994	
A2Q2	51.64	-103.2184	-1373.0812	2.617994	148.9240
A2Q1		-101.8529	-1375.4464	2.617994	
A2Q1	25.20	-101.3279	-1376.3557	2.617994	150.0765
A30		-88.2923	-1398.9340	2.617994	

A30	0.00	-88.2923	-1398.9340	2.617994	158.0230
A3Q1		-74.7317	-1422.4217	2.617994	
A3Q1	25.20	-74.2067	-1423.3310	2.617994	166.6096
A3Q2		-72.2903	-1426.6503	2.617994	
A3Q2	51.64	-71.2144	-1428.5137	2.617994	168.4336
A3Q3		-69.0637	-1432.2389	2.617994	
A3Q3	27.60	-68.4887	-1433.2348	2.617994	170.0952
A3B3		-65.7547	-1437.9703	2.617994	
A3B3	60.00	-64.6974	-1440.2375	2.705260	172.5234
A3Q4		-55.4738	-1460.0177	2.705260	
A3Q4	18.00	-55.1568	-1460.6974	2.705260	179.4043
A3Q5		-50.0613	-1471.6248	2.705260	
A3Q5	32.60	-49.4873	-1472.8558	2.705260	183.4933
A3Q6		-38.8132	-1495.7464	2.705260	
A3Q6	27.60	-38.3273	-1496.7885	2.705260	191.5421
A3Q7		-32.0356	-1510.2812	2.705260	
A3Q7	27.60	-31.5496	-1511.3234	2.705260	196.4303
A3B7		-27.3899	-1520.2437	2.705260	
A3B7	12.00	-27.1786	-1520.6969	2.705260	199.5827
A3B7		-23.2674	-1529.0846	2.705260	
A3B7	120.00	-21.9700	-1533.9266	2.879793	203.9237
A3Q8		-21.3445	-1536.2609	2.879793	
A3Q8	18.00	-21.1504	-1536.9853	2.879793	204.8889
A3B8		-18.1628	-1548.1351	2.879793	
A3B8	180.00	-18.1628	-1555.6783	3.141593	210.6801
A3Q9		-18.1628	-1558.0949	3.141593	
A3Q9	18.00	-18.1628	-1558.8449	3.141593	211.6453
A3B9		-18.1628	-1560.3449	3.141593	
A3B9	12.00	-18.1628	-1560.8449	3.141593	212.2549
A3B9		-18.1628	-1570.3881	3.141593	
A3B9	180.00	-20.1151	-1577.6742	3.403392	217.4365
A3Q10		-20.7406	-1580.0085	3.403392	
A3Q10	18.00	-20.9347	-1580.7329	3.403392	218.4017
A3B10		-23.3184	-1589.6289	3.403392	
A3B10	180.00	-27.0899	-1596.1615	3.665192	223.4817
A3B10		-27.8188	-1597.4238	3.665192	
A3B10	12.00	-28.0688	-1597.8569	3.665192	224.0784
A3Q11		-29.2643	-1599.9275	3.665192	
A3Q11	34.40	-29.9809	-1601.1688	3.665192	225.2441
A3Q12		-31.4689	-1603.7461	3.665192	
A3Q12	30.40	-32.1023	-1604.8431	3.665192	226.5372
A3B12		-32.7096	-1605.8949	3.665192	
A3B12	12.00	-32.9596	-1606.3279	3.665192	227.0598
A3Q13		-33.9502	-1608.0437	3.665192	
A3Q13	30.40	-34.5835	-1609.1407	3.665192	228.0498
A3Q14		-35.9262	-1611.4663	3.665192	
A3Q14	25.30	-36.4533	-1612.3793	3.665192	229.1896
A40		-49.3222	-1634.6689	3.665192	

A4O	0.00	-49.3222	-1634.6689	3.665192	237.0345
A4Q14		-62.7182	-1657.8715	3.665192	
A4Q14	25.30	-63.2453	-1658.7844	3.665192	245.5220
A4Q13		-64.6943	-1661.2941	3.665192	
A4Q13	30.40	-65.3276	-1662.3910	3.665192	246.7914
A4S12		-65.9349	-1663.4429	3.665192	
A4S12	12.00	-66.1849	-1663.8759	3.665192	247.3140
A4Q12		-67.1755	-1665.5917	3.665192	
A4Q12	30.40	-67.8088	-1666.6887	3.665192	248.3039
A4Q11		-69.3802	-1669.4103	3.665192	
A4Q11	34.40	-70.0968	-1670.6516	3.665192	249.6987
A4S10		-70.8257	-1671.9140	3.665192	
A4S10	12.00	-71.0757	-1672.3470	3.665192	250.2954
A4B10		-75.3261	-1679.7089	3.665192	
A4B10	180.00	-80.6599	-1685.0427	3.926991	255.1593
A4Q10		-82.3687	-1686.7515	3.926991	
A4Q10	18.00	-82.8990	-1687.2819	3.926991	256.1245
A4B9		-89.4114	-1693.7942	3.926991	
A4B9	180.00	-95.9439	-1697.5657	4.188790	261.2045
A4S9		-98.1090	-1698.8157	4.188790	
A4S9	12.00	-98.5420	-1699.0657	4.188790	262.1189
A4Q9		-100.0575	-1699.9407	4.188790	
A4Q9	18.00	-100.7070	-1700.3157	4.188790	262.8809
A4B8		-108.6830	-1704.9206	4.188790	
A4B8	180.00	-115.9691	-1706.8729	4.450590	267.9609
A4Q8		-120.5572	-1708.1023	4.450590	
A4Q8	18.00	-121.2817	-1708.2964	4.450590	269.6373
A4B7		-127.7335	-1710.0252	4.450590	
A4B7	120.00	-132.7271	-1710.4621	4.625123	273.1933
A4S7		-137.4512	-1710.8754	4.625123	
A4S7	12.00	-137.9493	-1710.9190	4.625123	274.7911
A4Q7		-148.4018	-1711.8334	4.625123	
A4Q7	27.60	-149.5474	-1711.9337	4.625123	278.3397
A4Q6		-164.3782	-1713.2312	4.625123	
A4Q6	27.60	-165.5238	-1713.3314	4.625123	283.2279
A4Q5		-190.8921	-1715.5509	4.625123	
A4Q5	32.60	-192.2452	-1715.6692	4.625123	291.4037
A4Q4		-203.6504	-1716.6671	4.625123	
A4Q4	18.00	-204.3976	-1716.7324	4.625123	295.1219
A4B3		-227.8845	-1718.7873	4.625123	
A4B3	60.00	-230.3860	-1718.7873	4.712389	303.0696
A4Q3		-234.5025	-1718.7873	4.712389	
A4Q3	27.60	-235.6524	-1718.7873	4.712389	304.6748
A4Q2		-240.9557	-1718.7873	4.712389	
A4Q2	51.64	-243.1074	-1718.7873	4.712389	306.9470
A4Q1		-245.8385	-1718.7873	4.712389	
A4Q1	25.20	-246.8885	-1718.7873	4.712389	308.0995
A5O		-272.9597	-1718.7873	4.712389	

A50	0.00	-272.9597	-1718.7873	4.712389	316.0460
A5Q1		-300.0809	-1718.7873	4.712389	
A5Q1	25.20	-301.1309	-1718.7873	4.712389	324.6326
A5Q2		-304.9636	-1718.7873	4.712389	
A5Q2	51.64	-307.1153	-1718.7873	4.712389	326.4566
A5Q3		-311.4168	-1718.7873	4.712389	
A5Q3	27.60	-312.5667	-1718.7873	4.712389	328.1182
A5B3		-318.0349	-1718.7873	4.712389	
A5B3	60.00	-320.5269	-1718.5692	4.799656	330.5464
A5Q4		-342.2689	-1716.6670	4.799656	
A5Q4	18.00	-343.0160	-1716.6017	4.799656	337.4273
A5Q5		-355.0272	-1715.5508	4.799656	
A5Q5	32.60	-356.3803	-1715.4325	4.799656	341.5163
A5Q6		-381.5411	-1713.2312	4.799656	
A5Q6	27.60	-382.6867	-1713.1309	4.799656	349.5651
A5Q7		-397.5175	-1711.8334	4.799656	
A5Q7	27.60	-398.6631	-1711.7332	4.799656	354.4533
A5B7		-408.4681	-1710.8754	4.799656	
A5B7	12.00	-408.9662	-1710.8318	4.799656	357.6057
A5B7		-418.1859	-1710.0252	4.799656	
A5B7	120.00	-423.0278	-1708.7278	4.974188	361.9467
A5Q8		-425.3621	-1708.1023	4.974188	
A5Q8	18.00	-426.0865	-1707.9082	4.974188	362.9119
A5B8		-437.2364	-1704.9206	4.974188	
A5B8	180.00	-443.7689	-1701.1490	5.235988	368.7031
A5Q9		-445.8618	-1699.9407	5.235988	
A5Q9	18.00	-446.5113	-1699.5657	5.235988	369.6683
A5B9		-447.8104	-1698.8157	5.235988	
A5B9	12.00	-448.2434	-1698.5657	5.235988	370.2779
A5B9		-456.5080	-1693.7941	5.235988	
A5B9	180.00	-461.8418	-1688.4603	5.497787	375.4595
A5Q10		-463.5506	-1686.7515	5.497787	
A5Q10	18.00	-464.0809	-1686.2212	5.497787	376.4247
A5B10		-470.5932	-1679.7088	5.497787	
A5B10	180.00	-474.3648	-1673.1763	5.759587	381.5047
A5B10		-475.0936	-1671.9139	5.759587	
A5B10	12.00	-475.3436	-1671.4809	5.759587	382.1014
A5Q11		-476.5391	-1669.4102	5.759587	
A5Q11	34.40	-477.2558	-1668.1689	5.759587	383.2671
A5Q12		-478.7438	-1665.5916	5.759587	
A5Q12	30.40	-479.3771	-1664.4947	5.759587	384.5602
A5B12		-479.9844	-1663.4428	5.759587	
A5B12	12.00	-480.2344	-1663.0098	5.759587	385.0828
A5Q13		-481.2250	-1661.2940	5.759587	
A5Q13	30.40	-481.8584	-1660.1971	5.759587	386.0728
A5Q14		-483.2011	-1657.8714	5.759587	
A5Q14	25.30	-483.7282	-1656.9585	5.759587	387.2126
A60		-496.5971	-1634.6688	5.759587	

A60	0.00	-496.5971	-1634.6688	5.759587	395.0575
A6Q14		-509.9931	-1611.4663	5.759587	
A6Q14	25.30	-510.5202	-1610.5533	5.759587	403.5450
A6Q13		-511.9691	-1608.0437	5.759587	
A6Q13	30.40	-512.6025	-1606.9467	5.759587	404.8144
A6S12		-513.2097	-1605.8949	5.759587	
A6S12	12.00	-513.4597	-1605.4619	5.759587	405.3370
A6Q12		-514.4504	-1603.7461	5.759587	
A6Q12	30.40	-515.0837	-1602.6491	5.759587	406.3269
A6Q11		-516.6550	-1599.9275	5.759587	
A6Q11	34.40	-517.3717	-1598.6862	5.759587	407.7217
A6S10		-518.1005	-1597.4238	5.759587	
A6S10	12.00	-518.3505	-1596.9908	5.759587	408.3184
A6B10		-522.6009	-1589.6289	5.759587	
A6B10	180.00	-524.5532	-1582.3427	6.021386	413.1823
A6Q10		-525.1787	-1580.0084	6.021386	
A6Q10	18.00	-525.3728	-1579.2840	6.021386	414.1475
A6B9		-527.7565	-1570.3880	6.021386	
A6B9	180.00	-527.7565	-1562.8449	6.283185	419.2275
A6S9		-527.7565	-1560.3449	.000000	
A6S9	12.00	-527.7565	-1559.8449	.000000	420.1419
A6Q9		-527.7565	-1558.0949	.000000	
A6Q9	18.00	-527.7565	-1557.3449	.000000	420.9039
A6B8		-527.7565	-1548.1351	.000000	
A6B8	180.00	-525.8042	-1540.8490	.261800	425.9839
A6Q8		-524.5748	-1536.2608	.261800	
A6Q8	18.00	-524.3807	-1535.5364	.261800	427.6603
A6B7		-522.6519	-1529.0846	.261800	
A6B7	120.00	-520.5334	-1524.5415	.436332	431.2163
A6S7		-518.5293	-1520.2437	.436332	
A6S7	12.00	-518.3180	-1519.7905	.436332	432.8141
A6Q7		-513.8837	-1510.2811	.436332	
A6Q7	27.60	-513.3977	-1509.2389	.436332	436.3627
A6Q6		-507.1060	-1495.7463	.436332	
A6Q6	27.60	-506.6200	-1494.7041	.436332	441.2509
A6Q5		-495.8580	-1471.6248	.436332	
A6Q5	32.60	-495.2839	-1470.3938	.436332	449.4267
A6Q4		-490.4455	-1460.0176	.436332	
A6Q4	18.00	-490.1285	-1459.3379	.436332	453.1449
A6B3		-480.1646	-1437.9702	.436332	
A6B3	60.00	-478.9138	-1435.8038	.523599	461.0926
A6Q3		-476.8556	-1432.2388	.523599	
A6Q3	27.60	-476.2806	-1431.2430	.523599	462.6978
A6Q2		-473.6290	-1426.6502	.523599	
A6Q2	51.64	-472.5531	-1424.7868	.523599	464.9700
A6Q1		-471.1876	-1422.4216	.523599	
A6Q1	25.20	-470.6626	-1421.5123	.523599	466.1225
A10		-457.6270	-1398.9340	.523599	
A10	0.00	-457.6270	-1398.9340	.523599	474.0690

15.21.50. UCLP, GQ, TB10, 0.346KLNS. ** END OF LISTING **

FINAL SITE COORDINATES FOR DEBUNCHER RING DE JOHSON 7-1-84

BEGIN -467.8520 -1393.0300 .5235987756

NAME	LENGTH(IN)	X(FEET)	Y(FEET)	THETA(RAD)	S(METERS)
D1O		-467.8520	-1393.0300	.523599	
D1O	0.00	-467.8520	-1393.0300	.523599	0.0000
D1Q1		-467.5645	-1392.5320	.523599	
D1Q1	13.80	-467.2770	-1392.0341	.523599	.3505
D1Q2		-460.9812	-1380.4365	.523599	
D1Q2	27.60	-460.0062	-1379.4406	.523599	4.7828
D1Q3		-453.3103	-1367.8431	.523599	
D1Q3	27.60	-452.7353	-1366.8472	.523599	9.2151
D1Q4		-446.0395	-1355.2496	.523599	
D1Q4	27.60	-445.4645	-1354.2537	.523599	13.6474
D1Q5		-438.7687	-1342.6562	.523599	
D1Q5	32.60	-438.0895	-1341.4798	.523599	18.1432
D1Q6		-431.4978	-1330.0627	.523599	
D1Q6	32.60	-430.8187	-1328.8864	.523599	22.5755
D1Q7		-424.2270	-1317.4693	.523599	
D1Q7	27.60	-423.6520	-1316.4734	.523599	26.9443
D1B7		-420.9906	-1311.1708	.523599	
D1B7	65.37	-419.0094	-1308.9504	.618799	29.6402
D1Q8		-416.3719	-1305.2465	.618799	
D1Q8	27.60	-415.7048	-1304.3097	.618799	31.3766
D1B8		-412.1532	-1299.3221	.618799	
D1B8	65.37	-410.3681	-1297.2621	.713998	34.0725
D1Q9		-407.3904	-1293.8256	.713998	
D1Q9	27.60	-406.6373	-1292.9565	.713998	35.8089
D1Q10		-397.8677	-1282.8358	.713998	
D1Q10	27.60	-397.1146	-1281.9667	.713998	40.2412
D1Q11		-388.3449	-1271.8459	.713998	
D1Q11	27.60	-387.5918	-1270.9768	.713998	44.6735
D1B11		-383.5822	-1266.3494	.713998	
D1B11	65.37	-381.6094	-1264.4684	.809198	47.3693
D1Q12		-378.3185	-1261.3306	.809198	
D1Q12	27.60	-377.4862	-1260.5370	.809198	49.1058
D1B12		-373.0549	-1256.3117	.809198	
D1B12	65.37	-370.9123	-1254.6267	.904398	51.8016
D1Q13		-367.3380	-1251.8159	.904398	
D1Q13	27.60	-366.4341	-1251.1050	.904398	53.5381
D1B13		-361.6211	-1247.3201	.904398	
D1B13	65.37	-359.3280	-1245.8464	.999598	56.2339
D1Q14		-355.5028	-1243.3881	.999598	
D1Q14	27.60	-354.5353	-1242.7663	.999598	57.9704
D1B14		-349.3844	-1239.4560	.999598	

D1B14	65.37	-346.9616	-1238.2070	1.094797	60.6662
D1Q15		-342.9200	-1236.1234	1.094797	
D1Q15	27.60	-341.8979	-1235.5965	1.094797	62.4027
D1B15		-336.4556	-1232.7908	1.094797	
D1B15	65.37	-333.9291	-1231.7777	1.189997	65.0985
D1Q16		-329.7037	-1230.0877	1.189997	
D1Q16	27.60	-328.6361	-1229.6603	1.189997	66.8350
D1B16		-322.9518	-1227.3847	1.189997	
D1B16	65.37	-320.3364	-1226.6167	1.285197	69.5308
D1Q17		-315.9735	-1225.3357	1.285197	
D1Q17	27.60	-314.8701	-1225.0117	1.285197	71.2673
D1B17		-308.9952	-1223.2866	1.285197	
D1B17	65.37	-306.3187	-1222.7708	1.380397	73.9631
D1Q18		-301.8538	-1221.9102	1.380397	
D1Q18	27.60	-300.7245	-1221.6926	1.380397	75.6996
D1B18		-294.7123	-1220.5338	1.380397	
D1B18	65.37	-291.9988	-1220.2747	1.475597	78.3954
D1Q19		-287.4723	-1219.8425	1.475597	
D1Q19	27.60	-286.3275	-1219.7332	1.475597	80.1319
D1B19		-280.2324	-1219.1512	1.475597	
D1B19	65.37	-277.5066	-1219.1512	1.570796	82.8277
D1Q20		-272.9595	-1219.1512	1.570796	
D1Q20	27.60	-271.8095	-1219.1512	1.570796	84.5642
D2B19		-265.6866	-1219.1512	1.570796	
D2B19	65.37	-262.9731	-1219.4103	1.665996	87.2600
D2Q19		-258.4466	-1219.8425	1.665996	
D2Q19	27.60	-257.3018	-1219.9518	1.665996	88.9965
D2B18		-251.2067	-1220.5338	1.665996	
D2B18	65.37	-248.5301	-1221.0497	1.761196	91.6923
D2Q18		-244.0652	-1221.9102	1.761196	
D2Q18	27.60	-242.9360	-1222.1279	1.761196	93.4288
D2B17		-236.9237	-1223.2866	1.761196	
D2B17	65.37	-234.3083	-1224.0546	1.856396	96.1246
D2Q17		-229.9455	-1225.3357	1.856396	
D2Q17	27.60	-228.8420	-1225.6596	1.856396	97.8611
D2B16		-222.9672	-1227.3847	1.856396	
D2B16	65.37	-220.4366	-1228.3977	1.951595	100.5570
D2Q16		-216.2152	-1230.0877	1.951595	
D2Q16	27.60	-215.1476	-1230.5151	1.951595	102.2934
D2B15		-209.4633	-1232.7908	1.951595	
D2B15	65.37	-207.0405	-1234.0398	2.046795	104.9893
D2Q15		-202.9989	-1236.1234	2.046795	
D2Q15	27.60	-201.9768	-1236.6504	2.046795	106.7257
D2B14		-196.5345	-1239.4561	2.046795	
D2B14	65.37	-194.2414	-1240.9297	2.141995	109.4216

D2Q14		-190.4162	-1243.3881	2.141995	
D2Q14	27.60	-189.4487	-1244.0098	2.141995	111.1580
D2B13		-184.2978	-1247.3201	2.141995	
D2B13	65.37	-182.1552	-1249.0051	2.237195	113.8539
D2Q13		-178.5809	-1251.8159	2.237195	
D2Q13	27.60	-177.6770	-1252.5268	2.237195	115.5903
D2B12		-172.8641	-1256.3117	2.237195	
D2B12	65.37	-170.8913	-1258.1927	2.332395	118.2862
D2Q12		-167.6004	-1261.3306	2.332395	
D2Q12	27.60	-166.7681	-1262.1242	2.332395	120.0226
D2B11		-162.3368	-1266.3494	2.332395	
D2B11	65.37	-160.5518	-1268.4095	2.427594	122.7185
D2Q11		-157.5741	-1271.8459	2.427594	
D2Q11	27.60	-156.8210	-1272.7150	2.427594	124.4549
D2Q10		-148.0513	-1282.8358	2.427594	
D2Q10	27.60	-147.2982	-1283.7049	2.427594	128.8872
D2Q9		-138.5285	-1293.8257	2.427594	
D2Q9	27.60	-137.7754	-1294.6948	2.427594	133.3195
D2B8		-133.7658	-1299.3221	2.427594	
D2B8	65.37	-132.1847	-1301.5425	2.522794	136.0153
D2Q8		-129.5471	-1305.2465	2.522794	
D2Q8	27.60	-128.8800	-1306.1832	2.522794	137.7518
D2B7		-125.3284	-1311.1708	2.522794	
D2B7	65.37	-123.9655	-1313.5314	2.617994	140.4476
D2Q7		-121.6920	-1317.4693	2.617994	
D2Q7	27.60	-121.1170	-1318.4652	2.617994	142.1841
D2Q6		-114.4211	-1330.0627	2.617994	
D2Q6	32.60	-113.7420	-1331.2391	2.617994	146.6799
D2Q5		-107.1503	-1342.6562	2.617994	
D2Q5	32.60	-106.4711	-1343.8326	2.617994	151.1122
D2Q4		-99.8795	-1355.2497	2.617994	
D2Q4	27.60	-99.3045	-1356.2456	2.617994	155.4810
D2Q3		-92.6086	-1367.8431	2.617994	
D2Q3	27.60	-92.0336	-1368.8390	2.617994	159.9133
D2Q2		-85.3378	-1380.4366	2.617994	
D2Q2	27.60	-84.7628	-1381.4325	2.617994	164.3456
D2Q1		-78.3545	-1392.5321	2.617994	
D2Q1	13.80	-78.0670	-1393.0300	2.617994	168.4274
D30		-78.0670	-1393.0300	2.617994	
D30	0.00	-78.0670	-1393.0300	2.617994	168.4274
D3Q1		-77.7795	-1393.5280	2.617994	
D3Q1	13.80	-77.4920	-1394.0259	2.617994	168.7779
D3Q2		-70.7961	-1405.6235	2.617994	
D3Q2	27.60	-70.2211	-1406.6194	2.617994	173.2102
D3Q3		-63.5253	-1418.2169	2.617994	

D3Q3	27.60	-62.9503	-1419.2129	2.617994	177.6425
D3Q4		-56.2545	-1430.8104	2.617994	
D3Q4	27.60	-55.6795	-1431.8063	2.617994	182.0748
D3Q5		-48.9836	-1443.4038	2.617994	
D3Q5	32.60	-48.3045	-1444.5802	2.617994	186.5706
D3Q6		-41.7128	-1455.9973	2.617994	
D3Q6	32.60	-41.0336	-1457.1736	2.617994	191.0029
D3Q7		-34.4420	-1468.5907	2.617994	
D3Q7	27.60	-33.8670	-1469.5867	2.617994	195.3717
D3B7		-30.8055	-1474.8892	2.617994	
D3B7	65.37	-29.6732	-1477.3687	2.713194	198.0675
D3Q8		-27.7843	-1481.5049	2.713194	
D3Q8	27.60	-27.3065	-1482.5510	2.713194	199.8040
D3B8		-24.7630	-1488.1206	2.713194	
D3B8	65.37	-23.8715	-1490.6965	2.808394	202.4998
D3Q9		-22.3843	-1494.9934	2.808394	
D3Q9	27.60	-22.0081	-1496.0802	2.808394	204.2363
D3Q10		-17.6282	-1508.7353	2.808394	
D3Q10	27.60	-17.2520	-1509.8221	2.808394	208.6686
D3Q11		-12.8720	-1522.4772	2.808394	
D3Q11	27.60	-12.4959	-1523.5640	2.808394	213.1009
D3B11		-10.4933	-1529.3501	2.808394	
D3B11	65.37	-9.8507	-1531.9991	2.903593	215.7967
D3Q12		-8.7787	-1536.4180	2.903593	
D3Q12	27.60	-8.5075	-1537.5356	2.903593	217.5332
D3B12		-7.0640	-1543.4859	2.903593	
D3B12	65.37	-6.6761	-1546.1839	2.998793	220.2290
D3Q13		-6.0290	-1550.6847	2.998793	
D3Q13	27.60	-5.8653	-1551.8230	2.998793	221.9655
D3B13		-4.9939	-1557.8836	2.998793	
D3B13	65.37	-4.8642	-1560.6063	3.093993	224.6613
D3Q14		-4.6479	-1565.1483	3.093993	
D3Q14	27.60	-4.5932	-1566.2970	3.093993	226.3978
D3B14		-4.3018	-1572.4129	3.093993	
D3B14	65.37	-4.4315	-1575.1356	3.189193	229.0936
D3Q15		-4.6479	-1579.6776	3.189193	
D3Q15	27.60	-4.7026	-1580.8263	3.189193	230.8301
D3B15		-4.9939	-1586.9422	3.189193	
D3B15	65.37	-5.3819	-1589.6403	3.284392	233.5259
D3Q16		-6.0290	-1594.1411	3.284392	
D3Q16	27.60	-6.1926	-1595.2794	3.284392	235.2624
D3B16		-7.0640	-1601.3400	3.284392	
D3B16	65.37	-7.7067	-1603.9889	3.379592	237.9582
D3Q17		-8.7787	-1608.4078	3.379592	
D3Q17	27.60	-9.0498	-1609.5254	3.379592	239.6947

D3B17		-10.4933	-1615.4757	3.379592	
D3B17	65.37	-11.3848	-1618.0516	3.474792	242.3905
D3Q18		-12.8721	-1622.3486	3.474792	
D3Q18	27.60	-13.2482	-1623.4354	3.474792	244.1270
D3B18		-15.2508	-1629.2215	3.474792	
D3B18	65.37	-16.3831	-1631.7010	3.569992	246.8228
D3Q19		-18.2721	-1635.8371	3.569992	
D3Q19	27.60	-18.7498	-1636.8832	3.569992	248.5593
D3B19		-21.2933	-1642.4528	3.569992	
D3B19	65.37	-22.6562	-1644.8134	3.665192	251.2551
D3Q20		-24.9298	-1648.7513	3.665192	
D3Q20	27.60	-25.5048	-1649.7472	3.665192	252.9916
D4B19		-28.5662	-1655.0498	3.665192	
D4B19	65.37	-30.1473	-1657.2702	3.760391	255.6874
D4Q19		-32.7849	-1660.9741	3.760391	
D4Q19	27.60	-33.4520	-1661.9109	3.760391	257.4239
D4B18		-37.0036	-1666.8985	3.760391	
D4B18	65.37	-38.7886	-1668.9585	3.855591	260.1197
D4Q18		-41.7663	-1672.3949	3.855591	
D4Q18	27.60	-42.5194	-1673.2641	3.855591	261.8562
D4B17		-46.5291	-1677.8914	3.855591	
D4B17	65.37	-48.5018	-1679.7725	3.950791	264.5520
D4Q17		-51.7927	-1682.9103	3.950791	
D4Q17	27.60	-52.6250	-1683.7039	3.950791	266.2885
D4B16		-57.0563	-1687.9292	3.950791	
D4B16	65.37	-59.1990	-1689.6142	4.045991	268.9843
D4Q16		-62.7732	-1692.4250	4.045991	
D4Q16	27.60	-63.6772	-1693.1359	4.045991	270.7208
D4B15		-68.4901	-1696.9208	4.045991	
D4B15	65.37	-70.7832	-1698.3945	4.141190	273.4166
D4Q15		-74.6085	-1700.8528	4.141190	
D4Q15	27.60	-75.5759	-1701.4745	4.141190	275.1531
D4B14		-80.7268	-1704.7848	4.141190	
D4B14	65.37	-83.1496	-1706.0339	4.236390	277.8489
D4Q14		-87.1912	-1708.1175	4.236390	
D4Q14	27.60	-88.2134	-1708.6444	4.236390	279.5854
D4B13		-93.6556	-1711.4501	4.236390	
D4B13	65.37	-96.1862	-1712.4632	4.331590	282.2812
D4Q13		-100.4075	-1714.1531	4.331590	
D4Q13	27.60	-101.4752	-1714.5806	4.331590	284.0177
D4B12		-107.1595	-1716.8562	4.331590	
D4B12	65.37	-109.7749	-1717.6242	4.426790	286.7135
D4Q12		-114.1377	-1718.9052	4.426790	
D4Q12	27.60	-115.2412	-1719.2292	4.426790	288.4500
D4B11		-121.1160	-1720.9542	4.426790	

D4B11	65.37	-123.7926	-1721.4701	4.521990	291.1458
D4Q11		-128.2575	-1722.3306	4.521990	
D4Q11	27.60	-129.3867	-1722.5483	4.521990	292.8823
D4Q10		-142.5364	-1725.0827	4.521990	
D4Q10	27.60	-143.6656	-1725.3003	4.521990	297.3146
D4Q9		-156.8153	-1727.8347	4.521990	
D4Q9	27.60	-157.9445	-1728.0523	4.521990	301.7469
D4B8		-163.9567	-1729.2111	4.521990	
D4B8	65.37	-166.6702	-1729.4702	4.617189	304.4427
D4Q8		-171.1967	-1729.9024	4.617189	
D4Q8	27.60	-172.3415	-1730.0117	4.617189	306.1792
D4B7		-178.4366	-1730.5937	4.617189	
D4B7	65.37	-181.1624	-1730.5937	4.712389	308.8750
D4Q7		-185.7095	-1730.5937	4.712389	
D4Q7	27.60	-186.8595	-1730.5937	4.712389	310.6115
D4Q6		-200.2512	-1730.5937	4.712389	
D4Q6	32.60	-201.6095	-1730.5937	4.712389	315.1073
D4Q5		-214.7929	-1730.5937	4.712389	
D4Q5	32.60	-216.1512	-1730.5937	4.712389	319.5396
D4Q4		-229.3345	-1730.5937	4.712389	
D4Q4	27.60	-230.4845	-1730.5937	4.712389	323.9084
LQRF		-236.6054	-1730.5937	4.712389	
LQRF	84.00	-240.1054	-1730.5937	4.712389	326.8408
D4Q3		-243.8762	-1730.5937	4.712389	
D4Q3	27.60	-245.0262	-1730.5937	4.712389	328.3407
D4Q2		-258.4179	-1730.5937	4.712389	
D4Q2	27.60	-259.5679	-1730.5937	4.712389	332.7730
LQRF		-265.6887	-1730.5937	4.712389	
LQRF	84.00	-269.1887	-1730.5937	4.712389	335.7054
D5Q0		-272.3845	-1730.5937	4.712389	
D5Q0	13.80	-272.9595	-1730.5937	4.712389	336.8548
D50		-272.9595	-1730.5937	4.712389	
D50	0.00	-272.9595	-1730.5937	4.712389	336.8548
D5Q0		-273.5345	-1730.5937	4.712389	
D5Q0	13.80	-274.1095	-1730.5937	4.712389	337.2053
LQRF		-280.2304	-1730.5937	4.712389	
LQRF	84.00	-283.7304	-1730.5937	4.712389	340.1377
D5Q2		-287.5012	-1730.5937	4.712389	
D5Q2	27.60	-288.6512	-1730.5937	4.712389	341.6376
LQRF		-294.7720	-1730.5937	4.712389	
LQRF	84.00	-298.2720	-1730.5937	4.712389	344.5700
D5Q3		-302.0429	-1730.5937	4.712389	
D5Q3	27.60	-303.1929	-1730.5937	4.712389	346.0699
LQRF		-309.3137	-1730.5937	4.712389	
LQRF	84.00	-312.8137	-1730.5937	4.712389	349.0023

D5Q4		-316.5845	-1730.5937	4.712389	
D5Q4	27.60	-317.7345	-1730.5937	4.712389	350.5022
LQRF		-323.7512	-1730.5937	4.712389	
LQRF	84.00	-327.2512	-1730.5937	4.712389	353.4029
D5Q5		-331.1262	-1730.5937	4.712389	
D5Q5	32.60	-332.4845	-1730.5937	4.712389	354.9980
LQRF		-338.3970	-1730.5937	4.712389	
LQRF	84.00	-341.8970	-1730.5937	4.712389	357.8669
D5Q6		-345.6679	-1730.5937	4.712389	
D5Q6	32.60	-347.0262	-1730.5937	4.712389	359.4303
LQRF		-353.0429	-1730.5937	4.712389	
LQRF	84.00	-356.5429	-1730.5937	4.712389	362.3310
D5Q7		-360.2095	-1730.5937	4.712389	
D5Q7	27.60	-361.3595	-1730.5937	4.712389	363.7991
D5B7		-367.4824	-1730.5937	4.712389	
D5B7	65.37	-370.1959	-1730.3346	4.807589	366.4949
D5Q8		-374.7224	-1729.9024	4.807589	
D5Q8	27.60	-375.8672	-1729.7931	4.807589	368.2314
D5B8		-381.9623	-1729.2110	4.807589	
D5B8	65.37	-384.6389	-1728.6952	4.902789	370.9272
D5Q9		-389.1038	-1727.8346	4.902789	
D5Q9	27.60	-390.2330	-1727.6170	4.902789	372.6637
SMRF		-393.8271	-1726.9243	4.902789	
SMRF	59.06	-396.2432	-1726.4586	4.902789	374.5293
SMRF		-398.6594	-1725.9929	4.902789	
SMRF	59.06	-401.0756	-1725.5273	4.902789	376.0293
D5Q10		-403.3827	-1725.0826	4.902789	
D5Q10	27.60	-404.5119	-1724.8650	4.902789	377.0960
SMRF		-408.1060	-1724.1723	4.902789	
SMRF	59.06	-410.5221	-1723.7066	4.902789	378.9616
D5Q11		-417.6616	-1722.3306	4.902789	
D5Q11	27.60	-418.7908	-1722.1129	4.902789	381.5283
D5B11		-424.8030	-1720.9542	4.902789	
D5B11	65.37	-427.4184	-1720.1862	4.997988	384.2241
D5Q12		-431.7813	-1718.9052	4.997988	
D5Q12	27.60	-432.8847	-1718.5812	4.997988	385.9606
D5B12		-438.7596	-1716.8561	4.997988	
D5B12	65.37	-441.2902	-1715.8431	5.093188	388.6564
D5Q13		-445.5115	-1714.1531	5.093188	
D5Q13	27.60	-446.5791	-1713.7257	5.093188	390.3929
D5B13		-452.2634	-1711.4500	5.093188	
D5B13	65.37	-454.6862	-1710.2010	5.188388	393.0887
D5Q14		-458.7278	-1708.1174	5.188388	
D5Q14	27.60	-459.7500	-1707.5904	5.188388	394.8252
D5B14		-465.1922	-1704.7848	5.188388	

D5B14	65.37	-467.4853	-1703.3111	5.283588	397.5210
D5Q15		-471.3106	-1700.8527	5.283588	
D5Q15	27.60	-472.2780	-1700.2310	5.283588	399.2575
D5B15		-477.4289	-1696.9207	5.283588	
D5B15	65.37	-479.5716	-1695.2357	5.378788	401.9533
D5Q16		-483.1458	-1692.4249	5.378788	
D5Q16	27.60	-484.0498	-1691.7140	5.378788	403.6898
D5B16		-488.8627	-1687.9291	5.378788	
D5B16	65.37	-490.8355	-1686.0481	5.473987	406.3856
D5Q17		-494.1263	-1682.9102	5.473987	
D5Q17	27.60	-494.9586	-1682.1166	5.473987	408.1221
D5B17		-499.3900	-1677.8914	5.473987	
D5B17	65.37	-501.1750	-1675.8313	5.569187	410.8179
D5Q18		-504.1527	-1672.3949	5.569187	
D5Q18	27.60	-504.9058	-1671.5258	5.569187	412.5544
D5B18		-508.9154	-1666.8984	5.569187	
D5B18	65.37	-510.4966	-1664.6780	5.664387	415.2502
D5Q19		-513.1341	-1660.9741	5.664387	
D5Q19	27.60	-513.8012	-1660.0373	5.664387	416.9867
D5B19		-517.3528	-1655.0497	5.664387	
D5B19	65.37	-518.7157	-1652.6891	5.759587	419.6825
D5Q20		-520.9893	-1648.7512	5.759587	
D5Q20	27.60	-521.5643	-1647.7553	5.759587	421.4190
D6B19		-524.6257	-1642.4527	5.759587	
D6B19	65.37	-525.7580	-1639.9732	5.854787	424.1148
D6Q19		-527.6470	-1635.8371	5.854787	
D6Q19	27.60	-528.1247	-1634.7910	5.854787	425.8513
D6B18		-530.6682	-1629.2214	5.854787	
D6B18	65.37	-531.5598	-1626.6455	5.949986	428.5471
D6Q18		-533.0470	-1622.3485	5.949986	
D6Q18	27.60	-533.4231	-1621.2618	5.949986	430.2836
D6B17		-535.4257	-1615.4756	5.949986	
D6B17	65.37	-536.0683	-1612.8266	6.045186	432.9794
D6Q17		-537.1403	-1608.4077	6.045186	
D6Q17	27.60	-537.4115	-1607.2902	6.045186	434.7159
D6B16		-538.8550	-1601.3399	6.045186	
D6B16	65.37	-539.2429	-1598.6418	6.140386	437.4117
D6Q16		-539.8900	-1594.1410	6.140386	
D6Q16	27.60	-540.0537	-1593.0027	6.140386	439.1482
D6B15		-540.9251	-1586.9421	6.140386	
D6B15	65.37	-541.0548	-1584.2194	6.235586	441.8440
D6Q15		-541.2711	-1579.6775	6.235586	
D6Q15	27.60	-541.3258	-1578.5288	6.235586	443.5805
D6B14		-541.6172	-1572.4128	6.235586	
D6B14	65.37	-541.4875	-1569.6901	6.330785	446.2763

D6Q14		-541.2711	-1565.1482	.047600	
D6Q14	27.60	-541.2164	-1563.9995	.047600	448.0128
D6B13		-540.9251	-1557.8835	.047600	
D6B13	65.37	-540.5371	-1555.1854	.142800	450.7086
D6Q13		-539.8900	-1550.6846	.142800	
D6Q13	27.60	-539.7264	-1549.5464	.142800	452.4451
D6B12		-538.8550	-1543.4858	.142800	
D6B12	65.37	-538.2123	-1540.8368	.238000	455.1409
D6Q12		-537.1403	-1536.4179	.238000	
D6Q12	27.60	-536.8692	-1535.3003	.238000	456.8774
D6B11		-535.4257	-1529.3500	.238000	
D6B11	65.37	-534.5341	-1526.7741	.333199	459.5732
D6Q11		-533.0469	-1522.4771	.333199	
D6Q11	27.60	-532.6708	-1521.3904	.333199	461.3097
D6Q10		-528.2908	-1508.7352	.333199	
D6Q10	27.60	-527.9147	-1507.6485	.333199	465.7420
D6Q9		-523.5347	-1494.9934	.333199	
D6Q9	27.60	-523.1586	-1493.9066	.333199	470.1743
D6B8		-521.1560	-1488.1205	.333199	
D6B8	65.37	-520.0236	-1485.6410	.428399	472.8701
D6Q8		-518.1347	-1481.5048	.428399	
D6Q8	27.60	-517.6570	-1480.4587	.428399	474.6066
D6B7		-515.1134	-1474.8892	.428399	
D6B7	65.37	-513.7505	-1472.5285	.523599	477.3024
D6Q7		-511.4770	-1468.5907	.523599	
D6Q7	27.60	-510.9020	-1467.5947	.523599	479.0389
D6Q6		-504.2062	-1455.9972	.523599	
D6Q6	32.60	-503.5270	-1454.8209	.523599	483.5347
D6Q5		-496.9353	-1443.4038	.523599	
D6Q5	32.60	-496.2562	-1442.2274	.523599	487.9670
D6Q4		-489.6645	-1430.8103	.523599	
D6Q4	27.60	-489.0895	-1429.8144	.523599	492.3358
D6Q3		-482.3936	-1418.2169	.523599	
D6Q3	27.60	-481.8186	-1417.2209	.523599	496.7681
D6Q2		-475.1228	-1405.6234	.523599	
D6Q2	27.60	-474.5478	-1404.6275	.523599	501.2004
D6Q1		-468.1395	-1393.5279	.523599	
D6Q1	13.80	-467.8520	-1393.0300	.523599	505.2822
D10		-467.8520	-1393.0300	.523599	
D10	0.00	-467.8520	-1393.0300	.523599	505.2822

15.23.23. UCLP, QQ, TB10, 0.452KLNS. ** END OF LISTING **

APPENDIX D

BEGIN -467.852 -1393.030 [illegible]

FINAL SITE COORDINATES FOR DEBUNCHER RING.
COORDINATES ARE GIVEN AT BEND CENTER
AND DOWNSTREAM END OF EACH MAGNET.
COORDINATES ARE LISTED IN CLOCKWISE MANNER.

MAIN RING STATION A0 IS X=0.0, Y=0.0

3 OCT 1983. DE JOHNSON

NAME	LENGTH(IN)	X(FEET)	Y(FEET)	THETA(RAD)	S(METERS)
D1O		-467.852	-1393.030	.523599	0.0000
D1OQ	27.60	-467.277	-1392.034	.523599	.3505
D1Q2		-460.581	-1380.437	.523599	
D1Q2	27.60	-460.006	-1379.441	.523599	4.7828
D1Q3		-453.310	-1367.843	.523599	
D1Q3	27.60	-452.735	-1366.847	.523599	9.2151
D1Q4		-446.039	-1355.250	.523599	
D1Q4	27.60	-445.464	-1354.254	.523599	13.6474
D1Q5		-438.769	-1342.656	.523599	
D1Q5	32.60	-438.089	-1341.480	.523599	18.1432
D1Q6		-431.498	-1330.063	.523599	
D1Q6	32.60	-430.819	-1328.886	.523599	22.5755
D1Q7		-424.227	-1317.469	.523599	
D1Q7	27.60	-423.652	-1316.473	.523599	26.9443
D1B7		-420.591	-1311.171	.523599	
D1B7	65.37	-419.009	-1308.950	.618799	29.6402
D1Q8		-416.372	-1305.246	.618799	
D1Q8	27.60	-415.705	-1304.310	.618799	31.3766
D1B8		-412.153	-1299.322	.618799	
D1B8	65.37	-410.368	-1297.262	.713998	34.0725
D1Q9		-407.390	-1293.826	.713998	
D1Q9	27.60	-406.637	-1292.957	.713998	35.8089
D1Q10		-397.868	-1282.836	.713998	
D1Q10	27.60	-397.115	-1281.967	.713998	40.2412
D1Q11		-388.345	-1271.846	.713998	
D1Q11	27.60	-387.592	-1270.977	.713998	44.6735
D1B11		-383.582	-1266.349	.713998	
D1B11	65.37	-381.609	-1264.468	.809198	47.3693
D1Q12		-378.319	-1261.331	.809198	
D1Q12	27.60	-377.486	-1260.537	.809198	49.1058
D1B12		-373.055	-1256.312	.809198	
D1B12	65.37	-370.912	-1254.627	.904398	51.8016
D1Q13		-367.338	-1251.816	.904398	
D1Q13	27.60	-366.434	-1251.105	.904398	53.5381
D1B13		-361.621	-1247.320	.904398	
D1B13	65.37	-359.328	-1245.846	.999598	56.2339
D1Q14		-355.503	-1243.388	.999598	
D1Q14	27.60	-354.535	-1242.766	.999598	57.9704
D1B14		-349.384	-1239.456	.999598	
D1B14	65.37	-346.962	-1238.207	1.094797	60.6662
D1Q15		-342.920	-1236.123	1.094797	
D1Q15	27.60	-341.898	-1235.596	1.094797	62.4027
D1B15		-336.456	-1232.791	1.094797	
D1B15	65.37	-333.925	-1231.778	1.189997	65.0985
D1Q16		-329.704	-1230.088	1.189997	
D1Q16	27.60	-328.636	-1229.660	1.189997	66.8350
D1B16		-322.952	-1227.385	1.189997	
D1B16	65.37	-320.336	-1226.617	1.285197	69.5308
D1Q17		-315.974	-1225.336	1.285197	
D1Q17	27.60	-314.870	-1225.012	1.285197	71.2673
D1B17		-308.995	-1223.287	1.285197	
D1B17	65.37	-306.319	-1222.771	1.380397	73.9631
D1Q18		-301.854	-1221.910	1.380397	
D1Q18	27.60	-300.725	-1221.693	1.380397	75.6996
D1B18		-294.712	-1220.534	1.380397	
D1B18	65.37	-291.999	-1220.275	1.475597	78.3954
D1Q19		-287.472	-1219.843	1.475597	
D1Q19	27.60	-286.328	-1219.733	1.475597	80.1319
D1B19		-280.232	-1219.151	1.475597	
D1B19	65.37	-277.507	-1219.151	1.570796	82.8277

NAME	LENGTH(IN)	X(FEET)	Y(FEET)	THETA(RAD)	S(METERS)
D20Q		-272.959	-1219.151	1.570796	
D20		-272.959	-1219.151	1.570796	
D20Q	27.60	-271.809	-1219.151	1.570796	84.5642
D2B19		-265.687	-1219.151	1.570796	
D2B19	65.37	-262.973	-1219.410	1.665996	87.2600
D2Q19		-258.447	-1219.843	1.665996	
D2Q19	27.60	-257.302	-1219.952	1.665996	88.9965
D2B18		-251.207	-1220.534	1.665996	
D2B18	65.37	-248.530	-1221.050	1.761196	91.6923
D2Q18		-244.065	-1221.910	1.761196	
D2Q18	27.60	-242.936	-1222.128	1.761196	93.4288
D2B17		-236.924	-1223.287	1.761196	
D2B17	65.37	-234.308	-1224.055	1.856396	96.1246
D2Q17		-229.945	-1225.336	1.856396	
D2Q17	27.60	-228.842	-1225.660	1.856396	97.8611
D2B16		-222.967	-1227.385	1.856396	
D2B16	65.37	-220.437	-1228.398	1.951595	100.5570
D2Q16		-216.215	-1230.088	1.951595	
D2Q16	27.60	-215.148	-1230.515	1.951595	102.2934
D2B15		-209.463	-1232.791	1.951595	
D2B15	65.37	-207.041	-1234.040	2.046795	104.9893
D2Q15		-202.999	-1236.123	2.046795	
D2Q15	27.60	-201.977	-1236.650	2.046795	106.7257
D2B14		-196.535	-1239.456	2.046795	
D2B14	65.37	-194.241	-1240.930	2.141995	109.4216
D2Q14		-190.416	-1243.388	2.141995	
D2Q14	27.60	-189.449	-1244.010	2.141995	111.1580
D2B13		-184.298	-1247.320	2.141995	
D2B13	65.37	-182.155	-1249.005	2.237195	113.8539
D2Q13		-178.581	-1251.816	2.237195	
D2Q13	27.60	-177.677	-1252.527	2.237195	115.5903
D2B12		-172.864	-1256.312	2.237195	
D2B12	65.37	-170.891	-1258.193	2.332395	118.2862
D2Q12		-167.600	-1261.331	2.332395	
D2Q12	27.60	-166.768	-1262.124	2.332395	120.0226
D2B11		-162.337	-1266.349	2.332395	
D2B11	65.37	-160.552	-1268.409	2.427594	122.7185
D2Q11		-157.574	-1271.846	2.427594	
D2Q11	27.60	-156.821	-1272.715	2.427594	124.4549
D2Q10		-148.051	-1282.836	2.427594	
D2Q10	27.60	-147.298	-1283.705	2.427594	128.8872
D2Q9		-138.529	-1293.826	2.427594	
D2Q9	27.60	-137.775	-1294.695	2.427594	133.3195
D2B8		-133.766	-1299.322	2.427594	
D2B8	65.37	-132.185	-1301.543	2.522794	136.0153
D2Q8		-129.547	-1305.246	2.522794	
D2Q8	27.60	-128.880	-1306.183	2.522794	137.7518
D2B7		-125.328	-1311.171	2.522794	
D2B7	65.37	-123.966	-1313.531	2.617994	140.4476
D2Q7		-121.692	-1317.469	2.617994	
D2Q7	27.60	-121.117	-1318.465	2.617994	142.1841
D2Q6		-114.421	-1330.063	2.617994	
D2Q6	32.60	-113.742	-1331.239	2.617994	146.6799
D2Q5		-107.150	-1342.656	2.617994	
D2Q5	32.60	-106.471	-1343.833	2.617994	151.1122
D2Q4		-99.879	-1355.250	2.617994	
D2Q4	27.60	-99.304	-1356.246	2.617994	155.4810
D2Q3		-92.609	-1367.843	2.617994	
D2Q3	27.60	-92.034	-1368.839	2.617994	159.9133
D2Q2		-85.338	-1380.437	2.617994	
D2Q2	27.60	-84.763	-1381.432	2.617994	164.3456

NAME	LENGTH(IN)	X(FEET)	Y(FEET)	THETA(RAD)	S(METERS)
D3QQ		-78.067	-1393.030	2.617994	
D3Q		-78.067	-1393.030	2.617994	
D3QQ	27.60	-77.492	-1394.026	2.617994	168.7779
D3Q2		-70.796	-1405.623	2.617994	
D3Q2	27.60	-70.221	-1406.619	2.617994	173.2102
D3Q3		-63.525	-1418.217	2.617994	
D3Q3	27.60	-62.950	-1419.213	2.617994	177.6425
D3Q4		-56.254	-1430.810	2.617994	
D3Q4	27.60	-55.679	-1431.806	2.617994	182.0748
D3Q5		-48.984	-1443.404	2.617994	
D3Q5	32.60	-48.304	-1444.580	2.617994	186.5706
D3Q6		-41.713	-1455.997	2.617994	
D3Q6	32.60	-41.034	-1457.174	2.617994	191.0029
D3Q7		-34.442	-1468.591	2.617994	
D3Q7	27.60	-33.867	-1469.587	2.617994	195.3717
D3B7		-30.806	-1474.889	2.617994	
D3B7	65.37	-29.673	-1477.369	2.713194	198.0675
D3Q8		-27.784	-1481.505	2.713194	
D3Q8	27.60	-27.307	-1482.551	2.713194	199.8040
D3B8		-24.763	-1488.121	2.713194	
D3B8	65.37	-23.871	-1490.696	2.808394	202.4998
D3Q9		-22.384	-1494.993	2.808394	
D3Q9	27.60	-22.008	-1496.080	2.808394	204.2363
D3Q10		-17.628	-1508.735	2.808394	
D3Q10	27.60	-17.252	-1509.822	2.808394	208.6686
D3Q11		-12.872	-1522.477	2.808394	
D3Q11	27.60	-12.496	-1523.564	2.808394	213.1009
D3B11		-10.493	-1529.350	2.808394	
D3B11	65.37	-9.851	-1531.999	2.903593	215.7967
D3Q12		-8.779	-1536.418	2.903593	
D3Q12	27.60	-8.508	-1537.536	2.903593	217.5332
D3B12		-7.064	-1543.486	2.903593	
D3B12	65.37	-6.676	-1546.184	2.998793	220.2290
D3Q13		-6.029	-1550.685	2.998793	
D3Q13	27.60	-5.865	-1551.823	2.998793	221.9655
D3B13		-4.994	-1557.884	2.998793	
D3B13	65.37	-4.864	-1560.606	3.093993	224.6613
D3Q14		-4.648	-1565.148	3.093993	
D3Q14	27.60	-4.593	-1566.297	3.093993	226.3978
D3B14		-4.302	-1572.413	3.093993	
D3B14	65.37	-4.432	-1575.136	3.189193	229.0936
D3Q15		-4.648	-1579.678	3.189193	
D3Q15	27.60	-4.703	-1580.826	3.189193	230.8301
D3B15		-4.994	-1586.942	3.189193	
D3B15	65.37	-5.382	-1589.640	3.284392	233.5259
D3Q16		-6.029	-1594.141	3.284392	
D3Q16	27.60	-6.193	-1595.279	3.284392	235.2624
D3B16		-7.064	-1601.340	3.284392	
D3B16	65.37	-7.707	-1603.989	3.379592	237.9582
D3Q17		-8.779	-1608.408	3.379592	
D3Q17	27.60	-9.050	-1609.525	3.379592	239.6947
D3B17		-10.493	-1615.476	3.379592	
D3B17	65.37	-11.385	-1618.052	3.474792	242.3905
D3Q18		-12.872	-1622.349	3.474792	
D3Q18	27.60	-13.248	-1623.435	3.474792	244.1270
D3B18		-15.251	-1629.221	3.474792	
D3B18	65.37	-16.383	-1631.701	3.569992	246.8228
D3Q19		-18.272	-1635.837	3.569992	
D3Q19	27.60	-18.750	-1636.883	3.569992	248.5593
D3B19		-21.293	-1642.453	3.569992	
D3B19	65.37	-22.656	-1644.813	3.665192	251.2551

NAME	LENGTH(IN)	X(FEET)	Y(FEET)	THETA(RAD)	S(METERS)
D4OQ		-24.930	-1648.751	3.665192	
D4O		-24.930	-1648.751	3.665192	
D4OQ	27.60	-25.505	-1649.747	3.665192	252.9916
D4B19		-28.566	-1655.050	3.665192	
D4B19	65.37	-30.147	-1657.270	3.760391	255.6874
D4Q19		-32.785	-1660.974	3.760391	
D4Q19	27.60	-33.452	-1661.911	3.760391	257.4239
D4B18		-37.004	-1666.898	3.760391	
D4B18	65.37	-38.789	-1668.958	3.855591	260.1197
D4Q18		-41.766	-1672.395	3.855591	
D4Q18	27.60	-42.519	-1673.264	3.855591	261.8562
D4B17		-46.529	-1677.891	3.855591	
D4B17	65.37	-48.502	-1679.772	3.950791	264.5520
D4Q17		-51.793	-1682.910	3.950791	
D4Q17	27.60	-52.625	-1683.704	3.950791	266.2885
D4B16		-57.056	-1687.929	3.950791	
D4B16	65.37	-59.199	-1689.614	4.045991	268.9843
D4Q16		-62.773	-1692.425	4.045991	
D4Q16	27.60	-63.677	-1693.136	4.045991	270.7208
D4B15		-68.490	-1696.921	4.045991	
D4B15	65.37	-70.783	-1698.394	4.141190	273.4166
D4Q15		-74.608	-1700.853	4.141190	
D4Q15	27.60	-75.576	-1701.475	4.141190	275.1531
D4B14		-80.727	-1704.785	4.141190	
D4B14	65.37	-83.150	-1706.034	4.236390	277.8489
D4Q14		-87.191	-1708.117	4.236390	
D4Q14	27.60	-88.213	-1708.644	4.236390	279.5854
D4B13		-93.656	-1711.450	4.236390	
D4B13	65.37	-96.186	-1712.463	4.331590	282.2812
D4Q13		-100.408	-1714.153	4.331590	
D4Q13	27.60	-101.475	-1714.581	4.331590	284.0177
D4B12		-107.159	-1716.856	4.331590	
D4B12	65.37	-109.775	-1717.624	4.426790	286.7135
D4Q12		-114.138	-1718.905	4.426790	
D4Q12	27.60	-115.241	-1719.229	4.426790	288.4500
D4B11		-121.116	-1720.954	4.426790	
D4B11	65.37	-123.793	-1721.470	4.521990	291.1458
D4Q11		-128.257	-1722.331	4.521990	
D4Q11	27.60	-129.387	-1722.548	4.521990	292.8823
D4Q10		-142.536	-1725.083	4.521990	
D4Q10	27.60	-143.666	-1725.300	4.521990	297.3146
D4Q9		-156.815	-1727.835	4.521990	
D4Q9	27.60	-157.944	-1728.052	4.521990	301.7469
D4B8		-163.957	-1729.211	4.521990	
D4B8	65.37	-166.670	-1729.470	4.617189	304.4427
D4Q8		-171.197	-1729.902	4.617189	
D4Q8	27.60	-172.341	-1730.012	4.617189	306.1792
D4B7		-178.437	-1730.594	4.617189	
D4B7	65.37	-181.162	-1730.594	4.712389	308.8750
D4Q7		-185.710	-1730.594	4.712389	
D4Q7	27.60	-186.860	-1730.594	4.712389	310.6115
D4Q6		-200.251	-1730.594	4.712389	
D4Q6	32.60	-201.610	-1730.594	4.712389	315.1073
D4Q5		-214.793	-1730.594	4.712389	
D4Q5	32.60	-216.151	-1730.594	4.712389	319.5396
D4Q4		-229.335	-1730.594	4.712389	
D4Q4	27.60	-230.485	-1730.594	4.712389	323.9084
LGRF		-236.605	-1730.594	4.712389	
LGRF	84.00	-240.105	-1730.594	4.712389	326.8408
D4Q3		-243.876	-1730.594	4.712389	
D4Q3	27.60	-245.026	-1730.594	4.712389	328.3407
D4Q2		-258.418	-1730.594	4.712389	
D4Q2	27.60	-259.568	-1730.594	4.712389	332.7730
LGRF		-265.689	-1730.594	4.712389	
LGRF	84.00	-269.189	-1730.594	4.712389	335.7054

NAME	LENGTH(IN)	X(FEET)	Y(FEET)	THETA(RAD)	S(METERS)
D5QG		-272.960	-1730.594	4.712389	
D5Q		-272.960	-1730.594	4.712389	
D5QG	27.60	-274.110	-1730.594	4.712389	337.2053
LGRF		-280.230	-1730.594	4.712389	
LGRF	84.00	-283.730	-1730.594	4.712389	340.1377
D5Q2		-287.501	-1730.594	4.712389	
D5Q2	27.60	-288.651	-1730.594	4.712389	341.6376
LGRF		-294.772	-1730.594	4.712389	
LGRF	84.00	-298.272	-1730.594	4.712389	344.5700
D5Q3		-302.043	-1730.594	4.712389	
D5Q3	27.60	-303.193	-1730.594	4.712389	346.0699
LGRF		-309.314	-1730.594	4.712389	
LGRF	84.00	-312.814	-1730.594	4.712389	349.0023
D5Q4		-316.585	-1730.594	4.712389	
D5Q4	27.60	-317.735	-1730.594	4.712389	350.5022
LGRF		-323.751	-1730.594	4.712389	
LGRF	84.00	-327.251	-1730.594	4.712389	353.4029
D5Q5		-331.126	-1730.594	4.712389	
D5Q5	32.60	-332.485	-1730.594	4.712389	354.9980
LGRF		-338.397	-1730.594	4.712389	
LGRF	84.00	-341.897	-1730.594	4.712389	357.8669
D5Q6		-345.668	-1730.594	4.712389	
D5Q6	32.60	-347.026	-1730.594	4.712389	359.4303
LGRF		-353.043	-1730.594	4.712389	
LGRF	84.00	-356.543	-1730.594	4.712389	362.3310
D5Q7		-360.210	-1730.594	4.712389	
D5Q7	27.60	-361.360	-1730.594	4.712389	363.7991
D5B7		-367.482	-1730.594	4.712389	
D5B7	65.37	-370.196	-1730.335	4.807589	366.4949
D5Q8		-374.722	-1729.902	4.807589	
D5Q8	27.60	-375.867	-1729.793	4.807589	368.2314
D5B8		-381.962	-1729.211	4.807589	
D5B8	65.37	-384.639	-1728.695	4.902789	370.9272
D5Q9		-389.104	-1727.835	4.902789	
D5Q9	27.60	-390.233	-1727.617	4.902789	372.6637
SMRF		-393.827	-1726.924	4.902789	
SMRF	59.06	-396.243	-1726.459	4.902789	374.5293
SMRF		-398.659	-1725.993	4.902789	
SMRF	59.06	-401.076	-1725.527	4.902789	376.0293
D5Q10		-403.383	-1725.083	4.902789	
D5Q10	27.60	-404.512	-1724.865	4.902789	377.0960
SMRF		-408.106	-1724.172	4.902789	
SMRF	59.06	-410.522	-1723.707	4.902789	378.9616
D5Q11		-417.662	-1722.331	4.902789	
D5Q11	27.60	-418.791	-1722.113	4.902789	381.5283
D5B11		-424.803	-1720.954	4.902789	
D5B11	65.37	-427.418	-1720.186	4.997988	384.2241
D5Q12		-431.781	-1718.905	4.997988	
D5Q12	27.60	-432.885	-1718.581	4.997988	385.9606
D5B12		-438.760	-1716.856	4.997988	
D5B12	65.37	-441.290	-1715.843	5.093188	388.6564
D5Q13		-445.512	-1714.153	5.093188	
D5Q13	27.60	-446.579	-1713.726	5.093188	390.3929
D5B13		-452.263	-1711.450	5.093188	
D5B13	65.37	-454.686	-1710.201	5.188388	393.0887
D5Q14		-458.728	-1708.117	5.188388	
D5Q14	27.60	-459.750	-1707.590	5.188388	394.8252
D5B14		-465.192	-1704.785	5.188388	
D5B14	65.37	-467.485	-1703.311	5.283588	397.5210
D5Q15		-471.311	-1700.853	5.283588	
D5Q15	27.60	-472.278	-1700.231	5.283588	399.2575
D5B15		-477.429	-1696.921	5.283588	
D5B15	65.37	-479.572	-1695.236	5.378788	401.9533
D5Q16		-483.146	-1692.425	5.378788	
D5Q16	27.60	-484.050	-1691.714	5.378788	403.6898
D5B16		-488.863	-1687.929	5.378788	
D5B16	65.37	-490.835	-1686.048	5.473987	406.3856
D5Q17		-494.126	-1682.910	5.473987	
D5Q17	27.60	-494.959	-1682.117	5.473987	408.1221
D5B17		-499.390	-1677.891	5.473987	
D5B17	65.37	-501.175	-1675.831	5.569187	410.8179
D5Q18		-504.153	-1672.395	5.569187	
D5Q18	27.60	-504.906	-1671.526	5.569187	412.5544
D5B18		-508.915	-1666.898	5.569187	
D5B18	65.37	-510.497	-1664.678	5.664387	415.2502
D5Q19		-513.134	-1660.974	5.664387	
D5Q19	27.60	-513.801	-1660.037	5.664387	416.9867
D5B19		-517.353	-1655.050	5.664387	
D5B19	65.37	-518.716	-1652.689	5.759587	419.6825

NAME	LENGTH(IN)	X(FEET)	Y(FEET)	THETA(RAD)	S(METERS)
D60Q		-520.989	-1648.751	5.759587	
D60		-520.989	-1648.751	5.759587	
D60Q	27.60	-521.564	-1647.755	5.759587	421.4190
D6B19		-524.626	-1642.453	5.759587	
D6B19	65.37	-525.758	-1639.973	5.854787	424.1148
D6Q19		-527.647	-1635.837	5.854787	
D6Q19	27.60	-528.125	-1634.791	5.854787	425.8513
D6B18		-530.668	-1629.221	5.854787	
D6B18	65.37	-531.560	-1626.646	5.949986	428.5471
D6Q18		-533.047	-1622.349	5.949986	
D6Q18	27.60	-533.423	-1621.262	5.949986	430.2836
D6B17		-535.426	-1615.476	5.949986	
D6B17	65.37	-536.068	-1612.827	6.045186	432.9794
D6Q17		-537.140	-1608.408	6.045186	
D6Q17	27.60	-537.411	-1607.290	6.045186	434.7159
D6B16		-538.855	-1601.340	6.045186	
D6B16	65.37	-539.243	-1598.642	6.140386	437.4117
D6Q16		-539.890	-1594.141	6.140386	
D6Q16	27.60	-540.054	-1593.003	6.140386	439.1482
D6B15		-540.925	-1586.942	6.140386	
D6B15	65.37	-541.055	-1584.219	6.235586	441.8440
D6Q15		-541.271	-1579.677	6.235586	
D6Q15	27.60	-541.326	-1578.529	6.235586	443.5805
D6B14		-541.617	-1572.413	6.235586	
D6B14	65.37	-541.487	-1569.690	6.330785	446.2763
D6Q14		-541.271	-1565.148	.047600	
D6Q14	27.60	-541.216	-1563.999	.047600	448.0128
D6B13		-540.925	-1557.884	.047600	
D6B13	65.37	-540.537	-1555.185	.142800	450.7086
D6Q13		-539.890	-1550.685	.142800	
D6Q13	27.60	-539.726	-1549.546	.142800	452.4451
D6B12		-538.855	-1543.486	.142800	
D6B12	65.37	-538.212	-1540.837	.238000	455.1409
D6Q12		-537.140	-1536.418	.238000	
D6Q12	27.60	-536.869	-1535.300	.238000	456.8774
D6B11		-535.426	-1529.350	.238000	
D6B11	65.37	-534.534	-1526.774	.333199	459.5732
D6Q11		-533.047	-1522.477	.333199	
D6Q11	27.60	-532.671	-1521.390	.333199	461.3097
D6Q10		-528.291	-1508.735	.333199	
D6Q10	27.60	-527.915	-1507.648	.333199	465.7420
D6Q9		-523.535	-1494.993	.333199	
D6Q9	27.60	-523.159	-1493.907	.333199	470.1743
D6B8		-521.156	-1488.120	.333199	
D6B8	65.37	-520.024	-1485.641	.428399	472.8701
D6Q8		-518.135	-1481.505	.428399	
D6Q8	27.60	-517.657	-1480.459	.428399	474.6066
D6B7		-515.113	-1474.889	.428399	
D6B7	65.37	-513.751	-1472.529	.523599	477.3024
D6Q7		-511.477	-1468.591	.523599	
D6Q7	27.60	-510.902	-1467.595	.523599	479.0389
D6Q6		-504.206	-1455.997	.523599	
D6Q6	32.60	-503.527	-1454.821	.523599	483.5347
D6Q5		-496.935	-1443.404	.523599	
D6Q5	32.60	-496.256	-1442.227	.523599	487.9670
D6Q4		-489.664	-1430.810	.523599	
D6Q4	27.60	-489.089	-1429.814	.523599	492.3358
D6Q3		-482.394	-1418.217	.523599	
D6Q3	27.60	-481.819	-1417.221	.523599	496.7681
D6Q2		-475.123	-1405.623	.523599	
D6Q2	27.60	-474.548	-1404.627	.523599	501.2004
D10Q		-467.852	-1393.030	.523599	
D10	0.00	-467.852	-1393.030	.523599	505.2822

** END OF LISTING **

APPENDIX D.

Synch Run Debuncher Lattice

```
 DRSN   RUN
C       DEBUNCHER RING LATTICE     A. G. RUGGIERO
C       THERE ARE --- THREE --- LONG STRAIGHT SECTIONS WITH ZERO DISPERSION
C       EACH LONG STRAIGHT SECTION HAS BEEN BRIDGED WITH REGULAR CELL QUADS
C       HARMONIC NUMBER IS          99
C       TWO QUADRUPOLE LENGTHS :  27.6 AND 32.6 INCHES
C       APRIL 9,1983.              A. G. RUGGIERO
C
 BRHO   =           29.4501
 BO     =           1.7
 RHOI   =           BO          /          BRHO
 LB     =           1.660402
C
 LQ     =           0.35052
 LQS    =           0.41402
C
 KF     =           0.336518
 KD     =           -0.329203
C
 QD     DRF         1.0354310
 QS     DRF         0.3
 D      DRF         0.7354310
 LC     DRF         1.660402
 S      DRF         0.3731264
 B      DRF         0.1467744
 Z      DRF         0.3604264
C
 B      MAG         LB          0.          1.          RHOI        S
C
 QF     MAG         LQ          KF          1.
 QD     MAG         LQ          KD          1.
C
 SF     SXTP        0.0         0.14071     1.
 SD     SXTP        0.0         -0.21342    1.
 .QFI   BNL         QS    SF    QD
 .QDI   BNL         QS    SD    QD
 .QFX   BNL         QD    SF    QS
 .QDD2  BNL         QD    SD    QS
 .C     BNL         QF    .QF1  B     #.QD2 QD    QD    .QD1 B     .QF2 QF
 .C1    BNL         QF    QD    B     QD    QD    QD    QD   B     .QF2 QF
 .LA    BNL         S     S     S     S     S     S     S    S     S    S
 .LB    BNL         B     F     B     B     B     B     B    B     B    B
 .LZ    BNL         Z     Z     Z     Z     Z     Z     Z    Z     Z    Z
 .CH    BNL         QF    .QF1  B     .QD2  QD
 .CS    BNL         QF    .QF1  LC    .QD2  QD    QD    .QD1 LC    .QF2 QF
 .CS1   BNL         QF1   .LA   QD1   QD1   .LA   QF2
 .CS2   BNL         QF2   .LA   QD2   QD2   .LB   QF3
 .CS3   BNL         QF3   .LZ   QD3   QD3   .LB   QF
 .C     BNL         .CS1  .CS2  .CS3  .C1    .CS
 KF1    =           0.377469
 KD1    =           0.347140
 KF2    =           0.358812
 KD2    =           0.386791
 KF3    =           0.324942
 KD3    =           0.324586
 QF1    MAG         LQ          KF1         1.
 QF2    MAG         LQ          KF2         1.
 QF3    MAG         LQS         KF3         1.
 QD1    MAG         LQ          -KD1        1.
 QD2    MAG         LQ          -KD2        1.
 QD3    MAG         LQS         -KD3        1.
 .SP    BNL         .CT   .C    .C    .C    .C    .CH
        CYC    -3   .SP
 DP     =           -3.02
```

```
V       PVEC
CHR     SUB
AGR     FXPT    2   -3 V     .SP            1
        INCR    1       DR       .005
        END
        CALL    9       CHR
        FIN
        STOP
```

SYNCH RUN ORSM

```
*****************************************************************************
                DEBUNCHER RING LATTICE    A. G. RUGGIERO
                THERE ARE ---- THREE (---- LONG STRAIGHT SECTIONS WITH ZERO DISPERSION
                EACH LONG STRAIGHT SECTION HAS BEEN BRIDGED WITH REGULAR CELL QUADS
                HARMONIC NUMBER IS      90
                TWO QUADRUPOLE LENGTHS :  27.6 AND 32.6 INCHES
                APRIL 9,1983.           A. G. RUGGIERO

***  BRHO    =              //  29.6501
***  BO      =              //  1.7
***  BHOI    =              //  BO          /          BRHO
***  LB      =              //  1.660402

***  LQ      =              //  0.35052
***  LQS     =              //  0.41402

***  KF      =              //  0.336518
***  KD      =              //  -0.329283

***  DD      DRF            //  1.0354310
***  DF      DRF            //  0.3
***  DF      DRF            //  0.7354310
***  LB      DRF            //  1.660402
***  X       DRF            //  0.3731264
***  Y       DRF            //  0.3667764
***  Z       DRF            //  0.3604264

***  B       MAG            //  LB          0.          1.          BHOI     $

***  QF      MAG            //  LQ          KF          1.
***  QD      MAG            //  LQ          KD          1.

***  SF      SXTP           //  0.0         0.14073     1.
***  SD      SXTP           //  0.0         -0.21342    1.
***  .QF1    BNL            //  QS      SF      D
***  .QD1    BNL            //  QS      SD      QS
***  .QF2    BNL            //  QS      SF      QS
***  .QD2    BNL            //  QS      SD      QS
***  .C      BNL            //  QF      .QF1    B       .QD2    QD      QD      .QD1    B       .QF2    QF      B
***  .C1     BNL            //  QF      QD      B       QD      QD      QD      QD      B       .QF2    QF
***  .LA     BNL            //  X       X       B       X       X       X       X       B       X       X
***  .LB     BNL            //  Z       Z       B       Z       Z       Z       Z       B       Z       Z
***  .CH     BNL            //  QF      .QF1    B       .QD2    QD
***  .CS1    BNL            //  QF      .QF1    LC      .QD2    QD      QD      .QD1    LC      .QF2    QF
***  .CS2    BNL            //  QF1     .LA     QD1     QD2     .LB     QF2
***  .CS3    BNL            //  QF3     .LZ     QD3     QD3     .LB     QF3
***  .CT     BNL            //  .CS1    .CS2    .CS3    .C1     .CS     QF
***  KF1     =              //  0.377469
***  KD1     =              //  -0.347140
***  KF2     =              //  0.358812
***  KD2     =              //  -0.386791
***  KF3     =              //  0.325942
***  KD3     =              //  -0.334884
***  QF1     MAG            //  LQ          KF1         1.
***  QF2     MAG            //  LQ          KF2         1.
***  QF3     MAG            //  LQS         KF3         1.
***  QD1     MAG            //  LQ          -KD1        1.
***  QD2     MAG            //  LQ          -KD2        1.
***  QD3     MAG            //  LQS         -KD3        1.
***  .SP     BHL            //  .CT   .C    .C    .C    .C    .CH
```

POS		S(M)	NUX	NUY	BETAX(M)	BETAY(M)	ETAX(M)	ETAY(M)	ETAS(M)	ALPHAX	ALPHAY	DETAX	DETAY
0		0.0000	0.00000	0.00000	17.83321	5.73406	-.00091	0.00000	0.00000	0.00000	0.00000	-.00000	0.00000
1	QF1	.3505	.00318	.00957	17.92564	6.02589	-.00089	0.00000	0.00000	2.26819	-.84539	.00012	0.00000
2		.7216	.00688	.01892	18.38125	6.69638	-.00085	0.00000	0.00000	2.13352	-.95130	.00012	0.00000
3		1.0969	.01092	.02734	19.86133	7.44610	-.00080	0.00000	0.00000	1.99886	-1.05774	.00012	0.00000
4		1.4699	.01548	.03492	12.39904	8.27506	-.00076	0.00000	0.00000	1.86420	-1.16391	.00012	0.00000
5		1.8408	.02033	.04173	11.08902	9.18324	-.00071	0.00000	0.00000	1.72953	-1.27008	.00012	0.00000
6		2.2162	.02622	.04787	9.81860	10.17066	-.00067	0.00000	0.00000	1.59487	-1.37626	.00012	0.00000
7		2.5893	.03266	.05342	8.67867	11.23732	-.00062	0.00000	0.00000	1.46020	-1.48243	.00012	0.00000
8		2.9624	.03995	.05846	7.63924	12.38320	-.00058	0.00000	0.00000	1.32554	-1.58861	.00012	0.00000
9		3.3358	.04826	.06303	6.70030	13.60832	-.00054	0.00000	0.00000	1.19088	-1.69478	.00012	0.00000
10	S	3.7087	.05774	.06720	5.86185	14.91267	-.00049	0.00000	0.00000	1.05621	-1.80096	.00012	0.00000
11	S	4.0818	.06858	.07101	5.12390	16.29626	-.00045	0.00000	0.00000	.92155	-1.90713	.00012	0.00000
12	QD1	4.4548	.08081	.07445	4.48647	17.75907	-.00041	0.00000	0.00000	.22980	-.08134	.00002	0.00000
13	QD1	4.7838	.09183	.07767	4.79248	16.16270	-.00040	0.00000	0.00000	-.42219	2.05979	.00002	0.00000
14	S	5.1360	.10380	.08154	5.14179	14.69048	-.00039	0.00000	0.00000	-.51343	1.93891	.00002	0.00000
15	S	5.4291	.11403	.08579	5.55950	13.28886	-.00038	0.00000	0.00000	-.60566	1.81803	.00002	0.00000
16	S	5.7222	.12411	.09050	6.04289	11.97726	-.00038	0.00000	0.00000	-.69739	1.69715	.00002	0.00000
17	S	6.0153	.13427	.09573	6.60017	10.75586	-.00037	0.00000	0.00000	-.78913	1.57626	.00002	0.00000
18	S	6.3083	.14470	.10159	7.23748	9.62468	-.00036	0.00000	0.00000	-.88086	1.45538	.00002	0.00000
19	S	6.6014	.15561	.10811	7.96506	8.58370	-.00035	0.00000	0.00000	-.97260	1.33450	.00002	0.00000
20	S	7.3947	.15829	.11345	8.67509	7.63293	-.00035	0.00000	0.00000	-1.06433	1.21361	.00002	0.00000
21	S	7.7678	.16475	.12371	9.30358	6.77237	-.00034	0.00000	0.00000	-1.15607	1.09273	.00002	0.00000
22	S	8.1410	.17073	.13303	10.00033	6.00202	-.00033	0.00000	0.00000	-1.24780	.97185	.00002	0.00000
23	S	8.5141	.17618	.14156	10.76503	5.32188	-.00033	0.00000	0.00000	-1.33954	.85097	.00002	0.00000
24	QF2	8.8869	.18096	.14946	11.61366	4.98611	-.00031	0.00000	0.00000	.08104	.12100	.00006	0.00000
25	QF2	9.2151	.18377	.15654	11.28583	5.14721	-.00029	0.00000	0.00000	1.58743	-.28732	.00010	0.00000
26		9.5883	.19117	.17021	10.18526	5.62188	-.00025	0.00000	0.00000	1.38103	-.68482	.00010	0.00000
27		9.9614	.19745	.18670	9.19443	6.16930	-.00021	0.00000	0.00000	1.27452	-.78232	.00010	0.00000
28		10.3345	.20426	.19588	8.28305	6.78949	-.00018	0.00000	0.00000	1.16802	-.87981	.00010	0.00000
29		10.7076	.21162	.20422	7.45114	7.48243	-.00014	0.00000	0.00000	1.06152	-.97731	.00010	0.00000
30	S	11.0808	.22063	.21178	6.69873	8.24812	-.00010	0.00000	0.00000	.95501	-1.07481	.00010	0.00000
31	S	11.4539	.22988	.21865	6.02579	9.08658	-.00007	0.00000	0.00000	.84851	-1.17230	.00010	0.00000
32	S	11.8270	.23948	.22488	5.43233	9.99778	-.00003	0.00000	0.00000	.74201	-1.26980	.00010	0.00000
33	S	12.2001	.25157	.23052	4.91833	11.98176	.00000	0.00000	0.00000	.63550	-1.36729	.00010	0.00000
34	S	12.5733	.26413	.23571	4.48383	12.03649	.00004	0.00000	0.00000	.52900	-1.46479	.00010	0.00000
35	S	12.9464	.27795	.24043	4.12881	13.16757	.00008	0.00000	0.00000	.42250	-1.56229	.00010	0.00000
36	QD2	13.2969	.29170	.24456	4.05811	13.64450	.00011	0.00000	0.00000	.21764	-.22641	.00011	0.00000
37	QD2	13.6474	.30495	.24873	4.46371	12.86320	.00015	0.00000	0.00000	-.89980	1.86912	.00013	0.00000
38	QF3	13.9979	.31715	.25356	5.19854	11.46976	.00020	0.00000	-1.04916	1.03005	.00013	0.00000
39	QF3	14.3484	.32760	.25898	6.40294	10.17834	.00025	0.00000	0.00000	-1.19833	1.69097	.00013	0.00000
40	R	14.7478	.33676	.26505	6.91691	8.98853	.00030	0.00000	0.00000	-1.34749	1.55190	.00013	0.00000
41	R	15.1145	.34463	.27198	7.96044	7.90154	.00034	0.00000	0.00000	-1.49726	1.41283	.00013	0.00000
42	R	15.4813	.35148	.27988	9.11344	6.91616	.00039	0.00000	0.00000	-1.64605	1.27375	.00013	0.00000
43	R	15.8481	.35749	.28892	10.37621	6.03280	.00044	0.00000	0.00000	-1.79480	1.13468	.00013	0.00000
44	R	16.2148	.36277	.29930	11.74844	5.25147	.00048	0.00000	0.00000	-1.94535	.99561	.00013	0.00000
45	R	16.5816	.36746	.31128	13.23024	4.57214	.00053	0.00000	0.00000	-2.09471	.85653	.00013	0.00000
46	R	16.9484	.37163	.32520	12.82161	3.99484	.00058	0.00000	0.00000	-2.24408	.71746	.00013	0.00000
47	R	17.3152	.37536	.34049	10.52254	3.51953	.00062	0.00000	0.00000	-2.39344	.57839	.00013	0.00000
48	QF3	17.7292	.37919	.36009	11.50682	3.28856	.00066	0.00000	0.00000	-.15295	-.01013	.00004	0.00000
49	QF3	18.1432	.38299	.37964	10.76634	3.53696	.00066	0.00000	0.00000	2.12099	-.60095	-.00002	0.00000

POS		S(M)	NUX	NUY	BETAX(M)	BETAY(M)	ETAX(M)	ETAY(M)	ETAS(M)	ALPHAX	ALPHAY	DETAX	DETAY
50	I	18.5037	.38657	.39487	15.28022	4.02015	.00064	0.00000	0.00000	2.00279	-.73965	-.00005	0.00000
51	I	18.8641	.39051	.40822	13.87911	4.60332	.00062	0.00000	0.00000	1.88459	-.87836	-.00005	0.00000
52	I	19.2245	.39446	.41986	12.56320	5.28648	.00061	0.00000	0.00000	1.76639	-1.01706	-.00005	0.00000
53	I	19.5849	.39840	.43000	11.33250	6.06962	.00059	0.00000	0.00000	1.64818	-1.15576	-.00005	0.00000
54	I	19.9454	.40300	.43883	10.18701	6.95275	.00057	0.00000	0.00000	1.52998	-1.29447	-.00005	0.00000
55	I	20.3058	.41005	.44656	9.12672	7.93586	.00055	0.00000	0.00000	1.41178	-1.43317	-.00005	0.00000
56	I	20.6662	.41761	.45334	8.15164	9.01896	.00054	0.00000	0.00000	1.29358	-1.57187	-.00005	0.00000
57	I	21.0266	.42507	.45937	7.26176	10.20204	.00052	0.00000	0.00000	1.17537	-1.71058	-.00005	0.00000
58	I	21.3871	.43343	.46482	6.45709	11.48511	.00050	0.00000	0.00000	1.05717	-1.84928	-.00005	0.00000
59	I	21.7475	.44284	.46984	5.73763	12.86816	.00049	0.00000	0.00000	.93897	-1.98799	-.00005	0.00000
60	QD3	22.1612	.45493	.47454	5.31343	13.81588	.00048	0.00000	0.00000	.10456	-.25847	.00002	0.00000
61	QD3	22.5550	.46716	.47906	5.35797	13.28051	.00050	0.00000	0.00000	.70614	1.52791	.00008	0.00000
62	R	22.9489	.47720	.48365	6.11223	12.19176	.00053	0.00000	0.00000	.60503	1.43545	.00008	0.00000
63	R	23.3091	.48631	.48865	6.73904	11.17455	.00056	0.00000	0.00000	-.90393	1.34339	.00008	0.00000
64	R	23.6759	.49495	.49411	7.43839	10.22286	.00059	0.00000	0.00000	-1.00283	1.25134	.00008	0.00000
65	R	24.0426	.50202	.50000	8.21029	9.33671	.00062	0.00000	0.00000	-1.10172	1.15928	.00008	0.00000
66	R	24.4094	.50880	.50663	9.05474	8.52208	.00065	0.00000	0.00000	-1.20062	1.06722	.00008	0.00000
67	R	24.7762	.51494	.51381	9.97174	7.76288	.00068	0.00000	0.00000	-1.29951	.97516	.00008	0.00000
68	R	25.1430	.52053	.52167	10.96129	7.09141	.00071	0.00000	0.00000	-1.39841	.88311	.00008	0.00000
69	R	25.5098	.52561	.53029	12.02334	6.47737	.00074	0.00000	0.00000	-1.49731	.79105	.00008	0.00000
70	R	25.8765	.53026	.53971	13.15796	5.93086	.00077	0.00000	0.00000	-1.59620	.69899	.00008	0.00000
71	R	26.2433	.53450	.54999	14.36514	5.45187	.00080	0.00000	0.00000	-1.69510	.60693	.00008	0.00000
72	QF	26.6038	.53829	.56047	14.86786	5.27437	.00081	0.00000	0.00000	-.00064	-.03376	-.00001	0.00000
73	QF	26.9643	.54206	.57092	14.36601	5.44670	.00079	0.00000	0.00000	1.69372	-.80714	-.00011	0.00000
74	QD	27.3798	.54810	.58025	13.24640	5.91116	.00068	0.00000	0.00000	1.41504	-1.11660	-.00011	0.00000
75	R	27.7952	.55473	.62408	7.19929	12.02048	.00968	0.00000	.00256	.96850	-1.54511	.09516	0.00000
76	QD	30.6756	.61110	.63617	5.47840	15.52277	.17801	0.00000	.00256	.68961	-1.83688	.09516	0.00000
77	QD	31.0261	.62159	.63965	5.23099	16.19062	.21521	0.00000	.00256	-.00032	-.04267	.11778	0.00000
78	QD	31.3766	.63208	.64314	5.47886	15.58099	.26114	0.00000	.00256	-.69031	1.75896	.14518	0.00000
79	QD	31.7271	.64244	.65509	7.10732	12.22123	.41146	0.00000	.00256	-.96935	1.48644	.14518	0.00000
80	R	32.0785	.65206	.68208	11.15227	7.92087	.73112	0.00000	.05574	-1.41614	1.09177	.24443	0.00000
81	QD	34.1079	.69765	.69844	13.38015	6.32246	.84996	0.00000	.05574	-1.61436	.88825	.24443	0.00000
82	SF	34.1079	.69765	.69844	13.38015	6.32246	.84996	0.00000	.05574	-1.61436	.88825	.24443	0.00000
83	QS	35.1079	.70109	.70616	14.37378	5.92668	.98009	0.00000	.05574	-1.69519	.80523	.24443	0.00000
84	QF	35.4584	.70487	.71584	14.97619	5.66064	1.04360	0.00000	.05574	.00032	.05089	.12068	0.00000
85	QF	35.8090	.70865	.72558	14.37335	5.88332	1.06411	0.00000	.05574	1.69277	-.69492	-.00406	0.00000
86	QS	36.1090	.71209	.73341	13.38015	6.32246	1.06290	0.00000	.05574	1.61488	-.77033	-.00406	0.00000
87	SF	36.1090	.71209	.73341	13.38015	6.32246	1.06290	0.00000	.05574	1.61488	-.77033	-.00406	0.00000
88	QD	36.4595	.71568	.73935	13.15073	7.00263	1.05991	0.00000	.05574	1.41628	-.96590	-.00406	0.00000
89	LC	36.8048	.71934	.77882	9.18903	11.42188	1.05318	0.00000	.05574	.96887	-1.37441	-.00406	0.00000
90	D	39.2402	.76936	.78819	5.91070	13.61977	1.05019	0.00000	.05574	.77056	-1.55978	-.00406	0.00000
91	SD	39.2402	.76936	.78819	5.91070	13.61977	1.05019	0.00000	.05574	.77056	-1.55978	-.00406	0.00000
92	QS	39.5402	.77226	.79158	5.92261	14.57832	1.04898	0.00000	.05574	.68967	-1.63539	-.00406	0.00000
93	QD	39.8907	.78026	.79931	5.93399	15.74279	1.06184	0.00000	.05574	-.00032	-.01679	.11777	0.00000
94	QD	40.2413	.79870	.79989	5.97217	15.81447	1.11208	0.00000	.05574	-.68898	1.72150	.24434	0.00000
95	QS	40.5413	.80716	.80246	5.90981	13.60618	1.20538	0.00000	.05574	-.76983	1.63958	.24434	0.00000
96	SD	40.5413	.80716	.80246	5.90981	13.60618	1.20538	0.00000	.05574	-.76983	1.63958	.24434	0.00000
97	D	41.2767	.82516	.81196	5.18788	11.24229	1.38508	0.00000	.05574	-.96802	1.43875	.24434	0.00000
98	LC	42.9371	.85485	.84147	11.14544	7.21730	1.79079	0.00000	.05574	-1.41548	.98533	.24434	0.00000
99	D	43.6725	.86445	.85942	13.37317	5.91571	1.97048	0.00000	.05574	-1.61367	.78450	.24434	0.00000

POS		S(M)	NUX	NUY	BETAX(M)	BETAY(M)	ETAX(M)	ETAY(M)	ETAS(M)	ALPHAX	ALPHAY	DETAX	DETAY
100	SF	43.6723	.86445	.85942	13.37317	5.91571	1.97048	0.00000	.05574	-1.61367	.78450	.24434	0.00000
101	QS	43.9723	.86789	.86782	14.36562	5.46959	2.04378	0.00000	.05574	-1.69451	.70258	.24434	0.00000
102	QF	44.2820	.87167	.87833	14.96291	5.22668	2.08673	0.00000	.05574	.00000	-.00000	-.00011	0.00000
103	QF	44.6736	.87548	.88884	14.96291	5.22668	2.08673	0.00000	.05574	1.69451	-.70258	-.24434	0.00000
104	QS	44.9736	.87889	.89724	13.37317	5.91571	1.97048	0.00000	.05574	1.61367	-.78450	-.24434	0.00000
105	SF	45.2736	.87889	.89724	13.37317	5.91571	1.97048	0.00000	.05574	1.61367	-.78450	-.24434	0.00000
106	Q	45.7090	.88849	.91519	11.14544	7.21730	1.79048	0.00000	.05574	1.41548	-.98533	-.24434	0.00000
107	B	47.3694	.91813	.94481	7.19273	11.16210	1.46400	0.00000	.20951	.96869	-1.37970	-.14429	0.00000
108	D	48.1048	.93611	.95441	5.91368	13.33215	1.35421	0.00000	.20951	.77050	-1.57101	-.14429	0.00000
109	SD	48.1048	.93611	.95441	5.91368	13.33215	1.35421	0.00000	.20951	.77050	-1.57101	-.14429	0.00000
110	QS	48.4048	.94431	.95786	5.47563	14.29817	1.30942	0.00000	.20951	.68966	-1.64905	-.14929	0.00000
111	QD	48.7348	.95306	.96166	5.23710	14.88417	1.28248	0.00000	.20951	.00000	-.00000	-.00016	0.00000
112	QD	48.7348	.95306	.96166	5.23710	14.88417	1.28248	0.00000	.20951	-.68965	1.64905	-.14895	0.00000
113	QS	49.1059	.97389	.96892	5.91367	13.33215	1.35399	0.00000	.20951	-.77050	1.57101	-.14895	0.00000
114	SD	49.1059	.97389	.96892	5.91367	13.33215	1.35399	0.00000	.20951	-.77050	1.57101	-.14895	0.00000
115	D	50.1413	.99188	.97852	7.19272	11.16211	1.46354	0.00000	.20951	-.96869	1.37970	-.14895	0.00000
116	B	51.7017	1.01778	1.00813	11.14541	7.21733	1.78931	0.00000	.26321	-1.41547	.98534	-.24434	0.00000
117	Q	52.1460	1.02611	1.02602	13.37313	5.91573	1.96907	0.00000	.26321	-1.61366	.78450	-.24434	0.00000
118	SF	52.4460	1.03111	1.03444	13.37313	5.91573	1.96907	0.00000	.26321	-1.61366	.78450	-.24434	0.00000
119	QS	52.8179	1.03456	1.03444	14.36888	5.46960	2.04236	0.00000	.26321	-1.69451	.70258	-.24434	0.00000
120	QF	53.1876	1.03834	1.04500	14.96786	5.22668	2.08528	0.00000	.36321	.00000	-.00000	-.00006	0.00000
121	QF	53.5582	1.04212	1.05551	14.36557	5.46961	2.04230	0.00000	.36321	1.69451	-.70258	-.24434	0.00000
122	QS	53.8582	1.04556	1.06301	13.37312	5.91573	1.96900	0.00000	.36321	1.61367	-.78451	-.24434	0.00000
123	SF	54.1582	1.04856	1.06301	13.37312	5.91573	1.96900	0.00000	.36321	1.61367	-.78451	-.24434	0.00000
124	Q	54.5716	1.05315	1.06186	11.14540	7.21733	1.78931	0.00000	.36321	1.41547	-.98534	-.24434	0.00000
125	B	55.0549	1.05888	1.11447	7.19271	11.16210	1.46320	0.00000	.51690	.96869	-1.37971	-.14906	0.00000
126	D	55.9694	1.10278	1.12107	5.91369	13.33220	1.35357	0.00000	.51690	.77050	-1.57102	-.14906	0.00000
127	SD	56.9694	1.10278	1.12107	5.91369	13.33220	1.35357	0.00000	.51690	.77050	-1.57102	-.14906	0.00000
128	QS	57.2694	1.11117	1.12493	5.47561	14.29822	1.30886	0.00000	.51690	.68965	-1.64905	-.14908	0.00000
129	QD	57.6200	1.12167	1.12833	5.23708	14.88417	1.28282	0.00000	.51690	-.00000	.00000	-.00000	0.00000
130	QD	57.9708	1.13217	1.13213	5.47561	14.29822	1.30886	0.00000	.51690	-.68965	1.64905	-.14906	0.00000
131	QS	58.2708	1.14056	1.13598	5.91362	13.33220	1.35357	0.00000	.51690	-.77050	1.57102	-.14906	0.00000
132	SD	58.6408	1.14844	1.14059	5.91362	13.33220	1.35357	0.00000	.51690	-.77050	1.57102	-.14906	0.00000
133	D	59.0059	1.15655	1.14519	7.19271	11.16215	1.46320	0.00000	.51690	-.96869	1.37971	-.14906	0.00000
134	B	60.6663	1.18819	1.17480	11.14540	7.21733	1.78931	0.00000	.67058	-1.41547	.98534	-.24434	0.00000
135	Q	61.1017	1.19778	1.19275	13.37312	5.91573	1.96900	0.00000	.67058	-1.61367	.78451	-.24434	0.00000
136	SF	61.5017	1.19778	1.19275	13.37312	5.91573	1.96900	0.00000	.67058	-1.61367	.78451	-.24434	0.00000
137	QS	61.7017	1.20123	1.20115	14.36557	5.46961	2.04230	0.00000	.67058	-1.69451	.70258	-.24434	0.00000
138	QF	62.0401	1.20500	1.21166	14.96786	5.22668	2.08528	0.00000	.67058	.00000	-.00000	-.00006	0.00000
139	QF	62.4028	1.20878	1.22218	14.36558	5.46960	2.04236	0.00000	.67058	1.69451	-.70258	-.25423	0.00000
140	QS	62.7028	1.21223	1.23057	13.37313	5.91573	1.96907	0.00000	.67058	1.61366	-.78450	-.24423	0.00000
141	SF	62.7028	1.21223	1.23057	13.37313	5.91573	1.96907	0.00000	.67058	1.61366	-.78450	-.24423	0.00000
142	Q	63.4382	1.22182	1.24852	11.14561	7.21732	1.78946	0.00000	.67058	1.41547	-.98533	-.24423	0.00000
143	B	65.0986	1.25146	1.27814	7.19272	11.16211	1.46354	0.00000	.82428	.96869	-1.37970	-.14895	0.00000
144	D	65.8164	1.26445	1.28774	5.91367	13.33215	1.35399	0.00000	.82428	.77050	-1.57101	-.14895	0.00000
145	SD	65.8164	1.26445	1.28774	5.91367	13.33215	1.35399	0.00000	.82428	.77050	-1.57101	-.14895	0.00000
146	QS	66.1340	1.27784	1.29120	5.47563	14.29817	1.30930	0.00000	.82428	.68965	-1.64905	-.14895	0.00000
147	QD	66.4846	1.28834	1.29500	5.23710	14.88414	1.28325	0.00000	.82428	.00000	-.00000	-.00016	0.00000
148	QD	66.8351	1.29883	1.29879	5.47563	14.29817	1.30942	0.00000	.82428	-.68966	1.64905	-.14929	0.00000
149	QS	67.1351	1.30723	1.30225	5.91368	13.33215	1.35421	0.00000	.82428	-.77050	1.57101	-.14929	0.00000

POS		S(M)	NUX	NUY	BETAX(M)	BETAY(M)	ETAX(M)	ETAY(M)	ETAS(M)	ALPHAX	ALPHAY	DETAX	DETAY
150	SD	67.1351	1.30723	1.30225	5.91368	13.33213	1.35421	0.00000	.82428	-.77050	1.57101	.14929	0.00000
151	D	67.6705	1.32521	1.31165	7.19273	11.16210	1.46400	0.00000	.82428	-.96869	1.37970	.14929	0.00000
152	B	69.5309	1.35485	1.34167	11.14544	7.21730	1.79068	0.00000	.97806	-1.41548	.98533	.24436	0.00000
153	D	70.2663	1.36443	1.35942	13.37317	5.91571	1.97034	0.00000	.97806	-1.61367	.78450	.24456	0.00000
154	SF	70.2663	1.36443	1.35942	13.37317	5.91571	1.97034	0.00000	.97806	-1.61367	.78450	.24456	0.00000
155	DS	70.5663	1.36749	1.36782	14.36462	5.46959	2.04371	0.00000	.97806	-1.69452	.70258	.24456	0.00000
156	QF	70.9169	1.37167	1.37833	14.96791	5.22666	2.08673	0.00000	.97806	.00000	-.00000	.00011	0.00000
157	QF	71.2674	1.37545	1.38884	14.36562	5.46959	2.04378	0.00000	.97806	1.69452	-.70258	-.24434	0.00000
158	DS	71.5674	1.37889	1.39724	13.37317	5.91571	1.97048	0.00000	.97806	1.61367	-.78450	-.24434	0.00000
159	SF	71.5674	1.37889	1.39724	13.37317	5.91571	1.97048	0.00000	.97806	1.61367	-.78450	-.24434	0.00000
160	D	72.3028	1.38849	1.41210	11.14544	7.21730	1.79079	0.00000	.97806	1.41548	-.98533	-.24435	0.00000
161	B	[illegible]	[illegible]	[illegible]	7.19273	11.16210	1.46467	0.00000	1.13188	.96869	-1.37970	-.14907	0.00000
162	D	[illegible]	[illegible]	[illegible]	5.91368	13.33215	1.35506	0.00000	1.13188	.77050	-1.57101	-.14907	0.00000
163	SD	74.6986	1.43611	1.45440	5.91368	13.33215	1.35504	0.00000	1.13188	.77050	-1.57101	-.14907	0.00000
164	DS	74.9986	1.44451	1.45786	5.47563	14.29817	1.31032	0.00000	1.13188	.68966	-1.64905	-.14907	0.00000
165	QD	75.3492	1.45600	1.46166	5.23710	14.88611	1.28431	0.00000	1.13188	.00000	-.00000	.00016	0.00000
166	QD	[illegible]	[illegible]	[illegible]	5.47563	14.29817	1.31043	0.00000	1.13188	-.68965	1.64905	.14940	0.00000
167	DS	[illegible]	1.47389	[illegible]	5.91367	13.33212	1.35526	0.00000	1.13188	-.77050	1.57101	.14940	0.00000
168	SD	[illegible]	1.47389	[illegible]	5.91367	13.33212	1.35526	0.00000	1.13188	-.77050	1.57101	.14940	0.00000
169	D	[illegible]	[illegible]	[illegible]	7.19272	11.16211	1.46513	0.00000	1.13188	-.96869	1.37970	.14940	0.00000
170	B	78.3955	1.52152	1.50813	11.14541	7.21732	1.79180	0.00000	1.28577	-1.41547	.98533	.24468	0.00000
171	D	79.1310	1.53111	1.52608	13.37313	5.91573	1.97175	0.00000	1.28577	-1.61366	.78450	.24468	0.00000
172	SF	79.1310	1.53111	1.52608	13.37313	5.91573	1.97175	0.00000	1.28577	-1.61366	.78450	.24468	0.00000
173	DS	79.4310	[illegible]	[illegible]	14.36[illegible]	5.46960	2.04515	0.00000	1.28577	-1.69451	.70258	.24468	0.00000
174	QF	79.7816	[illegible]	[illegible]	14.96786	5.22668	2.08819	0.00000	1.28577	.00000	-.00000	.00006	0.00000
175	QF	80.1320	[illegible]	[illegible]	14.36587	5.46961	2.04519	0.00000	1.28577	1.69451	-.70258	-.24457	0.00000
176	DS	80.4320	1.54556	1.56391	13.37312	5.91573	1.97182	0.00000	1.28577	1.61367	-.78451	-.24457	0.00000
177	SF	80.4320	1.54556	1.56391	13.37312	5.91573	1.97182	0.00000	1.28577	1.61367	-.78451	-.24457	0.00000
178	D	81.1674	1.55215	1.58786	11.14540	7.21733	1.79196	0.00000	1.28577	1.41547	-.98534	-.24457	0.00000
179	B	82.8278	1.58479	1.61167	7.19271	11.16215	1.46567	0.00000	1.43968	.96869	-1.37971	-.14929	0.00000
180	D	83.5633	1.60278	1.62107	5.91365	13.33220	1.35567	0.00000	1.43968	.77050	-1.57102	-.14929	0.00000
181	SD	83.5633	1.60278	1.62107	5.91365	13.33220	1.35567	0.00000	1.43968	.77050	-1.57102	-.14929	0.00000
182	DS	83.8633	1.61117	[illegible]	5.47561	14.29828	1.31088	0.00000	1.43968	.68965	-1.64909	-.14929	0.00000
183	QD	84.2138	1.62167	1.62833	5.23708	14.88417	1.28481	0.00000	1.43968	.00000	-.00000	-.00000	0.00000
184	REFL	168.4276	3.24534	3.25666	17.83321	5.73406	-.00091	0.00000	2.87937	.00000	-.00000	-.00000	0.00000

CIRCUMFERENCE = 505.2827 M THETX = 6.28318638 RAD NUX = 9.73002 DNUX/(DP/P) = .39620
(DS/S)/ERRORS = .00[illegible] M THETY(183) = 0.00000000 RAD NUY = 9.76997 DNUY/(DP/P) = .39105
TGAM = (7.64818, 0.00000)

MAXIMA ---- BETX(1) = 17.83321 BETY(12) = 16.94478 ETAX(174) = 2.08819 ETAY(184) = 0.00000
MINIMA ---- BETX(36) = 4.05811 BETY(48) = 3.28656 ETAX(33) = .C0000 ETAY(184) = 0.00000

```
***  DP          //  -0.02
***  V     PVEC  //                          DP
***  CHR   SUP   0    0 //
***  AGR   FXPT  ?   -3 //  V    .SP        1
*                        //
***        INCR  1      //  DP      .005
***        END   0    0 //
```

CALCULATION OF THE EQUILIBRIUM ORBIT AND BETATRON FUNCTIONS OF AGR .

INITIAL REFERENCE RAY DEFINED BY V

X = 0.00000000 DX = 0.00000000 Y = 0.00000000 DY = 0.00000000 DS = 0.00000000 DP/P = -.02000000 1.00000000

2

7X7 MATRIX FOR AGR

.06055299	17.87971570	0.00000000	0.00000000	0.00000000	.03138991	.00026699
-.05572423	.06055299	0.00000000	0.00000000	0.00000000	.00186192	.00001584
0.00000000	0.00000000	-.02881698	5.10131547	0.00000000	0.00000000	0.00000000
0.00000000	0.00000000	-.19586508	-.02881698	0.00000000	0.00000000	0.00000000
-.00185192	-.03138991	0.00000000	0.00000000	1.00000000	-2.83177215	.06130947
0.00000000	0.00000000	0.00000000	0.00000000	0.00000000	1.00000000	0.00000000
0.00000000	0.00000000	0.00000000	0.00000000	0.00000000	0.00000000	1.00000000

EIGENVALUES OF THE 4X4 SUBMATRIX

X... LMD1 = (.06055299 -.99816498); C(1) = 1.00000000; MU(1) = -1.51020627 RAD; Q(1) = .72107038
1/LMD1 = (.06055299 -.99816498); C(2) = 1.00000000; MU(2) = -1.51020627 RAD; Q(2) = .27892962

Y... LMD3 = (-.02881698 .99958470); C(3) = 1.00000000; MU(3) = -1.59861729 RAD; Q(3) = .76376100
1/LMD3 = (-.02881698 -.99958470); C(4) = 1.00000000; MU(4) = -1.59861729 RAD; Q(4) = .23623900

EIGENVALUE = (.06055299, .99816498), EIGENVECTOR = { 4.23232626, 0.00000000 }
{ .00000000, -.23627668 }
{ 0.00000000, 0.00000000 }
{ 0.00000000, 0.00000000 }

EIGENVALUE = (.06055299, -.99816498), EIGENVECTOR = { 4.23232626, 0.00000000 }
{ .00000000, -.23627668 }
{ 0.00000000, 0.00000000 }
{ 0.00000000, 0.00000000 }

EIGENVALUE = (-.02881698, .99958470), EIGENVECTOR = { 0.00000000, 0.00000000 }
{ 0.00000000, 0.00000000 }
{ 2.25907833, 0.00000000 }
{ .00000000, .44265840 }

EIGENVALUE = (-.02881698, -.99958470), EIGENVECTOR = { 0.00000000, 0.00000000 }
{ 0.00000000, 0.00000000 }
{ 2.25907833, 0.00000000 }
{ .00000000, -.44265840 }

	X	DX	Y	DY	DS	DP/P	
EQ ORBIT	-.00036772	0.00000000	0.00000000	0.00000000	0.00000000	-.02000000	1.00000000
ETA ORBIT	.03341310	.00000000	0.00000000	0.00000000	0.00000000	1.00000000	0.00000000

EIGENVECTORS 1 AND 3 IN POLAR COORDINATES

POS	X1 X3		DX1 DX3		Y1 Y3		DY1 DY3	
0	1.232326 0.000000	0.000000 0.000000	-.236277 0.000000	1.570796 0.000000	0.000000 2.259078	0.000000 0.000000	0.000000 .442658	0.000000 1.570796

BETATRON FUNCTIONS OF AGR

POS		S (M)	QX	QY	BX (M)	BY (M)	AX	AY	EX (M)	EXP	EY (M)	EYP	XCO (MM)	DXCO (MR)	YCO (MM)	DYCO (MR)
0		0.00	0.00	0.00	17.91	5.10	0.00	0.00	.03341	.00000	0.000000	0.000000	-.3477	0.0000	0.0000	0.0000
1	QF1	.36	.00	.01	17.08	6.37	2.32	-.78	.03262	-.00452	0.000000	0.000000	-.3395	.0466	0.0000	0.0000
2		.72	.01	.02	15.40	8.00	2.18	-.89	.03093	-.00452	0.000000	0.000000	-.3222	.0466	0.0000	0.0000
3		1.10	.01	.03	13.83	9.71	2.04	-1.01	.02924	-.00452	0.000000	0.000000	-.3048	.0466	0.0000	0.0000
4	S	1.47	.02	.04	12.39	11.50	1.90	-1.12	.02756	-.00452	0.000000	0.000000	-.2874	.0466	0.0000	0.0000
5	S	1.84	.02	.05	10.98	8.37	1.76	-1.23	.02587	-.00452	0.000000	0.000000	-.2700	.0466	0.0000	0.0000
6		2.22	.03	.05	9.72	9.33	1.62	-1.34	.02418	-.00452	0.000000	0.000000	-.2526	.0466	0.0000	0.0000
7		2.59	.03	.06	8.56	10.38	1.49	-1.45	.02249	-.00452	0.000000	0.000000	-.2353	.0466	0.0000	0.0000
8		2.96	.04	.06	7.50	11.60	1.35	-1.57	.02081	-.00452	0.000000	0.000000	-.2179	.0466	0.0000	0.0000
9	S	3.34	.05	.07	6.55	12.91	1.21	-1.68	.01912	-.00452	0.000000	0.000000	-.2005	.0466	0.0000	0.0000
10	S	3.71	.06	.07	5.70	14.01	1.07	-1.79	.01743	-.00452	0.000000	0.000000	-.1831	.0466	0.0000	0.0000
11		4.08	.07	.08	4.96	14.98	.93	-1.90	.01575	-.00452	0.000000	0.000000	-.1657	.0466	0.0000	0.0000
12	QD1	4.43	.08	.08	4.36	15.82	.79	-2.01	.01450	-.00263	0.000000	0.000000	-.1529	.0269	0.0000	0.0000
13	QD1	4.78	.09	.09	4.01	16.39	.41	-1.93	.01389	-.00086	0.000000	0.000000	-.1468	.0083	0.0000	0.0000
14	S	5.16	.11	.09	4.05	13.97	-.50	1.81	.01357	-.00086	0.000000	0.000000	-.1437	.0083	0.0000	0.0000
15	S	5.53	.12	.09	4.36	12.65	-.59	1.70	.01325	-.00086	0.000000	0.000000	-.1406	.0083	0.0000	0.0000
16		5.90	.13	.10	4.74	11.53	-.69	1.58	.01293	-.00086	0.000000	0.000000	-.1374	.0083	0.0000	0.0000
17		6.28	.14	.10	5.19	10.55	-.78	1.47	.01261	-.00086	0.000000	0.000000	-.1343	.0083	0.0000	0.0000
18		6.65	.15	.11	5.71	9.68	-.88	1.36	.01229	-.00086	0.000000	0.000000	-.1312	.0083	0.0000	0.0000
19	S	7.02	.15	.12	7.70	8.27	-.97	1.24	.01197	-.00086	0.000000	0.000000	-.1281	.0083	0.0000	0.0000
20	S	7.39	.16	.12	8.46	7.38	-1.07	1.13	.01165	-.00086	0.000000	0.000000	-.1250	.0083	0.0000	0.0000
21		7.77	.17	.13	9.29	6.59	-1.16	1.01	.01133	-.00086	0.000000	0.000000	-.1219	.0083	0.0000	0.0000
22		8.14	.18	.13	10.19	5.87	-1.26	.90	.01101	-.00086	0.000000	0.000000	-.1188	.0083	0.0000	0.0000
23		8.51	.18	.14	11.19	5.23	-1.35	.78	.01069	-.00086	0.000000	0.000000	-.1157	.0083	0.0000	0.0000
24	QF2	8.86	.19	.15	11.84	4.96	-1.08	.03	.01019	-.00221	0.000000	0.000000	-.1102	.0214	0.0000	0.0000
25	QF2	9.22	.19	.15	11.05	5.18	1.48	-.68	.00915	-.00347	0.000000	0.000000	-.0998	.0364	0.0000	0.0000
26		9.59	.20	.16	9.99	5.72	1.38	-.78	.00785	-.00347	0.000000	0.000000	-.0862	.0364	0.0000	0.0000
27		9.96	.20	.17	9.00	6.36	1.27	-.89	.00656	-.00347	0.000000	0.000000	-.0726	.0364	0.0000	0.0000
28		10.33	.21	.17	8.09	7.04	1.16	-.99	.00526	-.00347	0.000000	0.000000	-.0590	.0364	0.0000	0.0000
29	S	10.71	.22	.18	7.27	7.82	1.05	-1.10	.00397	-.00347	0.000000	0.000000	-.0454	.0364	0.0000	0.0000
30	S	11.08	.23	.19	6.32	8.97	.94	-1.20	.00267	-.00347	0.000000	0.000000	-.0319	.0364	0.0000	0.0000
31		11.46	.24	.19	5.46	9.93	.84	-1.31	.00138	-.00347	0.000000	0.000000	-.0183	.0364	0.0000	0.0000
32		11.83	.25	.20	5.28	10.62	.73	-1.41	.00008	-.00347	0.000000	0.000000	-.0047	.0364	0.0000	0.0000
33		12.20	.26	.20	4.77	11.71	.62	-1.51	-.00121	-.00347	0.000000	0.000000	.0089	.0364	0.0000	0.0000
34	S	12.57	.27	.21	4.35	12.68	.51	-1.62	-.00251	-.00347	0.000000	0.000000	.0225	.0364	0.0000	0.0000
35	S	12.95	.28	.22	4.01	14.13	.40	-1.72	-.00380	-.00347	0.000000	0.000000	.0361	.0364	0.0000	0.0000
36	QD2	13.30	.30	.22	3.93	14.66	.23	.24	-.00512	-.00409	0.000000	0.000000	.0498	.0429	0.0000	0.0000
37	QD2	13.65	.31	.23	4.35	14.81	.02	2.15	-.00669	-.00491	0.000000	0.000000	.0660	.0503	0.0000	0.0000
38		14.01	.32	.24	5.08	14.38	-.18	2.00	-.00840	-.00491	0.000000	0.000000	.0845	.0503	0.0000	0.0000
39	R	14.38	.34	.26	5.93	10.87	-1.23	1.85	-.01030	-.00491	0.000000	0.000000	.1029	.0503	0.0000	0.0000
40	R	14.75	.35	.27	6.89	9.47	-1.39	1.70	-.01210	-.00491	0.000000	0.000000	.1213	.0503	0.0000	0.0000
41	R	15.12	.36	.28	7.96	8.37	-1.54	1.55	-.01390	-.00491	0.000000	0.000000	.1398	.0503	0.0000	0.0000
42	R	15.48	.37	.29	9.14	7.59	-1.70	1.40	-.01570	-.00491	0.000000	0.000000	.1582	.0503	0.0000	0.0000
43	R	15.85	.38	.30	10.42	6.97	-1.85	1.26	-.01750	-.00491	0.000000	0.000000	.1766	.0503	0.0000	0.0000
44	R	16.22	.37	.30	11.82	6.44	-2.01	1.11	-.01931	-.00491	0.000000	0.000000	.1951	.0503	0.0000	0.0000
45	R	16.58	.38	.31	13.40	4.69	-2.16	.96	-.02111	-.00491	0.000000	0.000000	.2135	.0503	0.0000	0.0000
46	R	16.95	.39	.33	15.04	4.04	-2.32	.81	-.02291	-.00491	0.000000	0.000000	.2320	.0503	0.0000	0.0000
47	R	17.32	.38	.34	16.80	3.51	-2.48	.66	-.02471	-.00491	0.000000	0.000000	.2504	.0503	0.0000	0.0000
48	QF3	17.73	.19	.36	17.01	3.22	-.15	.06	-.02602	-.00138	0.000000	0.000000	.2640	.0148	0.0000	0.0000
49	QF3	18.14	.19	.38	17.04	3.41	2.21	-.53	-.02584	.00223	0.000000	0.000000	.2626	-.0219	0.0000	0.0000

PDS		S (M)	QX	QY	BX (M)	BY (M)	AX	AY	EX (M)	EXP	EY	EYP	XCO (MM)	DXCO (MR)	YCO (MM)	DYCO (MR)
50	Z	18.50	.39	.40	15.49	3.84	2.09	-.66	-.02504	.00223	0.000000	0.000000	.2540	-.0215	0.0000	0.0000
51	Z	18.66	.40	.41	14.03	4.36	1.96	-.80	-.02423	.00223	0.000000	0.000000	.2471	-.0215	0.0000	0.0000
52	Z	19.22	.40	.43	12.66	4.99	1.84	-.93	-.02343	.00223	0.000000	0.000000	.2342	-.0215	0.0000	0.0000
53	Z	19.88	.41	.44	11.38	5.71	1.71	-1.07	-.02262	.00223	0.000000	0.000000	.2316	-.0215	0.0000	0.0000
54	Z	19.95	.41	.45	10.19	6.53	1.59	-1.21	-.02181	.00223	0.000000	0.000000	.2238	-.0215	0.0000	0.0000
55	Z	20.81	.42	.46	9.09	7.45	1.46	-1.36	-.02101	.00223	0.000000	0.000000	.2161	-.0215	0.0000	0.0000
56	Z	20.67	.43	.46	8.08	8.47	1.34	-1.48	-.02020	.00223	0.000000	0.000000	.2083	-.0215	0.0000	0.0000
57	Z	21.03	.43	.47	7.16	9.58	1.21	-1.61	-.01940	.00223	0.000000	0.000000	.2006	-.0215	0.0000	0.0000
58	Z	21.39	.44	.47	6.33	10.79	1.09	-1.75	-.01859	.00223	0.000000	0.000000	.1929	-.0215	0.0000	0.0000
59	Z	21.75	.45	.48	5.58	12.10	.97	-1.88	-.01779	.00223	0.000000	0.000000	.1851	-.0215	0.0000	0.0000
60	QD3	22.16	.46	.48	5.15	12.99	.13	-.24	-.01347	-.00019	0.000000	0.000000	.1814	.0039	0.0000	0.0000
61	QD3	22.48	.46	.49	5.36	12.48	.07	-.18	-.01799	.00262	0.000000	0.000000	.1880	.0287	0.0000	0.0000
62	R	22.64	.48	.49	5.88	11.40	-.07	.07	-.01881	.00262	0.000000	0.000000	.1986	.0287	0.0000	0.0000
63	R	23.31	.50	.50	6.48	10.42	-.87	.29	-.01967	-.00262	0.000000	0.000000	.2091	.0287	0.0000	0.0000
64	R	23.68	.50	.50	7.15	9.51	-.97	1.20	-.02083	-.00262	0.000000	0.000000	.2196	.0287	0.0000	0.0000
65	R	24.04	.51	.51	7.90	8.66	-1.06	1.11	-.02179	-.00262	0.000000	0.000000	.2302	.0287	0.0000	0.0000
66	R	24.41	.52	.52	8.71	7.88	-1.16	1.01	-.02276	-.00262	0.000000	0.000000	.2407	.0287	0.0000	0.0000
67	R	24.78	.53	.53	9.60	7.18	-1.26	.92	-.02372	-.00262	0.000000	0.000000	.2512	.0287	0.0000	0.0000
68	R	25.14	.53	.53	10.57	6.54	-1.36	.82	-.02468	-.00262	0.000000	0.000000	.2618	.0287	0.0000	0.0000
69	R	25.51	.54	.54	11.60	5.97	-1.46	.73	-.02564	-.00262	0.000000	0.000000	.2723	.0287	0.0000	0.0000
70	R	25.88	.54	.55	12.71	5.47	-1.56	.63	-.02661	-.00262	0.000000	0.000000	.2829	.0287	0.0000	0.0000
71	R	26.24	.55	.57	13.89	5.04	-1.66	.54	-.02757	-.00262	0.000000	0.000000	.2934	.0287	0.0000	0.0000
72	QF	26.59	.56	.58	14.48	4.90	-1.71	.49	-.02790	.00076	0.000000	0.000000	.2972	.0069	0.0000	0.0000
73	QF	26.94	.57	.59	13.87	5.23	-1.68	.51	-.02743	.00412	0.000000	0.000000	.2886	-.0423	0.0000	0.0000
74	QD	27.98	.59	.61	10.69	7.27	1.40	-1.15	-.02278	.00412	0.000000	0.000000	.2447	-.0423	0.0000	0.0000
75	R	29.64	.60	.64	6.81	11.89	.94	-1.62	-.01463	.10134	0.000000	0.000000	-1.4371	-1.9867	0.0000	0.0000
76	QD	30.68	.63	.66	5.17	15.57	.65	-1.93	.16956	.10134	0.000000	0.000000	-3.4943	-1.9867	0.0000	0.0000
77	QD	31.03	.64	.66	4.95	16.30	-.02	-.10	.20892	.12401	0.000000	0.000000	-4.2678	-2.4423	0.0000	0.0000
78	QD	31.38	.65	.66	5.19	15.71	-.69	1.76	.25711	.15191	0.000000	0.000000	-5.2102	-2.9990	0.0000	0.0000
79	QD	32.41	.68	.67	6.93	12.35	-.99	1.49	.31440	.15191	0.000000	0.000000	-6.3234	-2.9990	0.0000	0.0000
80	R	34.07	.71	.70	10.97	8.08	-1.46	1.10	.74646	.24921	0.000000	0.000000	-14.9031	-4.9441	0.0000	0.0000
81	QF	34.81	.72	.72	13.28	6.93	-1.67	.90	.92211	.24921	0.000000	0.000000	-18.2302	-4.9441	0.0000	0.0000
82	QF	34.81	.72	.72	13.26	6.98	-1.70	.92	.92211	.29121	0.000000	0.000000	-18.2302	-4.9688	0.0000	0.0000
83	QS	35.11	.72	.72	14.31	6.05	-1.79	.83	1.00522	.25171	0.000000	0.000000	-20.0200	-4.9688	0.0000	0.0000
84	QF	35.46	.72	.73	14.97	5.74	-.07	.05	1.07128	.12379	0.000000	0.000000	-21.3382	-2.4704	0.0000	0.0000
85	QE	35.81	.73	.74	14.40	5.97	1.67	-.72	1.09139	-.00943	0.000000	0.000000	-21.7452	.1319	0.0000	0.0000
86	QS	36.11	.73	.75	13.42	6.68	1.59	-.79	1.08856	-.00943	0.000000	0.000000	-21.7099	.1319	0.0000	0.0000
87	SF	36.11	.73	.75	13.42	6.62	1.55	-.77	1.08856	-.00601	0.000000	0.000000	-21.7099	.0980	0.0000	0.0000
88	D	36.84	.74	.77	11.28	7.89	1.36	-.95	1.08419	-.00601	0.000000	0.000000	-21.6378	.0980	0.0000	0.0000
89	LC	38.30	.77	.80	7.46	11.85	.94	-1.37	1.07417	-.00601	0.000000	0.000000	-21.4751	.0980	0.0000	0.0000
90	D	39.24	.79	.81	6.21	13.69	.76	-1.55	1.06976	-.00601	0.000000	0.000000	-21.4030	.0980	0.0000	0.0000
91	SD	39.24	.79	.81	6.21	13.69	.78	-1.61	1.06976	-.01104	0.000000	0.000000	-21.4030	.1479	0.0000	0.0000
92	QS	39.54	.79	.81	5.76	14.69	.71	-1.69	1.06643	-.01104	0.000000	0.000000	-21.3506	.1479	0.0000	0.0000
93	QD	39.89	.80	.81	5.53	15.28	.03	.04	1.06508	.11774	0.000000	0.000000	-21.7488	-2.3819	0.0000	0.0000
94	QD	40.24	.81	.82	5.80	14.64	-.76	1.76	1.14956	.25151	0.000000	0.000000	-23.0400	-5.0104	0.0000	0.0000
95	QF	40.54	.82	.82	6.28	13.60	-.84	1.68	1.22501	.25151	0.000000	0.000000	-24.5431	-5.0104	0.0000	0.0000
96	SD	40.54	.82	.82	6.28	13.60	-.81	1.61	1.22501	.24490	0.000000	0.000000	-24.5431	-4.9448	0.0000	0.0000
97	D	41.28	.84	.84	7.62	11.38	-1.00	1.41	1.40512	.24490	0.000000	0.000000	-28.1796	-4.9448	0.0000	0.0000
98	LC	42.94	.87	.86	11.64	7.42	-1.44	.98	1.81174	.24490	0.000000	0.000000	-36.3900	-4.9448	0.0000	0.0000
99	D	43.67	.88	.88	13.95	6.12	-1.64	.78	1.99185	.24490	0.000000	0.000000	-40.0265	-4.9448	0.0000	0.0000

POS
SI
DX
DY
BX
BY
AX
AY
EX
EXP
EY
KCD

POS		S (M)	QX	QY	BX (M)	BY (M)	AX	AY	EX (M)	EXP	EY (M)	EYP	XCO (MM)	DXCO (MR)	YCO (MM)	DYCO (MR)
150	SD	67.12	1.31	1.31	6.28	13.40	-.81	1.53	1.37187	.15040	0.000000	0.000000	-27.5352	-3.0255	0.0000	0.0000
151	O	67.85	1.33	1.32	7.62	11.28	-1.01	1.35	1.48248	.15040	0.000000	0.000000	-29.7603	-3.0255	0.0000	0.0000
152	B	69.61	1.36	1.35	11.68	7.42	-1.45	.98	1.81118	.24770	0.000000	0.000000	-36.3757	-4.9706	0.0000	0.0000
153	O	70.25	1.37	1.36	13.95	6.12	-1.64	.78	1.99335	.24770	0.000000	0.000000	-40.0313	-4.9706	0.0000	0.0000
154	SF	70.25	1.37	1.36	13.95	6.12	-1.72	.82	1.99335	.25927	0.000000	0.000000	-40.0313	-5.0857	0.0000	0.0000
155	DS	70.55	1.37	1.37	15.01	5.66	-1.81	.74	2.07113	.28927	0.000000	0.000000	-41.5570	-5.0857	0.0000	0.0000
156	QF	70.90	1.37	1.38	15.65	5.40	.00	.00	2.11697	.00124	0.000000	0.000000	-42.4535	-.0119	0.0000	0.0000
157	QF	71.25	1.38	1.39	15.00	5.66	1.81	-.74	2.07199	-.25684	0.000000	0.000000	-41.5653	5.0623	0.0000	0.0000
158	DS	71.55	1.38	1.40	13.94	6.12	1.73	-.82	1.99494	-.25684	0.000000	0.000000	-40.0466	5.0623	0.0000	0.0000
159	SF	71.55	1.38	1.40	13.94	6.12	1.65	-.78	1.99494	-.24526	0.000000	0.000000	-40.0466	4.9472	0.0000	0.0000
160	O	72.20	1.39	1.42	11.67	7.42	1.49	-.98	1.81657	-.24526	0.000000	0.000000	-36.4083	4.9472	0.0000	0.0000
161	B	73.96	1.42	1.45	7.60	11.28	1.01	-1.35	1.48990	-.14796	0.000000	0.000000	-29.8316	3.0020	0.0000	0.0000
162	O	74.60	1.44	1.46	6.26	13.40	.81	-1.53	1.38109	-.14796	0.000000	0.000000	-27.6238	3.0020	0.0000	0.0000
163	SD	74.60	1.44	1.46	6.26	13.40	.85	-1.61	1.38109	-.15635	0.000000	0.000000	-27.6238	3.0851	0.0000	0.0000
164	DS	74.98	1.44	1.46	5.77	14.39	.77	-1.69	1.33418	-.15635	0.000000	0.000000	-26.6983	3.0851	0.0000	0.0000
165	QD	75.33	1.45	1.46	5.50	14.92	.04	.00	1.30718	.00175	0.000000	0.000000	-26.1624	-.0171	0.0000	0.0000
166	QD	75.68	1.46	1.47	5.72	14.39	-.69	1.70	1.33242	.15993	0.000000	0.000000	-26.7103	-3.1199	0.0000	0.0000
167	DS	75.98	1.47	1.47	6.16	13.40	-.77	1.62	1.38340	.15993	0.000000	0.000000	-27.6963	-3.1199	0.0000	0.0000
168	SD	75.98	1.47	1.47	6.16	13.40	-.73	1.53	1.38340	.15182	0.000000	0.000000	-27.6462	-3.0367	0.0000	0.0000
169	O	76.71	1.47	1.48	7.37	11.27	-.92	1.35	1.49403	.15182	0.000000	0.000000	-29.8796	-3.0367	0.0000	0.0000
170	B	78.37	1.52	1.51	11.08	7.41	-1.33	.98	1.82537	.24882	0.000000	0.000000	-36.5136	-4.9819	0.0000	0.0000
171	O	79.10	1.53	1.53	13.17	6.11	-1.51	.78	2.00836	.24882	0.000000	0.000000	-40.1774	-4.9819	0.0000	0.0000
172	SF	79.10	1.53	1.53	13.17	6.11	-1.59	.82	2.00836	.26052	0.000000	0.000000	-40.1774	-5.0978	0.0000	0.0000
173	DS	79.40	1.53	1.54	14.15	5.65	-1.67	.76	2.08652	.26052	0.000000	0.000000	-41.7068	-5.0978	0.0000	0.0000
174	QF	79.76	1.54	1.55	14.73	5.39	.03	.00	2.13247	.00080	0.000000	0.000000	-42.6044	-.0059	0.0000	0.0000
175	QF	80.11	1.54	1.56	14.10	5.65	1.73	-.73	2.08604	-.25936	0.000000	0.000000	-41.7109	5.0863	0.0000	0.0000
176	DS	80.41	1.54	1.56	13.09	6.11	1.65	-.81	2.00914	-.25936	0.000000	0.000000	-40.1850	5.0863	0.0000	0.0000
177	SF	80.41	1.54	1.56	13.09	6.11	1.57	-.78	2.00914	-.24763	0.000000	0.000000	-40.1850	4.9703	0.0000	0.0000
178	O	81.14	1.55	1.58	10.92	7.40	1.38	-.97	1.82703	-.24763	0.000000	0.000000	-36.5256	4.9703	0.0000	0.0000
179	B	82.80	1.58	1.61	7.10	11.25	.94	-1.35	1.49865	-.15033	0.000000	0.000000	-29.9147	3.0252	0.0000	0.0000
180	O	83.53	1.60	1.62	5.86	13.37	.74	-1.53	1.38789	-.15033	0.000000	0.000000	-27.6898	3.0252	0.0000	0.0000
181	SD	83.53	1.60	1.62	5.86	13.37	.78	-1.61	1.38789	-.15878	0.000000	0.000000	-27.6898	3.1087	0.0000	0.0000
182	DS	83.83	1.61	1.63	5.42	14.36	.70	-1.60	1.34026	-.15878	0.000000	0.000000	-26.7572	3.1087	0.0000	0.0000
183	QD	84.18	1.62	1.63	5.18	14.96	.00	-.00	1.31253	-.00000	0.000000	0.000000	-26.2143	.0000	0.0000	0.0000
184	REFL	168.37	3.24	3.25	17.91	5.10	-.00	-.00	.03341	-.00000	0.000000	0.000000	-.3477	0.0000	0.0000	0.0000

CIRCUMFERENCE = [illegible] M THETX = 6.28318638 RAD NUX = 9.72107 DNUX/(DP/P) = .32692
[illegible] = [illegible] M THETY(183) = 0.00000000 RAD NUY = 9.76376 DNUY/(DP/P) = .43820
TGAM = (7.71077, 0.00000)

MAXIMA --- BETX(1) = 17.91259 BETY(77) = 16.29623 ETAX(174) = 2.13247 ETAY(184) = 0.00000
MINIMA --- BETX(36) = 3.95271 BETY(48) = 3.21594 ETAX(32) = .00000 ETAY(184) = 0.00000

*** IMCA 1 // DP .005000 VALUE = -.015000

SUB. CHR , ITER. 2

CALCULATION OF THE EQUILIBRIUM ORBIT AND BETATRON FUNCTIONS OF AGR .

INITIAL REFERENCE RAY DEFINED BY V

X = -.00034772 DX = 0.00000000 Y = 0.00000000 DY = 0.00000000 DS = 0.00000000 DP/P = -.01500000 1.00000000

7X7 MATRIX FOR AGR

.05547951	17.88030476	0.00000000	0.00000000	0.00000000	.02442197	.00016680
-.05575532	.05547951	0.00000000	0.00000000	0.00000000	.00144164	.00000985
0.00000000	0.00000000	-.03127569	5.75435790	0.00000000	0.00000000	0.00000000
0.00000000	0.00000000	-.19013207	-.03127569	0.00000000	0.00000000	0.00000000
-.00144164	-.02442197	0.00000000	0.00000000	1.00000000	-2.84351346	.04525735
0.00000000	0.00000000	0.00000000	0.00000000	0.00000000	1.00000000	0.00000000
0.00000000	0.00000000	0.00000000	0.00000000	0.00000000	0.00000000	1.00000000

EIGENVALUES OF THE 4X4 SUBMATRIX

X--- LMD1 = (.05547951 -.99845983); C(1) = 1.00000000; MU(1) = 1.31328832 RAD; Q(1) = .77357588
1/LMD1 = (.05547951 -.99845983); C(2) = 1.00000000; MU(2) = -1.31328832 RAD; Q(2) = .27630312

Y--- LMD3 = (-.03127569 .99951080); C(3) = 1.00000000; MU(3) = 1.60207712 RAD; Q(3) = .76493248
1/LMD3 = (-.03127569 -.99951080); C(4) = 1.00000000; MU(4) = -1.60207712 RAD; Q(4) = .23506752

EIGENVALUE = (.05547951, -.99845983), EIGENVECTOR = (4.23177103, 0.00000000)
(-.00000000, -.23630768)
(0.00000000, 0.00000000)
(0.00000000, 0.00000000)

EIGENVALUE = (.05547951, -.99845983), EIGENVECTOR = (4.23177103, 0.00000000)
(-.00000000, -.23630768)
(0.00000000, 0.00000000)
(0.00000000, 0.00000000)

EIGENVALUE = (-.03127569, .99951080), EIGENVECTOR = (0.00000000, 0.00000000)
(0.00000000, 0.00000000)
(2.29279938, 0.00000000)
(-.00000000, .43614806)

EIGENVALUE = (-.03127569, -.99951080), EIGENVECTOR = (0.00000000, 0.00000000)
(0.00000000, 0.00000000)
(2.29279938, 0.00000000)
(-.00000000, -.43614806)

	X	DX	Y	DY	DS	DP/P	
EQ ORBIT	-.00019630	0.00000000	0.00000000	0.00000000	0.00000000	-.01500000	1.00000000
EYA ORBIT	.02885647	.00000000	0.00000000	0.00000000	0.00000000	1.00000000	0.00000000

EIGENVECTORS 1 AND 3 IN POLAR COORDINATES

POS	X1 X3		DX1 DX3		Y1 Y3		DY1 DY3	
0	4.231771 0.000000	0.000000 0.000000	.236308 0.000000	1.570796 0.000000	0.000000 2.292799	0.000000 0.000000	0.000000 .436148	0.000000 1.570796

BETATRON FUNCTIONS OF AGR

POS		S (M)	QX	QY	BX (M)	BY (M)	AX	AY	EX (M)	EXP	EY (M)	EYP	XCO (MM)	DXCO (MRT)	YCO (MM)	DYCO (MRT)
0		0.00	0.00	0.00	17.91	9.26	0.00	0.00	.02586	.00000	0.000000	0.000000	-.1963	0.0000	0.0000	0.0000
1	QF1	.28	.00	.01	17.08	8.83	-.31	-.80	.02525	-.00347	0.000000	0.000000	-.1917	-.0262	0.0000	0.0000
2		.78	.01	.01	15.41	8.17	-.77	-.91	.02302	-.00347	0.000000	0.000000	-.1819	-.0262	0.0000	0.0000
3		1.30	.01	.03	13.86	8.05	-2.03	-1.02	.02262	-.00347	0.000000	0.000000	-.1724	-.0262	0.0000	0.0000
4	S	1.62	.02	.04	12.93	7.69	-1.90	-1.15	.02136	-.00347	0.000000	0.000000	-.1624	-.0262	0.0000	0.0000
5	S	1.84	.02	.05	11.01	8.27	1.76	-1.24	.02006	-.00347	0.000000	0.000000	-.1526	-.0262	0.0000	0.0000
6	S	2.22	.03	.05	9.74	9.34	1.62	-1.35	.01877	-.00347	0.000000	0.000000	-.1429	-.0262	0.0000	0.0000
7	S	2.59	.03	.06	8.59	10.58	1.48	-1.46	.01747	-.00347	0.000000	0.000000	-.1331	-.0262	0.0000	0.0000
8	S	2.96	.04	.06	7.84	11.71	1.34	-1.57	.01618	-.00347	0.000000	0.000000	-.1234	-.0262	0.0000	0.0000
9	S	3.33	.05	.07	6.29	12.93	1.20	-1.68	.01488	-.00347	0.000000	0.000000	-.1136	-.0262	0.0000	0.0000
10	S	3.75	.06	.07	5.78	14.22	1.06	-1.79	.01359	-.00347	0.000000	0.000000	-.1038	-.0262	0.0000	0.0000
11	S	4.08	.07	.08	5.60	15.48	.93	-1.90	.01229	-.00347	0.000000	0.000000	-.0941	-.0262	0.0000	0.0000
12	QD1	4.43	.08	.08	5.60	16.26	.24	.03	.01133	-.00201	0.000000	0.000000	-.0869	-.0150	0.0000	0.0000
13	QD1	4.78	.09	.08	5.88	17.15	-.31	1.00	.01067	-.00063	0.000000	0.000000	-.0825	-.0047	0.0000	0.0000
14	S	5.16	.11	.09	6.08	14.13	-.90	1.04	.01064	-.00063	0.000000	0.000000	-.0818	-.0049	0.0000	0.0000
15	S	5.53	.12	.09	6.33	17.80	-.60	1.73	.01040	-.00063	0.000000	0.000000	-.0801	-.0047	0.0000	0.0000
16	S	5.90	.13	.10	6.62	11.52	-.59	1.41	.01017	-.00063	0.000000	0.000000	-.0784	-.0047	0.0000	0.0000
17	S	6.28	.14	.10	6.96	10.40	-.78	1.30	.00993	-.00063	0.000000	0.000000	-.0767	-.0047	0.0000	0.0000
18	S	6.65	.14	.11	7.36	9.32	-.88	1.18	.00970	-.00063	0.000000	0.000000	-.0750	-.0047	0.0000	0.0000
19	S	7.02	.15	.11	7.75	8.34	-.97	1.26	.00946	-.00063	0.000000	0.000000	-.0733	-.0045	0.0000	0.0000
20	S	7.39	.16	.12	8.51	7.44	-1.06	1.15	.00923	-.00063	0.000000	0.000000	-.0716	-.0045	0.0000	0.0000
21	S	7.77	.17	.13	9.36	6.62	-1.16	1.03	.00899	-.00063	0.000000	0.000000	-.0699	-.0045	0.0000	0.0000
22	S	8.14	.17	.13	10.20	5.90	-1.25	.91	.00876	-.00063	0.000000	0.000000	-.0682	-.0045	0.0000	0.0000
23	S	8.51	.18	.14	11.23	5.29	-1.34	.80	.00852	-.00063	0.000000	0.000000	-.0665	-.0045	0.0000	0.0000
24	QF2	8.88	.19	.14	11.83	4.96	-.08	.07	.00611	-.00170	0.000000	0.000000	-.0638	-.0124	0.0000	0.0000
25	QF2	9.22	.19	.17	11.10	5.16	1.49	-.65	.00734	-.00270	0.000000	0.000000	-.0716	-.0206	0.0000	0.0000
26	S	9.59	.19	.18	10.03	5.69	1.38	-.76	.00633	-.00270	0.000000	0.000000	-.0649	-.0206	0.0000	0.0000
27	S	9.96	.20	.19	9.02	6.29	1.27	-.86	.00532	-.00270	0.000000	0.000000	-.0582	-.0206	0.0000	0.0000
28	S	10.33	.21	.20	8.13	6.97	1.17	-.96	.00431	-.00270	0.000000	0.000000	-.0515	-.0206	0.0000	0.0000
29	S	10.71	.21	.20	7.33	7.71	1.06	-1.06	.00331	-.00270	0.000000	0.000000	-.0448	-.0206	0.0000	0.0000
30	S	11.08	.22	.22	6.60	8.46	.98	-1.17	.00230	-.00270	0.000000	0.000000	-.0381	-.0206	0.0000	0.0000
31	S	11.45	.23	.23	5.80	9.44	.86	-1.27	.00129	-.00270	0.000000	0.000000	-.0314	-.0206	0.0000	0.0000
32	S	11.83	.23	.23	5.31	10.45	.73	-1.37	.00028	-.00270	0.000000	0.000000	-.0247	-.0206	0.0000	0.0000
33	S	12.20	.24	.24	4.80	11.52	.62	-1.48	-.00073	-.00270	0.000000	0.000000	-.0180	-.0206	0.0000	0.0000
34	S	12.57	.25	.24	4.38	12.66	.52	-1.58	-.00174	-.00270	0.000000	0.000000	-.0117	-.0206	0.0000	0.0000
35	S	12.95	.26	.25	4.05	13.88	.41	-1.68	-.00274	-.00270	0.000000	0.000000	-.0194	-.0206	0.0000	0.0000
36	QD2	13.30	.30	.25	4.08	14.39	-.23	.23	-.00377	-.00313	0.000000	0.000000	-.0271	-.0238	0.0000	0.0000
37	QD2	13.65	.34	.26	4.31	13.56	-.91	2.10	-.00497	-.00375	0.000000	0.000000	-.0362	-.0282	0.0000	0.0000
38	S	14.01	.36	.26	4.69	12.07	-1.07	1.96	-.00635	-.00375	0.000000	0.000000	-.0465	-.0282	0.0000	0.0000
39	S	14.38	.33	.26	5.94	10.69	-1.22	1.81	-.00773	-.00375	0.000000	0.000000	-.0569	-.0282	0.0000	0.0000
40	S	14.75	.34	.27	6.89	9.42	-1.38	1.66	-.00910	-.00375	0.000000	0.000000	-.0672	-.0282	0.0000	0.0000
41	S	15.11	.35	.28	7.84	8.25	-1.53	1.52	-.01048	-.00375	0.000000	0.000000	-.0775	-.0282	0.0000	0.0000
42	S	15.48	.36	.29	8.79	7.19	-1.68	1.37	-.01186	-.00375	0.000000	0.000000	-.0879	-.0282	0.0000	0.0000
43	S	15.85	.36	.30	9.74	6.24	-1.83	1.22	-.01323	-.00375	0.000000	0.000000	-.0982	-.0282	0.0000	0.0000
44	S	16.21	.37	.30	10.83	5.40	-1.99	1.08	-.01461	-.00375	0.000000	0.000000	-.1085	-.0282	0.0000	0.0000
45	S	16.58	.37	.31	12.35	4.66	-2.15	.93	-.01599	-.00375	0.000000	0.000000	-.1188	-.0282	0.0000	0.0000
46	S	16.95	.38	.33	14.98	4.03	-2.30	.78	-.01737	-.00375	0.000000	0.000000	-.1292	-.0282	0.0000	0.0000
47	S	17.32	.38	.34	16.73	3.51	-2.46	.64	-.01874	-.00375	0.000000	0.000000	-.1395	-.0282	0.0000	0.0000
48	QF3	17.72	.39	.36	17.83	3.24	-.15	-.04	-.01975	-.00101	0.000000	0.000000	-.1474	-.0085	0.0000	0.0000
49	QF3	18.14	.39	.38	16.97	3.44	2.19	-.95	-.01964	.00163	0.000000	0.000000	-.1469	-.0117	0.0000	0.0000

POS		S (M)	QX	QY	BX (M)	BY (M)	AX	AY	EX (M)	EXP	EY (M)	EYP	XCO (MM)	DXCO (MR)	YCO (MM)	DYCO (MR)
50	Z	18.50	.39	.40	15.44	3.89	2.06	-.68	-.01905	.00163	0.000000	0.000000	.1423	-.0117	0.0000	0.0000
51	Z	18.86	.40	.41	13.99	4.43	1.94	-.82	-.01847	.00163	0.000000	0.000000	.1381	-.0117	0.0000	0.0000
52	Z	19.22	.40	.42	12.64	5.07	1.82	-.96	-.01788	.00163	0.000000	0.000000	.1339	-.0117	0.0000	0.0000
53	Z	19.58	.41	.43	11.37	5.81	1.70	-1.09	-.01729	.00163	0.000000	0.000000	.1297	-.0117	0.0000	0.0000
54	Z	19.95	.41	.44	10.19	6.64	1.57	-1.23	-.01670	.00163	0.000000	0.000000	.1255	-.0117	0.0000	0.0000
55	Z	20.31	.42	.45	9.10	7.58	1.45	-1.36	-.01612	.00163	0.000000	0.000000	.1213	-.0117	0.0000	0.0000
56	Z	20.67	.42	.46	8.10	8.61	1.33	-1.50	-.01553	.00163	0.000000	0.000000	.1171	-.0117	0.0000	0.0000
57	Z	21.03	.43	.47	7.19	9.74	1.20	-1.64	-.01494	.00163	0.000000	0.000000	.1129	-.0117	0.0000	0.0000
58	Z	21.39	.44	.47	6.36	10.97	1.08	-1.77	-.01436	.00163	0.000000	0.000000	.1087	-.0117	0.0000	0.0000
59	Z	21.75	.45	.48	5.63	12.30	.96	-1.91	-.01377	.00163	0.000000	0.000000	.1045	-.0117	0.0000	0.0000
60	QD3	22.16	.46	.48	3.19	13.20	-.13	-.23	-.01846	-.00023	0.000000	0.000000	.1026	.0025	0.0000	0.0000
61	QD3	22.58	.47	.49	5.51	12.67	-.68	1.50	-.01696	-.00211	0.000000	0.000000	.1065	.0166	0.0000	0.0000
62	R	22.94	.48	.49	[illegible]	11.60	-.78	1.40	-.01574	-.00211	0.000000	0.000000	.1126	.0166	0.0000	0.0000
63	R	23.31	.49	.50	6.55	10.61	-.88	1.31	-.01551	-.00211	0.000000	0.000000	.1187	.0166	0.0000	0.0000
64	R	23.68	.50	.50	7.23	9.68	-.98	1.21	-.01629	-.00211	0.000000	0.000000	.1248	.0166	0.0000	0.0000
65	R	24.04	.51	.51	7.99	8.83	-1.08	1.12	-.01706	-.00211	0.000000	0.000000	.1308	.0166	0.0000	0.0000
66	R	24.41	.52	.52	8.81	8.04	-1.17	1.03	-.01784	-.00211	0.000000	0.000000	.1369	.0166	0.0000	0.0000
67	R	24.78	.52	.52	9.71	7.34	-1.27	.93	-.01861	-.00211	0.000000	0.000000	.1430	.0166	0.0000	0.0000
68	R	25.14	.53	.53	10.68	6.67	-1.37	.84	-.01939	-.00211	0.000000	0.000000	.1491	.0166	0.0000	0.0000
69	R	25.51	.53	.54	11.72	6.09	-1.47	.78	-.02016	-.00211	0.000000	0.000000	.1552	.0166	0.0000	0.0000
70	R	25.88	.54	.55	12.84	5.58	-1.57	.65	-.02094	-.00211	0.000000	0.000000	.1613	.0166	0.0000	0.0000
71	R	26.24	.54	.56	14.03	5.13	-1.67	.56	-.02171	-.00211	0.000000	0.000000	.1674	.0166	0.0000	0.0000
72	QF	26.59	.55	.57	14.62	4.98	-.01	-.12	-.02199	.00053	0.000000	0.000000	.1696	-.0037	0.0000	0.0000
73	QF	26.94	.55	.58	13.01	5.30	1.69	-.81	-.02185	.00316	0.000000	0.000000	.1648	-.0237	0.0000	0.0000
74	QD	27.98	.56	.61	10.81	7.33	1.40	-1.14	-.01807	.00316	0.000000	0.000000	.1402	-.0237	0.0000	0.0000
75	B	30.33	.60	.64	3.91	11.88	.95	-1.60	.00736	.09989	0.000000	0.000000	-1.1018	-1.4746	0.0000	0.0000
76	QD	30.68	.62	.65	3.24	13.52	.66	-1.91	.17076	.09989	0.000000	0.000000	-2.6287	-1.4746	0.0000	0.0000
77	QD	31.03	.63	.65	3.02	16.23	-.01	-.08	.20960	.12244	0.000000	0.000000	-3.2033	-1.8152	0.0000	0.0000
78	QD	31.38	.64	.66	5.26	15.63	-.69	1.75	.25720	.15011	0.000000	0.000000	-3.9099	-2.2305	0.0000	0.0000
79	QD	32.41	.67	.67	6.99	12.28	-.98	1.48	.41262	.15011	0.000000	0.000000	-6.2194	-2.2305	0.0000	0.0000
80	B	34.07	.70	.70	11.00	7.99	-1.44	1.09	.73136	.24089	0.000000	0.000000	-11.1178	-3.6818	0.0000	0.0000
81	D	34.81	.71	.71	13.27	6.53	-1.65	.89	.82291	.24089	0.000000	0.000000	-13.8255	-3.6818	0.0000	0.0000
82	SF	34.81	.71	.71	13.27	6.53	-1.68	.90	.82291	.24873	0.000000	0.000000	-13.8255	-3.6954	0.0000	0.0000
83	QS	35.11	.72	.72	14.30	6.02	-1.76	.82	.99753	.24873	0.000000	0.000000	-14.9341	-3.6954	0.0000	0.0000
84	QF	35.46	.72	.73	14.94	5.72	-.05	.05	1.06294	.12306	0.000000	0.000000	-15.9080	-1.8422	0.0000	0.0000
85	QF	35.81	.72	.74	14.37	5.95	1.67	-.71	1.08321	-.00783	0.000000	0.000000	-16.2166	.0880	0.0000	0.0000
86	QS	36.11	.73	.75	13.39	6.40	1.59	-.79	1.08086	-.00783	0.000000	0.000000	-16.1901	.0880	0.0000	0.0000
87	SF	36.11	.73	.75	13.39	6.40	1.59	-.77	1.08086	-.00532	0.000000	0.000000	-16.1901	.0693	0.0000	0.0000
88	D	36.95	.74	.76	11.28	7.67	1.37	-.96	1.07695	-.00532	0.000000	0.000000	-16.1392	.0693	0.0000	0.0000
89	LC	38.80	.76	.79	7.38	11.54	.95	-1.37	1.06812	-.00532	0.000000	0.000000	-16.0251	.0693	0.0000	0.0000
90	D	39.24	.78	.80	6.12	13.70	.76	-1.56	1.06421	-.00532	0.000000	0.000000	-15.9732	.0693	0.0000	0.0000
91	SD	39.24	.78	.80	6.12	13.70	.78	-1.60	1.06421	-.00903	0.000000	0.000000	-15.9732	.0969	0.0000	0.0000
92	QS	39.54	.79	.80	5.68	14.68	.70	-1.68	1.06150	-.00903	0.000000	0.000000	-15.9441	.0969	0.0000	0.0000
93	QD	39.89	.80	.81	3.84	15.27	-.02	.06	1.08052	.11792	0.000000	0.000000	-16.2386	-1.7822	0.0000	0.0000
94	QD	40.24	.81	.81	3.71	14.63	-.79	1.75	1.14474	.24980	0.000000	0.000000	-17.2020	-3.7347	0.0000	0.0000
95	QS	40.54	.82	.82	6.18	13.61	-.83	1.67	1.21968	.24980	0.000000	0.000000	-18.3224	-3.7347	0.0000	0.0000
96	SD	40.54	.82	.82	6.18	13.61	-.80	1.62	1.21968	.24492	0.000000	0.000000	-18.3224	-3.6984	0.0000	0.0000
97	D	41.28	.84	.82	7.50	11.37	-1.00	1.42	1.39980	.24492	0.000000	0.000000	-21.0423	-3.6984	0.0000	0.0000
98	LC	42.94	.86	.85	11.54	7.39	-1.44	.98	1.80646	.24492	0.000000	0.000000	-27.1831	-3.6984	0.0000	0.0000
99	D	43.67	.87	.87	13.80	6.09	-1.63	.78	1.98658	.24492	0.000000	0.000000	-29.9030	-3.6984	0.0000	0.0000

POS		S (M)	QX	QY	BX (M)	BY (M)	AX	AY	EX (M)	EXP	EY (M)	EYP	XCO (MM)	DXCO (MR)	YCO (MM)	DYCO (MR)
100	SF	43.67	.87	.87	13.80	6.09	-1.69	.81	1.98658	.25347	0.000000	0.000000	-29.9030	-3.7622	0.0000	0.0000
101	OS	43.97	.88	.88	14.84	5.63	-1.78	.73	2.06262	.25347	0.000000	0.000000	-31.0317	-3.7622	0.0000	0.0000
102	QF	44.32	.88	.89	15.47	5.37	.00	.00	2.10706	-.00086	0.000000	0.000000	-31.6522	.0066	0.0000	0.0000
103	QF	44.67	.88	.90	14.84	5.62	1.78	-.73	2.06262	-.25518	0.000000	0.000000	-31.0271	3.7752	0.0000	0.0000
104	OS	44.97	.89	.91	13.79	6.09	1.70	-.81	1.98568	-.25518	0.000000	0.000000	-29.8945	3.7752	0.0000	0.0000
105	SF	44.97	.89	.91	13.79	6.09	1.64	-.78	1.98548	-.24660	0.000000	0.000000	-29.8945	3.7114	0.0000	0.0000
106	O	45.71	.90	.93	11.52	7.38	1.44	-.98	1.80412	-.24660	0.000000	0.000000	-27.1650	3.7114	0.0000	0.0000
107	B	47.37	.93	.95	7.48	11.27	1.00	-1.36	1.57657	-.14982	0.000000	0.000000	-22.2222	2.2601	0.0000	0.0000
108	O	48.10	.94	.96	6.16	13.40	.80	-1.54	1.36628	-.14982	0.000000	0.000000	-20.5601	2.2601	0.0000	0.0000
109	SD	48.10	.94	.96	6.16	13.40	.82	-1.60	1.36628	-.15595	0.000000	0.000000	-20.5601	2.3059	0.0000	0.0000
110	OS	48.40	.95	.97	5.60	14.38	.73	-1.68	1.31980	-.15595	0.000000	0.000000	-19.8683	2.3059	0.0000	0.0000
111	QD	48.75	.96	.97	5.42	14.98	.03	.00	1.29209	-.00118	0.000000	0.000000	-19.4640	.0091	0.0000	0.0000
112	QD	49.10	.97	.98	5.64	14.38	-.69	1.69	1.31887	.15355	0.000000	0.000000	-19.8618	-2.2869	0.0000	0.0000
113	OS	49.40	.98	.98	6.08	13.39	-.77	1.61	1.36474	.15355	0.000000	0.000000	-20.5478	-2.2869	0.0000	0.0000
114	SD	49.40	.98	.98	6.08	13.39	-.74	1.55	1.36474	.14743	0.000000	0.000000	-20.5478	-2.2412	0.0000	0.0000
115	O	50.14	1.00	.99	7.31	11.25	-.93	1.36	1.47316	.14743	0.000000	0.000000	-22.1961	-2.2412	0.0000	0.0000
116	B	51.80	1.02	1.02	11.07	7.35	-1.35	.98	1.79686	.24421	0.000000	0.000000	-27.1016	-3.6925	0.0000	0.0000
117	O	52.54	1.04	1.03	13.19	6.05	-1.54	.78	1.97656	.24421	0.000000	0.000000	-29.8236	-3.6925	0.0000	0.0000
118	SF	52.54	1.04	1.03	13.19	6.05	-1.59	.81	1.97656	.25270	0.000000	0.000000	-29.8236	-3.7560	0.0000	0.0000
119	OS	52.83	1.04	1.04	14.21	5.59	-1.67	.73	2.05216	.25270	0.000000	0.000000	-30.9500	-3.7560	0.0000	0.0000
120	QF	53.18	1.04	1.05	14.76	5.34	.02	.00	2.09667	-.00037	0.000000	0.000000	-31.6100	.0030	0.0000	0.0000
121	QF	53.53	1.05	1.06	14.14	5.59	1.72	-.72	2.05201	-.25363	0.000000	0.000000	-30.9479	3.7619	0.0000	0.0000
122	OS	53.83	1.05	1.07	13.13	6.04	1.63	-.80	1.97599	-.25363	0.000000	0.000000	-29.8193	3.7619	0.0000	0.0000
123	SF	53.83	1.05	1.07	13.13	6.05	1.58	-.79	1.97598	-.24694	0.000000	0.000000	-29.8193	3.6986	0.0000	0.0000
124	O	54.57	1.06	1.09	10.96	7.33	1.38	-.97	1.79609	-.24694	0.000000	0.000000	-27.0994	3.6986	0.0000	0.0000
125	B	56.23	1.09	1.12	7.11	11.30	.96	-1.35	1.49098	-.14616	0.000000	0.000000	-22.1780	2.2471	0.0000	0.0000
126	O	56.96	1.11	1.13	5.87	13.32	.75	-1.54	1.36198	-.14616	0.000000	0.000000	-20.5236	2.2471	0.0000	0.0000
127	SD	56.96	1.11	1.13	5.87	13.32	.77	-1.60	1.36198	-.15426	0.000000	0.000000	-20.5236	2.2927	0.0000	0.0000
128	OS	57.26	1.12	1.13	5.43	14.30	.69	-1.68	1.31570	-.15426	0.000000	0.000000	-19.8376	2.2927	0.0000	0.0000
129	QD	57.61	1.13	1.14	5.19	14.90	-.00	-.00	1.28877	.00010	0.000000	0.000000	-19.4372	-.0005	0.0000	0.0000
130	QD	57.96	1.14	1.14	5.44	14.30	-.70	1.68	1.31277	.15446	0.000000	0.000000	-19.8380	-2.2937	0.0000	0.0000
131	OS	58.26	1.14	1.15	5.88	13.32	-.78	1.60	1.36210	.15446	0.000000	0.000000	-20.5261	-2.2937	0.0000	0.0000
132	SD	58.26	1.14	1.15	5.88	13.32	-.75	1.56	1.36210	.14836	0.000000	0.000000	-20.5261	-2.2481	0.0000	0.0000
133	O	59.00	1.15	1.15	7.13	11.20	-.95	1.35	1.47121	.14836	0.000000	0.000000	-22.1794	-2.2481	0.0000	0.0000
134	B	60.66	1.19	1.18	11.00	7.33	-1.39	.97	1.79644	.24514	0.000000	0.000000	-27.1024	-3.6994	0.0000	0.0000
135	O	61.39	1.20	1.20	13.19	6.05	-1.59	.78	1.97672	.24514	0.000000	0.000000	-29.8231	-3.6994	0.0000	0.0000
136	SF	61.39	1.20	1.20	13.19	6.05	-1.64	.80	1.97672	.25362	0.000000	0.000000	-29.8231	-3.7629	0.0000	0.0000
137	OS	61.69	1.21	1.21	14.20	5.59	-1.73	.72	2.05201	.25362	0.000000	0.000000	-30.9519	-3.7629	0.0000	0.0000
138	QF	62.04	1.21	1.22	14.82	5.34	-.03	-.00	2.09752	.00047	0.000000	0.000000	-31.6144	-.0033	0.0000	0.0000
139	QF	62.39	1.22	1.23	14.24	5.60	1.68	-.73	2.05316	-.25270	0.000000	0.000000	-30.9544	3.7560	0.0000	0.0000
140	OS	62.69	1.22	1.24	13.25	6.06	1.60	-.81	1.97733	-.25270	0.000000	0.000000	-29.8276	3.7560	0.0000	0.0000
141	SF	62.69	1.22	1.24	13.25	6.06	1.54	-.79	1.97733	-.24421	0.000000	0.000000	-29.8276	3.6925	0.0000	0.0000
142	O	63.43	1.23	1.25	11.13	7.36	1.35	-.98	1.79773	-.24421	0.000000	0.000000	-27.1120	3.6925	0.0000	0.0000
143	B	65.09	1.26	1.28	7.35	11.26	.93	-1.36	1.47503	-.14743	0.000000	0.000000	-22.2005	2.2412	0.0000	0.0000
144	O	65.82	1.28	1.29	6.11	13.40	.73	-1.55	1.36361	-.14743	0.000000	0.000000	-20.5523	2.2412	0.0000	0.0000
145	SD	65.82	1.28	1.29	6.11	13.40	.77	-1.61	1.36361	-.15356	0.000000	0.000000	-20.5523	2.2869	0.0000	0.0000
146	OS	66.12	1.28	1.30	5.67	14.39	.69	-1.69	1.31936	-.15356	0.000000	0.000000	-19.8662	2.2869	0.0000	0.0000
147	QD	66.47	1.29	1.30	5.44	14.99	-.03	-.00	1.29295	.00127	0.000000	0.000000	-19.4685	-.0098	0.0000	0.0000
148	QD	66.82	1.30	1.30	5.71	14.39	-.75	1.68	1.32044	.15616	0.000000	0.000000	-19.8731	-2.3069	0.0000	0.0000
149	OS	67.12	1.31	1.31	6.18	13.41	-.83	1.60	1.36729	.15616	0.000000	0.000000	-20.5632	-2.3069	0.0000	0.0000

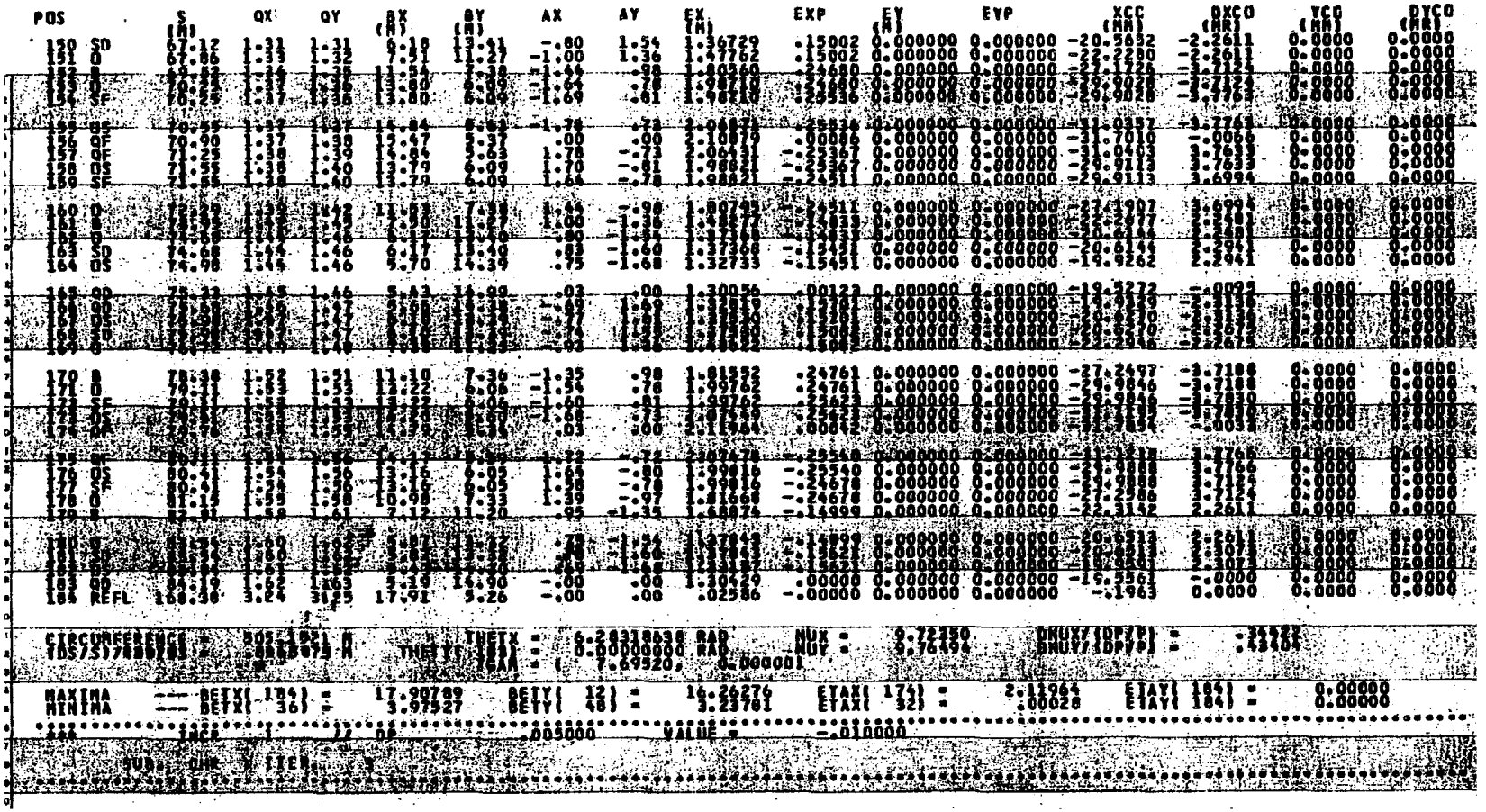

CALCULATION OF THE EQUILIBRIUM ORBIT AND BETATRON FUNCTIONS OF AGR .

INITIAL REFERENCE RAY DEFINED BY V

X = -.00018430 DX = 0.00000000 Y = 0.00000000 DY = 0.00000000 DS = 0.00000000 DP/P = -.01000000 1.00000000

7X7 MATRIX FOR AGR

.05067066	17.86977943	0.00000000	0.00000000	0.00000000	.01668046	.00008116
-.05581672	.05067066	0.00000000	0.00000000	0.00000000	.00098074	.00000477
0.00000000	0.00000000	-.03433320	5.41052687	0.00000000	0.00000000	0.00000000
0.00000000	0.00000000	-.18660702	-.03433320	0.00000000	0.00000000	0.00000000
-.00098074	-.01668046	0.00000000	0.00000000	1.00000000	-2.85536107	.02970060
0.00000000	0.00000000	0.00000000	0.00000000	0.00000000	1.00000000	0.00000000
0.00000000	0.00000000	0.00000000	0.00000000	0.00000000	0.00000000	1.00000000

EIGENVALUES OF THE 4X4 SUBMATRIX

X... LMD1 = (.05067066 .99871542); C(1) = 1.00000000; MU(1) = 1.52010396 RAD; Q(1) = .77179618
1/LMD1 = (.05567066 -.99871542); C(2) = 1.00000000; MU(2) = -1.52010396 RAD; Q(2) = .27420382

Y... LMD3 = (-.03433320 .99941044); C(3) = 1.00000000; MU(3) = 1.60513628 RAD; Q(3) = .76639612
1/LMD3 = (-.03433320 -.99941044); C(4) = 1.00000000; MU(4) = -1.60513628 RAD; Q(4) = .23360388

EIGENVALUE = (.05067066, .99871542), EIGENVECTOR = { 4.22998394, 0.00000000
0.00000000, -.23660752
0.00000000, 0.00000000
0.00000000, 0.00000000 }

EIGENVALUE = (.05067066, -.99871542), EIGENVECTOR = { 4.22998394, 0.00000000
0.00000000, -.23660752
0.00000000, 0.00000000
0.00000000, 0.00000000 }

EIGENVALUE = (-.03433320, .99941044), EIGENVECTOR = { 0.00000000, 0.00000000
0.00000000, 0.00000000
2.32673990, -.00000000
.00000000, .42978590 }

EIGENVALUE = (-.03433320, -.99941044), EIGENVECTOR = { 0.00000000, 0.00000000
0.00000000, 0.00000000
2.32673990, -.00000000
.00000000, -.42978590 }

	X	DX	Y	DY	DS	DP/P	
EQ ORBIT	-.00000590	0.00000000	0.00000000	0.00000000	0.00000000	-.01000000	1.00000000
ETA ORBIT	.01797078	.00000000	0.00000000	0.00000000	0.00000000	1.00000000	0.00000000

EIGENVECTORS 1 AND 3 IN POLAR COORDINATES

POS	X1 X3			DX1 DX3		Y1 Y3		DY1 DY3	
0	4.229986 0.000000	0.000000 0.000000	-.236405 0.000000	1.570796 0.000000	0.000000 2.324740	0.000000 -.000000	0.000000 .429786	0.000000 1.570796	

BETATRON FUNCTIONS OF AGR

POS	S (M)	QX	QY	BX (M)	BY (M)	AX	AY	EX (M)	EXP	EY (M)	EYP	XCO (MM)	DXCO (MR)	YCO (MM)	DYCO (MR)
0	0.00	0.00	0.00	17.89	5.41	0.00	0.00	.01757	.00000	0.000000	0.000000	-.0859	0.0000	0.0000	0.0000
1 QF1	.35	.00	.01	17.07	5.69	2.30	-.81	.01716	-.00234	0.000000	0.000000	-.0639	.0114	0.0000	0.0000
2 S	[illegible]	.01	.02	[illegible]	[illegible]	2.16	-.92	.01629	-.00234	0.000000	0.000000	-.0796	.0114	0.0000	0.0000
3 S	1.10	.01	.03	[illegible]	7.07	2.02	-1.03	.01551	-.00234	0.000000	0.000000	-.0754	.0114	0.0000	0.0000
4 S	1.47	.02	.04	[illegible]	7.88	1.89	-1.14	.01456	-.00234	0.000000	0.000000	-.0711	.0114	0.0000	0.0000
5 S	1.84	.02	.04	11.03	8.77	1.75	-1.25	.01366	-.00234	0.000000	0.000000	-.0669	.0114	0.0000	0.0000
6 S	2.22	.03	.05	9.78	9.74	1.61	-1.36	.01279	-.00234	0.000000	0.000000	-.0626	.0114	0.0000	0.0000
7 S	2.59	.03	.06	8.63	10.80	1.47	-1.47	.01192	-.00234	0.000000	0.000000	-.0584	.0114	0.0000	0.0000
8 S	2.96	.04	.06	7.58	11.93	1.36	-1.58	.01106	-.00234	0.000000	0.000000	-.0541	.0114	0.0000	0.0000
9 S	3.34	.05	.07	6.61	13.15	1.20	-1.68	.01017	-.00234	0.000000	0.000000	-.0499	.0114	0.0000	0.0000
10 S	3.71	.06	.07	[illegible]	14.45	1.06	-1.79	.00930	-.00234	0.000000	0.000000	-.0456	.0114	0.0000	0.0000
11 S	4.08	.07	.07	[illegible]	[illegible]	.93	-1.90	.00842	-.00234	0.000000	0.000000	[illegible]	.0114	0.0000	0.0000
12 QD1	4.43	.08	.08	4.65	16.48	.24	.05	.00778	-.00134	0.000000	0.000000	-.0383	.0065	0.0000	0.0000
13 QD1	4.78	.09	.08	4.71	15.76	-.41	1.99	.00747	-.00041	0.000000	0.000000	-.0368	.0019	0.0000	0.0000
14 S	5.16	.10	.09	5.05	14.31	-.51	1.88	.00732	-.00041	0.000000	0.000000	-.0361	.0019	0.0000	0.0000
15 S	[illegible]	.12	.09	[illegible]	12.96	-.60	1.76	.00717	-.00041	0.000000	0.000000	-.0354	.0019	0.0000	0.0000
16 S	[illegible]	[illegible]	.09	[illegible]	[illegible]	-.69	1.64	.00702	-.00041	0.000000	0.000000	-.0347	.0019	0.0000	0.0000
17 S	[illegible]	[illegible]	.10	[illegible]	[illegible]	-.78	1.52	[illegible]	-.00041	0.000000	0.000000	-.0339	.0019	0.0000	0.0000
18 S	[illegible]	[illegible]	.11	[illegible]	[illegible]	-.88	1.40	[illegible]	-.00041	0.000000	0.000000	-.0332	.0019	0.0000	0.0000
19 S	7.02	.15	.11	7.80	8.41	-.97	1.29	.00657	-.00041	0.000000	0.000000	-.0325	.0019	0.0000	0.0000
20 S	7.39	.16	.12	8.56	7.50	-1.06	1.17	.00641	-.00041	0.000000	0.000000	-.0318	.0019	0.0000	0.0000
21 S	7.77	.17	.13	9.39	6.67	-1.16	1.05	.00626	-.00041	0.000000	0.000000	-.0311	.0019	0.0000	0.0000
22 S	[illegible]	.17	.14	[illegible]	[illegible]	-1.25	.93	.00611	-.00041	0.000000	0.000000	-.0304	.0019	0.0000	0.0000
23 S	[illegible]	.18	.15	[illegible]	[illegible]	-1.34	.82	.00596	-.00041	0.000000	0.000000	-.0296	.0019	0.0000	0.0000
24 QF2	[illegible]	.18	.16	[illegible]	4.84	[illegible]	.00	.00569	-.00119	0.000000	0.000000	-.0283	.0056	0.0000	0.0000
25 QF2	9.22	.19	.17	11.15	5.15	1.49	-.63	.00516	-.00185	0.000000	0.000000	-.0257	.0091	0.0000	0.0000
26 S	9.59	.19	.18	10.08	5.66	1.38	-.73	.00447	-.00185	0.000000	0.000000	-.0224	.0091	0.0000	0.0000
27 S	9.96	.20	.19	9.09	6.24	1.27	-.83	.00378	-.00185	0.000000	0.000000	-.0190	.0091	0.0000	0.0000
28 S	10.33	.21	.20	8.18	6.90	1.16	-.93	.00309	-.00185	0.000000	0.000000	-.0156	.0091	0.0000	0.0000
29 S	10.71	.21	.21	7.35	7.64	1.06	-1.03	.00240	-.00185	0.000000	0.000000	-.0122	.0091	0.0000	0.0000
30 S	11.08	.22	.22	6.60	[illegible]	.95	-1.14	.00171	-.00185	0.000000	0.000000	-.0088	.0091	0.0000	0.0000
31 S	[illegible]	.23	[illegible]	[illegible]	[illegible]	.84	-1.24	.00102	-.00185	0.000000	0.000000	-.0055	.0091	0.0000	0.0000
32 S	11.83	.24	.23	5.35	10.29	.73	-1.34	.00033	-.00185	0.000000	0.000000	-.0021	.0091	0.0000	0.0000
33 S	12.20	.25	.23	4.86	11.33	.63	-1.44	-.00035	-.00185	0.000000	0.000000	.0013	.0091	0.0000	0.0000
34 S	12.57	.27	.24	4.41	12.44	.52	-1.54	-.00104	-.00185	0.000000	0.000000	.0047	.0091	0.0000	0.0000
35 S	[illegible]	.28	[illegible]	4.06	13.61	.41	-1.64	-.00173	-.00185	0.000000	0.000000	.0081	.0091	0.0000	0.0000
36 QD2	13.30	.30	[illegible]	4.00	[illegible]	[illegible]	.23	-.00243	-.00213	0.000000	0.000000	.0115	.0104	0.0000	0.0000
37 QD2	[illegible]	[illegible]	[illegible]	4.50	[illegible]	-.91	2.06	-.00324	-.00252	0.000000	0.000000	.0154	.0122	0.0000	0.0000
38 R	[illegible]	.32	[illegible]	[illegible]	[illegible]	-1.06	1.91	-.00416	-.00252	0.000000	0.000000	.0199	.0122	0.0000	0.0000
39 R	14.38	.33	.26	5.93	10.51	-1.21	1.77	-.00509	-.00252	0.000000	0.000000	.0244	.0122	0.0000	0.0000
40 R	14.75	.34	.27	6.90	9.27	-1.37	1.62	-.00601	-.00252	0.000000	0.000000	.0289	.0122	0.0000	0.0000
41 R	[illegible]	[illegible]	.27	7.96	8.13	-1.52	1.48	-.00694	-.00252	0.000000	0.000000	.0333	.0122	0.0000	0.0000
42 R	[illegible]	[illegible]	.28	[illegible]	7.10	-1.67	1.34	-.00786	-.00252	0.000000	0.000000	.0378	.0122	0.0000	0.0000
43 R	[illegible]	.36	.29	10.41	6.17	-1.82	1.19	-.00878	-.00252	0.000000	0.000000	.0423	.0122	0.0000	0.0000
44 R	[illegible]	[illegible]	.30	11.80	5.35	-1.98	1.05	-.00971	-.00252	0.000000	0.000000	.0468	.0122	0.0000	0.0000
45 R	16.58	.37	.31	13.31	4.63	-2.13	.90	-.01063	-.00252	0.000000	0.000000	.0513	.0122	0.0000	0.0000
46 R	16.95	.38	.33	14.93	4.02	-2.28	.76	-.01156	-.00252	0.000000	0.000000	.0558	.0122	0.0000	0.0000
47 R	17.32	.38	.34	16.66	3.52	-2.43	.62	-.01248	-.00252	0.000000	0.000000	.0602	.0122	0.0000	0.0000
48 QF3	17.73	.38	.36	17.75	3.26	-.15	.02	-.01316	-.00076	0.000000	0.000000	.0636	.0038	0.0000	0.0000
49 QF3	18.14	.39	.38	16.90	3.48	2.16	-.57	-.01311	.00104	0.000000	0.000000	.0633	-.0049	0.0000	0.0000

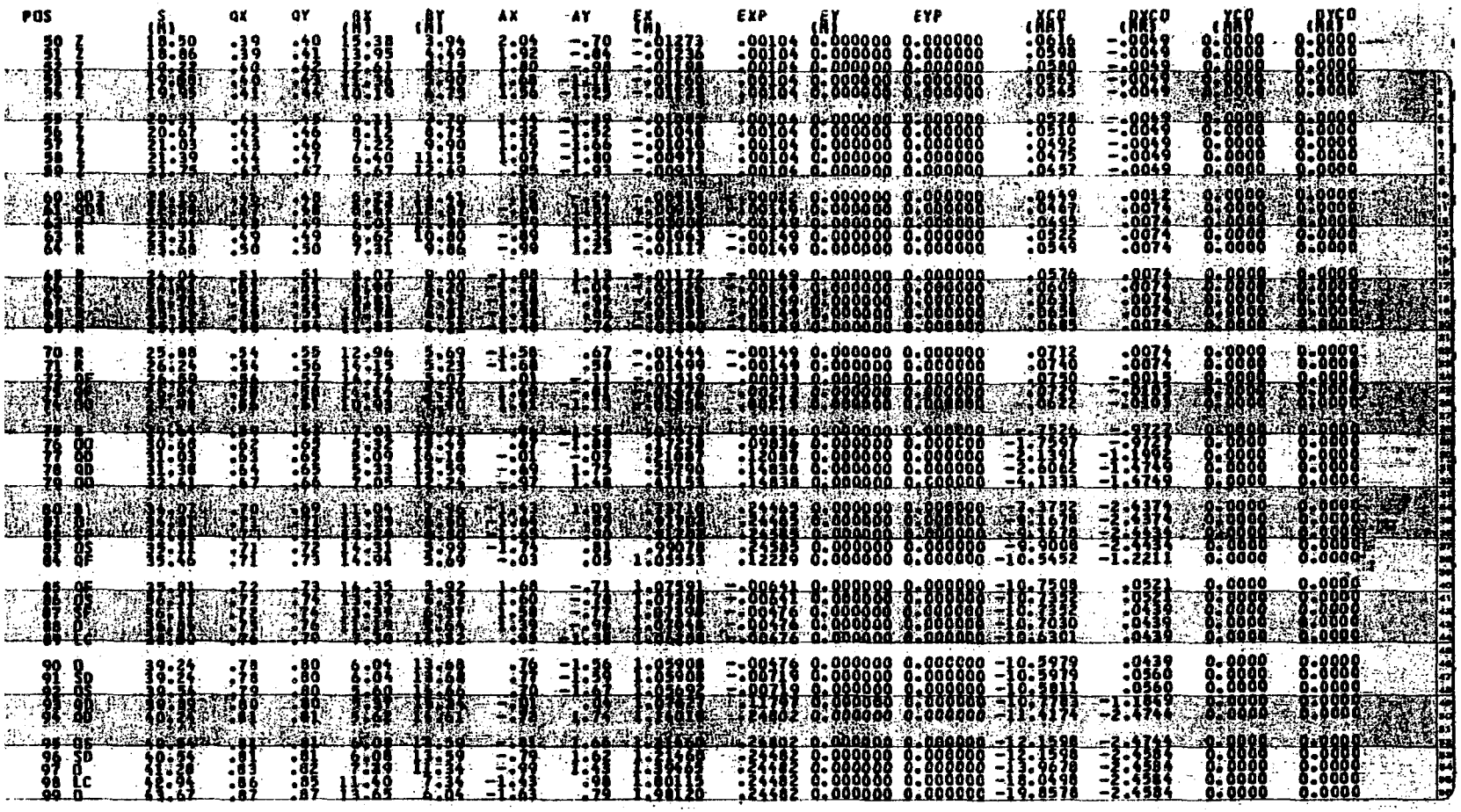

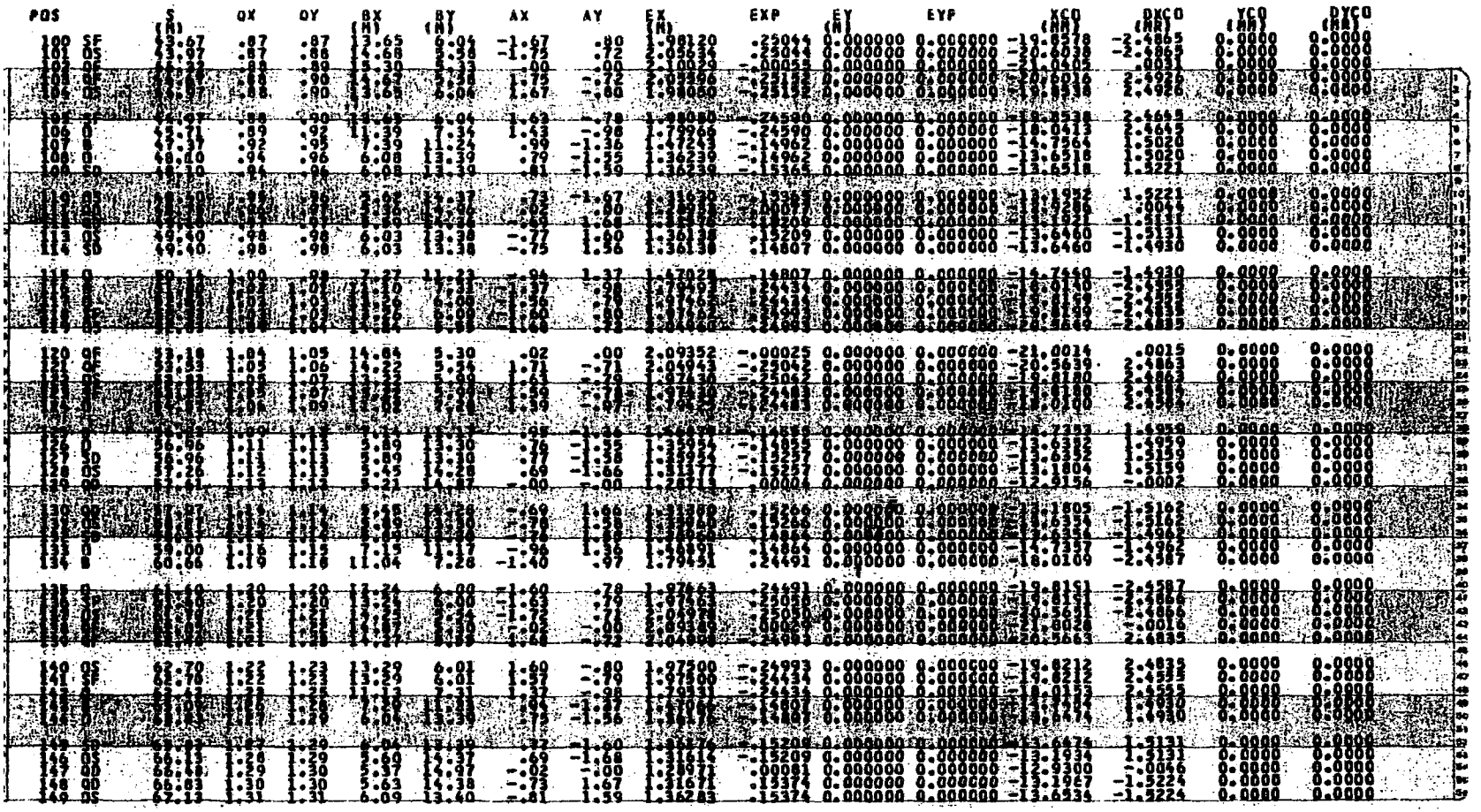

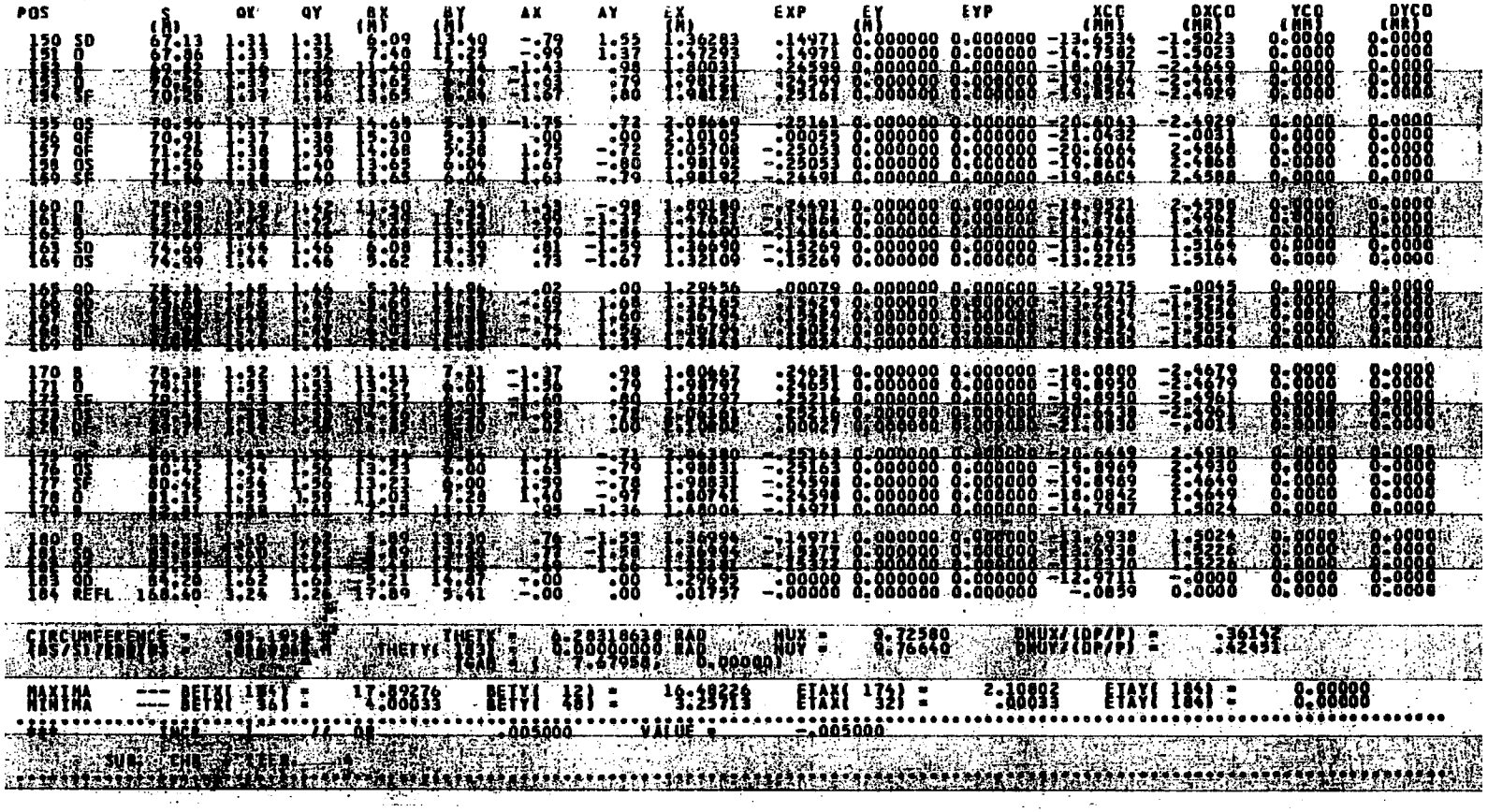

CALCULATION OF THE EQUILIBRIUM ORBIT AND BETATRON FUNCTIONS OF AGR .
INITIAL REFERENCE RAY DEFINED BY V

X_2 = -.00008500 DX = 0.00000000 Y = 0.00000000 DY = 0.00000000 DS = 0.00000000 DP/P = -.00500000 1.00000000

7X7 MATRIX FOR AGR

.04612244	17.84869784	0.00000000	0.00000000	0.00000000	.00822691	.00002195
-.05590731	.04612244	0.00000000	0.00000000	0.00000000	.00048218	.00000129
0.00000000	0.00000000	-.03787803	5.56903798	0.00000000	0.00000000	0.00000000
0.00000000	0.00000000	-.17930660	-.03787803	0.00000000	0.00000000	0.00000000
-.00049218	-.00822691	0.00000000	0.00000000	1.00000000	-2.86731298	.01462072
0.00000000	0.00000000	0.00000000	0.00000000	0.00000000	1.00000000	0.00000000
0.00000000	0.00000000	0.00000000	0.00000000	0.00000000	0.00000000	1.00000000

EIGENVALUES OF THE 4X4 SUBMATRIX

X... LMD1 = (.04612244 .77893579); C(1) = 1.00000000, MU(1) = 1.52465752 RAD, Q(1) = .72797034
1/LMD1 = (.04612244 -.99893579); C(2) = 1.00000000, MU(2) = -1.52465752 RAD, Q(2) = .27202966

Y... LMD3 = (-.03787803 .99928237); C(3) = 1.00000000, MU(3) = 1.60868342 RAD, Q(3) = .76808976
1/LMD3 = (-.03787803 -.99928237); C(4) = 1.00000000, MU(4) = -1.60868342 RAD, Q(4) = .23191024

EIGENVALUE = (.04612244, .99893579), EIGENVECTOR = (4.22702174, -.00000000)
(0.00000000, -.23657319)
(0.00000000, 0.00000000)
(0.00000000, 0.00000000)

EIGENVALUE = (.04612244, -.99893579), EIGENVECTOR = (4.22702174, .00000000)
(0.00000000, -.23657319)
(0.00000000, 0.00000000)
(0.00000000, 0.00000000)

EIGENVALUE = (-.03787803, .99928237), EIGENVECTOR = (0.00000000, 0.00000000)
(0.00000000, 0.00000000)
(2.36072814, 0.00000000)
(-.00000000, .42359812)

EIGENVALUE = (-.03787803, -.99928237), EIGENVECTOR = (0.00000000, 0.00000000)
(0.00000000, 0.00000000)
(2.36072814, 0.00000000)
(-.00000000, -.42359812)

	X	DX	Y	DY	DS	DP/P	
EQ ORBIT	-.00001959	0.00000000	0.00000000	0.00000000	0.00000000	-.00500000	1.00000000
ETA ORBIT	.00862470	.00000000	0.00000000	0.00000000	0.00000000	1.00000000	0.00000000

EIGENVECTORS 1 AND 3 IN POLAR COORDINATES

POS	X1 X3		DX1 DX3		Y1 Y3		DY1 DY3	
0	4.227022 0.000000	-.000000 0.000000	.236573 0.000000	1.570796 0.000000	0.000000 2.360728	0.000000 0.000000	0.000000 .423598	0.000000 1.570796

BETATRON FUNCTIONS OF AGR

POS		S (M)	DX	QY	BX (M)	BY (M)	AX	AY	EX (M)	EXP	EY (M)	EYP	XCO (MM)	DXCO (MR)	YCO (MM)	DYCO (MR)
0		0.00	0.00	0.00	17.87	5.57	0.00	0.00	.00862	.00000	0.000000	0.000000	-.0156	0.0000	0.0000	0.0000
1	QF1	.35	.00	.01	17.05	5.86	2.28	-.83	.00862	-.00114	0.000000	0.000000	-.0151	.0026	0.0000	0.0000
2	S	.72	.01	.02	15.40	6.52	2.15	-.94	.00800	-.00114	0.000000	0.000000	-.0142	.0026	0.0000	0.0000
3	S	1.10	.01	.03	13.85	7.26	2.01	-1.04	.00757	-.00114	0.000000	0.000000	-.0132	.0026	0.0000	0.0000
4	S	1.47	.02	.04	12.40	8.08	1.88	-1.15	.00715	-.00114	0.000000	0.000000	-.0122	.0026	0.0000	0.0000
5	S	1.84	.02	.04	11.05	8.98	1.74	-1.26	.00672	-.00114	0.000000	0.000000	-.0113	.0026	0.0000	0.0000
6	S	2.22	.03	.05	9.80	9.96	1.60	-1.37	.00630	-.00114	0.000000	0.000000	-.0103	.0026	0.0000	0.0000
7	S	2.59	.03	.05	8.66	11.02	1.47	-1.47	.00587	-.00114	0.000000	0.000000	-.0093	.0026	0.0000	0.0000
8	S	2.96	.04	.06	7.61	12.16	1.33	-1.58	.00545	-.00114	0.000000	0.000000	-.0084	.0026	0.0000	0.0000
9	S	3.34	.05	.06	6.67	13.38	1.20	-1.69	.00502	-.00114	0.000000	0.000000	-.0074	.0026	0.0000	0.0000
10	S	3.71	.06	.07	5.83	14.68	1.06	-1.80	.00459	-.00114	0.000000	0.000000	-.0065	.0026	0.0000	0.0000
11	S	4.08	.07	.07	5.09	16.06	.92	-1.90	.00417	-.00114	0.000000	0.000000	-.0055	.0026	0.0000	0.0000
12	QD1	4.53	.08	.08	4.69	16.71	.23	.07	.00386	-.00065	0.000000	0.000000	-.0048	.0015	0.0000	0.0000
13	QD1	4.78	.09	.08	4.75	12.97	-.42	2.03	.00371	-.00019	0.000000	0.000000	-.0045	.0004	0.0000	0.0000
14	S	5.16	.10	.08	5.10	14.50	-.51	1.91	.00364	-.00019	0.000000	0.000000	-.0043	.0004	0.0000	0.0000
15	S	5.53	.12	.09	5.51	13.12	-.60	1.79	.00357	-.00019	0.000000	0.000000	-.0041	.0004	0.0000	0.0000
16	S	5.90	.13	.09	5.99	11.83	-.69	1.67	.00350	-.00019	0.000000	0.000000	-.0040	.0004	0.0000	0.0000
17	S	6.28	.14	.10	6.54	10.63	-.79	1.55	.00343	-.00019	0.000000	0.000000	-.0038	.0004	0.0000	0.0000
18	S	6.65	.14	.10	7.17	9.52	-.88	1.43	.00336	-.00019	0.000000	0.000000	-.0037	.0004	0.0000	0.0000
19	S	7.02	.15	.11	7.86	8.50	-.97	1.31	.00329	-.00019	0.000000	0.000000	-.0075	.0004	0.0000	0.0000
20	S	7.39	.16	.12	8.62	7.56	-1.06	1.19	.00322	-.00019	0.000000	0.000000	-.0073	.0004	0.0000	0.0000
21	S	7.77	.17	.13	9.45	6.72	-1.16	1.07	.00315	-.00019	0.000000	0.000000	-.0072	.0004	0.0000	0.0000
22	S	8.14	.17	.14	10.34	5.96	-1.25	.95	.00308	-.00019	0.000000	0.000000	-.0070	.0004	0.0000	0.0000
23	S	8.51	.18	.15	11.31	5.30	-1.34	.83	.00301	-.00019	0.000000	0.000000	-.0069	.0004	0.0000	0.0000
24	QF2	8.86	.18	.16	11.76	4.97	-.08	.10	.00287	-.00036	0.000000	0.000000	-.0066	.0013	0.0000	0.0000
25	QF2	9.22	.19	.17	11.20	5.15	1.49	-.61	.00261	-.00091	0.000000	0.000000	-.0060	.0021	0.0000	0.0000
26	S	9.59	.19	.18	10.13	5.44	1.38	-.71	.00227	-.00091	0.000000	0.000000	-.0052	.0021	0.0000	0.0000
27	S	9.96	.20	.19	9.14	6.20	1.27	-.81	.00193	-.00091	0.000000	0.000000	-.0044	.0021	0.0000	0.0000
28	S	10.33	.21	.20	8.22	6.84	1.17	-.91	.00159	-.00091	0.000000	0.000000	-.0037	.0021	0.0000	0.0000
29	S	10.71	.21	.21	7.40	7.56	1.06	-1.01	.00125	-.00091	0.000000	0.000000	-.0029	.0021	0.0000	0.0000
30	S	11.08	.22	.21	6.65	8.34	.95	-1.10	.00091	-.00091	0.000000	0.000000	-.0021	.0021	0.0000	0.0000
31	S	11.45	.23	.22	6.08	9.21	.84	-1.20	.00057	-.00091	0.000000	0.000000	-.0014	.0021	0.0000	0.0000
32	S	11.83	.24	.23	5.39	10.16	.74	-1.30	.00023	-.00091	0.000000	0.000000	-.0006	.0021	0.0000	0.0000
33	S	12.20	.25	.23	4.88	11.15	.63	-1.40	-.00011	-.00091	0.000000	0.000000	.0002	.0021	0.0000	0.0000
34	S	12.57	.27	.24	4.49	12.23	.52	-1.50	-.00045	-.00091	0.000000	0.000000	.0010	.0021	0.0000	0.0000
35	S	12.95	.28	.24	4.10	13.39	.42	-1.60	-.00079	-.00091	0.000000	0.000000	.0017	.0021	0.0000	0.0000
36	QD2	13.30	.29	.25	4.03	13.88	-.22	.23	-.00113	-.00104	0.000000	0.000000	.0025	.0024	0.0000	0.0000
37	QD2	13.65	.31	.25	4.42	13.09	-.90	2.01	-.00152	-.00122	0.000000	0.000000	.0034	.0028	0.0000	0.0000
38	R	14.01	.32	.26	5.21	11.46	-1.06	1.87	-.00197	-.00122	0.000000	0.000000	.0044	.0028	0.0000	0.0000
39	R	14.38	.33	.26	5.97	10.34	-1.21	1.73	-.00242	-.00122	0.000000	0.000000	.0054	.0028	0.0000	0.0000
40	R	14.73	.34	.27	6.91	9.13	-1.36	1.59	-.00287	-.00122	0.000000	0.000000	.0065	.0028	0.0000	0.0000
41	R	15.11	.35	.27	7.96	8.01	-1.51	1.45	-.00331	-.00122	0.000000	0.000000	.0075	.0028	0.0000	0.0000
42	R	15.48	.36	.28	9.16	7.01	-1.66	1.30	-.00376	-.00122	0.000000	0.000000	.0085	.0028	0.0000	0.0000
43	R	15.85	.36	.28	10.47	6.10	-1.81	1.16	-.00421	-.00122	0.000000	0.000000	.0095	.0028	0.0000	0.0000
44	R	16.21	.36	.30	11.77	5.30	-1.96	1.02	-.00466	-.00122	0.000000	0.000000	.0105	.0028	0.0000	0.0000
45	R	16.58	.37	.31	13.27	4.60	-2.11	.88	-.00511	-.00122	0.000000	0.000000	.0115	.0028	0.0000	0.0000
46	R	16.95	.37	.33	14.87	4.01	-2.26	.74	-.00555	-.00122	0.000000	0.000000	.0125	.0028	0.0000	0.0000
47	R	17.32	.38	.34	16.59	3.52	-2.41	.60	-.00600	-.00122	0.000000	0.000000	.0135	.0028	0.0000	0.0000
48	QF3	17.73	.38	.36	17.47	3.27	-.15	.01	-.00636	-.00038	0.000000	0.000000	.0143	.0009	0.0000	0.0000
49	QF3	18.14	.39	.38	16.83	3.51	2.14	-.56	-.00632	.00046	0.000000	0.000000	.0143	-.0011	0.0000	0.0000

POS		S (M)	QX	QY	BX (M)	BY (M)	AX	AY	EX (M)	EXP	EY (M)	EYP	XCC (M)	DXCO (MM)	YCO (MM)	DYCO (MM)
50	Z	18.50	.33	.40	15.33	3.98	2.02	-.72	-.00614	.00048	0.000000	0.000000	.0139	-.0011	0.0000	0.0000
51	Z	18.86	.39	.41	13.92	4.55	1.90	-.86	-.00597	.00048	0.000000	0.000000	.0135	-.0011	0.0000	0.0000
52	Z	19.22	.40	.42	12.59	5.22	1.78	-1.00	-.00580	.00048	0.000000	0.000000	.0131	-.0011	0.0000	0.0000
53	Z	19.58	.40	.43	11.35	5.99	1.66	-1.14	-.00562	.00048	0.000000	0.000000	.0127	-.0011	0.0000	0.0000
54	Z	19.95	.41	.44	10.19	6.86	1.54	-1.27	-.00545	.00048	0.000000	0.000000	.0123	-.0011	0.0000	0.0000
55	Z	20.31	.41	.45	9.12	7.82	1.42	-1.41	-.00528	.00048	0.000000	0.000000	.0120	-.0011	0.0000	0.0000
56	Z	20.67	.42	.46	8.14	8.89	1.30	-1.55	-.00511	.00048	0.000000	0.000000	.0116	-.0011	0.0000	0.0000
57	Z	21.03	.43	.46	7.24	10.05	1.18	-1.69	-.00493	.00048	0.000000	0.000000	.0112	-.0011	0.0000	0.0000
58	Z	21.39	.44	.47	6.43	11.32	1.07	-1.82	-.00476	.00048	0.000000	0.000000	.0108	-.0011	0.0000	0.0000
59	Z	21.75	.44	.47	5.70	12.68	.95	-1.96	-.00459	.00048	0.000000	0.000000	.0104	-.0011	0.0000	0.0000
60	QQ3	22.16	.46	.48	5.28	13.62	-.11	-.25	-.00482	-.00013	0.000000	0.000000	.0103	.0003	0.0000	0.0000
61	QQ3	22.58	.47	.48	5.51	13.08	-.70	1.42	-.00470	-.00075	0.000000	0.000000	.0107	.0017	0.0000	0.0000
62	R	22.94	.48	.49	6.06	12.99	-.80	1.43	-.00498	-.00075	0.000000	0.000000	.0113	.0017	0.0000	0.0000
63	R	23.31	.49	.49	6.68	12.99	-.90	1.33	-.00525	-.00075	0.000000	0.000000	.0119	.0017	0.0000	0.0000
64	R	23.68	.50	.50	7.38	13.04	-.99	1.24	-.00553	-.00075	0.000000	0.000000	.0126	.0017	0.0000	0.0000
65	R	24.04	.50	.50	8.14	13.12	-1.09	1.15	-.00580	-.00075	0.000000	0.000000	.0132	.0017	0.0000	0.0000
66	R	24.41	.51	.51	8.98	13.36	-1.19	1.06	-.00608	-.00075	0.000000	0.000000	.0139	.0017	0.0000	0.0000
67	R	24.78	.52	.52	9.89	13.62	-1.29	.96	-.00636	-.00075	0.000000	0.000000	.0145	.0017	0.0000	0.0000
68	R	25.14	.52	.52	10.88	14.03	-1.39	.87	-.00663	-.00075	0.000000	0.000000	.0151	.0017	0.0000	0.0000
69	R	25.51	.53	.53	11.93	14.56	-1.49	.78	-.00691	-.00075	0.000000	0.000000	.0158	.0017	0.0000	0.0000
70	R	25.88	.53	.54	13.06	15.21	-1.59	.68	-.00719	-.00075	0.000000	0.000000	.0164	.0017	0.0000	0.0000
71	R	26.24	.54	.55	14.26	15.96	-1.69	.59	-.00746	-.00075	0.000000	0.000000	.0170	.0017	0.0000	0.0000
72	QE	26.59	.54	.56	14.86	16.17	-.00	-.10	-.00757	-.00014	0.000000	0.000000	.0173	-.0003	0.0000	0.0000
73	QF	26.94	.55	.57	15.26	16.39	1.69	-.81	-.00737	.00103	0.000000	0.000000	.0168	-.0023	0.0000	0.0000
74	QQ	27.28	.56	.60	15.64	17.48	1.41	-1.12	-.00630	.00103	0.000000	0.000000	.0144	-.0023	0.0000	0.0000
75	R	29.64	.59	.62	7.10	11.96	-.96	-1.56	.07429	.09679	0.000000	0.000000	-.3863	-.4811	0.0000	0.0000
76	QQ	30.69	.61	.64	5.40	15.13	-.68	-1.86	.17500	.09679	0.000000	0.000000	-.8845	-.4811	0.0000	0.0000
77	QQ	31.03	.61	.64	5.17	16.37	-.00	-.96	.21277	.11931	0.000000	0.000000	-1.0725	-.5962	0.0000	0.0000
78	QQ	31.38	.62	.63	5.40	15.37	-.69	1.75	.23922	.14673	0.000000	0.000000	-1.2039	-.7316	0.0000	0.0000
79	QQ	32.41	.64	.66	7.12	12.22	-.97	1.48	.41114	.14673	0.000000	0.000000	-2.0614	-.7316	0.0000	0.0000
80	R	34.07	.69	.69	11.09	7.93	-1.42	1.09	.73368	.24250	0.000000	0.000000	-3.6708	-1.2104	0.0000	0.0000
81	Q	34.81	.70	.70	13.33	6.48	-1.62	.89	.91202	.24250	0.000000	0.000000	-4.5610	-1.2104	0.0000	0.0000
82	QF	34.81	.70	.70	13.33	6.48	-1.63	.89	.91202	.24309	0.000000	0.000000	-4.5610	-1.2118	0.0000	0.0000
83	QS	35.11	.71	.71	14.33	5.97	-1.71	.81	.98495	.24309	0.000000	0.000000	-4.9245	-1.2118	0.0000	0.0000
84	QF	35.46	.71	.72	14.95	5.67	-.02	.05	1.04907	.12150	0.000000	0.000000	-5.2444	-.6070	0.0000	0.0000
85	QE	35.81	.71	.73	14.36	5.90	1.69	-.70	1.06953	-.00515	0.000000	0.000000	-5.3471	.0230	0.0000	0.0000
86	QS	36.11	.72	.74	13.37	6.34	1.61	-.78	1.06799	-.00515	0.000000	0.000000	-5.3402	.0230	0.0000	0.0000
87	SF	36.11	.72	.74	13.37	6.34	1.60	-.77	1.06799	-.00434	0.000000	0.000000	-5.3402	.0210	0.0000	0.0000
88	D	36.84	.73	.75	11.16	7.62	1.40	-.96	1.06680	-.00434	0.000000	0.000000	-5.3248	.0210	0.0000	0.0000
89	LC	38.50	.76	.78	7.26	11.48	.96	-1.38	1.05759	-.00634	0.000000	0.000000	-5.2899	.0210	0.0000	0.0000
90	Q	39.24	.77	.79	5.97	13.66	.77	-1.56	1.05439	-.00434	0.000000	0.000000	-5.2745	.0210	0.0000	0.0000
91	SQ	39.24	.77	.79	5.97	13.66	.77	-1.58	1.05439	-.00554	0.000000	0.000000	-5.2745	.0240	0.0000	0.0000
92	QS	39.56	.78	.80	5.53	14.43	.69	-1.65	1.05273	-.00554	0.000000	0.000000	-5.2673	.0240	0.0000	0.0000
93	QQ	39.89	.79	.80	5.30	15.29	-.01	.04	1.01236	.11791	0.000000	0.000000	-5.3663	-.5907	0.0000	0.0000
94	QQ	40.24	.80	.80	5.54	14.57	-.71	1.73	1.13596	.24620	0.000000	0.000000	-5.8842	-1.2295	0.0000	0.0000
95	QS	40.54	.81	.81	5.99	13.55	-.79	1.65	1.20982	.24620	0.000000	0.000000	-6.0530	-1.2295	0.0000	0.0000
96	SD	40.54	.81	.81	5.99	13.55	-.78	1.63	1.20982	.24469	0.000000	0.000000	-6.0530	-1.2255	0.0000	0.0000
97	D	41.28	.83	.82	7.29	11.30	-.98	1.43	1.38973	.24463	0.000000	0.000000	-6.9543	-1.2255	0.0000	0.0000
98	LC	42.94	.86	.85	11.27	7.28	-1.42	.98	1.79591	.24463	0.000000	0.000000	-8.9892	-1.2255	0.0000	0.0000
99	D	43.67	.87	.86	13.51	5.98	-1.62	.79	1.97581	.24463	0.000000	0.000000	-9.8905	-1.2255	0.0000	0.0000

POS		S (M)	QX	QY	BX (M)	BY (M)	AX	AY	EX (M)	EXP	EY (M)	EYP	XCC (MM)	QXCQ (MM)	YCC (MM)	QYCQ (MM)
100	SF	43.67	.87	.86	13.51	5.98	-1.64	.79	1.97581	.24740	0.000000	0.000000	-9.8965	-1.2324	0.0000	0.0000
101	QS	43.97	.87	.87	14.52	5.53	-1.72	.71	2.05003	.24740	0.000000	0.000000	-10.2602	-1.2324	0.0000	0.0000
102	QF	44.32	.87	.88	15.11	5.28	.00	.00	2.09349	-.00030	0.000000	0.000000	-10.4768	.0010	0.0000	0.0000
103	QF	44.67	.88	.89	14.52	5.53	1.72	-.71	2.04982	-.24798	0.000000	0.000000	-10.2565	1.2344	0.0000	0.0000
104	QS	44.97	.88	.90	13.51	5.98	1.64	-.79	1.97543	-.24798	0.000000	0.000000	-9.8842	1.2344	0.0000	0.0000
105	SF	44.97	.88	.90	13.51	5.98	1.62	-.79	1.97543	-.24521	0.000000	0.000000	-9.8852	1.2275	0.0000	0.0000
106	D	45.71	.89	.92	11.27	7.28	1.42	-.98	1.79509	-.24521	0.000000	0.000000	-8.9864	1.2275	0.0000	0.0000
107	B	47.37	.92	.95	7.23	11.21	.98	-1.37	1.46826	-.14944	0.000000	0.000000	-7.3461	.7487	0.0000	0.0000
108	D	48.10	.94	.96	6.00	13.37	.78	-1.56	1.35835	-.14944	0.000000	0.000000	-6.7984	.7487	0.0000	0.0000
109	SD	48.10	.94	.96	6.00	13.37	.79	-1.58	1.35835	-.15143	0.000000	0.000000	-6.7984	.7536	0.0000	0.0000
110	QS	48.40	.95	.96	5.55	14.34	.71	-1.66	1.31292	-.15143	0.000000	0.000000	-6.5724	.7536	0.0000	0.0000
111	QD	48.71	.96	.96	5.30	14.33	.01	.00	1.26640	-.00043	0.000000	0.000000	-6.4405	.0015	0.0000	0.0000
112	QD	49.10	.97	.97	5.53	14.34	-.69	1.67	1.31342	-.15056	0.000000	0.000000	-6.5713	-.7507	0.0000	0.0000
113	QS	49.40	.98	.97	5.97	13.36	-.77	1.59	1.35779	-.15056	0.000000	0.000000	-6.7965	-.7507	0.0000	0.0000
114	SD	49.40	.98	.97	5.97	13.36	-.76	1.57	1.35779	-.14857	0.000000	0.000000	-6.7965	-.7457	0.0000	0.0000
115	D	50.14	.99	.98	7.23	11.20	-.96	1.38	1.44705	-.14857	0.000000	0.000000	-7.3430	-.7457	0.0000	0.0000
116	B	51.80	1.02	1.01	11.13	7.26	-1.39	.99	1.79244	-.24534	0.000000	0.000000	-8.9774	-1.2244	0.0000	0.0000
117	D	52.36	1.03	1.03	13.32	5.96	-1.59	.79	1.97214	-.24534	0.000000	0.000000	-9.8780	-1.2244	0.0000	0.0000
118	SF	52.36	1.03	1.03	13.32	5.96	-1.61	.79	1.97214	-.24710	0.000000	0.000000	-9.8780	-1.2314	0.0000	0.0000
119	QS	52.84	1.04	1.04	14.31	5.51	-1.69	.71	2.04627	-.24710	0.000000	0.000000	-10.2474	-1.2314	0.0000	0.0000
120	QF	53.19	1.04	1.05	14.91	5.26	-.01	.00	2.08971	-.00014	0.000000	0.000000	-10.4639	.0005	0.0000	0.0000
121	QF	53.54	1.04	1.06	14.30	5.50	1.70	-.71	2.04617	-.24738	0.000000	0.000000	-10.2471	1.2324	0.0000	0.0000
122	QS	53.84	1.05	1.07	13.30	5.95	1.62	-.79	1.97186	-.24738	0.000000	0.000000	-9.8774	1.2324	0.0000	0.0000
123	SF	53.84	1.05	1.07	13.30	5.95	1.60	-.78	1.97186	-.24462	0.000000	0.000000	-9.8774	1.2255	0.0000	0.0000
124	D	54.39	1.06	1.08	11.09	7.24	1.41	-.98	1.79208	-.24462	0.000000	0.000000	-8.9761	1.2255	0.0000	0.0000
125	B	55.93	1.09	1.11	7.17	11.15	.96	-1.37	1.46620	-.14885	0.000000	0.000000	-7.3421	.7467	0.0000	0.0000
126	D	56.57	1.10	1.12	5.90	13.31	.76	-1.56	1.35673	-.14885	0.000000	0.000000	-6.7939	.7467	0.0000	0.0000
127	SD	56.97	1.10	1.12	5.90	13.31	.77	-1.58	1.35673	-.15083	0.000000	0.000000	-6.7939	.7516	0.0000	0.0000
128	QS	57.27	1.11	1.13	5.46	14.27	.69	-1.65	1.31148	-.15083	0.000000	0.000000	-6.5674	.7516	0.0000	0.0000
129	QD	57.42	1.12	1.13	5.22	14.86	-.00	-.00	1.28514	.00001	0.000000	0.000000	-6.4361	-.0000	0.0000	0.0000
130	QD	57.97	1.13	1.13	5.46	14.27	-.69	1.65	1.31149	-.15086	0.000000	0.000000	-6.5674	-.7517	0.0000	0.0000
131	QS	58.27	1.14	1.14	5.90	13.31	-.77	1.58	1.35673	-.15086	0.000000	0.000000	-6.7930	-.7517	0.0000	0.0000
132	SD	58.27	1.14	1.14	5.90	13.31	-.76	1.56	1.35673	-.14888	0.000000	0.000000	-6.7930	-.7467	0.0000	0.0000
133	D	59.00	1.16	1.15	7.17	11.15	-.96	1.37	1.46624	-.14888	0.000000	0.000000	-7.3421	-.7467	0.0000	0.0000
134	B	60.66	1.19	1.18	11.09	7.24	-1.41	.98	1.79213	-.24465	0.000000	0.000000	-8.9763	-1.2255	0.0000	0.0000
135	D	61.40	1.20	1.20	13.31	5.95	-1.60	.78	1.97205	-.24465	0.000000	0.000000	-9.8776	-1.2255	0.0000	0.0000
136	SF	61.40	1.20	1.20	13.31	5.95	-1.62	.79	1.97205	-.24741	0.000000	0.000000	-9.8776	-1.2324	0.0000	0.0000
137	QS	61.70	1.20	1.20	14.30	5.50	-1.70	.71	2.04627	-.24741	0.000000	0.000000	-10.2473	-1.2324	0.0000	0.0000
138	QF	62.05	1.21	1.21	14.91	5.26	-.01	-.00	2.08981	-.00027	0.000000	0.000000	-10.4641	-.0005	0.0000	0.0000
139	QF	62.40	1.21	1.22	14.32	5.51	1.69	-.71	2.04638	-.24711	0.000000	0.000000	-10.2477	1.2314	0.0000	0.0000
140	QS	62.70	1.21	1.23	13.33	5.96	1.61	-.79	1.97225	-.24711	0.000000	0.000000	-9.8782	1.2314	0.0000	0.0000
141	SF	62.70	1.21	1.23	13.33	5.96	1.59	-.79	1.97225	-.24434	0.000000	0.000000	-9.8782	1.2245	0.0000	0.0000
142	D	63.44	1.22	1.25	11.13	7.26	1.39	-.99	1.79255	-.24434	0.000000	0.000000	-8.9797	1.2245	0.0000	0.0000
143	B	65.09	1.25	1.28	7.24	11.20	.96	-1.38	1.46716	-.14857	0.000000	0.000000	-7.3452	.7437	0.0000	0.0000
144	D	65.83	1.27	1.29	5.97	13.36	.76	-1.57	1.35790	-.14857	0.000000	0.000000	-6.7968	.7457	0.0000	0.0000
145	SD	65.83	1.27	1.29	5.97	13.36	.77	-1.59	1.35790	-.15056	0.000000	0.000000	-6.7968	.7507	0.0000	0.0000
146	QS	66.13	1.28	1.29	5.54	14.34	.69	-1.67	1.31273	-.15056	0.000000	0.000000	-6.5715	.7507	0.0000	0.0000
147	QD	66.48	1.29	1.30	5.30	14.33	-.01	-.00	1.26651	.00044	0.000000	0.000000	-6.4407	-.0015	0.0000	0.0000
148	QD	66.83	1.30	1.30	5.55	14.34	-.71	1.66	1.31304	-.15146	0.000000	0.000000	-6.5726	-.7537	0.0000	0.0000
149	QS	67.13	1.31	1.30	6.00	13.37	-.79	1.58	1.35848	-.15146	0.000000	0.000000	-6.7987	-.7237	0.0000	0.0000

CALCULATION OF THE EQUILIBRIUM ORBIT AND BETATRON FUNCTIONS OF AGR .
INITIAL REFERENCE RAY DEFINED BY V

X = -.00001959 DX = 0.00000000 Y = 0.00000000 DY = 0.00000000 DS = 0.CCCCCCCC DP/P = 0.00000000 1.0000000
2

7X7 MATRIX FOR AGR

.04182933	17.81760225	C.00000000	0.00000000	0.00000C00	-.00087646	-.00000000
-.05602607	.04182933	0.00000000	0.00000000	0.00000C00	-.00005125	-.00000000
0.00000000	0.00000000	-.04180826	5.72904571	0.00000C00	0.00000000	0.00000000
0.00000000	0.00000000	-.17424404	-.04180826	0.00000000	0.00000000	0.00000000
.00005125	.00087646	0.00000000	0.00000000	1.00000C00	-2.87936746	-.00000000
0.00000000	0.00000000	0.00000000	0.00000000	0.00000000	1.00000000	0.00000000
0.00000000	0.00000000	0.00000000	0.00000000	0.00000000	0.00000000	1.00000000

EIGENVALUES OF THE 4X4 SUBMATRIX

X... LMD1 = (.04182933 -.99912477); C(1) = 1.00000000; MU(1) = 1.52895479 RAD; Q(1) = .73002214
1/LMD1 = (.04182933 -.99912477); C(2) = 1.00000000; MU(2) = -1.52895479 RAD; Q(2) = .26997786

Y... LMD3 = (-.04180826 -.99912565); C(3) = 1.00000000; MU(3) = 1.61261677 RAD; Q(3) = .76996779
1/LMD3 = (-.04180826 -.99912565); C(4) = 1.00000000; MU(4) = -1.61261677 RAD; Q(4) = .23003221

EIGENVALUE = (.04182933, .99912477), EIGENVECTOR = { 4.22293860, 0.00000000 }
{ 0.00000000, -.23680193 }
{ 0.00000000, 0.00000000 }
{ 0.00000000, 0.00000000 }

EIGENVALUE = (.04182933, -.99912477), EIGENVECTOR = { 4.22293860, 0.00000000 }
{ 0.00000000, -.23680193 }
{ 0.00000000, 0.00000000 }
{ 0.00000000, 0.00000000 }

EIGENVALUE = (-.04180826, .99912565), EIGENVECTOR = { 0.00000000, 0.00000000 }
{ 0.00000000, 0.00000000 }
{ 2.39458958, 0.00000000 }
{ .00000000, .41760810 }

EIGENVALUE = (-.04180826, -.99912565), EIGENVECTOR = { 0.00000000, 0.00000000 }
{ 0.00000000, 0.00000000 }
{ 2.39458958, 0.00000000 }
{ .00000000, -.41760810 }

	X	DX	Y	DY	DS	DP/P	
EQ ORBIT	-.00000000	0.00000000	0.00000000	0.00000000	0.00000000	0.00000000	1.00000000
ETA ORBIT	-.00091473	-.00000000	0.00000000	0.00000000	0.00000000	1.00000000	0.00000000

POS		S (M)	QX	QY	BX (M)	BY (M)	AX	AY	EX (M)	EXP	EY (M)	EYP	XCO (MM)	DXCO (MR)	YCO (MM)	DYCO (MR)
150	SD	67.13	1.31	1.30	6.00	13.37	-.78	1.56	1.35848	.14947	0.000000	0.000000	-6.7987	-.7487	0.0000	0.0000
151	D	67.87	1.33	1.31	7.29	11.21	-.93	1.37	1.46840	.14947	0.000000	0.000000	-7.3493	-.7487	0.0000	0.0000
152	B	69.53	1.36	1.34	11.27	7.28	-1.42	.98	1.79528	.24524	0.000000	0.000000	-8.9860	-1.2273	0.0000	0.0000
153	D	70.26	1.37	1.36	13.51	5.98	-1.62	.79	1.97863	.24524	0.000000	0.000000	-9.8896	-1.2273	0.0000	0.0000
154	SF	70.26	1.37	1.36	13.51	5.98	-1.64	.79	1.97863	.24801	0.000000	0.000000	-9.8896	-1.2345	0.0000	0.0000
155	QS	70.56	1.37	1.37	14.52	5.53	-1.72	.71	2.05004	.24801	0.000000	0.000000	-10.2599	-1.2345	0.0000	0.0000
156	QF	70.91	1.37	1.38	15.13	5.28	.00	.00	2.09371	.00030	0.000000	0.000000	-10.4772	-.0010	0.0000	0.0000
157	QF	71.26	1.38	1.39	14.52	5.53	1.72	-.71	2.05025	-.24742	0.000000	0.000000	-10.2606	1.2325	0.0000	0.0000
158	QS	71.56	1.38	1.40	13.51	5.98	1.64	-.79	1.97602	-.24742	0.000000	0.000000	-9.8909	1.2325	0.0000	0.0000
159	SF	71.56	1.38	1.40	13.51	5.98	1.62	-.79	1.97602	-.24465	0.000000	0.000000	-9.8509	1.2256	0.0000	0.0000
160	D	72.30	1.39	1.42	11.27	7.28	1.42	-.98	1.79609	-.24465	0.000000	0.000000	-8.9895	1.2256	0.0000	0.0000
161	B	73.96	1.42	1.45	7.29	11.21	.98	-1.37	1.47019	-.14888	0.000000	0.000000	-7.3554	.7468	0.0000	0.0000
162	D	74.69	1.44	1.45	6.00	13.37	.78	-1.56	1.36070	-.14888	0.000000	0.000000	-6.8062	.7468	0.0000	0.0000
163	SD	74.69	1.44	1.45	6.00	13.37	.79	-1.58	1.36070	-.15087	0.000000	0.000000	-6.8062	.7517	0.0000	0.0000
164	QS	74.99	1.44	1.46	5.55	14.34	.71	-1.66	1.31543	-.15087	0.000000	0.000000	-6.5806	.7517	0.0000	0.0000
165	QD	75.34	1.45	1.46	5.30	14.93	-.01	.00	1.28916	.00043	0.000000	0.000000	-6.4496	-.0015	0.0000	0.0000
166	QD	75.69	1.47	1.47	5.54	14.34	-.69	1.67	1.31575	.15176	0.000000	0.000000	-6.5817	-.7547	0.0000	0.0000
167	QS	75.99	1.47	1.47	5.97	13.36	-.77	1.59	1.36127	.15176	0.000000	0.000000	-6.8081	-.7547	0.0000	0.0000
168	SD	75.99	1.47	1.47	5.97	13.36	-.76	1.57	1.36127	.14977	0.000000	0.000000	-6.8081	-.7498	0.0000	0.0000
169	D	76.73	1.49	1.48	7.24	11.20	-.96	1.38	1.47141	.14977	0.000000	0.000000	-7.3595	-.7498	0.0000	0.0000
170	B	78.39	1.52	1.51	11.13	7.26	-1.39	.99	1.79878	.24554	0.000000	0.000000	-8.9986	-1.2286	0.0000	0.0000
171	D	79.12	1.53	1.53	13.32	5.96	-1.59	.79	1.97935	.24554	0.000000	0.000000	-9.9021	-1.2286	0.0000	0.0000
172	SF	79.12	1.53	1.53	13.32	5.96	-1.61	.79	1.97935	.24832	0.000000	0.000000	-9.9021	-1.2355	0.0000	0.0000
173	QS	79.42	1.53	1.53	14.31	5.51	-1.69	.71	2.05385	.24832	0.000000	0.000000	-10.2728	-1.2355	0.0000	0.0000
174	QF	79.78	1.54	1.56	14.91	5.26	.01	.00	2.09755	.00015	0.000000	0.000000	-10.4901	-.0005	0.0000	0.0000
175	QF	80.13	1.54	1.56	14.30	5.50	1.70	-.71	2.05395	-.24802	0.000000	0.000000	-10.2731	1.2345	0.0000	0.0000
176	QS	80.43	1.54	1.56	13.30	5.95	1.62	-.79	1.97955	-.24802	0.000000	0.000000	-9.9028	1.2345	0.0000	0.0000
177	SF	80.43	1.55	1.56	13.30	5.95	1.60	-.78	1.97955	-.24525	0.000000	0.000000	-9.9028	1.2276	0.0000	0.0000
178	D	81.16	1.55	1.58	11.09	7.24	1.41	-.98	1.79918	-.24525	0.000000	0.000000	-9.0060	1.2276	0.0000	0.0000
179	B	82.82	1.58	1.61	7.17	11.15	.96	-1.37	1.47230	-.14947	0.000000	0.000000	-7.3625	.7488	0.0000	0.0000
180	D	83.56	1.60	1.62	5.90	13.31	.76	-1.56	1.36237	-.14947	0.000000	0.000000	-6.8118	.7488	0.0000	0.0000
181	SD	83.56	1.60	1.62	5.90	13.31	.77	-1.58	1.36237	-.15147	0.000000	0.000000	-6.8118	.7538	0.0000	0.0000
182	QS	83.86	1.61	1.62	5.46	14.31	.69	-1.65	1.31693	-.15147	0.000000	0.000000	-6.5857	.7538	0.0000	0.0000
183	QD	84.21	1.62	1.63	5.22	14.86	-.00	.00	1.29047	.00000	0.000000	0.000000	-6.4540	-.0000	0.0000	0.0000
184	REFL	168.41	3.24	3.26	17.87	5.37	-.00	.00	.00862	-.00000	0.000000	0.000000	-.0196	0.0000	0.0000	0.0000

CIRCUMFERENCE = 505.2394 M THETX = 6.28318638 RAD NUX = 9.72797 DNUX/(DP/P) = .37870
(DS/S)/EBDZDS = .00870253 M THETY(183) = 0.00000000 RAD NUY = 9.76809 DNUY/(DP/P) = .41000
TGAM = (7.66390, 0.00000)

MAXIMA --- BETX(184) = 17.86771 BETY(12) = 16.71017 ETAX(174) = 2.09755 ETAY(184) = 0.00000
MINIMA --- BETX(36) = 4.02794 BETY(48) = 3.27399 ETAX(33) = -.00011 ETAY(184) = 0.00000

*** INCR 1 // DP .005000 VALUE = 0.000000

SUB. CHR , ITER. 5

EIGENVECTORS 1 AND 3 IN POLAR COORDINATES

POS	X1 X3		DX1 DX3		Y1 Y3		DY1 DY3	
0	1.222933 0.000000	0.000000 0.000000	.236d02 0.000000	1.570796 0.000000	0.000000 2.394590	0.000000 0.000000	0.000000 .417608	0.000000 1.570796

BETATRON FUNCTIONS OF AGR

POS		S (M)	QX	QY	BX (M)	BY (M)	AX	AY	EX (M)	EXP	EY (M)	EYP	XCO (MM)	DXCO (MR)	YCO (MM)	DYCO (MR)
0		0.00	0.00	0.00	17.83	5.73	0.00	0.00	-.00091	-.00000	0.000000	0.000000	-.0000	0.0000	0.0000	0.0000
1	QF1	.35	.00	.01	17.01	6.03	2.27	-.85	-.00089	.00012	0.000000	0.000000	-.0000	.0000	0.0000	0.0000
2		.72	.01	.02	15.38	6.70	2.13	-.95	-.00085	.00012	0.000000	0.000000	-.0000	.0000	0.0000	0.0000
3		1.10	.01	.03	13.84	7.45	2.00	-1.06	-.00080	.00012	0.000000	0.000000	-.0000	.0000	0.0000	0.0000
4	S	1.47	.02	.03	12.40	8.28	1.86	-1.16	-.00076	.00012	0.000000	0.000000	-.0000	.0000	0.0000	0.0000
5	S	1.84	.02	.04	11.06	9.18	1.73	-1.27	-.00071	.00012	0.000000	0.000000	-.0000	.0000	0.0000	0.0000
6	S	2.22	.03	.05	9.82	10.17	1.59	-1.38	-.00067	.00012	0.000000	0.000000	-.0000	.0000	0.0000	0.0000
7	S	2.59	.03	.05	8.68	11.24	1.46	-1.48	-.00062	.00012	0.000000	0.000000	-.0000	.0000	0.0000	0.0000
8	S	2.96	.04	.06	7.64	12.38	1.33	-1.59	-.00058	.00012	0.000000	0.000000	-.0000	.0000	0.0000	0.0000
9	S	3.34	.05	.06	6.70	13.61	1.19	-1.69	-.00054	.00012	0.000000	0.000000	-.0000	.0000	0.0000	0.0000
10	S	3.71	.06	.07	5.86	14.91	1.06	-1.80	-.00049	.00012	0.000000	0.000000	-.0000	.0000	0.0000	0.0000
11	S	4.08	.07	.07	5.12	16.20	.92	-1.91	-.00045	.00012	0.000000	0.000000	-.0000	.0000	0.0000	0.0000
12	QD1	4.43	.08	.07	4.73	16.94	.23	.08	-.00041	.00007	0.000000	0.000000	-.0000	.0000	0.0000	0.0000
13	QD1	4.78	.09	.08	4.79	16.18	-.42	2.06	-.00040	.00002	0.000000	0.000000	-.0000	.0000	0.0000	0.0000
14	S	5.16	.10	.08	5.14	14.69	-.51	1.94	-.00039	.00002	0.000000	0.000000	-.0000	.0000	0.0000	0.0000
15	S	5.53	.11	.09	5.56	13.29	-.61	1.82	-.00038	.00002	0.000000	0.000000	-.0000	.0000	0.0000	0.0000
16	S	5.90	.11	.09	6.08	11.98	-.70	1.70	-.00038	.00002	0.000000	0.000000	-.0000	.0000	0.0000	0.0000
17	S	6.28	.12	.10	6.69	10.76	-.79	1.58	-.00037	.00002	0.000000	0.000000	-.0000	.0000	0.0000	0.0000
18	S	6.64	.13	.10	7.39	9.67	-.88	1.46	-.00036	.00002	0.000000	0.000000	-.0000	.0000	0.0000	0.0000
19	S	7.02	.13	.11	7.92	8.58	-.97	1.33	-.00035	.00002	0.000000	0.000000	-.0000	.0000	0.0000	0.0000
20	S	7.39	.14	.12	8.68	7.63	-1.06	1.21	-.00035	.00002	0.000000	0.000000	-.0000	.0000	0.0000	0.0000
21	S	7.77	.15	.13	9.50	6.77	-1.16	1.09	-.00034	.00002	0.000000	0.000000	-.0000	.0000	0.0000	0.0000
22	S	8.14	.17	.13	10.48	6.00	-1.25	.97	-.00033	.00002	0.000000	0.000000	-.0000	.0000	0.0000	0.0000
23	S	8.51	.18	.14	11.77	5.32	-1.34	.85	-.00033	.00002	0.000000	0.000000	-.0000	.0000	0.0000	0.0000
24	QF2	8.86	.18	.15	11.81	4.99	.08	.12	-.00031	.00006	0.000000	0.000000	-.0000	.0000	0.0000	0.0000
25	QF2	9.22	.19	.17	11.26	5.15	1.49	-.59	-.00029	.00010	0.000000	0.000000	-.0000	.0000	0.0000	0.0000
26	S	9.59	.19	.18	10.19	5.62	1.38	-.68	-.00025	.00010	0.000000	0.000000	-.0000	.0000	0.0000	0.0000
27	S	9.96	.20	.19	9.19	6.17	1.27	-.78	-.00021	.00010	0.000000	0.000000	-.0000	.0000	0.0000	0.0000
28	S	10.33	.20	.20	8.28	6.79	1.17	-.88	-.00018	.00010	0.000000	0.000000	-.0000	.0000	0.0000	0.0000
29	S	10.71	.21	.20	7.63	7.40	1.06	-.98	-.00014	.00010	0.000000	0.000000	-.0000	.0000	0.0000	0.0000
30	S	11.08	.22	.21	6.70	8.25	.96	-1.07	-.00010	.00010	0.000000	0.000000	-.0000	.0000	0.0000	0.0000
31	S	11.45	.23	.22	6.03	9.09	.85	-1.17	-.00007	.00010	0.000000	0.000000	-.0000	.0000	0.0000	0.0000
32	S	11.83	.24	.23	5.43	10.00	.74	-1.27	-.00003	.00010	0.000000	0.000000	-.0000	.0000	0.0000	0.0000
33	S	12.20	.25	.23	4.92	10.98	.64	-1.37	.00000	.00010	0.000000	0.000000	.0000	.0000	0.0000	0.0000
34	S	12.57	.26	.24	4.48	12.04	.53	-1.46	.00004	.00010	0.000000	0.000000	.0000	.0000	0.0000	0.0000
35	S	12.95	.28	.24	4.13	13.17	-.42	-1.56	.00008	.00010	0.000000	0.000000	.0000	.0000	0.0000	0.0000
36	QD2	13.30	.29	.25	3.86	14.37	-.53	-.22	.00011	.00011	0.000000	0.000000	.0000	.0000	0.0000	0.0000
37	QD2	13.65	.30	.25	3.67	15.06	-.90	.97	.00015	.00013	0.000000	0.000000	.0000	.0000	0.0000	0.0000
38	R	14.01	.32	.25	3.56	14.47	-1.05	1.03	.00020	.00013	0.000000	0.000000	.0000	.0000	0.0000	0.0000
39	R	14.38	.33	.26	3.98	10.18	-1.20	1.69	.00025	.00013	0.000000	0.000000	.0000	.0000	0.0000	0.0000
40	R	14.75	.34	.27	4.92	8.99	-1.35	1.55	.00030	.00013	0.000000	0.000000	.0000	.0000	0.0000	0.0000
41	R	15.11	.34	.27	5.96	7.90	-1.50	1.41	.00034	.00013	0.000000	0.000000	.0000	.0000	0.0000	0.0000
42	R	15.48	.35	.28	6.11	6.92	-1.65	1.27	.00039	.00013	0.000000	0.000000	.0000	.0000	0.0000	0.0000
43	R	15.85	.36	.29	10.38	6.03	-1.80	1.13	.00044	.00013	0.000000	0.000000	.0000	.0000	0.0000	0.0000
44	R	16.21	.36	.30	11.24	5.25	-1.95	1.00	.00048	.00013	0.000000	0.000000	.0000	.0000	0.0000	0.0000
45	R	16.58	.37	.31	13.23	4.57	-2.09	.86	.00053	.00013	0.000000	0.000000	.0000	.0000	0.0000	0.0000
46	R	16.95	.37	.32	14.82	3.99	-2.24	.72	.00058	.00013	0.000000	0.000000	.0000	.0000	0.0000	0.0000
47	R	17.32	.38	.34	16.52	3.52	-2.39	.58	.00062	.00013	0.000000	0.000000	.0000	.0000	0.0000	0.0000
48	QF3	17.74	.38	.36	17.60	3.26	-.15	-.01	.00066	.00004	0.000000	0.000000	.0000	.0000	0.0000	0.0000
49	QF3	18.14	.38	.38	16.77	3.54	2.12	-.60	.00066	-.00005	0.000000	0.000000	.0000	-.0000	0.0000	0.0000

POS		S (M)	QX	QY	BX (M)	BY (M)	AX	AY	EX (M)	EXP	EY (M)	EYP	XCO (MM)	DXCO (MR)	YCO (MR)	DYCO (MR)
50	Z	18.50	.37	.39	15.29	4.02	2.00	-.74	.00064	-.00005	0.000000	0.000000	.0000	-.0000	0.0000	0.0000
51	Z	18.86	.39	.41	13.88	4.60	1.88	-.88	.00062	-.00005	0.000000	0.000000	.0000	-.0000	0.0000	0.0000
52	Z	19.22	.39	.42	12.56	5.24	1.77	-1.02	.00061	-.00005	0.000000	0.000000	.0000	-.0000	0.0000	0.0000
53	Z	19.58	.40	.43	11.33	6.07	1.65	-1.16	.00059	-.00005	0.000000	0.000000	.0000	-.0000	0.0000	0.0000
54	Z	19.95	.41	.44	10.19	6.95	1.53	-1.26	.00057	-.00005	0.000000	0.000000	.0000	-.0000	0.0000	0.0000
55	Z	20.31	.41	.46	9.13	7.94	1.41	-1.43	.00055	-.00005	0.000000	0.000000	.0000	-.0000	0.0000	0.0000
56	Z	20.67	.42	.45	8.15	9.02	1.29	-1.57	.00034	-.00002	0.000000	0.000000	.0000	-.0000	0.0000	0.0000
57	Z	21.03	.43	.46	7.26	10.20	1.18	-1.71	.00032	-.00005	0.000000	0.000000	.0000	-.0000	0.0000	0.0000
58	Z	21.39	.43	.46	6.46	11.49	1.06	-1.85	.00050	-.00005	0.000000	0.000000	.0000	-.0000	0.0000	0.0000
59	Z	21.75	.44	.47	5.74	12.87	.94	-1.99	.00049	-.00005	0.000000	0.000000	.0000	-.0000	0.0000	0.0000
60	QD3	22.16	.45	.47	5.31	13.82	.10	-.26	.00048	.00002	0.000000	0.000000	.0000	.0000	0.0000	0.0000
61	QD3	22.58	.47	.48	5.56	13.28	-.71	1.53	.00050	.00006	0.000000	0.000000	.0000	.0000	0.0000	0.0000
62	R	22.94	.48	.48	6.11	12.19	-.81	1.46	.00053	.00008	0.000000	0.000000	.0000	.0000	0.0000	0.0000
63	R	23.31	.49	.49	6.74	11.17	-.90	1.34	.00056	.00008	0.000000	0.000000	.0000	.0000	0.0000	0.0000
64	R	23.68	.49	.49	7.44	10.22	-1.00	1.23	.00059	.00008	0.000000	0.000000	.0000	.0000	0.0000	0.0000
65	R	24.04	.50	.50	8.21	9.34	-1.10	1.16	.00062	.00008	0.000000	0.000000	.0000	.0000	0.0000	0.0000
66	R	24.41	.51	.51	9.05	8.53	-1.20	1.07	.00065	.00008	0.000000	0.000000	.0000	.0000	0.0000	0.0000
67	R	24.78	.51	.51	9.97	7.80	-1.30	.98	.00068	.00008	0.000000	0.000000	.0000	.0000	0.0000	0.0000
68	R	25.14	.52	.52	10.96	7.08	-1.40	.88	.00071	.00008	0.000000	0.000000	.0000	.0000	0.0000	0.0000
69	R	25.51	.53	.53	12.02	6.43	-1.50	.79	.00074	.00008	0.000000	0.000000	.0000	.0000	0.0000	0.0000
70	R	25.88	.53	.54	13.16	5.93	-1.60	.70	.00077	.00008	0.000000	0.000000	.0000	.0000	0.0000	0.0000
71	R	26.24	.53	.55	14.37	5.45	-1.70	.61	.00080	.00008	0.000000	0.000000	.0000	.0000	0.0000	0.0000
72	QF	26.59	.54	.56	14.97	5.27	-.00	-.09	.00081	-.00001	0.000000	0.000000	.0000	-.0000	0.0000	0.0000
73	QF	26.94	.56	.57	14.37	5.39	1.69	-1.81	.00079	-.00011	0.000000	0.000000	.0000	-.0000	0.0000	0.0000
74	QD	27.98	.58	.60	11.15	7.38	1.42	-1.12	.00068	-.00011	0.000000	0.000000	.0000	-.0000	0.0000	0.0000
75	R	29.44	.58	.62	7.20	12.02	.97	-1.55	.97848	.09516	0.000000	0.000000	.0000	-.0000	0.0000	0.0000
76	QD	30.68	.61	.64	5.48	13.42	.69	-1.84	.17801	.09516	0.000000	0.000000	.0000	-.0000	0.0000	0.0000
77	QD	31.03	.62	.64	5.24	14.19	-.00	-.04	.21521	.11778	0.000000	0.000000	.0000	.0000	0.0000	0.0000
78	QD	31.38	.63	.64	5.48	15.38	-.69	1.76	.26114	.14518	0.000000	0.000000	.0000	.0000	0.0000	0.0000
79	QD	32.41	.66	.66	7.20	12.22	-.97	1.49	.31156	.14518	0.000000	0.000000	.0000	.0000	0.0000	0.0000
80	R	34.07	.69	.68	11.13	7.92	-1.42	1.09	.73113	.24045	0.000000	0.000000	.0000	.0000	0.0000	0.0000
81	QD	34.81	.70	.70	13.28	6.76	-1.61	.89	.90744	.24045	0.000000	0.000000	.0000	.0000	0.0000	0.0000
82	QF	34.81	.70	.70	13.28	6.46	-1.61	.89	.90744	.24045	0.000000	0.000000	.0000	.0000	0.0000	0.0000
83	QS	34.81	.70	.71	14.37	5.96	-1.70	.81	.98009	.24045	0.000000	0.000000	.0000	-.0000	0.0000	0.0000
84	QF	35.46	.70	.72	14.98	5.66	.00	.05	1.04360	.12068	0.000000	0.000000	.0000	-.0000	0.0000	0.0000
85	QF	35.81	.71	.73	14.37	5.88	1.70	-.69	1.04411	-.00406	0.000000	0.000000	.0000	-.0000	0.0000	0.0000
86	QS	36.11	.71	.73	13.38	6.32	1.61	-.77	1.06290	-.00406	0.000000	0.000000	.0000	-.0000	0.0000	0.0000
87	SF	36.11	.71	.73	13.38	6.32	1.61	-.77	1.06290	-.00406	0.000000	0.000000	.0000	-.0000	0.0000	0.0000
88	D	36.86	.72	.75	11.19	7.56	1.42	-.96	1.05991	-.00406	0.000000	0.000000	.0000	-.0000	0.0000	0.0000
89	LC	38.50	.75	.78	7.19	11.46	.97	-1.37	1.05318	-.00406	0.000000	0.000000	.0000	-.0000	0.0000	0.0000
90	D	39.24	.77	.79	5.91	13.62	.77	-1.56	1.05019	-.00406	0.000000	0.000000	.0000	-.0000	0.0000	0.0000
91	SD	39.24	.77	.79	5.91	13.62	.77	-1.56	1.05019	-.00406	0.000000	0.000000	.0000	-.0000	0.0000	0.0000
92	QS	39.54	.78	.79	5.47	14.58	.69	-1.64	1.04898	-.00406	0.000000	0.000000	.0000	-.0000	0.0000	0.0000
93	QD	39.89	.79	.80	5.23	15.14	.00	-.05	1.06884	.11779	0.000000	0.000000	.0000	-.0000	0.0000	0.0000
94	QD	40.24	.80	.80	5.47	14.51	-.69	1.72	1.13208	.24434	0.000000	0.000000	.0000	-.0000	0.0000	0.0000
95	QS	40.54	.81	.80	5.91	13.51	-.77	1.64	1.20338	.24434	0.000000	0.000000	.0000	-.0000	0.0000	0.0000
96	SD	40.54	.81	.80	5.91	13.51	-.77	1.64	1.20338	.24434	0.000000	0.000000	.0000	-.0000	0.0000	0.0000
97	D	41.28	.83	.81	7.19	11.24	-.97	1.44	1.38208	.24434	0.000000	0.000000	.0000	-.0000	0.0000	0.0000
98	LC	42.94	.85	.84	11.15	7.22	-1.42	.99	1.79079	.24434	0.000000	0.000000	.0000	-.0000	0.0000	0.0000
99	D	43.67	.86	.86	13.37	5.92	-1.61	.78	1.97068	.24434	0.000000	0.000000	.0000	-.0000	0.0000	0.0000

POS		S (M)	QX	QY	BX (M)	BY (M)	AX	AY	EX (M)	EXP	EY (M)	EYP	XCO (MM)	DXCO (MR)	YCO (MM)	DYCO (MR)
100	SF	43.67	.86	.86	13.37	5.92	-1.61	.78	1.97048	.24434	0.000000	0.000000	.0000	-.0000	0.0000	0.0000
101	QS	43.97	.87	.87	14.37	5.47	-1.69	.70	2.04378	.24434	0.000000	0.000000	.0000	-.0000	0.0000	0.0000
102	QF	44.32	.87	.88	14.97	5.23	.00	-.00	2.08673	-.00011	0.000000	0.000000	.0000	-.0000	0.0000	0.0000
103	QF	44.67	.88	.89	14.37	5.47	1.69	-.70	2.04371	-.24436	0.000000	0.000000	.0000	-.0000	0.0000	0.0000
104	QS	44.97	.88	.90	13.37	5.92	1.61	-.78	1.97034	-.24436	0.000000	0.000000	.0000	-.0000	0.0000	0.0000
105	SF	44.97	.88	.90	13.37	5.92	1.61	-.78	1.97034	-.24436	0.000000	0.000000	.0000	-.0000	0.0000	0.0000
106	D	45.71	.89	.92	11.15	7.22	1.42	-.99	1.79048	-.24436	0.000000	0.000000	.0000	-.0000	0.0000	0.0000
107	B	47.37	.92	.96	7.19	11.16	.97	-1.38	1.46400	-.14929	0.000000	0.000000	.0000	-.0000	0.0000	0.0000
108	D	48.10	.94	.95	5.91	13.33	.77	-1.57	1.35421	-.14929	0.000000	0.000000	.0000	-.0000	0.0000	0.0000
109	SD	48.10	.94	.95	5.91	13.33	.77	-1.57	1.35421	-.14929	0.000000	0.000000	.0000	-.0000	0.0000	0.0000
110	QS	48.40	.94	.96	5.48	14.30	.69	-1.65	1.30942	-.14929	0.000000	0.000000	.0000	-.0000	0.0000	0.0000
111	QD	48.76	.95	.96	5.24	14.88	.00	-.00	1.28332	-.00016	0.000000	0.000000	.0000	-.0000	0.0000	0.0000
112	QD	49.11	.95	.97	5.48	14.30	-.69	1.65	1.30920	.14898	0.000000	0.000000	.0000	-.0000	0.0000	0.0000
113	QS	49.41	.97	.97	5.91	13.33	-.77	1.57	1.35399	.14895	0.000000	0.000000	.0000	-.0000	0.0000	0.0000
114	SD	49.41	.97	.97	5.91	13.33	-.77	1.57	1.35399	.14895	0.000000	0.000000	.0000	-.0000	0.0000	0.0000
115	D	50.14	.98	.98	7.19	11.16	-.97	1.38	1.46354	.14895	0.000000	0.000000	.0000	-.0000	0.0000	0.0000
116	B	51.80	1.02	1.01	11.15	7.22	-1.42	.99	1.78946	.24423	0.000000	0.000000	.0000	-.0000	0.0000	0.0000
117	D	52.54	1.03	1.03	13.37	5.92	-1.61	.78	1.96907	.24423	0.000000	0.000000	.0000	-.0000	0.0000	0.0000
118	SF	52.54	1.03	1.03	13.37	5.92	-1.61	.78	1.96907	.24423	0.000000	0.000000	.0000	-.0000	0.0000	0.0000
119	QS	52.84	1.03	1.03	14.37	5.47	-1.69	.70	2.04284	.24423	0.000000	0.000000	.0000	-.0000	0.0000	0.0000
120	QF	53.19	1.04	1.04	14.97	5.23	.00	-.00	2.08528	-.00006	0.000000	0.000000	.0000	-.0000	0.0000	0.0000
121	QF	53.54	1.04	1.06	14.37	5.47	1.69	-.70	2.04230	-.24434	0.000000	0.000000	.0000	-.0000	0.0000	0.0000
122	QS	53.84	1.05	1.06	13.37	5.92	1.61	-.78	1.96900	-.24436	0.000000	0.000000	.0000	-.0000	0.0000	0.0000
123	SF	53.84	1.05	1.06	13.37	5.92	1.61	-.78	1.96900	-.24434	0.000000	0.000000	.0000	-.0000	0.0000	0.0000
124	D	54.57	1.06	1.08	11.15	7.22	1.42	-.99	1.78931	-.24434	0.000000	0.000000	.0000	-.0000	0.0000	0.0000
125	B	56.23	1.08	1.11	7.19	11.16	.97	-1.38	1.46320	-.14906	0.000000	0.000000	.0000	-.0000	0.0000	0.0000
126	D	56.97	1.10	1.12	5.91	13.33	.77	-1.57	1.35357	-.14906	0.000000	0.000000	.0000	-.0000	0.0000	0.0000
127	SD	56.97	1.10	1.12	5.91	13.33	.77	-1.57	1.35357	-.14906	0.000000	0.000000	.0000	-.0000	0.0000	0.0000
128	QS	57.27	1.11	1.12	5.48	14.30	.69	-1.65	1.30886	-.14906	0.000000	0.000000	.0000	-.0000	0.0000	0.0000
129	QD	57.62	1.12	1.13	5.24	14.88	-.00	.00	1.28282	.00000	0.000000	0.000000	.0000	-.0000	0.0000	0.0000
130	QD	57.97	1.13	1.13	5.48	14.30	-.69	1.65	1.30886	.14906	0.000000	0.000000	.0000	-.0000	0.0000	0.0000
131	QS	58.27	1.14	1.14	5.91	13.33	-.77	1.57	1.35357	.14906	0.000000	0.000000	.0000	-.0000	0.0000	0.0000
132	SD	58.27	1.14	1.14	5.91	13.33	-.77	1.57	1.35357	.14906	0.000000	0.000000	.0000	-.0000	0.0000	0.0000
133	D	59.01	1.15	1.15	7.19	11.16	-.97	1.38	1.46320	.14906	0.000000	0.000000	.0000	-.0000	0.0000	0.0000
134	B	60.67	1.19	1.17	11.15	7.22	-1.42	.99	1.78931	.24434	0.000000	0.000000	.0000	-.0000	0.0000	0.0000
135	D	61.40	1.20	1.19	13.37	5.92	-1.61	.78	1.96900	.24434	0.000000	0.000000	.0000	-.0000	0.0000	0.0000
136	SF	61.40	1.20	1.19	13.37	5.92	-1.61	.78	1.96900	.24434	0.000000	0.000000	.0000	-.0000	0.0000	0.0000
137	QS	61.70	1.20	1.20	14.37	5.47	-1.69	.70	2.04230	.24434	0.000000	0.000000	.0000	-.0000	0.0000	0.0000
138	QF	62.05	1.21	1.21	14.97	5.23	-.00	.00	2.08528	-.00006	0.000000	0.000000	.0000	-.0000	0.0000	0.0000
139	QF	62.40	1.21	1.22	14.37	5.47	1.69	-.70	2.04284	-.24423	0.000000	0.000000	.0000	-.0000	0.0000	0.0000
140	QS	62.70	1.21	1.23	13.37	5.92	1.61	-.78	1.96907	-.24423	0.000000	0.000000	.0000	-.0000	0.0000	0.0000
141	SF	62.70	1.21	1.23	13.37	5.92	1.61	-.78	1.96907	-.24423	0.000000	0.000000	.0000	-.0000	0.0000	0.0000
142	D	63.44	1.23	1.25	11.15	7.22	1.42	-.99	1.78946	-.24423	0.000000	0.000000	.0000	-.0000	0.0000	0.0000
143	B	65.10	1.26	1.28	7.19	11.16	.97	-1.38	1.46354	-.14895	0.000000	0.000000	.0000	-.0000	0.0000	0.0000
144	D	65.85	1.27	1.29	5.91	13.33	.77	-1.57	1.35399	-.14895	0.000000	0.000000	.0000	-.0000	0.0000	0.0000
145	SD	65.85	1.27	1.29	5.91	13.33	.77	-1.57	1.35399	-.14895	0.000000	0.000000	.0000	-.0000	0.0000	0.0000
146	QS	66.13	1.28	1.29	5.48	14.30	.69	-1.65	1.30930	-.14895	0.000000	0.000000	.0000	-.0000	0.0000	0.0000
147	QD	66.48	1.29	1.29	5.24	14.88	-.00	.00	1.28332	.00016	0.000000	0.000000	.0000	-.0000	0.0000	0.0000
148	QD	66.84	1.30	1.30	5.48	14.30	-.69	1.65	1.30942	.14929	0.000000	0.000000	.0000	-.0000	0.0000	0.0000
149	QS	67.14	1.31	1.30	5.91	13.33	-.77	1.57	1.35421	.14929	0.000000	0.000000	.0000	-.0000	0.0000	0.0000

POS		S (M)	QX	QY	BX (M)	BY (M)	AX	AY	EX (M)	EXP	EY (M)	EYP	XCO (MM)	DXCO (MR)	YCO (MM)	DYCO (MR)
150	SD	67.14	1.31	1.30	5.91	13.33	-.77	1.57	1.35421	.14929	0.000000	0.000000	.0000	-.0000	0.0000	0.0000
151	D	67.87	1.33	1.31	7.19	11.16	-.97	1.38	1.46400	.14929	0.000000	0.000000	.0000	-.0000	0.0000	0.0000
152	B	69.83	1.35	1.34	11.15	7.22	-1.42	.99	1.79068	.24456	0.000000	0.000000	.0000	-.0000	0.0000	0.0000
153	D	70.27	1.36	1.36	13.37	5.92	-1.61	.78	1.97034	.24456	0.000000	0.000000	.0000	-.0000	0.0000	0.0000
154	SF	70.27	1.36	1.36	13.37	5.92	-1.61	.78	1.97034	.24456	0.000000	0.000000	.0000	-.0000	0.0000	0.0000
155	QS	70.57	1.37	1.37	14.37	5.47	-1.69	.70	2.04371	.24456	0.000000	0.000000	.0000	-.0000	0.0000	0.0000
156	QF	70.92	1.37	1.38	14.97	5.23	.00	-.00	2.06673	.00011	0.000000	0.000000	.0000	-.0000	0.0000	0.0000
157	QF	71.27	1.38	1.39	14.37	5.47	1.69	-.70	2.04378	-.24434	0.000000	0.000000	.0000	-.0000	0.0000	0.0000
158	QS	71.57	1.38	1.40	13.37	5.92	1.61	-.78	1.97048	-.24434	0.000000	0.000000	.0000	-.0000	0.0000	0.0000
159	SF	71.57	1.38	1.40	13.37	5.92	1.61	-.78	1.97048	-.24434	0.000000	0.000000	.0000	-.0000	0.0000	0.0000
160	D	72.30	1.39	1.42	11.15	7.22	1.42	-.99	1.79079	-.24434	0.000000	0.000000	.0000	-.0000	0.0000	0.0000
161	B	73.96	1.42	1.44	7.19	11.16	.97	-1.38	1.46467	-.14907	0.000000	0.000000	.0000	-.0000	0.0000	0.0000
162	D	74.40	1.44	1.45	5.91	13.33	.77	-1.57	1.35506	-.14907	0.000000	0.000000	.0000	-.0000	0.0000	0.0000
163	SD	74.70	1.44	1.45	5.91	13.33	.77	-1.57	1.35505	-.14907	0.000000	0.000000	.0000	-.0000	0.0000	0.0000
164	QS	75.00	1.44	1.46	5.48	14.30	.69	-1.65	1.31032	-.14907	0.000000	0.000000	.0000	-.0000	0.0000	0.0000
165	QD	75.35	1.46	1.46	5.24	14.88	.00	-.00	1.28431	.00016	0.000000	0.000000	.0000	-.0000	0.0000	0.0000
166	QD	75.70	1.47	1.47	5.48	14.30	-.69	1.65	1.31043	.14940	0.000000	0.000000	.0000	-.0000	0.0000	0.0000
167	QS	76.00	1.47	1.47	5.91	13.33	-.77	1.57	1.35526	.14940	0.000000	0.000000	.0000	-.0000	0.0000	0.0000
168	SD	76.00	1.47	1.47	5.91	13.33	-.77	1.57	1.35526	.14940	0.000000	0.000000	.0000	-.0000	0.0000	0.0000
169	D	76.74	1.49	1.48	7.19	11.16	-.97	1.38	1.46513	.14940	0.000000	0.000000	.0000	-.0000	0.0000	0.0000
170	B	78.40	1.52	1.51	11.15	7.22	-1.42	.99	1.79180	.24468	0.000000	0.000000	.0000	-.0000	0.0000	0.0000
171	D	79.13	1.53	1.53	13.37	5.92	-1.61	.78	1.97175	.24468	0.000000	0.000000	.0000	-.0000	0.0000	0.0000
172	SF	79.13	1.53	1.53	13.37	5.92	-1.61	.78	1.97175	.24468	0.000000	0.000000	.0000	-.0000	0.0000	0.0000
173	QS	79.43	1.53	1.54	14.37	5.47	-1.69	.70	2.04515	.24468	0.000000	0.000000	.0000	-.0000	0.0000	0.0000
174	QF	79.78	1.54	1.55	14.97	5.23	.00	-.00	2.06819	.00006	0.000000	0.000000	.0000	-.0000	0.0000	0.0000
175	QF	80.13	1.54	1.56	14.37	5.47	1.69	-.70	2.04519	-.24457	0.000000	0.000000	.0000	-.0000	0.0000	0.0000
176	QS	80.43	1.55	1.56	13.37	5.92	1.61	-.78	1.97182	-.24457	0.000000	0.000000	.0000	-.0000	0.0000	0.0000
177	SF	80.43	1.55	1.56	13.37	5.92	1.61	-.78	1.97182	-.24457	0.000000	0.000000	.0000	-.0000	0.0000	0.0000
178	D	81.17	1.56	1.58	11.15	7.22	1.42	-.99	1.79196	-.24457	0.000000	0.000000	.0000	-.0000	0.0000	0.0000
179	B	82.83	1.58	1.61	7.19	11.16	.97	-1.38	1.46547	-.14929	0.000000	0.000000	.0000	-.0000	0.0000	0.0000
180	D	83.56	1.60	1.62	5.91	13.33	.77	-1.57	1.35567	-.14929	0.000000	0.000000	.0000	-.0000	0.0000	0.0000
181	SD	83.56	1.60	1.62	5.91	13.33	.77	-1.57	1.35567	-.14929	0.000000	0.000000	.0000	-.0000	0.0000	0.0000
182	QS	83.86	1.61	1.62	5.48	14.30	.69	-1.65	1.31088	-.14929	0.000000	0.000000	.0000	-.0000	0.0000	0.0000
183	QD	84.21	1.62	1.63	5.24	14.88	-.00	.00	1.28481	.00000	0.000000	0.000000	.0000	-.0000	0.0000	0.0000
184	REFL	168.43	3.24	3.26	17.83	5.73	-.00	.00	-.00091	.00000	0.000000	0.000000	-.0000	0.0000	0.0000	0.0000

CIRCUMFERENCE = 505.2827 M THETX = 6.28318638 RAD NUX = 9.73002 DNUX/(DP/P) = .39620
(DS7S)/(RADIUS) = .8378958 M THETY(183) = 0.00000000 RAD NUY = 9.76997 DNUY/(DP/P) = .39105
TGAM = (7.64818, 0.00000)

MAXIMA --- BETX(184) = 17.83321 BETY(12) = 16.94478 ETAX(174) = 2.08819 ETAY(184) = 0.00000
MINIMA --- BETX(36) = 4.05811 BETY(48) = 3.28856 ETAX(33) = .00000 ETAY(184) = 0.00000

*** INCR 1 // QD .005000 VALUE = .005000

SUB. CHR , ITER. 6

CALCULATION OF THE EQUILIBRIUM ORBIT AND BETATRON FUNCTIONS OF AGR .
INITIAL REFERENCE RAY DEFINED BY V

X = -.00000000 DX = 0.00000000 Y = 0.00000000 DY = 0.00000000 DS = 0.00000000 DP/P = .00500000 1.00000000

7X7 MATRIX FOR AGR

.03778456	17.77701740	0.00000000	0.00000000	0.00000000	-.01056744	.00002498
-.05617210	.03778456	0.00000000	0.00000000	0.00000000	-.00001690	.00000146
0.00000000	0.00000000	-.04603245	5.88965712	0.00000000	0.00000000	0.00000000
0.00000000	0.00000000	-.16942939	-.04603245	0.00000000	0.00000000	0.00000000
.00001690	.01056744	0.00000000	0.00000000	1.00000000	-2.89152294	-.01417647
0.00000000	0.00000000	0.00000000	0.00000000	0.00000000	1.00000000	0.00000000
0.00000000	0.00000000	0.00000000	0.00000000	0.00000000	0.00000000	1.00000000

EIGENVALUES OF THE 4X4 SUBMATRIX

X... LMD1 = (.03778456 -.99928591); C(1) = 1.00000000; MU(1) = -1.53300277 RAD; Q(1) = .73195490
1/LMD1 = (.03778456 -.99928591); C(2) = 1.00000000; MU(2) = -1.53300277 RAD; Q(2) = .26804510

Y... LMD3 = (-.04603245 .99893995); C(3) = 1.00000000; MU(3) = 1.61684505 RAD; Q(3) = .77198664
1/LMD3 = (-.04603245 -.99893995); C(4) = 1.00000000; MU(4) = -1.61684505 RAD; Q(4) = .22801336

EIGENVALUE = (.03778456, .99928591), EIGENVECTOR = { 4.21778626, 0.00000000 }
{ .00000000, .23709120 }
{ 0.00000000, 0.00000000 }
{ 0.00000000, 0.00000000 }

EIGENVALUE = (.03778456, -.99928591), EIGENVECTOR = { 4.21778626, 0.00000000 }
{ .00000000, -.23709120 }
{ 0.00000000, 0.00000000 }
{ 0.00000000, 0.00000000 }

EIGENVALUE = (-.04603245, .99893995), EIGENVECTOR = { 0.00000000, 0.00000000 }
{ 0.00000000, 0.00000000 }
{ 2.42814890, .00000000 }
{ .00000000, .41183636 }

EIGENVALUE = (-.04603245, -.99893995), EIGENVECTOR = { 0.00000000, 0.00000000 }
{ 0.00000000, 0.00000000 }
{ 2.42814890, -.00000000 }
{ .00000000, -.41183636 }

	X	DX	Y	DY	DS	DP/P	
EQ ORBIT	-.00002944	0.00000000	0.00000000	0.00000000	0.00000000	.00500000	1.00000000
ETA ORBIT	-.01098241	-.00000000	0.00000000	0.00000000	0.00000000	1.00000000	0.00000000

BETATRON FUNCTIONS OF AGR

POS		S (M)	QX	QY	BX (M)	BY (M)	AX	AY	EX (M)	EXP	EY (M)	EYP	XCO (MM)	DXCO (MR)	YCO (MM)	DYCO (MR)
0		0.00	0.00	0.00	17.79	5.90	0.00	0.00	-.01098	-.00000	0.000000	0.000000	-.0294	0.0000	0.0000	0.0000
1	QF1	.38	.00	.01	16.99	6.19	2.25	-.86	-.01073	.00143	0.000000	0.000000	-.0288	.0038	0.0000	0.0000
2	S	.72	.01	.02	15.36	6.88	2.12	-.97	-.01020	.00143	0.000000	0.000000	-.0273	.0038	0.0000	0.0000
3	S	1.10	.01	.03	13.83	7.64	1.98	-1.07	-.00966	.00143	0.000000	0.000000	-.0259	.0038	0.0000	0.0000
4	S	1.47	.02	.03	12.40	8.47	1.85	-1.18	-.00913	.00143	0.000000	0.000000	-.0245	.0038	0.0000	0.0000
5	S	1.84	.02	.04	11.06	9.39	1.72	-1.28	-.00859	.00143	0.000000	0.000000	-.0230	.0038	0.0000	0.0000
6	S	2.22	.03	.05	9.83	10.39	1.59	-1.39	-.00806	.00143	0.000000	0.000000	-.0216	.0038	0.0000	0.0000
7	S	2.59	.03	.05	8.70	11.46	1.45	-1.49	-.00753	.00143	0.000000	0.000000	-.0202	.0038	0.0000	0.0000
8	S	2.96	.04	.06	7.66	12.61	1.32	-1.60	-.00699	.00143	0.000000	0.000000	-.0187	.0038	0.0000	0.0000
9	S	3.34	.05	.06	6.73	13.84	1.19	-1.70	-.00646	.00143	0.000000	0.000000	-.0173	.0038	0.0000	0.0000
10	S	3.71	.06	.07	5.90	15.15	1.05	-1.81	-.00593	.00143	0.000000	0.000000	-.0158	.0038	0.0000	0.0000
11	S	4.08	.07	.07	5.16	16.54	.92	-1.91	-.00539	.00143	0.000000	0.000000	-.0144	.0038	0.0000	0.0000
12	QD1	4.43	.08	.07	4.76	17.10	.23	-.10	-.00500	.00081	0.000000	0.000000	-.0134	.0022	0.0000	0.0000
13	QD1	4.78	.09	.08	4.83	16.40	-.53	2.09	-.00482	.00021	0.000000	0.000000	-.0129	.0006	0.0000	0.0000
14	S	5.16	.10	.08	5.19	14.89	-.52	1.97	-.00474	.00021	0.000000	0.000000	-.0127	.0006	0.0000	0.0000
15	S	5.53	.11	.08	5.61	13.46	-.61	1.85	-.00466	.00021	0.000000	0.000000	-.0124	.0006	0.0000	0.0000
16	S	5.90	.11	.09	6.10	12.13	-.70	1.73	-.00458	.00021	0.000000	0.000000	-.0122	.0006	0.0000	0.0000
17	S	6.28	.12	.09	6.65	10.89	-.79	1.60	-.00450	.00021	0.000000	0.000000	-.0120	.0006	0.0000	0.0000
18	S	6.65	.13	.10	7.28	9.74	-.88	1.48	-.00442	.00021	0.000000	0.000000	-.0118	.0006	0.0000	0.0000
19	S	7.02	.13	.11	7.97	8.68	-.97	1.36	-.00434	.00021	0.000000	0.000000	-.0116	.0006	0.0000	0.0000
20	S	7.39	.14	.11	8.73	7.71	-1.07	1.24	-.00426	.00021	0.000000	0.000000	-.0113	.0006	0.0000	0.0000
21	S	7.77	.15	.12	9.56	6.83	-1.16	1.11	-.00418	.00021	0.000000	0.000000	-.0111	.0006	0.0000	0.0000
22	S	8.14	.17	.12	10.46	6.02	-1.25	.99	-.00410	.00021	0.000000	0.000000	-.0109	.0006	0.0000	0.0000
23	S	8.51	.18	.13	11.43	5.35	-1.34	.87	-.00402	.00021	0.000000	0.000000	-.0107	.0006	0.0000	0.0000
24	QF2	8.86	.18	.13	11.88	5.00	.08	.14	-.00386	.00071	0.000000	0.000000	-.0102	.0019	0.0000	0.0000
25	QF2	9.22	.19	.16	11.32	5.15	1.49	-.57	-.00353	.00117	0.000000	0.000000	-.0094	.0031	0.0000	0.0000
26	S	9.59	.19	.17	10.25	5.61	1.38	-.66	-.00309	.00117	0.000000	0.000000	-.0082	.0031	0.0000	0.0000
27	S	9.96	.20	.18	9.25	6.14	1.28	-.76	-.00265	.00117	0.000000	0.000000	-.0070	.0031	0.0000	0.0000
28	S	10.33	.20	.19	8.34	6.74	1.17	-.85	-.00222	.00117	0.000000	0.000000	-.0059	.0031	0.0000	0.0000
29	S	10.71	.21	.20	7.51	7.42	1.06	-.95	-.00178	.00117	0.000000	0.000000	-.0047	.0031	0.0000	0.0000
30	S	11.08	.22	.21	6.75	8.16	.96	-1.03	-.00134	.00117	0.000000	0.000000	-.0035	.0031	0.0000	0.0000
31	S	11.45	.23	.22	6.08	8.98	.85	-1.14	-.00091	.00117	0.000000	0.000000	-.0023	.0031	0.0000	0.0000
32	S	11.83	.24	.22	5.48	9.86	.75	-1.24	-.00047	.00117	0.000000	0.000000	-.0012	.0031	0.0000	0.0000
33	S	12.20	.25	.23	4.96	10.82	.64	-1.33	-.00003	.00117	0.000000	0.000000	-.0000	.0031	0.0000	0.0000
34	S	12.57	.26	.23	4.52	11.85	.53	-1.43	.00040	.00117	0.000000	0.000000	.0012	.0031	0.0000	0.0000
35	S	12.95	.28	.24	4.17	12.96	.43	-1.52	.00084	.00117	0.000000	0.000000	.0023	.0031	0.0000	0.0000
36	QD2	13.30	.29	.24	4.09	13.42	-.21	.22	.00127	.00131	0.000000	0.000000	.0035	.0035	0.0000	0.0000
37	QD2	13.65	.30	.25	4.47	12.65	-.80	1.96	.00177	.00152	0.000000	0.000000	.0048	.0041	0.0000	0.0000
38	R	14.01	.32	.25	5.18	11.29	-1.04	1.72	.00222	.00152	0.000000	0.000000	.0063	.0041	0.0000	0.0000
39	R	14.38	.33	.26	6.00	10.02	-1.19	1.66	.00288	.00152	0.000000	0.000000	.0078	.0041	0.0000	0.0000
40	R	14.75	.33	.26	6.93	8.86	-1.34	1.52	.00344	.00152	0.000000	0.000000	.0093	.0041	0.0000	0.0000
41	R	15.11	.34	.27	7.97	7.79	-1.49	1.38	.00399	.00152	0.000000	0.000000	.0108	.0041	0.0000	0.0000
42	R	15.48	.35	.28	9.11	6.83	-1.63	1.25	.00455	.00152	0.000000	0.000000	.0123	.0041	0.0000	0.0000
43	R	15.85	.36	.29	10.36	5.97	-1.78	1.11	.00511	.00152	0.000000	0.000000	.0138	.0041	0.0000	0.0000
44	R	16.21	.36	.30	11.73	5.20	-1.93	.97	.00566	.00152	0.000000	0.000000	.0153	.0041	0.0000	0.0000
45	R	16.58	.37	.31	13.20	4.54	-2.08	.83	.00622	.00152	0.000000	0.000000	.0168	.0041	0.0000	0.0000
46	R	16.95	.37	.32	14.77	3.98	-2.22	.70	.00677	.00152	0.000000	0.000000	.0183	.0041	0.0000	0.0000
47	R	17.32	.37	.34	16.46	3.52	-2.37	.56	.00733	.00152	0.000000	0.000000	.0198	.0041	0.0000	0.0000
48	QF3	17.72	.38	.36	17.53	3.30	-.15	-.03	.00775	.00051	0.000000	0.000000	.0209	.0013	0.0000	0.0000
49	QF3	18.14	.38	.38	16.70	3.56	2.10	-.62	.00775	-.00053	0.000000	0.000000	.0209	-.0015	0.0000	0.0000

EIGENVECTORS 1 AND 3 IN POLAR COORDINATES

POS	X1 X3		DX1 DX3		Y1 Y3		DY1 DY3	
0	4.217786 0.000000	0.000000 0.000000	-.237091 0.000000	1.570796 0.000000	0.000000 2.428149	0.000000 .000000	0.000000 .411836	0.000000 1.570796

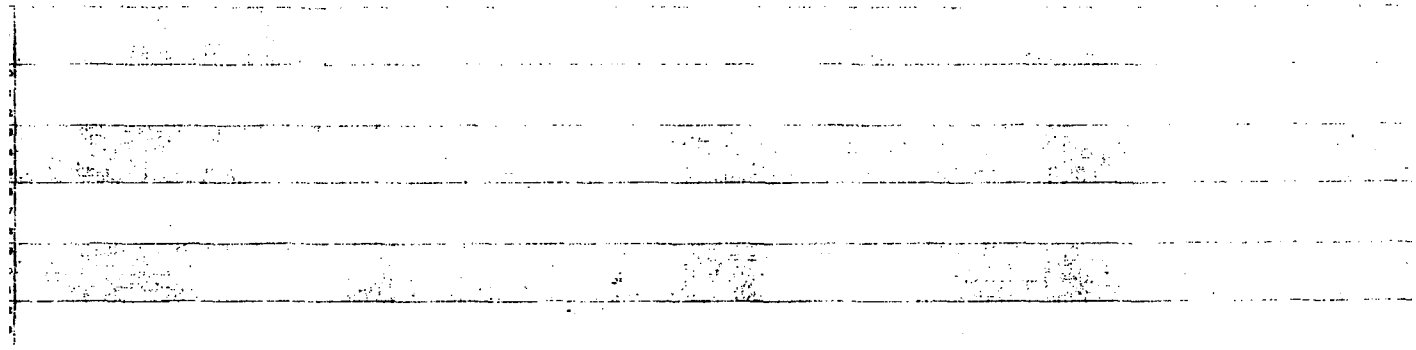

POS		S (M)	QX	QY	BX (M)	BY (M)	AX	AY	EX (M)	EXP	EY (M)	EYP	XCO (MR)	QXCO (MR)	YCO (MR)	QYCO (MR)
50	Z	18.50	.38	.39	15.23	4.06	1.98	-.76	.00759	-.00053	0.000000	0.000000	.0204	-.0015	0.0000	0.0000
51	Z	18.86	.39	.41	13.64	4.65	1.87	-.90	.00736	-.00053	0.000000	0.000000	.0198	-.0015	0.0000	0.0000
52	Z	19.22	.39	.42	12.54	5.35	1.75	-1.04	.00717	-.00053	0.000000	0.000000	.0193	-.0015	0.0000	0.0000
53	Z	19.58	.40	.43	11.32	6.19	1.63	-1.18	.00698	-.00053	0.000000	0.000000	.0188	-.0015	0.0000	0.0000
54	Z	19.95	.40	.44	10.14	7.04	1.92	-1.32	.00678	-.00053	0.000000	0.000000	.0183	-.0015	0.0000	0.0000
55	Z	20.31	.41	.44	9.13	8.04	1.40	-1.45	.00659	-.00053	0.000000	0.000000	.0177	-.0015	0.0000	0.0000
56	Z	20.67	.42	.45	8.16	9.14	1.28	-1.59	.00640	-.00053	0.000000	0.000000	.0172	-.0015	0.0000	0.0000
57	Z	21.03	.42	.46	7.28	10.34	1.17	-1.73	.00621	-.00053	0.000000	0.000000	.0167	-.0015	0.0000	0.0000
58	Z	21.39	.43	.46	6.48	11.64	1.05	-1.87	.00601	-.00053	0.000000	0.000000	.0161	-.0015	0.0000	0.0000
59	Z	21.75	.44	.47	5.77	13.04	.93	-2.01	.00582	-.00053	0.000000	0.000000	.0156	-.0015	0.0000	0.0000
60	QD3	22.16	.45	.47	5.35	14.01	-.10	-.27	.00576	.00023	0.000000	0.000000	.0154	.0006	0.0000	0.0000
61	QD3	22.58	.46	.48	5.60	13.47	-.21	1.53	.00602	.00102	0.000000	0.000000	.0161	.0027	0.0000	0.0000
62	R	22.94	.47	.48	6.16	12.38	-.91	1.44	.00639	.00102	0.000000	0.000000	.0171	.0027	0.0000	0.0000
63	R	23.31	.48	.49	6.79	11.16	-.91	1.35	.00676	.00102	0.000000	0.000000	.0181	.0027	0.0000	0.0000
64	R	23.68	.49	.49	7.49	10.40	-1.01	1.26	.00713	.00102	0.000000	0.000000	.0191	.0027	0.0000	0.0000
65	R	24.04	.50	.50	8.27	9.51	-1.11	1.17	.00751	.00102	0.000000	0.000000	.0201	.0027	0.0000	0.0000
66	R	24.91	.51	.50	9.12	8.68	-1.21	1.08	.00788	.00102	0.000000	0.000000	.0211	.0027	0.0000	0.0000
67	R	24.78	.51	.51	10.04	7.93	-1.31	.99	.00825	.00102	0.000000	0.000000	.0221	.0027	0.0000	0.0000
68	R	25.15	.52	.52	11.04	7.25	-1.41	.90	.00863	.00102	0.000000	0.000000	.0230	.0027	0.0000	0.0000
69	R	25.51	.52	.53	12.10	6.61	-1.50	.80	.00900	.00102	0.000000	0.000000	.0240	.0027	0.0000	0.0000
70	R	25.89	.53	.54	13.24	6.06	-1.60	-.71	.00937	.00102	0.000000	0.000000	.0250	.0027	0.0000	0.0000
71	R	26.24	.53	.55	14.46	5.57	-1.70	.62	.00974	.00102	0.000000	0.000000	.0260	.0027	0.0000	0.0000
72	QF	26.59	.54	.56	15.06	5.38	-.00	-.09	.00990	-.00014	0.000000	0.000000	.0264	-.0004	0.0000	0.0000
73	QF	26.94	.55	.57	14.46	5.69	1.69	-.81	.00963	-.00124	0.000000	0.000000	.0257	-.0033	0.0000	0.0000
74	QD	27.98	.55	.59	11.24	7.89	1.42	-1.11	.00832	-.00129	0.000000	0.000000	.0222	-.0035	0.0000	0.0000
75	R	29.64	.58	.63	7.28	12.11	.97	-1.53	.08427	.09351	0.000000	0.000000	.4093	.4705	0.0000	0.0000
76	QD	30.68	.61	.63	5.56	15.39	.70	-1.82	.18159	.09351	0.000000	0.000000	.8965	.4705	0.0000	0.0000
77	QD	31.03	.62	.63	5.31	16.24	.00	-.93	.21824	.11628	0.000000	0.000000	1.0807	.5837	0.0000	0.0000
78	QD	31.38	.63	.64	5.53	15.62	-.69	1.77	.26366	.14372	0.000000	0.000000	1.3085	.7204	0.0000	0.0000
79	QD	32.41	.65	.65	7.27	12.24	-.97	1.49	.41247	.14372	0.000000	0.000000	2.0344	.7204	0.0000	0.0000
80	R	34.07	.68	.68	11.22	7.92	-1.41	1.10	.72943	.23850	0.000000	0.000000	3.6419	1.1944	0.0000	0.0000
81	R	34.81	.69	.69	13.64	6.46	-1.61	.89	.90483	.23850	0.000000	0.000000	4.5203	1.1944	0.0000	0.0000
82	SF	34.81	.69	.69	13.64	6.46	-1.60	.89	.90483	.23793	0.000000	0.000000	4.5203	1.1929	0.0000	0.0000
83	DS	35.11	.70	.70	14.43	5.95	-1.68	.80	.97621	.23793	0.000000	0.000000	4.8762	1.1929	0.0000	0.0000
84	QF	35.46	.70	.71	15.02	5.65	.02	.05	1.03913	.11985	0.000000	0.000000	5.1935	.5998	0.0000	0.0000
85	QF	35.81	.70	.72	14.60	5.87	1.71	-.49	1.05966	-.00312	0.000000	0.000000	5.2958	-.0178	0.0000	0.0000
86	QS	36.11	.71	.73	13.41	6.31	1.62	-.76	1.05872	-.00312	0.000000	0.000000	5.2905	-.0178	0.0000	0.0000
87	SF	36.11	.71	.73	13.41	6.31	1.63	-.77	1.05872	-.00390	0.000000	0.000000	5.2905	-.0198	0.0000	0.0000
88	DS	36.46	.72	.73	11.75	7.29	1.53	-.95	1.05365	-.00390	0.000000	0.000000	5.2750	-.0198	0.0000	0.0000
89	LC	38.91	.76	.77	7.15	11.43	-.98	-1.37	1.04937	-.00390	0.000000	0.000000	5.2430	-.0198	0.0000	0.0000
90	D	39.24	.77	.78	5.86	13.58	-.78	-1.56	1.04650	-.00390	0.000000	0.000000	5.2285	-.0198	0.0000	0.0000
91	SD	39.24	.77	.78	5.86	13.58	-.77	-1.54	1.04650	-.00274	0.000000	0.000000	5.2285	-.0169	0.0000	0.0000
92	DS	39.46	.77	.79	5.42	14.53	-.69	-1.61	1.04268	-.00274	0.000000	0.000000	5.2234	-.0169	0.0000	0.0000
93	QD	39.89	.78	.79	5.18	15.08	-.01	-.05	1.06512	.11749	0.000000	0.000000	5.3259	.5867	0.0000	0.0000
94	QD	40.24	.79	.79	5.41	14.45	-.87	1.71	1.12859	.24245	0.000000	0.000000	5.6374	1.2140	0.0000	0.0000
95	DS	40.54	.80	.80	5.83	13.45	-.75	1.63	1.20133	.24245	0.000000	0.000000	6.0016	1.2140	0.0000	0.0000
96	SD	40.54	.80	.80	5.83	13.45	-.76	1.65	1.20133	.24398	0.000000	0.000000	6.0016	1.2178	0.0000	0.0000
97	D	41.28	.82	.81	7.10	11.19	-.96	1.44	1.38075	.24398	0.000000	0.000000	6.8972	1.2178	0.0000	0.0000
98	LC	42.94	.85	.84	11.03	7.14	-1.41	.99	1.78585	.24398	0.000000	0.000000	8.9192	1.2178	0.0000	0.0000
99	D	43.67	.86	.86	13.24	5.84	-1.61	.78	1.96528	.24398	0.000000	0.000000	9.8148	1.2178	0.0000	0.0000

POS		S (IN)	QX	QY	BX (IN)	BY (IN)	AX	AY	EX (IN)	EXP	EY (IN)	EYP	XCG (INR)	DXCG (INR)	YCG (INR)	DYCG (INR)
100	SF	43.67	.86	.86	13.24	5.84	-1.59	.77	1.96528	.24128	0.000000	0.000000	9.8146	1.2110	0.0000	0.0000
101	QS	43.97	.86	.86	14.22	5.40	-1.67	.69	2.03767	.24128	0.000000	0.000000	10.1761	1.2110	0.0000	0.0000
102	QF	44.32	.87	.87	14.81	5.16	.00	.00	2.08010	.00002	0.000000	0.000000	10.3511	-.0002	0.0000	0.0000
103	QF	44.67	.89	.89	14.22	5.40	1.67	-.69	2.03768	-.24125	0.000000	0.000000	10.1760	-1.2113	0.0000	0.0000
104	QS	44.97	.90	.89	13.24	5.84	1.59	-.77	1.96530	-.24125	0.000000	0.000000	9.8146	-1.2115	0.0000	0.0000
105	SF	44.97	.84	.89	13.24	5.84	1.61	-.78	1.96530	-.24395	0.000000	0.000000	9.8146	-1.2182	0.0000	0.0000
106	Q	45.71	.89	.91	11.02	7.14	1.41	-.99	1.78590	-.24395	0.000000	0.000000	8.9167	-1.2182	0.0000	0.0000
107	S	47.37	.92	.94	7.10	11.10	.96	-1.39	1.45971	-.14917	0.000000	0.000000	7.2911	-.7443	0.0000	0.0000
108	Q	48.11	.93	.95	5.83	13.28	.76	-1.58	1.35001	-.14917	0.000000	0.000000	6.7437	-.7443	0.0000	0.0000
109	SD	48.11	.93	.95	5.83	13.28	.75	-1.56	1.35001	-.14724	0.000000	0.000000	6.7437	-.7394	0.0000	0.0000
110	QS	48.41	.94	.95	5.40	14.24	-.67	-1.64	1.30584	-.14724	0.000000	0.000000	6.5219	-.7394	0.0000	0.0000
111	QD	48.76	.95	.96	5.18	14.82	-.01	-.00	1.28013	.00002	0.000000	0.000000	6.3927	-.0003	0.0000	0.0000
112	QD	49.11	.96	.96	5.42	14.24	-.69	1.63	1.30586	.14728	0.000000	0.000000	6.5217	.7388	0.0000	0.0000
113	QS	49.41	.97	.97	5.85	13.29	-.77	1.55	1.35004	.14729	0.000000	0.000000	6.7433	.7388	0.0000	0.0000
114	SD	49.41	.97	.97	5.85	13.29	-.78	1.57	1.35004	.14921	0.000000	0.000000	6.7433	.7436	0.0000	0.0000
115	D	50.14	.99	.98	7.15	11.12	-.98	1.38	1.45978	.14921	0.000000	0.000000	7.2902	.7436	0.0000	0.0000
116	S	51.80	1.02	1.01	11.16	7.17	-1.44	.98	1.78603	.24399	0.000000	0.000000	8.9167	1.2175	0.0000	0.0000
117	QS	52.34	1.03	1.02	13.42	5.88	-1.64	.78	1.96547	.24399	0.000000	0.000000	9.8121	1.2175	0.0000	0.0000
118	SF	52.54	1.03	1.02	13.42	5.88	-1.62	.77	1.96547	.24130	0.000000	0.000000	9.8121	1.2108	0.0000	0.0000
119	QS	52.84	1.03	1.03	14.41	5.44	-1.70	.69	2.03786	.24130	0.000000	0.000000	10.1753	1.2108	0.0000	0.0000
120	QF	53.19	1.04	1.04	15.02	5.20	-.01	-.00	2.08030	.00001	0.000000	0.000000	10.3882	-.0001	0.0000	0.0000
121	QF	53.54	1.04	1.05	14.43	5.44	1.68	-.70	2.03787	-.24128	0.000000	0.000000	10.1752	-1.2110	0.0000	0.0000
122	QS	53.84	1.04	1.06	13.44	5.89	1.60	-.78	1.96548	-.24128	0.000000	0.000000	9.8119	-1.2110	0.0000	0.0000
123	SF	53.84	1.04	1.06	13.44	5.89	1.62	-.79	1.96548	-.24398	0.000000	0.000000	9.8119	-1.2178	0.0000	0.0000
124	Q	54.58	1.05	1.08	11.20	7.20	1.42	-.99	1.78605	-.24398	0.000000	0.000000	8.9163	-1.2178	0.0000	0.0000
125	S	56.24	1.08	1.11	7.23	11.19	.98	-1.39	1.46982	-.14920	0.000000	0.000000	7.2895	-.7438	0.0000	0.0000
126	D	56.97	1.10	1.12	5.93	13.38	.78	-1.59	1.35010	-.14920	0.000000	0.000000	6.7425	-.7438	0.0000	0.0000
127	SD	56.97	1.10	1.12	5.93	13.38	.77	-1.57	1.35010	-.14727	0.000000	0.000000	6.7425	-.7390	0.0000	0.0000
128	QS	57.27	1.11	1.12	5.49	14.35	.69	-1.65	1.30592	-.14727	0.000000	0.000000	6.5208	-.7390	0.0000	0.0000
129	QD	57.62	1.12	1.13	5.25	14.93	-.00	-.00	1.28019	-.00000	0.000000	0.000000	6.3917	-.0000	0.0000	0.0000
130	QD	57.97	1.13	1.13	5.49	14.35	-.69	1.65	1.30592	.14727	0.000000	0.000000	6.5208	.7390	0.0000	0.0000
131	QS	58.27	1.14	1.13	5.93	13.38	-.77	1.57	1.35010	.14727	0.000000	0.000000	6.7425	.7390	0.0000	0.0000
132	SD	58.27	1.14	1.13	5.93	13.38	-.78	1.59	1.35010	.14920	0.000000	0.000000	6.7425	.7438	0.0000	0.0000
133	D	59.01	1.16	1.14	7.22	11.19	-.98	1.39	1.46982	.14920	0.000000	0.000000	7.2895	.7438	0.0000	0.0000
134	S	60.67	1.19	1.17	11.20	7.20	-1.43	.99	1.78605	.24398	0.000000	0.000000	8.9163	1.2178	0.0000	0.0000
135	Q	61.41	1.20	1.19	13.44	5.89	-1.62	.79	1.96548	.24398	0.000000	0.000000	9.8119	1.2178	0.0000	0.0000
136	SF	61.41	1.20	1.19	13.44	5.89	-1.61	.78	1.96548	.24128	0.000000	0.000000	9.8119	1.2110	0.0000	0.0000
137	QS	61.71	1.20	1.20	14.43	5.44	-1.68	.70	2.03786	.24128	0.000000	0.000000	10.1752	1.2110	0.0000	0.0000
138	QF	62.06	1.20	1.21	15.03	5.20	.01	.00	2.08029	-.00001	0.000000	0.000000	10.3882	.0001	0.0000	0.0000
139	QF	62.41	1.21	1.22	14.42	5.44	1.70	-.69	2.03786	-.24130	0.000000	0.000000	10.1753	-1.2108	0.0000	0.0000
140	QS	62.71	1.21	1.23	13.42	5.88	1.62	-.77	1.96547	-.24130	0.000000	0.000000	9.8120	-1.2108	0.0000	0.0000
141	SF	62.71	1.21	1.23	13.42	5.88	1.64	-.78	1.96547	-.24399	0.000000	0.000000	9.8120	-1.2175	0.0000	0.0000
142	Q	63.44	1.22	1.25	11.16	7.18	1.44	-.98	1.78603	-.24399	0.000000	0.000000	8.9166	-1.2175	0.0000	0.0000
143	S	65.10	1.25	1.28	7.12	11.12	.98	-1.38	1.45977	-.14921	0.000000	0.000000	7.2901	-.7436	0.0000	0.0000
144	D	65.84	1.27	1.29	5.86	13.29	.78	-1.57	1.35004	-.14921	0.000000	0.000000	6.7433	-.7436	0.0000	0.0000
145	SD	65.84	1.27	1.29	5.86	13.29	.77	-1.55	1.35004	-.14728	0.000000	0.000000	6.7433	-.7388	0.0000	0.0000
146	QS	66.14	1.28	1.29	5.42	14.25	.69	-1.63	1.30585	0.000000	0.000000	0.000000	6.5216	-.7388	0.0000	0.0000
147	QD	66.49	1.29	1.29	5.16	14.83	.01	.00	1.28012	-.00002	0.000000	0.000000	6.3926	.0003	0.0000	0.0000
148	QD	66.84	1.30	1.30	5.41	14.24	-.67	1.64	1.30583	.14724	0.000000	0.000000	6.5218	.7394	0.0000	0.0000
149	QS	67.14	1.31	1.30	5.83	13.28	-.75	1.56	1.35001	.14724	0.000000	0.000000	6.7437	.7394	0.0000	0.0000

POS		S (IN)	QX	QY	BX (IN)	BY (IN)	AX	AY	EX (IN)	EXP	EY (IN)	EYP	XCC (MM)	DXCO (MR)	YCO (MR)	DYCO (MR)
150	SD	67.14	1:31	1:30	5.83	13.28	-.76	1.58	1.35001	.14917	0.000000	0.000000	9.7437	.7443	0.0000	0.0000
151	O	67.87	1:32	1:31	7.10	11.10	-.96	1.39	1.45971	.14917	0.000000	0.000000	7.2910	.7443	0.0000	0.0000
152	B	69.64	1:35	1:34	11.03	7.14	-1.41	.99	1.78589	.24394	0.000000	0.000000	8.9186	1.2182	0.0000	0.0000
153	O	70.27	1:36	1:36	13.24	5.84	-1.61	.78	1.96529	.24394	0.000000	0.000000	9.8145	1.2182	0.0000	0.0000
154	SF	70.27	1:36	1:36	13.24	5.84	-1.59	.77	1.96529	.24125	0.000000	0.000000	9.8145	1.2115	0.0000	0.0000
155	OS	70.57	1:37	1:37	14.22	5.40	-1.67	.69	2.03767	.24125	0.000000	0.000000	10.1779	1.2115	0.0000	0.0000
156	OF	70.92	1:37	1:38	14.81	5.16	.00	.00	2.08009	-.00002	0.000000	0.000000	10.3910	.0002	0.0000	0.0000
157	OF	71.29	1:37	1:39	14.22	5.40	1.67	-.69	2.03765	-.24128	0.000000	0.000000	10.1781	-1.2110	0.0000	0.0000
158	OS	71.57	1:38	1:40	13.24	5.84	1.59	-.77	1.96527	-.24128	0.000000	0.000000	9.8147	-1.2110	0.0000	0.0000
159	SF	71.57	1:38	1:40	13.24	5.84	1.61	-.78	1.96527	-.24398	0.000000	0.000000	9.8147	-1.2178	0.0000	0.0000
160	O	72.31	1:39	1:41	11.02	7.14	1.41	-.99	1.78584	-.24398	0.000000	0.000000	8.9192	-1.2178	0.0000	0.0000
161	B	73.97	1:42	1:44	7.10	11.10	.96	-1.39	1.45961	-.14920	0.000000	0.000000	7.2923	-.7438	0.0000	0.0000
162	O	74.70	1:43	1:45	5.83	13.28	.76	-1.56	1.34989	-.14920	0.000000	0.000000	6.7493	-.7438	0.0000	0.0000
163	SD	74.70	1:44	1:45	5.83	13.28	.75	-1.56	1.34989	-.14727	0.000000	0.000000	6.7493	-.7390	0.0000	0.0000
164	OS	75.00	1:44	1:46	5.41	14.24	.67	-1.64	1.30571	-.14727	0.000000	0.000000	6.5236	-.7390	0.0000	0.0000
165	OD	75.26	1:46	1:46	5.18	14.82	-.01	-.00	1.27998	-.00002	0.000000	0.000000	6.3946	-.0003	0.0000	0.0000
166	OD	75.71	1:47	1:47	5.42	14.25	-.69	1.63	1.30569	.14722	0.000000	0.000000	6.5238	.7397	0.0000	0.0000
167	OS	76.01	1:47	1:47	5.86	13.29	-.77	1.55	1.34986	.14722	0.000000	0.000000	6.7457	.7397	0.0000	0.0000
168	SD	76.01	1:47	1:47	5.86	13.29	-.78	1.57	1.34986	.14913	0.000000	0.000000	6.7457	.7445	0.0000	0.0000
169	O	76.44	1:48	1:48	7.18	11.12	-.98	1.38	1.45958	.14913	0.000000	0.000000	7.2932	.7445	0.0000	0.0000
170	B	78.40	1:52	1:51	11.16	7.17	-1.44	.98	1.78570	.24393	0.000000	0.000000	8.9211	1.2184	0.0000	0.0000
171	O	79.14	1:53	1:53	13.42	5.88	-1.64	.78	1.96510	.24393	0.000000	0.000000	9.8172	1.2184	0.0000	0.0000
172	SF	79.14	1:53	1:53	13.42	5.88	-1.62	.77	1.96510	.24123	0.000000	0.000000	9.8172	1.2117	0.0000	0.0000
173	OS	79.44	1:54	1:54	14.43	5.44	-1.70	.69	2.03747	.24123	0.000000	0.000000	10.1807	1.2117	0.0000	0.0000
174	OF	79.79	1:55	1:55	15.02	5.20	-.01	-.00	2.07989	-.00001	0.000000	0.000000	10.3938	.0001	0.0000	0.0000
175	OF	80.14	1:55	1:56	14.43	5.44	1.69	-.70	2.02746	-.24125	0.000000	0.000000	10.1808	-1.2115	0.0000	0.0000
176	OS	80.44	1:55	1:56	13.44	5.89	1.61	-.78	1.96509	-.24125	0.000000	0.000000	9.8174	-1.2115	0.0000	0.0000
177	SF	80.44	1:55	1:56	13.44	5.89	1.62	-.79	1.96509	-.24394	0.000000	0.000000	9.8174	-1.2182	0.0000	0.0000
178	O	81.17	1:56	1:58	11.20	7.20	1.42	-.99	1.78568	-.24394	0.000000	0.000000	8.9214	-1.2182	0.0000	0.0000
179	B	83.84	1:59	1:61	7.23	11.19	.98	-1.39	1.45950	-.14917	0.000000	0.000000	7.2939	-.7443	0.0000	0.0000
180	O	85.57	2:00	1:62	5.93	13.38	.78	-1.59	1.34980	-.14917	0.000000	0.000000	6.7465	-.7443	0.0000	0.0000
181	SD	85.87	2:00	1:62	5.93	13.38	.77	-1.57	1.34980	-.14724	0.000000	0.000000	6.7465	-.7394	0.0000	0.0000
182	OS	86.22	2:01	1:63	5.49	14.34	.69	-1.65	1.30563	-.14724	0.000000	0.000000	6.5247	-.7394	0.0000	0.0000
183	OD	87.22	2:02	1:63	5.25	14.93	-.00	.00	1.27991	.00000	0.000000	0.000000	6.3955	-.0000	0.0000	0.0000
184	REFL	168.44	3.24	3.26	17.79	5.90	-.00	.00	-.01098	.00000	0.000000	0.000000	-.0294	0.0000	0.0000	0.0000

CIRCUMFERENCE = 505.3257 M THETY(1831) = 6.28318638 RAD NUX = 9.73193 DNUX/(DP/P) = .41404
(25751/4096)PI = .0074883 M THETY(1831) = 0.00000000 RAD NUY = 9.77149 DNUY/(DP/P) = .36032
THEAM = (7.63240, 0.00000)

MAXIMA --- BETX(134) = 17.78972 BETY(12) = 17.18421 ETAX(120) = 2.08030 ETAY(184) = 0.00000
MINIMA --- BETX(36) = 4.09089 BETY(48) = 3.30098 ETAX(33) = -.00003 ETAY(184) = 0.00000

*** TUCB 1 // DR .005000 VALUE = .010000

SUB. CHR ; ITER. 7

CALCULATION OF THE EQUILIBRIUM ORBIT AND BETATRON FUNCTIONS OF AGR .
INITIAL REFERENCE RAY DEFINED BY V
X_2 = -.00332944 DX = 0.00000000 Y = 0.00000000 DY = 0.00000000 DS = 0.00000000 DP/P = .01000000 1.00000000

7X7 MATRIX FOR AGR

	.03398034	17.72745044	0.00000000	0.00000000	0.00000000	-.02078433	.00010538
	-.05634456	.03398034	0.00000000	0.00000000	0.00000000	-.00121228	.00000615
	0.00000000	0.00000000	-.05047040	6.04994201	0.00000000	0.00000000	0.00000000
	0.00000000	0.00000000	-.16486980	-.05047040	0.00000000	0.00000000	0.00000000
	.00121228	.02078433	0.00000000	0.00000000	1.00000000	-2.90377804	-.02793087
	0.00000000	0.00000000	0.00000000	0.00000000	0.00000000	1.00000000	0.00000000
	0.00000000	0.00000000	0.00000000	0.00000000	0.00000000	0.00000000	1.00000000

EIGENVALUES OF THE 4X4 SUBMATRIX

X... LMD1 = (.03398034 .99942250); C(1) = 1.00000000; MU(1) = 1.53680944 RAD, Q(1) = .73377246
1/LMD1 = (.03398034 -.99942250); C(2) = 1.00000000; MU(2) = -1.53680944 RAD, Q(2) = .26622754

Y... LMD3 = (-.05047040 .99872556); C(3) = 1.00000000; MU(3) = 1.62128618 RAD, Q(3) = .77410808
1/LMD3 = (-.05047040 -.99872556); C(4) = 1.00000000; MU(4) = -1.62128618 RAD, Q(4) = .22589192

EIGENVALUE = (.03398034, .99942250), EIGENVECTOR = (4.21161417, 0.00000000)
(0.00000000, -.23743865)
(0.00000000, 0.00000000)
(0.00000000, 0.00000000)

EIGENVALUE = (.03398034, -.99942250), EIGENVECTOR = (4.21161417, 0.00000000)
(0.00000000, -.23743865)
(0.00000000, 0.00000000)
(0.00000000, 0.00000000)

EIGENVALUE = (-.05047040, .99872556), EIGENVECTOR = (0.00000000, 0.00000000)
(0.00000000, 0.00000000)
(2.46123184, 0.00000000)
(.00000000, .40630061)

EIGENVALUE = (-.05047040, -.99872556), EIGENVECTOR = (0.00000000, 0.00000000)
(0.00000000, 0.00000000)
(2.46123184, 0.00000000)
(.00000000, -.40630061)

	X	DX	Y	DY	DS	DP/P	
EQ ORBIT	-.00010986	0.00000000	0.00000000	0.00000000	0.00000000	.01000000	1.00000000
ETA ORBIT	-.02151543	-.00000000	0.00000000	0.00000000	0.00000000	1.00000000	0.00000000

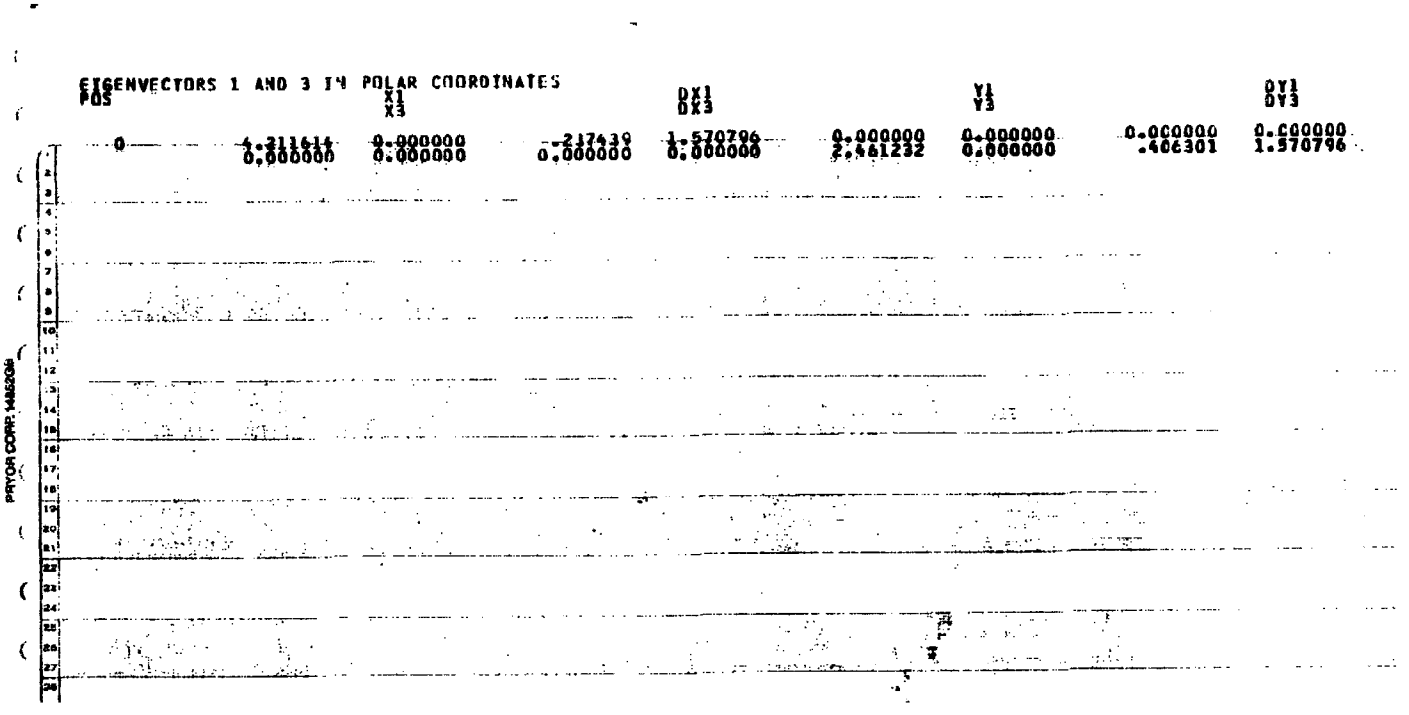

BETATRON FUNCTIONS OF AGR

POS		S (M)	QX	QY	BX (M)	BY (M)	AX	AY	EX (M)	EXP	EY (M)	EYP	XCO (MM)	DXCO (MM)	YCO (MM)	DYCO (MM)
0		0.00	0.00	0.00	17.74	6.06	0.00	0.00	-.02152	-.00000	0.000000	0.000000	-.1099	0.0000	0.0000	0.0000
1	QF1	.38	.00	.01	16.94	6.36	2.23	-.88	-.02103	.00278	0.000000	0.000000	-.1073	.0143	0.0000	0.0000
2	S	.72	.01	.02	15.32	7.05	2.10	-.98	-.01999	.00278	0.000000	0.000000	-.1020	.0143	0.0000	0.0000
3	S	1.10	.01	.03	13.81	7.83	1.97	-1.09	-.01895	.00278	0.000000	0.000000	-.0967	.0143	0.0000	0.0000
4	S	1.47	.02	.03	12.38	8.67	1.84	-1.19	-.01791	.00278	0.000000	0.000000	-.0914	.0143	0.0000	0.0000
5	S	1.84	.02	.04	11.06	9.60	1.71	-1.29	-.01687	.00278	0.000000	0.000000	-.0860	.0143	0.0000	0.0000
6	S	2.22	.03	.05	9.84	10.60	1.57	-1.40	-.01583	.00278	0.000000	0.000000	-.0807	.0143	0.0000	0.0000
7	S	2.59	.03	.05	8.71	11.69	1.44	-1.50	-.01480	.00278	0.000000	0.000000	-.0754	.0143	0.0000	0.0000
8	S	2.96	.04	.06	7.68	12.84	1.31	-1.60	-.01376	.00278	0.000000	0.000000	-.0700	.0143	0.0000	0.0000
9	S	3.34	.05	.06	6.76	14.08	1.18	-1.71	-.01272	.00278	0.000000	0.000000	-.0647	.0143	0.0000	0.0000
10	S	3.71	.06	.06	5.93	15.39	1.05	-1.81	-.01168	.00278	0.000000	0.000000	-.0594	.0143	0.0000	0.0000
11	S	4.08	.07	.07	5.19	16.79	.91	-1.92	-.01064	.00278	0.000000	0.000000	-.0541	.0143	0.0000	0.0000
12	QD1	4.43	.08	.07	4.60	17.43	.22	.11	-.00988	.00156	0.000000	0.000000	-.0502	.0080	0.0000	0.0000
13	QD1	4.78	.09	.07	4.87	16.63	-.43	2.13	-.00954	.00040	0.000000	0.000000	-.0484	.0021	0.0000	0.0000
14	S	5.16	.10	.08	5.23	15.09	-.52	2.00	-.00940	.00040	0.000000	0.000000	-.0476	.0021	0.0000	0.0000
15	S	5.53	.11	.08	5.66	13.64	-.61	1.88	-.00925	.00040	0.000000	0.000000	-.0468	.0021	0.0000	0.0000
16	S	5.90	.12	.09	6.15	12.29	-.71	1.75	-.00910	.00040	0.000000	0.000000	-.0460	.0021	0.0000	0.0000
17	S	6.28	.13	.09	6.71	11.02	-.80	1.63	-.00895	.00040	0.000000	0.000000	-.0452	.0021	0.0000	0.0000
18	S	6.65	.14	.10	7.34	9.85	-.89	1.51	-.00880	.00040	0.000000	0.000000	-.0445	.0021	0.0000	0.0000
19	S	7.02	.15	.10	8.03	8.78	-.98	1.38	-.00866	.00040	0.000000	0.000000	-.0437	.0021	0.0000	0.0000
20	S	7.39	.16	.11	8.80	7.79	-1.07	1.26	-.00851	.00040	0.000000	0.000000	-.0429	.0021	0.0000	0.0000
21	S	7.77	.16	.12	9.63	6.90	-1.16	1.14	-.00836	.00040	0.000000	0.000000	-.0421	.0021	0.0000	0.0000
22	S	8.14	.17	.12	10.53	6.10	-1.25	1.01	-.00821	.00040	0.000000	0.000000	-.0413	.0021	0.0000	0.0000
23	S	8.51	.17	.13	11.50	5.39	-1.34	.89	-.00806	.00040	0.000000	0.000000	-.0405	.0021	0.0000	0.0000
24	QF2	8.86	.18	.13	12.34	5.03	.08	.16	-.00775	.00138	0.000000	0.000000	-.0389	.0071	0.0000	0.0000
25	QF2	9.22	.18	.16	11.38	5.16	1.49	-.55	-.00710	.00230	0.000000	0.000000	-.0356	.0117	0.0000	0.0000
26	S	9.59	.19	.17	10.31	5.61	1.38	-.64	-.00624	.00230	0.000000	0.000000	-.0312	.0117	0.0000	0.0000
27	S	9.96	.20	.18	9.32	6.12	1.28	-.74	-.00538	.00230	0.000000	0.000000	-.0268	.0117	0.0000	0.0000
28	S	10.33	.20	.19	8.40	6.70	1.17	-.83	-.00452	.00230	0.000000	0.000000	-.0225	.0117	0.0000	0.0000
29	S	10.71	.21	.20	7.57	7.36	1.07	-.92	-.00366	.00230	0.000000	0.000000	-.0181	.0117	0.0000	0.0000
30	S	11.08	.22	.21	6.81	8.08	.96	-1.02	-.00281	.00230	0.000000	0.000000	-.0137	.0117	0.0000	0.0000
31	S	11.45	.23	.21	6.13	8.88	.86	-1.11	-.00195	.00230	0.000000	0.000000	-.0093	.0117	0.0000	0.0000
32	S	11.83	.24	.22	5.53	9.74	.75	-1.21	-.00109	.00230	0.000000	0.000000	-.0050	.0117	0.0000	0.0000
33	S	12.20	.25	.23	5.01	10.63	.65	-1.30	-.00023	.00230	0.000000	0.000000	-.0006	.0117	0.0000	0.0000
34	S	12.57	.26	.23	4.57	11.68	.54	-1.39	.00063	.00230	0.000000	0.000000	.0038	.0117	0.0000	0.0000
35	S	12.95	.27	.24	4.20	12.76	-.43	-1.49	.00149	.00230	0.000000	0.000000	.0082	.0117	0.0000	0.0000
36	QD2	13.30	.29	.24	4.13	13.21	-.21	.22	.00234	.00256	0.000000	0.000000	.0125	.0131	0.0000	0.0000
37	QD2	13.65	.30	.25	4.31	13.46	-.89	1.89	.00330	.00293	0.000000	0.000000	.0174	.0151	0.0000	0.0000
38	R	14.01	.31	.25	4.81	13.15	-1.04	1.76	.00438	.00293	0.000000	0.000000	.0230	.0151	0.0000	0.0000
39	R	14.38	.32	.26	5.03	9.87	-1.18	1.62	.00545	.00293	0.000000	0.000000	.0285	.0151	0.0000	0.0000
40	R	14.75	.33	.26	6.95	8.73	-1.33	1.49	.00653	.00293	0.000000	0.000000	.0341	.0151	0.0000	0.0000
41	R	15.11	.34	.27	7.98	7.80	-1.48	1.35	.00760	.00293	0.000000	0.000000	.0396	.0151	0.0000	0.0000
42	R	15.48	.35	.28	9.11	6.93	-1.62	1.22	.00868	.00293	0.000000	0.000000	.0451	.0151	0.0000	0.0000
43	R	15.85	.35	.29	10.36	5.90	-1.77	1.08	.00975	.00293	0.000000	0.000000	.0507	.0151	0.0000	0.0000
44	R	16.21	.36	.30	11.71	5.16	-1.91	.95	.01083	.00293	0.000000	0.000000	.0562	.0151	0.0000	0.0000
45	R	16.58	.36	.31	13.17	4.51	-2.06	.81	.01191	.00293	0.000000	0.000000	.0618	.0151	0.0000	0.0000
46	R	16.95	.37	.32	14.73	3.96	-2.21	.68	.01298	.00293	0.000000	0.000000	.0673	.0151	0.0000	0.0000
47	R	17.32	.37	.34	16.40	3.52	-2.35	.54	.01406	.00293	0.000000	0.000000	.0729	.0151	0.0000	0.0000
48	QF3	17.73	.37	.36	17.46	3.31	-.15	-.04	.01488	-.00101	0.000000	0.000000	.0771	-.0051	0.0000	0.0000
49	QF3	18.12	.38	.38	16.64	3.58	2.08	-.63	.01488	-.00097	0.000000	0.000000	.0770	-.0052	0.0000	0.0000

POS		S (M)	DX	DY	BX (M)	BY (M)	AX	AY	EX (M)	EXP	EY (M)	EYP	XCC (MM)	DXCO (MM)	YCC (MM)	DYCO (MM)
50	Z	18.50	.38	.39	15.18	4.09	1.97	-.77	.01453	-.00097	0.000000	0.000000	.0751	-.0052	0.0000	0.0000
51	Z	18.86	.39	.41	13.81	4.70	1.85	-.91	.01418	-.00097	0.000000	0.000000	.0733	-.0052	0.0000	0.0000
52	Z	19.22	.39	.42	12.52	5.41	1.74	-1.04	.01383	-.00097	0.000000	0.000000	.0714	-.0052	0.0000	0.0000
53	Z	19.58	.40	.43	11.30	6.25	1.62	-1.19	.01348	-.00097	0.000000	0.000000	.0695	-.0052	0.0000	0.0000
54	Z	19.95	.40	.44	10.18	7.13	1.50	-1.33	.01313	-.00097	0.000000	0.000000	.0676	-.0052	0.0000	0.0000
55	Z	20.31	.41	.44	9.13	8.14	1.39	-1.48	.01278	-.00097	0.000000	0.000000	.0657	-.0052	0.0000	0.0000
56	Z	20.67	.41	.45	8.17	9.26	1.27	-1.62	.01243	-.00097	0.000000	0.000000	.0638	-.0052	0.0000	0.0000
57	Z	21.03	.42	.46	7.30	10.47	1.16	-1.76	.01208	-.00097	0.000000	0.000000	.0620	-.0052	0.0000	0.0000
58	Z	21.39	.43	.46	6.51	11.79	1.04	-1.90	.01173	-.00097	0.000000	0.000000	.0601	-.0052	0.0000	0.0000
59	Z	21.75	.44	.47	5.80	13.21	.93	-2.04	.01138	-.00097	0.000000	0.000000	.0582	-.0052	0.0000	0.0000
60	QD3	22.16	.45	.47	5.36	14.18	.09	-.28	.01128	.00052	0.000000	0.000000	.0576	.0024	0.0000	0.0000
61	QD3	22.58	.46	.47	5.64	13.65	-.72	1.54	.01181	.00204	0.000000	0.000000	.0602	.0102	0.0000	0.0000
62	F	23.04	.47	.48	6.20	12.86	-.82	1.45	.01256	.00204	0.000000	0.000000	.0640	.0102	0.0000	0.0000
63	R	23.31	.48	.48	6.84	11.53	-.92	1.36	.01331	.00204	0.000000	0.000000	.0677	.0102	0.0000	0.0000
64	R	23.68	.49	.49	7.54	10.57	-1.02	1.27	.01405	.00204	0.000000	0.000000	.0715	.0102	0.0000	0.0000
65	R	24.04	.50	.50	8.33	9.67	-1.11	1.18	.01480	.00204	0.000000	0.000000	.0752	.0102	0.0000	0.0000
66	R	24.41	.50	.50	9.18	8.84	-1.21	1.09	.01555	.00204	0.000000	0.000000	.0790	.0102	0.0000	0.0000
67	R	24.78	.51	.51	10.10	8.03	-1.31	1.00	.01630	.00204	0.000000	0.000000	.0828	.0102	0.0000	0.0000
68	R	25.14	.52	.52	11.10	7.38	-1.41	.91	.01705	.00204	0.000000	0.000000	.0865	.0102	0.0000	0.0000
69	R	25.51	.52	.52	12.17	6.75	-1.51	.82	.01780	.00204	0.000000	0.000000	.0903	.0102	0.0000	0.0000
70	R	25.88	.52	.53	13.32	6.18	-1.61	.72	.01855	.00204	0.000000	0.000000	.0940	.0102	0.0000	0.0000
71	R	26.24	.53	.54	14.53	5.68	-1.71	.63	.01929	.00204	0.000000	0.000000	.0978	.0102	0.0000	0.0000
72	QF	26.59	.53	.55	15.14	5.49	-.01	-.08	.01961	-.00023	0.000000	0.000000	.0995	-.0013	0.0000	0.0000
73	QF	26.94	.54	.56	14.55	5.81	1.69	-.82	.01916	-.00249	0.000000	0.000000	.0969	-.0128	0.0000	0.0000
74	QD	27.98	.55	.59	11.33	7.80	1.42	-1.11	.01656	-.00249	0.000000	0.000000	.0836	-.0128	0.0000	0.0000
75	B	29.64	.58	.62	7.32	12.21	.98	-1.53	.09064	.09184	0.000000	0.000000	.8443	.9305	0.0000	0.0000
76	QD	30.68	.60	.63	5.63	15.66	.70	-1.81	.18573	.09184	0.000000	0.000000	1.8078	.9305	0.0000	0.0000
77	QD	31.03	.61	.63	5.39	16.31	.00	-.02	.22183	.11482	0.000000	0.000000	2.1724	1.1571	0.0000	0.0000
78	QD	31.38	.62	.63	5.61	15.69	-.70	1.78	.26675	.14237	0.000000	0.000000	2.6244	1.4303	0.0000	0.0000
79	QD	32.41	.65	.65	7.35	12.29	-.97	1.50	.41417	.14237	0.000000	0.000000	4.1054	1.4303	0.0000	0.0000
80	B	34.07	.68	.67	11.30	7.94	-1.41	1.10	.72860	.23667	0.000000	0.000000	7.2595	2.3734	0.0000	0.0000
81	QF	34.81	.69	.69	13.51	6.47	-1.60	.90	.90268	.23667	0.000000	0.000000	9.0050	2.3734	0.0000	0.0000
82	QF	34.81	.69	.69	13.51	6.47	-1.58	.89	.90268	.23554	0.000000	0.000000	9.0050	2.3677	0.0000	0.0000
83	QS	35.11	.69	.70	14.49	5.96	-1.66	.81	.97131	.23554	0.000000	0.000000	9.7133	2.3677	0.0000	0.0000
84	QF	35.46	.70	.71	15.07	5.66	.03	.06	1.03566	.11900	0.000000	0.000000	10.3414	1.1925	0.0000	0.0000
85	QF	35.81	.70	.72	14.45	5.87	1.72	-.68	1.05618	-.00234	0.000000	0.000000	10.5456	-.0313	0.0000	0.0000
86	QS	36.11	.70	.72	13.44	6.30	1.61	-.75	1.05548	-.00234	0.000000	0.000000	10.5362	-.0313	0.0000	0.0000
87	SF	36.11	.70	.72	13.44	6.30	1.65	-.76	1.03548	-.00388	0.000000	0.000000	10.3362	-.0391	0.0000	0.0000
88	D	36.81	.71	.74	11.16	7.56	1.45	-.99	1.05263	-.00388	0.000000	0.000000	10.5079	-.0391	0.0000	0.0000
89	LC	38.81	.74	.77	7.11	11.40	.99	-1.36	1.04618	-.00388	0.000000	0.000000	10.4427	-.0391	0.0000	0.0000
90	Q	39.24	.74	.78	5.81	13.54	.78	-1.55	1.04333	-.00388	0.000000	0.000000	10.4139	-.0391	0.0000	0.0000
91	SD	39.24	.76	.78	5.81	13.54	.77	-1.52	1.04333	-.00160	0.000000	0.000000	10.4139	-.0276	0.0000	0.0000
92	DS	39.86	.77	.78	5.97	14.47	.69	-1.59	1.04285	-.00160	0.000000	0.000000	10.4057	-.0276	0.0000	0.0000
93	QD	40.89	.78	.79	9.13	15.02	.02	-.06	1.06303	.11714	0.000000	0.000000	10.6050	1.1664	0.0000	0.0000
94	QD	40.24	.79	.79	5.35	14.39	-.66	1.70	1.12551	.24054	0.000000	0.000000	11.2306	2.4125	0.0000	0.0000
95	DS	40.84	.80	.79	6.77	13.39	-.74	1.62	1.19767	.24054	0.000000	0.000000	11.9544	2.4125	0.0000	0.0000
96	SD	40.84	.80	.79	6.77	13.39	-.75	1.66	1.19767	.24355	0.000000	0.000000	11.9544	2.4275	0.0000	0.0000
97	D	41.28	.82	.80	7.01	11.11	-.95	1.39	1.17670	.24355	0.000000	0.000000	11.7307	2.4275	0.0000	0.0000
98	LC	42.94	.85	.83	10.91	7.06	-1.40	.99	1.20117	.24355	0.000000	0.000000	11.7704	2.4275	0.0000	0.0000
99	O	43.67	.86	.85	13.12	5.76	-1.60	.78	1.96028	.24355	0.000000	0.000000	19.5557	2.4275	0.0000	0.0000

POS		S (M)	QX	QY	BX (M)	BY (M)	AX	AY	EX (M)	EXP	EY (M)	EYP	XCO (MM)	DXCO (MR)	YCO (MM)	DYCO (MR)
100	SF	43.67	.86	.85	13.12	5.76	-1.56	.77	1.96028	.23823	0.000000	0.000000	19.5557	2.4009	0.0000	0.0000
101	QS	43.97	.86	.86	14.08	5.33	-1.64	.68	2.03175	.23823	0.000000	0.000000	20.2759	2.4009	0.0000	0.0000
102	QF	44.32	.87	.87	14.66	5.00	.00	.00	2.07367	.00009	0.000000	0.000000	20.6982	.0001	0.0000	0.0000
103	QF	44.67	.87	.88	14.08	5.33	1.64	-.68	2.03181	-.23806	0.000000	0.000000	20.2760	-2.4008	0.0000	0.0000
104	QS	44.97	.87	.89	13.11	5.76	1.57	-.76	1.96039	-.23806	0.000000	0.000000	19.5557	-2.4008	0.0000	0.0000
105	SF	44.97	.87	.89	13.11	5.76	1.60	-.78	1.96039	-.24338	0.000000	0.000000	19.5557	-2.4274	0.0000	0.0000
106	Q	45.71	.88	.91	10.91	7.05	1.40	-.98	1.78140	-.24338	0.000000	0.000000	17.7765	-2.4274	0.0000	0.0000
107	B	47.37	.91	.94	7.00	11.02	.95	-1.39	1.43546	-.14909	0.000000	0.000000	14.5248	-1.4843	0.0000	0.0000
108	Q	48.11	.93	.95	5.75	13.21	.75	-1.59	1.34581	-.14909	0.000000	0.000000	13.4332	-1.4843	0.0000	0.0000
109	SD	48.11	.93	.95	5.75	13.21	.73	-1.55	1.34581	-.14529	0.000000	0.000000	13.4332	-1.4653	0.0000	0.0000
110	QS	48.41	.94	.95	5.33	14.16	.65	-1.63	1.30223	-.14529	0.000000	0.000000	12.9936	-1.4653	0.0000	0.0000
111	QF	48.76	.95	.96	5.11	14.74	.02	-.01	1.27687	.00013	0.000000	0.000000	12.7377	.0001	0.0000	0.0000
112	QF	49.11	.96	.96	5.36	14.17	-.69	1.61	1.30232	.14555	0.000000	0.000000	12.9937	1.4655	0.0000	0.0000
113	QS	49.41	.97	.96	5.79	13.23	-.77	1.53	1.34598	.14555	0.000000	0.000000	13.4333	1.4655	0.0000	0.0000
114	SD	49.41	.97	.96	5.79	13.23	-.79	1.57	1.34598	.14935	0.000000	0.000000	13.4333	1.4845	0.0000	0.0000
115	Q	50.14	.98	.97	7.10	11.06	-.99	1.38	1.45582	.14935	0.000000	0.000000	14.5251	1.4845	0.0000	0.0000
116	B	51.81	1.02	1.00	11.16	7.13	-1.46	.98	1.78221	.24364	0.000000	0.000000	17.7711	2.4276	0.0000	0.0000
117	Q	52.56	1.03	1.02	13.46	5.84	-1.66	.78	1.96140	.24364	0.000000	0.000000	19.5565	2.4276	0.0000	0.0000
118	SF	52.56	1.03	1.02	13.46	5.84	-1.62	.76	1.96140	.23833	0.000000	0.000000	19.5564	2.4010	0.0000	0.0000
119	QS	52.84	1.03	1.03	14.45	5.40	-1.70	.68	2.03290	.23833	0.000000	0.000000	20.2767	2.4010	0.0000	0.0000
120	QF	53.19	1.04	1.04	15.07	5.17	-.02	-.01	2.07482	-.00005	0.000000	0.000000	20.6990	.0000	0.0000	0.0000
121	QF	53.54	1.04	1.05	14.48	5.42	1.67	-.70	2.03293	-.23824	0.000000	0.000000	20.2768	-2.4009	0.0000	0.0000
122	SF	53.84	1.04	1.06	13.50	5.86	1.59	-.78	1.96146	-.23824	0.000000	0.000000	19.5565	-2.4009	0.0000	0.0000
123	SF	53.84	1.04	1.06	13.50	5.86	1.63	-.80	1.96146	-.24339	0.000000	0.000000	19.5565	-2.4276	0.0000	0.0000
124	Q	54.58	1.06	1.08	11.24	7.19	1.43	-1.01	1.78234	-.24339	0.000000	0.000000	17.7712	-2.4276	0.0000	0.0000
125	B	56.24	1.08	1.13	7.23	11.21	.98	-1.41	1.46610	-.14926	0.000000	0.000000	14.5252	-1.4845	0.0000	0.0000
126	Q	56.97	1.10	1.13	5.04	13.45	.78	-1.61	1.34832	-.14926	0.000000	0.000000	13.4335	-1.4845	0.0000	0.0000
127	SD	56.97	1.10	1.13	5.04	13.45	.77	-1.57	1.34832	-.14546	0.000000	0.000000	13.4335	-1.4654	0.0000	0.0000
128	QS	57.27	1.11	1.13	5.50	14.42	.69	-1.65	1.30269	-.14546	0.000000	0.000000	12.9939	-1.4654	0.0000	0.0000
129	QS	57.61	1.12	1.13	5.27	15.00	-.00	-.00	1.27728	.00000	0.000000	0.000000	12.7379	.0000	0.0000	0.0000
130	QD	57.98	1.13	1.13	5.50	14.42	-.69	1.65	1.30269	.14547	0.000000	0.000000	12.9939	1.4654	0.0000	0.0000
131	QS	58.28	1.14	1.13	5.04	13.45	-.77	1.57	1.34833	.14547	0.000000	0.000000	13.4335	1.4654	0.0000	0.0000
132	SF	58.28	1.14	1.13	5.04	13.45	-.78	1.61	1.34833	.14927	0.000000	0.000000	13.4335	1.4845	0.0000	0.0000
133	Q	59.01	1.15	1.14	7.24	11.23	-.98	1.41	1.45911	.14927	0.000000	0.000000	14.5253	1.4845	0.0000	0.0000
134	B	60.67	1.18	1.17	11.26	7.20	-1.44	1.00	1.78237	.24356	0.000000	0.000000	17.7712	2.4276	0.0000	0.0000
135	Q	61.41	1.19	1.19	13.52	5.87	-1.64	.80	1.96149	.24356	0.000000	0.000000	19.5565	2.4276	0.0000	0.0000
136	SF	61.71	1.19	1.19	13.52	5.87	-1.60	.78	1.96149	.23824	0.000000	0.000000	19.5565	2.4009	0.0000	0.0000
137	QS	61.71	1.20	1.20	14.50	5.42	-1.68	.70	2.03296	.23824	0.000000	0.000000	20.2768	2.4009	0.0000	0.0000
138	QF	62.06	1.20	1.21	15.09	5.18	.02	.01	2.07865	.00004	0.000000	0.000000	20.6950	.0000	0.0000	0.0000
139	QF	62.41	1.20	1.22	14.48	5.41	1.71	-.68	2.03294	-.23833	0.000000	0.000000	20.2768	-2.4010	0.0000	0.0000
140	QS	62.71	1.21	1.23	13.48	5.84	1.63	-.76	1.96144	-.23833	0.000000	0.000000	19.5565	-2.4010	0.0000	0.0000
141	SF	62.71	1.21	1.23	13.48	5.84	1.66	-.78	1.96144	-.24364	0.000000	0.000000	19.5565	-2.4276	0.0000	0.0000
142	Q	63.46	1.22	1.24	11.19	7.14	1.46	-.98	1.78225	-.24364	0.000000	0.000000	17.7711	-2.4276	0.0000	0.0000
143	B	65.11	1.25	1.27	7.12	11.08	.99	-1.38	1.45586	-.14935	0.000000	0.000000	14.5251	-1.4845	0.0000	0.0000
144	Q	65.86	1.27	1.28	5.01	13.25	.79	-1.57	1.34602	-.14935	0.000000	0.000000	13.4333	-1.4845	0.0000	0.0000
145	SD	65.86	1.28	1.28	5.01	13.25	.77	-1.53	1.34602	-.14555	0.000000	0.000000	13.4333	-1.4655	0.0000	0.0000
146	QS	66.16	1.27	1.29	5.37	14.19	.69	-1.61	1.30236	-.14555	0.000000	0.000000	12.9937	-1.4655	0.0000	0.0000
147	QD	66.49	1.28	1.29	5.12	14.76	.02	.01	1.27694	-.00013	0.000000	0.000000	12.7377	-.0001	0.0000	0.0000
148	QD	66.84	1.30	1.30	5.34	14.18	-.69	1.63	1.30227	.14539	0.000000	0.000000	12.9936	1.4653	0.0000	0.0000
149	QS	67.14	1.30	1.30	5.76	13.22	-.73	1.55	1.34586	.14529	0.000000	0.000000	13.4332	1.4653	0.0000	0.0000

POS		S (M)	QX	QY	BX (M)	BY (M)	AX	AY	EX (M)	EXP	EY (M)	EYP	XCC (MM)	DXCO (MR)	YCO (MM)	DYCG (MR)
150	SD	67.14	1.30	1.30	5.76	13.22	-.75	1.59	1.34586	.14910	0.000000	0.000000	13.4332	1.4843	0.0000	0.0000
151	D	67.88	1.32	1.31	7.01	11.03	-.95	1.39	1.45551	.14910	0.000000	0.000000	14.5248	1.4843	0.0000	0.0000
152	B	69.54	1.35	1.34	10.91	7.06	-1.40	.99	1.78147	.24339	0.000000	0.000000	17.7706	2.4274	0.0000	0.0000
153	D	70.28	1.36	1.36	13.11	5.76	-1.60	.78	1.96046	.24339	0.000000	0.000000	19.5558	2.4274	0.0000	0.0000
154	SF	70.28	1.36	1.36	13.11	5.76	-1.56	.76	1.96046	.23807	0.000000	0.000000	19.5558	2.4008	0.0000	0.0000
155	DS	70.58	1.37	1.37	14.08	5.33	-1.64	.68	2.03189	-.23807	0.000000	0.000000	20.2760	2.4008	0.0000	0.0000
156	QF	70.93	1.37	1.38	14.66	5.09	.00	.00	2.07374	-.00009	0.000000	0.COCCOC	20.6982	-.0001	0.0000	0.0000
157	QF	71.28	1.37	1.39	14.08	5.33	1.64	-.68	2.03183	-.23824	0.000000	0.000000	20.2760	-2.4009	0.0000	0.0000
158	DS	71.58	1.38	1.40	13.11	5.76	1.56	-.76	1.96035	-.23824	0.000000	0.00000C	19.5557	-2.4009	0.0000	0.0000
159	SF	71.58	1.38	1.40	13.11	5.76	1.60	-.78	1.96035	-.24356	0.000000	0.000000	19.5557	-2.4276	0.0000	0.0000
160	D	72.31	1.39	1.41	10.91	7.06	1.40	-.98	1.78123	-.24356	0.000000	0.000000	17.77C4	-2.4276	0.0000	0.0000
161	B	73.97	1.42	1.44	7.00	11.03	.95	-1.39	1.45599	-.14927	0.000000	0.000000	14.5249	-1.4845	0.0000	0.0000
162	D	74.71	1.44	1.45	5.75	13.22	.75	-1.59	1.34522	-.14927	0.000000	0.000000	13.4327	-1.4845	0.0000	0.0000
163	SD	74.71	1.44	1.45	5.75	13.22	.73	-1.55	1.34522	-.14547	0.000000	0.000000	13.4327	-1.4654	0.0000	0.0000
164	DS	75.01	1.44	1.46	5.34	14.17	.65	-1.63	1.30158	-.14547	0.000000	0.000000	12.9931	-1.4654	0.0000	0.0000
165	QD	75.36	1.46	1.46	5.12	14.25	-.02	-.01	1.27615	-.00013	0.000000	0.000000	12.7371	-.0001	0.0000	0.0000
166	QD	75.71	1.47	1.47	5.36	14.18	-.69	1.61	1.30149	.14520	0.000000	0.000000	12.9931	1.4652	0.0000	0.0000
167	DS	76.01	1.47	1.47	5.80	13.24	-.77	1.55	1.34505	.14520	0.000000	0.000000	13.4326	1.4652	0.0000	0.0000
168	SD	76.01	1.47	1.47	5.80	13.24	-.79	1.57	1.34505	.14900	0.000000	0.000000	13.4326	1.4843	0.0000	0.0000
169	D	76.75	1.49	1.48	7.11	11.07	-.99	1.38	1.45463	.14900	0.000000	0.000000	14.5242	1.4843	0.0000	0.0000
170	B	78.41	1.52	1.51	11.18	7.13	-1.46	.98	1.78044	.24329	0.000000	0.000000	17.7698	2.4274	0.0000	0.0000
171	D	79.14	1.53	1.53	13.47	5.84	-1.66	.78	1.95936	.24329	0.000000	0.000C00	19.5550	2.4274	0.0000	0.0000
172	SF	79.14	1.53	1.53	13.47	5.84	-1.62	.76	1.95936	.23798	0.000000	0.000C0C	19.5550	2.4007	0.0000	0.0000
173	DS	79.44	1.54	1.53	14.47	5.41	-1.71	.68	2.03076	.23798	0.000000	0.000000	20.2752	2.4007	0.0000	0.0000
174	QF	79.79	1.54	1.55	15.08	5.18	-.02	-.01	2.07261	-.00004	0.000000	0.000000	20.6974	-.0000	0.0000	0.0000
175	QF	80.14	1.54	1.56	14.49	5.42	1.68	-.70	2.03073	-.23807	0.000000	0.000000	20.2752	-2.4008	0.0000	0.0000
176	DS	80.44	1.55	1.56	13.51	5.87	1.60	-.78	1.95931	-.23807	0.000000	0.000000	19.5550	-2.4008	0.0000	0.0000
177	SF	80.44	1.55	1.56	13.51	5.87	1.63	-.80	1.95931	-.24338	0.000000	0.000000	19.5550	-2.4274	0.0000	0.0000
178	D	81.18	1.56	1.58	11.25	7.19	1.43	-1.01	1.78032	-.24338	0.000000	0.000000	17.7698	-2.4274	0.0000	0.0000
179	B	82.84	1.59	1.61	7.24	11.23	.98	-1.41	1.45637	-.14909	0.000000	0.000000	14.5240	-1.4843	0.0000	0.0000
180	D	83.58	1.60	1.62	5.94	13.45	.78	-1.61	1.34472	-.14909	0.000000	0.000000	13.4324	-1.4853	0.0000	0.0000
181	SD	83.58	1.60	1.62	5.94	13.45	.77	-1.57	1.34472	-.14529	0.000000	0.000000	13.4324	-1.4653	0.0000	0.0000
182	DS	83.88	1.61	1.63	5.50	14.23	.69	-1.65	1.30114	-.14529	0.000000	0.000000	12.9928	-1.4653	0.0000	0.0000
183	QD	84.23	1.62	1.63	5.27	15.00	-.00	.00	1.27576	.00000	0.000000	0.000000	12.7369	-.0000	0.0000	0.0000
184	REFL	168.46	3.24	3.26	17.74	6.06	-.00	-.00	-.02152	.00000	0.000000	0.000000	-.1099	0.0000	0.0000	0.0000

CIRCUMFERENCE = 505.3686 M THETX = 6.28318638 RAD NUX = 9.73377 DNUX/(DP/P) = .43232
(DS/S)/CORDES = .0828329 M THETY(183) = 0.00000000 RAD NUY = 9.77411 DNUY/(DP/P) = .34253
TGAM = (7.61658, 0.00000)

MAXIMA --- BETX(184) = 17.73769 BETY(12) = 17.42648 ETAX(138) = 2.07486 ETAY(184) = 0.00000
MINIMA --- BETX(36) = 4.12630 BETY(48) = 3.31143 ETAX(33) = -.00023 ETAY(184) = 0.00C00

*** INCR 1 // DP .005000 VALUE = .015000

SUB.: CHR , ITER. 8

CALCULATION OF THE EQUILIBRIUM ORBIT AND BETATRON FUNCTIONS OF AGR .
INITIAL REFERENCE RAY DEFINED BY V

X = -.00010986 DX = 0.00000000 Y = 0.00000000 DY = 0.00000000 DS = 0.00000000 DP/P = .01500000 1.00000000
2

7X7 MATRIX FOR AGR

.03040808	17.66939186	0.00000000	0.00000000	0.00000000	-.03146645	.00024846
-.05654271	.03040808	0.00000000	0.00000000	0.00000000	-.00183500	.00001449
0.00000000	0.00000000	-.05505360	6.20894356	0.00000000	0.00000000	0.00000000
0.00000000	0.00000000	-.16056984	-.05505360	0.00000000	0.00000000	0.00000000
.00183500	.03146645	0.00000000	0.00000000	1.00000000	-2.91613147	-.04127261
0.00000000	0.00000000	0.00000000	0.00000000	0.00000000	1.00000000	0.00000000
0.00000000	0.00000000	0.00000000	0.00000000	0.00000000	0.00000000	1.00000000

EIGENVALUES OF THE 4X4 SUBMATRIX

X... LMD1 = (.03040808 -.99953737); C(1) = 1.00000000; MU(1) = 1.54038355 RAD; Q(1) = .73547897
1/LMD1 = (.03040808 -.99953737); C(2) = 1.00000000; MU(2) = -1.54038355 RAD; Q(2) = .26452103

Y... LMD3 = (-.05505360 -.99848340); C(3) = 1.00000000; MU(3) = 1.62587778 RAD; Q(3) = .77629945
1/LMD3 = (-.05505360 -.99848340); C(4) = 1.00000000; MU(4) = -1.62587778 RAD; Q(4) = .22370055

EIGENVALUE = (.03040808, .99953737), EIGENVECTOR = (4.20446983, 0.00000000)
(0.00000000, .23784212)
(0.00000000, 0.00000000)
(0.00000000, 0.00000000)

EIGENVALUE = (.03040808, -.99953737), EIGENVECTOR = (4.20446983, 0.00000000)
(0.00000000, -.23784212)
(0.00000000, 0.00000000)
(0.00000000, 0.00000000)

EIGENVALUE = (-.05505360, .99848340), EIGENVECTOR = (0.00000000, 0.00000000)
(0.00000000, 0.00000000)
(2.49366685, .00000000)
(.00000000, .40101588)

EIGENVALUE = (-.05505360, -.99848340), EIGENVECTOR = (0.00000000, 0.00000000)
(0.00000000, 0.00000000)
(2.49366685, -.00000000)
(.00000000, -.40101588)

	X	DX	Y	DY	DS	DP/P	
EQ ORBIT	-.00024288	0.00000000	0.00000000	0.00000000	0.00000000	.01500000	1.00000000
ETA ORBIT	-.03245329	-.00000000	0.00000000	0.00000000	0.00000000	1.00000000	0.00000000

EIGENVECTORS 1 AND 3 IN POLAR COORDINATES

POS	X1 X3		DX1 DX3		Y1 Y3		DY1 DY3	
0	4.204479 0.000000	0.000000 0.000000	-.237842 0.000000	1.570796 0.000000	0.000000 2.443667	0.000000 .000000	0.000000 .401016	0.000000 1.570796

BETATRON FUNCTIONS OF AGR

POS		S (M)	QX	QY	BX (M)	BY (M)	AX	AY	EX (M)	EXP	EY (M)	EYP	XCO (MM)	DXCO (MR)	YCO (MM)	DYCO (MR)
0		0.00	0.30	0.00	17.68	6.22	0.00	0.00	-.03245	-.00000	0.000000	0.000000	-.2429	0.0000	0.0000	0.0000
1	QF1	.35	.03	.01	16.89	6.53	2.22	-.89	-.03172	.00417	0.000000	0.000000	-.2374	.0314	0.0000	0.0000
2		.72	.01	.02	15.28	7.23	2.09	-1.00	-.03017	.00417	0.000000	0.000000	-.2256	.0314	0.0000	0.0000
3		1.10	.01	.03	13.78	8.01	1.95	-1.10	-.02861	.00417	0.000000	0.000000	-.2139	.0314	0.0000	0.0000
4	S	1.47	.02	.03	12.37	8.87	1.82	-1.20	-.02706	.00417	0.000000	0.000000	-.2022	.0314	0.0000	0.0000
5	S	1.84	.02	.04	11.05	9.81	1.69	-1.30	-.02550	.00417	0.000000	0.000000	-.1905	.0314	0.0000	0.0000
6	S	2.22	.03	.04	9.84	10.82	1.56	-1.41	-.02395	.00417	0.000000	0.000000	-.1787	.0314	0.0000	0.0000
7	S	2.59	.03	.05	8.72	11.91	1.43	-1.51	-.02239	.00417	0.000000	0.000000	-.1670	.0314	0.0000	0.0000
8	S	2.96	.04	.05	7.70	13.07	1.30	-1.61	-.02084	.00417	0.000000	0.000000	-.1553	.0314	0.0000	0.0000
9	S	3.34	.05	.06	6.78	14.32	1.17	-1.72	-.01928	.00417	0.000000	0.000000	-.1436	.0314	0.0000	0.0000
10	S	3.71	.06	.06	5.95	15.64	1.04	-1.82	-.01773	.00417	0.000000	0.000000	-.1318	.0314	0.0000	0.0000
11	S	4.08	.07	.07	5.23	17.03	.91	-1.92	-.01617	.00417	0.000000	0.000000	-.1201	.0314	0.0000	0.0000
12	QD1	4.33	.08	.07	4.84	17.67	.22	.13	-.01504	.00232	0.000000	0.000000	-.1116	.0176	0.0000	0.0000
13	QD1	4.58	.09	.07	4.91	16.86	-.44	2.16	-.01554	.00056	0.000000	0.000000	-.1077	.0045	0.0000	0.0000
14	S	5.16	.10	.08	5.27	15.29	-.53	2.03	-.01433	.00056	0.000000	0.000000	-.1060	.0045	0.0000	0.0000
15	S	5.53	.11	.08	5.70	13.82	-.62	1.91	-.01412	.00056	0.000000	0.000000	-.1044	.0045	0.0000	0.0000
16	S	5.90	.12	.09	6.20	12.45	-.71	1.78	-.01391	.00056	0.000000	0.000000	-.1027	.0045	0.0000	0.0000
17	S	6.28	.13	.09	6.76	11.16	-.80	1.66	-.01370	.00056	0.000000	0.000000	-.1010	.0045	0.0000	0.0000
18	S	6.65	.14	.10	7.39	9.97	-.89	1.53	-.01349	.00056	0.000000	0.000000	-.0993	.0045	0.0000	0.0000
19	S	7.02	.15	.10	8.09	8.88	-.98	1.41	-.01328	.00056	0.000000	0.000000	-.0977	.0045	0.0000	0.0000
20	S	7.39	.16	.11	8.86	7.87	-1.07	1.28	-.01307	.00056	0.000000	0.000000	-.0960	.0045	0.0000	0.0000
21	S	7.77	.16	.12	9.69	6.96	-1.16	1.16	-.01286	.00056	0.000000	0.000000	-.0943	.0045	0.0000	0.0000
22	S	8.14	.17	.13	10.59	6.15	-1.25	1.03	-.01265	.00056	0.000000	0.000000	-.0926	.0045	0.0000	0.0000
23	S	8.51	.17	.14	11.56	5.43	-1.34	.91	-.01244	.00056	0.000000	0.000000	-.0910	.0045	0.0000	0.0000
24	QF2	8.86	.18	.15	12.61	5.05	.08	.17	-.01197	.00207	0.000000	0.000000	-.0874	.0196	0.0000	0.0000
25	QF2	9.22	.18	.16	11.45	5.18	1.49	-.53	-.01099	.00349	0.000000	0.000000	-.0801	.0260	0.0000	0.0000
26	S	9.59	.19	.17	10.38	5.61	1.39	-.62	-.00969	.00349	0.000000	0.000000	-.0704	.0260	0.0000	0.0000
27	S	9.96	.19	.18	9.38	6.11	1.28	-.71	-.00839	.00349	0.000000	0.000000	-.0607	.0260	0.0000	0.0000
28	S	10.33	.20	.19	8.47	6.67	1.18	-.81	-.00709	.00349	0.000000	0.000000	-.0510	.0260	0.0000	0.0000
29	S	10.71	.21	.20	7.63	7.31	1.07	-.90	-.00579	.00349	0.000000	0.000000	-.0413	.0260	0.0000	0.0000
30	S	11.08	.22	.21	6.87	8.02	.97	-.99	-.00449	.00349	0.000000	0.000000	-.0316	.0260	0.0000	0.0000
31	S	11.45	.23	.21	6.19	8.79	.86	-1.08	-.00319	.00349	0.000000	0.000000	-.0219	.0260	0.0000	0.0000
32	S	11.82	.24	.22	5.59	9.63	.76	-1.18	-.00189	.00349	0.000000	0.000000	-.0122	.0260	0.0000	0.0000
33	S	12.20	.25	.22	5.06	10.55	.65	-1.27	-.00058	.00349	0.000000	0.000000	-.0025	.0260	0.0000	0.0000
34	S	12.57	.26	.23	4.61	11.53	.55	-1.36	.00072	.00349	0.000000	0.000000	.0072	.0260	0.0000	0.0000
35	S	12.93	.27	.23	4.25	12.58	-.44	-1.45	.00202	.00349	0.000000	0.000000	.0169	.0260	0.0000	0.0000
36	QD2	13.30	.28	.24	4.16	13.01	-.20	.22	.00330	.00384	0.000000	0.000000	.0265	.0289	0.0000	0.0000
37	QD2	13.65	.30	.24	4.54	12.27	-.89	1.86	.00473	.00437	0.000000	0.000000	.0373	.0331	0.0000	0.0000
38	R	14.01	.31	.25	5.25	10.96	-1.03	1.73	.00633	.00437	0.000000	0.000000	.0494	.0331	0.0000	0.0000
39	R	14.38	.32	.25	6.06	9.74	-1.18	1.59	.00793	.00437	0.000000	0.000000	.0616	.0331	0.0000	0.0000
40	R	14.75	.33	.26	6.97	8.62	-1.32	1.46	.00953	.00437	0.000000	0.000000	.0737	.0331	0.0000	0.0000
41	R	15.11	.34	.27	7.99	7.59	-1.47	1.33	.01114	.00437	0.000000	0.000000	.0859	.0331	0.0000	0.0000
42	R	15.48	.34	.28	9.12	6.67	-1.61	1.19	.01274	.00437	0.000000	0.000000	.0980	.0331	0.0000	0.0000
43	R	15.85	.35	.28	10.35	5.84	-1.75	1.06	.01434	.00437	0.000000	0.000000	.1102	.0331	0.0000	0.0000
44	R	16.21	.36	.30	11.69	5.11	-1.90	.93	.01594	.00437	0.000000	0.000000	.1223	.0331	0.0000	0.0000
45	R	16.59	.36	.31	13.14	4.48	-2.04	.79	.01754	.00437	0.000000	0.000000	.1345	.0331	0.0000	0.0000
46	R	16.93	.37	.32	14.69	3.93	-2.19	.66	.01915	.00437	0.000000	0.000000	.1466	.0331	0.0000	0.0000
47	R	17.32	.37	.34	16.35	3.51	-2.33	.53	.02075	.00437	0.000000	0.000000	.1588	.0331	0.0000	0.0000
48	QF3	17.70	.32	.36	17.30	3.32	-.15	-.05	.02198	-.00154	0.000000	0.000000	.1680	-.0114	0.0000	0.0000
49	QF3	18.14	.38	.38	16.59	3.60	2.07	-.65	.02202	-.00136	0.000000	0.000000	.1681	-.0110	0.0000	0.0000

POS		S (M)	DX	DY	BX (M)	BY (M)	AX	AY	EX (M)	EXP	EY (M)	EYP	XCO (MM)	DXCO (MM)	YCO (MM)	DYCO (MM)
50	Z	18.50	.38	.39	15.14	4.12	1.95	-.79	.02152	-.00136	0.000000	0.000000	.1641	-.0110	0.0000	0.0000
51	Z	18.86	.38	.40	13.77	4.74	1.84	-.93	.02103	-.00136	0.000000	0.000000	.1602	-.0110	0.0000	0.0000
52	Z	19.22	.39	.42	12.49	5.46	1.72	-1.07	.02054	-.00136	0.000000	0.000000	.1562	-.0110	0.0000	0.0000
53	Z	19.58	.39	.43	11.29	6.28	1.61	-1.21	.02004	-.00136	0.000000	0.000000	.1522	-.0110	0.0000	0.0000
54	Z	19.95	.40	.43	10.17	7.20	1.49	-1.35	.01956	-.00136	0.000000	0.000000	.1483	-.0110	0.0000	0.0000
55	Z	20.31	.40	.44	9.14	8.23	1.38	-1.49	.01907	-.00136	0.000000	0.000000	.1443	-.0110	0.0000	0.0000
56	Z	20.67	.41	.45	8.18	9.38	1.26	-1.64	.01858	-.00136	0.000000	0.000000	.1403	-.0110	0.0000	0.0000
57	Z	21.03	.42	.45	7.31	10.63	1.15	-1.78	.01809	-.00136	0.000000	0.000000	.1363	-.0110	0.0000	0.0000
58	Z	21.39	.43	.46	6.53	11.92	1.04	-1.92	.01760	-.00136	0.000000	0.000000	.1324	-.0110	0.0000	0.0000
59	Z	21.75	.44	.46	5.82	13.36	.92	-2.06	.01711	-.00136	0.000000	0.000000	.1284	-.0110	0.0000	0.0000
60	QD3	22.16	.45	.47	5.41	14.35	.09	-.29	.01701	.00087	0.000000	0.000000	.1273	.0058	0.0000	0.0000
61	QD3	22.58	.46	.47	5.67	13.82	-.72	1.54	.01784	.00315	0.000000	0.000000	.1333	.0230	0.0000	0.0000
62	R	23.04	.47	.48	6.24	12.73	-.82	1.45	.01899	.00315	0.000000	0.000000	.1417	.0230	0.0000	0.0000
63	R	23.31	.48	.48	6.89	11.69	-.92	1.36	.02014	.00315	0.000000	0.000000	.1502	.0230	0.0000	0.0000
64	R	23.68	.49	.49	7.59	10.73	-1.02	1.27	.02130	.00315	0.000000	0.000000	.1586	.0230	0.0000	0.0000
65	R	24.04	.49	.49	8.37	9.83	-1.12	1.18	.02245	.00315	0.000000	0.000000	.1671	.0230	0.0000	0.0000
66	R	24.41	.50	.50	9.23	8.99	-1.22	1.09	.02361	.00315	0.000000	0.000000	.1755	.0230	0.0000	0.0000
67	R	24.78	.51	.51	10.16	8.22	-1.32	1.00	.02476	.00315	0.000000	0.000000	.1839	.0230	0.0000	0.0000
68	R	25.14	.51	.51	11.16	7.52	-1.41	.91	.02592	.00315	0.000000	0.000000	.1924	.0230	0.0000	0.0000
69	R	25.51	.52	.52	12.23	6.88	-1.51	.82	.02707	.00315	0.000000	0.000000	.2008	.0230	0.0000	0.0000
70	R	25.88	.52	.53	13.38	6.31	-1.61	.74	.02823	.00315	0.000000	0.000000	.2093	.0230	0.0000	0.0000
71	R	26.24	.53	.54	14.60	5.80	-1.71	.65	.02938	.00315	0.000000	0.000000	.2177	.0230	0.0000	0.0000
72	QF	26.59	.53	.55	15.21	5.61	-1.01	-.08	.02989	-.00028	0.000000	0.000000	.2214	-.0026	0.0000	0.0000
73	QF	26.94	.53	.56	14.62	5.92	-1.69	-.92	.02919	-.00370	0.000000	0.000000	.2159	-.0281	0.0000	0.0000
74	QD	27.48	.55	.58	11.41	7.93	-1.41	-1.12	.02936	-.00370	0.000000	0.000000	.1868	-.0281	0.0000	0.0000
75	B	29.64	.58	.61	7.45	12.38	-.98	-1.52	.09704	.09016	0.000000	0.000000	1.3075	1.3798	0.0000	0.0000
76	QD	30.68	.60	.62	5.71	15.77	-.71	-1.80	.19039	.09016	0.000000	0.000000	2.7362	1.3798	0.0000	0.0000
77	QD	31.03	.61	.63	5.46	16.41	-.00	-.01	.22905	.11341	0.000000	0.000000	3.2778	1.7206	0.0000	0.0000
78	QD	31.38	.62	.63	5.70	15.78	-.70	1.79	.27041	.14113	0.000000	0.000000	3.9505	2.1303	0.0000	0.0000
79	QD	32.61	.65	.64	7.44	12.36	-.97	1.52	.41654	.14113	0.000000	0.000000	6.1562	2.1303	0.0000	0.0000
80	B	34.07	.68	.67	11.38	7.97	-1.41	1.11	.72862	.23494	0.000000	0.000000	10.8573	3.5378	0.0000	0.0000
81	Q	34.81	.68	.68	13.58	6.48	-1.60	.91	.90146	.23494	0.000000	0.000000	13.4591	3.5378	0.0000	0.0000
82	SF	34.81	.68	.68	13.58	6.48	-1.57	.89	.90140	.23327	0.000000	0.000000	13.4591	3.5253	0.0000	0.0000
83	DS	35.11	.69	.69	14.56	5.97	-1.65	.81	.97138	.23327	0.000000	0.000000	14.5167	3.5253	0.0000	0.0000
84	DF	35.46	.69	.70	15.13	5.87	.04	.06	1.03319	.11819	0.000000	0.000000	15.4493	1.7781	0.0000	0.0000
85	QF	35.81	.70	.71	14.50	5.88	1.73	-.67	1.05367	-.00170	0.000000	0.000000	15.7547	-.0412	0.0000	0.0000
86	DS	36.11	.70	.72	13.49	6.30	1.62	-.74	1.03316	-.00170	0.000000	0.000000	15.7229	-.0412	0.0000	0.0000
87	SF	36.11	.70	.72	13.49	6.30	1.67	-.76	1.04316	-.00398	0.000000	0.000000	15.7229	-.0964	0.0000	0.0000
88	D	36.85	.71	.74	11.18	7.85	1.47	-.96	1.05023	-.00398	0.000000	0.000000	15.6944	-.0964	0.0000	0.0000
89	LC	38.51	.74	.76	7.04	11.37	1.00	-1.36	1.04362	-.00398	0.000000	0.000000	15.6023	-.0964	0.0000	0.0000
90	D	39.24	.76	.77	5.77	13.50	.79	-1.54	1.04070	-.00398	0.000000	0.000000	15.5595	-.0964	0.0000	0.0000
91	SD	39.24	.76	.77	5.77	13.50	.77	-1.50	1.04070	-.00060	0.000000	0.000000	15.5505	-.0330	0.0000	0.0000
92	DS	39.54	.77	.78	5.33	14.42	.69	-1.57	1.04052	-.00060	0.000000	0.000000	15.5456	-.0330	0.0000	0.0000
93	QD	39.89	.78	.78	5.08	14.96	.02	-.07	1.06060	.11671	0.000000	0.000000	15.8469	1.7464	0.0000	0.0000
94	QD	40.24	.79	.79	5.30	14.33	-.64	1.70	1.12286	.23861	0.000000	0.000000	16.7820	3.5955	0.0000	0.0000
95	DS	40.54	.80	.79	5.70	13.33	-.72	1.62	1.19444	.23861	0.000000	0.000000	17.8607	3.5955	0.0000	0.0000
96	SD	40.54	.80	.79	5.70	13.33	-.74	1.67	1.19444	.24306	0.000000	0.000000	17.8607	3.6291	0.0000	0.0000
97	D	41.28	.81	.80	6.94	11.04	-.94	1.46	1.37320	.24306	0.000000	0.000000	20.5296	3.6291	0.0000	0.0000
98	LC	42.94	.84	.83	10.81	6.98	-1.39	.99	1.77678	.24306	0.000000	0.000000	26.5554	3.6291	0.0000	0.0000
99	D	43.67	.85	.85	13.00	5.68	-1.59	.78	1.95553	.24306	0.000000	0.000000	29.2243	3.6291	0.0000	0.0000

POS		S (M)	QX	QY	BX (M)	BY (M)	AX	AY	EX (M)	EXP	EY (M)	EYP	XCO (MM)	DXCO (MR)	YCO (MM)	DYCO (MR)
100	SF	43.67	.85	.85	13.00	5.63	-1.54	.76	1.95553	.23520	0.000000	0.000000	29.2243	3.5699	0.0000	0.0000
101	OS	43.97	.86	.86	13.94	5.25	-1.61	.67	2.02609	.23520	0.000000	0.000000	30.2953	3.5699	0.0000	0.0000
102	QF	44.32	.86	.87	14.52	5.01	.00	.00	2.06748	.00010	0.000000	0.000000	30.9232	.0006	0.0000	0.0000
103	QF	44.67	.87	.88	13.94	5.24	1.62	-.67	2.02616	-.23499	0.000000	0.000000	30.2957	-3.5688	0.0000	0.0000
104	OS	44.97	.87	.89	12.99	5.67	1.54	-.75	1.95567	-.23499	0.000000	0.000000	29.2250	-3.5688	0.0000	0.0000
105	SF	44.97	.87	.89	12.99	5.67	1.60	-.77	1.955.67	-.24286	0.000000	0.000000	29.2250	-3.6280	0.0000	0.0000
106	Q	45.71	.88	.91	10.79	6.96	1.60	-.98	1.77706	-.24286	0.000000	0.000000	26.5569	-3.6280	0.0000	0.0000
107	Q	47.37	.91	.94	6.91	10.02	.94	-1.39	1.45127	-.14905	0.000000	0.000000	21.7019	-2.2205	0.0000	0.0000
108	Q	48.11	.93	.95	5.67	13.12	.74	-1.53	1.34165	-.14905	0.000000	0.000000	20.0660	-2.2205	0.0000	0.0000
109	SD	48.11	.93	.95	5.67	13.12	.72	-1.53	1.34165	-.14343	0.000000	0.000000	20.0690	-2.1781	0.0000	0.0000
110	OS	48.41	.94	.95	5.26	14.06	.64	-1.61	1.29862	-.14343	0.000000	0.000000	19.4155	-2.1781	0.0000	0.0000
111	QD	48.76	.95	.95	5.03	14.64	-.02	-.02	1.27356	.00010	0.000000	0.000000	19.0352	.0009	0.0000	0.0000
112	QD	49.11	.96	.96	5.29	14.08	-.69	1.48	1.29871	.14376	0.000000	0.000000	19.4161	2.1799	0.0000	0.0000
113	QS	49.41	.97	.96	5.73	13.15	-.77	1.51	1.34186	.14376	0.000000	0.000000	20.0701	2.1799	0.0000	0.0000
114	SD	49.41	.97	.96	5.73	13.15	-.79	1.56	1.34186	.14938	0.000000	0.000000	20.0701	2.2222	0.0000	0.0000
115	Q	50.14	.99	.97	7.05	10.99	-1.00	1.37	1.45172	.14938	0.000000	0.000000	21.7043	2.2222	0.0000	0.0000
116	Q	51.81	1.02	1.00	11.16	7.08	-1.47	.97	1.77805	.24319	0.000000	0.000000	26.5622	3.6297	0.0000	0.0000
117	QF	52.56	1.03	1.02	13.48	5.80	-1.68	.77	1.95690	.24319	0.000000	0.000000	29.2316	3.6297	0.0000	0.0000
118	QF	52.54	1.03	1.02	13.48	5.80	-1.63	.75	1.95690	.23532	0.000000	0.000000	29.2316	3.5705	0.0000	0.0000
119	OS	52.84	1.03	1.05	14.49	5.37	-1.71	.67	2.02750	.23532	0.000000	0.000000	30.3028	3.5705	0.0000	0.0000
120	QF	53.19	1.03	1.04	12.10	5.15	-.03	-.02	2.06890	.00006	0.000000	0.000000	30.9307	.0003	0.0000	0.0000
121	QF	53.54	1.04	1.05	14.52	5.40	1.66	-.78	2.02754	-.23520	0.000000	0.000000	30.3030	-3.5699	0.0000	0.0000
122	OS	53.84	1.04	1.06	13.55	5.86	1.58	-.79	1.95698	-.23520	0.000000	0.000000	29.2320	-3.5699	0.0000	0.0000
123	SF	53.84	1.04	1.06	13.55	5.86	1.64	-.81	1.95698	-.24307	0.000000	0.000000	29.2320	-3.6291	0.0000	0.0000
124	Q	54.58	1.05	1.08	11.26	7.13	1.44	-1.02	1.77827	-.24307	0.000000	0.000000	26.5630	-3.6291	0.0000	0.0000
125	Q	56.24	1.08	1.10	7.33	11.29	.99	-1.43	1.45206	-.14927	0.000000	0.000000	21.7062	-2.2216	0.0000	0.0000
126	Q	56.98	1.10	1.11	5.92	13.34	.79	-1.63	1.34229	-.14927	0.000000	0.000000	20.0723	-2.2216	0.0000	0.0000
127	SD	56.98	1.10	1.11	5.95	13.34	.76	-1.57	1.34229	-.14364	0.000000	0.000000	20.0723	-2.1793	0.0000	0.0000
128	OS	57.28	1.11	1.12	5.51	14.51	.68	-1.65	1.29819	-.14364	0.000000	0.000000	19.4186	-2.1793	0.0000	0.0000
129	QD	57.63	1.12	1.12	5.28	15.09	-.00	-.00	1.27411	.00001	0.000000	0.000000	19.0379	.0000	0.0000	0.0000
130	QD	57.98	1.13	1.13	5.28	14.51	-.69	1.65	1.29829	.14367	0.000000	0.000000	19.4186	2.1793	0.0000	0.0000
131	QS	58.28	1.13	1.13	5.95	13.34	-.77	1.57	1.34230	.14367	0.000000	0.000000	20.0724	2.1793	0.0000	0.0000
132	SD	58.28	1.13	1.13	5.95	13.34	-.79	1.62	1.34230	.14929	0.000000	0.000000	20.0724	2.2217	0.0000	0.0000
133	Q	59.01	1.15	1.14	7.27	11.30	-.99	1.43	1.45209	.14929	0.000000	0.000000	21.7063	2.2217	0.0000	0.0000
134	B	60.68	1.19	1.17	11.32	7.20	-1.45	1.02	1.77827	.24310	0.000000	0.000000	26.5633	3.6292	0.0000	0.0000
135	Q	61.41	1.19	1.19	13.60	5.86	-1.65	.81	1.95703	.24310	0.000000	0.000000	29.2323	3.6292	0.0000	0.0000
136	SF	61.41	1.19	1.19	13.60	5.86	-1.59	.79	1.95703	.23522	0.000000	0.000000	29.2323	3.5700	0.0000	0.0000
137	OS	61.71	1.19	1.19	14.58	5.31	-1.67	.70	2.02768	.23522	0.000000	0.000000	30.3033	3.5700	0.0000	0.0000
138	QF	62.06	1.20	1.20	15.16	5.17	-.02	.02	2.06899	-.00005	0.000000	0.000000	30.9311	-.0003	0.0000	0.0000
139	QF	62.41	1.20	1.22	14.58	5.39	1.71	-.67	2.02759	-.23532	0.000000	0.000000	30.3031	-3.5705	0.0000	0.0000
140	OS	62.71	1.21	1.22	13.54	5.82	1.63	-.75	1.95699	-.23532	0.000000	0.000000	29.2320	-3.5705	0.0000	0.0000
141	SF	62.71	1.21	1.22	13.54	5.82	1.69	-.77	1.95699	-.24319	0.000000	0.000000	29.2320	-3.6297	0.0000	0.0000
142	Q	63.47	1.22	1.24	11.23	7.10	1.48	-.98	1.77815	-.24319	0.000000	0.000000	26.5626	-3.6297	0.0000	0.0000
143	QB	65.11	1.25	1.27	7.08	11.03	1.01	-1.39	1.45183	-.14938	0.000000	0.000000	21.7047	-2.2222	0.0000	0.0000
144	Q	65.85	1.26	1.28	5.76	13.20	.80	-1.57	1.34199	-.14938	0.000000	0.000000	20.0704	-2.2222	0.0000	0.0000
145	SD	65.85	1.26	1.28	5.76	13.20	.77	-1.51	1.34195	-.14376	0.000000	0.000000	20.0704	-2.1799	0.0000	0.0000
146	OS	66.15	1.27	1.29	5.32	14.13	.69	-1.59	1.29882	-.14376	0.000000	0.000000	19.4165	-2.1799	0.0000	0.0000
147	QD	66.50	1.28	1.29	5.07	14.69	.02	-.02	1.27369	-.00015	0.000000	0.000000	19.0355	-.0008	0.0000	0.0000
148	QD	66.85	1.29	1.29	5.28	14.11	-.64	1.62	1.29871	.14345	0.000000	0.000000	19.4159	2.1782	0.0000	0.0000
149	QS	67.15	1.30	1.30	5.69	13.16	-.72	1.54	1.34175	.14345	0.000000	0.000000	20.0694	2.1782	0.0000	0.0000

POS		S (M)	QX	QY	BX (M)	BY (M)	AX	AY	EX (M)	EXP	EY (M)	EYP	XCO (MM)	DXCO (MR)	YCO (MM)	DYCO (MR)
150	SD	67.15	1.30	1.30	5.69	13.16	-.74	1.60	1.34175	.14907	0.000000	0.000000	20.0694	2.2205	0.0000	0.0000
151	D	67.88	1.32	1.31	6.92	10.95	-.94	1.40	1.45138	.14907	0.000000	0.000000	21.7024	2.2205	0.0000	0.0000
152	B	69.55	1.35	1.34	10.80	6.97	-1.39	.99	1.77721	.24288	0.000000	0.000000	26.5575	3.6281	0.0000	0.0000
153	D	70.28	1.36	1.36	12.99	5.67	-1.59	.78	1.95583	.24288	0.000000	0.000000	29.2237	3.6281	0.0000	0.0000
154	SF	70.28	1.36	1.36	12.99	5.67	-1.54	.75	1.95583	.23501	0.000000	0.000000	29.2237	3.5689	0.0000	0.0000
155	QS	70.58	1.37	1.36	13.94	5.25	-1.62	.67	2.02634	.23501	0.000000	0.000000	30.2564	3.5689	0.0000	0.0000
156	QF	70.93	1.37	1.38	14.51	5.01	.00	.00	2.06766	-.00010	0.000000	0.000000	30.9239	-.0006	0.0000	0.0000
157	QF	71.28	1.37	1.39	13.94	5.24	1.62	-.67	2.02627	-.23522	0.000000	0.000000	30.2960	-3.5700	0.0000	0.0000
158	QS	71.58	1.38	1.40	12.99	5.67	1.54	-.75	1.95570	-.23522	0.000000	0.000000	29.2250	-3.5700	0.0000	0.0000
159	SF	71.58	1.38	1.40	12.99	5.67	1.59	-.77	1.95570	-.24308	0.000000	0.000000	29.2250	-3.6292	0.0000	0.0000
160	D	72.32	1.39	1.41	10.79	6.96	1.39	-.98	1.77693	-.24308	0.000000	0.000000	26.5560	-3.6292	0.0000	0.0000
161	B	73.98	1.42	1.46	6.91	10.94	.94	-1.40	1.45077	-.14928	0.000000	0.000000	21.6991	-2.2216	0.0000	0.0000
162	B	74.72	1.43	1.48	5.68	13.14	.74	-1.59	1.34098	-.14928	0.000000	0.000000	20.0652	-2.2216	0.0000	0.0000
163	SD	74.72	1.44	1.45	5.69	13.14	.72	-1.54	1.34098	-.14366	0.000000	0.000000	20.0652	-2.1793	0.0000	0.0000
164	QS	75.02	1.44	1.46	5.27	14.08	.64	-1.62	1.29789	-.14366	0.000000	0.000000	19.4114	-2.1793	0.0000	0.0000
165	QD	75.37	1.46	1.46	5.06	14.46	-.02	-.02	1.27277	-.00016	0.000000	0.000000	19.0306	-.0008	0.0000	0.0000
166	QD	75.72	1.47	1.47	5.31	14.11	-.69	1.59	1.29778	.14235	0.000000	0.000000	19.4108	2.1776	0.0000	0.0000
167	QS	76.02	1.48	1.47	5.74	13.18	-.77	1.51	1.34078	.14235	0.000000	0.000000	20.0641	2.1776	0.0000	0.0000
168	SD	76.02	1.48	1.47	5.74	13.18	-.80	1.57	1.34078	.14896	0.000000	0.000000	20.0641	2.2199	0.0000	0.0000
169	D	76.75	1.49	1.48	7.07	11.01	-1.00	1.37	1.45033	.14896	0.000000	0.000000	21.6967	2.2199	0.0000	0.0000
170	B	78.41	1.52	1.51	11.19	7.09	-1.48	.97	1.77596	.24277	0.000000	0.000000	26.5508	3.6275	0.0000	0.0000
171	D	79.15	1.53	1.53	13.51	5.81	-1.68	.77	1.95450	.24277	0.000000	0.000000	29.2186	3.6275	0.0000	0.0000
172	SF	79.15	1.53	1.53	13.51	5.81	-1.63	.75	1.95450	.23691	0.000000	0.000000	29.2186	3.5683	0.0000	0.0000
173	QS	79.45	1.54	1.54	14.52	5.38	-1.71	.67	2.02497	.23691	0.000000	0.000000	30.2890	3.5683	0.0000	0.0000
174	QF	79.80	1.54	1.55	15.13	5.16	-.02	-.02	2.06629	-.00005	0.000000	0.000000	30.9165	-.0003	0.0000	0.0000
175	QF	80.15	1.54	1.56	14.55	5.41	1.67	-.70	2.02493	-.23501	0.000000	0.000000	30.2889	-3.5688	0.0000	0.0000
176	QS	80.45	1.55	1.57	13.57	5.85	1.59	-.79	1.95443	-.23501	0.000000	0.000000	29.2182	-3.5688	0.0000	0.0000
177	SF	80.45	1.55	1.57	13.57	5.85	1.64	-.81	1.95443	-.24287	0.000000	0.000000	29.2182	-3.6280	0.0000	0.0000
178	D	81.19	1.56	1.58	11.30	7.20	1.44	-1.02	1.77582	-.24287	0.000000	0.000000	26.5500	-3.6280	0.0000	0.0000
179	B	82.85	1.60	1.61	7.26	11.29	.00	-1.43	1.45001	-.14906	0.000000	0.000000	21.6950	-2.2205	0.0000	0.0000
180	D	83.58	1.60	1.62	5.95	13.54	.79	-1.63	1.34039	-.14906	0.000000	0.000000	20.0620	-2.2205	0.0000	0.0000
181	SD	83.58	1.60	1.62	5.95	13.54	.76	-1.57	1.34039	-.14345	0.000000	0.000000	20.0620	-2.1782	0.0000	0.0000
182	QS	83.88	1.61	1.62	5.62	14.51	.68	-1.66	1.29738	-.14345	0.000000	0.000000	19.4086	-2.1782	0.0000	0.0000
183	QD	84.24	1.62	1.63	5.28	15.09	-.00	.00	1.27230	.00000	0.000000	0.000000	19.0281	-.0000	0.0000	0.0000
184	REFL	168.47	3.25	3.26	17.68	6.22	-.00	-.00	-.03245	.00000	0.000000	0.000000	-.2429	0.0000	0.0000	0.0000

CIRCUMFERENCE = 505.4313 M THETX = 6.28318638 RAD NUX = 9.73548 DNUX/(DP/P) = .45114
(DS/S)/[illegible] = .0474808 M THETY(183) = 0.00000000 RAD NUY = 9.77630 DNUY/(DP/P) = .31448
TGAM = (7.60070, 0.00000)

MAXIMA --- BETX(184) = 17.67757 BETY(12) = 17.66947 ETAX(138) = 2.06899 ETAY(184) = 0.00000
MINIMA --- BETX(36) = 4.16436 BETY(48) = 3.32012 ETAX(33) = -.00058 ETAY(184) = 0.00000

*** [illegible] INCR 1 // DP .005C00 VALUE = .020000

SUB.(CHR , ITER. 9

CALCULATION OF THE EQUILIBRIUM ORBIT AND BETATRON FUNCTIONS OF AGR .

INITIAL REFERENCE RAY DEFINED BY V

X = -.00024288 DX = 0.00000000 Y = 0.00000000 DY = 0.00000000 DS = 0.00000000 DP/P = .02000000 1.00000000

7X7 MATRIX FOR AGR

.02705862	17.60331730	0.00000000	0.00000000	0.00000000	-.04255458	.00046025
-.05676588	.02705862	0.00000000	0.00000000	0.00000000	-.00248283	.00002685
0.00000000	0.00000000	-.05972548	6.36568879	0.00000000	0.00000000	0.00000000
0.00000000	0.00000000	-.15653182	-.05972548	0.00000000	0.00000000	0.00000000
.00243283	.04255458	0.00000000	0.00000000	1.00000000	-2.92858206	-.05421840
0.00000000	0.00000000	0.00000000	0.00000000	0.00000000	1.00000000	0.00000000
0.00000000	0.00000000	0.00000000	0.00000000	0.00000000	0.00000000	1.00000000

EIGENVALUES OF THE 4X4 SUBMATRIX

X... LMD1 = (.02705862 -.99963385); C(1) = 1.00000000; MU(1) = 1.54373440 RAD; Q(1) = .73707888
1/LMD1 = (.02705862 -.99963385); C(2) = 1.00000000; MU(2) = -1.54373440 RAD; Q(2) = .26292112

Y... LMD3 = (-.05972548 .99821484); C(3) = 1.00000000; MU(3) = 1.63055738 RAD; Q(3) = .77623380
1/LMD3 = (-.05972548 -.99821484); C(4) = 1.00000000; MU(4) = -1.63055738 RAD; Q(4) = .22376620

EIGENVALUE = (.02705862, .99963385), EIGENVECTOR = (4.19639907, -.00000000)
(0.00000000, -.23829955)
(0.00000000, 0.00000000)
(0.00000000, 0.00000000)

EIGENVALUE = (.02705862, -.99963385), EIGENVECTOR = (4.19639907, -.00000000)
(0.00000000, -.23829955)
(0.00000000, 0.00000000)
(0.00000000, 0.00000000)

EIGENVALUE = (-.05972548, .99821484), EIGENVECTOR = (0.00000000, 0.00000000)
(0.00000000, 0.00000000)
(2.52528669, 0.00000000)
(-.00000000, -.39599464)

EIGENVALUE = (-.05972548, -.99821484), EIGENVECTOR = (0.00000000, 0.00000000)
(0.00000000, 0.00000000)
(2.52528669, 0.00000000)
(-.00000000, -.39599464)

	X	DX	Y	DY	DS	DP/P	
EQ ORBIT	-.00042983	0.00000000	0.00000000	0.00000000	0.00000000	.02000000	1.00000000
ETA ORBIT	-.04373807	-.00000000	0.00000000	0.00000000	0.00000000	1.00000000	0.00000000

EIGENVECTORS 1 AND 3 IN POLAR COORDINATES

POS	X1 X3			DX1 DX3		Y1 Y3		DY1 DY3	
0	4.104393 0.000000	-.000000 0.000000	-.238300 0.000000	1.570796 0.000000	0.000000 2.525287	0.000000 0.000000	0.000000 .345995	0.000000 1.570796	

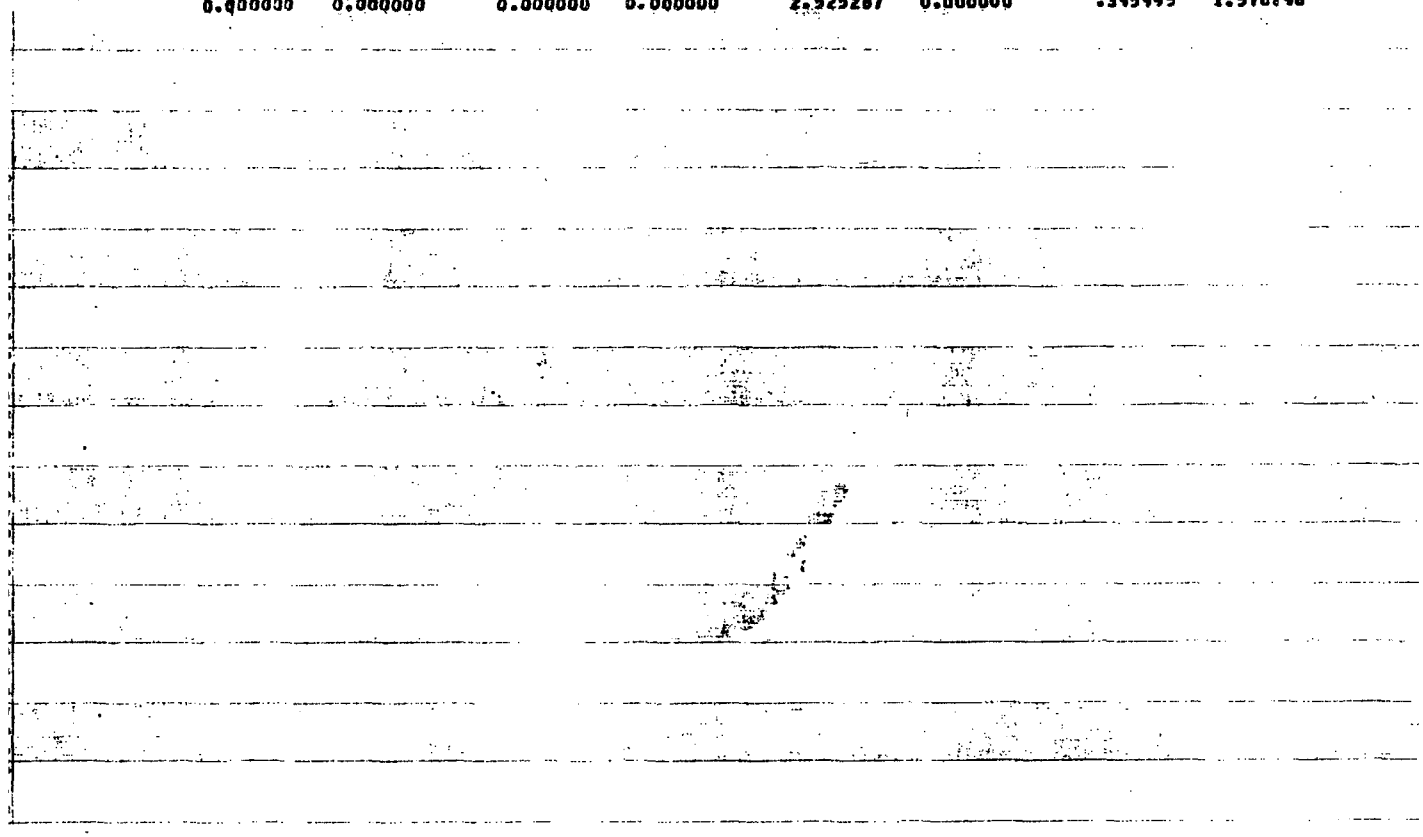

BETATRON FUNCTIONS OF AGR

POS		S (M)	QX	QY	BX (M)	BY (M)	AX	AY	EX (M)	EXP	EY (M)	EYP	XCO (MR)	DXCO (MR)	YCO (MR)	DYCO (MR)
0		0.00	0.00	0.00	17.61	6.38	0.00	0.00	-.04374	-.00000	0.000000	0.000000	-.4298	0.0000	0.0000	0.0000
1	QF1	.38	.00	.01	16.82	6.69	2.20	-.91	-.04276	.00558	0.000000	0.000000	-.4201	.0553	0.0000	0.0000
2	S	.77	.01	.02	15.24	7.41	2.07	-1.01	-.04068	.00558	0.000000	0.000000	-.3994	.0553	0.0000	0.0000
3	S	1.10	.01	.02	13.74	8.20	1.94	-1.11	-.03860	.00558	0.000000	0.000000	-.3788	.0553	0.0000	0.0000
4	S	1.47	.02	.03	12.34	9.07	1.81	-1.21	-.03652	.00558	0.000000	0.000000	-.3582	.0553	0.0000	0.0000
5	S	1.84	.02	.04	11.04	10.01	1.68	-1.32	-.03444	.00558	0.000000	0.000000	-.3375	.0553	0.0000	0.0000
6	S	2.22	.03	.04	9.84	11.03	1.55	-1.42	-.03235	.00558	0.000000	0.000000	-.3169	.0553	0.0000	0.0000
7	S	2.59	.03	.05	8.73	12.13	1.42	-1.52	-.03027	.00558	0.000000	0.000000	-.2962	.0553	0.0000	0.0000
8	S	2.96	.04	.05	7.72	13.30	1.29	-1.62	-.02819	.00558	0.000000	0.000000	-.2756	.0553	0.0000	0.0000
9	S	3.34	.05	.06	6.80	14.55	1.16	-1.72	-.02611	.00558	0.000000	0.000000	-.2549	.0553	0.0000	0.0000
10	S	3.71	.06	.06	5.98	15.88	1.03	-1.83	-.02403	.00558	0.000000	0.000000	-.2343	.0553	0.0000	0.0000
11	S	4.00	.07	.07	5.36	17.28	.91	-1.93	-.02195	.00558	0.000000	0.000000	-.2136	.0553	0.0000	0.0000
12	QD1	4.43	.08	.07	4.87	17.01	.21	.16	-.02044	.00308	0.000000	0.000000	-.1986	.0308	0.0000	0.0000
13	QD1	4.78	.09	.07	4.95	17.08	-.44	4.19	-.01978	.00071	0.000000	0.000000	-.1919	.0076	0.0000	0.0000
14	S	5.16	.10	.07	5.32	15.50	-.93	2.06	-.01951	.00071	0.000000	0.000000	-.1840	.0076	0.0000	0.0000
15	S	5.53	.11	.08	5.75	14.00	-.62	1.94	-.01925	.00071	0.000000	0.000000	-.1862	.0076	0.0000	0.0000
16	S	5.90	.11	.08	6.25	12.61	-.71	1.81	-.01898	.00071	0.000000	0.000000	-.1833	.0076	0.0000	0.0000
17	S	6.28	.12	.09	6.81	11.30	-.81	1.68	-.01871	.00071	0.000000	0.000000	-.1805	.0076	0.0000	0.0000
18	S	6.65	.13	.09	7.45	10.10	-.90	1.56	-.01845	.00071	0.000000	0.000000	-.1776	.0076	0.0000	0.0000
19	S	7.02	.15	.10	8.15	8.98	-.99	1.43	-.01818	.00071	0.000000	0.000000	-.1748	.0076	0.0000	0.0000
20	S	7.39	.16	.11	8.92	7.96	-1.08	1.30	-.01792	.00071	0.000000	0.000000	-.1719	.0076	0.0000	0.0000
21	S	7.77	.16	.12	9.76	7.04	-1.17	1.18	-.01765	.00071	0.000000	0.000000	-.1691	.0076	0.0000	0.0000
22	S	8.14	.17	.12	10.66	6.21	-1.26	1.05	-.01738	.00071	0.000000	0.000000	-.1663	.0076	0.0000	0.0000
23	S	8.51	.18	.13	11.63	5.47	-1.35	.92	-.01712	.00071	0.000000	0.000000	-.1634	.0076	0.0000	0.0000
24	QF2	8.86	.19	.13	12.08	5.08	.08	.19	-.01651	.00227	0.000000	0.000000	-.1572	.0279	0.0000	0.0000
25	QF2	9.22	.18	.14	11.82	5.20	1.49	-.51	-.01519	.00472	0.000000	0.000000	-.1443	.0461	0.0000	0.0000
26	S	9.59	.19	.14	10.45	5.61	1.39	-.60	-.01343	.00472	0.000000	0.000000	-.1271	.0461	0.0000	0.0000
27	S	9.96	.19	.15	9.15	6.10	1.28	-.69	-.01167	.00472	0.000000	0.000000	-.1099	.0461	0.0000	0.0000
28	S	10.33	.20	.16	7.95	6.68	1.18	-.79	-.00991	.00472	0.000000	0.000000	-.0927	.0461	0.0000	0.0000
29	S	10.71	.21	.20	7.70	7.27	1.07	-.88	-.00815	.00472	0.000000	0.000000	-.0755	.0461	0.0000	0.0000
30	S	11.08	.22	.20	6.93	7.96	.97	-.97	-.00639	.00472	0.000000	0.000000	-.0582	.0461	0.0000	0.0000
31	S	11.45	.23	.21	6.28	8.71	.86	-1.06	-.00463	.00472	0.000000	0.000000	-.0410	.0461	0.0000	0.0000
32	S	11.83	.23	.22	5.64	9.54	.76	-1.15	-.00287	.00472	0.000000	0.000000	-.0238	.0461	0.0000	0.0000
33	S	12.20	.24	.22	5.11	10.53	.66	-1.24	-.00111	.00472	0.000000	0.000000	-.0066	.0461	0.0000	0.0000
34	S	12.57	.25	.23	4.66	11.39	.55	-1.33	.00065	.00472	0.000000	0.000000	.0106	.0461	0.0000	0.0000
35	S	12.95	.27	.23	4.29	12.41	.45	-1.42	.00241	.00472	0.000000	0.000000	.0278	.0461	0.0000	0.0000
36	QD2	13.30	.28	.24	4.21	12.84	-.20	.23	.00413	.00514	0.000000	0.000000	.0447	.0509	0.0000	0.0000
37	QD2	13.65	.30	.24	4.58	12.10	-.88	1.83	.00604	.00581	0.000000	0.000000	.0638	.0581	0.0000	0.0000
38	R	14.01	.31	.24	5.28	10.81	-1.03	1.70	.00817	.00581	0.000000	0.000000	.0851	.0581	0.0000	0.0000
39	R	14.38	.32	.25	6.09	9.61	-1.17	1.57	.01030	.00581	0.000000	0.000000	.1064	.0581	0.0000	0.0000
40	R	14.75	.33	.26	7.00	8.51	-1.31	1.44	.01243	.00581	0.000000	0.000000	.1277	.0581	0.0000	0.0000
41	R	15.11	.34	.27	8.01	7.50	-1.46	1.30	.01456	.00581	0.000000	0.000000	.1490	.0581	0.0000	0.0000
42	R	15.48	.34	.27	9.13	6.60	-1.60	1.17	.01670	.00581	0.000000	0.000000	.1703	.0581	0.0000	0.0000
43	R	15.85	.35	.28	10.36	5.79	-1.75	1.04	.01883	.00581	0.000000	0.000000	.1917	.0581	0.0000	0.0000
44	R	16.21	.36	.29	11.68	5.07	-1.88	.91	.02096	.00581	0.000000	0.000000	.2130	.0581	0.0000	0.0000
45	R	16.58	.36	.31	13.12	4.45	-2.03	.78	.02309	.00581	0.000000	0.000000	.2343	.0581	0.0000	0.0000
46	R	16.95	.36	.32	14.66	3.93	-2.17	.64	.02522	.00581	0.000000	0.000000	.2556	.0581	0.0000	0.0000
47	R	17.32	.37	.34	16.30	3.51	-2.31	.51	.02735	.00581	0.000000	0.000000	.2769	.0581	0.0000	0.0000
48	QF3	17.73	.37	.36	17.34	3.33	-.15	-.07	.02900	.00211	0.000000	0.000000	.2932	.0203	0.0000	0.0000
49	QF3	18.14	.37	.38	16.93	3.62	2.05	-.66	.02909	-.00169	0.000000	0.000000	.2936	-.0185	0.0000	0.0000

POS		S (M)	DX	DY	BX (M)	BY (M)	AX	AY	EX (M)	EXP	EY (M)	EYP	XCO (MM)	DXCO (MR)	YCO (MM)	DYCO (MR)
50	Z	18.50	.38	.39	15.10	4.15	1.94	-.80	.02847	-.00169	0.000000	0.000000	.2869	-.0185	0.0000	0.0000
51	Z	18.86	.38	.40	13.74	4.77	1.82	-.94	.02786	-.00169	0.000000	0.000000	.2802	-.0185	0.0000	0.0000
52	Z	19.22	.39	.41	12.47	5.50	1.71	-1.08	.02725	-.00169	0.000000	0.000000	.2736	-.0185	0.0000	0.0000
53	Z	19.58	.39	.42	11.28	6.34	1.60	-1.23	.02664	-.00169	0.000000	0.000000	.2669	-.0185	0.0000	0.0000
54	Z	19.95	.40	.43	10.17	7.27	1.48	-1.37	.02603	-.00169	0.000000	0.000000	.2602	-.0185	0.0000	0.0000
55	Z	20.31	.40	.44	9.14	8.31	1.37	-1.51	.02542	-.00169	0.000000	0.000000	.2535	-.0185	0.0000	0.0000
56	Z	20.67	.41	.45	8.19	9.45	1.26	-1.65	.02481	-.00169	0.000000	0.000000	.2468	-.0185	0.0000	0.0000
57	Z	21.03	.42	.45	7.33	10.70	1.14	-1.80	.02420	-.00169	0.000000	0.000000	.2401	-.0185	0.0000	0.0000
58	Z	21.39	.42	.46	6.54	12.05	1.03	-1.94	.02359	-.00169	0.000000	0.000000	.2335	-.0185	0.0000	0.0000
59	Z	21.75	.43	.46	5.84	13.49	.92	-2.08	.02298	-.00169	0.000000	0.000000	.2268	-.0185	0.0000	0.0000
60	QD3	22.16	.45	.47	5.44	14.50	-.08	-.30	.02289	.00128	0.000000	0.000000	.2723	.0111	0.0000	0.0000
61	QD3	22.58	.46	.47	5.70	13.08	-.73	1.54	.02405	.00433	0.000000	0.000000	.2561	.0414	0.0000	0.0000
62	R	22.94	.47	.48	6.23	12.88	-.83	1.45	.02564	.00433	0.000000	0.000000	.2512	.0414	0.0000	0.0000
63	R	23.31	.48	.48	6.91	11.85	-.93	1.36	.02723	.00433	0.000000	0.000000	.2664	.0414	0.0000	0.0000
64	R	23.68	.49	.49	7.63	10.88	-1.02	1.28	.02882	.00433	0.000000	0.000000	.2816	.0414	0.0000	0.0000
65	R	24.04	.49	.49	8.41	9.98	-1.12	1.19	.03041	.00433	0.000000	0.000000	.2967	.0414	0.0000	0.0000
66	R	24.41	.50	.50	9.22	9.15	-1.22	1.10	.03200	.00433	0.000000	0.000000	.3119	.0414	0.0000	0.0000
67	R	24.78	.50	.50	10.11	8.36	-1.32	1.01	.03359	.00433	0.000000	0.000000	.3271	.0414	0.0000	0.0000
68	R	25.15	.51	.51	11.04	7.66	-1.42	.92	.03518	.00433	0.000000	0.000000	.3422	.0414	0.0000	0.0000
69	R	25.51	.52	.52	12.04	7.01	-1.52	.83	.03677	.00433	0.000000	0.000000	.3574	.0414	0.0000	0.0000
70	R	25.88	.52	.53	13.43	6.43	-1.62	.74	.03836	.00433	0.000000	0.000000	.3726	.0414	0.0000	0.0000
71	R	26.25	.53	.54	14.66	5.92	-1.71	.66	.03995	.00433	0.000000	0.000000	.3878	.0414	0.0000	0.0000
72	QF	26.56	.53	.55	15.27	5.72	-1.02	-.08	.04046	-.00030	0.000000	0.000000	.3943	-.0040	0.0000	0.0000
73	QF	26.94	.53	.56	14.68	6.05	-1.08	-.03	.03975	-.00492	0.000000	0.000000	.3840	-.0492	0.0000	0.0000
74	QD	27.98	.55	.58	13.68	6.06	-1.41	-1.12	.03469	-.00492	0.000000	0.000000	.3340	-.0492	0.0000	0.0000
75	R	29.44	.57	.60	7.84	12.47	-.98	-1.52	.10393	.08848	0.000000	0.000000	1.8010	1.8188	0.0000	0.0000
76	QD	30.68	.60	.62	5.78	15.90	.71	-1.80	.19555	.08848	0.000000	0.000000	3.6842	1.8188	0.0000	0.0000
77	QD	31.03	.61	.62	5.53	16.54	.00	.00	.23058	.11206	0.000000	0.000000	4.3902	2.2746	0.0000	0.0000
78	QD	31.38	.62	.63	5.78	15.90	-.71	1.81	.27461	.14000	0.000000	0.000000	5.2844	2.8210	0.0000	0.0000
79	QD	32.41	.64	.64	7.52	12.44	-.98	1.53	.41957	.14000	0.000000	0.000000	8.2103	2.8210	0.0000	0.0000
80	R	34.07	.67	.66	11.47	8.01	-1.41	1.12	.72947	.23333	0.000000	0.000000	14.4395	4.6883	0.0000	0.0000
81	Q	34.01	.66	.66	13.68	6.31	-1.60	.92	.90108	.23333	0.000000	0.000000	17.8874	4.6883	0.0000	0.0000
82	SK	34.01	.66	.66	13.68	6.31	-1.56	.88	.90108	.23113	0.000000	0.000000	17.8874	4.6663	0.0000	0.0000
83	QS	35.11	.67	.69	15.61	6.00	-1.65	.82	.97042	.23113	0.000000	0.000000	19.2873	4.6663	0.0000	0.0000
84	QF	35.46	.69	.70	15.20	5.69	-.05	.07	1.03176	.11724	0.000000	0.000000	20.5223	2.3566	0.0000	0.0000
85	QF	35.81	.69	.71	14.57	5.90	1.74	-.46	1.02212	-.00119	0.000000	0.000000	20.9282	-.0483	0.0000	0.0000
86	QS	36.11	.69	.71	13.95	6.32	1.66	-.75	1.03176	-.00119	0.000000	0.000000	20.9138	-.0483	0.0000	0.0000
87	SF	36.11	.69	.71	13.95	6.32	1.70	-.75	1.03176	-.00420	0.000000	0.000000	20.9138	-.0784	0.0000	0.0000
88	D	36.05	.70	.71	17.21	9.66	1.48	-.94	1.04867	-.00420	0.000000	0.000000	20.8561	-.0784	0.0000	0.0000
89	LC	38.91	.73	.76	7.01	11.36	1.01	-1.35	1.04170	-.00420	0.000000	0.000000	20.7258	-.0784	0.0000	0.0000
90	D	39.24	.75	.77	5.73	13.48	.80	-1.23	1.03861	-.00420	0.000000	0.000000	20.6682	-.0784	0.0000	0.0000
91	SD	39.24	.75	.77	5.73	13.48	.76	-1.47	1.03861	.00025	0.000000	0.000000	20.6682	-.0337	0.0000	0.0000
92	QS	39.54	.76	.77	5.20	14.38	.69	-1.54	1.03868	.00025	0.000000	0.000000	20.6280	-.0337	0.0000	0.0000
93	QD	39.89	.77	.78	5.04	14.90	.03	-.08	1.04902	.11620	0.000000	0.000000	21.0572	2.3167	0.0000	0.0000
94	QD	40.24	.78	.78	5.23	14.27	-.62	1.69	1.12065	.23668	0.000000	0.000000	22.2643	4.7634	0.0000	0.0000
95	QS	40.54	.79	.78	5.49	13.28	-.70	1.61	1.19165	.23668	0.000000	0.000000	23.1233	4.7634	0.0000	0.0000
96	SD	40.54	.79	.78	5.65	13.28	-.73	1.68	1.19165	.24253	0.000000	0.000000	23.1233	4.8222	0.0000	0.0000
97	D	41.28	.81	.79	6.87	10.97	-.93	1.47	1.37002	.24253	0.000000	0.000000	27.2607	4.8222	0.0000	0.0000
98	LC	42.94	.84	.82	10.71	6.89	-1.38	.99	1.77273	.24253	0.000000	0.000000	35.2766	4.8222	0.0000	0.0000
99	D	43.67	.85	.84	12.89	5.59	-1.58	.78	1.95110	.24253	0.000000	0.000000	38.8230	4.8222	0.0000	0.0000

POS		S (M)	QX	QY	BX (M)	BY (M)	AX	AY	EX (M)	EXP	EY (M)	EYP	XCO (MM)	DXCO (MR)	YCO (MM)	DYCO (MR)
100	SF	43.67	.95	.84	12.89	5.59	-1.51	.75	1.95110	-.23219	0.000000	0.000000	38.8230	4.7183	0.0000	0.0000
101	OS	43.97	.96	.85	13.82	5.16	-1.50	.66	2.02075	-.23219	0.000000	0.000000	40.2385	4.7183	0.0000	0.0000
102	QF	44.32	.86	.86	14.38	4.93	-.01	.01	2.06162	-.00007	0.000000	0.000000	41.0684	-.0010	0.0000	0.0000
103	QF	44.67	.86	.87	13.81	5.16	1.60	-.69	2.02080	-.23205	0.000000	0.000000	40.2392	-4.7163	0.0000	0.0000
104	QS	44.97	.87	.88	12.87	5.57	1.52	-.74	1.95118	-.23205	0.000000	0.000000	38.8243	-4.7163	0.0000	0.0000
105	SF	44.97	.87	.88	12.87	5.57	1.69	-.77	1.95118	-.24240	0.000000	0.000000	38.8243	-4.8203	0.0000	0.0000
106	Q	45.71	.88	.90	10.68	6.85	1.39	-.97	1.77292	-.24240	0.000000	0.000000	35.2793	-4.8203	0.0000	0.0000
107	Q	47.31	.91	.93	6.81	10.81	.93	-1.39	1.44719	-.14907	0.000000	0.000000	28.8236	-2.9529	0.0000	0.0000
108	Q	48.11	.93	.94	5.59	13.01	.73	-1.59	1.33756	-.14907	0.000000	0.000000	26.6519	-2.9529	0.0000	0.0000
109	SD	48.11	.93	.94	5.59	13.01	.70	-1.52	1.33756	-.14169	0.000000	0.000000	26.6519	-2.8786	0.0000	0.0000
110	OS	48.41	.94	.95	5.19	12.94	-.62	-1.69	1.29505	-.14169	0.000000	0.000000	25.7883	-2.8786	0.0000	0.0000
111	QD	48.76	.95	.95	4.99	14.52	-.03	-.02	1.27033	.00011	0.000000	0.000000	25.2697	.0016	0.0000	0.0000
112	QS	49.11	.96	.95	5.23	13.97	-.68	1.86	1.29519	-.14191	0.000000	0.000000	25.7846	2.8818	0.0000	0.0000
113	OS	49.41	.97	.96	5.67	13.06	-.77	1.58	1.33771	.14191	0.000000	0.000000	26.6540	2.8818	0.0000	0.0000
114	SD	49.41	.97	.96	5.67	13.06	-.80	1.56	1.33771	.14930	0.000000	0.000000	26.6540	2.9561	0.0000	0.0000
115	Q	50.15	.99	.97	7.00	10.91	-1.01	1.36	1.44750	.14930	0.000000	0.000000	28.8280	2.9561	0.0000	0.0000
116	Q	51.81	1.02	1.00	11.16	7.02	-1.59	.96	1.77361	.24263	0.000000	0.000000	35.2891	4.8235	0.0000	0.0000
117	Q	52.54	1.02	1.02	12.81	5.75	-1.70	.76	1.95204	.24263	0.000000	0.000000	38.8364	4.8235	0.0000	0.0000
118	SF	52.54	1.02	1.02	12.81	5.75	-1.63	.73	1.95204	.23227	0.000000	0.000000	38.8364	4.7194	0.0000	0.0000
119	QS	52.84	1.03	1.03	13.41	5.34	-1.71	.68	2.02142	.23227	0.000000	0.000000	40.2922	4.7194	0.0000	0.0000
120	QF	53.19	1.03	1.04	15.13	5.12	-.03	-.03	2.06260	.00004	0.000000	0.000000	41.0823	.0006	0.0000	0.0000
121	QF	53.53	1.04	1.05	14.56	5.38	1.65	-.71	2.02175	-.23219	0.000000	0.000000	40.2526	-4.7183	0.0000	0.0000
122	QS	53.85	1.04	1.06	13.59	5.83	1.57	-.79	1.95209	-.23219	0.000000	0.000000	38.8371	-4.7183	0.0000	0.0000
123	QF	53.85	1.04	1.06	13.59	5.83	1.64	-.83	1.95209	-.24255	0.000000	0.000000	38.8371	-4.8224	0.0000	0.0000
124	QS	54.88	1.05	1.07	11.82	7.19	1.41	-1.03	1.77372	-.24255	0.000000	0.000000	35.2906	-4.8224	0.0000	0.0000
125	Q	56.24	1.08	1.10	7.26	11.26	.99	-1.45	1.44775	-.14922	0.000000	0.000000	28.8314	-2.9550	0.0000	0.0000
126	Q	56.98	1.10	1.11	5.95	13.65	.79	-1.66	1.33801	-.14922	0.000000	0.000000	26.6581	-2.9550	0.0000	0.0000
127	SD	56.98	1.10	1.11	5.95	13.65	.76	-1.58	1.33801	-.14183	0.000000	0.000000	26.6581	-2.8807	0.0000	0.0000
128	OS	57.28	1.10	1.12	5.52	14.62	.68	-1.66	1.29546	-.14183	0.000000	0.000000	25.7939	-2.8807	0.0000	0.0000
129	QD	57.63	1.11	1.12	5.29	15.21	-.00	-.00	1.27069	.00001	0.000000	0.000000	25.2907	.0001	0.0000	0.0000
130	QD	57.98	1.12	1.12	5.53	14.62	-.69	1.65	1.29544	.14185	0.000000	0.000000	25.7940	2.8809	0.0000	0.0000
131	QS	58.28	1.13	1.13	6.97	13.66	-.77	1.97	1.33805	.14185	0.000000	0.000000	26.6583	2.8809	0.0000	0.0000
132	SD	58.28	1.13	1.13	6.97	13.66	-.80	1.65	1.33805	.14924	0.000000	0.000000	26.6583	2.9552	0.0000	0.0000
133	D	59.02	1.15	1.14	7.29	11.38	-1.00	1.42	1.44778	.14924	0.000000	0.000000	28.8316	2.9552	0.0000	0.0000
134	S	60.68	1.18	1.17	11.39	7.22	-1.48	1.03	1.77379	.24257	0.000000	0.000000	35.2912	4.8226	0.0000	0.0000
135	Q	61.42	1.19	1.18	13.68	5.86	-1.66	.82	1.95218	.24257	0.000000	0.000000	38.8379	4.8226	0.0000	0.0000
136	SF	61.42	1.19	1.18	13.68	5.86	-1.59	.79	1.95218	.23221	0.000000	0.000000	38.8379	4.7185	0.0000	0.0000
137	QS	61.75	1.19	1.19	14.66	5.41	-1.66	.77	2.02185	.23221	0.000000	0.000000	40.2534	4.7185	0.0000	0.0000
138	QF	62.07	1.20	1.20	15.24	5.16	-.03	.02	2.06270	-.00003	0.000000	0.000000	41.0831	-.0005	0.0000	0.0000
139	QF	62.42	1.20	1.21	14.62	5.38	1.72	-.86	2.02183	-.23227	0.000000	0.000000	40.2531	-4.7194	0.0000	0.0000
140	QS	62.72	1.20	1.22	13.61	5.80	1.64	-.74	1.95214	-.23227	0.000000	0.000000	38.8373	-4.7194	0.0000	0.0000
141	SF	62.72	1.20	1.22	13.61	5.80	1.71	-.77	1.95214	-.24263	0.000000	0.000000	38.8373	-4.8235	0.0000	0.0000
142	Q	63.45	1.21	1.24	11.25	7.08	1.30	-.97	1.77371	-.24263	0.000000	0.000000	35.2890	-4.8235	0.0000	0.0000
143	Q	65.11	1.24	1.27	7.06	10.99	1.02	-1.37	1.44761	-.14930	0.000000	0.000000	28.8249	-2.9561	0.0000	0.0000
144	Q	65.85	1.26	1.28	5.71	13.15	.81	-1.56	1.33781	-.14930	0.000000	0.000000	26.6548	-2.9561	0.0000	0.0000
145	SD	65.85	1.26	1.28	5.71	13.15	.77	-1.49	1.33781	-.14191	0.000000	0.000000	26.6548	-2.8818	0.0000	0.0000
146	OS	66.15	1.27	1.28	5.27	14.07	.69	-1.56	1.29523	-.14191	0.000000	0.000000	25.7903	-2.8818	0.0000	0.0000
147	QD	66.50	1.28	1.29	5.02	14.61	.03	.03	1.27043	-.00010	0.000000	0.000000	25.2866	-.0015	0.0000	0.0000
148	QD	66.85	1.29	1.29	5.23	14.03	-.62	1.61	1.29516	.14171	0.000000	0.000000	25.7892	2.8788	0.0000	0.0000
149	OS	67.15	1.30	1.29	5.62	13.09	-.70	1.53	1.33767	.14171	0.000000	0.000000	26.6529	2.8788	0.0000	0.0000

POS		S (M)	QX	QY	BX (M)	BY (M)	AX	AY	EX (M)	EXP	EY (M)	EYP	XCO (MM)	DXCO (MR)	YCO (MM)	DYCO (MR)
150	SD	67.15	1.30	1.29	9.62	13.03	-.73	1.61	1.33767	.14910	0.000000	0.000000	26.6529	2.9531	0.0000	0.0000
151	Q	67.89	1.32	1.30	6.84	10.87	-.93	1.41	1.44732	.14910	0.000000	0.000000	28.8247	2.9531	0.0000	0.0000
152	B	69.55	1.35	1.34	10.69	6.87	-1.38	.98	1.77309	.24242	0.000000	0.000000	35.2808	4.8205	0.0000	0.0000
153	Q	70.29	1.36	1.35	12.88	5.58	-1.58	.77	1.95137	.24242	0.000000	0.000000	38.8259	4.8205	0.0000	0.0000
154	SF	70.29	1.36	1.35	12.88	5.58	-1.52	.74	1.95137	.23208	0.000000	0.000000	38.8259	4.7165	0.0000	0.0000
155	OS	70.59	1.36	1.36	13.81	5.16	-1.59	.66	2.02100	.23208	0.000000	0.000000	40.2408	4.7165	0.0000	0.0000
156	QF	70.94	1.37	1.37	14.37	4.93	.00	.00	2.06182	-.00007	0.000000	0.000000	41.0701	-.0010	0.0000	0.0000
157	QF	71.29	1.37	1.39	13.81	5.16	1.60	-.66	2.02095	-.23221	0.000000	0.000000	40.2401	-4.7185	0.0000	0.0000
158	OS	71.59	1.38	1.39	12.87	5.57	1.52	-.74	1.95128	-.23221	0.000000	0.000000	38.8246	-4.7185	0.0000	0.0000
159	SF	71.59	1.38	1.39	12.87	5.57	1.59	-.77	1.95128	-.24256	0.000000	0.000000	38.8246	-4.8224	0.0000	0.0000
160	Q	72.32	1.39	1.41	10.68	6.86	1.39	-.98	1.77290	-.24256	0.000000	0.000000	35.2780	-4.8224	0.0000	0.0000
161	B	73.99	1.42	1.44	6.83	10.84	.93	-1.40	1.44691	-.14923	0.000000	0.000000	28.8186	-2.9551	0.0000	0.0000
162	B	74.72	1.44	1.45	5.60	13.05	.73	-1.60	1.33716	-.14923	0.000000	0.000000	26.6453	-2.9551	0.0000	0.0000
163	SD	74.72	1.44	1.45	5.60	13.05	.70	-1.53	1.33716	-.14185	0.000000	0.000000	26.6453	-2.8808	0.0000	0.0000
164	OS	75.02	1.44	1.46	5.21	13.99	.62	-1.60	1.29461	-.14185	0.000000	0.000000	25.7811	-2.8808	0.0000	0.0000
165	QD	75.37	1.46	1.46	5.00	14.56	-.03	-.02	1.26982	-.00011	0.000000	0.000000	25.2776	-.0015	0.0000	0.0000
166	QD	75.72	1.47	1.47	5.25	14.02	-.69	1.56	1.29453	.14163	0.000000	0.000000	25.7800	2.8777	0.0000	0.0000
167	OS	76.02	1.48	1.47	5.69	13.11	-.77	1.49	1.33702	.14163	0.000000	0.000000	26.6433	2.8777	0.0000	0.0000
168	SD	76.02	1.48	1.47	5.69	13.11	-.80	1.56	1.33702	.14901	0.000000	0.000000	26.6433	2.9520	0.0000	0.0000
169	B	76.76	1.49	1.48	7.03	10.95	-1.02	1.37	1.44661	.14901	0.000000	0.000000	28.8143	2.9520	0.0000	0.0000
170	B	78.42	1.52	1.51	11.20	7.05	-1.50	.97	1.77224	.24234	0.000000	0.000000	35.2685	4.8193	0.0000	0.0000
171	Q	79.16	1.53	1.53	13.56	5.78	-1.71	.76	1.95047	.24234	0.000000	0.000000	38.8128	4.8193	0.0000	0.0000
172	SF	79.16	1.53	1.53	13.56	5.78	-1.63	.73	1.95047	.23200	0.000000	0.000000	38.8128	4.7154	0.0000	0.0000
173	OS	79.46	1.54	1.54	14.56	5.36	-1.72	.65	2.02007	.23200	0.000000	0.000000	40.2274	4.7154	0.0000	0.0000
174	QF	79.81	1.54	1.55	15.19	5.14	-.03	-.02	2.06088	-.00004	0.000000	0.000000	41.0566	-.0005	0.0000	0.0000
175	QF	80.16	1.54	1.56	14.61	5.40	1.66	-.71	2.02004	-.23207	0.000000	0.000000	40.2271	-4.7164	0.0000	0.0000
176	OS	80.46	1.55	1.57	13.64	5.85	1.58	-.79	1.95042	-.23207	0.000000	0.000000	38.8121	-4.7164	0.0000	0.0000
177	SF	80.46	1.55	1.57	13.64	5.85	1.65	-.82	1.95042	-.24241	0.000000	0.000000	38.8121	-4.8203	0.0000	0.0000
178	Q	81.19	1.56	1.58	11.35	7.21	1.45	-1.03	1.77214	-.24241	0.000000	0.000000	35.2671	-4.8203	0.0000	0.0000
179	B	82.86	1.59	1.61	7.28	11.37	1.00	-1.45	1.44640	-.14908	0.000000	0.000000	28.8112	-2.9530	0.0000	0.0000
180	Q	83.59	1.60	1.62	5.96	13.65	.80	-1.65	1.33676	-.14908	0.000000	0.000000	26.6395	-2.9530	0.0000	0.0000
181	SD	83.59	1.60	1.62	5.96	13.65	.76	-1.58	1.33676	-.14171	0.000000	0.000000	26.6395	-2.8788	0.0000	0.0000
182	OS	83.89	1.61	1.63	5.53	14.62	.68	-1.65	1.29425	-.14171	0.000000	0.000000	25.7759	-2.8788	0.0000	0.0000
183	QD	84.24	1.62	1.63	5.29	15.21	-.00	.00	1.26950	.00000	0.000000	0.000000	25.2730	-.0000	0.0000	0.0000
184	REFL	158.48	3.25	3.26	17.61	6.38	.00	-.00	-.04374	.00000	0.000000	0.000000	-.4298	0.0000	0.0000	0.0000

```
CIRCUMFERENCE =   505.4538 M          THETX =   6.28318638 RAD      NUX =   9.73708      DNUX/(DP/P) =   .47056
[illegible] =   .[illegible] M   THETY( 183) =   0.00000000 RAD      NUY =   9.77653      DNUY/(DP/P) =   .28502
                                      TGAM = (   7.58479,   0.00000)

MAXIMA   --- BETX( 184) =   17.60977   BETY(  12) =   17.91103   ETAX( 138) =   2.06270   ETAY( 184) =   0.00000
MINIMA   --- BETX(  36) =    4.20509   BETY(  48) =    3.32724   ETAX(  34) =    .00065   ETAY( 184) =   0.00000
*****************************************************************************************************************
***      INCR     1,   // DP        0.000000     VALUE =        -.020000

***      FIN     0   0  // CORE USE SUMMARY                         MAXIMUM              USED      UNUSED
                           STORE  (ELEMENT STORAGE)                   9600 (LMAX)         1911       7689
                           INFF   (ELEMENT DEFINITIONS)                400 (MAX)            79        321

=================================================================================================================
END OF SYNCH RUN DRSM
15.03.03.MYJ11,T1000,HP.
15.03.03.JOB CLASS = P3, PRIORITY = HP.
15.03.03.USER,91046,.
15.03.03.CHARGE,6112.
```

APPENDIX E

APPENDIX E.

Synch Run Accumulator Lattice

```
                                8 0 GEV KINETIC EXTRACTION ORBIT
                                7.92767 GEV KINETIC CENTRAL ENERGY.
                                8 MARCH 83.  A. ANDO,  DE JOHNSON

***   BRHO      =               //  294.0756
***   RO        =               //  16.8391978
***   BL        =               //  0.3048
***   BL1       =               //  1.5240
***   BL2       =               //  3.0480
***   BL3       =               //  4.5720

***   A10       DRF             //  0.0
***   A20       DRF             //  0.0

***   LS        DRF             //  7.946495
***   LS*       DRF             //  7.84408
***   Q1        DRF             //  0.512413
***   Q2        DRF             //  0.960396
***   Q3        DRF             //  0.9042
***   QB3       DRF             //  6.42366
***   Q4        DRF             //  3.2610
***   Q5        DRF             //  7.34776
***   Q6        DRF             //  4.18716
***   Q7        DRF             //  2.8476
***   QS7       DRF             //  1.29304
***   QB7       DRF             //  0.5080
***   Q8        DRF             //  1.2192
***   QB8       DRF             //  0.5080
***   Q9        DRF             //  0.3048
***   Q99       DRF             //  0.6096
***   QB9       DRF             //  0.5080
***   Q10       DRF             //  0.3080
***   QB10      DRF             //  0.2919
***   QS10      DRF             //  0.2919
***   Q11       DRF             //  0.52102
***   Q12       DRF             //  0.2178
***   QS12      DRF             //  0.2178
***   Q13       DRF             //  0.49722

                                SMALL APERTURE DIPOLES

***   B3        MAG             //  BL1        0.0         BRHO        BO          $
***   B7        MAG             //  BL2        0.0         BRHO        BO          $
***   B8        MAG             //  BL3        0.0         BRHO        BO          $

                                LARGE APERTURE DIPOLES

***   B9        MAG             //  BL3        0.0         BRHO        BO          $
***   B10       MAG             //  BL3        0.0         BRHO        BO          $

                                SMALL APERTURE QUADRUPOLES
                                HALF QUAD LENGTHS LISTED

***   GF        =               //  96.6333
***   GD        =               //  -97.4126
***   GT        =               //  103.8087

***   Q1        MAG             //  0.32004    GT          BRHO
***   Q2        MAG             //  0.655828   -GT         BRHO
***   Q3        MAG             //  0.35052    GT          BRHO
***   Q4        MAG             //  0.2286     GF          BRHO
***   Q5        MAG             //  0.41402    GD          BRHO
***   Q6        MAG             //  0.35052    GF          BRHO
***   Q7        MAG             //  0.35052    GD          BRHO
***   Q8        MAG             //  0.2286     GF          BRHO
***   Q9        MAG             //  0.2286     GD          BRHO

                                LARGE APERTURE QUADRUPOLES

***   G10       =               //  40.8765
***   GF1       =               //  89.3989
***   GD1       =               //  -89.3989

***   G10       MAG             //  0.2286     G10         BRHO
***   G11       MAG             //  0.43688    GF1         BRHO
***   G12       MAG             //  0.3861     GD1         BRHO
***   G13       MAG             //  0.3861     GD1         BRHO
***   G14       MAG             //  0.32131    GF1         BRHO

                                SEXTUPOLES
```

```
***  S7      SXTP          //  SL        0.0       BRHD
***  S9      SXTP          //  SL        0.0       BRHD
***  S10     SXTP          //  SL        0.0       BRHD
***  S12     SXTP          //  SL        0.0       BRHD

***  R/6     BML           //  A10  LS   Q1   Q1   Q1   Q2   Q2   Q2   Q3   Q3   Q3   B3
  *                        //  QB3  Q4   Q4   Q4   Q5   Q5   Q5   Q6   Q6   Q6   Q7   Q7
  *                        //  Q7   S7   QS7  B7   QB7  Q8   Q8   Q8   B8   QB8  Q9   Q9
  *                        //  Q9   S9   QS9  B9   QB9  Q10  Q10  Q10  B10  QB10 S10  QS10
  *                        //  Q11  Q11  Q11  Q12  Q12  Q12  S12  QS12 Q13  Q13  Q13  Q14
  *                        //  Q14  LS*  A20
***                 CYC   -3 //  R/6
```

POS		S(M)	NUX	NUY	BETAX(M)	BETAY(M)	ETAX(M)	ETAY(M)	ETAS(M)	ALPHAX	ALPHAY	DETAX	DETAY
0		0.0000	0.00000	0.00000	7.56400	7.26661	.00155	0.00000	0.00000	0.00000	0.00000	-.00000	0.00000
1	A10	0.0000	0.00000	0.00000	7.56400	7.26661	.00155	0.00000	0.00000	0.00000	0.00000	-.00000	0.00000
2	LS	7.9465	.12892	.13211	15.91233	15.95660	.00155	0.00000	0.00000	-1.09057	-1.09356	-.00000	0.00000
3	Q1	8.2665	.13210	.13519	16.01364	17.27175	.00152	0.00000	0.00000	.73785	-3.06516	-.00017	0.00000
4	Q1	8.5866	.13536	.13795	14.99036	19.97577	.00144	0.00000	0.00000	2.42084	-5.48543	-.00034	0.00000
5	Q1	9.0990	.14129	.14153	12.62959	26.00603	.00126	0.00000	0.00000	2.18633	-6.28294	-.00034	0.00000
6	Q2	9.7548	.15011	.14516	11.68624	30.32147	.00113	0.00000	0.00000	-.67585	.03924	-.00007	0.00000
7	Q2	10.4106	.15831	.14879	14.50755	25.91321	.00117	0.00000	0.00000	-3.96970	6.33876	.00020	0.00000
8	Q2	11.3712	.16661	.15649	23.27416	15.20161	.00136	0.00000	0.00000	-5.07325	4.81223	.00020	0.00000
9	Q3	11.7218	.16887	.16035	25.87297	12.59663	.00140	0.00000	0.00000	-2.23340	2.72664	.00002	0.00000
10	Q3	12.0723	.17099	.16327	26.31581	11.26714	.00138	0.00000	0.00000	.98833	1.12096	-.00015	0.00000
11	Q3	12.9765	.17665	.17927	24.58992	9.40373	.00124	0.00000	0.00000	.92041	.93987	-.00015	0.00000
12	B3	14.5005	.18708	.20947	21.96209	6.94355	.06747	0.00000	.00203	.80608	.66827	.08717	0.00000
13	QB3	20.9241	.24525	.39718	14.70981	6.95470	.62745	0.00000	.00203	.32354	-.67000	.08717	0.00000
14	Q4	21.1527	.24776	.40227	14.31239	7.39561	.64194	0.00000	.00203	1.38758	-1.26974	.03943	0.00000
15	Q4	21.3813	.25037	.40697	13.45148	8.12909	.64542	0.00000	.00203	2.35686	-1.95720	-.00899	0.00000
16	Q4	24.6423	.33229	.44215	3.26194	27.21314	.61610	0.00000	.00203	.76780	-3.89501	-.00899	0.00000
17	Q5	25.0564	.35408	.44448	2.87570	28.90145	.62991	0.00000	.00203	.18270	-.10537	.07605	0.00000
18	Q5	25.4704	.37700	.44680	2.94779	27.38111	.67966	0.00000	.00203	-.36012	3.70775	.16542	0.00000
19	Q5	32.8181	.52344	.69382	28.93029	1.97247	1.89516	0.00000	.00203	-3.17600	-.24974	.16542	0.00000
20	Q6	33.1687	.52532	.72031	29.99143	2.30008	1.91463	0.00000	.00203	.18953	-.69745	-.05472	0.00000
21	Q6	33.5192	.52721	.74184	28.67165	2.97688	1.85705	0.00000	.00203	3.52486	-1.25931	-.27267	0.00000
22	Q6	37.7063	.57374	.81659	7.36233	28.75210	.71534	0.00000	.00203	1.56435	-4.89647	-.27267	0.00000
23	Q7	38.0569	.58180	.81845	6.59770	31.04324	.63372	0.00000	.00203	.64659	-1.55101	-.19462	0.00000
24	Q7	38.4074	.59043	.82024	6.43097	30.86822	.57798	0.00000	.00203	-.16448	2.04353	-.12451	0.00000
25	Q7	41.2550	.65273	.83825	8.66271	20.58959	.22342	0.00000	.00203	-.61925	1.56604	-.12451	0.00000
26	B7	41.5998	.65821	.84066	9.03904	19.65091	.18547	0.00000	.00203	-.66793	1.51493	-.12451	0.00000
27	QB7	42.8328	.67884	.85228	11.04937	16.01312	.02448	0.00000	.00203	-.87443	1.29812	-.12451	0.00000
28	B7	45.9008	.71351	.89247	17.82159	9.29316	-.08779	0.00000	-.01127	-1.35874	.87293	.05047	0.00000
29	QB7	46.4088	.71787	.90159	19.24328	8.45519	-.06215	0.00000	-.01127	-1.43987	.77661	.05047	0.00000
30	Q8	46.6374	.71974	.90596	19.57382	8.25203	-.05012	0.00000	-.01127	.00223	.11716	.05469	0.00000
31	Q8	46.8660	.72161	.91036	19.24127	8.34682	-.03722	0.00000	-.01127	1.44418	-.53419	.05798	0.00000
32	Q8	49.0852	.73270	.93179	15.95816	9.87830	.03346	0.00000	-.01127	1.24866	-.72194	.05798	0.00000
33	B8	52.6572	.79843	.98624	7.94667	18.80195	.89057	0.00000	.08409	.52381	-1.16259	.32128	0.00000
34	QB8	53.1652	.80894	.99041	7.45586	20.01542	1.05379	0.00000	.08409	.44235	-1.22613	.32128	0.00000
35	Q9	53.3938	.81386	.99221	7.38952	20.23158	1.13658	0.00000	.08409	-.15046	.28603	.40409	0.00000
36	Q9	53.6224	.81873	.99403	7.59503	19.75689	1.23907	0.00000	.08409	-.75374	1.77849	.49391	0.00000
37	Q9	53.9272	.82492	.99655	8.07370	18.69230	1.38961	0.00000	.08409	-.81667	1.71427	.49391	0.00000
38	B9	54.2320	.83075	.99922	8.59072	17.66686	1.54016	0.00000	.08409	-.87961	1.65004	.49391	0.00000
39	QB9	54.8416	.84137	1.00504	9.73986	15.73343	1.84124	0.00000	.08409	-1.00547	1.52159	.49391	0.00000
40	B9	59.4136	.89014	1.08571	23.04733	5.63827	4.66875	0.00000	.91485	-1.93869	.61035	.75721	0.00000
41	QB9	59.9216	.89390	1.10084	25.07033	5.08097	5.05342	0.00000	.91485	-2.04358	.48669	.75721	0.00000
42	B10	60.1502	.89493	1.10814	25.82923	4.90713	5.20797	0.00000	.91485	-1.26816	.27562	.59409	0.00000
43	Q10	60.3788	.89633	1.11562	26.22433	4.82772	5.32471	0.00000	.91485	-.45599	.07259	.42664	0.00000
44	B10	60.8868	.89938	1.13244	26.69950	4.80771	5.54144	0.00000	.91485	-.47939	-.03319	.42664	0.00000
45	B10	65.4588	.92410	1.25367	31.97419	9.12771	8.06492	0.00000	2.67987	-.68759	-.87912	.68995	0.00000
46	QB10	65.7307	.92555	1.25862	32.37953	9.65749	8.26631	0.00000	2.67987	-.70103	-.93582	.68995	0.00000
47	B10	66.0555	.92704	1.26350	32.81116	10.24601	8.47661	0.00000	2.67987	-.71507	-.99502	.68995	0.00000
48	QB10	66.3474	.92844	1.26790	33.23255	10.84345	8.67801	0.00000	2.67987	-.72852	-1.05171	.68995	0.00000
49	Q11	66.7843	.93056	1.27394	31.96215	12.47757	8.72598	0.00000	2.67987	3.57995	-2.76080	-.47140	0.00000

POS		S(M)	NUX	NUY	BETAX(M)	BETAY(M)	ETAX(M)	ETAY(M)	ETAS(M)	ALPHAX	ALPHAY	DETAX	DETAY
50	Q11	67.2212	.93289	1.27893	27.21571	15.85680	8.27009	0.00000	2.67987	7.07349	-5.12314	-1.60552	0.00000
51	Q11	67.7422	.93641	1.28341	20.35389	21.66177	7.43358	0.00000	2.67987	6.09649	-6.01840	-1.60552	0.00000
52	Q12	68.1283	.93977	1.28601	16.72287	25.45541	6.97807	0.00000	2.67987	3.44951	-3.65826	-.76292	0.00000
53	Q12	68.5144	.94370	1.28833	14.86405	27.14243	6.84000	0.00000	2.67987	1.43734	-.64493	.04497	0.00000
54	Q12	68.7322	.94608	1.28960	14.24773	27.42584	6.84979	0.00000	2.67987	1.39242	-.65629	.04497	0.00000
55	S12	69.0370	.94959	1.29135	13.41807	27.83076	6.86350	0.00000	2.67987	1.32955	-.67219	.04497	0.00000
56	QS12	69.2548	.95223	1.29259	12.84871	28.12604	6.87329	0.00000	2.67987	1.28462	-.68356	.04497	0.00000
57	Q13	69.6409	.95712	1.29479	12.44883	27.39026	7.04712	0.00000	2.67987	-.23333	2.56037	.85885	0.00000
58	Q13	70.0270	.96195	1.29715	13.22005	24.29020	7.34152	0.00000	2.67987	-1.79422	5.34713	1.71180	0.00000
59	Q13	70.3242	.96756	1.30081	15.08319	19.27399	8.39266	0.00000	2.67987	-1.95291	4.74139	1.71180	0.00000
60	Q14	70.8455	.97084	1.30366	15.87623	16.90129	8.80845	0.00000	2.67987	-.48935	2.72016	.86951	0.00000
61	Q14	71.1668	.97407	1.30681	15.69904	15.70432	8.94851	0.00000	2.67987	1.03500	1.04401	.00000	0.00000
62	LS*	79.0117	1.10180	1.43524	7.97960	7.91415	8.94851	0.00000	2.67987	-.00000	.00000	.00000	0.00000
63	A20	79.0117	1.10180	1.43524	7.57960	7.91415	8.94851	0.00000	2.67987	-.00000	.00000	.00000	0.00000
64	REFL	158.0234	2.20361	2.87048	7.56400	7.26661	.00155	0.00000	5.35974	.00000	.00000	.00000	0.00000

CIRCUMFERENCE = 474.0703 M THETX = 6.28318533 RAD NUX = 6.61082 DNUX/(DP/P) = -8.47593
RADIUS = 75.4506 M THETY(63) = 0.00000000 RAD NUY = 8.61144 DNUY/(DP/P) = -12.88242
(DS/S)/(DP/P) = .0339174 TGAM = (5.42986, 0.00000)

MAXIMA --- BETX(48) = 33.23255 BETY(23) = 31.04324 ETAX(63) = 8.94851 ETAY(64) = 0.00000
MINIMA --- BETX(17) = 2.87570 BETY(19) = 1.97247 ETAX(28) = -.08779 ETAY(64) = 0.00000

SEXTUPOLE CORRECTIONS

```
***  KS7      =          //  35.7175
***  KS9      =          //  -219.5244
***  KS10     =          //  134.7943
***  KS12     =          //  -170.5021

***  S7       SXTP       //  SL        KS7       BRHO
***  S9       SXTP       //  SL        KS9       BRHO
***  S10      SXTP       //  SL        KS10      BRHO
***  S12      SXTP       //  SL        KS12      BRHO

***           CYC     -3 //  R/6
```

PUG		S(M)	NUX	NUY	BETAX(M)	BETAY(M)	ETAX(M)	ETAY(M)	ETAS(M)	ALPHAX	ALPHAY	DETAX	DETAY
0		0.0000	0.00000	0.00000	7.56400	7.26661	.00155	0.00000	0.00000	0.00000	0.00000	-.00000	0.00000
1	A10	0.0000	0.00000	0.00000	7.56400	7.26661	.00155	0.00000	0.00000	0.00000	0.00000	-.00000	0.00000
2	LS	7.9465	.12892	.13211	15.91233	15.95460	.00155	0.00000	0.00000	-1.05057	-1.09356	-.00000	0.00000
3	Q1	8.2665	.13210	.13519	16.01364	17.27175	.00152	0.00000	0.00000	.73785	-3.06216	-.00017	0.00000
4	Q1	8.5866	.13536	.13795	14.99036	19.97577	.00144	0.00000	0.00000	2.42084	-5.48543	.00034	0.00000
5	Q1	9.0990	.14129	.14153	12.62959	26.00603	.00126	0.00000	0.00000	2.18633	-6.28294	-.00034	0.00000
6	Q2	9.7548	.15011	.14516	11.68624	30.32147	.00113	0.00000	0.00000	-.67585	.03924	-.00007	0.00000
7	Q2	10.4106	.15831	.14879	14.58755	25.91321	.00117	0.00000	0.00000	-3.96970	6.33876	.00020	0.00000
8	Q2	11.3712	.16661	.15649	23.27416	15.20161	.00136	0.00000	0.00000	-5.07325	4.81223	.00020	0.00000
9	Q3	11.7218	.16887	.16055	25.87297	12.59663	.00140	0.00000	0.00000	-2.23340	2.72664	.00002	0.00000
10	Q3	12.0723	.17099	.16527	26.31581	11.26714	.00138	0.00000	0.00000	.98833	1.12096	-.00015	0.00000
11	Q3	12.9765	.17663	.17927	24.38992	9.40373	.00124	0.00000	0.00000	.92041	.93987	-.00015	0.00000
12	B3	14.3005	.18708	.20947	21.96209	6.94355	.06747	0.00000	.00203	.80608	.66827	.08717	0.00000
13	QB3	20.9241	.24525	.39718	14.70581	6.95470	.62745	0.00000	.00203	.32354	-.67000	.08717	0.00000
14	Q4	21.1527	.24776	.40227	14.31239	7.39561	.64194	0.00000	.00203	1.38758	-1.26974	.03943	0.00000
15	Q4	21.3813	.25037	.40697	13.45148	8.12909	.64542	0.00000	.00203	2.35686	-1.95720	-.00899	0.00000
16	Q4	24.6423	.33229	.44215	3.26194	27.21314	.61610	0.00000	.00203	.76780	-3.89501	-.00899	0.00000
17	Q5	25.0564	.35408	.44448	2.87570	28.90145	.62991	0.00000	.00203	.18270	-.10537	.07605	0.00000
18	Q5	25.4704	.37700	.44680	2.94779	27.38111	.67966	0.00000	.00203	-.36012	3.70775	.16542	0.00000
19	Q5	32.8181	.52344	.69382	28.93029	1.97247	1.89516	0.00000	.00203	-3.17600	-.24974	.16542	0.00000
20	Q6	33.1687	.52532	.72031	29.99143	2.30008	1.91463	0.00000	.00203	.18953	-.69745	-.05472	0.00000
21	Q6	33.5192	.52721	.74184	28.67165	2.97688	1.85705	0.00000	.00203	3.52486	-1.25931	-.27267	0.00000
22	Q6	37.7063	.57374	.81659	7.36233	28.75210	.71534	0.00000	.00203	1.56435	-4.89647	-.27267	0.00000
23	Q7	38.0569	.58180	.81845	6.59770	31.04324	.63372	0.00000	.00203	.64659	-1.55101	-.19462	0.00000
24	Q7	38.4074	.59043	.82024	6.43097	30.86822	.57798	0.00000	.00203	-.16448	2.04353	-.12451	0.00000
25	Q7	41.2550	.65273	.83825	8.66271	20.58959	.22342	0.00000	.00203	-.61925	1.56604	-.12451	0.00000
26	S7	41.5598	.65821	.84066	9.05504	19.65051	.18547	0.00000	.00203	-.66793	1.51493	-.12451	0.00000
27	QS7	42.8528	.67884	.85228	11.04937	16.01312	.02448	0.00000	.00203	-.87443	1.29812	-.12451	0.00000
28	B7	45.9008	.71351	.89247	17.82159	9.29316	-.08779	0.00000	-.01127	-1.35874	.87293	.05047	0.00000
29	QB7	46.4088	.71787	.90159	19.24328	8.45519	-.06215	0.00000	-.01127	-1.43987	.77661	.05047	0.00000
30	Q8	46.6374	.71974	.90596	19.57382	8.25203	-.05012	0.00000	-.01127	.00223	.11716	.05469	0.00000
31	Q8	46.8660	.72161	.91036	19.24127	8.34682	-.03722	0.00000	-.01127	1.44418	-.53419	.05798	0.00000
32	Q8	48.0852	.73270	.93179	15.95816	9.87830	.03346	0.00000	-.01127	1.24866	-.72194	.05798	0.00000
33	B8	52.6572	.79843	.98624	7.94667	18.80195	.89037	0.00000	.08409	.52381	-1.16259	.32128	0.00000
34	QB8	53.1652	.80894	.99041	7.45586	20.01542	1.05379	0.00000	.08409	.44235	-1.22613	.32128	0.00000
35	Q9	53.3938	.81386	.99221	7.38952	20.23158	1.13658	0.00000	.08409	-.15046	.28603	.40409	0.00000
36	Q9	53.6224	.81873	.99403	7.59503	19.75689	1.23907	0.00000	.08409	-.75374	1.77849	.49391	0.00000
37	Q9	53.9272	.82492	.99655	8.07370	18.69230	1.38961	0.00000	.08409	-.81667	1.71427	.49391	0.00000
38	S9	54.2320	.83075	.99922	8.59072	17.66486	1.54016	0.00000	.08409	-.87961	1.65004	.49391	0.00000
39	QS9	54.8416	.84137	1.00504	9.73986	15.73343	1.84124	0.00000	.08409	-1.00547	1.52159	.49391	0.00000
40	B9	59.4136	.89014	1.08571	23.04733	5.63827	4.66875	0.00000	.91485	-1.93869	.61035	.75721	0.00000
41	Q09	59.9216	.89350	1.10084	25.07033	5.08097	5.05342	0.00000	.91485	-2.04358	.48669	.75721	0.00000
42	Q10	60.1502	.89493	1.10814	25.82923	4.90713	5.20797	0.00000	.91485	-1.26816	.27562	.59409	0.00000
43	Q10	60.3788	.89633	1.11562	26.22433	4.82772	5.32471	0.00000	.91485	-.45599	.07259	.42664	0.00000
44	Q10	60.8868	.89938	1.13244	26.69950	4.80771	5.54144	0.00000	.91485	-.47939	-.03319	.42664	0.00000
45	B10	65.4588	.92410	1.25367	31.97419	9.12771	8.06492	0.00000	2.67987	-.68759	-.87912	.68995	0.00000
46	QB10	65.7507	.92555	1.25862	32.37953	9.65749	8.26631	0.00000	2.67987	-.70103	-.93582	.68995	0.00000
47	S10	66.0355	.92704	1.26350	32.81116	10.24601	8.47661	0.00000	2.67987	-.71507	-.99502	.68995	0.00000
48	QS10	66.3474	.92844	1.26790	33.23255	10.84345	8.67801	0.00000	2.67987	-.72852	-1.05171	.68995	0.00000
49	Q11	66.7843	.93056	1.27394	31.96215	12.47757	8.72598	0.00000	2.67987	3.57995	-2.76080	-.47140	0.00000

POS		S(M)	NUX	NUY	BETAX(M)	BETAY(M)	ETAX(M)	ETAY(M)	ETAS(M)	ALPHAX	ALPHAY	DETAX	DETAY
50	Q11	67.2212	.93289	1.27893	27.21571	15.85680	8.27609	0.00000	2.67987	7.07349	-5.12314 -1	.60552	0.00000
51	D11	67.7422	.93641	1.28341	20.35389	21.66177	7.43358	0.00000	2.67987	6.09649	-6.01840 -1	.60552	0.00000
52	Q12	68.1283	.93977	1.28601	16.72287	25.45541	6.97807	0.00000	2.67987	3.44951	-3.65826	.76292	0.00000
53	Q12	68.5144	.94370	1.28833	14.86405	27.14243	6.84000	0.00000	2.67987	1.43734	-.64493	.04497	0.00000
54	D12	68.7322	.94608	1.28960	14.24773	27.42584	6.84979	0.00000	2.67987	1.39242	-.65629	.04497	0.00000
55	S12	69.0370	.94959	1.29135	13.41807	27.83076	6.86350	0.00000	2.67987	1.32955	-.67219	.04497	0.00000
56	DS12	69.2548	.95223	1.29259	12.84871	28.12604	6.87329	0.00000	2.67987	1.28462	-.68356	.04497	0.00000
57	Q13	69.6409	.95712	1.29479	12.44883	27.39026	7.04712	0.00000	2.67987	-.23333	2.56037	.89885	0.00000
58	Q13	70.0270	.96195	1.29715	13.22005	24.29020	7.54152	0.00000	2.67987	-1.79422	5.34713 1	.71180	0.00000
59	D13	70.3242	.96756	1.30081	15.08319	19.27399	8.39266	0.00000	2.67987	-1.95291	4.74139 1	.71180	0.00000
60	Q14	70.8455	.97084	1.30366	15.87623	16.90129	8.80845	0.00000	2.67987	-.48935	2.72016	.86951	0.00000
61	Q14	71.1668	.97407	1.30681	15.69904	15.70432	8.94851	0.00000	2.67987	1.03500	1.04401	.00000	0.00000
62	LS*	79.0117	1.10180	1.43524	7.57960	7.51415	8.94851	0.00000	2.67987	-.00000	.00000	.00000	0.00000
63	A20	79.0117	1.10180	1.43524	7.57960	7.51415	8.94851	0.00000	2.67987	-.00000	.00000	.00000	0.00000
64	REFL	158.0234	2.20361	2.87048	7.56400	7.26661	.00155	0.00000	5.35974	.00000	.00000	.00000	0.00000

CIRCUMFERENCE = 474.0703 M
RADIUS = 75.4506 M
(DS/S)/(DP/P) = .0339174

THETX = 6.28318533 RAD
THETY(63) = 0.00000000 RAD
TQAM = (5.42986, 0.00000)

NUX = 6.61082
NUY = 8.61144

DNUX/(DP/P) = .89856
DNUY/(DP/P) = .33310

MAXIMA	--- BETX(48) =	33.23255	BETY(23) =	31.04324	ETAX(63) =	8.94851	ETAY(64) =	0.00000
MINIMA	--- BETX(17) =	2.87570	BETY(19) =	1.97247	ETAX(28) =	-.08779	ETAY(64) =	0.00000

```
                                  INJECTION ORBIT
                                  8.00920 GEV KINETIC
***  DI'      =                   //     00930
***  V        PVEC                //
***  INJ      FXPT    2   -3      //  V     R/6              1                    DP
*                                 //
```

CALCULATION OF THE EQUILIBRIUM ORBIT AND BETATRON FUNCTIONS OF INJ
INITIAL REFERENCE RAY DEFINED BY V

X = 0.00000000 DX = 0.00000000 Y = 0.00000000 DY = 0.00000000 DS = 0.00000000 DP/P = .00930000 1.00000000

3

7X7 MATRIX FOR INJ

.26824382	8.69314725	0.00000000	0.00000000	0.00000000	-.15380901	.00079763
-.10675596	.26824382	0.00000000	0.00000000	0.00000000	-.02243921	.00011637
0.00000000	0.00000000	.71018489	-5.07291413	0.00000000	0.00000000	0.00000000
0.00000000	0.00000000	.09770270	.71018489	0.00000000	0.00000000	0.00000000
.02243921	.15380901	0.00000000	0.00000000	1.00000000	-5.47427891	-.04757677
0.00000000	0.00000000	0.00000000	0.00000000	0.00000000	1.00000000	0.00000000
0.00000000	0.00000000	0.00000000	0.00000000	0.00000000	0.00000000	1.00000000

EIGENVALUES OF THE 4X4 SUBMATRIX

X... LMD1 = (.26824382 .96335105), C(1) = 1.00000000, MU(1) = 1.29922675 RAD., Q(1) = .62033508
1/LMD1 = (.26824382 -.96335105), C(2) = 1.00000000, MU(2) = -1.29922675 RAD., Q(2) = .37966492

Y... LMD3 = (.71018489 .70401522), C(3) = 1.00000000, MU(3) = .78103554 RAD., Q(3) = .37291700
1/LMD3 = (.71018489 -.70401522), C(4) = 1.00000000, MU(4) = -.78103554 RAD., Q(4) = .62708300

EIGENVALUE = (.26824382, .96335105), EIGENVECTOR = (3.00397442, -.00000000)
(.00000000, .33289232)
(0.00000000, 0.00000000)
(0.00000000, 0.00000000)

EIGENVALUE = (.26824382, -.96335105), EIGENVECTOR = (3.00397442, .00000000)
(.00000000, -.33289232)
(0.00000000, 0.00000000)
(0.00000000, 0.00000000)

EIGENVALUE = (.71018489, .70401522), EIGENVECTOR = (0.00000000, 0.00000000)
(0.00000000, 0.00000000)
(2.68434129, .00000000)
(0.00000000, -.37253087)

EIGENVALUE = (.71018489, -.70401522), EIGENVECTOR = (0.00000000, 0.00000000)
(0.00000000, 0.00000000)
(2.68434129, -.00000000)
(0.00000000, .37253087)

	X	DX	Y	DY	DS	DP/P	
EQ. ORBIT	-.00088124	0.00000000	0.00000000	0.00000000	0.00000000	.00930000	1.00000000
ETA ORBIT	-.21019162	-.00000000	0.00000000	0.00000000	0.00000000	1.00000000	0.00000000

EIGENVECTORS 1 AND 3 IN POLAR COORDINATES

POS	X1 X3		DX1 DX3		Y1 Y3		DY1 DY3	
0	3.003974 0.000000	-.000000 0.000000	.332892 0.000000	1.570796 0.000000	0.000000 2.684341	0.000000 .000000	0.000000 .372531	0.000000 -1.570796

OPTIMIZATION FUNCTIONS OF INJ

POS		S (M)	QX	QY	BX (M)	BY (M)	AX	AY	EX (M)	EXP	EY (M)	EYP	XCO (MM)	DXCO (MR)	YCO (MM)	DYCO (MR)
0		0.00	0.000	0.000	9.0239	7.2057	0.0000	0.0000	-.2102	-.0000	0.0000	0.0000	-.8812	0.0000	0.0000	0.0000
1	A10	0.00	0.000	0.000	9.0239	7.2057	0.0000	0.0000	-.2102	-.0000	0.0000	0.0000	-.8812	0.0000	0.0000	0.0000
2	LS	7.95	.115	.133	16.0216	15.9692	-.8806	-1.1028	-.2102	-.0000	0.0000	0.0000	-.8812	0.0000	0.0000	0.0000
3	Q1	8.27	.118	.136	16.0160	17.2853	.8979	-3.0587	-.2065	.0233	0.0000	0.0000	-.8655	.0981	0.0000	0.0000
4	Q1	8.59	.121	.139	14.8994	19.9790	2.5493	-5.4582	-.1954	.0458	0.0000	0.0000	-.8189	.1926	0.0000	0.0000
5	Q1	9.10	.127	.142	12.4189	25.9774	2.2914	-6.2479	-.1719	.0458	0.0000	0.0000	-.7202	.1926	0.0000	0.0000
6	Q2	9.75	.136	.146	11.2940	30.2896	-.4911	.0057	-.1542	.0090	0.0000	0.0000	-.6455	.0379	0.0000	0.0000
7	Q2	10.41	.145	.149	13.8403	25.9638	-3.3842	6.2561	-.1599	-.0265	0.0000	0.0000	-.6692	-.1110	0.0000	0.0000
8	Q2	11.37	.154	.157	21.6493	15.3711	-4.5452	4.7711	-.1853	-.0265	0.0000	0.0000	-.7758	-.1110	0.0000	0.0000
9	Q3	11.72	.156	.161	23.9492	12.7925	-1.9222	2.6906	-.1906	-.0034	0.0000	0.0000	-.7978	-.0142	0.0000	0.0000
10	Q3	12.07	.159	.166	24.2677	11.4897	1.0266	1.0793	-.1877	.0197	0.0000	0.0000	-.7857	.0832	0.0000	0.0000
11	Q3	12.98	.165	.179	22.4805	9.6919	.9300	.9089	-.1699	.0197	0.0000	0.0000	-.7104	.0832	0.0000	0.0000
12	B3	14.30	.176	.208	19.7863	7.2965	.8212	.6366	-.0740	.1062	0.0000	0.0000	.0285	.8878	0.0000	0.0000
13	QB3	20.92	.243	.387	12.7277	6.9544	-.2776	-.6033	.6085	.1062	0.0000	0.0000	5.7315	.8878	0.0000	0.0000
14	Q4	21.15	.245	.392	12.3913	7.3627	1.1857	-1.1928	.6276	.0606	0.0000	0.0000	5.8852	.4549	0.0000	0.0000
15	Q4	21.38	.248	.397	11.6558	8.0575	2.0135	-1.8639	.6361	.0140	0.0000	0.0000	5.9389	.0143	0.0000	0.0000
16	Q4	24.64	.339	.433	3.1350	26.1187	.5995	-3.6746	.6816	.0140	0.0000	0.0000	5.9854	.0143	0.0000	0.0000
17	Q5	25.06	.361	.436	2.8752	27.7000	.0397	-.0728	.7066	.1070	0.0000	0.0000	6.1606	.8356	0.0000	0.0000
18	Q5	25.47	.384	.438	3.0667	26.2348	-.3109	3.5451	.7711	.2061	0.0000	0.0000	6.6839	1.7042	0.0000	0.0000
19	Q5	32.82	.515	.684	32.7759	2.0593	-3.5324	-.2549	2.2853	.2061	0.0000	0.0000	19.2060	1.7042	0.0000	0.0000
20	Q6	33.17	.516	.709	33.9429	2.3906	.2476	-.7030	2.3119	-.0549	0.0000	0.0000	19.4165	-.5070	0.0000	0.0000
21	Q6	33.52	.518	.730	32.4378	3.0715	3.9884	-1.2651	2.2471	-.3137	0.0000	0.0000	18.8530	-2.6979	0.0000	0.0000
22	Q6	37.71	.559	.804	8.1757	28.5098	1.8060	-4.8102	.9336	-.3137	0.0000	0.0000	7.5563	-2.6979	0.0000	0.0000
23	Q7	38.06	.567	.806	7.2744	30.7603	-.7999	-1.5240	.8416	-.2128	0.0000	0.0000	6.7572	-1.8774	0.0000	0.0000
24	Q7	38.41	.575	.808	7.0239	30.5894	-.0754	2.0048	.7834	-.1203	0.0000	0.0000	6.2314	-1.1328	0.0000	0.0000
25	Q7	41.25	.634	.826	8.6144	20.5023	-.4831	1.5375	.4407	-.1203	0.0000	0.0000	3.0057	-1.1328	0.0000	0.0000
26	B7	41.56	.640	.828	8.9220	19.5809	-.5259	1.4855	.4041	-.1204	0.0000	0.0000	2.6604	-1.1329	0.0000	0.0000
27	QB7	42.85	.661	.840	10.3211	16.0131	-.7109	1.2737	.2484	-.1204	0.0000	0.0000	1.1955	-1.1329	0.0000	0.0000
28	B7	45.90	.698	.880	16.1477	9.4111	-1.1448	.8603	.1461	.0530	0.0000	0.0000	.2044	.4793	0.0000	0.0000
29	QB7	46.41	.703	.889	17.3478	8.5847	-1.2175	.7663	.1731	.0530	0.0000	0.0000	.4479	.4793	0.0000	0.0000
30	Q8	46.64	.705	.893	17.6121	8.3870	.0679	.1036	.1837	.0397	0.0000	0.0000	.5534	.4420	0.0000	0.0000
31	Q8	46.87	.707	.897	17.2864	8.4889	1.3487	-.5520	.1912	.0258	0.0000	0.0000	.6494	.3972	0.0000	0.0000
32	Q8	48.09	.720	.919	14.2402	10.0634	1.1498	-.7394	.2226	.0258	0.0000	0.0000	1.1337	.3972	0.0000	0.0000
33	B8	52.66	.794	.972	7.1832	19.1305	.4128	-1.1790	.9292	.2866	0.0000	0.0000	8.4140	2.8228	0.0000	0.0000
34	QB8	53.17	.805	.976	6.8059	20.3606	.3300	-1.2425	1.0748	.2866	0.0000	0.0000	9.8480	2.8228	0.0000	0.0000
35	Q9	53.39	.811	.978	6.7792	20.5816	-.2128	.2819	1.1496	.3691	0.0000	0.0000	10.5797	3.5880	0.0000	0.0000
36	Q9	53.62	.816	.980	7.0026	20.1060	-.7702	1.7870	1.2440	.4580	0.0000	0.0000	11.4931	4.4149	0.0000	0.0000
37	Q9	53.93	.823	.982	7.4933	19.0360	-.8396	1.7235	1.3836	.4580	0.0000	0.0000	12.8388	4.4149	0.0000	0.0000
38	S9	54.23	.829	.985	8.0335	17.9878	-.9334	1.7147	1.5238	.4624	0.0000	0.0000	14.1876	4.4355	0.0000	0.0000
39	QS9	54.84	.840	.990	9.2580	15.9787	-1.0753	1.5812	1.8057	.4624	0.0000	0.0000	16.8914	4.4355	0.0000	0.0000
40	B9	59.42	.889	1.072	23.8158	5.4921	-2.1286	.6241	4.4932	.7223	0.0000	0.0000	42.4612	6.8573	0.0000	0.0000
41	QB9	59.93	.893	1.087	26.0383	4.9233	-2.2465	.4956	4.8602	.7223	0.0000	0.0000	45.9447	6.8573	0.0000	0.0000
42	Q10	60.16	.894	1.095	26.8861	4.7443	-1.4513	.2889	5.0079	.5684	0.0000	0.0000	47.3451	5.3879	0.0000	0.0000
43	Q10	60.39	.895	1.103	27.3598	4.6577	-.6143	.0906	5.1198	.4104	0.0000	0.0000	48.4051	3.8798	0.0000	0.0000
44	Q10	60.90	.898	1.120	27.9970	4.6215	-.6399	-.0194	5.3283	.4104	0.0000	0.0000	50.3760	3.8798	0.0000	0.0000
45	B10	65.48	.921	1.246	34.9220	9.0280	-.8680	-.9126	7.7893	.6705	0.0000	0.0000	73.4742	6.3024	0.0000	0.0000
46	QB10	65.78	.923	1.251	35.4330	9.5781	-.8827	-.9719	7.9850	.6705	0.0000	0.0000	75.3138	6.3024	0.0000	0.0000
47	S10	66.08	.924	1.256	35.8605	10.2217	-.5188	-1.1414	8.1764	.5855	0.0000	0.0000	77.1734	5.8997	0.0000	0.0000
48	QS10	66.37	.925	1.260	36.1663	10.9072	-.5291	-1.2072	8.3473	.5855	0.0000	0.0000	78.8955	5.8997	0.0000	0.0000
49	Q11	66.81	.927	1.266	34.5786	12.6845	4.0946	-2.9386	8.3642	-.5088	0.0000	0.0000	79.1914	-4.5516	0.0000	0.0000

		S (M)	GX	GY	BX (M)	BY (M)	AX	AY	EX (M)	EXP	EY (M)	EYP	XCO (MM)	DXCO (MR)	YCO (MM)	DYCO (MR)
50	Q11	67.25	.929	1.271	29.2765	16.2440	7.7941	-5.3577	7.9062	-1.5744	0.0000	0.0000	74.9566	-14.7424	0.0000	0.0000
51	Q11	67.77	.933	1.275	21.7273	22.3234	6.6952	-6.3105	7.0859	-1.5744	0.0000	0.0000	67.2755	-14.7424	0.0000	0.0000
52	Q12	68.15	.936	1.278	17.7138	26.3275	3.8634	-3.9148	6.6323	-.7871	0.0000	0.0000	63.0567	-7.1923	0.0000	0.0000
53	Q12	68.34	.940	1.280	15.9846	28.1845	1.7357	-.8262	6.4743	-.0350	0.0000	0.0000	61.6799	.0337	0.0000	0.0000
54	Q12	68.76	.942	1.281	14.8408	28.9473	1.6796	-.8393	6.4667	-.0350	0.0000	0.0000	61.6872	.0337	0.0000	0.0000
55	S12	69.06	.945	1.283	13.8872	28.9693	1.4514	-.5440	6.4666	.0345	0.0000	0.0000	61.7483	.3669	0.0000	0.0000
56	QS12	69.28	.948	1.284	13.2656	29.2084	1.4027	-.5538	6.4741	.0345	0.0000	0.0000	61.8282	.3669	0.0000	0.0000
57	Q13	69.67	.953	1.286	12.7874	28.3381	-.1477	2.7783	6.6318	.7865	0.0000	0.0000	63.3642	7.6192	0.0000	0.0000
58	Q13	70.05	.957	1.289	13.4975	25.0911	-1.7248	5.6189	7.0851	1.5736	0.0000	0.0000	67.7559	15.2150	0.0000	0.0000
59	Q13	70.35	.963	1.292	15.2856	19.7849	-1.8712	4.9724	7.8676	1.5736	0.0000	0.0000	75.3211	15.2150	0.0000	0.0000
60	Q14	70.87	.966	1.295	16.0236	17.2759	-.3998	2.9069	8.2505	.7991	0.0000	0.0000	79.0165	7.7273	0.0000	0.0000
61	Q14	71.19	.969	1.298	15.7924	15.9667	1.1211	1.2064	8.3794	-.0000	0.0000	0.0000	80.2611	-.0000	0.0000	0.0000
62	LS*	79.04	1.103	1.438	6.9975	6.9028	.0000	-.0000	8.3794	-.0000	0.0000	0.0000	80.2611	-.0000	0.0000	0.0000
63	A20	79.04	1.103	1.438	6.9975	6.9028	.0000	-.0000	8.3794	-.0000	0.0000	0.0000	80.2611	-.0000	0.0000	0.0000
64	REFL	158.07	2.207	2.876	9.0239	7.2057	.0000	-.0000	-.2102	.0000	0.0000	0.0000	-.8812	0.0000	0.0000	0.0000

CIRCUMFERENCE = 474.2191 M THETX = 6.28318533 RAD NUX = 6.62034 DNUX/(DP/P) = 2.04842
RADIUS = 75.4743 M THETY(63) = 0.00000000 RAD NUY = 8.62708 DNUY/(DP/P) = .21319
(DS/S)/(DP/P) = .0346612 TGAM = (5.37129, 0.00000)

MAXIMA	---	BETX(48) =	36.16635	BETY(23) =	30.76032	ETAX(61) =	8.37941	ETAY(64) =	0.00000
MINIMA	---	BETX(17) =	2.87519	BETY(19) =	2.05926	ETAX(2) =	-.21019	ETAY(64) =	0.00000

STACKING ORBIT
7.94214 GEV KINETIC

```
***  DP      =                 //     00165
***  V       PVEC              //
***  STK     FXPT    2   -3    //  V     R/A            1                                  DP
  *                            //
```

CALCULATION OF THE EQUILIBRIUM ORBIT AND BETATRON FUNCTIONS OF STK
INITIAL REFERENCE RAY DEFINED BY V
X = 0.00000000 DX = 0.00000000 Y = 0.00000000 DY = 0.00000000 DS = 0.00000000 DP/P = .00165000 1.00000000

7X7 MATRIX FOR STK

.28561963	7.47013149	0.00000000	0.00000000	0.00000000	-.02038452	.00001813
-.12294582	.28561963	0.00000000	0.00000000	0.00000000	-.00350820	.00000312
0.00000000	0.00000000	.68819753	-5.27775387	0.00000000	0.00000000	0.00000000
0.00000000	0.00000000	.09973640	.68819753	0.00000000	0.00000000	0.00000000
.00350820	.02038452	0.00000000	0.00000000	1.00000000	-5.38532999	-.00876629
0.00000000	0.00000000	0.00000000	0.00000000	0.00000000	1.00000000	0.00000000
0.00000000	0.00000000	0.00000000	0.00000000	0.00000000	0.00000000	1.00000000

EIGENVALUES OF THE 4X4 SUBMATRIX

X. LMD1 = (.28561963 .95834306), C(1) = 1.00000000, MU(1) = 1.28114340 RAD, Q(1) = .61170091
1/LMD1 = (.28561963 -.95834306), C(2) = 1.00000000, MU(2) = -1.28114340 RAD, Q(2) = .38829909

Y... LMD3 = (.68819753 .72552337), C(3) = 1.00000000, MU(3) = .81179458 RAD, Q(3) = .38760336
1/LMD3 = (.68819753 -.72552337), C(4) = 1.00000000, MU(4) = -.81179458 RAD, Q(4) = .61239664

EIGENVALUE = (.28561963, .95834306), EIGENVECTOR = (2.79192419, -.00000000)
(.00000000, .35817591)
(0.00000000, 0.00000000)
(0.00000000, 0.00000000)

EIGENVALUE = (.28561963, -.95834306), EIGENVECTOR = (2.79192419, .00000000)
(.00000000, -.35817591)
(0.00000000, 0.00000000)
(0.00000000, 0.00000000)

EIGENVALUE = (.68819753, .72552337), EIGENVECTOR = (0.00000000, 0.00000000)
(0.00000000, 0.00000000)
(2.69711127, 0.00000000)
(.00000000, -.37076705)

EIGENVALUE = (.68819753, -.72552337), EIGENVECTOR = (0.00000000, 0.00000000)
(0.00000000, 0.00000000)
(2.69711127, 0.00000000)
(.00000000, .37076705)

	X	DX	Y	DY	DS	DP/P	
EQ ORBIT	-.00002178	0.00000000	0.00000000	0.00000000	0.00000000	.00165000	1.00000000
ETA ORBIT	-.02853455	.00000000	0.00000000	0.00000000	0.00000000	1.00000000	0.00000000

EIGENVECTORS 1 AND 3 IN POLAR COORDINATES

PUN	X1 X3			DX1 DX3		Y1 Y3			DY1 DY3	
0	2 791924 0 000000	-. 000000 0. 000000	.358176 0. 000000	1. 570796 0. 000000	0 000000 2 697111	0. 000000 0. 000000	0 000000 370767		0. 000000 -1. 570796	

RELATIVE FUNCTIONS OF STR

POS		S (M)	GX	GY	BX (M)	BY (M)	AX	AY	RA (M)	EXP	EXP (R)	EXP	XCG (MM)	DXCG (MM)	YCG (MM)	DYCG (MM)
0		0.00	0.000	0.000	7.7948	7.2744	0.0000	0.0000	-.0285	0000	0.0000	0.0000	-.0218	0.0000	0.0000	0.0000
1	A10	0.00	0.000	0.000	7.7948	7.2744	0.0000	0.0000	-.0285	0000	0.0000	0.0000	-.0218	0.0000	0.0000	0.0000
2	LS	7.95	.127	.132	15.8959	15.9551	-1.0195	-1.0924	-.0285	0000	0.0000	0.0000	-.0218	0.0000	0.0000	0.0000
3	G1	8.27	.130	.135	15.9789	17.2684	.7632	-3.0604	-.0280	0032	0.0000	0.0000	-.0214	.0024	0.0000	0.0000
4	G1	8.59	.133	.138	14.9422	19.9679	2.4370	-5.4757	-.0265	0063	0.0000	0.0000	-.0202	.0048	0.0000	0.0000
5	G1	9.10	.139	.141	12.3667	25.9869	2.1991	-6.2708	-.0233	.0063	0.0000	0.0000	-.0178	.0048	0.0000	0.0000
6	G2	9.75	.148	.145	11.3949	30.2960	-.6432	.0357	-.0208	.0012	0.0000	0.0000	-.0159	.0010	0.0000	0.0000
7	G2	10.41	.156	.149	14.4297	25.9025	-3.8956	6.3216	-.0216	-.0036	0.0000	0.0000	-.0165	-.0027	0.0000	0.0000
8	G2	11.37	.164	.156	22.9482	15.2167	-4.9724	4.8025	-.0231	-.0036	0.0000	0.0000	-.0191	-.0027	0.0000	0.0000
9	G3	11.72	.167	.160	25.4906	12.6174	-2.1760	2.7195	-.0258	-.0004	0.0000	0.0000	-.0197	.0003	0.0000	0.0000
10	G3	12.07	.169	.165	25.9118	11.2926	.9919	1.1144	-.0254	.0027	0.0000	0.0000	-.0194	.0021	0.0000	0.0000
11	G3	12.98	.173	.179	24.1806	9.4396	.9227	.9349	-.0229	.0027	0.0000	0.0000	-.0175	.0021	0.0000	0.0000
12	B3	14.50	.185	.209	21.5495	6.9903	.8062	.6661	.0476	.0899	0.0000	0.0000	.0952	.1459	0.0000	0.0000
13	G83	20.92	.245	.396	14.3518	6.9548	.3143	-.6606	.6251	.0899	0.0000	0.0000	1.0325	.1459	0.0000	0.0000
14	G4	21.15	.247	.401	13.9691	7.3910	1.3504	-1.2586	.6402	.0425	0.0000	0.0000	1.0569	.0675	0.0000	0.0000
15	G4	21.38	.250	.405	13.1311	8.1189	2.2943	-1.9435	.6444	-.0057	0.0000	0.0000	1.0633	-.0122	0.0000	0.0000
16	G4	24.64	.333	.441	3.2403	27.0518	.7387	-3.8624	.6258	-.0057	0.0000	0.0000	1.0236	-.0122	0.0000	0.0000
17	G5	25.06	.355	.443	2.8758	28.7248	.1584	-.1017	.6413	.0805	0.0000	0.0000	1.0477	.1290	0.0000	0.0000
18	G5	25.47	.378	.445	2.9680	27.2140	-.3853	3.6816	.6931	.1713	0.0000	0.0000	1.1315	.2775	0.0000	0.0000
19	G5	32.82	.522	.692	29.5216	1.9849	-3.2285	-.2480	1.9517	.1713	0.0000	0.0000	3.1702	.2775	0.0000	0.0000
20	G6	33.17	.524	.718	30.5975	2.3111	.2005	-.6952	1.9722	-.0547	0.0000	0.0000	3.2031	-.0902	0.0000	0.0000
21	G6	33.52	.525	.740	29.2480	2.9860	3.5976	-1.2561	1.9136	-.2785	0.0000	0.0000	3.1074	-.4543	0.0000	0.0000
22	G6	37.71	.571	.814	7.4784	28.6395	1.6016	-4.8706	.7474	-.2785	0.0000	0.0000	1.2053	-.4543	0.0000	0.0000
23	G7	38.06	.579	.816	6.6924	30.9189	-.6713	-1.5440	.6643	-.1971	0.0000	0.0000	1.0696	-.3229	0.0000	0.0000
24	G7	38.41	.588	.818	6.5116	30.7461	-.1485	2.0303	.6083	-.1237	0.0000	0.0000	.9775	-.2046	0.0000	0.0000
25	G7	41.25	.650	.836	8.6298	20.5342	-.5954	1.3539	.2560	-.1237	0.0000	0.0000	.3948	-.2046	0.0000	0.0000
26	S7	41.56	.655	.839	9.0073	19.6013	-.6431	1.5048	.2183	-.1237	0.0000	0.0000	.3325	-.2046	0.0000	0.0000
27	OS7	42.85	.676	.850	10.9329	15.9881	-.8461	1.2895	.0583	-.1237	0.0000	0.0000	.0679	-.2046	0.0000	0.0000
28	B7	45.90	.711	.890	17.5075	9.3116	-1.3220	.8677	-.0520	.0510	0.0000	0.0000	-.1155	.0836	0.0000	0.0000
29	OB7	46.41	.716	.900	18.8911	8.4786	-1.4017	.7721	-.0261	.0510	0.0000	0.0000	-.0731	.0836	0.0000	0.0000
30	G8	46.64	.717	.904	19.2109	8.2776	.0112	.1120	-.0143	.0525	0.0000	0.0000	-.0534	.0884	0.0000	0.0000
31	G8	46.87	.719	.908	18.8810	8.3790	1.4233	-.5403	-.0022	.0531	0.0000	0.0000	-.0328	.0916	0.0000	0.0000
32	G8	48.09	.731	.930	15.6486	9.9216	1.2279	-.7283	.0626	.0531	0.0000	0.0000	.0789	.0916	0.0000	0.0000
33	B8	52.66	.798	.984	7.8236	18.9055	.5036	-1.1696	.8967	.3159	0.0000	0.0000	1.4733	.5253	0.0000	0.0000
34	OB8	53.17	.808	.988	7.3533	20.1261	.4222	-1.2332	1.0572	.3159	0.0000	0.0000	1.7402	.5253	0.0000	0.0000
35	G9	53.39	.813	.990	7.2943	20.3442	-.1625	.2849	1.1388	.3987	0.0000	0.0000	1.8756	.6618	0.0000	0.0000
36	G9	53.62	.818	.992	7.5036	19.8686	-.7585	1.7834	1.2400	.4883	0.0000	0.0000	2.0436	.8097	0.0000	0.0000
37	G9	53.93	.824	.994	7.9855	18.9010	-.8225	1.7193	1.3889	.4883	0.0000	0.0000	2.2904	.8097	0.0000	0.0000
38	S9	54.23	.830	.997	8.5078	17.7694	-.8912	1.6649	1.5378	.4891	0.0000	0.0000	2.5373	.8104	0.0000	0.0000
39	OS9	54.84	.841	1.002	9.6727	15.8184	-1.0197	1.5355	1.8360	.4891	0.0000	0.0000	3.0313	.8104	0.0000	0.0000
40	B9	59.42	.890	1.083	23.2132	5.6229	-1.9730	.6159	4.6425	.7518	0.0000	0.0000	7.6758	1.2440	0.0000	0.0000
41	OB9	59.92	.893	1.098	25.2722	5.0605	-2.0801	.4913	5.0244	.7518	0.0000	0.0000	8.3078	1.2440	0.0000	0.0000
42	G10	60.15	.895	1.106	26.0467	4.8844	-1.3001	.2808	5.1779	.5902	0.0000	0.0000	8.5617	.9763	0.0000	0.0000
43	G10	60.38	.896	1.113	26.4552	4.9025	-.4825	.0784	5.2939	.4243	0.0000	0.0000	8.7536	.7014	0.0000	0.0000
44	O10	60.89	.899	1.130	26.9575	4.7769	-.5061	-.0280	5.5095	.4243	0.0000	0.0000	9.1099	.7014	0.0000	0.0000
45	B10	65.46	.923	1.252	32.5035	9.0838	-.7169	-.8818	8.0242	.6870	0.0000	0.0000	13.2632	1.1351	0.0000	0.0000
46	OB10	65.76	.925	1.257	32.9260	9.6153	-.7305	-.9390	8.2248	.6870	0.0000	0.0000	13.5945	1.1351	0.0000	0.0000
47	S10	66.06	.926	1.262	33.3562	10.2118	-.6806	-1.0182	8.4317	.6710	0.0000	0.0000	13.9385	1.1218	0.0000	0.0000
48	OS10	66.35	.928	1.266	33.7572	10.8232	-.6934	-1.0764	8.6276	.6710	0.0000	0.0000	14.2659	1.1218	0.0000	0.0000
49	G11	66.79	.930	1.273	32.4302	12.4784	3.6721	-2.7851	8.6697	-.4794	0.0000	0.0000	14.3401	-.7838	0.0000	0.0000

POS		S (M)	GX	GY	BX (M)	BY (M)	AX	AY	EX (M)	EXP	EY (M)	EYP	XCO (MM)	DXCO (MR)	YCO (MM)	DYCO (MR)
50	Q11	67.23	.932	1.277	27.5850	15.8805	7.2030	-5.1517	8.2127	-1.6022	0.0000	0.0000	13.5876	-2.6443	0.0000	0.0000
51	Q11	67.75	.936	1.282	20.5996	21.7196	6.2041	-6.0553	7.3779	-1.6022	0.0000	0.0000	12.2099	-2.6443	0.0000	0.0000
52	Q12	68.13	.939	1.285	16.8993	25.5422	3.5240	-3.6960	6.9219	-.7689	0.0000	0.0000	11.4585	-1.2628	0.0000	0.0000
53	Q12	68.52	.943	1.287	14.9917	27.2569	1.4912	-.6778	6.7798	.0296	0.0000	0.0000	11.2274	.0614	0.0000	0.0000
54	Q12	68.74	.945	1.288	14.3523	27.5547	1.4444	-.6895	6.7862	.0296	0.0000	0.0000	11.2408	.0614	0.0000	0.0000
55	S12	69.04	.949	1.290	13.5001	27.9631	1.3521	-.6503	6.7973	.0430	0.0000	0.0000	11.2612	.0725	0.0000	0.0000
56	QS12	69.26	.951	1.291	12.9211	28.2488	1.3064	-.6614	6.8066	.0430	0.0000	0.0000	11.2770	.0725	0.0000	0.0000
57	Q13	69.65	.956	1.293	12.3067	27.4928	-.2171	2.5899	6.9777	.8463	0.0000	0.0000	11.5613	1.4056	0.0000	0.0000
58	Q13	70.03	.961	1.296	13.2664	24.3686	-1.7805	5.3795	7.4651	1.6880	0.0000	0.0000	12.3706	2.8025	0.0000	0.0000
59	Q13	70.53	.966	1.299	15.1147	19.3228	-1.9368	4.7686	8.3043	1.6880	0.0000	0.0000	13.7641	2.8025	0.0000	0.0000
60	Q14	70.85	.970	1.302	15.8970	16.9338	-.4722	2.7438	8.7144	.8574	0.0000	0.0000	14.4448	1.4235	0.0000	0.0000
61	Q14	71.17	.973	1.305	15.7091	15.7221	1.0509	1.0663	8.8525	-.0000	0.0000	0.0000	14.6741	.0000	0.0000	0.0000
62	LS*	79.02	1.102	1.435	7.4647	7.3569	.0000	-.0000	8.8525	-.0000	0.0000	0.0000	14.6741	.0000	0.0000	0.0000
63	A20	79.02	1.102	1.435	7.4647	7.3569	.0000	-.0000	8.8525	-.0000	0.0000	0.0000	14.6741	.0000	0.0000	0.0000
64	REFL	158.03	2.204	2.871	7.7948	7.2744	.0000	-.0000	-.0285	-.0000	0.0000	0.0000	-.0218	0.0000	0.0000	0.0000

CIRCUMFERENCE = 474.0968 M THETX = 6.28318533 RAD NUX = 6.61170 DNUX/(DP/P) = 1.13607
RADIUS = 75.4549 M THETY(63) = 0.00000000 RAD NUY = 8.61240 DNUY/(DP/P) = 31979
(DS/S)/(DP/P) = .0340780 TGAM = (5.41705, 0.00000)

MAXIMA --- BETX(48) = 33.75723 BETY(23) = 30.91887 ETAX(61) = 8.85247 ETAY(64) = 0.00000
MINIMA --- BETX(17) = 2.87575 BETY(19) = 1.98486 ETAX(28) = -.05199 ETAY(64) = 0.00000

```
                                   CORE
                                   7.06718 GEV KINETIC
***  DP       =                    //     -.00690
***  V        PVEC                 //                                          DP
***  CORE     FXPT     2    -3     //  V     R/6              1
*                                  //
```

CALCULATION OF THE EQUILIBRIUM ORBIT AND BETATRON FUNCTIONS OF CORE
INITIAL REFERENCE RAY DEFINED BY V

X = 0.00000000 DX = 0.00000000 Y = 0.00000000 DY = 0.00000000 DS = 0.00000000 DP/P = -.00690000 1.00000000

7X7 MATRIX FOR CORE

.28548057	6.43517268	0.00000000	0.00000000	0.00000000	.06679535	.00019826
-.14273134	.28548057	0.00000000	0.00000000	0.00000000	.01334294	.00003960
0.00000000	0.00000000	.69555851	-5.15560016	0.00000000	0.00000000	0.00000000
0.00000000	0.00000000	.10012382	.69555851	0.00000000	0.00000000	0.00000000
-.01334294	-.06679535	0.00000000	0.00000000	1.00000000	-5.22016486	.03847210
0.00000000	0.00000000	0.00000000	0.00000000	0.00000000	1.00000000	0.00000000
0.00000000	0.00000000	0.00000000	0.00000000	0.00000000	0.00000000	1.00000000

EIGENVALUES OF THE 4X4 SUBMATRIX

X... LMD1 = (.28548057 .95838450), C(1) = 1.00000000, MU(1) = 1.28128850 RAD, Q(1) = .61177020
1/LMD1 = (.28548057 -.95838450), C(2) = 1.00000000, MU(2) = -1.28128850 RAD, Q(2) = .38822980

Y.. LMD3 = (.69555851 .71846946), C(3) = 1.00000000, MU(3) = .80159936 RAD, Q(3) = .38273550
1/LMD3 = (.69555851 -.71846946), C(4) = 1.00000000, MU(4) = -.80159936 RAD, Q(4) = .61726450

EIGENVALUE = (.28548057, .95838450), EIGENVECTOR = (2.59125536, 0.00000000)
(-.00000000, .38591334)
(0.00000000, 0.00000000)
(0.00000000, 0.00000000)

EIGENVALUE = (.28548057, -.95838450), EIGENVECTOR = (2.59125536, 0.00000000)
(-.00000000, -.38591334)
(0.00000000, 0.00000000)
(0.00000000, 0.00000000)

EIGENVALUE = (.69555851, .71846946), EIGENVECTOR = (0.00000000, 0.00000000)
(0.00000000, 0.00000000)
(2.67877020, 0.00000000)
(-.00000000, -.37330563)

EIGENVALUE = (.69555851, -.71846946), EIGENVECTOR = (0.00000000, 0.00000000)
(0.00000000, 0.00000000)
(2.67877020, 0.00000000)
(-.00000000, .37330563)

	X	DX	Y	DY	DS	DP/P	
EQ ORBIT	-.00036225	0.00000000	0.00000000	0.00000000	0.00000000	-.00690000	1.00000000
ETA ORBIT	.09348290	.00000000	0.00000000	0.00000000	0.00000000	1.00000000	0.00000000

EIGENVECTORS 1 AND 3 IN POLAR COORDINATES

POS	X1 X3		DX1 DX3		Y1 Y3		DY1 DY3	
0	2.591255 0.000000	0.000000 0.000000	.385913 0.000000	1.570796 0.000000	0.000000 2.678770	0.000000 0.000000	0.000000 .373306	0.000000 -1.570796

BETATRON FUNCTIONS OF CORE

POS		S (M)	QX	QY	BX (M)	BY (M)	AX	AY	EX (M)	EXP	EY (M)	EYP	XCO (MM)	DXCO (MR)	YCO (MM)	DYCO (MR)
0		0.00	0.000	0.000	6.7146	7.1758	0.0000	0.0000	.0935	.0000	0.0000	0.0000	-.3622	0.0000	0.0000	0.0000
1	A10	0.00	0.000	0.000	6.7146	7.1758	0.0000	0.0000	.0935	.0000	0.0000	0.0000	-.3622	0.0000	0.0000	0.0000
2	LS	7.95	.138	.133	16.1190	15.9758	-1.1835	-1.1074	.0935	.0000	0.0000	0.0000	-.3622	0.0000	0.0000	0.0000
3	Q1	8.27	.141	.136	16.2936	17.3051	.6447	-3.0965	.0918	-.0106	0.0000	0.0000	-.3557	.0410	0.0000	0.0000
4	Q1	8.59	.145	.139	15.3136	20.0367	2.3800	-5.5421	.0867	-.0208	0.0000	0.0000	-.3362	.0804	0.0000	0.0000
5	Q1	9.10	.150	.143	12.9888	26.1320	2.1570	-6.3532	.0761	-.0208	0.0000	0.0000	-.2950	.0804	0.0000	0.0000
6	Q2	9.75	.159	.146	12.1482	30.4926	-.8106	.0466	.0680	-.0042	0.0000	0.0000	-.2637	.0161	0.0000	0.0000
7	Q2	10.41	.167	.150	15.3387	26.0219	-4.2998	6.4193	.0704	.0118	0.0000	0.0000	-.2733	-.0457	0.0000	0.0000
8	Q2	11.37	.175	.157	24.7717	15.1860	-5.5202	4.8612	.0817	.0118	0.0000	0.0000	-.3171	-.0457	0.0000	0.0000
9	Q3	11.72	.177	.161	27.6176	12.5531	-2.4802	2.7591	.0841	.0014	0.0000	0.0000	-.3261	-.0055	0.0000	0.0000
10	Q3	12.07	.179	.166	28.1488	11.2038	.9868	1.1461	.0827	-.0091	0.0000	0.0000	-.3209	.0350	0.0000	0.0000
11	Q3	12.98	.184	.180	26.4215	9.3000	.9234	.9594	.0745	-.0091	0.0000	0.0000	-.2893	.0350	0.0000	0.0000
12	B3	14.50	.194	.211	23.7719	6.7953	.8167	.6780	.1276	.0788	0.0000	0.0000	-.6977	-.5717	0.0000	0.0000
13	QB3	20.92	.247	.403	16.1731	6.9484	.3662	-.7019	.6341	.0788	0.0000	0.0000	-4.3702	-.5717	0.0000	0.0000
14	Q4	21.15	.249	.408	15.7332	7.4052	1.5471	-1.3076	.6465	.0300	0.0000	0.0000	-4.4628	-.2372	0.0000	0.0000
15	Q4	21.38	.252	.413	14.7747	8.1580	2.6215	-2.0043	.6477	-.0193	0.0000	0.0000	-4.4783	.1015	0.0000	0.0000
16	Q4	24.64	.328	.448	3.3433	27.7703	.8840	-4.0099	.5846	-.0193	0.0000	0.0000	-4.1474	.1015	0.0000	0.0000
17	Q5	25.06	.350	.450	2.8710	29.5112	.2784	-.1146	.5935	.0622	0.0000	0.0000	-4.2241	-.4738	0.0000	0.0000
18	Q5	25.47	.373	.452	2.8645	27.9529	-.2623	3.8065	.6366	.1473	0.0000	0.0000	-4.5435	-1.0763	0.0000	0.0000
19	Q5	32.82	.591	.703	26.8640	1.9315	-3.0039	-.2651	1.7191	.1473	0.0000	0.0000	-12.4522	-1.0763	0.0000	0.0000
20	Q6	33.17	.633	.730	27.8812	2.2710	.1417	-.7166	1.7353	-.0551	0.0000	0.0000	-12.5747	.3799	0.0000	0.0000
21	Q6	33.52	.635	.751	26.6706	2.7634	3.2646	-1.2862	1.6807	-.2554	0.0000	0.0000	-12.1877	1.8208	0.0000	0.0000
22	Q6	37.71	.785	.825	6.9951	29.4367	1.4344	-5.0363	.6115	-.2554	0.0000	0.0000	-4.5638	1.8208	0.0000	0.0000
23	Q7	38.06	.793	.827	6.3068	31.7902	.3558	-1.5861	.5340	-.1881	0.0000	0.0000	-4.0150	1.3210	0.0000	0.0000
24	Q7	38.41	.802	.829	6.1943	31.6002	-.2305	2.1205	.4787	-.1287	0.0000	0.0000	-3.6314	.8755	0.0000	0.0000
25	Q7	41.25	.865	.847	8.8855	20.9340	-.7146	1.6252	.1122	-.1287	0.0000	0.0000	-1.1382	.8755	0.0000	0.0000
26	B7	41.56	.870	.849	9.3370	19.9592	-.7668	1.5729	.0730	-.1287	0.0000	0.0000	-.8714	.8755	0.0000	0.0000
27	QB7	42.85	.890	.860	11.6042	16.1825	-.9867	1.3479	-.0934	-.1287	0.0000	0.0000	.2607	.8755	0.0000	0.0000
28	B7	45.90	.723	.901	19.1536	9.2116	-1.3024	.9033	-.2165	.0475	0.0000	0.0000	1.0722	-.3403	0.0000	0.0000
29	QB7	46.41	.727	.910	20.7239	8.3448	-1.5888	.8031	-.1924	.0475	0.0000	0.0000	.8994	-.3403	0.0000	0.0000
30	Q8	46.64	.728	.914	21.0945	8.1289	-.0230	.1470	-.1799	.0617	0.0000	0.0000	.8140	-.4052	0.0000	0.0000
31	Q8	46.87	.730	.919	20.7447	8.2089	1.3443	-.4990	-.1642	.0748	0.0000	0.0000	.7147	-.4631	0.0000	0.0000
32	Q8	48.09	.740	.941	17.2216	9.6517	1.3454	-.6845	-.0731	.0748	0.0000	0.0000	.1501	-.4631	0.0000	0.0000
33	B8	52.66	.802	.997	8.3864	18.2172	.6078	-1.1215	.8638	.3400	0.0000	0.0000	-6.0764	-2.2929	0.0000	0.0000
34	QB8	53.16	.812	1.001	7.8111	19.3885	.5249	-1.1844	1.0365	.3400	0.0000	0.0000	-7.2412	-2.2929	0.0000	0.0000
35	Q9	53.39	.817	1.003	7.7138	19.5943	-.0970	.2899	1.1236	.4228	0.0000	0.0000	-7.8300	-2.8666	0.0000	0.0000
36	Q9	53.62	.821	1.005	7.9008	19.1266	-.7257	1.7442	1.2304	.5131	0.0000	0.0000	-8.5556	-3.4904	0.0000	0.0000
37	Q9	53.93	.827	1.007	8.3611	18.0830	-.7846	1.6798	1.3868	.5131	0.0000	0.0000	-9.6195	-3.4904	0.0000	0.0000
38	B9	54.23	.833	1.010	8.8512	17.0910	-.8230	1.5756	1.5426	.5096	0.0000	0.0000	-10.6815	-3.4786	0.0000	0.0000
39	QB9	54.84	.843	1.016	9.9250	15.2457	-.9385	1.4914	1.8533	.5096	0.0000	0.0000	-12.8021	-3.4786	0.0000	0.0000
40	B9	59.41	.892	1.098	22.2238	5.6755	-1.7947	.5767	4.7495	.7756	0.0000	0.0000	-32.6371	-5.3107	0.0000	0.0000
41	QB9	59.92	.896	1.113	24.0962	5.1502	-1.8912	.4574	5.1434	.7756	0.0000	0.0000	-35.3349	-5.3107	0.0000	0.0000
42	Q10	60.14	.897	1.120	24.7911	4.9901	-1.1396	.2446	5.3016	.6072	0.0000	0.0000	-36.4183	-4.1621	0.0000	0.0000
43	Q10	60.37	.899	1.127	25.1337	4.9253	-.3547	.0390	5.4208	.4344	0.0000	0.0000	-37.2355	-2.9830	0.0000	0.0000
44	Q10	60.88	.902	1.144	25.5056	4.9382	-.3775	-.0643	5.6414	.4344	0.0000	0.0000	-38.7509	-2.9830	0.0000	0.0000
45	B10	65.44	.928	1.260	29.7616	9.4050	-.5795	-.8778	8.1905	.7001	0.0000	0.0000	-56.3225	-4.8146	0.0000	0.0000
46	QB10	65.73	.930	1.265	30.1038	9.9335	-.5926	-.9327	8.3949	.7001	0.0000	0.0000	-57.7279	-4.8146	0.0000	0.0000
47	B10	66.04	.931	1.270	30.5455	10.4936	-.8572	-.9037	8.6190	.7703	0.0000	0.0000	-59.2321	-5.0550	0.0000	0.0000
48	QB10	66.33	.933	1.274	31.0507	11.0399	-.8738	-.9542	8.8438	.7703	0.0000	0.0000	-60.7076	-5.0550	0.0000	0.0000
49	Q11	66.77	.935	1.280	30.0168	12.5927	3.1952	-2.6786	8.9183	-.4315	0.0000	0.0000	-61.1298	3.1318	0.0000	0.0000

PHS	S (M)	QX	QY	BX (M)	BY (M)	AX	AY	DX (M)	EYP	EY (M)	EYP	XCO (MM)	DXCO (MR)	YCO (MM)	DYCO (MR)
50 Q11	67.20	.937	1.285	25.6794	15.9026	6.5318	-5.0407	8.4701	-1.6000	0.0000	0.0000	-57.9975	11.1365	0.0000	0.0000
51 Q11	67.72	.941	1.290	19.3346	21.6060	5.6458	-5.9039	7.6323	-1.6000	0.0000	0.0000	-52.1954	11.1365	0.0000	0.0000
52 Q12	68.11	.945	1.292	15.9959	25.2987	3.1369	-3.5181	7.1831	-.7298	0.0000	0.0000	-49.0582	5.1756	0.0000	0.0000
53 Q12	68.90	.949	1.294	14.3433	26.8726	1.2093	-.4978	7.0649	.1147	0.0000	0.0000	-48.1603	-.5482	0.0000	0.0000
54 Q12	68.71	.951	1.296	13.8247	27.0917	1.1719	-.3079	7.0899	.1147	0.0000	0.0000	-48.2877	-.5482	0.0000	0.0000
55 S12	69.02	.955	1.298	13.0914	27.4774	1.2324	-.7583	7.1155	.0533	0.0000	0.0000	-48.4231	-.3401	0.0000	0.0000
56 OS12	69.24	.958	1.299	12.3637	27.8104	1.1905	-.7707	7.1271	.0533	0.0000	0.0000	-48.4972	-.3401	0.0000	0.0000
57 Q13	69.62	.963	1.301	12.2270	27.1462	-.3043	2.4672	7.3121	.9092	0.0000	0.0000	-49.7402	-6.1234	0.0000	0.0000
58 Q13	70.01	.967	1.303	13.0493	24.1187	-1.8396	5.2618	7.8340	1.8070	0.0000	0.0000	-53.2617	-12.1873	0.0000	0.0000
59 Q13	70.51	.973	1.307	14.9831	19.1801	-2.0295	4.6704	8.7325	1.8070	0.0000	0.0000	-59.3214	-12.1873	0.0000	0.0000
60 Q14	70.83	.976	1.310	15.8280	16.8492	-.5671	2.6540	9.1719	.9180	0.0000	0.0000	-62.2818	-6.1912	0.0000	0.0000
61 Q14	71.15	.980	1.313	15.4990	15.6942	.9663	-.9764	9.3199	-.0000	0.0000	0.0000	-63.2791	.0000	0.0000	0.0000
62 LS*	78.99	1.102	1.436	8.1182	8.0343	.0000	-.0000	9.3199	-.0000	0.0000	0.0000	-63.2791	.0000	0.0000	0.0000
63 A20	78.99	1.102	1.436	8.1182	8.0343	.0000	-.0000	9.3199	-.0000	0.0000	0.0000	-.3622	0.0000	0.0000	0.0000
64 REFL	157.99	2.204	2.872	6.7146	7.1758	.0000	-.0000	.0935	-.0000	0.0000	0.0000	-.3622	0.0000	0.0000	0.0000

CIRCUMFERENCE = 473.9592 M THETX = 6.28318533 RAD NUX = 6.61177 DNUX/(DP/P) = -.22134
RADIUS = 75.4330 M THETY(63) = 0.00000000 RAD NUY = 8.61726 DNUY/(DP/P) = .32513
(DS/S)/(DP/P) = .0330498 TGAM = (5.50067, 0.00000)

MAXIMA --- BETX(48) = 31.05075 BETY(23) = 31.79018 ETAX(61) = 9.31994 ETAY(64) = 0.00000
MINIMA --- BETX(18) = 2.86447 BETY(19) = 1.93146 ETAX(28) = -.21650 ETAY(64) = 0.00000

```
                                  EXTRACTION ORBIT
                                  8.0 GEV KINETIC

***  DP      =                    //    .00825
***  V       PVEC                 //
***  EXT     FXPT    2   -3       //  V     R/6          1
   *                               //
```

DP

CALCULATION OF THE EQUILIBRIUM ORBIT AND BETATRON FUNCTIONS OF EXT
INITIAL REFERENCE RAY DEFINED BY V
X = 0.00000000 DX = 0.00000000 Y = 0.00000000 DY = 0.00000000 DS = 0.00000000 DP/P = .00825000 1.00000000
3

7X7 MATRIX FOR EXT

.27141873	8.50707256	0.00000000	0.00000000	0.00000000	-.13191220	.00060208
-.10888962	.27141873	0.00000000	0.00000000	0.00000000	-.01971485	.00008998
0.00000000	0.00000000	.70581336	-5.11973196	0.00000000	0.00000000	0.00000000
0.00000000	0.00000000	.09801832	.70581336	0.00000000	0.00000000	0.00000000
.01971485	.13191220	0.00000000	0.00000000	1.00000000	-5.46449632	.04241407
0.00000000	0.00000000	0.00000000	0.00000000	0.00000000	1.00000000	0.00000000
0.00000000	0.00000000	0.00000000	0.00000000	0.00000000	0.00000000	1.00000000

EIGENVALUES OF THE 4X4 SUBMATRIX

X... LMD1 = (.27141873 .96246136), C(1) = 1.00000000, MU(1) = 1.29592953 RAD, Q(1) = .61876077
1/LMD1 = (.27141873 -.96246136), C(2) = 1.00000000, MU(2) = -1.29592953 RAD, Q(2) = .38123923

Y... LMD3 = (.70581336 .70839784), C(3) = 1.00000000, MU(3) = .78722567 RAD, Q(3) = .37587257
1/LMD3 = (.70581336 -.70839784), C(4) = 1.00000000, MU(4) = -.78722567 RAD, Q(4) = .62412743

EIGENVALUE = (.27141873, .96246136), EIGENVECTOR = (2.97302401, -.00000000)
(.00000000, .33635786)
(0.00000000, 0.00000000)
(0.00000000, 0.00000000)

EIGENVALUE = (.27141873, -.96246136), EIGENVECTOR = (2.97302401, .00000000)
(.00000000, -.33635786)
(0.00000000, 0.00000000)
(0.00000000, 0.00000000)

EIGENVALUE = (.70581336, .70839784), EIGENVECTOR = (0.00000000, 0.00000000)
(0.00000000, 0.00000000)
(2.68834497, .00000000)
(.00000000, -.37197607)

EIGENVALUE = (.70581336, -.70839784), EIGENVECTOR = (0.00000000, 0.00000000)
(0.00000000, 0.00000000)
(2.68834497, -.00000000)
(.00000000, .37197607)

	X	DX	Y	DY	DS	DP/P	
EQ ORBIT	-.00067869	0.00000000	0.00000000	0.00000000	0.00000000	.00825000	1.00000000
ETA ORBIT	-.18105351	-.00000000	0.00000000	0.00000000	0.00000000	1.00000000	0.00000000

EIGENVECTORS 1 AND 3 IN POLAR COORDINATES

PLUS	X1 X3		DX1 DX3		Y1 Y3		DY1 DY3	
0	2.973024 0.000000	-.000000 0.000000	.336358 0.000000	1.570796 0.000000	0.000000 2.688345	0.000000 .000000	0.000000 .371976	0.000000 -1.570796

BETATRON FUNCTIONS OF EXT

POS		S (M)	QX	QY	BX (M)	BY (M)	AX	AY	EX (M)	EXP	EY (M)	EYP	XCO (MM)	DXCO (MR)	YCO (MM)	DYCO (MR)
0		0.00	0.000	0.000	8.8389	7.2272	0.0000	0.0000	-.1811	-.0000	0.0000	0.0000	-.6787	0.0000	0.0000	0.0000
1	A10	0.00	0.000	0.000	8.8389	7.2272	0.0000	0.0000	-.1811	-.0000	0.0000	0.0000	-.6787	0.0000	0.0000	0.0000
2	LS	7.95	.117	.133	15.9831	15.9646	-.8990	-1.0995	-.1811	-.0000	0.0000	0.0000	-.6787	0.0000	0.0000	0.0000
3	Q1	8.27	.120	.136	15.9900	17.2790	-.8777	-3.0566	.1778	.0201	0.0000	0.0000	-.6666	.0756	0.0000	0.0000
4	Q1	8.59	.123	.138	14.8861	19.9717	-2.5301	-5.4573	-.1683	.0395	0.0000	0.0000	-.6306	.1485	0.0000	0.0000
5	D1	9.10	.129	.142	12.4238	25.9692	2.2753	-6.2471	-.1480	.0395	0.0000	0.0000	-.5545	.1485	0.0000	0.0000
6	Q2	9.75	.138	.146	11.3221	30.2772	-.5119	.0114	-.1328	.0077	0.0000	0.0000	-.4969	.0293	0.0000	0.0000
7	Q2	10.41	.147	.149	13.9058	25.9422	-3.6234	6.2634	-.1376	-.0228	0.0000	0.0000	-.5152	-.0855	0.0000	0.0000
8	D2	11.37	.155	.157	21.8045	15.3399	-4.5994	4.7738	-.1595	-.0228	0.0000	0.0000	-.5973	-.0855	0.0000	0.0000
9	Q3	11.72	.158	.161	24.1356	12.7591	-1.9555	2.6941	-.1641	-.0029	0.0000	0.0000	-.6142	-.0109	0.0000	0.0000
10	Q3	12.07	.160	.166	24.4683	11.4532	1.0200	1.0847	-.1616	.0170	0.0000	0.0000	-.6049	.0642	0.0000	0.0000
11	D3	12.98	.166	.179	22.6920	9.6471	.9446	.9129	-.1462	.0170	0.0000	0.0000	-.5468	.0642	0.0000	0.0000
12	B3	14.50	.178	.208	20.0113	7.2437	.8177	.6578	-.0544	.1036	0.0000	0.0000	-.0946	.7787	0.0000	0.0000
13	D83	20.92	.243	.389	12.9472	6.9538	.2820	-.6127	.6113	.1036	0.0000	0.0000	5.0966	.7787	0.0000	0.0000
14	Q4	21.15	.246	.394	12.6048	7.3666	1.2073	-1.2034	.6298	.0577	0.0000	0.0000	5.2308	.3934	0.0000	0.0000
15	Q4	21.38	.249	.398	11.8557	8.0667	2.0509	-1.8766	.6377	.0108	0.0000	0.0000	5.2760	.0015	0.0000	0.0000
16	D4	24.64	.338	.434	3.1496	26.2662	.6189	-3.7044	.6730	.0108	0.0000	0.0000	5.2808	.0015	0.0000	0.0000
17	Q5	25.06	.360	.437	2.8751	27.8624	.0565	-.0782	.6964	.1028	0.0000	0.0000	5.4308	.7266	0.0000	0.0000
18	Q5	25.47	.383	.439	3.0524	26.3909	-.4928	3.5653	.7589	.2006	0.0000	0.0000	5.8881	1.4928	0.0000	0.0000
19	D5	32.82	.516	.685	32.2786	2.0472	-3.4847	-.2522	2.2325	.2006	0.0000	0.0000	16.8568	1.4928	0.0000	0.0000
20	Q6	33.17	.517	.711	33.4309	2.3765	.2415	-.6998	2.2581	-.0549	0.0000	0.0000	17.0402	-.4499	0.0000	0.0000
21	Q6	33.52	.519	.731	31.9489	3.0548	3.9296	-1.2610	2.1943	-.3081	0.0000	0.0000	16.5435	-2.3746	0.0000	0.0000
22	D6	37.71	.561	.806	8.0638	28.4810	1.7748	-4.8114	.9042	-.3081	0.0000	0.0000	6.6008	-2.3746	0.0000	0.0000
23	Q7	38.06	.568	.807	7.1799	30.7323	.7809	-1.5251	.8137	-.2102	0.0000	0.0000	5.8966	-1.6574	0.0000	0.0000
24	Q7	38.41	.576	.809	6.9393	30.5620	-.0852	2.0042	.7559	-.1208	0.0000	0.0000	5.4311	-1.0073	0.0000	0.0000
25	Q7	41.25	.636	.827	8.6015	20.4789	-.4985	1.5367	.4119	-.1208	0.0000	0.0000	2.5627	-1.0073	0.0000	0.0000
26	S7	41.56	.642	.830	8.9187	19.3379	-.5420	1.4850	.3751	-.1208	0.0000	0.0000	2.2556	-1.0074	0.0000	0.0000
27	D87	42.85	.663	.841	10.5629	15.9916	-.7296	1.2731	.2188	-.1208	0.0000	0.0000	.9530	-1.0074	0.0000	0.0000
28	B7	45.90	.700	.881	16.3211	9.3944	-1.1695	.8593	.1155	.0527	0.0000	0.0000	.0687	.4243	0.0000	0.0000
29	D87	46.41	.705	.890	17.5468	8.5692	-1.2432	.7653	.1422	.0527	0.0000	0.0000	.2843	.4243	0.0000	0.0000
30	Q8	46.64	.707	.895	17.8191	8.3718	.0586	-.1030	.1530	.0417	0.0000	0.0000	.3786	.3996	0.0000	0.0000
31	Q8	46.87	.709	.899	17.4938	8.4739	1.3564	-.3522	.1613	.0300	0.0000	0.0000	.4664	.3680	0.0000	0.0000
32	D8	48.09	.721	.920	14.4276	10.0494	1.1585	-.7400	.1978	.0300	0.0000	0.0000	.9151	.3680	0.0000	0.0000
33	B8	52.66	.794	.974	7.2767	19.1277	.4247	-1.1804	.9241	.2911	0.0000	0.0000	7.4493	2.5221	0.0000	0.0000
34	D88	53.17	.806	.978	6.8870	20.3593	.3423	-1.2440	1.0719	.2911	0.0000	0.0000	8.7305	2.5221	0.0000	0.0000
35	Q9	53.39	.811	.980	6.8561	20.5806	-.2065	.2819	1.1478	.3736	0.0000	0.0000	9.3838	3.2014	0.0000	0.0000
36	Q9	53.62	.816	.981	7.0780	20.1047	-.7697	1.7885	1.2432	.4626	0.0000	0.0000	10.1984	3.9357	0.0000	0.0000
37	D9	53.93	.823	.984	7.5681	19.0339	-.8382	1.7248	1.3842	.4626	0.0000	0.0000	11.3979	3.9357	0.0000	0.0000
38	B9	54.23	.829	.986	8.1066	17.9868	-.9287	1.7099	1.5258	.4665	0.0000	0.0000	12.6000	3.9519	0.0000	0.0000
39	D89	54.84	.840	.992	9.3243	15.9831	-1.0688	1.5769	1.8102	.4665	0.0000	0.0000	15.0091	3.9519	0.0000	0.0000
40	B9	59.42	.889	1.073	23.7495	5.5174	-2.1077	.6250	4.5161	.7268	0.0000	0.0000	37.7711	6.1029	0.0000	0.0000
41	D89	59.93	.893	1.089	25.9300	4.9475	-2.2241	.4969	4.8653	.7268	0.0000	0.0000	40.8714	6.1029	0.0000	0.0000
42	Q10	60.16	.894	1.096	26.7878	4.7681	-1.4304	.2896	5.0338	.5717	0.0000	0.0000	42.1177	4.7944	0.0000	0.0000
43	Q10	60.39	.895	1.104	27.2523	4.6813	-.5955	.0906	5.1464	.4125	0.0000	0.0000	43.0608	3.4514	0.0000	0.0000
44	D10	60.89	.898	1.121	27.8702	4.6449	-.6207	-.0188	5.3560	.4125	0.0000	0.0000	44.8141	3.4514	0.0000	0.0000
45	B10	65.48	.922	1.247	34.5953	9.0192	-.8459	-.9062	7.8257	.6730	0.0000	0.0000	65.3457	5.6031	0.0000	0.0000
46	D810	65.77	.923	1.252	35.0933	9.3654	-.8604	-.9652	8.0222	.6730	0.0000	0.0000	66.9812	5.6031	0.0000	0.0000
47	S10	66.08	.924	1.257	35.5208	10.2013	-.5411	-1.1224	8.2157	.5970	0.0000	0.0000	68.6405	5.2843	0.0000	0.0000
48	DS10	66.37	.926	1.261	35.8398	10.8754	-.5517	-1.1871	8.3900	.5970	0.0000	0.0000	70.1829	5.2843	0.0000	0.0000
49	Q11	66.81	.928	1.267	34.2876	12.4328	4.0373	-2.9125	8.4101	-.5055	0.0000	0.0000	70.4597	-4.0235	0.0000	0.0000

POS		S (M)	GX	GY	BX (M)	BY (M)	AX	AY	LX (M)	LXP	LY (M)	LYP	XCO (MM)	DXCO (MR)	YCO (MM)	DY (MR)
50	Q11	67.24	930	1.272	29.0478	16.1645	7.7143	-5.3205	7.9519	-1.5793	0.0000	0.0000	56.7010	-13.1008	0.0000	0.0000
51	Q11	67.76	933	1.276	21.5747	22.2008	6.6290	-6.2651	7.1390	-1.5793	0.0000	0.0000	59.8752	13.1008	0.0000	0.0000
52	Q12	68.15	936	1.279	17.6032	26.1741	3.8176	-3.6790	6.6746	-.7855	0.0000	0.0000	56.1297	-6.3736	0.0000	0.0000
53	Q12	68.54	940	1.281	15.5038	28.0094	1.7027	-.8058	6.5185	-.0268	0.0000	0.0000	54.9166	.0659	0.0000	0.0000
54	Q12	68.75	942	1.282	14.7740	28.3632	1.6480	-.8186	6.5127	-.0268	0.0000	0.0000	54.9309	.0659	0.0000	0.0000
55	Q12	69.06	946	1.284	13.8340	28.7834	1.4383	-.5590	6.5140	.0356	0.0000	0.0000	54.9913	.3304	0.0000	0.0000
56	QS12	69.28	948	1.285	13.2180	29.0290	1.3900	-.3689	6.5218	.0356	0.0000	0.0000	55.0633	.3304	0.0000	0.0000
57	Q13	69.66	953	1.287	12.7482	28.1768	-.1566	2.7465	6.6813	.7948	0.0000	0.0000	56.4340	6.7962	0.0000	0.0000
58	Q13	70.05	958	1.290	13.4648	24.9183	-1.7317	5.5755	7.1395	1.5896	0.0000	0.0000	60.3507	13.5685	0.0000	0.0000
59	Q13	70.55	963	1.293	15.2603	19.6921	-1.8794	4.9353	7.9298	1.5896	0.0000	0.0000	67.0972	13.5685	0.0000	0.0000
60	Q14	70.87	967	1.296	16.0055	17.2047	-.4090	2.8783	8.3165	.8072	0.0000	0.0000	70.3927	6.8912	0.0000	0.0000
61	Q14	71.19	970	1.299	15.7781	15.9122	1.1119	1.1832	8.4467	.0000	0.0000	0.0000	71.5027	.0000	0.0000	0.0000
62	LS*	79.03	1.103	1.437	7.0555	6.6303	.0000	-.0000	8.4467	-.0000	0.0000	0.0000	71.5027	.0000	0.0000	0.0000
63	A20	79.03	1.103	1.437	7.0555	6.6303	.0000	-.0000	8.4467	-.0000	0.0000	0.0000	71.5027	.0000	0.0000	0.0000
64	REFL	158.07	2.206	2.875	8.8389	7.2272	.0000	-.0000	-.1811	.0000	0.0000	0.0000	-.6787	0.0000	0.0000	0.0000

CIRCUMFERENCE = 474.2024 M THETX = 6.28318533 RAD NUX = 6.61876 DNUX/(DP/P) = 1.94317
RADIUS = 75.4717 M THETY(63) = 0.00000000 RAD NUY = 8.42413 DNUY/(DP/P) = .23079
(DS/S)/(DP/P) = .0345932 TCAM = (5.37656, 0.00000)

MAXIMA --- BETX(48) = 35.83982 BETY(23) = 30.73231 ETAX(61) = 8.44668 ETAY(64) = 0.00000
MINIMA --- BETX(17) = 2.87511 BETY(19) = 2.04719 ETAX(2) = -.18105 ETAY(64) = 0.00000

*** PAGE //